FOSSIL

DOE/PC/79817-8
(DE91005868)

DIRECT CONVERSION OF METHANE TO C_2's AND LIQUID FUELS

Final Technical Progress Report for the Period
October 1, 1987—December 31, 1989

By
Barbara Knight Warren
Kenneth D. Campbell
J. L. Matherne
G. L. Culp
N. E. Kinkade

April 15, 1990

Work Performed Under Contract No. AC22-87PC79817

For
U.S. Department of Energy
Pittsburgh Energy Technology Center
Pittsburgh, Pennsylvania

By
Union Carbide Chemical and Plastics Company, Inc.
South Charleston, West Virginia

DISCLAIMER

This report was prepared as an account of work sponsored by an agency of the United States Government. Neither the United States Government nor any agency thereof, nor any of their employees, makes any warranty, express or implied, or assumes any legal liability or responsibility for the accuracy, completeness, or usefulness of any information, apparatus, product, or process disclosed, or represents that its use would not infringe privately owned rights. Reference herein to any specific commercial product, process, or service by trade name, trademark, manufacturer, or otherwise does not necessarily constitute or imply its endorsement, recommendation, or favoring by the United States Government or any agency thereof. The views and opinions of authors expressed herein do not necessarily state or reflect those of the United States Government or any agency thereof.

DISCLAIMER

Portions of this document may be illegible in electronic image products. Images are produced from the best available original document.

DOE/PC/79817--8

DE91 005868

DIRECT CONVERSION OF METHANE TO C_2's AND LIQUID FUELS

Final Technical Progress Report for the Period October 1, 1987 - December 31, 1989

April 15, 1990

By Barbara Knight Warren; Kenneth D. Campbell; J. L. Matherne;
G. L. Culp; N. E. Kinkade
Contributions from P. H. Tate

Work Performed Under DOE Contract Number DE-AC22-87PC79817

Prepared for U. S. Department of Energy
Assistant Secretary for Fossil Energy

Industrial Chemicals Division

Solvents and Coatings Materials Division

Union Carbide Chemical and Plastics Company Inc.
South Charleston Technical Center
South Charleston, West Virginia 25303

Patent cleared by Chicago OPC on June 19, 1990

CONTENTS

I.	Contract Objectives	1
II.	Abstract	2
III.	Organization	3
IV.	Summary of Progress	4
V.	Technical and Experimental Results	8
VI	References	187
VII.	Appendices	195
	A. Key to Tables and Definitions	195
	B. Experimental	197
	1. BKW Laboratory	198
	2. KDC Laboratory	201
	3. NEK Laboratory	203
	4. Tables	207
	5. Figures	218
	C. Catalyst Preparation Procedures	240
	1. BKW Laboratory	240
	a. Examples	244
	b. Sources of Materials	249
	3. KDC Laboratory	251
	4. NEK Laboratory	258
	D. Catalyst Compositions and Preparation Procedures, BKW Laboratory	259
	E. Catalyst Compositions and Preparation Procedures, KDC Laboratory	264
	F. Tables and Figures	270
	G. EDS Data - Weight and Atom Percent	308
	H. References for Selectivity/Conversion Plot	313
	I. Process Conceptualization - Methane to C_2's	337
	J. Process Conceptualization - Methane to Liquid Hydrocarbon Fuels	375
	K. Engineering Assumptions, Definitions, Methods, and Index of Cases	399
	1. Assumptions and Definitions	399
	2. Methods	400
	3. Index of Sensitivity Study Cases	402

I. CONTRACT OBJECTIVES

Methane is expensive to transport, so it is often flared or reinjected[1]. It is also a by-product from coal gasification. Conversion of methane to liquid hydrocarbon transportation fuels in an energy efficient, economical process would represent important technology for extending natural hydrocarbon fuel reserves. One route from methane to liquid fuels involves the conversion of methane through light hydrocarbon gases rich in ethylene to liquid fuels. Other routes, including one through methanol, are considered less technologically feasible[2]. The technological hurdle in the route through light hydrocarbon gases rich in ethylene is the direct conversion of methane to this ethylene-rich mixture. The light olefins may then, ideally, with little or no separation of products, be converted over molecular sieve catalysts to gasoline and distillates using Mobil's Olefins to Gasoline and Distillate (MOGD) Process[3].

The objectives of the project are to discover and evaluate novel catalytic systems for the conversion of methane or by-product light hydrocarbon gases (from natural gas, Lurgi Dry Bottom Gasifiers, or Fischer-Tropsch processes) either indirectly (through intermediate light gases rich in C_2's) or directly to liquid hydrocarbon fuels, and to evaluate, from an engineering perspective, different conceptualized schemes. The approach was to carry out catalyst testing on several specific classes of potential catalysts for the conversion of methane selectively to C_2 products, including metal oxide catalysts, catalysts containing metals in unusual oxidation states, and other novel catalysts and process ideas, and to provide appropriate engineering support to the catalyst design and testing effort. Promising catalysts and process ideas were further explored.

II. ABSTRACT

Conversion of methane to liquid hydrocarbon transportation fuels in an energy efficient, economical process would represent important technology for extending natural hydrocarbon fuel reserves. The technological hurdle in the route through light hydrocarbon gases rich in ethylene is the direct conversion of methane to this ethylene-rich mixture.

Methane coupling catalysts were explored which are the first reported catalysts to provide hundreds of hours of stable operation in the oxidation of methane to C_2's with high ethylene to ethane product ratios (2.5-10 or more). These catalysts contain alkaline earth components and require the presence of small amounts of halides, either as a catalyst component or as a periodic or continuous additive to the catalyst.

Other classes of catalysts studied include simple perovskites, layered perovskites, metal/molecular sieves, hydrotalcites, catalysts based on Pr/Ce oxygen carriers, low temperature silver catalysts, low temperature catalysts containing certain Group VIII metals, and superacids (in the cofeed mode), and a unique class of sequential mode double perovskite coupling catalysts. Catalyst systems were provided which demonstrate two concepts to avoid the heterogeneous/homogeneous reaction mechanism thought to be common to all reported catalyst systems. Some of these catalyst systems show enhanced surface reactions at lower temperatures, and others alter the reaction pathways in the vapor phase. These two concepts suggest future generations of methane coupling catalysts which might be economically viable.

Methane coupling products from low pressure coupling reactions (<25 psig) were oligomerized to liquid hydrocarbons without separation and/or compression of the product stream.

Economic assessments were completed for several cases of methane coupling, for a comparison case where gasoline and distillate fuels are produced from methane using conventional technology involving reforming, and for the economically best case from methane to gasoline and distillate fuels using methane coupling technology.

The economics of producing gasoline and distillate fuels from methane coupling are roughly equivalent to those for making these materials from methane using a synthesis gas and methanol route, but not currently competitive with the economics of producing these from petroleum. Given the early state of development of oxidative coupling catalysis and sufficient time and resources, future generations of catalysts or catalyst improvements should confer superior economics to the methane coupling route.

III. ORGANIZATION

Union Carbide Chemicals and Plastics Company Inc.'s (UCC&P, formerly Union Carbide Corporation) catalyst development, catalyst evaluation, and conceptual process design efforts for converting methane or by-product light hydrocarbon gases either indirectly or directly to liquid hydrocarbon fuels were being pursued by a group within the Solvents and Coatings Materials Division. During the initial portion of the contract, this group was part of the Engineering, Manufacturing and Technology Services Division.

The work was performed at UCC&P's South Charleston Technical Center, South Charleston, West Virginia 25303.

Project Manager and Principal Investigator is Dr. Barbara Knight Warren.

Program Manager is Dr. Donald C. Best.

IV. SUMMARY OF PROGRESS

TASK 1: Catalyst Design and Testing

Task 1 work involved the set-up of reactor equipment, the development and testing of catalysts for the direct conversion of methane to C_2's (ethylene and ethane), and (briefly) the conversion of C_2's to liquid fuels. Task 1 is completed. Seven Quarterly Reports have been written, and this is the Final Report under this contract.

Conversion of methane to liquid hydrocarbon transportation fuels in an energy efficient, economical process would represent important technology for extending natural hydrocarbon fuel reserves. The technological hurdle in the route through light hydrocarbon gases rich in ethylene is the direct conversion of methane to an ethylene-rich mixture. The literature on methane coupling catalysts has disclosed or claimed nearly all elements as methane coupling catalysts. The literature does not distinguish among the many materials used and claimed, which, if any, material would provide a stable catalyst for the conversion of methane to ethylene. Published literature reports contain no data which indicate the catalysts studied give stable, long-term performance. Most literature catalysts are operated at temperatures from 700-950 °C at pressures close to atmospheric pressure, and produce about equal amounts of ethane and ethylene, with carbon monoxide and carbon dioxide as the major by-products. These catalysts are proposed to operate by a heterogeneous/homogeneous reaction mechanism which may impose a C_2 yield limit and similar product distributions.

Methane coupling catalysts were provided which are comparable in selectivity, activity, and C_2 yield to the better literature catalysts, but which provide hundreds of hours of stable operation in the oxidation of methane to C_2's. These catalysts also produce high ethylene to ethane product ratios (2.5-10 or more). These catalysts contain alkaline earth components and require the presence of a small amount of halides, either as a catalyst component or as a periodic or continuous additive to the catalyst. The chloride appears to serve three distinct roles, resulting in suppression of carbon dioxide formation, increased rates to C_2 products, and in higher ethylene to ethane product ratios. Acidic supports result in higher ethylene to ethane product ratios.

Other classes of catalysts have also been tested. Some of these were less promising, although the concepts, such as that of locking an active metal into an unusual coordination or oxidation state within a framework, remain viable and interesting. Those catalysts tested within the catalyst classes of framework metal molecular sieves,

hydrotalcites, simple perovskites, catalysts based on Pr/Ce oxygen carriers, catalysts containing Fe and Cu, and superacids showed no advantages over literature catalysts.

Other catalysts were novel and have process advantages. These include layered perovskite catalysts, a unique class of double perovskite coupling catalysts which operate in the sequential mode, catalysts containing silver, catalysts containing certain Group VIII metals, and vapor phase catalysts. Layered perovskites of the form $A_2Ln_2Ti_3O_{10}$ (A = K, Rb, Na; Ln = La, Nd, Sm, Dy, Gd, Pr, Ce) represent a new type of methane coupling catalyst in which the alkali dopant is part of the crystal structure. Alkali carbonate doped $LaCaMnCoO_6$ catalysts showed very high C_{2+} selectivities and exhibited the unique characteristic in the sequential mode that the CH_4 conversions and C_2 selectivities were highest during the early stages of the catalyst reduction cycle. Catalysts containing $SrCl_2$, α-alumina, and Co, Ni, or Rh showed C_2 selectivities of 50-70% and C_2 yields of 13-18% at 650 °C.

Catalysts containing silver and Pd or Pt operate at lower temperatures than most methane coupling catalysts and show unusually high C_3 selectivities, demonstrating the concept of enhanced surface reactions, a move away from the heterogeneous/ homogeneous reaction mechanism with the apparent C_2 yield barrier. An alternate way to avoid the C_2 yield barrier is to change the chemistry in the vapor phase. The use of vapor phase catalysts was proposed and explored.

Methane coupling with an alkaline earth catalyst was demonstrated with a model processed natural gas mixture. Methane coupling products from low pressure coupling reactions (<25 psig) were oligomerized to liquid hydrocarbons without prior separation and/or compression of the C_2 containing stream. The integrated process gave substituted benzenes, substituted napthalenes, and xylenes as the main products. To obtain particular hydrocarbon fractions, higher ethylene pressures in the oligomerization reaction and/or separation of some components from the product stream would be required.

In summary, UCC&P has provided stable methane coupling systems which produce high (2.5-10) ethylene to ethane product ratios. Other catalyst systems were provided which are unique in their behavior, which show enhanced surface reactions at lower temperatures, and which alter the reaction pathways in the vapor phase.

TASK 2: Process Conceptualization

Task 2 covers all of the engineering studies. It involves evaluation and development of conceptual processes for converting methane to C_2's and C_2's to fuels, and also includes engineering assistance to catalyst design and testing. Task 2 is completed, and results are reported in this Final Report.

The purposes of the Task 2 engineering program have been to compare the economics of making gasoline and distillate fuels from methane, through olefins produced via methane coupling with a route utilizing synthesis gas and methanol as intermediates; and to provide economic direction to the methane coupling catalyst research program by quantifying the economic sensitivities to key process variables.

The key directions given to the catalyst screening program by the Task 2 engineering program were: (1) the yield to C_2's (alone) is not a good general predictor of economic performance, and (2) high selectivity to C_2's is more critical than high methane conversion. These conclusions stem from the finding that the Methane Diluent case (where no diluent is added, but high methane to oxygen feed ratios are used) is favored economically to any of the Nitrogen and Steam Diluent cases studied. Compared to any other diluent, methane provides the maximum selectivity to C_2's, the minimum methane conversion, the minimum C_2 yield, and the best economics. These conclusions are further reinforced by the finding that for both Nitrogen and Steam Diluent cases, the economics improve with increasing methane/oxygen feed ratio, which increases selectivity to C_2's at the expense of lower methane conversion and C_2 yield.

The best of the Sequential Feed cases have similar economics to the Co-feed Methane Diluent case. However, the Sequential Feed cases are based on literature results versus extrapolation of actual laboratory results for the Co-feed cases; they require a fluidized-bed reactor design, while Co-feed cases can use fixed-bed reactors; and they require a ready customer for the heavy co-products which are produced. Therefore, the Co-feed Methane Diluent case is preferred over the more technically and commercially complex Sequential Feed cases.

The economics favor the maximum concentration of oxygen in the reactor feed, up to the explosive limits of the mixture, in spite of the higher selectivity to C_2's that result from lower oxygen concentrations. Increasing the ethylene to ethane production ratio is important economically up to a ratio of 3.0; less so above this level. The best way to handle any level of co-product ethane is to provide conventional steam cracking hardware to convert it to additional ethylene within the process. All other things being equal, the economics favor a lower reactor temperature and a higher reactor pressure. However, the

impact of reactor pressure on the selectivity to C_2's has not been fully considered in this evaluation.

Hypothetical catalyst improvements that would allow both the selectivity to C_2's and the methane conversion to be increased from their current levels would greatly improve the economics of the resulting oxidative coupling process. Such improvements have the potential to reduce the Total Fixed Investment by 30%, and the Cash Cost by 17%. Given sufficient time and resources, future catalyst improvements should confer superior economics to the methane coupling process.

The best process configuration for oxidatively coupling methane to ethylene based on extrapolated catalyst results using a barium on alpha-alumina catalyst with low levels of ethyl chloride in the methane feed gas and a reactor pressure of 50 psig is to use a fixed bed reactor, no added diluent (methane diluent), a methane to oxygen feed ratio of 7, a reactor temperature of 725 °C, and to provide the capability to crack co-product ethane to ethylene. The methane diluent case assumes a methane conversion of 18.4%, a selectivity to C_2's of 76.7%, and an ethylene to ethane production ratio of 3, based on extrapolated laboratory results. The Total Fixed Investment for this cases would be $482MM for a plant producing one billion pounds per year olefins, and the Cash Cost per pound of olefins would be 12.4 ¢.

The Comparison Case is based upon a total production of 3320 metric tons per day of methanol in two parallel operating units followed by single train Methanol to Olefins (MTO) and MOGD facilities which produce a final product of 10,600 barrels per day of gasoline and distillate. The total fixed investment is $491MM, the total cash cost/lb is 13.6 ¢, and a sales price of $1.94/gallon of gasoline and distillate products will be required in order to generate a ten percent after tax return on investment based upon a natural gas cost of $2.15/MMBTU. For the same liquid fuels production rate, the total fixed investment for Case 2 is $538MM, the total cash cost/lb is 12.8 ¢, and the required sales price is $2.09/gallon. Thus, within the error of the estimates, both methane based routes to liquid fuels are judged to be about equal but the scope for improvement of the methane coupling process is probably greater since it is still in the very early stages of research and development.

This result is viewed as encouraging, given the early state of development of oxidative coupling catalysis. Given sufficient time and resources, future catalyst improvements should confer superior economics to the methane coupling route. However, enormous technological breakthroughs would be required for either process to be competitive with the present oil based route which currently produces liquid fuels at an average sales price of about $0.53/gallon.

V. TECHNICAL AND EXPERIMENTAL RESULTS

By B. K. Warren, K. D. Campbell, J. L. Matherne
G. L. Culp, N. E. Kinkade
Contibutions from P. H. Tate

TABLE OF CONTENTS

TASK 1: Catalyst Design and Testing 11
A. Introduction 11
1. Background 11
2. Approach 14
B. Experimental 15
C. Results and Discussion 16
1. BKW Laboratory 16
a. Control Studies 16
b. Alkali Chloride/Metal Oxide Catalysts 20
(1) Catalyst Deactivation 22
(2) Added Volatile Chloride to Retard Catalyst Deactivation .. 23
(3) Pure Components 24
(4) Other Anions 25
(5) Other Catalysts 25
c. Alkaline Earth Chloride/Alpha-Alumina Catalysts 26
(1) Concentration Studies 31
(2) Process Variable Studies 33
(3) Other Anions 35
d. Alkaline Earth Chloride/Metal Oxide Catalysts 38
(1) Support Acidity 39
(2) Pure Components 44
(3) Catalysts Containing Non-Group IA or IIA Metals 46
e. Alkaline Earth/Metal Oxide/Halide Catalysts 48
(1) Ethyl Chloride/Support Interactions 50
(2) Concentration Studies 52
(3) Catalyst Lifetimes 54

(4) Space Velocity 57
(5) Methane to Oxygen Ratios 59
(6) Added Ethane 60
(7) Higher Ethyl Chloride Levels 62
(8) Other Supports 67
(9) Non-Chloride Halides 67
(10) Role of Halide 73
(11) Vapor-Phase Catalyst-Derived Free Radicals 77
(12) Anions 84
(13) Pressure 92
(14) Catalyst Surface Analyses 93
(15) Natural Gas Mixture 95
f. Comparative Examples 99
g. Summary of Methane Coupling Catalyst Performance 101
h. Avoiding the Heterogeneous/Homogeneous Mechanism 103
(1) Silver Catalysts 103
(2) Vapor Phase Catalysts 111
i. Metals in Activated States 114
(1) Metal Molecular Sieve Catalysts 115
j. Base Catalysts - Hydrotalcites 116
2. KDC Laboratory 117
a. Homogeneous Methane Oxidation 117
b. Layered Perovskites 122
c. Low Temperature Catalysts 126
d. Double Perovskite Catalysts 131
e. Oligomerization 138
3. NEK Laboratory 144
a. Reactor Validation 144
b. Steam 145
c. High Pressure 150
D. Summary 151

TASK 2: Process Conceptualization 153
A. Introduction 153
B. Results and Discussion 154
1. Comparison of Methane Coupling and Conventional Routes to Fuels 154
a. Methane Coupling Simplified Block Diagram 154
b. Synthesis Gas/Methanol Process Simplified Block Diagram 156
c. Gasoline and Distillate Economics 157
2. Methane Coupling Sensitivity Studies 158
a. Sensitivity to Reactor Diluent 158
(1) Methane Coupling Process Simplified Block Diagram 159
(2) Reactor Diluent Case Descriptions 162
(3) Reactor Diluent Investment Costs 164
(4) Reactor Diluent Economics 165
b. Sensitivity to Methane/Oxygen Ratio 168
(1) Nitrogen Diluent Cases 168
(2) Methane Diluent Case 169
(3) Steam Diluent Cases 170
(4) Sequential Feed Cases 171
(5) Summary of Economic Sensitivity to Methane/Oxygen Ratio 172
c. Sensitivity to Oxygen Concentration in the Reactor Feed 173
d. Sensitivity to Ethylene to Ethane Product Ratio 174
e. Sensitivity to the Fate of Co-Product Ethane 175
f. Sensitivity to Reactor Temperature and Pressure 176
(1) Reactor Temperature Cases 176
(2) Reactor Pressure Cases 177
g. Hypothetical Catalyst Performance Economics 177
3. Comparison Case 178
4. Case 2 182
5. Economic Analysis 182
a. Comparison Case 182
b. Case 2 183
C. Summary 184

REFERENCES 187

V. TECHNICAL AND EXPERIMENTAL RESULTS

TASK 1: Catalyst Design and Testing

INTRODUCTION:

Background

Methane is expensive to transport, so it is often flared or reinjected[1]. It is also a by-product from coal gasification. Conversion of methane to liquid hydrocarbon transportation fuels in an energy efficient, economical process would represent important technology for extending natural hydrocarbon fuel reserves. One route from methane to liquid fuels involves the conversion of methane through light hydrocarbon gases rich in ethylene to liquid fuels. Other routes, including one through methanol, are considered less technologically feasible[2]. The technological hurdle in the route through light hydrocarbon gases rich in ethylene is the direct conversion of methane to this ethylene-rich mixture. The light olefins may then, ideally, with little or no separation of products, be converted over molecular sieve catalysts to gasoline and distillates.

Technology exists for converting methane to liquid fuels,

$$CH_4 \longrightarrow CO/H_2 \longrightarrow CH_3OH \longrightarrow C_2H_4 \longrightarrow \text{GASOLINE/DISTILLATES},$$

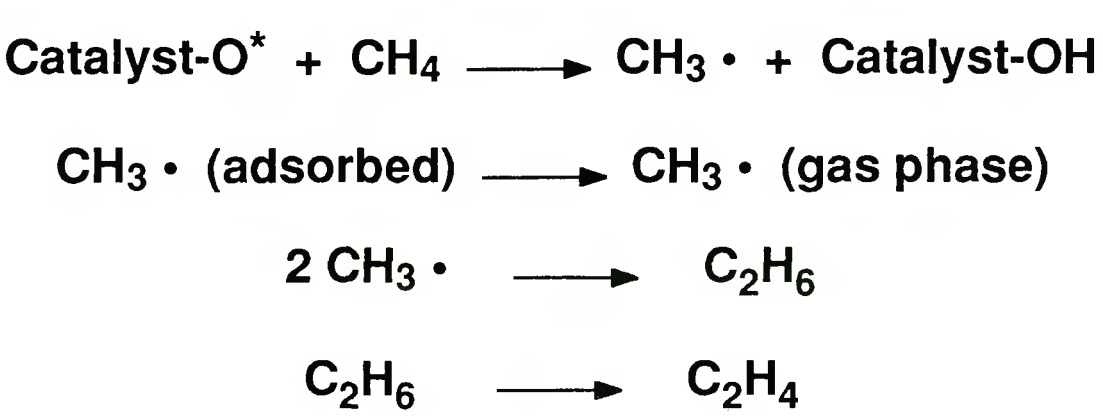
where C_2H_4 indicates light hydrocarbon gases rich in ethylene. UCC&P economic studies indicate that 75% of the cost of conversion of methane to fuels via commercial technology is in the conversion of methane through synthesis gas to methanol. The conversion of methanol to light olefins and the oligomerization of these olefins to liquid fuels with Mobil's Olefins to Gasoline and Distillate (MOGD) process[3] are a small portion of the investment and operating costs for this technology. Economic studies also indicate that a process to convert methane to fuels by direct oxidation of methane to light hydrocarbon gases rich in ethylene could be economically superior to the synthesis gas route in the near future (10-15 years). The economics of the conversion of methane to ethylene and/or liquid hydrocarbon fuels become more attractive for commercialization as the difference in costs of methane and higher hydrocarbons, currently used to produce ethylene or liquid fuels, becomes greater. This research proposes to invent the

technology necessary to avoid the reforming step which is required in existing technology to convert methane to liquid fuels, because it is capital intensive.

Methane can be converted to C_2's by a two-step process in which methane is reacted with a metal oxide to produce C_2's, then the reduced metal oxide is reoxidized[4-6] with air. Methane can also be converted to C_2's in a cofeed mode, where methane and oxygen, with or without a diluent, are fed simultaneously[7,8] to a reactor containing catalyst. Active sites on the catalyst are continuously regenerated by the oxygen present in this mode. In both cases, the major inefficiencies are the formation of CO and CO_2. Smaller amounts of C_3's, C_4's, and higher hydrocarbons are formed, and in some cases traces of acetylene and hydrogen are observed. In the cofeed mode, hydrocarbons higher than C_4 are rare. The cooxidation mode was preferred for all studies. Reported literature reactions are usually conducted at temperatures in the 700-950 °C range and operated at low pressures, 5-50 psig (135-440 kPa), in fixed bed or fluidized bed reactors. Quartz and alumina[9-11] materials have been used for reactors. Stainless steel and alonized stainless steel are suitable at lower pressures and temperatures. Oxygen concentration is limited to about 10 mole percent in any stream to avoid operation within the explosive limits.

Direct conversion of methane to C_2's is a very active area of research internationally[12], industrially[13], academically[14], and in government laboratories[15]. Although several different mechanisms have been proposed for the catalytic oxidative coupling of methane, Lunsford and coworkers[16-19] have elegantly and convincingly demonstrated, and others[5,20-23] have agreed, that the mechanism for conversion of methane to ethane and ethylene over the metal oxides studied (and probably over other selective methane coupling catalysts) involves abstraction of hydrogen from methane by the catalyst to produce methyl radicals and surface hydroxyls, followed by release of the methyl radicals into the gas phase where they couple to form ethane. Ethane is then converted to ethylene through known gas phase free radical chemistry. This is shown in Figure 1.

Figure 1. Methane to Ethylene Current Technology



Methyl radicals can also be produced in the gas phase without a catalyst, by initiation on surfaces, by direct reaction with oxygen, or by cracking of higher hydrocarbon impurities in the methane. Ethane produced by catalyzed or uncatalyzed reactions may be converted to ethylene through known gas phase free radical chemistry. This mechanism dictates much of the product distribution is controlled by gas phase chemistry, largely independent of catalyst, but dependent on the temperature and operating conditions. With this mechanism, one might at best approach C_2 yields of about 50% if certain reported models of the mechanism are correct[24]. Others[25,26] have proposed a yield barrier closer to 30%. Practically, literature results above a 30% yield to C_2's are very rare, and cannot be maintained.

Almost all of the reported literature catalysts rapidly deactivate. A few metal oxide catalysts which are less volatile (e.g., Sm_2O_3) undergo phase changes resulting in deactivation[27]. Most frequently, catalysts lose critical components due to volatilization at the high temperatures used for methane oxidation. Catalysts containing alkali metals lose the metal salts, e.g., the lithium is lost from the Li/MgO catalyst. As an example, a Li/MgO catalyst which contained less than 3% Li, and which had been roasted at >800 °C for 4 hours prior to exposure to methane and oxygen, exhibited a 12% loss in the rate to C_2's over 50 hours, presumably due to loss of Li. Often, initial results from literature catalysts indicate transient high selectivities to and/or yields of C_2's.

Literature reports contain no information which indicates that the catalysts studied give stable, long-term performance. Rapid deactivation is shown in most cases. Recently, one catalyst was reported to run for over 100 hours with about a 14% C_2 yield[28], but this yield is considered low, since there are many literature yields above the 18% range.

Approach

The plans at the beginning of this project, after control studies, were to explore simple catalyst systems which might be more active and/or stable than existing catalyst systems. Catalysts which might provide high (greater than 1) ethylene to ethane product ratios were of particular interest. Reported catalyst systems were predominantly variations on Li/MgO[16,17,29], the Mn-based ARCO catalyst[6,30,31], or lanthanide oxide systems[21,32-34]. Catalysts which might provide high ethylene to ethane product ratios were of particular interest. Studies began with exploration of a very simple NaCl on α-alumina catalyst discovered, but not reported, by UCC&P's G. E. Keller and M. M. Bhasin in the late 1960's. They explored this catalyst only in a pulsed, rather than a continuous mode. Specific ideas were to be explored by the examination of several types of catalyst systems. Plans were then to design catalyst systems to alter the currently accepted heterogeneous/homogeneous mechanism for methane oxidation through several specific approaches.

The NaCl/α-alumina catalyst system showed high initial methane conversions and C_2 selectivities, atypically high ethylene to ethane product ratios (3 to 20), low carbon dioxide to carbon monoxide ratios, catalyst deactivation, and changing product selectivities as a function of on-stream time. The high ethylene to ethane product ratios are desirable since ethylene is a more valuable product than ethane, and the conversion of ethylene into other products such as liquid fuels is possible. The low carbon dioxide to carbon monoxide ratios are advantageous for several reasons: less oxygen is required for the same methane conversion; the heat produced per unit of methane converted is lower when carbon monoxide rather than carbon dioxide is the product; and carbon monoxide is a more valuable product. Deactivation was observed to occur at different rates on alkali halide/α-alumina catalysts.

Other classes of potential methane oxidation catalysts of interest included several catalysts containing rigid structures which might stabilize metals in unusual oxidation or coordination states (e.g., perovskites or metal/molecular sieves), complex and mixed metal oxides, potential low temperature catalysts, such as those containing silver or promoting oxychlorination, catalysts containing rare earth oxides, solid base catalysts, and vapor phase catalysts.

Plans were to explore catalysts within these classes, and to explore other classes of catalysts conceived as a result of findings during exploration of these catalysts. Any catalysts yielding interesting results, or with potential, were to be explored in greater

detail. Process studies would include the study of major variables, including pressure, temperature, gas ratios, and diluent.

During the last few months of the contract, methane to C_2's and C_2's to fuels steps would be integrated, and the use of typical model processed natural gas mixtures would be demonstrated for a methane coupling catalyst.

EXPERIMENTAL:

Most abbreviations, keys to table terms and headings, and definitions are presented in Appendix A. Other abbreviations are obvious or are defined where used. Experimental procedures are described in Appendix B. Chemistry experiments were performed in three laboratories, and since the reactor systems, reactors, and procedures differed among these laboratories, equipment and procedures for each laboratory are described in Appendix B. The Results and Discussion Section for Task 1 below consists of three sections, corresponding to the three laboratories where work was performed, so that the particular equipment and experimental procedures may be known for each experiment.

Figures B1-B5 of Appendix B present illustrations of the various reactor systems used for methane coupling research. Figures B6 to B15 of Appendix B are drawings of the Reactors A through H, S, and V. The temperature distribution of Reactor A is shown in Figure B16 of Appendix B, and the oven configuration used with Reactor V is illustrated in Figure B17 of Appendix B.

Appendix C presents catalyst preparation procedures. Appendix D presents a list of all catalysts used in the BKW laboratory. Catalyst compositions and preparation procedures are included in the list. Appendix D presents a similar list of catalysts used in the KDC laboratory. All catalysts used in the NEK laboratory are described in the Results and Discussion Section below, except for a 4.77% $BaCO_3$ on Norton SA5451/ α-alumina catalyst (30/60 mesh); used to test the reactor, and prepared by Procedure B of Appendix C.

The First through the Seventh Quarterly Reports contain details of reactions runs, including table summaries of reaction conditions and results for all methane oxidation runs.

RESULTS AND DISCUSSION:

During the past two years, UCC&P developed continuous, unattended operation capabilities for the study of methane coupling[35,36] and pursued studies mainly in the cooxidation mode; however, limited studies were conducted in the pulsed, sequential reaction mode. Many classes of methane oxidation catalysts were explored.

In the literature, nearly all elements have been used or claimed for methane coupling catalysts. One patent in particular[37] claims an unusually large number of catalysts and components for "the oxidative conversion of organic compounds to other organic compounds," and includes two examples of methane oxidation to C_2's. This patent and the literature do not distinguish among the many materials used and claimed, which, if any, material would provide a stable, commercializable catalyst for the conversion of methane to ethylene. Only two examples of the oxidation of methane are presented, and these exhibit low ethylene to ethane product ratios, and no evidence of a long catalyst lifetime. A catalyst system which would provide a high ethylene to ethane product ratio would be more economical, from a commercial point of view, than a similar one which would not provide a high ethylene to ethane product ratio, since ethylene is more valuable as a raw material than ethane.

BKW Laboratory

Control Studies

Control studies were done to determine temperatures, reactors, and reaction conditions where gas phase methane oxidation reactions were slow enough that the homogeneous reaction would not interfere with catalyst results. Initial studies in Reactor A (Figure B6 of Appendix B) showed that new reactors were needed to reduce void volume in order to minimize the homogeneous component of the reaction (Tables F1 and F2 of Appendix F). Studies were continued to compare results of the new reactors, Reactors C, D, and E (Figures B8, B9, and B10, respectively, of Appendix B) with those of Reactor A, and to determine the effect of added volatile chloride (ethyl chloride) on the homogeneous (uncatalyzed) reaction, so that volatile chloride could be added to methane coupling reactions to replace chloride which might be lost from catalyst compositions containing chloride.

Results from all conditions of four control runs without catalyst but with quartz chips, using three reactors, are presented in Table F3 of Appendix F. The observed results are from homogeneous (uncatalyzed) gas phase oxidation of methane. Quartz surface area from the reactor and the quartz chips is low (the surface area of 14/30 Thomas Scientific quartz chips was measured at 0.08 m^2/g), but quartz initiation and quenching reactions are expected to contribute to some degree. Selectivity to C_2's is low at 700 °C and is in the 25-45% range at 750 °C. Further increases in temperature did not improve the selectivity. Methane conversion rises as the reaction temperature is increased.

Table 1 below shows the highest methane conversions for each experiment without added volatile ethyl chloride (ECl) in the gas feed. Appendix A defines terms and table headings. The symbol =/– refers to the ethylene to ethane product ratio. Time is the time of a run in minutes, unless specified otherwise. Ccm indicates the flow rate in ccm. Results depend on the history of the reactor (temperature and ethyl chloride level), and complete results are presented in Table F3 of Appendix F. The top part of Reactor E is the same width as Reactor A, but Reactor E narrows to a 3-mm i. d. capillary tube after the catalyst bed (see Appendix B Figures B6, B9, and B10). Reactor D has the same capillary tube in the lower part of the reactor and is narrower in the top part of the reactor than is Reactor A (for the least void volume).

Table 1. Blank Runs*

Reaction	ECl	Temp	Ccm	CH_4 C	Sel	Yield	O_2 C	=/-	Time	Reactor
30-49	0	750	50	6.76	26.3	1.73	9.2	0.63	195	A
30-79	0	750	50	4.12	43.7	1.75	6.54	0.27	400	D
30-82	0	750	50	9.92	35.1	3.38	12.8	1.05	1455	E
29-139	0	800	50	17.04	28.8	4.92	35.3	2.48	4260	A
30-79	0	800	50	6.63	41.2	2.68	12.1	0.65	315	D

* Appendix A describes table headings and defines terms used in tables and in this report. See Appendix B for experimental conditions.

The amount of reaction is smaller in Reactor D with the smaller void volume. At 750 °C and 50 sccm flow rate, reaction is at a sufficiently low level with this reactor that the homogeneous reaction does not interfere with catalyst testing (at this temperature or

lower temperatures with a 50 sccm or higher flow rate, with 10% methane and 5% oxygen at 11 psig pressure).

Table 2 below shows results with three reactors at two temperatures for the gas phase, uncatalyzed reaction with added ethyl chloride.

Table 2. Blank Runs

Reaction	ECl	Temp	Ccm	CH_4 C	Sel	Yield	O_2 C	=/-	Time	Reactor
30-82	50	800	50	27.18	23.6	6.26	54.7	3.43	330	E
30-79	50	750	50	2.15	41.8	0.89	0	0.54	540	D
30-82	50	750	50	12.77	33.2	4.01	19	1.17	420	E
30-49	100	750	50	12.53	29.2	3.54	20.4	1.6	1410	A
30-82	100	750	50	12.14	35.1	4.06	13.9	1.07	1545	E

Addition of ethyl chloride to the homogeneous gas phase, uncatalyzed reaction results in an increase in the ethylene to ethane product ratio (Figure 2), an increase in the selectivity to C_2 products (Figure 3), and an increase in methane conversion (Figure 4). For Figures 2, 3, and 4, Reactor A is used at 750 °C with a 50 ccm flow rate of gases, using 10% CH_4, 5% O_2, and nitrogen diluent at 11 psig.

Figure 2. Effect of Ethyl Chloride on the Ethylene to Ethane Ratio, 30-BKW-49

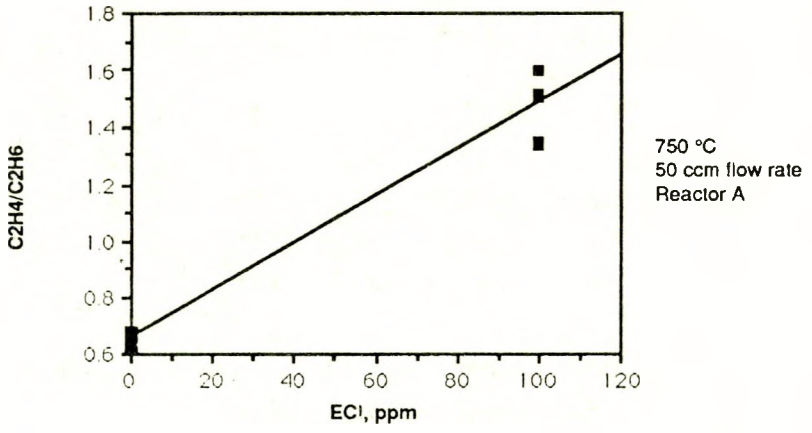


Figure 3. Effect of Ethyl Chloride on the Selectivity to C_2 Products, 30-BKW-49

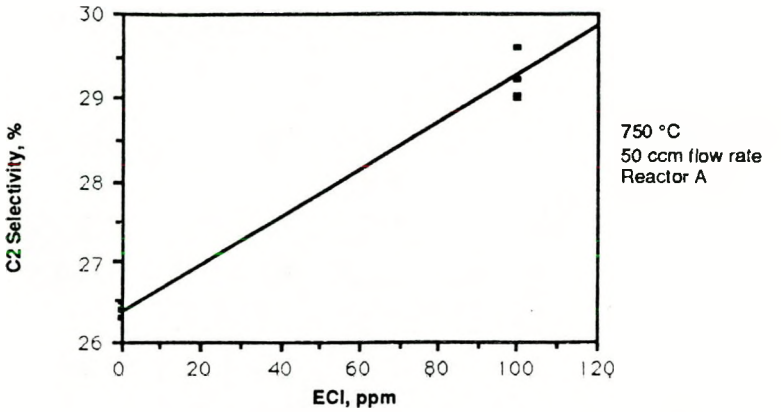
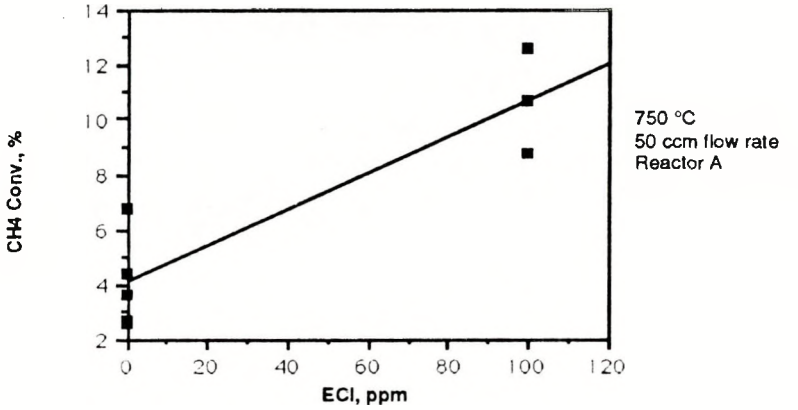


Figure 4. Effect of Ethyl Chloride on the Methane Conversion, 30-BKW-49



Reaction 30-BKW-79 was run in Reactor D with a flow rate of 50 sccm. Selected results, shown in Table 3, indicate that at 750 °C and flow rates of 50 ccm or greater, with 10% CH_4, 5% oxygen, and nitrogen balance, at 11 psig, methane conversions are below 5% with 0 or 50 ppm ECl.

Table 3. Control Studies without Catalyst

ECl	T	CH_4 C	Sel	Yield	O_2C	=/-	CO_2/CO	CH_4/O_2	CH_4 in	O_2 in	C Bal	Time
0	750	1.79	36.6	0.66	6.05	0.27	0.1	1.9	10.087	5.302	99.97	50
0	775	4.19	40.5	1.67	8.04	0.4	0.05	1.9	10.087	5.302	98.53	225
0	800	6.63	41.2	2.68	12.05	0.65	0.03	1.9	10.087	5.302	98.22	315
0	750	4.12	43.7	1.75	6.54	0.27	0.04	1.9	10.087	5.302	97.28	400
50	750	2.15	41.8	0.89	0	0.54	0.03	2.05	10.351	5.058	99.41	540
50	750	0.24	43.6	0.1	0.95	0.47	0.02	2.03	10.349	5.092	101.34	1260

Alkali Chloride/Metal Oxide Catalysts

For all reactions in the BKW laboratory, unless indicated otherwise, five grams of catalyst were used and 10% methane, 5% oxygen, and balance nitrogen were fed to quartz reactors, with or without ethyl chloride (ECl) in ppm as indicated.

Studies began with exploration of a very simple NaCl on α-alumina catalyst discovered, but not reported, by UCC&P's G. E. Keller and M. M. Bhasin in the late 1960's. They explored this catalyst only in a pulsed, rather than a continuous mode. Initial results for the cofeed mode with the NaCl on α-alumina catalyst showed high initial methane conversions and C_2 selectivities (C_2 yields of 18-20%), atypically high ethylene to ethane product ratios (3 to 20), low carbon dioxide to carbon monoxide ratios, catalyst deactivation, and changing product selectivities.

Further exploration of alkali/metal oxide catalysts was of interest, and new catalysts were sought, both to understand what was unique about alkali/metal chloride catalysts, as well as to provide superior catalysts to these. It was known that the support is not active or selective for C_2 production, but it was not known whether the alkali or chloride catalyst components were unique in some way, whether all of the catalyst components present were needed, or whether an unsupported catalyst would be active. Successful methane coupling with sodium chloride/α-alumina indicates that redox metals are not needed for this reaction, and it reasonable to assume that an oxide of sodium may abstract hydrogen from methane in the rate determining step of this reaction[38]. It was therefore likely that oxides of other alkali metals might activate methane. Catalysts similar to and different from the NaCl/α-alumina system were designed to identify what made NaCl/α-alumina catalysts unique.

At the time this work was begun in 1987, very few catalysts for methane coupling had been reported which contained chlorine[39-51]. Several of these resulted in methane oxidation to C_2's in yields reported to be as high as 20-30%, the highest in the literature, but the role and contribution of the chloride component in these catalysts was not apparent from these articles and patents. None of these catalysts were shown to exhibit C_2 yields of over 20% for periods of over a few hours.

Table 4 below shows that catalysts of NaCl/α-Al_2O_3 and KCl/α-Al_2O_3 were competitive with literature catalysts in methane conversion and C_2 selectivity, but showed product distributions containing ethylene to ethane product ratios of over 2.5, rather than the ethylene to ethane product ratios of about 1 which were typical for literature catalysts (e.g., references 16, 17, and 18). These catalysts deactivate rapidly under cooxidation conditions.

Table 4. Alkali Metal Chloride/α-Al_2O_3 Catalysts*

Ref	Cat	T	C C	Sel	Yield	=/-	CO_2/CO	Time	GHSV	ECl
29-95	NaCl/Al_2O_3	700	17	58	9.5	2.0	0.2	698	1305	5
29-95	NaCl/Al_2O_3	800	38	42	16	17.2	0.3	1116	1620	0
29-93	KCl/Al_2O_3	700	18	42	7.2	3.0	0.2	349	285	0

* Appendix A describes table headings and defines terms used in tables and in this report. See Appendix B for experimental conditions. Appendix D describes catalyst compositions. Appendix C describes catalyst preparation procedures. Five grams of catalyst were used and 10% methane, 5% oxygen, and balance nitrogen were fed to quartz reactors, with or without ethyl chloride (ECl) in ppm as indicated.

It was thought that catalyst deactivation might be due to the loss of chloride or alkali. Indeed, addition of parts per million of chloride in the form of ethyl chloride in the feed gas resulted in partial reactivation of deactivated catalysts.

The concentration of NaCl on Norton 5551 α-alumina was increased from 3.85% in 29-BKW-95 to 13.8% in 29-BKW-101. The catalyst with more NaCl was a lot less active under the same conditions. This might indicate an interaction of the NaCl with the support which requires optimum amounts of both to be exposed for higher activity.

KCl (4.85%) on Norton 5551 α-alumina in 29-BKW-106 was compared with an equal molar amount of NaCl on Norton 5551 α-alumina. Under similar conditions, the KCl catalyst was slightly less active and deactivated much faster than the NaCl catalyst. C_2 selectivities were approximately the same (Table 5).

In 29-BKW-107, a CsCl (7.06%) on Norton 5551 α-alumina catalyst was slightly less active and selective to C_2's than a similar NaCl catalyst, but the deactivation rates were similar. A similar catalyst containing LiCl (2.82%) on Norton 5551 α-alumina was much more active but less selective than the NaCl catalyst.

Table 5. Alkali Metal Chloride/α-Al_2O_3 Catalysts

Ref	Cat	T	C C	Sel	Yield	=/-	CO_2/CO	Time	GHSV	ECl
29-95	NaCl/Al_2O_3	700	22.2	48	11	4.2	0.3	390	349	0
29-106	KCl/Al_2O_3	700	20.9	45	9	3.6	0.2	90	366	0
29-107	CsCl/Al_2O_3	700	18.4	36	7	2.5	0.8	225	375	0
29-111	LiCl/Al_2O_3	700	43.5	33	14	15	0.5	100	366	0

For 5 grams of a 2.82% LiCl on Norton 5551 α-alumina catalyst (29-BKW-115) in Reactor A at 750 °C, rapid catalyst deactivation was observed, as shown in Table 6 below. Some very high ethylene to ethane product ratios were observed.

Table 6. Deactivation of a LiCl/α-Al_2O_3 Catalyst

Temp	CC	Sel	Yield	=/-	CO_2/CO	CH_4 in	O_2 in	Time	GHSV	ECl	R
750	47.0	36.1	16.8	19.7	0.3	10.0	4.8	430	1098	0	A
750	39.7	34.2	13.9	15.1	0.4	10.2	5.1	565	1098	0	A
750	21.7	28.6	6.2	1.6	1.0	10.2	5.1	715	1098	0	A

In reaction 29-BKW-119, the catalyst was 30 g of 3.85% NaCl on Norton 5551 α-alumina. A C_2 yield (selectivity x methane conversion) of 20.7% was obtained at 800 °C and 186 h^{-1} GHSV.

Catalysts containing Rb (30-BKW-64 and 74) and Cs (30-BKW-71 and 73) exhibited C_2 yields below 14% at 750 °C and 878 h^{-1} GHSV with 50 ppm ethyl chloride

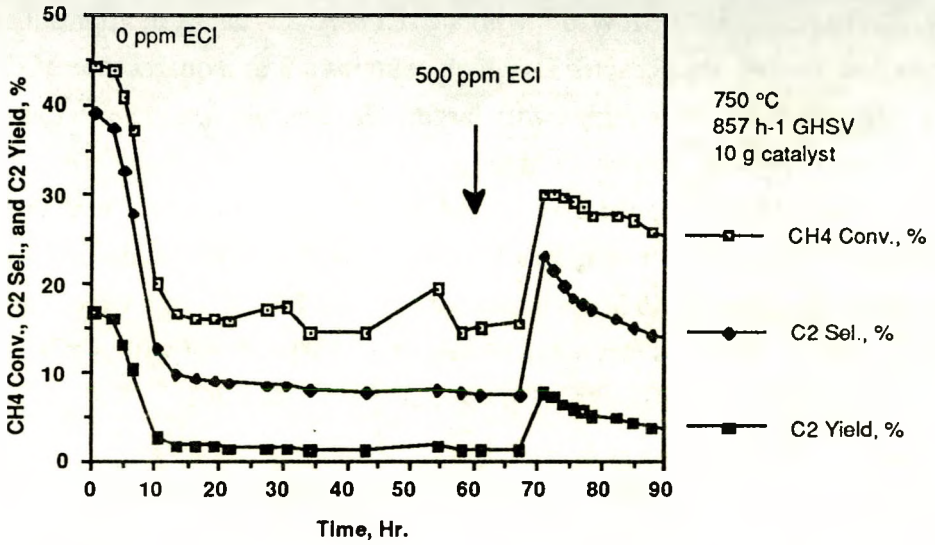
in the feed gas. They deactivated rapidly, and they were lower in activity at 750 °C than similar Na or Li catalysts. Initial C_2 selectivities were over 50% at the low conversions. An initial selectivity of 65% was obtained with a KCl/α-alumina catalyst in reaction 30-BKW-71. In reaction 30-BKW-65, with a CsCl/α-Al_2O_3 catalyst, after only a few hours of operation, the reactor (Reactor D, which contains a 3 mm quartz tube after the catalyst bed) plugged in the narrow region with large, clear crystals which were found (by powder x-ray diffraction) to be cesium chloride.

The NaCl/Al_2O_3 catalyst used in reaction 29-BKW-95, which was analyzed by ICP to contain 1.33% sodium prior to reaction, was found by ICP to contain 0.134% sodium after a reaction period of 46 hours at temperatures of 700-800 °C. Other catalysts containing alkali chlorides lost alkali metals (e.g., 30-BKW-64 with RbCl, 30-BKW-71 with KCl, and 30-BKW-70 with LiCl; see Table 8 on page 26).

Added Volatile Chloride to Retard Catalyst Deactivation

Since NaCl/α-alumina catalysts were observed to deactivate, and this was thought due in part to the loss of chloride from the catalyst, catalysts were tested without and with addition of ethyl chloride in the feed gas. Addition of 500 ppm of ethyl chloride to the feed gas resulted in increased selectivity to C_2's, methane conversion, and yield to C_2's (Figure 5 below), although the yield did not return to the original yield.

Figure 5. Addition of Ethyl Chloride to Retard Catalyst Deactivation, 30-BKW-29



Deactivation was then observed to continue. Selectivity and methane conversion began dropping after the initial increase upon addition of ethyl chloride, indicating that loss of chloride is not the only reason for catalyst deactivation.

A LiCl/α-alumina catalyst (30-BKW-70) showed an initial C_2 yield of 20.2% (41% C_2 selectivity) with an ethylene to ethane product ratio of nearly 20 (at 750 °C and a GHSV of 1463 h^{-1} with 50 ppm ethyl chloride in the feed gas). Even with the added ethyl chloride, catalyst deactivation was rapid.

Pure Components

Since NaCl/α-alumina catalysts provided active catalysts, NaCl alone was tested as catalyst in reactions 30-BKW-23 and 30-BKW-48. Two forms of pure sodium chloride were used. Selected results below in Table 7 show that activity is low at temperatures of interest (750 °C and below).

Table 7. Pure NaCl

Temp	CC	Sel	Yield	=/-	CO_2/CO	CH_4 in	O_2 in	Time	GHSV	ECl	Ref
700	4.5	39.6	1.8	0.5	0.2	10.5	5.0	90	652	0	30-23
700	4.4	25.4	1.1	0.4	0.2	10.0	4.9	15	423	0	30-48
750	12.3	46.5	5.7	2.0	0.1	10.5	5.0	270	652	0	30-23
750	9.9	40.4	3.9	1.5	0.1	10.0	4.9	105	423	0	30-48
800	33.0	26.5	8.8	9.1	0.1	10.5	5.0	360	326	0	30-23

Other Anions

A NaOH/α-alumina catalyst was shown to have initial activity and selectivity (at 35 minutes after the start of the experiment, 30-BKW-118) comparable to a NaCl/α-alumina catalyst, but results after the initial analysis were indistinguishable from homogeneous reaction results, most likely indicating loss of sodium from the catalyst.

Results for alkali catalysts with other anions, e.g., one with $LiBO_2$ (30-BKW-134), showed selectivities and activities which were not comparable to those of the catalysts containing NaCl. A catalyst consisting of NaCl on Ga_2O_3 (30-BKW-132) showed methane conversions, C_2 selectivities, and C_2 yields at least as good as similar catalysts on Norton SA5551 α-alumina.

Other Catalysts

It was concluded that alkali metal/metal oxide catalysts deactivated too rapidly for them to be practical catalysts for methane coupling. This was the case even when volatile chloride was added in the gas phase to replace any lost from the catalyst.

Catalyst components with higher melting points, which might be less volatile, were sought and explored. Catalysts were tested before and after reaction by ICP. Alkaline earth chloride containing catalysts (e.g., 30-BKW-129, with Ba) tested by ICP did not lose alkaline earth components. Unlike the $NaCl/Al_2O_3$ catalyst (29-BKW-95), which lost most of the Na during an overnight reaction, $BaCl_2/Al_2O_3$ (30-BKW-52) and $CaCl_2/Al_2O_3$ (31-BKW-13) catalysts did not lose significant amounts of Ba and Ca, although C_2 yields and ethylene to ethane product ratios had dropped during methane

coupling experiments. Results, including those for several catalysts containing alkali chlorides, are presented in Table 8 below.

Table 8. Loss of Metals in Catalysts Containing Metal Chlorides

Reaction	Catalyst	Chloride	Chloride mp, °C	% Metal in Fresh Catalyst	% Metal in Used Catalyst
30-BKW-52	$BaCl_2/\alpha$-Al_2O_3	$BaCl_2$	963	3.06	2.94
32-BKW-62	$BaCl_2/\alpha$-Al_2O_3	$BaCl_2$	963	2.3	2.4
34-BKW-19	$SrCl_2/\alpha$-Al_2O_3	$SrCl_2$	875	0.98	0.96
29-BKW-95	$NaCl/\alpha$-Al_2O_3	NaCl	801	1.33	0.134
30-BKW-129	$CaCl_2/\alpha$-Al_2O_3	$CaCl_2$	782	1.08	1.04
31-BKW-13	$CaCl_2/\alpha$-Al_2O_3	$CaCl_2$	782	1.19	1.10
30-BKW-71	KCl/α-Al_2O_3	KCl	770	1[a]	0.28
30-BKW-64	$RbCl/\alpha$-Al_2O_3	RbCl	718	5.33	0.93
30-BKW-83	$CsCl/\alpha$-Al_2O_3	CsCl	645	3.5	<1 ppm
30-BKW-70	$LiCl/\alpha$-Al_2O_3	LiCl	605	0.147	0.07

a. Estimated based on preparation and ICP of similar catalysts (no ICP of fresh catalyst).

Although the melting point of calcium chloride (782 °C) is lower than that of barium chloride (963 °C), the calcium chloride is not lost to a significantly greater degree. The melting point of sodium chloride (801 °C) is higher than that of calcium chloride, and sodium is lost rapidly compared with calcium. These catalysts were not all run the same length of time under the same conditions, but results clearly indicate rapid loss of alkali chlorides, and insignificant loss of alkaline earth chlorides, irrespective of melting point.

Alkaline Earth Chloride/Alpha-Alumina Catalysts

As described above, alkaline earth compounds are less volatile, and catalysts containing these were considered good candidates for methane coupling catalysts. Barium was of particular interest because a barium peroxide catalyst was found to

stoichiometrically convert methane to C_2's at temperatures less than 400 °C[52], so it was thought that barium salts might form peroxides under reaction conditions and form C_2's at faster rates (lower temperatures) than other catalysts. Selected literature articles and patents describing the use of alkaline earth components in catalysts for methane coupling are reviewed in References 16, 37, and 52-59.

$BaCl_2$ (12.43%) on Norton 5551 α-alumina (29-BKW-110) was compared with an equal molar amount of NaCl on Norton 5551 α-alumina (29-BKW-95). Under approximately the same conditions, the $BaCl_2$ catalyst was more active and selective to C_2's than the NaCl catalyst (see Table 9 below), and the deactivation rate appeared to be at least as good as that for the NaCl catalyst. This catalyst has the same interesting selectivity pattern as the $NaCl/Al_2O_3$ catalyst (high ethylene to ethane product ratio and low carbon dioxide to carbon monoxide product ratio compared with literature catalysts like the Li/MgO catalyst).

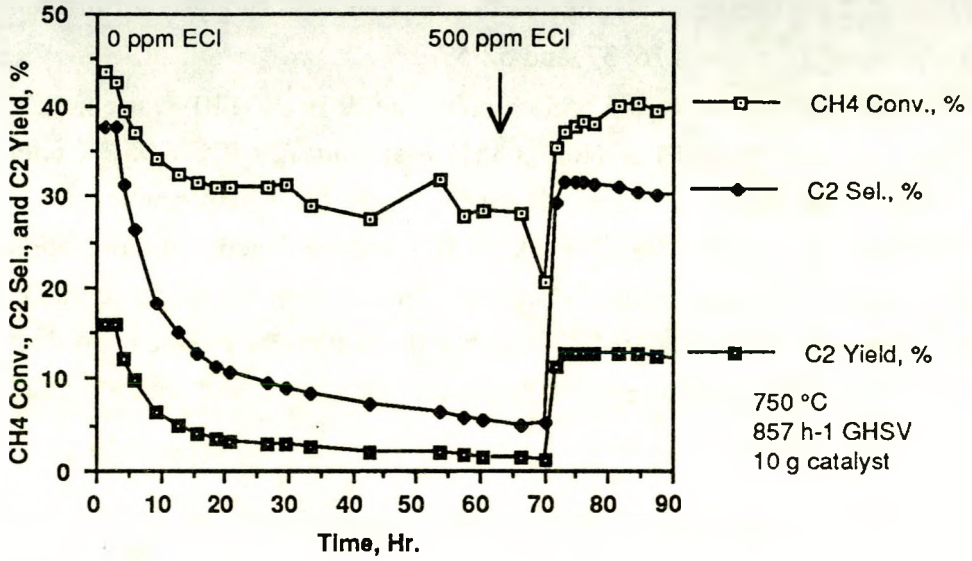
Table 9. Alkaline Earth and Alkali Metal Chloride/α-Al_2O_3 Catalysts

Ref	Cat	T	C C	Sel	Yield	=/-	CO_2/CO	Time	GHSV	ECl
29-95	$NaCl/Al_2O_3$	700	22	48	11	4.2	0.3	390	349	0
29-110	$BaCl_2/Al_2O_3$	700	31	46	13	7.6	0.3	55	366	0

The temperature of the reaction was raised to 800 °C, and at 1171 h^{-1} GHSV, the methane conversion dropped from 41 to 30% over a period of 11 hours, presumably due to loss of chloride.

Figure 6 shows deactivation of a 1.4% $BaCl_2/α\text{-}Al_2O_3$ catalyst followed by reactivation upon addition of 500 ppm ethyl chloride to the feed gas of the reaction.

Figure 6. Addition of Ethyl Chloride to Retard Catalyst Deactivation, $BaCl_2/\alpha$-Al_2O_3 Catalyst, 30-BKW-28



Whereas the catalyst containing sodium (Figure 5) deactivated rapidly after partial reactivation with ethyl chloride, the catalyst containing barium (Figure 6) does not deactivate at this fast rate after catalyst reactivation with ethyl chloride. In reaction 30-BKW-36, methane conversion was observed to increase upon reduction of ethyl chloride in the feed gas from 500 to 100 ppm. This indicated that 500 ppm ethyl chloride was above the optimum amount of ethyl chloride required in the feed gas for this catalyst under the reaction conditions used. Although chloride is needed to retain high activities for the alkaline earth chloride/alumina catalysts, too much chloride can poison at least certain catalysts, under certain conditions. An example of a $SrCl_2$ catalyst with different ethyl chloride levels in the feed gas is shown in Table 10 below. Although temperatures are higher (750-800 °C) than are typically used for experiments, and catalyst performance has not stabilized, C_2 yields above 20% are maintained for over 68 hours (C_2 selectivities 47-57%), and C_2 yields of 24-26% are maintained for over 17 hours.

Table 10. Selected Results, $SrCl_2/\alpha\text{-}Al_2O_3$ Catalyst, 32-BKW-41

Temp	CH_4 C	Sel	Yield	=/-	CO_2/CO	Time	GHSV	ECl
750	38.4	33.1	12.8	2.0	7.3	60	783	0
750	34.3	26.8	9.2	1.4	8.5	4200	2087	0
750	35.8	30.0	10.9	1.8	8.0	4290	2087	30
750	38.0	33.9	13.0	2.1	7.4	4380	2087	30
750	39.9	48.3	19.3	2.2	2.9	5820	2087	30
760	43.3	46.8	20.2	2.6	3.1	5895	2087	30
800	50.0	53.2	26.1	6.8	1.9	7485	2087	30
800	46.0	51.4	23.4	5.1	1.5	9925	2087	40
780	38.5	57.3	21.9	3.5	1.3	9960	2087	40
760	25.4	66.9	16.8	2.0	1.1	10005	2087	40
760	23.7	67.7	15.9	2.0	1.0	10065	2087	40
740	14.5	70.1	10.1	1.1	1.1	10095	2087	40
740	13.3	71.0	9.4	1.0	1.0	10180	2087	40
790	37.9	53.8	20.3	3.1	1.7	14725	2087	5
790	30.3	60.1	18.0	3.6	0.6	17425	2087	10

A variety of components and supports were used to create new catalysts similar to $BaCl_2/Al_2O_3$, to give C_2 yields of up to 26% with high (many >10) ethylene to ethane product ratios. A summary of results for alkaline earth/alpha-alumina catalysts is presented in Table 11 below. A 26% C_2 yield (51% selectivity, 16 ethylene to ethane product ratio) is obtained with a $CaCl_2/Al_2O_3$ catalyst (31-BKW-33). Several catalysts containing Sr or Ca exhibit C_2 selectivities of over 60% with C_2 yields of over 10% (e.g., 31-BKW-33).

Table 11. Best Results

Reference	Catalyst	Temp	CH_4 C	Sel	Yield	=/-	CO_2/CO	Time	GHSV	ECl
31-BKW-33	$CaCl_2/Al_2O_3$	700	51.6	51.3	25.9	16.2	0.6	195	1171	0
31-BKW-33	$CaCl_2/Al_2O_3$	700	50.6	52	25.9	14.6	0.6	235	1171	0
31 BKW 119	$BaCl_2/Al_2O_3$	750	46.5	52.6	24.3	9.8	2.5	170	1171	10
31-BKW-33	$CaCl_2/Al_2O_3$	700	36.6	64.6	23.4	6.0	0.6	275	2341	0
31-BKW-28	$SrCl_2/Al_2O_3$	750	46.8	47.4	22.1	17.3	0.5	40	837	50
31-BKW-34	$BaCl_2/Al_2O_3$	750	48.8	44.4	21.5	13.7	0.6	35	783	0
31-BKW-47	$SrCl_2/Al_2O_3$	750	49.3	44	21.5	19.1	0.6	65	783	0
31-BKW-47	$SrCl_2/Al_2O_3$	750	45.2	47.9	21.4	10.8	2.2	1100	783	0
31-BKW-47	$SrCl_2/Al_2O_3$	750	44.8	47.6	21.0	9.3	2.6	1410	783	0
31-BKW-28	$SrCl_2/Al_2O_3$	750	30.2	57.3	17.3	4.2	1.5	4320	837	50
31 BKW 35	$BaCl_2/Al_2O_3$	750	26.8	54.6	14.5	3.2	0.7	1360	783	0
31 BKW 59	$CaCl_2/Al_2O_3$	700	20.8	69.4	14.4	2.5	0.5	345	2341	0
31 BKW 134	$CaCl_2/Al_2O_3$	750	19.5	66.9	12.8	1.9	0.9	9105	1043	500

Table headings are defined in Appendix A and in the Experimental Section.

Catalysts containing Ca show some of the best C_2 yields and C_2 selectivities for methane coupling demonstrated here or elsewhere [4-8,16-26,52,53,60-71] (Table 11, above). Ca catalysts, however, have not been demonstrated to operate with stable behavior. In the absence of added ethyl chloride in the feed gas, $CaCl_2/Al_2O_3$ catalysts exhibit an initial increase in selectivity which then drops rapidly. C_2 yield, C_2 selectivity, and methane conversion do not proceed through maxima, but rather drop rapidly from the beginning of experiments. In reaction 31-BKW-63, addition of 500 ppm ethyl chloride to a $CaCl_2/Al_2O_3$ catalyst results in partial reactivation of a deactivated catalyst, with the selectivity, yield, and methane conversion then dropping only slowly for the next 15 hours. After addition of 500 ppm ethyl chloride to 31-BKW-5 ($CaCl_2/Al_2O_3$), C_2 yield is constant for 5 hours while selectivity to C_2's is dropping and methane conversion is rising. In 31-BKW-53, a $CaCl_2/Al_2O_3$ catalyst was run for an extended period of time at 500 ppm ECl in the feed gas, but deactivation was still observed. Stable behavior for 10 or more hours has not been demonstrated for $CaCl_2/Al_2O_3$ catalysts tested to date.

In contrast to the lack of stable performance in $CaCl_2/Al_2O_3$ catalysts, catalysts containing barium and strontium exhibit stable behavior or only low levels of catalyst deactivation for periods of tens of hours. This is important, since published literature reports contain no data which indicates that the catalysts studied give stable, long-term

performance. Stable performance for over 55 hours (C_2 yields over 17% and C_2 selectivities over 50%) is exhibited by a $SrCl_2/Al_2O_3$/ECl catalyst (31-BKW-28). A deactivated $BaCl_2/TiO_2$ catalyst is activated by addition of 500 ppm ethyl chloride in the gas feed (31-BKW-46). After this, a C_2 yield of over 16% with an ethylene to ethane molar ratio of 10 continue unchanged for over 15 hours (the duration of the experiment).

In reaction 31-BKW-119 ($BaCl_2/Al_2O_3$ catalyst), for a period of about 25 hours (with an ethyl chloride level of 30 ppm), C_2 selectivity remains constant, while methane conversion and C_2 yield drop only slightly. A similar catalyst containing Sr and run under the same reaction conditions (31-BKW-118) deactivates faster with 10 ppm ethyl chloride. Both catalysts respond to higher levels of ethyl chloride by a partial reversal of catalyst deactivation. C_2 selectivity of the catalyst with barium returns close to the initial value with 400 ppm ethyl chloride. Better overall catalyst performance was observed with the catalyst containing barium.

Concentration Studies

In experiments 29-BKW-124, 29-BKW-125, 29-BKW-128, and 29-BKW-129, four concentrations of $BaCl_2$ on Norton 5551 α-alumina are compared in Reactor A under the same conditions (Table 12 below). No ethyl chloride is added in the feed gas. The catalysts containing 0.145% (29-BKW-129) and 1.41% $BaCl_2$ (29-BKW-124) were more active than the catalysts with higher (12.43%, 29-BKW-128) and lower (0.019%, 29-BKW-125) amounts of $BaCl_2$.

Table 12. $BaCl_2/\alpha$-Al_2O_3 Catalyst with Different Concentrations of $BaCl_2$

Temp	CC	Sel	Yield	=/-	CO_2/CO	CH_4 in	O_2 in	Time	GHSV	$BaCl_2$,%
700	15.9	54.6	8.6	1.7	0.7	9.8	4.7	135	714	1.41
700	5.1	17.3	0.9	0.7	0.6	9.8	4.7	180	714	0.019
700	13.3	58.5	7.6	1.3	0.7	10.1	5.1	180	714	12.43
700	20.2	57.6	11.4	3.0	0.4	10.1	5.1	135	714	0.145
800	42.6	39.2	17.3	11.9	0.5	9.8	4.7	420	1143	1.41
800	11.0	26.1	2.9	1.6	0.5	9.8	4.7	465	1143	0.019
800	40.8	40.7	16.9	10.9	0.4	10.1	5.1	465	1143	12.43
800	37.3	36.1	13.7	9.2	0.5	10.1	5.1	405	1143	0.145

This might indicate an interaction of the $BaCl_2$ with the support which requires optimum amounts of both to be exposed for higher activity, as was proposed on page 21 for a catalyst containing NaCl.

The effect of catalyst loading on deactivation was determined using 3.28% (31-BKW-127), 6.35% (31-BKW-126), and 11.94% (31-BKW-134) $SrCl_2/Al_2O_3$ (on Norton SA5451 alpha-alumina). When running under the same reaction conditions, the 3.28% $SrCl_2$ catalyst exhibits C_2 yields of over 20% for under 4 hours, the 6.35% $SrCl_2$ catalyst exhibits a C_2 yields of over 20% for over 17 hours, while the 11.94% $SrCl_2$ catalyst exhibits C_2 yields of over 20% for over 93 hours. High ethylene to ethane product ratios, C_2 yields and C_2 selectivities are retained for a longer period of time with the catalyst with the higher loading of $SrCl_2$ (Table 13). No ethyl chloride was added during the time periods indicated, so these results may indicate that the catalyst with the higher initial loading of $SrCl_2$ stays active because it does not lose all of its chloride as fast as catalysts containing lower amounts of chloride; however, addition of 200 and 500 ppm chloride to experiment 31-BKW-134 after partial catalyst deactivation had no significant effect on catalyst performance.

Table 13. Different Catalyst Loadings

Temp	CH_4 C	Sel	Yield	=/-	CO_2/CO	Time	GHSV	ECl
			31-BKW-127, 3.28% $SrCl_2$					
750	49.3	48.2	23.6	18.5	0.5	70	1043	0
750	43.7	53.9	23.7	9.6	0.7	225	1043	0
750	28.4	59.3	17.0	4.0	0.7	315	1043	0
			31-BKW-126, 6.35% $SrCl_2$					
750	38.9	54.5	21.3	9.2	0.7	180	1043	0
750	45.3	52.0	23.2	7.3	3.1	1305	1043	0
750	40.8	55.0	22.3	5.0	3.2	1575	1043	0
750	38.5	55.6	21.4	4.2	3.2	1665	1043	0
750	34.4	57.3	19.5	3.2	2.8	1800	1043	0
			31-BKW-134, 11.94% $SrCl_2$					
750	47.7	49.8	23.3	13.8	0.6	35	1043	0
750	46.6	52.6	23.9	10.4	3.0	1490	1043	0
750	45.7	52.5	23.7	9.4	3.5	1805	1043	0
750	44.3	52.6	23.0	6.3	4.6	3335	1043	0
750	42.7	53.8	22.5	4.5	5.6	4550	1043	0
750	37.8	55.3	20.7	3.1	5.3	5450	1043	0
750	36.9	55.1	20.1	2.9	5.0	5630	1043	0
750	36.4	55.4	19.8	2.8	4.8	5720	1043	0

Table headings are defined in Appendix A.

Process Variable Studies

Catalyst mesh studies with 1.41% $BaCl_2/Al_2O_3$ catalysts (29-BKW-124, 14/30 mesh, 29-BKW-132, 100/140 mesh, and 29-BKW-138, 30/60 mesh) indicated differences in catalyst activity, but these could have resulted from slight differences in pressure drops, since additional studies (30-BKW-3, 30/60 mesh, 30-BKW-5, 60/100 mesh, and 30-BKW-7, 30/60 mesh) showed insignificantly different results.

Major process variables including methane to oxygen ratio, temperature, space velocity, and the amount of ethyl chloride in the feed gas were varied in experiment 30-BKW-36, which used a $BaCl_2/\alpha$-alumina catalyst. The selectivity, methane conversion, and yield varied as expected, with higher methane to oxygen ratios resulting in higher

selectivities and lower methane conversions (since methane conversion is limited by oxygen conversion at high methane to oxygen ratios), and with selectivity increasing and methane conversion decreasing with an increase in space velocity. Increases in temperature resulted in higher methane conversions and lower selectivities. The ethyl chloride level in the feed gas was 500 ppm for the first fifty hours of the experiment, then it was dropped to 100 ppm. In spite of the process changes, a 17% C_2 yield was obtained after 70 hours of catalyst time on-stream in reaction 30-BKW-36. The presence of ethyl chloride successfully retards catalyst deactivation.

Lower levels of ethyl chloride were used in reaction 30-BKW-52, since results in 30-BKW-36 showed 100 ppm ethyl chloride to be better than 500 ppm ethyl chloride. Results from 50 ppm ethyl chloride showed this level to result in higher methane conversions and C_2 yields than 100 ppm ethyl chloride at 750 °C and 918 or 434 h^{-1} space velocity. In Table 14 below, all results are for reaction 30-BKW-52 in Reactor A at 750 °C. The methane conversion and selectivity were similar for ethyl chloride levels of 10 and 50 ppm, and at the 10 ppm level, the methane conversion dropped very slowly for over 80 hours. The C_2 yield was over 15% after over 160 hours of operation. Although the ethyl chloride level was not optimized, the presence of ethyl chloride clearly extended the lifetime of the catalyst.

Table 14. $BaCl_2/\alpha$-Al_2O_3 Catalyst with Lower Levels of Ethyl Chloride, 30-BKW-52

CH_4 C	Sel	Yield	=/-	CO_2/CO	CH_4 in	O_2 in	Time	GHSV	ECl
41.9	37.8	16.3	9.2	0.5	10.3	4.9	2415	434	100
44.8	39.5	17.6	8.8	0.7	10.5	5.1	4080	434	50
30.1	50.0	15.1	5.3	0.4	10.6	5.3	2640	918	100
32.8	49.6	16.4	5.2	0.6	10.3	5.2	3000	918	50
45.7	39.6	17.7	9.0	0.7	10.5	5.1	4170	434	50
43.8	40.0	17.7	9.0	0.8	10.3	5.2	4350	434	10
44.1	40.4	17.8	8.8	0.8	10.3	5.2	4440	434	10
37.1	38.4	15.0	7.1	0.9	10.0	5.0	9615	434	10

In reaction 29-BKW-132, at 800 °C and 1705 h^{-1} GHSV with 5 g of a 1.4% $BaCl_2/\alpha$-Al_2O_3 catalyst, a 49% methane conversion at a 46% selectivity to C_2's was obtained (a 22% C_2 yield). In reactions 30-BKW-60 and 61, C_2 yields comparable to better literature results were obtained, even after hours of catalyst operation. Alkaline earth chloride/metal oxide catalysts appear to exhibit superior C_2 yield/ethylene to ethane

product ratio/catalyst lifetime combinations than literature catalysts. Selected results are presented in Table 15 below.

Table 15. Performance of $BaCl_2/\alpha$-Al_2O_3 Catalysts

Temp	CC	Sel	Yield	=/-	CO_2/CO	CH_4 in	O_2 in	Time	GHSV	ECl	R	Ref
750	43.1	48.8	21.0	9.2	0.3	10.2	4.9	25	878	50	D	30-60
800	44.5	47.0	20.8	8.4	0.4	10.8	5.2	1590	1463	50	D	30-60
800	25.8	62.1	16.0	2.8	0.5	10.5	5.1	2600	2341	50	D	30-60
750	40.3	48.8	19.7	7.2	0.4	10.2	4.9	65	878	50	C	30-61
775	45.8	41.7	19.0	12.5	0.6	10.8	5.2	1410	512	50	C	30-61
800	42.4	37.4	16.0	12.4	0.5	10.5	5.1	2560	585	50	C	30-61

The catalyst for reaction 30-BKW-53 had lower levels of $BaCl_2$ (0.5% $BaCl_2$ on Norton 5551 α-alumina) than catalysts for reactions 30-BKW-60 and 61 (5% $BaCl_2$ on Norton 5551 α-alumina). Although methane conversion was about the same with this catalyst as for the catalysts with higher levels of $BaCl_2$, selectivities were lower and ethylene to ethane product ratios were higher. With 30-BKW-53, the barium chloride to alumina ratio is lower, and alumina might catalyze decomposition of barium chloride to release chlorine radicals into the gas phase, which can initiate conversion of C_2's to both ethylene and combustion products.

In reaction 30-BKW-129, a 5% $CaCl_2$ on Norton 5551 α-alumina catalyst was found to exhibit C_2 yields, selectivities, and ethylene to ethane product ratios similar to those of $BaCl_2$ on α-alumina catalysts. Ethylene to ethane product ratios of close to 20 were observed at the low space velocity of 878 h^{-1} (750 °C).

Other Anions

Catalyst deactivation of catalysts containing Group IA and IIA metal chlorides was shown to occur both by loss of chloride and by loss of metal. If a catalyst can lose chloride and then be activated by addition of chloride to the feed gas (Figures 5 and 6 above), a non-chloride catalyst might be activated by addition of chloride to a catalyst made with anions other than chloride. Low selectivities and yields to C_2's were obtained with phosphate and sulfate anions in place of chloride anions in catalysts of reactions 30-BKW-87 ($Ba_3(PO_4)_2/Al_2O_3$) and 136 ($BaSO_4/Al_2O_3$), even in the presence of ethyl

chloride in the feed gas. Gas phase addition of ethyl chloride was used for this purpose. For alkaline earth/alpha-alumina catalysts, the same common mixture of anions could result from alkaline earth carbonates, nitrates, chlorides, aluminates, or other anions, most likely a mixture of alkaline earth hydroxide, carbonate, oxides, and chloride on the catalyst surface (plus aluminates if alumina were support, titanates if titania were support, etc.). One might therefore expect that after catalysts were run for a period of time in the presence of chloride (e.g., with ethyl chloride in the gas feed), catalyst performances (C_2 yields, C_2 selectivities, and ethylene to ethane product ratios) would be similar, the only differences being those of activity, from differences in dispersions of catalyst components during catalyst preparation with the different salts. The time required for catalyst activation or deactivation to the common state would vary with the stability of the salt used to make the catalyst, with the least stable salts reaching the common state faster.

Performance of the carbonate catalysts differed from that of the chloride catalysts, although maximum selectivities, activities, and ethylene to ethane product ratios reached after several hours of reaction were similar with the two types of catalysts. In general, methane conversions above 35% for 5 g of catalyst at 750 °C were not observed at space velocities above 1000 h^{-1} for chloride catalysts on α-alumina, whereas for carbonate catalysts on α-alumina, methane conversions above 35% could be obtained with 5 g of catalyst at 750 °C at space velocities above 2000 h^{-1} (10% methane, 5% oxygen, balance nitrogen, 11 psig).

The alkaline earth chloride/alumina catalysts as a rule show high initial activities, yields, and ethylene to ethane product ratios, which then drop. In the presence of added volatile chloride, catalyst performance may stabilize, but ethylene to ethane product ratios and C_2 yields will often not rise to the values observed early in the reaction. As an example, in reaction 30-BKW-53, 10 g of a catalyst prepared by impregnation of barium chloride on Norton α-alumina was tested at 750 °C and 429 h^{-1} GHSV. The initial C_2 yield was 17.1% and the initial ethylene to ethane product ratio was 12. These values dropped to 11.2% and 5, respectively, after 19.5 hours of reaction. Addition of 100 ppm of ethyl chloride caused both values to rise, but the maximum values reached under these conditions were a C_2 yield of 15.8% and a 9.3 ethylene to ethane product ratio. In contrast to this, catalysts prepared by impregnation of alkaline earth carbonate on α-alumina, in the presence or absence of added ethyl chloride in the feed gas, exhibit low C_2 selectivities, C_2 yields, and ethylene to ethane product ratios initially (e.g., 33%, 13%, and 2, respectively, 32-BKW-41, Table 10, above), but these values then rise in the presence of added ethyl chloride in the feed gas.

A $BaCl_2/\alpha$-Al_2O_3 catalyst (33-BKW-81) was compared with a $BaCO_3/Al_2O_3$ catalyst (33-BKW-74) to see if the catalysts reached a common state of mixed anions and the same catalyst performance. Both catalysts were prepared with the same support and were prepared to contain the same amount of barium. Table 16 below shows that the chloride catalyst is not as active as the carbonate catalyst under similar process conditions, which results in a lower C_2 yield.

Table 16. $BaCO_3/Al_2O_3$ (33-BKW-74) and $BaCl_2/Al_2O_3$ (33-BKW-81) Catalysts

Ref.	CH_4 C	Sel	Yield	O_2 C	=/-	CO_2/CO	Time, h	GHSV	ECl
33-74	29.1	59.0	17.0	45	1.6	1.8	208	2233	4
33-74	40.8	47.8	19.3	77	3.0	1.8	332	1116	8
33-81	19.7	58.7	11.5	27	1.6	0.7	115	1067	4

Analyses of these two catalysts by microscopy showed significant differences in distribution of the barium before and after reaction (see Catalyst Surface Analyses Section below). Larger clumps of barium were present before the reaction on the catalyst prepared with barium chloride than on the catalyst prepared with barium carbonate. After the reaction, the barium on the catalyst made with carbonate had further dispersed, whereas the barium was still in clumps on the catalyst made from chloride. The different dispersions of barium could explain differences in the activity of these two catalysts. The catalyst for reaction 33-BKW-74 ($BaCO_3/Al_2O_3$) contained 3.1% barium before and after reaction (by ICP). The catalyst for reaction 33-BKW-81 was analyzed by ICP to contain 3.8% barium before reaction and 3.3% barium after reaction. EDS analyses showed that the surface of the catalyst for reaction 33-BKW-74 contained 22 atom% barium before reaction and 15 atom% barium after reaction. The surface of the catalyst for 33-BKW-81 contained 6 atom% barium before and 11 atom% barium after reaction.

Alkaline earth/metal oxide catalysts with added Na, K, Rb, and Cs compounds did not exhibit increased selectivities, activities, or ethylene to ethane product ratios, when compared with alkaline earth/metal oxide catalysts without added alkali components (30-BKW-100, 101, 106, 107, and 111).

Alkaline Earth Chloride/Metal Oxide Catalysts

Reactions 30-BKW-86 (5% $BaCl_2$ on ZrO_2), 97 (5% $BaCl_2$ on ZnO), 133 (5% $BaCl_2$ on Ga_2O_3), and 31-BKW-7 (5% $BaCl_2$ on Ga_2O_3) used non-alumina supports for catalysts. Selected results are presented below in Table 17. The ethylene to ethane product ratios are high on catalysts using ZrO_2 and Ga_2O_3 supports. Methane coupling on the $BaCl_2/Ga_2O_3$ catalysts compete with the better literature results, even after over 20 hours of operation, and the ethylene to ethane product ratios remain high.

Table 17. Non-Alumina Supports

Temp	CC	Sel	Yield	=/-	CO_2/CO	CH_4 in	O_2 in	Time	GHSV	ECl	R	Ref.	Support
750	42.6	34.0	14.2	4.3	1.7	10.3	5.3	35	1200	0	D	30-86	ZrO_2
750	12.7	68.0	8.5	1.2	1.0	10.3	5.1	45	2000	50	D	30-97	ZnO
750	40.2	46.5	18.5	11.5	58.9	9.9	5.1	70	900	50	D	30-133	Ga_2O_3
750	42.6	49.0	20.5	7.3	183.5	9.9	5.1	275	900	50	D	30-133	Ga_2O_3
750	40.9	48.5	19.5	4.5	9.3	10.1	5.3	1125	1500	50	D	30-133	Ga_2O_3
750	34.9	47.8	16.6	3.8	4.9	10.3	5.2	1875	1500	50	C	31-7	Ga_2O_3
800	38.9	46.0	17.4	6.3	7.7	10.2	5.2	3030	1650	50	C	31-7	Ga_2O_3

Supports were shown to have dramatic effects on methane coupling reactions using $BaCl_2$/metal oxide catalysts. Alkaline earth chloride/Norton 5551 α-alumina catalysts show higher ethylene to ethane product ratios than literature catalysts such as Li/MgO, with comparable C_2 yields and C_2 selectivities. Similar catalysts on Norton support 5502 α-alumina, Ga_2O_3 and ZrO_2 show even higher ethylene to ethane product ratios, whereas a catalyst on ZnO did not. In reaction 30-BKW-93 ($BaCl_2$/Norton 5502 α-Al_2O_3), C_2 yields of 22-24% were obtained with ethylene to ethane product ratios of 8-12 using 50 ppm ECl at 750 °C and 783 h^{-1} GHSV. Catalysts on Norton 3232 and 3235 α-aluminas were inactive and unselective.

In reaction 30-BKW-37 ($BaCl_2$ on Norton support 5502 α-alumina), C_2 selectivity and C_2 yield are lower, and the ethylene to ethane product ratio is higher than in 30-BKW-36 (using Norton 5551 support) at the start of both reactions, under the same conditions. Under similar process conditions, the ethylene to ethane product ratio is higher for the catalyst on support 5502, with ratios of 20-25 observed. Norton support

5551 has a lower surface area (0.25 m^2/g, BET method) and is less acidic (0.27 μmoles/g by irreversible ammonia absorption) than Norton support 5502 (0.75m^2/g, 1.2 μmoles/g).

Support Acidity

The high yields obtained using the alkaline earth/metal oxide catalysts described above are surprising since the metal oxides used, such as titania, are relatively acidic. Almost all literature articles discussing the types of supports suitable for methane coupling state that basic supports are necessary[60-66] to obtain high C_2 selectivities and yields of C_2's. Indeed, one of the best literature catalysts, Li/MgO[16-19], contains the basic MgO support. Oxides of aluminum, gallium, titanium, zirconium, and zinc are considered amphoteric, having both acid and base sites and properties, whereas oxides of calcium, magnesium, praseodymium, and cerium are basic (with basicity according to, e.g., Sargent-Welch Scientific Companies periodic table) in the order of Ca > Mg > Pr ~ Ce). Measured acidities per unit of surface area are low for CeO_2 and Pr_6O_{11} (see Table 18 below). Measured acidities per weight of catalyst for these are relatively high (see Table 18).

The total (Lewis and Bronsted) surface acidity of metallic oxides used as supports were measured by ammonia chemisorption at 100 °C. The basic oxides (CaO and MgO) possess few or no acidic sites while the other oxides (three α-alumina samples, ZnO, TiO_2, ZrO_2, and Ga_2O_3) have a range of acidities up to 20 times that of MgO per weight of oxide. Surface areas (m^2/g) of the oxides are less than 1, except for the MgO (37.7) and Ga_2O_3 (4.22). Table 18 presents the acidity measurements and representative initial experimental results for catalysts with 5% $BaCl_2$ on the different supports (except for 31-BKW-113, which uses 6% $SrCl_2$).

Table 18. Acidity and Surface Areas of Selected Supports[a]

Support	Acidity µmole/g	S A m^2/g	Acidity/SA µmole/m^2	T	CC	Sel	Yield	=/-	GHSV	ECl	Ref[b]
Al_2O_3 5551	0.27	0.25	1.08	750	43.1	48.8	21.0	9.2	878	50	30-60
Al_2O_3 5451	0.31	0.28	1.11	750	48.8	44.4	21.5	13.7	783	0	31-34
Al_2O_3 5502	1.20	0.75	1.60	750	40.2	48.5	19.5	12.6	783	50	30-93
CaO	0.05	0.84	0.06	700	29.3	50.0	14.6	1.6	6857	0	31-113
MgO	0.15	37.8	0.00	700	43.9	39.1	16.9	1.7	9796	0	31-67
ZnO	0.16	<0.2	0.80	750	12.7	68.0	8.5	1.2	2000	50	30-97
TiO_2	1.08	0.82	1.32	750	38.2	47.9	18.1	11.0	878	0	31-46
ZrO_2	1.45	0.95	1.53	750	42.6	34.0	14.2	4.3	1200	0	30-86
Ga_2O_3	3.76	4.22	0.89	750	42.6	49.0	20.5	7.3	900	50	30-133
CeO_2	2.06	6.76	0.30	700	34.3	37.4	12.7	1.0	38400	200	32-1
Pr_6O_{11}	1.78	2.46	0.72	700	30.9	19.7	6.0	0.6	32000	0	32-2

a. Acidity is defined as irreversible ammonia adsorption in µmoles/gram. Surface area were determined with a BET method on a Quantasorb instrument. Table headings are defined in Appendix A.
b. References are abbreviated, e.g., 30-86 is 30-BKW-86.

Table 18 shows that higher molar ethylene to ethane product ratios are observed for methane coupling with catalysts on more acidic supports. Alkaline earth chlorides supported on CaO, MgO, Pr_6O_{11}, and CeO_2 gave much lower ethylene to ethane product ratios (<2) than those obtained when the other, more acidic, (per surface area) materials are used as supports (ethylene to ethane product ratios of 5 to 25). Catalysts on Pr_6O_{11} and CeO_2 (32-BKW-1 and 36-BKW-2), were tested at very high space velocities and low temperatures due to high activities, so ethylene to ethane product ratios are lower than they might be at higher temperatures or residence times. It is concluded that non-basic supports are preferred for higher ethylene to ethane product ratios.

The highest initial ethylene to ethane product ratios are observed for Sr and Ca catalysts on Al_2O_3 or TiO_2. Ethylene to ethane product ratios as high as 27 were observed. Table 19 shows some selected results with high ethylene to ethane product ratios with basic supports.

Table 19. Non-Basic, Non-Alumina Supports - Selected Results

Reference	Catalyst	Temp	CH_4 C	Sel	Yield	=/-	CO_2/CO	Time	GHSV	ECl
31-BKW-21	$CaCl_2/ZrO_2$	700	37.8	42.9	16.1	12.6	1.8	95	1000	50
31-BKW-40	$CaCl_2/Ga_2O_3$	700	22.2	38.9	8.6	8.8	0.4	35	1200	0
31-BKW-41	$SrCl_2/Ga_2O_3$	750	33.1	48.0	15.6	7.5	1.3	70	1200	0
31-BKW-46	$BaCl_2/TiO_2$	750	38.2	47.9	18.1	11.0	0.4	30	878	0
31-BKW-96	$CaCl_2/TiO_2$	700	20.7	35.0	7.2	23.7	0.2	30	1171	0
31-BKW-97	$SrCl_2/TiO_2$	750	38.4	32.7	12.4	22.6	0.2	60	878	0

The type of support appears to be important to both the initial and the final ethylene to ethane product ratios. Representative ethylene to ethane product ratios after several hours of reaction are presented for barium catalysts on four supports in Table 20, where =/– is the molar ethylene to ethane product ratio (Table 19 contained only initial results). Ethylene to ethane product ratios of more than 5 were not obtained using barium catalysts with more basic supports such as MgO, ZnO, or CaO under any conditions at temperatures below 760 °C. Addition of ethyl chloride to catalysts prepared using these basic supports does not appear to increase catalyst performance, rather performance drops in some cases with addition of volatile chloride. Activity, selectivity, and stability of catalysts on supports which are not significantly acidic or basic, e.g., Norton 5451 α-alumina, are higher in the presence of the right amount of added chloride than without added chloride after the catalyst has run for a period of time. Catalysts on more acidic supports, such as TiO_2, require higher levels of volatile chloride for stable performance and result in higher ethylene to ethane product ratios. Alkaline earth chloride/acidic support catalysts provide higher initial ethylene to ethane product ratios (e.g., 13.7 for 5451 α-alumina at 750 °C and 783 h^{-1} GHSV), but deactivate more rapidly when less than optimum amounts of volatile chloride are added in the feed gas.

Table 20. Ethylene to Ethane Product Ratios on Different Supports

Support	Acidity μm/g	Acidity $\mu m/m^2$	ECl ppm	GHSV h^{-1}	T °C	=/-	C_2 Yield %	Time h
MgO	0.15	0.004	1-500	9796	700	1.6	15	95
ZnO	0.16	0.80	50	2000	750	1.2	5	16
Norton 5451 α-Alumina	0.31	1.11	200	2087	750	2.2	19	234
TiO_2	1.08	1.31	500	2743	750	8.1	22	51

It is thought that chlorine radicals in the gas phase are responsible for higher ethylene to ethane product ratios[56]. In control runs, addition of ethyl chloride to an uncatalyzed (homogeneous) reaction of methane and oxygen results in only a slight increase in methane conversion or shift in product distribution, whereas large shifts in product distribution and large increases in methane conversion are observed upon addition of chloride to catalyzed methane coupling reactions. These results are consistent with the explanation that chlorine radicals are produced on the acidic catalyst surface and released into the gas phase.

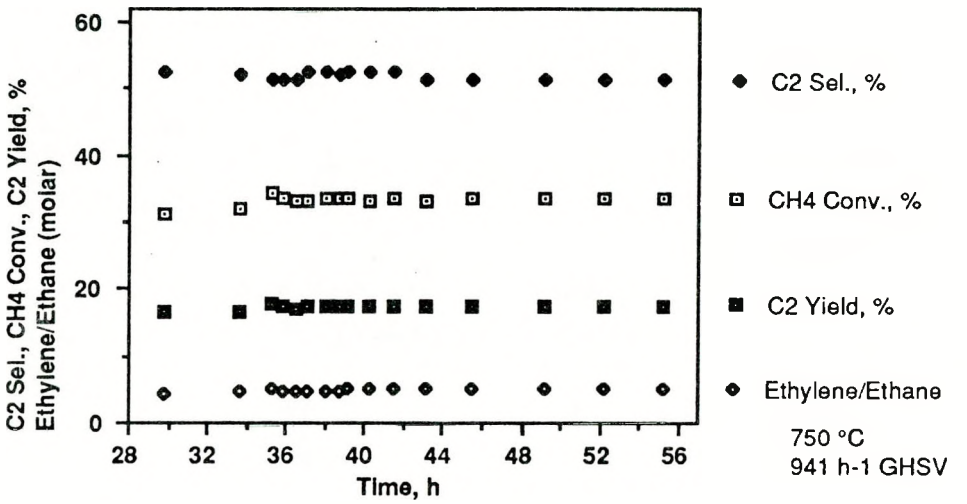
Catalysts were prepared on four additional α-alumina supports and tested for methane coupling activity and selectivity. Barium chloride was used as the source of alkaline earth. Catalysts were tested at three levels of added ethyl chloride, 0, 10, and 200 ppm. The supports used to prepare catalysts for these four reactions, 33-BKW-54, 55, 62, and 63, had surface areas of 0.19 (Norton 8855001, type 6596), 1.42 (Norton 8855011), 0.49 (Norton 8855002), and 0.12 m^2/g (Norton 8855003, type 5452), respectively.

A high C_2 selectivity was seen at low methane conversions for the catalyst in reaction 33-BKW-54. The initial C_2 yield was over 25%, but dropped to 5% after 87 hours. An increase in added ethyl chloride from 10 to 200 ppm in the feed gas resulted in a rise in selectivity, C_2 yield, methane conversion, and ethylene to ethane product ratio. The final C_2 yield, however, was only 5%, due to the low methane conversion. Although initial C_2 selectivity was not as high for the catalyst in reaction 33-BKW-55, activity did

not drop as sharply as it did for the catalyst in reaction 33-BKW-54. The final C_2 yield with 200 ppm ethyl chloride was only 3%.

Methane coupling with the catalyst in reaction 33-BKW-62 resulted in methane conversions of 29-34%, C_2 selectivities of 51-53%, and C_2 yields of 15-18%, with ethylene to ethane product ratios of 3-5, with 200 ppm ethyl chloride in the feed gas. Figure 7 shows the stability of catalyst performance from this reaction for the period during which 200 ppm ethyl chloride was used.

Figure 7. $BaCl_2$/Norton 8855002 α-Al_2O_3, 33-BKW-62



Methane coupling in reaction 33-BKW-63 also shows stable catalyst behavior with 200 ppm ethyl chloride in the gas feed, but the C_2 yield and C_2 selectivity are not as good as those for the reaction shown in Figure 7.

A physical mixture of $BaCl_2$ and $BaCO_3$ was melted, crushed, then used as a catalyst in reaction 33-BKW-121. At 750 °C and 2400 h^{-1} GHSV, a C_2 selectivity of 70% was obtained at a methane conversion of 12% with no added ethyl chloride. Addition of ethyl chloride of levels up to 500 ppm did not result in improved activity or selectivity. Ethylene to ethane product ratios were not greater than 0.7, suggesting the importance of an acidic support for high ethylene to ethane product ratios.

Pure Components

High initial selectivities are obtained with pure, unsupported $SrCl_2$ as catalyst (31-BKW-76, Table 21). Methane conversion is low, and the ethylene to ethane product ratio is also low, using 1 gram of catalyst at 750 °C and 3000 h^{-1} space velocity.

Table 21. Pure $SrCl_2$

Temp	CH_4 C	Sel	Yield	=/-	CO_2/CO	Time	GHSV	ECl
750	8.7	72.4	6.3	0.9	0.9	185	3000	0
750	10.6	72.2	7.6	1.0	1.0	545	3000	0
750	9.8	69.6	6.8	1.0	0.9	1125	3000	20
800	19.8	58.0	11.4	2.5	0.6	1200	3000	20
800	8.4	55.0	4.7	1.3	0.4	2580	3000	200

Much lower selectivities and methane conversions are observed using pure, unsupported $BaCl_2$ as catalyst (31-BKW-77, Table 22).

Table 22. Pure $BaCl_2$

Temp	CH_4C	Sel	Yield	=/-	CO_2/CO	Time	GHSV	ECl
750	1.7	49.3	0.8	0.2	0.4	95	5143	0
750	0.7	47.8	0.4	0.2	0.6	950	5143	0
750	1.9	45.7	0.9	0.3	0.3	1145	5143	20
800	5.1	49.2	2.5	0.6	0.2	1230	5143	20
800	4.5	57.4	2.6	0.6	0.4	2390	5143	0
800	4.5	52.8	2.4	1.0	0.1	2615	5143	200

Powder x-ray analyses of used alkaline earth/alpha alumina catalysts showed alkaline earth aluminates as the only significant components in these catalysts. Calcium aluminate was tested as a methane coupling catalyst. If it were the active species on these catalysts for methane coupling, high initial C_2 selectivities would be expected, although activities could vary depending on the surface area of the sample. Initial C_2 selectivities at 750 °C and 400 h^{-1} GHSV were low (under 5%). C_2 selectivity is strongly influenced

by the level of added ethyl chloride in the feed gas, but did not rise over 25% with 500 ppm of added ethyl chloride.

A barium oxide·aluminum oxide (barium aluminate) catalyst ($3BaO \cdot Al_2O_3$, from Alfa, with major powder x-ray phases of barium aluminate, barium oxide, and barium carbonate) was tested for methane coupling. The highest C_2 yield, C_2 selectivity, and ethylene to ethane product ratio obtained at 750 °C and 3429 h^{-1} GHSV (2 g catalyst) were 15.3%, 36.5%, and 2, respectively. This material was tested on an α-alumina support (32-BKW-116). The highest C_2 yield, C_2 selectivity, and ethylene to ethane product ratio obtained at 750 °C and 2087 h^{-1} GHSV were 11.5%, 63.2%, and 2-3, respectively. Although the C_2 selectivity was higher, the methane conversion was lower on the supported catalyst, so the supported catalyst was not superior to the unsupported barium aluminate for methane coupling, even in the presence of ethyl chloride.

In contrast to this, a $BaCl_2/Al_2O_3$ catalyst shows significantly higher C_2 yields and ethylene to ethane product ratios than either $BaCl_2$ or Al_2O_3, as shown in the Table 23 below.

Table 23. Performance for a Catalyst and the Individual Components

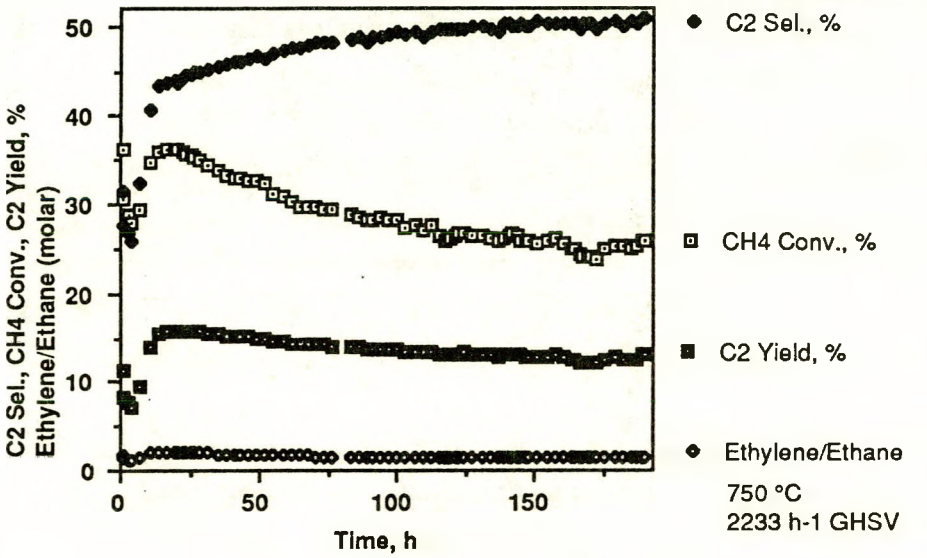
Reference	Catalyst	Temp	CH_4 C	Sel	Yield	=/-	Time	GHSV	ECl
31-BKW-77	$BaCl_2$	750	1.7	49.3	0.8	0.2	95	5143	0
31-BKW-77	$BaCl_2$	750	1.9	45.7	0.9	0.3	1070	5143	20
29-BKW-71	Al_2O_3	800	19.1	23	4.4	2.7	2650	-	0
30-BKW-52	$BaCl_2/Al_2O_3$	750	45.5	40.4	18.5	18.5	35	361	0

These results indicate a possible synergistic effect of support and catalyst components resulting in the high C_2 yields and ethylene to ethane product ratios.

The oxidation of methane over gamma-alumina at 650 °C is oxygen limited, and carbon dioxide is the major product, while carbon monoxide is the only significant minor product. Pure barium carbonate was surprisingly effective for methane coupling at 750 °C, a space velocity of 2233 h^{-1}, and with 7.5 ppm ethyl chloride in the feed gas (Figure 8 below). A peak C_2 yield of 15.7% was obtained at a C_2 selectivity of 43.8%. This indicates that a barium species is likely to be the active component for oxidizing methane in barium/metal oxide catalysts. The barium carbonate, 99.997%, had a surface area of 0.59 m^2/g prior to reaction and 0.26 m^2/g after reaction. The ethylene to ethane

product ratio was low for this unsupported barium compound. Again, this indicates that the support is involved in producing high ethylene to ethane product ratios.

Figure 8. $BaCO_3$, 33-BKW-75



Catalysts Containing Non-Group IA or IIA Metals

High ethylene to ethane product ratios were not obtained with most non-Group IA or IIA metals which were tested in place of alkali or alkaline earth metals. Some non-alkali and alkaline earth chlorides on alumina or titania were tested as catalysts for methane coupling. These resulted in low ethylene to ethane product ratios and low C_2 yields. A $LaCl_3/Al_2O_3$ catalyst exhibited a 10.1% yield to C_2's. $ZrCl_4/Al_2O_3$ and $CeCl_3/Al_2O_3$ catalysts resulted in low selectivities and yields to C_2's. Catalysts on alumina and titania which were made with a La/Nd nitrate solution exhibited 9-10% C_2 yields after ethyl chloride was added to the feed gas. Significant yields were not observed with these catalysts until the chloride was added to the feed gas.

Additional non-Group IA or IIA metals used to make catalysts for methane coupling contained chromium chloride, nickel chloride, and gallium nitrate on alpha-alumina, and gallium nitrate on magnesium oxide. Chromium and nickel are of interest because for each, more than one oxidation state is accessible. Chromium is an example of a metal which undergoes rapid 1-electron redox reactions, and it is associated with

rapid formation of free radicals from organic compounds. Nickel catalysts were among the best catalysts reported by Otsuka[43,44]. Redox properties may be important for adsorption or reaction of oxygen with the catalyst to provide active sites, for rapid transfer of electrons from the reaction site to the adsorption site for oxygen, when these sites are different, or for interconversion of oxygen from the initially adsorbed state to the reactive state, if these oxygen types are different. Gallium is of interest because gallium in molecular sieves successfully converts alkanes[72-75] including methane[72] to aromatics. It is therefore known that catalysts containing gallium can successfully abstract hydrogen from alkanes and produce products selectively other than those which are thermodynamically most stable (carbon in the absence of oxygen, and carbon dioxide in the presence of oxygen).

Methane coupling with a $CrCl_2/\alpha$-Al_2O_3 catalyst results in high activity for methane conversion, even at 600 °C, but carbon monoxide and carbon dioxide are the only significant products. With 10% methane, 5% oxygen, and without ethyl chloride in the feed gas, at 600 °C and 2087 h^{-1} GHSV, a 25.3% methane conversion is achieved at a 98.6% oxygen conversion. The CO_2/CO ratio in the products is 11. At 650 °C, the CO_2/CO ratio in the products is 12.7 without ethyl chloride, and 2.9 after 500 ppm ethyl chloride is added in the feed gas. Even in the presence of added ethyl chloride, carbon oxides are the only significant products. Chloride, either on the catalyst or in the gas phase, appears to inhibit total oxidation.

In contrast to the results with the catalyst containing Cr, methane conversions are less than 8% at 600 °C and 2087 h^{-1} GHSV using a $NiCl_2/\alpha$-Al_2O_3 catalyst. At 750 °C with 500 ppm ethyl chloride, methane conversions of 11-15% with C_2 selectivities of 26-33% are observed (C_2 yields of about 4%). At 800 °C, C_2 yields are 7-9%.

With a $Ga(NO_3)_3/\alpha$-Al_2O_3 without added ethyl chlorides, a 35% C_2 selectivity is obtained at 800 °C (6.4% methane conversion). Addition of 150 ppm ethyl chloride results in a slight increase in C_2 selectivity. C_2 yields remain low for this catalyst compared with alkaline earth catalysts.

With a $Ga(NO_3)_3$/MgO catalyst, methane conversion is 25% at 700 °C and a space velocity of 9796 h^{-1} (with 0.5 g of catalyst). High activity is expected from the higher surface area of 37.8 m^2/g for the MgO_2. In the presence of ethyl chloride, C_2 selectivities as high as 45% and C_2 yields as high as 15.6% are obtained (825 °C, 3673 h^{-1} GHSV). Ethylene to ethane product ratios are not above 2 at temperatures below 750 °C. An ethylene to ethane product ratio of 6.8 is observed at 825 °C, but an ethylene to ethane product ratio of over 10 was observed in an uncatalyzed reaction at 850 °C.

Zinc chloride was also tested as a methane coupling catalyst. Table 24 below shows that methane coupling results with pure zinc chloride were similar to results from alkali and alkaline earth/metal oxide catalysts, although C_2 yields were not as high. This catalyst did exhibit high ethylene to ethane product ratios. Deactivation occurs, along with a decrease in the ethylene to ethane product ratio, but both could be reversed by addition of ethyl chloride to the feed gas.

Table 24. Pure $ZnCl_2$

Temp	CC	Sel	Yield	=/-	CO_2/CO	CH_4 in	O_2 in	Time	GHSV	ECl	R
750	23.3	46.6	10.5	2.5	1.8	10.0	5.4	45	878	0	C
750	15.8	41.8	6.7	1.6	0.9	10.0	4.9	1005	878	0	C
750	19.5	48.5	9.4	2.4	1.2	10.1	4.7	1185	878	50	C
750	26.3	50.1	13.4	5.9	0.3	10.5	4.8	4060	878	500	C
750	25.8	49.8	13.1	5.8	0.2	10.5	4.8	4140	878	500	C
750	24.8	46.5	11.7	6.2	0.1	10.5	4.8	4325	878	500	C

Alkaline Earth/Metal Oxide/Halide Catalysts

It was concluded above that supports favoring high ethylene to ethane product ratios are the more acidic supports, with alkaline earth catalysts on TiO_2 and Ga_2O_3 providing some of the highest C_2 yield/selectivity/ethylene to ethane product ratio combinations for methane coupling. Barium carbonate catalysts were made and tested on these two supports. Higher ethylene to ethane product ratios were indeed observed using these catalysts under similar conditions to those of alkaline earth chloride catalysts. Ethylene to ethane product ratios above 5 were not observed under typical experimental conditions at 750 °C with alkaline earth carbonate catalysts on α-alumina. Ethylene to ethane product ratios above 5 were frequently observed at 750 °C with $BaCO_3/TiO_2$ (32-BKW-80) and $BaCO_3/Ga_2O_3$ (32-BKW-81) catalysts.

With a 5 weight percent barium carbonate (3.5 weight percent barium) on titanium dioxide catalyst, the amount of halogen component had a demonstrable effect on the performance of the catalyst. High selectivities, activities, and C_2 yields were not obtained with 6 ppm ethyl chloride in the feed gas (Table 25 below). The lower levels used were not sufficient to maintain high selectivities and yields to C_2's. After a period of over 350 hours, methane coupling with this catalyst at 750 °C and 2743 h^{-1} GHSV

exhibited a 22% C_2 yield, a C_2 selectivity of 58%, and an ethylene to ethane product ratio of 8. C_2 yields of over 20% were observed for this catalyst for 27 hours (18540 to 20160 minutes). With TiO_2 (31-BKW-46) and Ga_2O_3(30-BKW-133) supports, as well as with alumina supports, methane conversions were higher at comparable space velocities and temperatures with alkaline earth carbonate catalysts than they were with alkaline earth chloride catalysts.

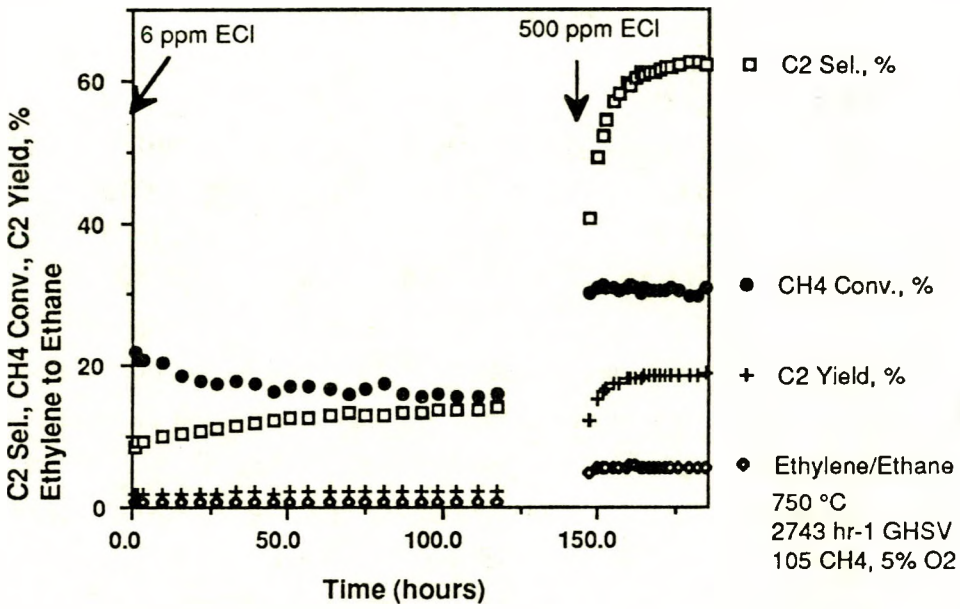
Table 25. 5% $BaCO_3/TiO_3$, 32-BKW-80

Temp	CH_4 C	Sel	Yield	=/-	CO_2/CO	Time	GHSV	ECl
750	22.0	8.5	1.9	0.7	0.9	30	2743	6
750	15.9	14.1	2.2	0.7	0.7	7050	2743	6
750	30.3	40.6	12.4	4.9	0.3	8850	2743	500
750	31.1	63.2	19.1	5.6	0.3	11430	2743	500
750	38.8	54.5	20.5	8.4	0.3	11520	1714	500
750	44.1	49.5	21.9	11.3	0.3	18610	1714	500
750	38.1	58.9	22.1	8.1	0.3	20070	2743	500
770	48.0	47.8	23.1	11.1	0.3	20160	2743	500
730	30.3	63.3	18.8	5.8	0.2	20210	2743	500
750	37.8	58.5	22.0	8.1	0.3	21105	2743	500
750	47.5	47.2	22.5	12.8	0.3	21330	1714	500

To summarize observations from the sections above, the best methane coupling catalysts for high ethylene to ethane product ratios, which exhibit C_2 selectivities and C_2 yields competitive with literature catalysts, and which are stable, were found to be catalysts which contain Ba or Sr, with chloride on the catalyst and/or in the feed gas, and a non-basic metal oxide combustion promoter. Combustion promoters are metal oxides which alone, with methane and oxygen under reaction conditions, burn methane; for example, oxides of Ti, Zr, Ga, or Al. Without the combustion promoter, alkaline earth catalysts did not result in high ethylene to ethane product ratios. Examples of these catalysts are $SrCO_3/TiO_2$/ethyl chloride and $BaCO_3$/α-alumina/ethyl chloride. The best supports are acidic. Without added chloride, these catalysts deactivate rapidly. Ethyl chloride was used as the chloride source for all experiments. More acidic supports require more chloride. Some basic supports result in combustion without added promoters. Even when these basic supports are promoted with Ba or Sr, the ratios of ethylene to ethane produced are not high.

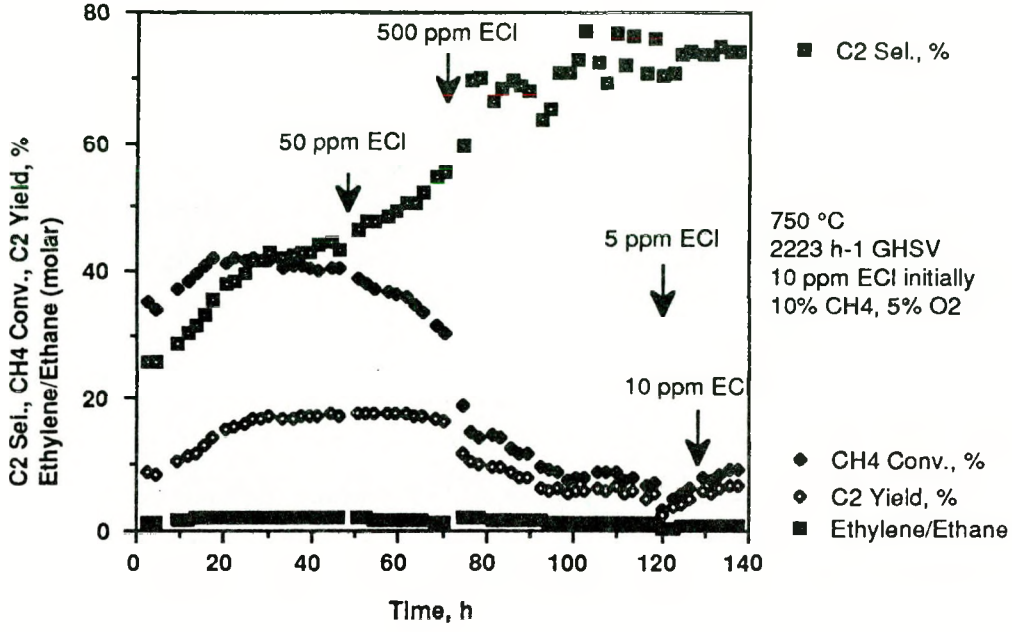
Ba or Sr catalysts with titanium dioxide combustion promoters require higher levels of ethyl chloride for high methane conversions and C_2 selectivities. This is illustrated in Figure 9, where a C_2 selectivity of 63%, methane conversion of 31%, and a C_2 yield of 19% are obtained with 500 ppm ethyl chloride in the gas feed using 5 g of a $BaCO_3/TiO_2$ catalyst at 750 °C, 11 psig (176 kPa), and a space velocity of 2743 h^{-1}. With 6 ppm ethyl chloride, C_2 selectivities and yields are very low.

Figure 9. $BaCO_3/TiO_2$ Catalyst, Effect of Ethyl Chloride, 32-BKW-80



In contrast to this example, Figure 10 shows that after an initial catalyst activation period with the low ethyl chloride level of 10 ppm in the feed gas, a $BaCO_3/\alpha\text{-}Al_2O_3$ catalyst exhibits a C_2 yield of 17% and a C_2 selectivity of 44%, using 5 g of catalyst, at 750 °C, 11 psig (176 kPa), and a space velocity of 2233 h^{-1}. With 500 ppm of ethyl chloride, rates to all products drop. The higher level of ethyl chloride, which promotes higher selectivities and activities for the catalyst containing titanium oxide, causes catalyst deactivation with this catalyst.

Figure 10. $BaCO_3/\alpha$-Al_2O_3 Catalyst, Effect of Ethyl Chloride, 34-BKW-125



Starting with the carbonate catalyst, which initially contains no chloride, Figure 10 shows lower selectivity to C_2's, lower methane conversion, and lower C_2 yields initially. The 10 ppm of ECl fed from the beginning of the reaction slowly increases the rate of methane activation and conversion to C_2 products. The chloride appears to affect the surface of the catalyst. These data are consistent with chloride catalyzing the conversion of inactive catalyst sites to active sites. For instance, chloride can react with stable barium or strontium salts to produce less stable intermediates, which can then be converted to active sites for hydrogen abstraction by reaction with oxygen. In this same figure, the selectivity rises slowly over a period of time while the rate to C_2's remains constant. During this time, the rate to CO_2 continues to drop. This observation can be explained by chloride blocking CO_2 formation on the surface of the catalyst. The reduction of the rate to CO_2 occurs over a long period of time, indicating a slow catalyst change.

Both the magnitude of changes in conversion and selectivity and the direction of these changes are different for catalysts on alumina (33-BKW-74) and titania (33-BKW-85) supports containing the same amount of barium. The change in ethyl chloride level from 200 to 4 ppm resulted in an increase in conversion for the catalyst containing

alumina, and a decrease in both selectivity and conversion for the catalyst containing titania. For both reactions, the change in concentrations of methane and oxygen fed to the reactors from 80 and 10%, respectively, to 10 and 5%, respectively, resulted in increased methane conversion (as a percentage of that fed) and decreased selectivity to C_2's. The ethylene to ethane product ratio rose as the ethyl chloride level was raised and as the methane to oxygen ratio was lowered on the catalyst containing titania. On the catalyst containing alumina, changes in the ethylene to ethane product ratio were lower for similar process changes. This shows that the ethylene to ethane product ratio depends on the process variables, including the level of ethyl chloride in the reaction, and on the support.

Concentration Studies

Figures 11 and 12 below display the first 140 hours of reaction with methane coupling reactions catalysts with 5% (33-BKW-6) and 30% (33-BKW-7) barium carbonate, respectively, on Norton 5451 alumina support.

Figure 11. 5%$BaCO_3/Al_2O_3$, 33-BKW-6

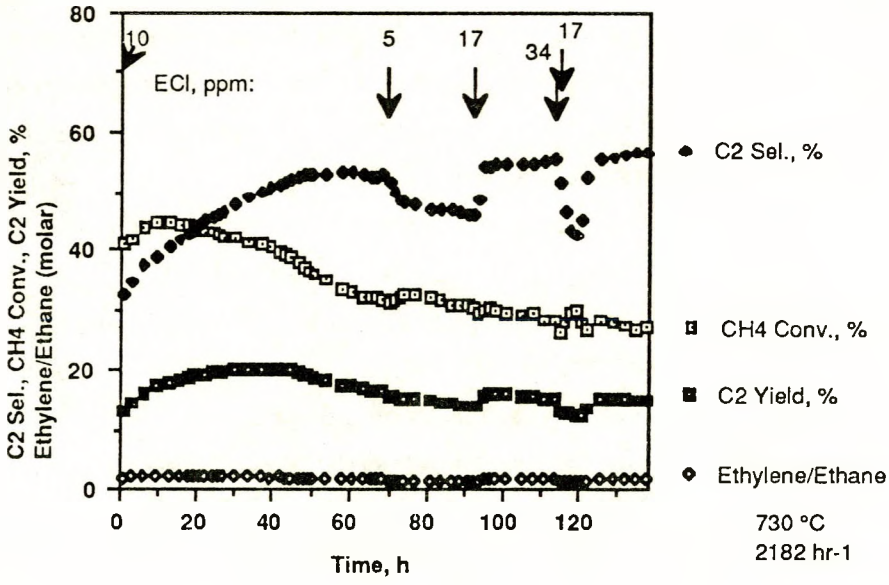
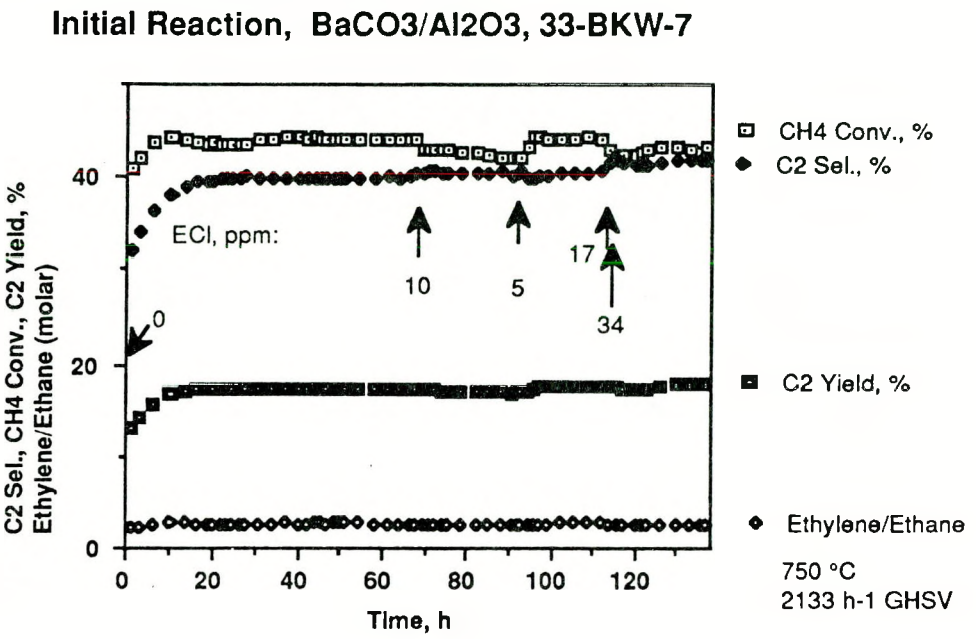


Figure 12. 30% $BaCO_3/Al_2O_3$, 33-BKW-7



After an initial period of activation for both of these catalysts, the methane conversion continued to drop for the catalyst containing only 5% barium carbonate with several levels of ethyl chloride (10, 5, 34, and 17 ppm). For both catalysts, C_2 selectivity and C_2 yield were superior to results from the catalysts on the more acidic support used in reactions 33-BKW-1 and 2. The selectivity was very sensitive to changes in the ethyl chloride level for the catalyst made with 5% barium carbonate, whereas the selectivity was relatively insensitive to ethyl chloride level (as may be seen in Figures 11 and 12) for the catalyst made with 30% barium carbonate.

A C_2 yield of over 20% was obtained in reaction 33-BKW-6. The C_2 yield then dropped (see Figure 11 above). A change in the ethyl chloride level from 10 to 5 ppm did not result in an improvement in catalyst performance. Ethyl chloride levels higher than 10 ppm also resulted in poor catalyst performance. It was thought that this 5% barium carbonate on alumina catalyst might be extremely sensitive to changes in ethyl chloride, and that 5 ppm ethyl chloride might have been lower than the optimum amount of ECl, whereas 10 ppm of ethyl chloride might have been too much.

Two catalyst levels of barium carbonate (5 wt% and 17 wt%) were explored for methane coupling on each of two kinds of titania supports (Norton and JM) to determine the effects of catalyst loading and of the kind of titania support on catalyst performance.

Table 26 below presents results. For the Norton support, the highest selectivity/yield combination for the catalyst containing less barium (reaction 33-BKW-85) is compared with results for the catalyst containing more barium (33-BKW-91) at the same temperature (750 °C), space velocity (1579 h^{-1}), and the same levels of methane (10 vol%) and oxygen (5 vol%) in the feed gas. The catalyst with the higher loading of barium is more active and selective than the catalyst with less barium on this support.

Table 26. $BaCO_3/TiO_2$ Catalysts with Different Types of Titania and Amounts of $BaCO_3$

Ref.	CH_4 C	Sel	Yield	O_2 C	=/-	$BaCO_3$	Type[a]	Time, h	GHSV	ECl
33-85	36.9	39.4	14.8	69	5.6	5	N	164	1579	200
33-91	44.3	44.6	19.9	73	8.6	17	N	249	1579	300
33-101	23.9	51.0	12.2	36	3.9	5	N	249	1579	300
33-114	34.7	56.4	19.3	52	6.4	17	J	148	1548	500
33-115	37.1	50.5	18.6	60	7.4	5	J	146	1548	500

a. N is Norton (0.6 m^2/g) and J is JM (0.82 m^2/g) titania (see Appendices D and E).

Table 26 also shows the highest yield obtained in reaction 33-BKW-85, which was 14%. The catalyst for this reaction was used again in reaction 33-BKW-101. Although higher levels of ethyl chloride were used, results for methane coupling were not significantly improved over those for reaction 33-BKW-85. Table 26 shows that the level of $BaCO_3$ alone does not correlate with methane conversion or selectivity to C_2's.

Catalyst Lifetimes

Methane coupling in reactions 32-BKW-62 and 32-BKW-63 was carried out under the same conditions, with the same catalysts ($BaCO_3/Al_2O_3$), except that the catalyst for reaction 32-BKW-62 was roasted in air at 850 °C whereas the other catalyst was not (see Appendix D). Although C_2 yields were similar, and the pattern of reactivity was the same for both reactions, initial lined-out selectivities with 10 ppm ethyl chloride were slightly lower and activities were slightly higher for the catalyst heated at 850 °C. For reaction 32-BKW-62, a C_2 yield of above 20% is observed at 775 °C and 2191 h^{-1} GHSV after 412 hours of methane coupling with this catalyst. For reaction 32-BKW-63, a C_2

yield of 19.7% and an ethylene to ethane product ratio of 2.9 is observed after 337 hours of methane coupling with this catalyst at 750 °C and 1304 h^{-1} GHSV. No comparable C_2 yields at reaction times this long were reported in the literature at the time this work was conducted.

Methane coupling was conducted in reaction 33-BKW-7 for over 400 hours. Table 27 below shows that at conditions identical to those used during the earlier portion of the reaction, results after 400 hours were almost the same as those immediately after activation (C_2 selectivity and C_2 yield were actually higher after 405 hours than they were at 13 or 96 hours). The temperature was 750 °C and the space velocity was 2133 h^{-1} for these examples. The catalyst was undergoing activation for the first 13 hours on-stream. Between 96 and 405 hours, the catalyst was tested at many methane to oxygen ratios, space velocities, and temperatures.

Table 27. Stability of a $BaCO_3/Al_2O_3$ Catalyst, 33-BKW-7

CH_4 C	Sel	Yield	=/-	CO_2/CO	Time, h	ECl
44.0	39.0	17.1	2.7	3.1	13	10
44.2	39.9	17.4	2.6	3.0	96	17
37.3	47.6	17.6	2.0	2.3	405	17

Figure 13 below shows that an intermediate level of ethyl chloride (7.5 ppm) was used in reaction 33-BKW-74, at 750 °C and 2233 h^{-1} GHSV. The C_2 yield remained between 16 and 18% for over 190 hours, at which time, the ethyl chloride level was adjusted to 4 ppm. The C_2 yield remained between 16 and 18% an additional 95 hours. Upon changing the space velocity to 1116 h^{-1}, the C_2 yield rose to above 19% and remained there for 70 hours, at which time a lowering of the space velocity coupled with an increase in the ethyl chloride level to 40 ppm resulted in a decrease in methane conversion and selectivity to C_2's. ICP analyses of fresh and used catalysts for this reaction showed 3.1% barium in each catalyst, indicating no loss of barium during the methane coupling reaction.

Figure 13. $BaCO_3/Al_2O_3$, 33-BKW-74

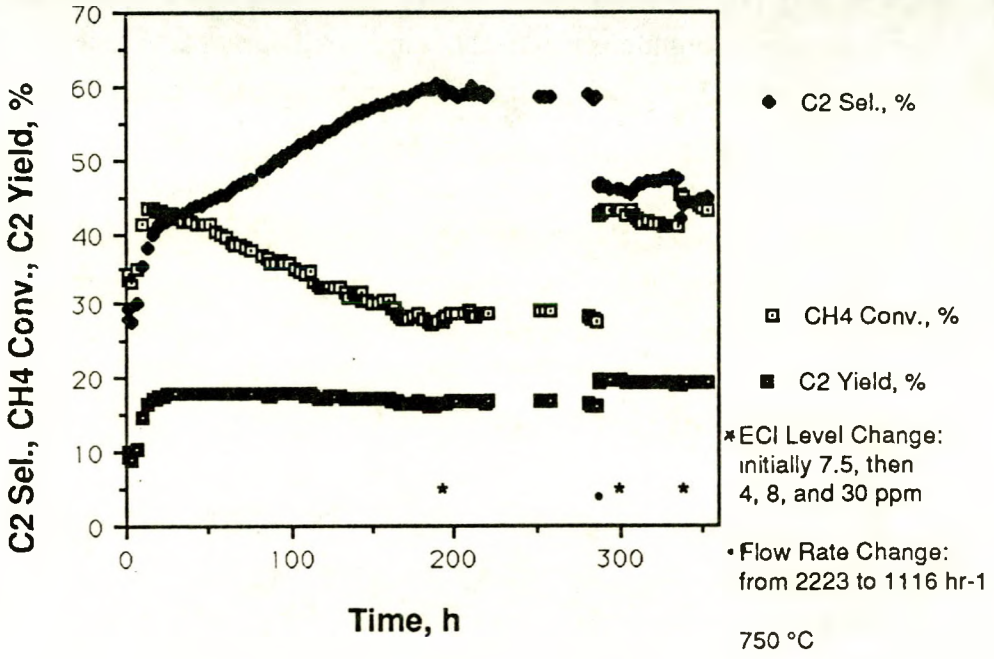
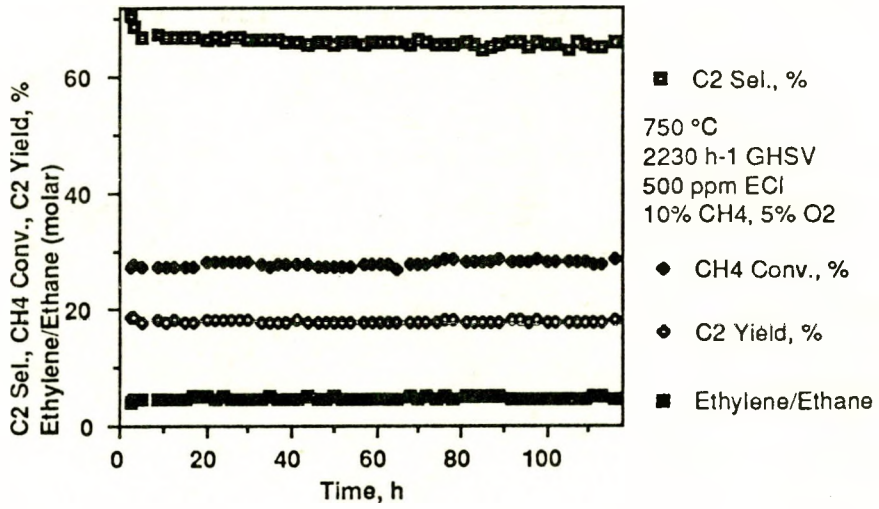


Figure 14 shows stable behavior in a Ba/TiO_2 catalyst, made from $Ba(OH)_2$.

Figure 14. Methane Coupling over a $Ba(OH)_2/TiO_2$ Catalyst, 36-BKW-29

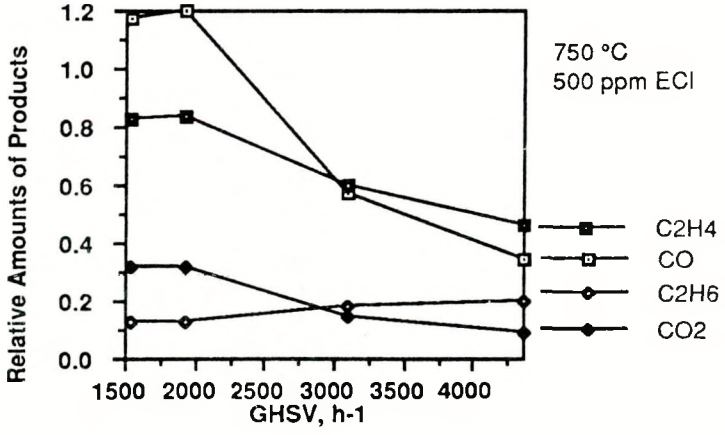


C_2 selectivity and methane conversion can be maintained for long periods of time over Ba and Sr catalysts. The optimum amount of a volatile chloride promoter must be used to obtain a stable rate to C_2's. This amount depends on the process conditions and the particular catalyst used. As described above, the amount depends on the type of metal oxide combustion promoter used. Catalyst stability is better, and higher C_2 selectivities and C_2 yields are obtained over long periods when catalysts are made with barium and strontium carbonates rather than the chlorides.

Space Velocity

Increases in space velocity at a given set of process conditions result in increased selectivity to C_2's, decreased methane conversion, decreased ethylene to ethane product ratios, and decreased C_2 yields. Figure 15 below shows that relative amounts of carbon monoxide, carbon dioxide, and ethylene are lower at higher space velocities (lower residence times). The drop in the relative amount of CO in the product is large compared with relative drops in amounts of other products. A slight increase in the relative amount of ethane is observed at the higher space velocities.

Figure 15. Space Velocity Changes with $BaCO_3/TiO_2$ Catalyst with 500 ppm Ethyl Chloride, 33-BKW-114

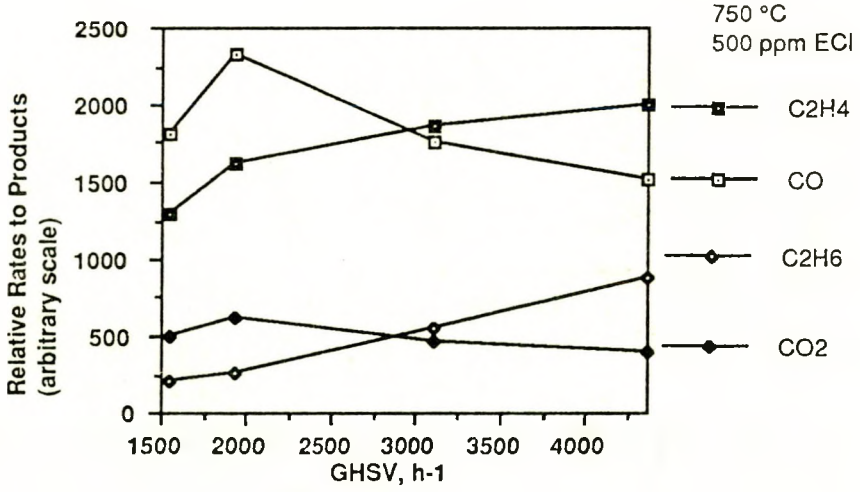


As the space velocity is lowered, the residence time is greater, so the conversion of primary to secondary products occurs to a larger extent, and gas phase reactions become

relatively more important (especially if chain branching reactions occur). Ethylene is a secondary product, and can be produced in the gas phase from ethane in the presence of radicals[56]. The amount of ethane is therefore relatively less at lower space velocities, and the amount of ethylene is relatively more. Carbon dioxide is also a secondary product from oxidation of ethane, ethylene, and carbon monoxide. Carbon dioxide is presumed to result mainly from reactions on surfaces (catalyst and quartz reactor packing and reactor walls). At low conversions, a significant amount of the carbon dioxide is presumed to result from catalytic oxidation of methyl radical. As space velocity is decreased, more carbon dioxide is observed. Carbon monoxide is a known product of gas phase combustion of methane.

In Figure 16, the relative amounts of products in the reaction outlet are multiplied by the space velocity, to give relative rates to products. The actual rates to ethylene and ethane increase as space velocity is raised, whereas the rates to CO and CO_2 decrease as the space velocity is raised (for the three higher space velocities). Results at the lowest space velocity are inconsistent with trends observed at the three higher space velocities in Figures 15 and 16, in that rates are lower than those of the next higher space velocity. Two of several possible explanations for this are diffusional or mass transfer problems at the lowest space velocity, or since the lowest space velocity was at the end of the time period for the data displayed, the lower rates could be due to catalyst deactivation (e.g., from non-optimum chloride levels - overchlorination).

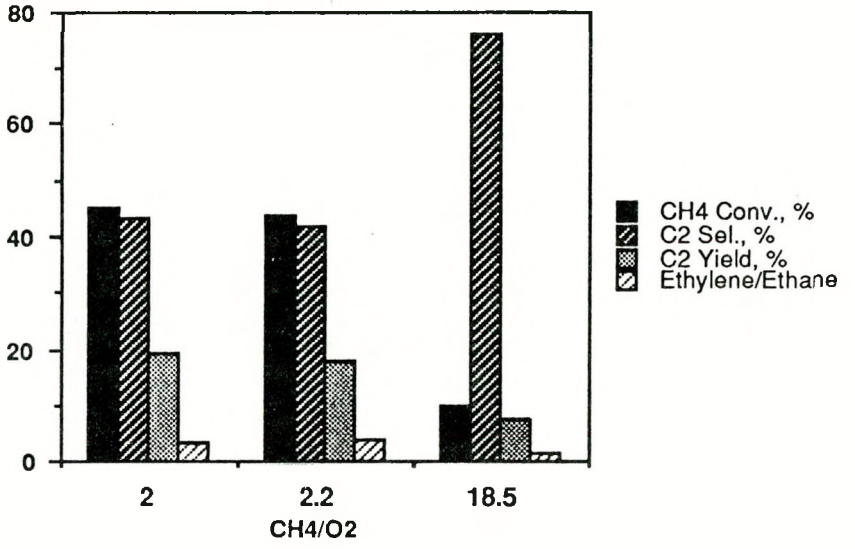
Figure 16. Space Velocity Changes with $BaCO_3/TiO_2$ Catalyst with 500 ppm Ethyl Chloride



Methane to Oxygen Ratios

Figure 17 shows that methane conversion, C_2 selectivity, C_2 yield, and the ethylene to ethane product ratio at 750 °C and 1667 h^{-1} GHSV are affected strongly by the methane to oxygen ratio in the feed gas, but only slightly by the concentrations of the feed gases at a given ratio, for the particular process conditions explored. The oxygen concentration was 5% for the methane to oxygen ratio of 2, 9% for the methane to oxygen ratio of 2.2, and 4.4% for the methane to oxygen ratio of 18.5 in Figure 17.

Figure 17. $BaCO_3/Al_2O_3$, 33-BKW-7



With a catalyst of 5% barium carbonate on Norton titania (33-BKW-85, 750 °C, 1589 h^{-1} GHSV, 200 ppm ECl), a change in the volume percentages of methane and oxygen fed from 80 and 10%, respectively, to 10 and 5%, respectively, resulted in a drop in C_2 selectivity from 48 to 39%. The expected rise in methane conversion (from 12 to 36%) was observed and resulted in a significant increase in the C_2 yield (from 6 to 14%). The ethylene to ethane product ratio rose from 2.1 to 5.4%.

Reactions 34-BKW-59 ($SrCO_3/Al_2O_3$ catalyst), 34-BKW-61 ($BaCO_3/Al_2O_3$ catalyst), and 34-BKW-63 ($BaCO_3/Al_2O_3$ catalyst) were run with 80% methane and 8% oxygen, which were conditions found to be favored in economic analyses of methane coupling processes (largely due to higher selectivities presumed to result from higher methane to oxygen feed gas ratios). Selectivities were not that much higher than have

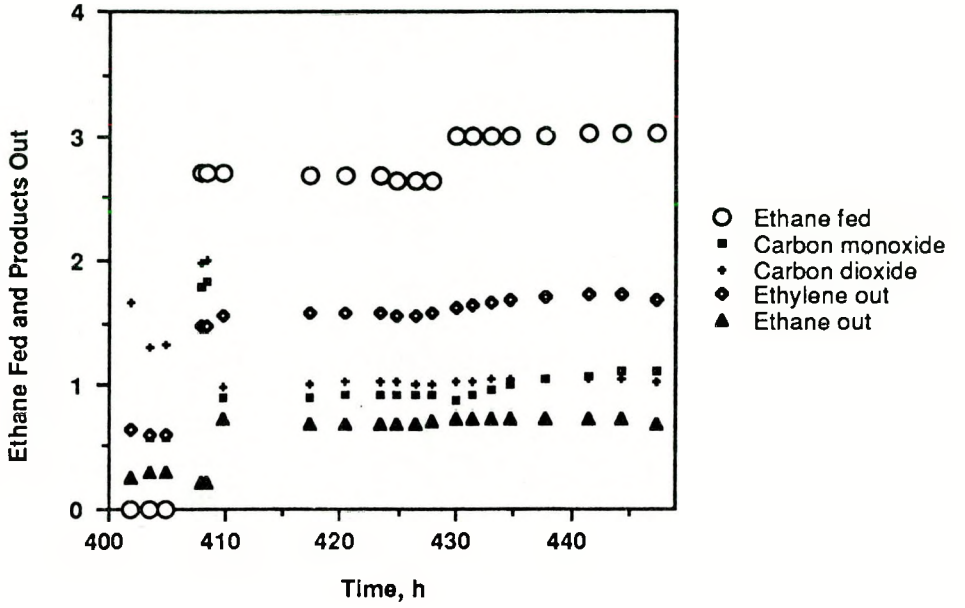
been observed for reactions with 10% methane and 5% oxygen in the feed gas (typical reaction conditions). The space velocities and concentrations of ethyl chloride in the feed gas were not optimized for these process conditions and catalysts. The amount of ethyl chloride could have been far from the optimum amount, resulting in selectivities and activities below those possible. Selectivities were lower for the Sr catalyst than for the Ba catalysts. No significant catalyst deactivation was observed for 70 hours on stream (after which, several process variable changes were made). The highest C_2 yield was 11.1% (reaction 34-BKW-61, 68% C_2 selectivity and 16.5% methane conversion). This was a transient result after an increase in space velocity, suggesting that the ethyl chloride level is not optimized.

Five grams of catalyst were used in reaction 34-BKW-63, whereas 2.5 g of the same catalyst were used in reaction 34-BKW-61. At 750 °C and 2820 h^{-1} GHSV, with the same feed gas, results for the two reactions were similar (8% C_2 yield, 63-66% C_2 selectivity, 13% methane conversion).

Added Ethane

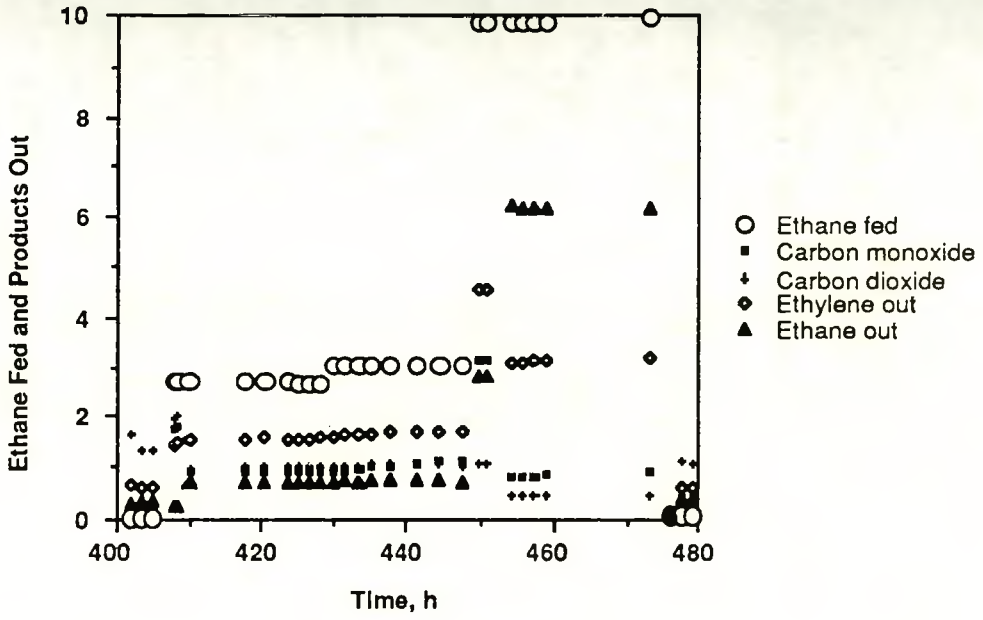
After the time period displayed in Figure 13 (page 56 above) for reaction 33-BKW-7, ethane was tested as a feed component in the methane coupling reaction. It is likely that some ethane would be recycled in a methane coupling process, since it is a major product of methane coupling. Therefore, different levels of ethane were added to a methane coupling reaction. Results are displayed below in Figures 18 and 19.

Figure 18. Added Ethane, $BaCO_3/Al_2O_3$, 33-BKW-7



When ethane is added at the level of 2.7%, the amount of ethane leaving the reactor is less than that added to the reactor. The ethylene amount is higher than without added ethane, as are the amounts of carbon dioxide and carbon monoxide. At a higher level of added ethane, the carbon dioxide to carbon monoxide ratio drops due to an increase in the rate to CO, so that more CO is produced than is CO_2. Figure 19 shows that when 10% ethane is fed, 3% ethylene is produced in the product mixture. CO and CO_2 are produced to a smaller extent. Since much of the ethane would burn if it were recycled, most of the ethane should be removed from a methane oxidation recycle.

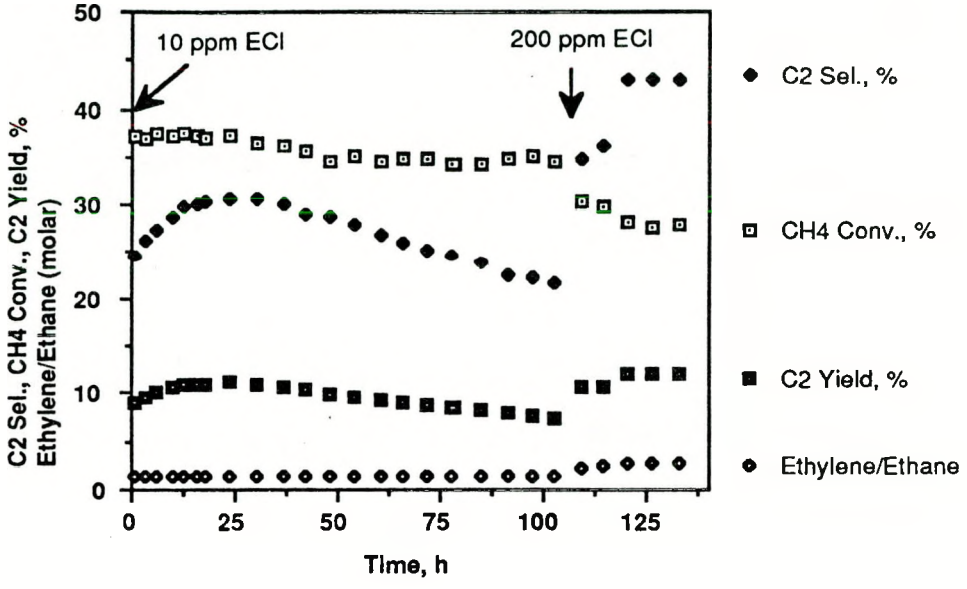
Figure 19. Added Ethane, $BaCO_3/Al_2O_3$, 33-BKW-7



Higher Ethyl Chloride Levels

Initial ethylene to ethane product ratios of 4 ($BaCl_2/ZrO_2$, 30-BKW-86) and 15 ($CaCl_2/ZrO_2$, 31-BKW-21) could be obtained at 750 °C and space velocities of 1000-1200 h^{-1} with alkaline earth/ZrO_2 catalysts. Ethyl chloride levels of greater than 50 ppm were not used to test these catalysts. Although chloride catalysts showed initially high ethylene to ethane product ratios, catalysts prepared from both alkaline earth carbonates and alkaline earth chlorides on the same support, showed similar ethylene to ethane product ratios after they had been run until performance stabilized. Catalysts prepared from carbonates generally exhibited higher lined-out activities, under similar conditions. A $BaCO_3/ZrO_2$ catalyst was tested with 10 and 200 ppm ethyl chloride at 750 °C and 5053 h^{-1} GHSV. Ethylene to ethane product ratios over 3 were not observed. After over 120 hours of reaction (over 30 hours with 200 ppm ethyl chloride), the C_2 yield was 12% with a C_2 selectivity of 42%. Figure 20 shows that the C_2 selectivity and C_2 yield are relatively stable with 200 ppm ethyl chloride in the feed gas.

Figure 20. $BaCO_3/ZrO_2$, 32-BKW-128



It was thought that the ethyl chloride levels might not have been high enough to sustain good C_2 selectivities and activities. Barium carbonate/metal oxide catalysts were made on a variety of supports which were relatively acidic, compared with Norton 5451 alpha-alumina. The same amount of barium was put on each support (by weight). These were tested for methane oxidation under standard conditions of 750 °C, 2000-2500 h^{-1} space velocity, with 10% methane, 5% oxygen, and balance nitrogen in the feed gas, at about 11 psig pressure in quartz reactors. In each case, the catalyst was run for 20-100 hours with 10 ppm ethyl chloride, the for over 20 hours with 50 ppm ethyl chloride in the feed gas, then finally for at least 50 hours with 500 ppm ethyl chloride in the feed gas.

Supports used included Norton aluminas 5502, 8855002, and 8855003, ZrO_2, and Ga_2O_3. The surface areas and acidities of these supports are shown in Table 28.

Table 28. Surface Areas and Acidities of Metal Oxides*

Metal Oxide	Surface Area, m^2/g	Acidity, μm/g	Acidity, $\mu m/m^2$
Norton 5502	0.75	1.2	1.6
ZrO_2	0.95	1.45	1.53
Ga_2O_3	4.22	3.76	0.89
Norton 8855002	0.485*		
Norton 8855003	1.047*		

* All numbers were measured, except for the two marked with a star, which were numbers supplied by Norton.

With all of these catalysts, the C_2 yield and the selectivity to C_2's were higher with 500 ppm ethyl chloride in the feed gas. Figures 21 and 22 show that the C_2 selectivity and C_2 yield were higher for the catalyst with the lower amount of barium carbonate on zirconia.

Figure 21. 15% $BaCO_3/ZrO_2$, 36-BKW-12

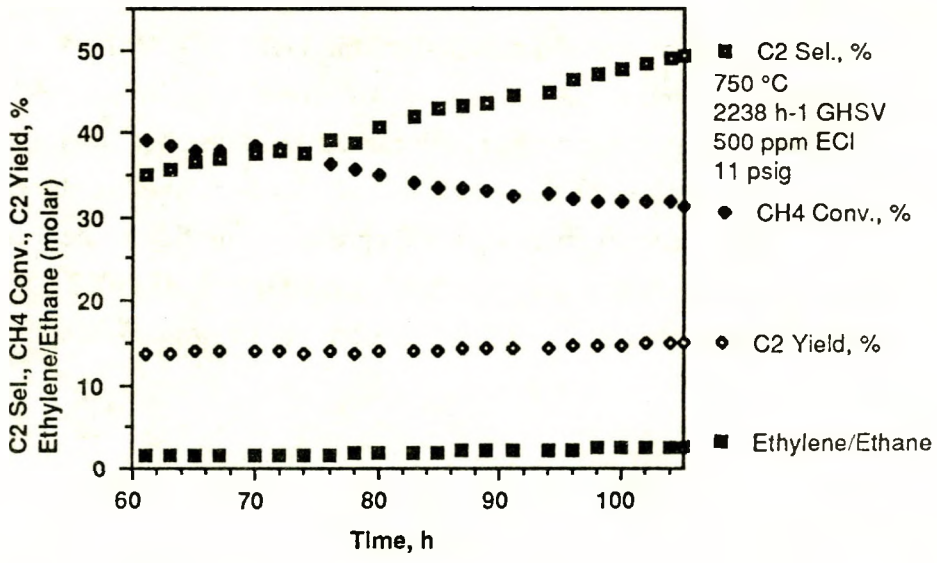
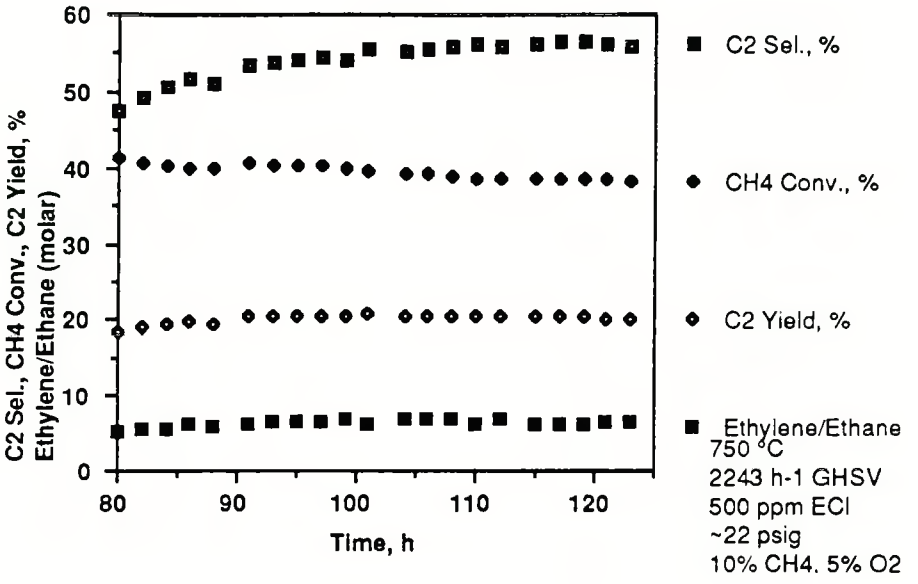
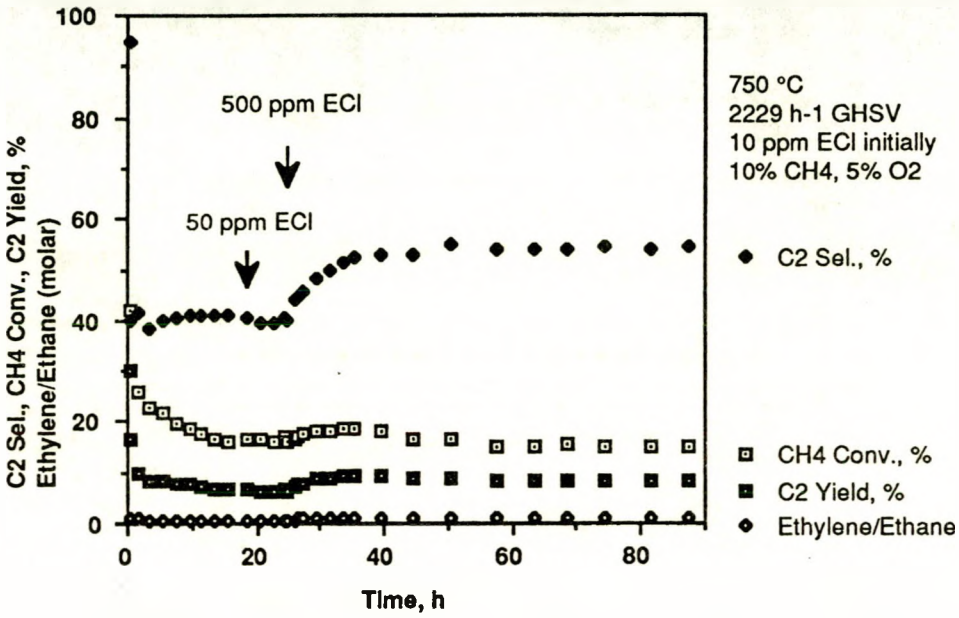


Figure 22. 5% $BaCO_3/ZrO_2$, 36-BKW-13



Results from the higher loading of barium carbonate are closer to results from unsupported barium oxide with similar reaction conditions, shown in Figure 23.

Figure 23. BaO Catalyst for Methane Coupling, 36-BKW-46



Of particular interest is the fact that the ethylene to ethane product ratio is low using the catalyst with a high loading of $BaCO_3$ (like unsupported $BaCO_3$, Figure 8 on page 46, and BaO, Figure 21 above), whereas the ethylene to ethane product ratio is higher for the catalyst with less $BaCO_3$. This is consistent with the proposal that the support is involved in producing chlorine radicals from ethyl chloride, which are then released into the gas phase where they initiate chain reactions.

Two levels of barium were also used on Norton 5502 alumina. Methane coupling results were not outstanding. C_2 yields of 10-15% were obtained with 50 ppm ethyl chloride in the feed gas with the catalyst containing 25% barium carbonate. Upon raising the ethyl chloride level to 500 ppm, the C_2 yield rapidly dropped. C_2 yields of 10-15% were not obtained until 500 ppm ethyl chloride was used with the catalyst prepared with only 5% barium carbonate. Selectivities to C_2's were then above 65%. Using 500 ppm ethyl chloride with Ga_2O_3 as support, C_2 yields were not over 13%, with selectivity to C_2's below 50%.

Other Supports

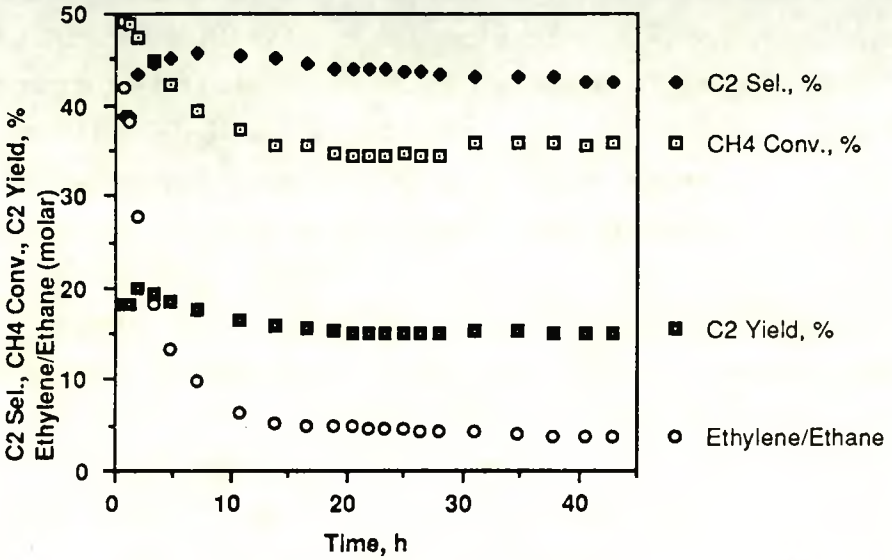
Methane coupling catalysts were prepared using other supports, including calcium aluminate (32-BKW-28), magnesium aluminate (32-BKW-105), and silica (32-BKW-110 and 111). Catalysts for reactions using these catalysts, except for reaction 32-BKW-111, contained barium chloride. The catalyst for reaction 32-BKW-111 contained barium carbonate. C_2 selectivities and C_2 yields were lower for catalysts on these supports than for those on α-aluminas, Ga_2O_3, TiO_2, and ZrO_2. Ethylene to ethane product ratios were highest for the $BaCl_2/CaAl_2O_4$ catalyst (13.1% C_2 yield, 32.5% C_2 selectivity, at 800 °C and 4000 h^{-1} GHSV with 500 ppm ECl in the feed gas). The initial C_2 yield (after 30 minutes of reaction) for reaction 32-BKW-110 ($BaCl_2/SiO_2$) was 11.3%, with a C_2 selectivity of 27%. The selectivity dropped to 6% and the C_2 yield dropped to 1.7% after 5.5 hours on-stream. It was thought that yields might be higher if higher levels of ethyl chloride were added to the feed gas, since a $BaCO_3/TiO_2$ catalyst exhibited C_2 yields of 18-22% with 250 and 500 ppm ethyl chloride. The used catalyst from reaction 32-BKW-110 was retested with 200 ppm ethyl chloride in the feed gas. A selectivity to C_2's of over 14% was not observed, and although the initial C_2 yield was 5%, it dropped to 0.5% after 90 hours of reaction (750 °C, 2217 h^{-1} GHSV).

Gamma-alumina was also used as support in the preparation of one catalyst. Barium carbonate, rather than barium chloride was used. At 650 °C and a space velocity of 6000 h^{-1}, carbon dioxide and carbon monoxide were the only significant products observed. Levels of both 10 and 200 ppm ethyl chloride were used in the feed gas.

Non-Chloride Halides

Methane coupling was studied with bromide or fluoride, rather than chloride as catalyst component and/or volatile halide additive. Figure 24 shows the results of methane oxidation with a $BaBr_2/Al_2O_3$ catalyst at 750 °C and a space velocity of 2087 h^{-1}. The first two data points on Figure 24 were with a space velocity of 1043 h^{-1} where the reaction was oxygen limited.

Figure 24. $BaBr_2$/5451 α-Al_2O_3, 32-BKW-122



The C_2 yield and C_2 selectivity line out to fairly constant values, where they remain for over 30 hours. For the $BaBr_2/Al_2O_3$ catalyst, the initial ethylene to ethane product ratios are among the highest observed. The lined-out ethylene to ethane product ratios for the space velocity and temperature used are higher than those typically observed for barium catalysts on Norton 5451 α-alumina support, with or without added volatile chloride (e.g., 32-BKW-63).

The maximum C_2 selectivity observed was 23% and the maximum C_2 yield observed was 8.5% for a BaF_2/Al_2O_3 catalyst at 750 °C and 1067 h^{-1} GHSV (either 0 or 10 ppm ethyl chloride), indicating that alkaline earth fluoride catalysts are inferior to chloride and bromide catalysts for methane coupling.

Ethyl bromide (EBr) was used in the feed gas in reactions 32-BKW-66, ($BaCl_2/Al_2O_3$ catalyst) and 32-BKW-67 ($BaCO_3/Al_2O_3$ catalyst). Both catalysts were tested at 750 °C with space velocities of slightly over 2000 h^{-1}. Results are shown in Figures 25 and 26.

Figure 25. $BaCl_2/Al_2O_3$, 33-BKW-66

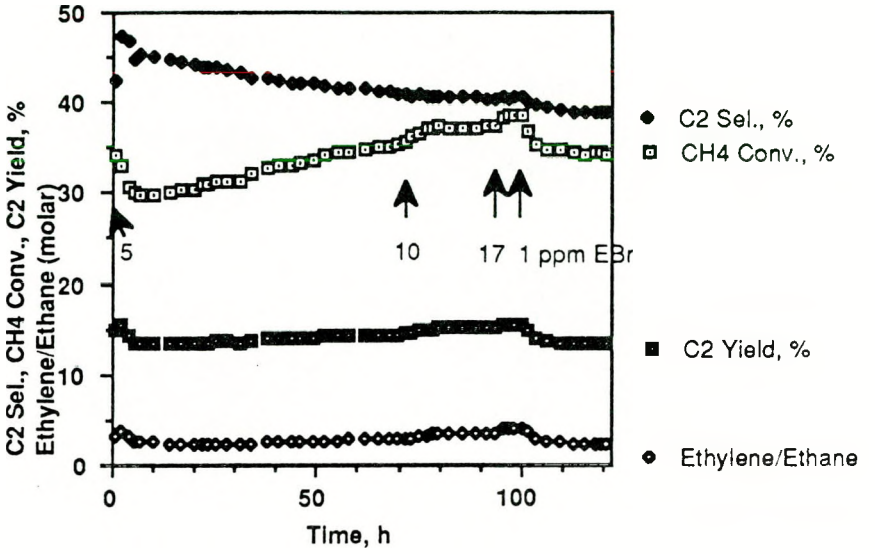
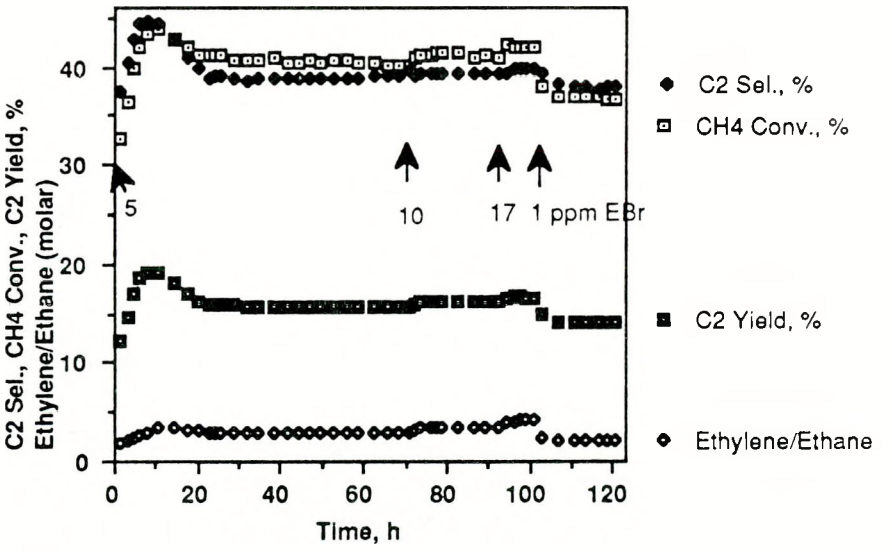


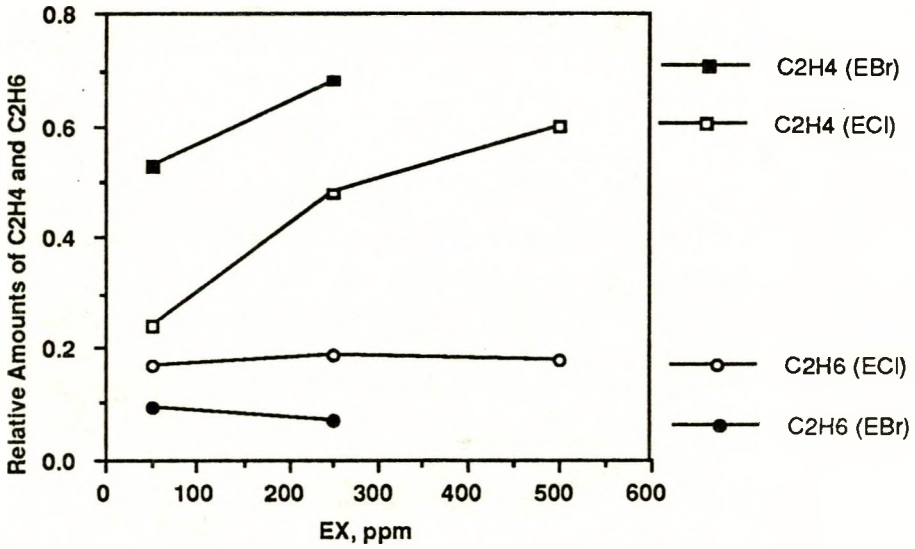
Figure 26. $BaCO_3/Al_2O_3$, 33-BKW-67



Four different low levels of ethyl bromide were used, and catalyst performance did not change much when the ethyl bromide level was changed. The carbonate catalyst was observed to undergo a period of activation. The highest C_2 selectivity, C_2 yield, methane conversion, and ethylene to ethane product ratio were observed after 10 hours of reaction. The performance of both catalysts then lined out with similar C_2 selectivities, C_2 yields, methane conversions, and ethylene to ethane product ratios.

Figure 27 shows the relative rates to ethylene and ethane for different concentrations of ethyl chloride and ethyl bromide in the feed gas for reaction

Figure 27. Rates to Ethylene and Ethane with Different Ethyl Bromide and Ethyl Chloride Levels, 33-BKW-114



33-BKW-114. Figure 28 shows the relative rates to carbon monoxide and carbon dioxide for different concentrations of ethyl halide (EX, X=Br or Cl) in the feed gas for this reaction.

Figure 28. Rates to Carbon Monoxide and Carbon Dioxide with Different Ethyl Bromide and Ethyl Chloride Levels, 33-BKW-114

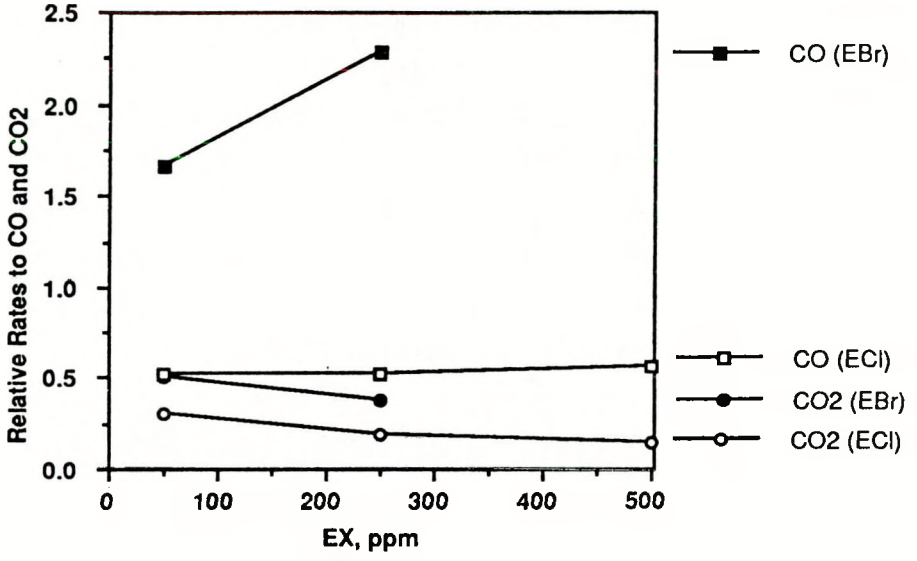


Figure 27 shows that the relative rates to ethylene increase as the amount of ethyl halide (EX) is increased. If one exceeds the optimum level of ECl for a particular catalyst under a particular set of process conditions, rates to all products decrease, as is shown in Figure 10 on page 51. Figure 28 shows that the amount of carbon monoxide increases when the ethyl halide level is raised, but the increase with ethyl chloride is slight compared to that with ethyl bromide.

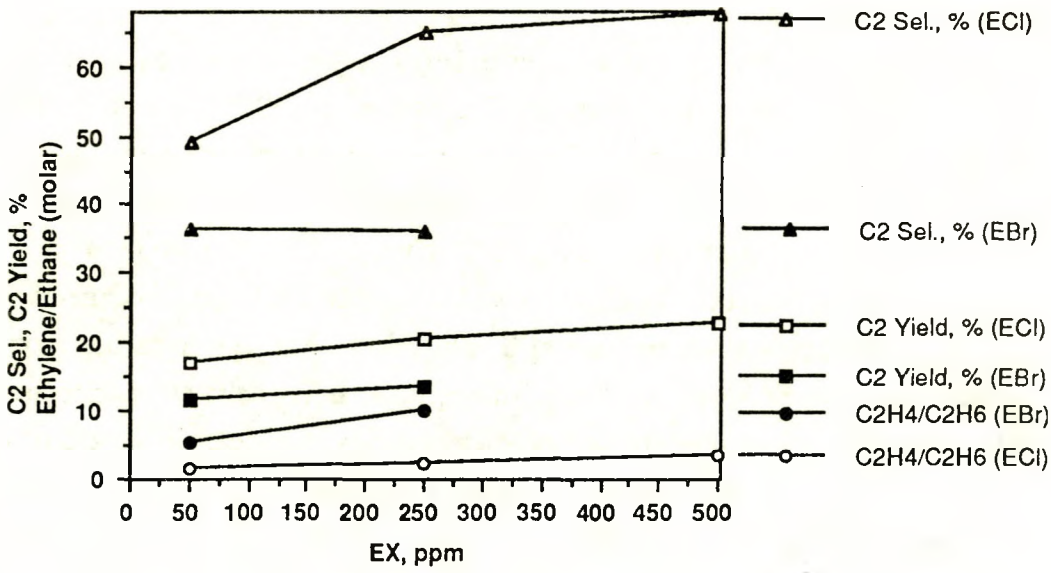
Under similar conditions, the rates to ethylene and carbon monoxide are higher with ethyl bromide than with ethyl chloride. The rates to total C_2's (the sum of ethane and ethylene) are also higher under a given set of reaction conditions with ethyl bromide rather than ethyl chloride in the feed gas (see Figure 27). Ethylene is considered to result primarily from gas phase conversion of ethane to ethylene. Carbon monoxide is considered to be primarily from gas phase (non-catalytic) oxidation of methane or other gas phase products and intermediates. The higher rates to C_2's, to carbon monoxide, and to ethylene in the presence of ethyl bromide (higher ethylene to ethane product ratios) are consistent with the presence of higher concentrations of radicals in the gas phase when ethyl bromide is present. Since the C-Br bond is weaker than the C-Cl bond, it is possible that ethyl bromide reacts with the catalyst to release bromine radicals into the gas phase at a more rapid rate (in higher concentration), or that homolytic dissociation of the C-Br

bond occurs to a significant degree without catalysis. These bromine radicals then initiate chain reactions which convert ethane to ethylene and methane to carbon monoxide, among other things.

A higher concentration of radicals in the gas phase would also be expected to result in higher rates of methane conversion, higher rates of product oxidation, and lower selectivities (from faster oxidation of the higher concentrations of products). Figure 29 below shows that the selectivity is higher under similar conditions with ethyl chloride rather than ethyl bromide in the feed gas [mainly from the exceptionally high rate to carbon monoxide in the presence of ethyl bromide (Figure 28 above)]. The C_2 yields are also higher with ethyl chloride (due to the higher selectivity), even though the actual rates to ethylene are higher with ethyl bromide (Figure 27 above).

With a $BaCO_3/TiO_2$ catalyst, ethylene to ethane product ratios as high as 25 (32% selectivity to C_2's, 51% methane conversion, 16.5% yield to C_2's) were observed (33-BKW-91). Ethylene to ethane product ratios were four times higher with ethyl bromide than with ethyl chloride (10 vs. 2.6 at 250 ppm and 5.7 vs. 1.4 at 50 ppm) with other conditions the same on a $BaCO_3/TiO_2$ catalyst (33-BKW-114). Selectivities to C_2's were lower with bromide (36% vs. 65%).

Figure 29. Effect of Ethyl Halide Levels on C_2 Selectivity, C_2 Yield, and Ethylene to Ethane 33-BKW-114



Role of Halide

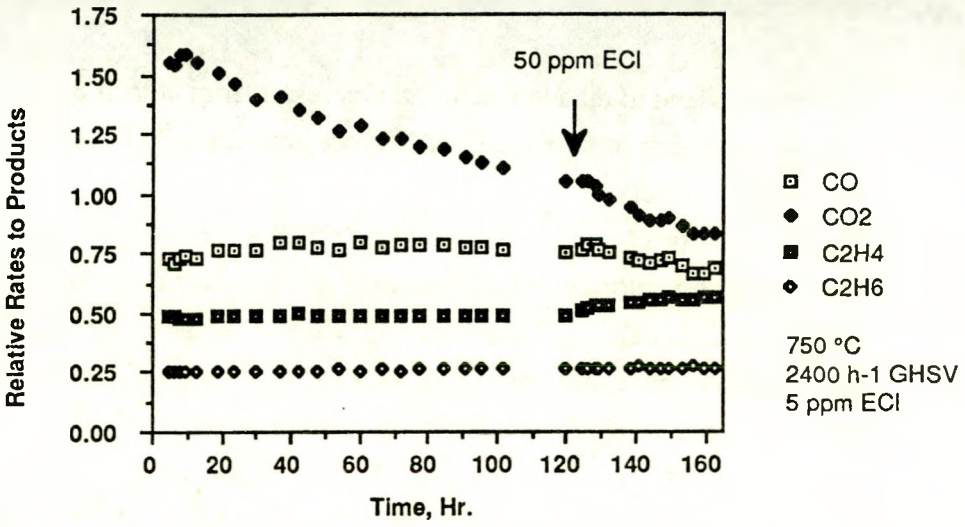
The following three roles for chloride are proposed for alkaline earth (or alkali) metal oxide/halide catalysts:

1. Higher ethylene to ethane product ratios result from chlorine radicals in the gas phase, which initiate reactions. These are proposed to be produced on the catalyst surface.
2. Higher activities (compared with no chloride) are consistent with the conversion by chloride of stable salts of alkaline earth metals, e.g., aluminates, titanates, or carbonates, into active oxygen species.
3. Higher selectivities are consistent with a slow catalyst change in which the chloride blocks CO_2 formation on the surface of the catalyst.

Different amounts of chloride were explored for $SrCO_3/Al_2O_3$ (34-BKW-18) and $SrCl_2/Al_2O_3$ (34-BKW-19) catalysts. It appears that 500 ppm ethyl chloride may not be too much for the Ba/TiO_2 catalysts tested (31-BKW-46 and 32-BKW-80), but a level of 500 ppm ethyl chloride was too much for the $SrCO_3/Al_2O_3$ catalyst, and even 50 ppm was too much for the $SrCl_2/Al_2O_3$ catalyst.

The relative rates to products for the first part of reaction 34-BKW-18 are shown in Figure 30 below.

Figure 30. $SrCO_3/Al_2O_3$ Catalyst



Three roles of chloride were described above.

1. When ethyl chloride is added in the feed gas to a barium catalyst, the rate to C_2's rises to a constant level slowly. Removal of ethyl chloride results in a rapid loss in rate to C_2's. The selectivity and activity increases are proposed to result from the halide on the catalyst reacting with and breaking up stable carbonates or other salts (aluminates, titanates, etc.) to allow the formation of active oxygen species on barium which can abstract hydrogen from methane to lead to C_2's. This is a slow change for a deactivated catalyst. Figure 30 shows that the strontium carbonate catalyst does not show the same initial increase in the rate of C_2 production in the presence of halide as did a similar barium catalyst (33-BKW-74, Figure 13 on page 56). This is consistent with the proposition that under similar reaction conditions, the strontium catalysts would have a lower requirement for chloride to catalyze decomposition of stable salts compared with barium catalysts. Strontium carbonate is less stable than barium carbonate[55], so this is reasonable.

2. With barium carbonate catalysts in the presence of ethyl chloride in the feed gas, the rate to carbon dioxide decreases slowly with addition of ethyl chloride

and increases by removal of ethyl chloride. The chloride is also proposed to react with and destroy surface catalyst species which oxidize C_2's or methyl radicals to carbon dioxide. Figure 30 shows that with the strontium carbonate catalyst, using 5 and 50 ppm ethyl chloride, the rate of carbon dioxide formation drops during a period of greater than 100 hours.

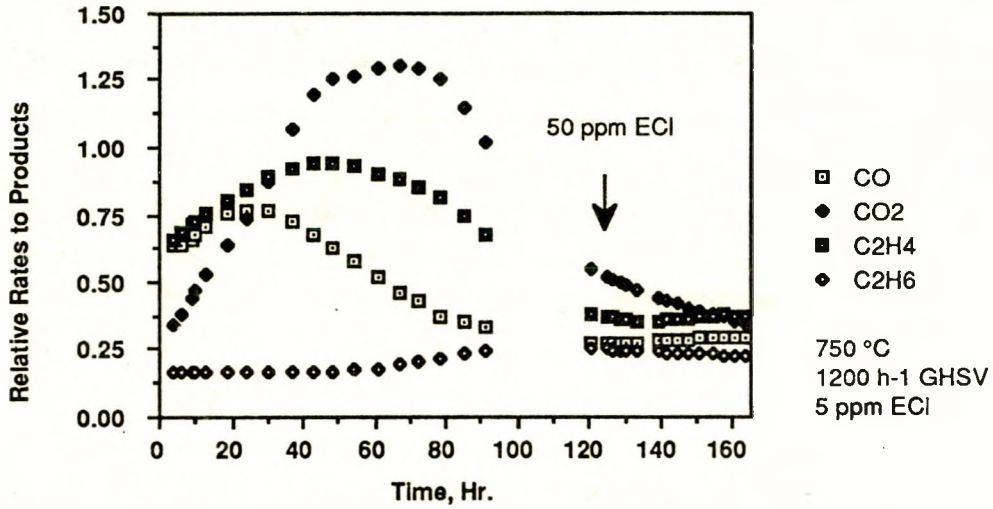
3. Increases in the ethylene to ethane product ratio from addition of ethyl chloride in the gas feed are consistent with gas phase, free radical reactions involving halide radicals produced on the catalyst surface and released into the gas phase, where free radical chain reactions occur. The changes in ethylene to ethane product ratios are fast when the level of ethyl chloride is changed, which would be expected from a gas phase reaction. Carbon monoxide is known to result from gas phase methane oxidation, and process changes on many alkaline earth/metal oxide catalysts which result in increased rates to CO generally result in higher ethylene to ethane product ratios. Ethane is known to be converted in the gas phase to ethylene in the presence of halides[56]. Figure 30 shows little change in the ethylene to ethane product ratio with an increase from 5 to 50 ppm ethyl chloride on the strontium carbonate/alpha-alumina catalyst, but little change is expected at these low levels of chloride on a relatively non-acidic alumina support.

Although catalysts containing strontium may not require chloride to form the active sites (since an initial increase in the rate of C_2 production was not observed for a catalyst with Sr, see 1. above), chloride is still required to lower the rate of carbon dioxide production to obtain good selectivities to C_2's. It is also required to produce high ethylene to ethane product ratios on supports where this is favored, e.g., titania.

Figure 31 shows the relative rates to products for the first part of a methane coupling reaction sequence over a $SrCl_2/Al_2O_3$ catalyst (34-BKW-19) under the same conditions (at the same time) as were used for the $SrCO_3/Al_2O_3$ catalyst in reaction 33-BKW-18 (Figure 30 above), except that the space velocity for the reaction over the chloride catalyst was one-half of that used for the reaction over the carbonate catalyst, in order to compare results under similar methane conversions (since the chloride catalyst is less active). The same amounts of catalyst were used, with the same Sr loading. Results for the catalyst made with chloride differed significantly from those of the catalyst made with carbonate. Rates to CO, CO_2, and ethylene rise and pass through maxima (at about

25, 60, and 45 hours, respectively), whereas the rate to ethane is fairly constant for about 40 hours, then rises only slightly for the next 25 hours.

Figure 31. $SrCl_2/Al_2O_3$ Catalyst



The methane conversion goes through a maximum at a reaction time of about 60 hours on-stream. This catalyst initially contains a large amount of chloride. An explanation consistent with the observed results is that catalyst surface changes occur slowly over a period of hours. These surface changes lead to increased methane conversion through formation of additional sites, perhaps by dispersion of alkaline earth metal, and to an increase in the rate of release of chlorine radicals from the catalyst surface. These chlorine radicals then initiate free radical chain reactions, resulting in higher rates to CO and higher rates of conversion of ethane to ethylene in the gas phase. The rate of release of chlorine radicals and the concentration of radicals in the gas phase are proposed to go through maxima. If, as described above under 2., the reaction of chloride with the catalyst surface results in slow catalyst changes, poisoning sites which convert methane, products, and intermediates to carbon dioxide (see discussion above), then loss of chloride from the catalyst should result in an increase in these sites and an increase in the rate to carbon dioxide. This is observed initially with reaction 34-BKW-19 (Figure 31 above).

The increase in sites which can oxidize methane, products, and intermediates to carbon dioxide on the catalyst surface can result in decreases in observed rates to CO and C_2's, because these are further oxidized as they are produced. When the concentration of

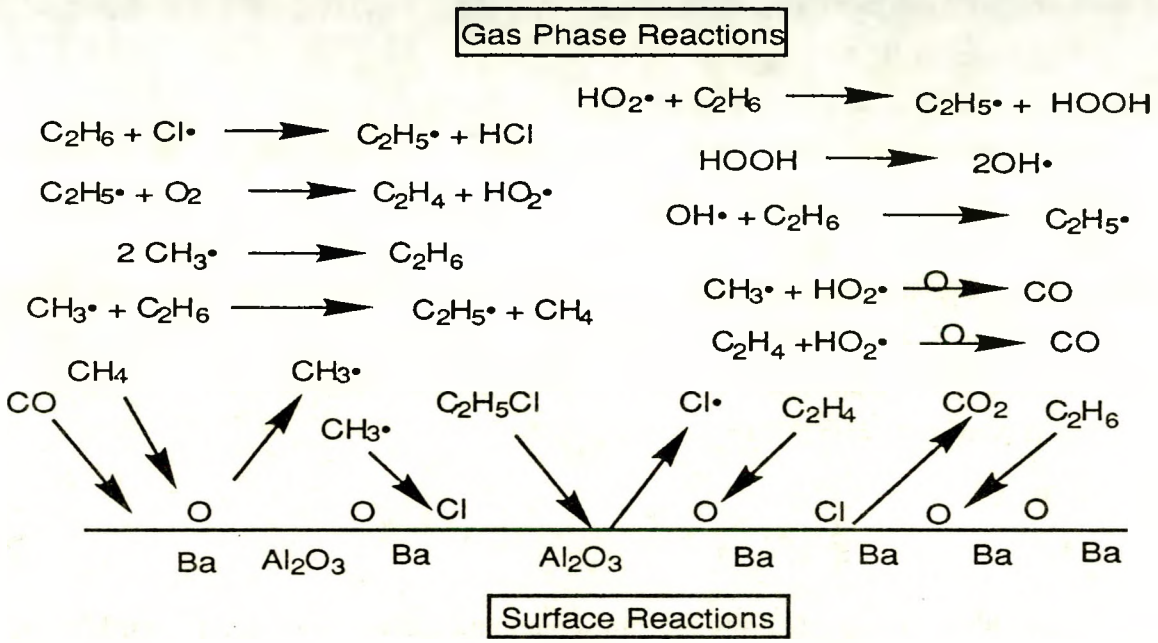
chloride on the catalyst is reduced to a level where the rate of release of chlorine radicals into the gas phase is lower, the rate of conversion of ethane to ethylene should be lower, resulting in lower ethylene to ethane product ratios. This is observed in Figure 31, where the rate to ethane after 60 hours increases, while the rate to ethylene and the overall rate to all other products decreases.

Similar maxima are not normally observed for reactions of barium chloride on alumina. This could reflect differences in the rates of transformations of alkaline earth compounds on the catalyst surface to form a steady state of metal dispersion and steady states of the concentrations of various anions. In the case of the catalysts containing barium, the maximum rate of release of chlorine radicals from the catalyst surface could be at or soon after the start of reactions. Indeed, the highest ethylene to ethane product ratios from $BaCl_2$/metal oxide catalysts is often observed at the start of the reaction, which is consistent with this explanation.

Vapor-Phase, Catalyst-Derived Free Radicals

Gas phase reactions during methane coupling reactions with alkaline earth/metal oxide catalysts appear to be altered by presence of chloride in the starting catalyst or by addition of ethyl chloride (or other sources of volatile chloride) to the catalyzed methane coupling reactions. Higher ethylene to ethane product ratios were observed in product compositions of methane coupling reactions which used alkaline earth/non-basic metal oxide supports, in the presence of chloride. This observation is consistent with the production of chlorine radicals on the catalyst surface which are released into the gas phase, with the conversion of ethane to ethylene in the gas phase, catalyzed by the chlorine radicals in the gas phase. Figure 32 below illustrates this and shows selected key gas phase and surface reactions. The conversion of ethane to ethylene in the gas phase catalyzed by chloride is a known reaction[56].

Figure 32. Role of Surface Generated Chlorine Radicals in Conversion of Ethane to Ethylene



The addition of volatile chloride to gas phase methane oxidation reactions results in only small changes in methane conversion without catalysts, indicating that methane oxidation in the gas phase under reaction conditions used for catalyzed reactions is not affected to a large extent by ethyl chloride in the gas phase in the absence of catalysts. Reactions 33-BKW-130 and 33-BKW-131 showed that in the reactor most commonly used (Reactor D), under typical conditions of 10% methane and 5% oxygen at 750 °C with flow rates of 80 or 160 ccm (typically used with 5 g of catalyst to give space velocities of 1000-3000 h^{-1}), methane conversions of over 5% are not observed with levels of ethyl chloride of from 0 to 150 ppm. Reaction 33-BKW-130 has a void space of 4.5 cc (between quartz chips) in the hottest part of the oven. Reactor 33-BKW-131 has quartz chips throughout the reactor (without any additional void spaces other than those present from the spaces among the quartz chips).

The concept of production of radicals on the catalyst surface and release of these into the gas phase was shown by Lunsford and coworkers[16-19] (through the trapping of methyl radicals released from catalyst surfaces and the correlation of the rates of methyl radical production with rates of C_2 formation) to be important in the catalyzed oxidation of methane to ethane. Radicals of hydrocarbon fragments higher than methane have

additional pathways of reaction available to them other than coupling (e.g., alkene formation through loss of a hydrogen atom), so they do not have lifetimes comparable to methyl radicals. They therefore cannot be detected by the esr methods employed by Lunsford and coworkers.

Since higher hydrocarbon radicals could not be directly detected, H. H. Kung[57] developed an indirect method to indicate the presence of enhancement of gas phase reactions due to the presence of free radicals produced on catalyst surfaces and released into the gas phase. He applied this method to the oxidation of butane. This method to detect radical enhancement of gas phase reactions from release of radicals produced on catalysts into the gas phase was applied to determine if radical enhancement of gas phase reactions could be observed during methane oxidation over $BaCO_3/Al_2O_3$ catalysts in the presence and absence of added chloride.

Two reactions were run simultaneously in two reactors with the same amount of the same $BaCO_3/\alpha$-Al_2O_3 catalyst, already activated in a previous experiment (32-BKW-63). In one case (34-BKW-1), the catalyst was placed after a 2.5 cc void space in the reactor. In the other case (34-BKW-2), the catalyst was placed before the 2.5 cc void space in the reactor.

Reactions 33-BKW-130 and 131 (Table 29) show us that methane conversion in the void space before the catalyst in reaction 34-BKW-2 will be negligible, so differences in catalyst activity and selectivity to products between reactions 34-BKW-1 and 2 are due to the void space after the catalyst. The same reactions occur to the same extent in the catalysts in both reactions, but in the case with the void volume after the catalyst, gas phase reactions of methane, products, and intermediates may occur to a greater extent after the catalyst bed.

Thus, differences in the reactions are due to increased contributions of gas phase reactions in reaction 33-BKW-2, from oxidation of products or from reactions of radicals produced on the catalyst and released into the gas phase. These radicals may cause chain reactions. If one sees an increase in the rate to a product in reaction 33-BKW-2 compared with reaction 33-BKW-1, it is likely that this is due to a gas phase reaction.

The following reactions (Figure 33) may occur (without consideration of relative rates of reaction, or whether these reactions occur on the catalyst surface, in the gas phase, or both):

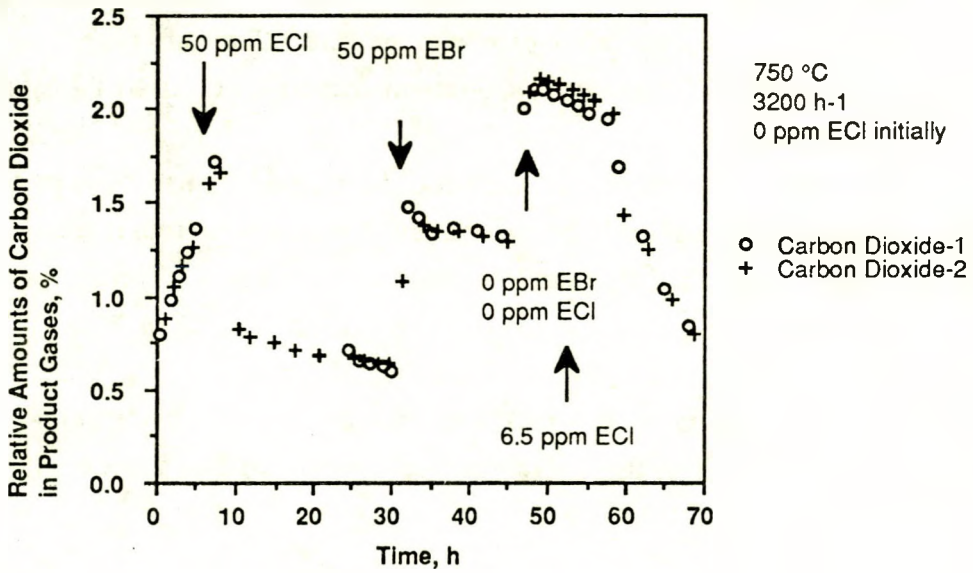
Figure 33. Some Reaction Steps Leading to Products during Methane Oxidation

CH_4	⟶	$CH_3\bullet$	(1)
$2CH_3\bullet$	⟶	C_2H_6	(2)
CH_4	⟶	CO	(3)
CH_4	⟶	CO_2	(4)
C_2H_6	⟶	C_2H_4	(5)
C_2H_6	⟶	CO_2	(6)
C_2H_6	⟶	CO	(7)
C_2H_4	⟶	CO_2	(8)
C_2H_4	⟶	CO	(9)
CO	⟶	CO_2	(10)

CO_2 may come from methane, ethane, ethylene, or CO. Ethylene is produced from ethane. CO is produced from methane, ethane, or ethylene.

Figure 34 below compares relative rates of CO_2 production for reactions 34-BKW-1 (void space after catalyst) and 34-BKW-2 (void space before catalyst).

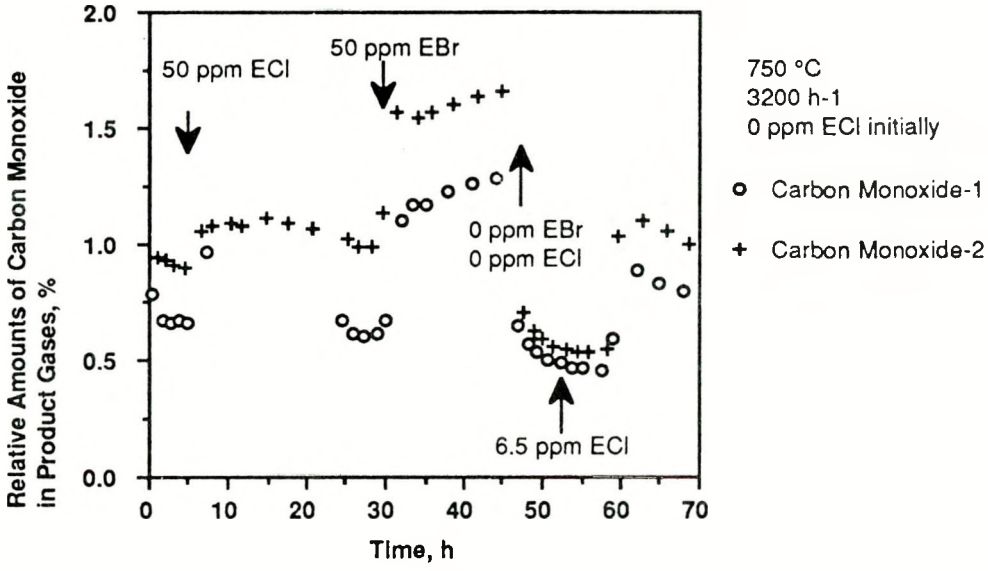
Figure 34. Relative Amounts of Carbon Dioxide Produced in Reactions 34-BKW-1 and 2



The rates to CO_2 are nearly the same for both reactions 34-BKW-1 and 2 for levels of 5 and 50 ppm of ECl and 50 ppm of EBr, under each of the same process conditions. This implies that no additional CO_2 is produced in reaction 33-BKW-2 from additional gas phase reactions, than is produced in reaction 33-BKW-1 over catalyst. This result is consistent with the formation of CO_2 from all sources on the catalyst surface, with little or no gas phase contribution to the rate determining step of oxidation of methane, intermediates, or products to CO_2.

Figure 35 below compares relative rates of CO production for these two reactions. The rate of CO production under each set of process conditions is significantly higher in

Figure 35. Relative Amounts of Carbon Monoxide Produced in Reactions 34-BKW-1 and 2



reaction 33-BKW-2 than it is in reaction 33-BKW-1. This is consistent with the production of CO resulting from gas phase reactions, which is known in combustion chemistry. The increased amount of CO produced in 34-BKW-2 with the 2.5 cc void space after the catalyst (relative to 34-BKW-1) with 50 ppm ECl in the feed gas was more than the total amount of CO produced in an uncatalyzed 4.5 cc void space (34-BKW-130, see Table 29 below). This indicates that the increase in CO production results from reactions other than exclusively gas phase reactions of methane and oxygen (which in

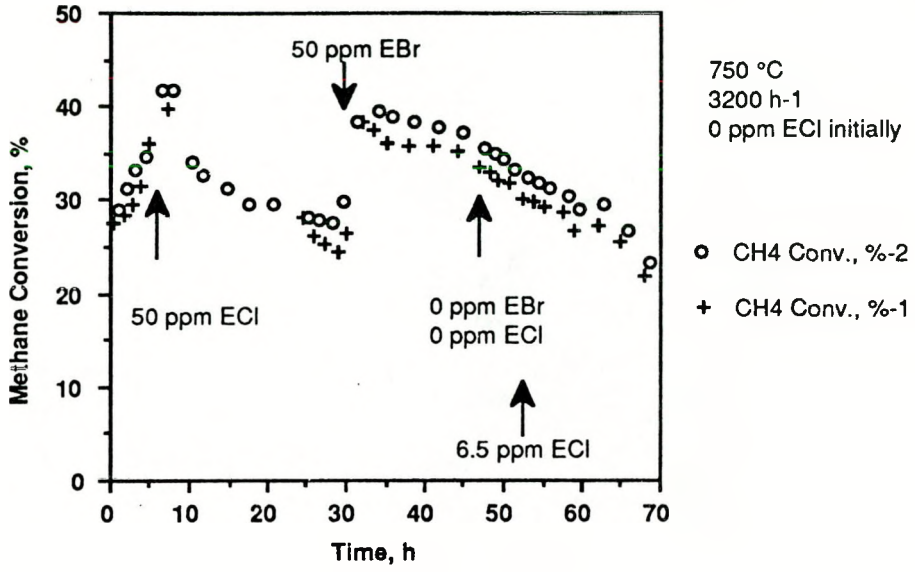
reactions 33-BKW-130 and 131 were observed to occur to only a small extent under reaction conditions). Possibilities include production of radicals (e.g., chlorine) on the catalyst surface followed by release of these into the gas phase to initiate chain reactions. These chain reactions would be expected to produce CO from Reactions 3, 7, and 9 of Figure 33 above. More ethylene would be expected from Reaction 5 of Figure 33. An increase in the observed methane coupling reaction to ethane might also be observed due to additional gas phase oxidation of methane from the increased concentration of free radicals. The actual amount of ethane observed would be that expected from reaction 34-BKW-1 plus that from the increase in gas phase methane oxidation minus that lost from reaction 5 in Figure 33 above.

Table 29. Enhanced Gas Phase Reactions, 34-BKW-1 and 2 and 33-BKW-130 and 131

Ref	CO	CO_2	C_2H_4	C_2H_6	CH_4C	EX	X	Time, m
34-BKW-1	0.7	1.2	0.4	0.2	31.7	0	0	235
34-BKW-2	0.9	1.3	0.5	0.2	34.5	0	0	270
34-BKW-1	0.6	0.6	0.3	0.2	24.6	50	Cl	1730
34-BKW-2	1.0	0.6	0.4	0.2	27.6	50	Cl	1695
34-BKW-1	1.3	1.3	0.4	0.1	35.2	50	Br	2640
34-BKW-2	1.7	1.3	0.5	0.1	37.8	50	Br	2685
33-BKW-130	0	0.002	0.001	0.01	1.3	0	0	170
33-BKW-131	0	0	0	0	0.8	0	0	195
33-BKW-130	0.09	0.002	0.01	0.03	2.6	50	Cl	1250
33-BKW-131	0.01	0.0004	0.006	0.01	1.2	50	Cl	1295
33-BKW-130	0.15	0.003	0.02	0.05	3.8	50	Br	3210
33-BKW-131	0.05	0.0006	0.008	0.03	2.2	50	Br	3190

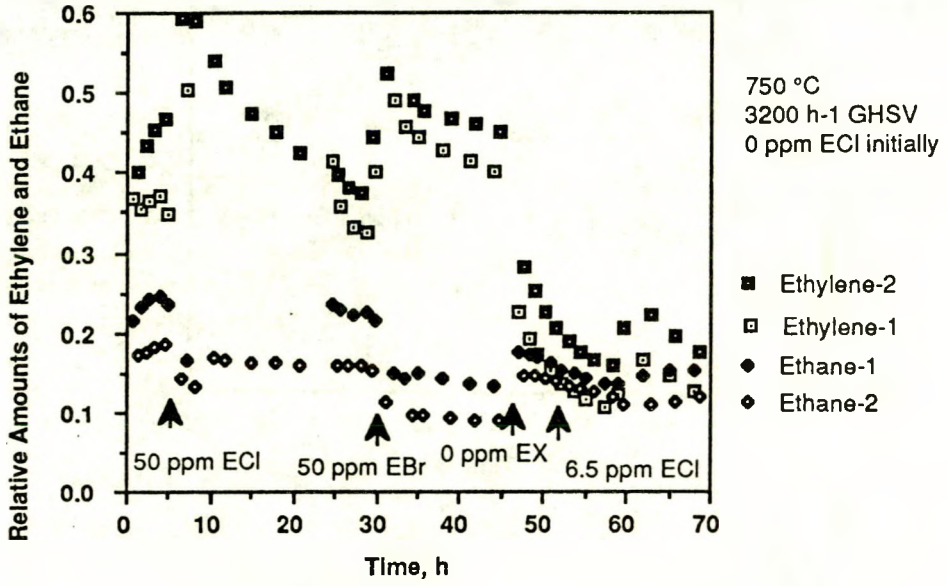
Table 29 shows the increase in methane conversion in reaction 34-BKW-2 with the void space after the reactor, compared to the reaction with the void space before the reactor, 34-BKW-1. Looking at Table 29, it may be seen that increases and decreases in ethylene and carbon dioxide levels roughly track changes in methane conversion. The amounts of CO with different amounts of ethyl halide in the feed gas in reaction 34-BKW-2 do not correlate with methane conversion. The amount of CO produced is higher with 50 ppm than it is with no ECl in the feed gas, even though methane conversion is less with 50 ppm ECl than it is without added ECl in the feed gas.

Figure 36. Relative Amounts of Methane Conversion in Reactions 34-BKW-1 and 2



As expected, the amounts of ethylene are higher in reaction 34-BKW-2 than 1, and the amounts of ethane are lower, due to conversion of ethane to ethylene in the gas phase after the catalyst bed in reaction 34-BKW-2 (Figure 37).

Figure 37. Relative Amounts of Ethane and Ethylene Produced in Reactions 34-BKW-1 and 2



An explanation consistent with observed results is that the catalyst generates radicals which are released into the gas phase to start chain reactions. Lunsford has shown that methyl radicals are released into the gas phase in this manner[16-19]. It is reasonable to expect chlorine radicals could also be released from the catalyst surface into the gas phase. Since thermolysis and/or oxidation of C_2's can also initiate chain reactions, it is not known what portion of the enhancement in gas phase reactions is initiated by decomposition of C_2's and what portion is initiated by free radicals lost from the catalyst surface. Experiments with added C_2's would help clarify roles of gas and surface reactions. Even in the absence of added volatile chloride, residual chloride on the catalyst surface could be released for a period of time from the catalyst into the gas phase.

Anions

Alkaline earth/metal oxide/halide catalysts for the oxidation of methane to C_2's were made with different anions. Electron microscopy showed that preparation of these catalysts with different anions resulted in different dispersions of the alkaline earth

components on the metal oxide. This not only varied with the anion used, but the same anion resulted in different dispersions with different alkaline earth metals. Electron microscopy further showed changes in the dispersion of alkaline earth metals during methane coupling reactions depended upon the anion for each alkaline earth. For instance, the barium on a catalyst made using barium carbonate and alpha-alumina was initially in smaller particles than the barium on a $BaCl_2/\alpha\text{-}Al_2O_3$ catalyst. The barium on the carbonate catalyst dispersed further and migrated into the catalyst particle during the reaction. The barium on a $BaCl_2/\alpha\text{-}Al_2O_3$ catalyst remained in clumps during the reaction, and barium was not observed to migrate into the catalyst particle during reaction.

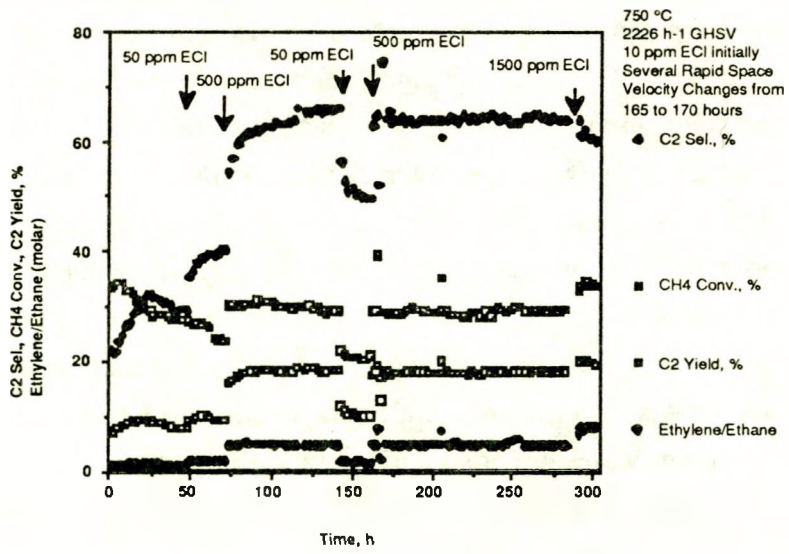
A barium nitrate on α–alumina catalyst was tested in reaction 33-BKW-49. Selectivity and activity were low without added ethyl chloride, so ethyl chloride levels of 0, 10, 2, and then 200 ppm were used. The 10 ppm level of ethyl chloride was too low to sustain good activities and C_2 selectivities, but with 200 ppm ethyl chloride, C_2 yields as high as 16.3% and C_2 selectivities as high as 69% were observed.

Differences in dispersions are likely to result from different solubilities of and crystallization behavior of different alkaline earth salts during drying of fresh catalysts. Differences in reactivity of different catalysts may be attributed in part to the dispersion of the alkaline earth metals on supports. The catalysts prepared from barium carbonate and alpha-alumina result in an increase in the rate to C_2's during the initial period of the methane coupling reaction, in the presence of small amounts of ethyl chloride in the feed gas, and they are more active than catalysts prepared from the same amount of barium, but using barium chloride (not carbonate) and alpha-alumina. These differences are consistent with different rates in the conversion of the starting anions to the final state of the activated catalyst, which is a slow process with certain alkaline earth salt/metal oxide combinations, but which is rapid with other combinations of salts and metal oxides. Although the only crystalline substances containing alkaline earth components which were detected in significant amounts by powder x-ray after reactions were alkaline earth metallates, e.g., aluminates from catalysts containing an aluminum oxide component, or titanates from catalysts containing a titanium oxide component, it is likely that catalysts prepared with different anions were converted during reaction to a common state of anions (e.g., hydroxide, oxides, carbonate, etc.). EDS analyses and XPS analyses were consistent with the presence of oxide (2-), hydroxide, carbonate, and chloride on used catalysts. Peroxide may have been present also.

Figure 14 on page 56 shows that selectivity to C_2's, methane conversion, yield to C_2's, and the ethylene to ethane product ratio remain fairly constant during a period of over 100 hours for methane oxidation over a catalyst prepared from barium hydroxide and titanium oxide, at 750 °C, 2230 h^{-1} space velocity, with 10% methane, 5% oxygen, and 500 ppm ethyl chloride in the feed gas (in a quartz reactor with 5 grams of catalyst).

The selectivity and C_2 yield drop initially for a few hours. This is in contrast to the initial behavior with a catalyst containing the same amount of barium, but prepared using barium carbonate, rather than barium hydroxide. Figure 38 shows that initially (with 10 ppm ethyl chloride in the feed gas), then again upon changing the amount of ethyl chloride in the feed gas from 10 to 50 ppm and from 50 to 500 ppm, the selectivity to C_2's increases slowly over a period of hours. The carbonate is therefore associated with low selectivity and the hydroxide with high selectivity on the surface of the catalyst. The rate of change to a level value of selectivity with 500 ppm ethyl chloride in the feed gas is faster for the catalyst prepared with hydroxide than it is for the catalyst prepared with carbonate. This is consistent with the carbonate being more stable on the catalyst surface than is the hydroxide, so the hydroxide is converted at a more rapid rate to the common mixture of anions.

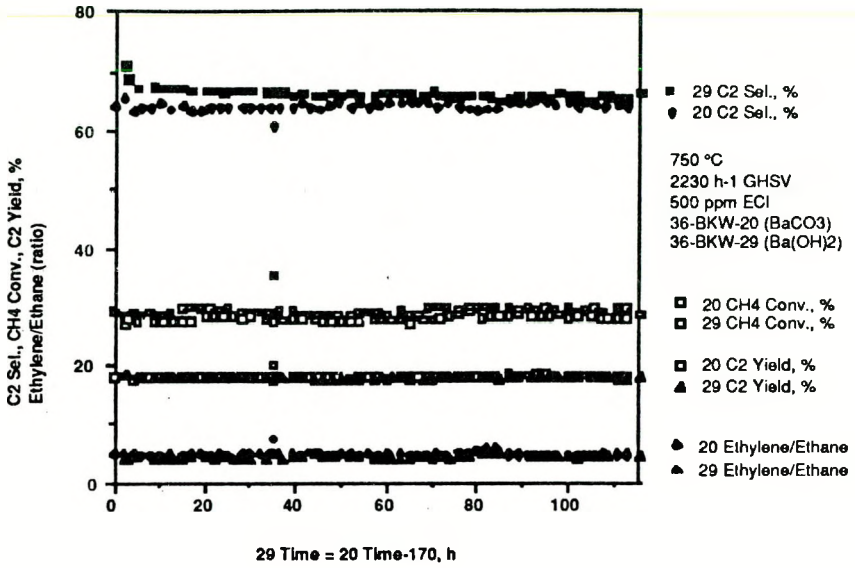
Figure 38. Methane Oxidation with a $BaCO_3/TiO_2$ Catalyst, 36-BKW-20



Although the initial reactivity of the two catalysts (from barium hydroxide and barium carbonate) are different, Figure 39 shows that the selectivity, methane conversion,

C_2 yield, and ethylene to ethane product ratios for these two catalysts (which contain the same amount of barium) under the same conditions, are the same.

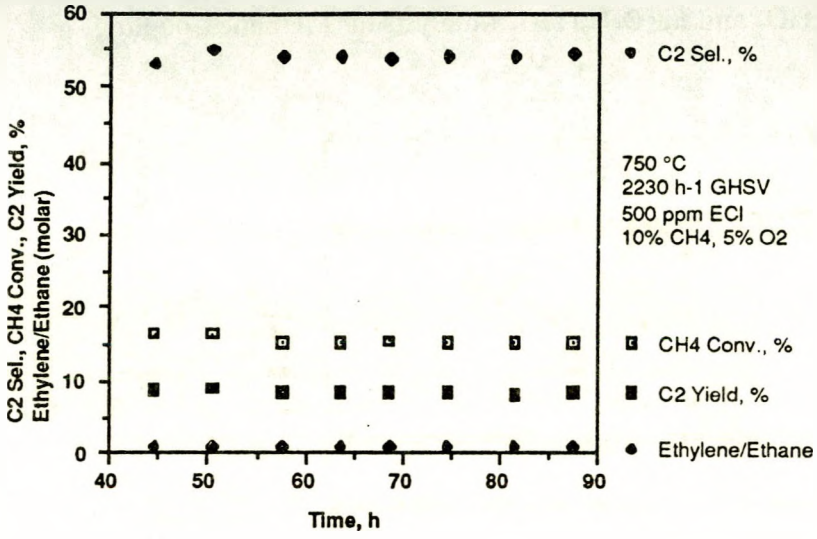
Figure 39. $BaCO_3/TiO_2$ and $Ba(OH)_2/TiO_2$ Catalysts for Methane Coupling



Reaction 36-BKW-20 is shown from the time of 170 hours (so actual run times are those shown plus 170 hours).

High ethylene to ethane product ratios are not observed with alkaline earth catalysts without non-basic metal oxide supports. Since it was proposed above that chlorine radical is released from the catalyst surface to allow chain reactions in the gas phase, resulting in the conversion of ethane to ethylene, it is likely that the support is required to react with ethyl chloride to release chlorine radicals. Figure 23 on page 66 shows methane oxidation results using a catalyst consisting of only barium oxide (no support). Low ethylene to ethane product ratios are obtained under all conditions used.
Figure 40 shows that portion of the reaction run under the same conditions as those used for the reactions in Figure 39. The methane conversion, yield to C_2's, and selectivity to C_2's are lower with barium oxide than they are with barium (from the carbonate or the hydroxide, as shown in Figure 39) on titanium oxide. It is known that barium hydroxide may be heated to form barium oxide.

Figure 40. BaO Catalyst for Methane Coupling, 36-BKW-46



Figures 41 and 42 compare catalysts containing the same amount of barium (from barium oxide and barium carbonate) on alpha-aluminum oxide (Norton 5451) for methane coupling. These catalysts were run simultaneously under the same sequence of process changes, and it may be seen that the patterns of reactivity for both catalysts are the same.

Figure 41. BaO/Al_2O_3-5451, 34-BKW-124

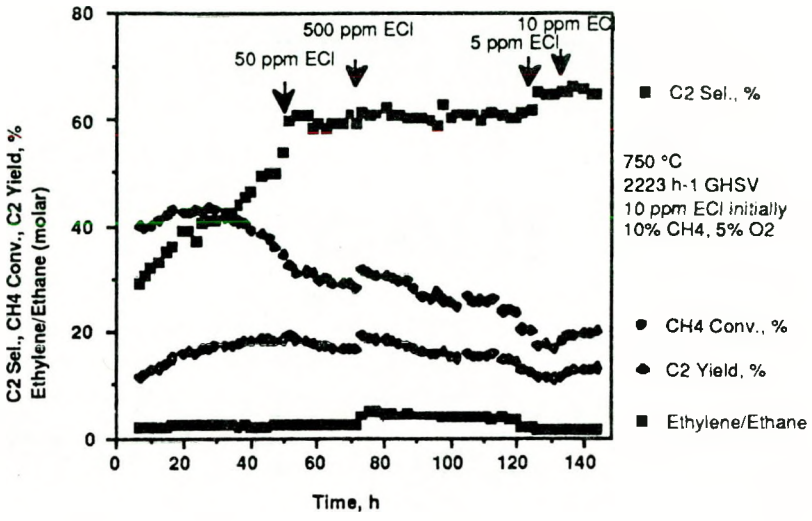


Figure 42. $BaCO_3/Al_2O_3$-5451, 34-BKW-125

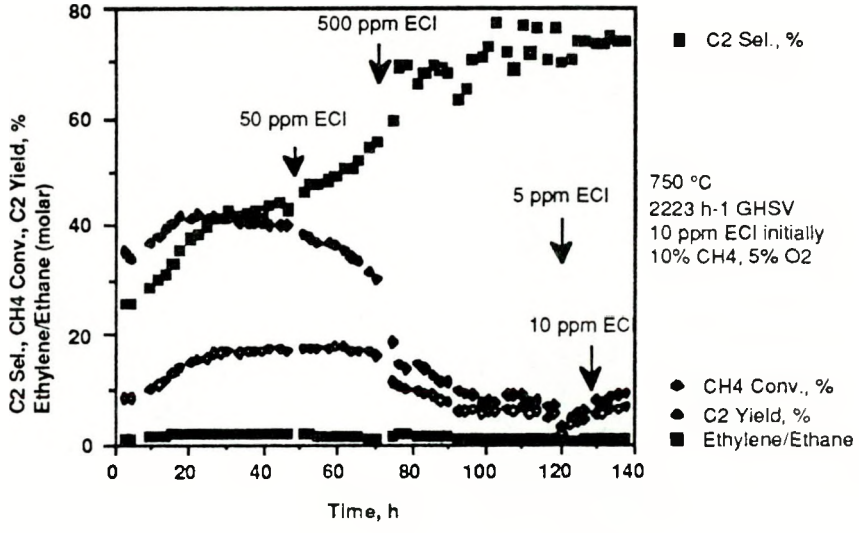


Figure 43 compares the portions of the reactions shown in Figures 41 and 42 which had 10 ppm ethyl chloride in the feed gas. Figure 44 compares the portions of these two reactions with 50 ppm ethyl chloride in the feed gas.

Figure 43. BaO/Al_2O_3-5451 and $BaCO_3/Al_2O_3$-5451, 34-BKW-124 and 125

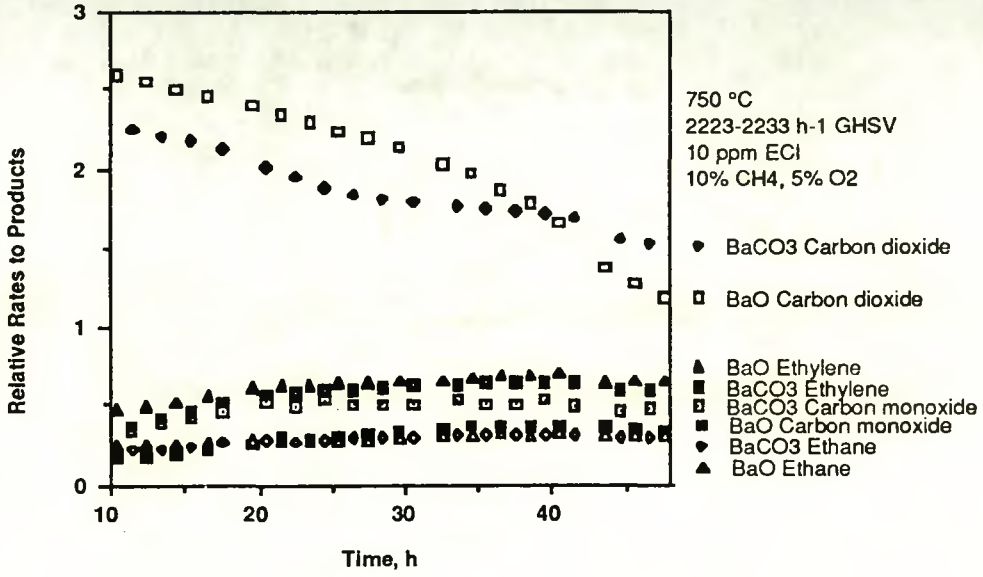
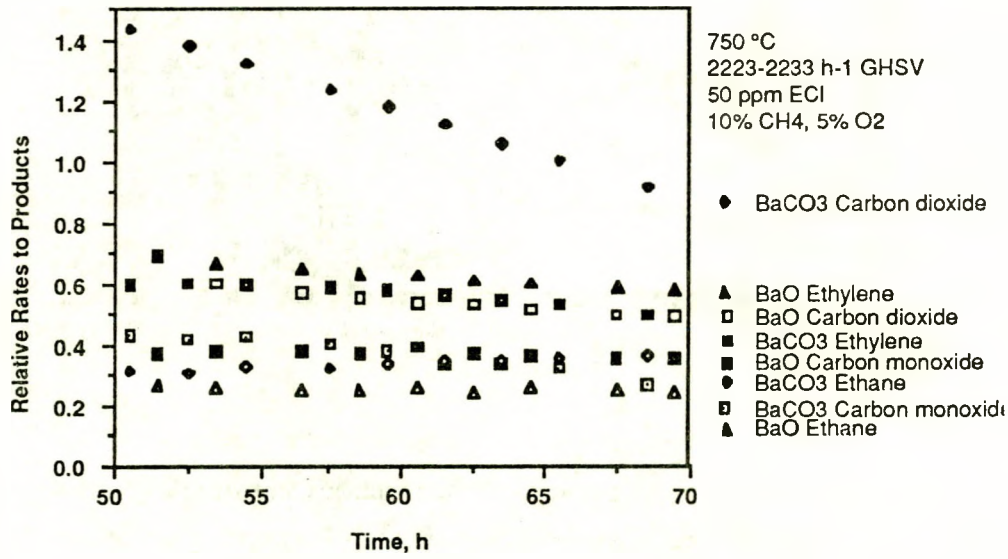


Figure 44. BaO/Al_2O_3-5451 and $BaCO_3/Al_2O_3$-5451, 34-BKW-124 and 125



Considering that the dispersions of barium on these catalysts must be quite different, and that different dispersions of barium probably have different optimum

concentrations of ethyl chloride, the relative rates to products are surprisingly similar. With 10 ppm ethyl chloride in the feed gas, the amounts of ethylene and ethane produced with the two catalysts are about the same. When the ethyl chloride level is raised to 50 ppm, the total amounts of C_2's produced over both catalysts are approximately the same, however the catalyst prepared with BaO produces a higher ethylene to ethane product ratio than does the catalyst prepared with $BaCO_3$. This might indicate that the catalyst prepared with BaO releases higher concentrations of ethyl chloride into the gas phase to allow faster conversion of ethane to ethylene in the gas phase (from different dispersions of barium or different acidities of the catalysts).

The relative rates of production of various products on barium oxide alone (without a metal oxide support) with 10 ppm ethyl chloride in the feed gas are shown in Figure 45. Higher levels of ethane than ethylene are present in product mixtures, which is consistent with the proposition that the support is involved in the production of higher ethylene to ethane product ratios.

Figure 45. BaO, 36-BKW-46

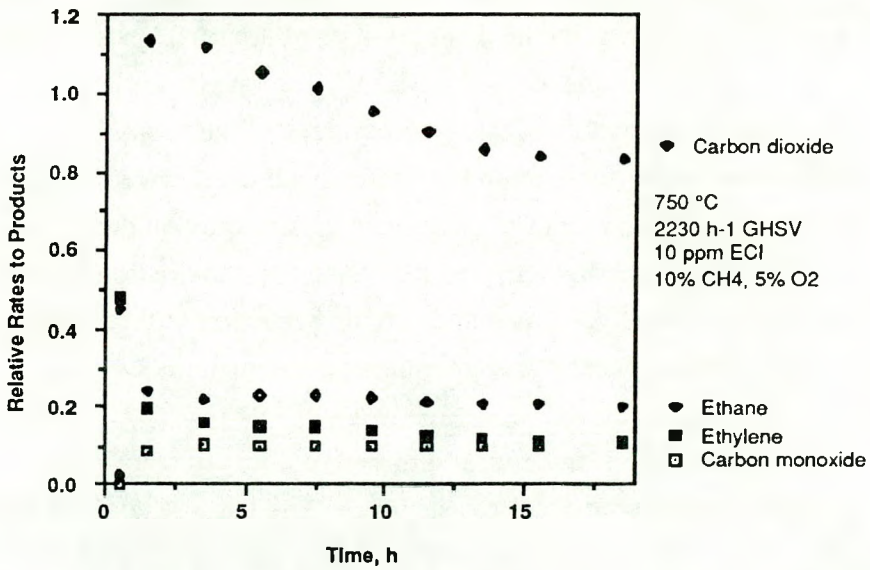
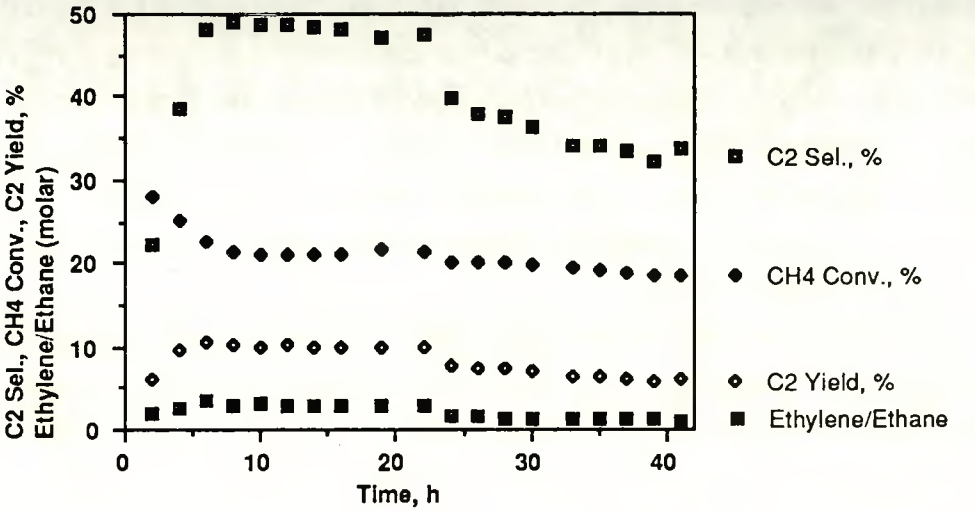


Figure 46 shows that the performance of a $SrCO_3/TiO_2$ catalyst is not as good as that of a $BaCO_3/TiO_2$ catalyst (see Figures 38 and 39 above) with the same molar amount of alkaline earth carbonate and the same reaction conditions. Results with 500 ppm ethyl chloride in the feed gas are better than with 50 ppm ethyl chloride in the feed gas.

Figure 46. $SrCO_3/TiO_2$, 36-BKW-26



Pressure

Although reactions were normally run at about 11 psig (176 kPa), a C_2 yield of 21% with a C_2 selectivity of 57% was obtained at pressures of about 22 psig (236 kPa) with a $BaCO_3/ZrO_2$ catalyst at 750 °C and 2243 h^{-1} GHSV. The rate of the homogeneous, gas-phase reaction is increased with an increase in pressure, and the catalytic and/or quenching effects of the reactor wall are more pronounced at otherwise constant conditions. Therefore, the high rate of the homogeneous reaction and the increased importance of wall effects under higher pressures using the cooxidation mode make it unlikely that studies of the catalyzed methane coupling reaction will provide meaningful results without significant engineering, reactor design, and materials science contributions.

Methane coupling reactions under pressure will require a reactor material which will remain intact under pressure. Stainless steel was tested as a reactor material (at the usual 11 psig pressure) without a catalyst (packed with quartz chips, 32-BKW-95) and with a $BaCO_3/TiO_2$ used (activated) catalyst (from reaction 32-BKW-80). At flow rates which correspond to space velocities of 1000-4000 h^{-1} with charges of 5g of catalyst, methane conversion was 3-5% at 750 °C without added ethyl chloride in the feed gas. With 500 ppm added ethyl chloride, methane conversion rose to 30-38% (limited by 98%

oxygen conversion). When ethyl chloride was no longer fed to the reactor, methane conversion remained above 30% for hours.

C_2 yields, C_2 selectivities, and ethylene to ethane product ratios for the $BaCO_3/TiO_2$ catalyst run in the stainless steel reactor were significantly lower than the values of these variables in reaction 32-BKW-80, where a quartz reactor was used. The stainless steel reactor was highly pitted and corroded after the reaction.

Catalyst Surface Analyses

Electron Microscopy [energy dispersive spectroscopy (EDS), secondary electron image (SEI), and backscattered electron image (BEI)] was applied to fresh and used alkaline earth/metal oxide catalysts. In SEI pictures, barium is not distinct from aluminum in Ba/Al_2O_3 catalysts. In BEI pictures, chunks of barium (light) are present on the alumina (darker). Large, light areas of caked-looking barium are visible by BEI in a fresh $BaCl_2/Al_2O_3$ catalyst, 33-BKW-79A. The used catalyst, 33-BKW-81, looks largely the same as the fresh catalyst. For the fresh $BaCO_3/Al_2O_3$ catalyst, 32-BKW-20I, BEI shows smaller Ba particles which are better dispersed than the Ba particles on the $BaCl_2$ catalyst. After reaction, Ba particles look even smaller (32-BKW-62), and there appear by BEI to be fewer barium particles. EDS analyses clearly indicate that the barium is well dispersed on alumina.

The weight and atom percents of Al, Si, Cl, and Ba for the surface of Ba/Al_2O_3 catalysts which were prepared with nitrate, carbonate, and chloride catalysts were determined. The amount of surface barium detected by EDS for used chloride (33-BKW-81, 11.8 wt%) and carbonate (33-BKW-74, 12.6 wt%) catalysts was similar after reactions. For catalysts made from nitrates and chlorides, the surface amount of barium increased during the reaction (from 5.6 to 11.8 wt% for the chloride). For the catalyst prepared with barium carbonate, the surface amount of barium decreased during the reaction (from 19.0 to 12.7 wt%).

Since ICP analyses of used barium catalysts showed no loss of barium, catalyst particle cross sections were examined by SEI, BEI, and EDS to determine if barium migrated into the catalyst during reaction over $BaCO_3/Al_2O_3$ catalysts. For a cross section of fresh $BaCO_3/Al_2O_3$ catalyst, BEI shows that the light particles of barium are concentrated on the outside of the sliced catalyst. For used catalyst 32-BKW-62, there is no concentration of barium on the outside of the catalyst. By EDS analyses of catalyst

surfaces and catalyst cross sections, the barium concentration increases in the middle of the catalyst particles during methane coupling reactions.

Table G1 of Appendix G shows EDS data for fresh and used $BaCO_3/Al_2O_3$ catalysts, illustrating the decrease in the amount of barium on the surface of the catalyst during reaction. Figure G1 of Appendix G shows BEI micrographs of fresh and used $BaCO_3/Al_2O_3$ catalysts, illustrating the clumps of barium before reaction and the dispersed barium after reaction.

Table G2 of Appendix G presents EDS results from used BaO/Al_2O_3 and $BaCO_3/Al_2O_3$ catalysts. Figures G2 and G3 of Appendix G are BEI micrographs of these used catalysts. Both EDS and BEI micrographs show less uniform distribution of barium in the catalyst made from BaO, compared to the one made from $BaCO_3$.

Barium appeared to be better dispersed on alumina on the fresh $Ba(NO_3)_2/Al_2O_3$ catalyst, 33-BKW-47B than on the fresh carbonate catalyst. Very little distinct barium was visible in the used $Ba(NO_3)_2/Al_2O_3$ catalyst, 33-BKW-49, whereas by EDS it is present, suggesting that the barium is dispersed uniformly over alumina particles.

In fresh catalyst 30-BKW-68C, certain areas analyzed contained 26 atom% Ba and 16 atom% Cl by EDS, whereas other areas contained as little as 1 atom% Ba or no chlorine. This suggests poor dispersion of barium, or clumps of barium, on the $BaCl_2/Al_2O_3$ catalyst. EDS analyses show relatively little chloride on used Ba/Al_2O_3 catalysts from reactions 30-BKW-52 (0.44 wt%), 30-BKW-93 (0.00 wt%), 32-BKW-62 (0.01 wt%), and 33-BKW-74 (0.08 wt%). The amounts of chlorine observed on used Sr catalysts are much higher (0.98 wt% or 7 atom% for 34-BKW-18, and 2.75 wt% or 13 atom% for 34-BKW-19) than amounts observed for used barium catalysts.

For the $SrCO_3/Al_2O_3$ catalyst, surface Sr (light areas in BEI) remained in clumps during the methane coupling reaction. For the fresh $SrCl_2/Al_2O_3$ catalyst, lighter areas of more concentrated, but relatively well dispersed Sr are observed by BEI (34-BKW-16B). Patches of more concentrated Sr cannot be detected by BEI in the used catalyst (34-BKW-19).

Catalysts 30-BKW-68C and D are on different alumina supports. Catalyst C uses Norton 5551 alumina, and catalyst D uses Norton 5502 alumina. The Norton 5502 support is more acidic and has a higher surface area. The concentration of Ba on a fresh catalyst on this higher surface area support is lower (2.7 wt%) than that on the Norton 5551 support (5.2 wt%), most likely due to the fact that the same amount of Ba is spread out over a larger surface. A used $CaCl_2$ catalyst (31-BKW-13) had 1.09 wt% Ca on the surface by EDS compared with 0.88 wt% Ca on the fresh catalyst.

In summary, fresh barium chloride and carbonate catalysts on alumina have different dispersions of barium. The barium in a carbonate catalyst moves from the surface into the particle as the reaction proceeds, and Ba clumps disappear as the barium disperses to more uniformly coat alumina particles. Barium on fresh catalysts prepared from barium chloride and alumina is in larger clumps than is the barium on fresh catalysts prepared from barium carbonate and alumina. The barium remains in clumps during methane oxidation reactions over $BaCl_2/Al_2O_3$ catalysts. In contrast to the barium catalysts, strontium catalysts from $SrCO_3$ have larger Sr clumps which do not disperse well, whereas the $SrCl_2$ is dispersed fairly well on fresh catalysts, and it appears to spread out even more as the reaction proceeds.

The $BaCO_3/Al_2O_3$ catalyst used in reaction 32-BKW-62 was analyzed by XPS. No chlorine was found on the catalyst surface. Trace amounts (<0.10 atom%) of Ca, Ag, and N were detected. From XPS analysis, the top layer on the catalyst surface most likely is BaO with O^{2-} anion, mixed with a small amount of $BaCO_3$. 6.4% Ba, 51.7% O, 21.9% C, and 19.9% Al are present.

Natural Gas Mixture

Methane oxidation over two used catalysts with a mixture representative of a processed natural gas mixture resulted in the same rates to ethane and slightly increased rates to ethylene, carbon monoxide, and carbon dioxide, compared with pure methane in the feed gas.

Table 30. Mixture Representative of a Processed Natural Gas Mixture

Component	Mole%	Weight%
Nitrogen	1.65200	2.78054
Carbon Dioxide	0.03782	0.10001
Propane	0.17400	0.46102
Hydrogen Sulfide	0.00024	0.00050
Ethane	2.45200	4.43010
Methane	95.67091	92.22006
Oxygen	0.00077	0.00149
Water	0.00048	0.00052
Isobutane	0.00061	0.00213
N-Butane	0.00033	0.00116
Propylene	0.00000	0.00000
Ethylene	0.00074	0.00124
Hydrogen	0.01009	0.00122

Figures 47-50 show results. Pure methane was first used, then the mixture representative of a processed natural gas mixture was substituted for pure methane.

Figure 47. $BaCO_3/TiO_2$, 36-BKW-50

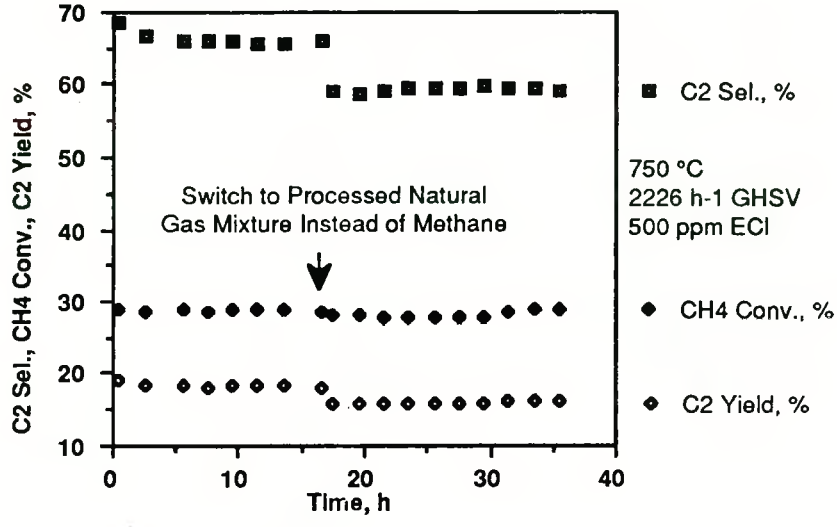


Figure 48. $BaCO_3/TiO_2$, 36-BKW-50

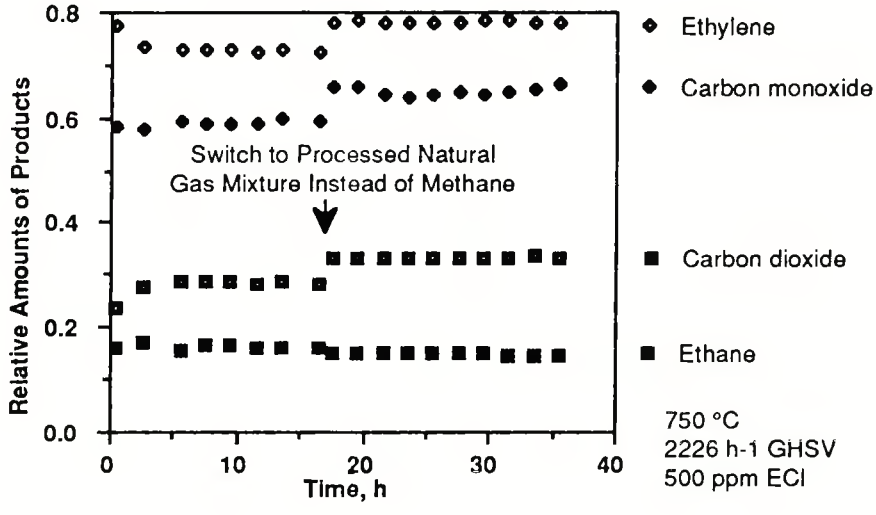


Figure 49. $BaCO_3/ZrO_2$, 36-BKW-51

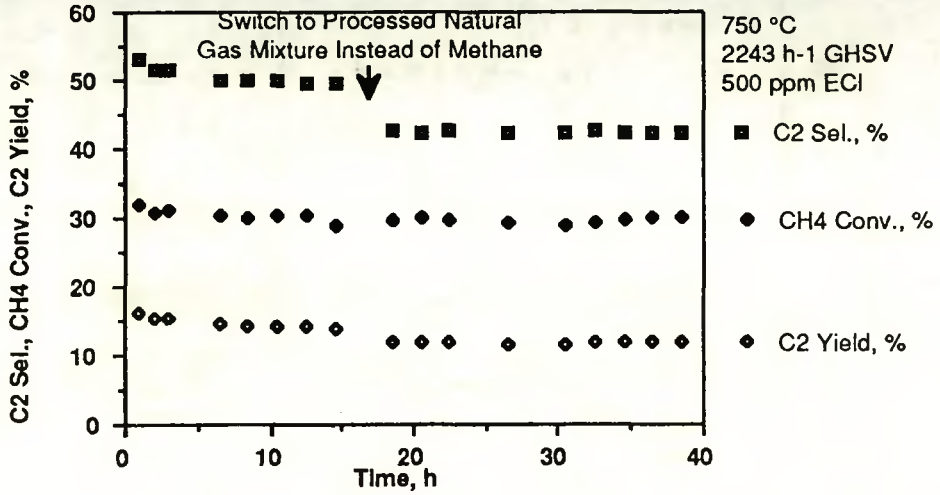
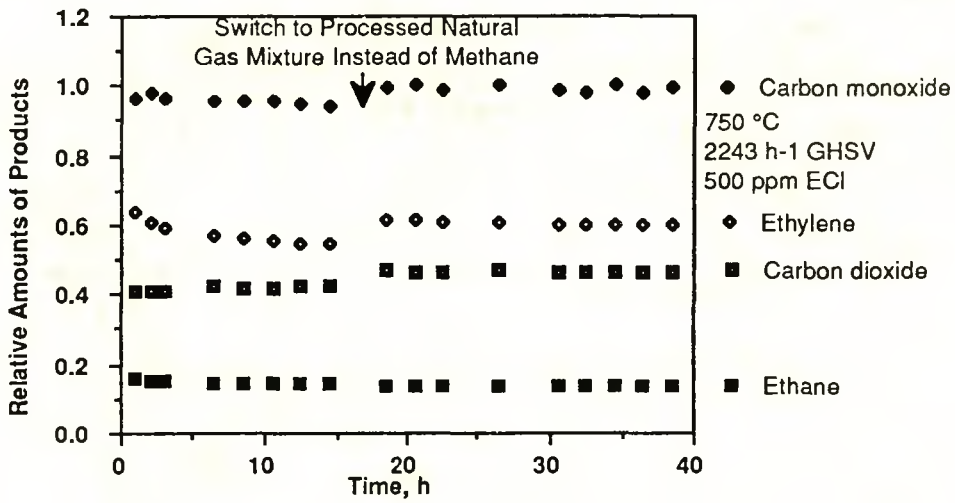


Figure 50. $BaCO_3/ZrO_2$, 36-BKW-51



The overall methane conversion remained approximately the same, so the increase in relative amounts of products more oxidized than ethane is presumed to result from decomposition of the non-methane components of the processed gas mixture (ethane and higher alkanes) to generate some ethylene, carbon monoxide, and carbon dioxide. Table 30 presents the mixture representative of a processed natural gas mixture.

Comparative Examples

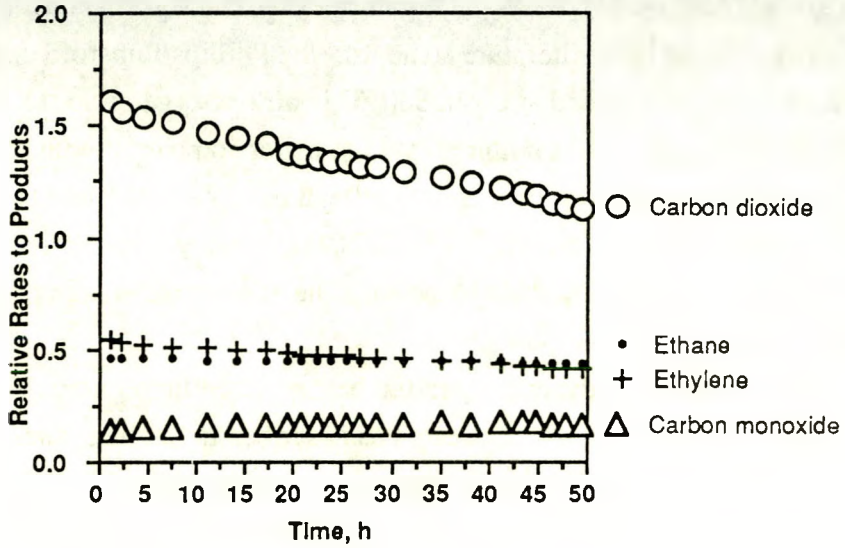
The importance of catalyst preparation or "pretreatment" is demonstrated by a test of a LiCl/MgO catalyst (31-BKW-83) against a Li_2CO_3/MgO catalyst (31-BKW-84)[16-20]. The latter catalyst is the literature standard - the Phillips/Lunsford catalyst. Normally, the literature catalyst is heated at about 800 °C in air or oxygen prior to reaction. The Li_2CO_3/MgO catalyst was not pretreated to better compare it with the LiCl/MgO catalyst. The Li_2CO_3/MgO catalyst (not pretreated) gave only a 10% yield to C_2's and deactivated to very low selectivity and activity. The LiCl/MgO catalyst gave a 16% C_2 yield initially, which decreased to 10.2% after 68 hours. The ethylene to ethane product ratio is low, as expected on this basic support.

Two Li/MgO catalysts (among the best reported literature catalysts[16-20]) were prepared using Li_2CO_3, and pretreated as described in the literature. The catalyst used for reaction 32-BKW-135 was the same as the one used for 32-BKW-134, except that the catalyst for 32-BKW-135 was heated at 850 °C in air for 2 hours, and the catalyst for 32-BKW-134 was heated in air for 600 °C for 12 hours. The surface area of the catalyst heated at 850 °C was 1.6 m^2/g before reaction, whereas the surface area of the catalyst for 32-BKW-134, heated only to 600 °C was 32.7 m^2/g. After reaction, the catalyst used in reaction 32-BKW-134 had a surface area of 0.98 m^2/g, and the catalyst used for reaction 32-BKW-135 had a surface area of 1.18 m^2/g. The rate of methane conversion in the catalyst with the higher surface area (32-BKW-134) was higher initially but it dropped to a level comparable to that of the catalyst in 32-BKW-135 after a few hours.

Although the pattern of reactivity for both catalysts with process changes was similar, the catalyst for reaction 32-BKW-135 was slightly more selective in forming C_2's, and it deactivated at a slightly lower rate after the first few hours of reaction. One gram of catalyst was tested in both cases, but the catalyst heated at 850 °C was twice as dense, therefore, although the same flow rates are used in experiments, the space velocities in 32-BKW-135 (Figure 51) are twice those in 32-BKW-134.

Methane conversion dropped rapidly during the first fifty hours of reaction, mainly due to a drop in the rate to CO_2. The C_2 yield drops 12% during this time period, predominately due to the drop in rate to ethylene, as shown in Figure 51 (700 °C, 9600 h^{-1} GHSV, 1 g catalyst, 10% CH_4, 5% O_2, nitrogen diluent). The rate to ethane remains fairly constant during the first fifty hours of this reaction, and the rate to CO rises slightly.

Figure 51. Li_2CO_3/MgO, 32-BKW-135



The addition of 10 ppm of ethyl chloride to reaction 32-BKW-135 at 74.1 h resulted in no significant changes in methane conversion, C_2 selectivity, C_2 yield, or in the ethylene to ethane product ratio. In reaction 31-BKW-87, addition of 500 ppm ethyl chloride to a LiCl/MgO catalyst resulted in a significant drop in methane conversion (from 26 to 11%) which rose upon removal of ethyl chloride from the feed gas (to 20%). This indicates that ethyl chloride in the feed gas may be absent under optimum conditions for a Li/MgO catalyst, whereas it is required for optimum catalyst performance in the alkaline earth/acidic metal oxide catalysts.

Both $LiCO_3$/MgO catalysts lost lithium during the reaction. The catalyst for reaction 32-BKW-134 contained 2.5% lithium prior to reaction, and 1.1% lithium after reaction. The catalyst for 32-BKW-135 contained 2.2% lithium before reaction and 1.6% lithium after reaction. In contrast, the catalyst used for the long reaction 33-BKW-74 ($BaCO_3/Al_2O_3$) did not lose a significant amount of barium in the reaction, even though the reaction was conducted at higher temperatures. It contained 3.1% barium before and after reaction. A major difference in the alkaline earth/non-basic metal oxide/chloride catalysts and the Li/MgO catalysts is that the Li/MgO catalyst irreversibly deactivates by the loss of Li, whereas the alkaline earth catalysts do not lose alkaline earth metals.

Although optimum conditions for the Li/MgO catalysts are not the same as those for the alkaline earth/metal oxide/Cl catalysts, (Li/MgO catalysts lose lithium rapidly at

temperatures above 720 °C and require no added chloride), Table 31 below shows for different methane to oxygen ratios that a Li/MgO (33-BKW-135) catalyst can be run at lower temperatures and higher space velocities than barium/α-alumina catalysts 33-BKW-7 and 33-BKW-74, with similar selectivities and activities for the two types of catalysts, and with similar maximum C_2 yields. The Li/MgO catalyst is more active.

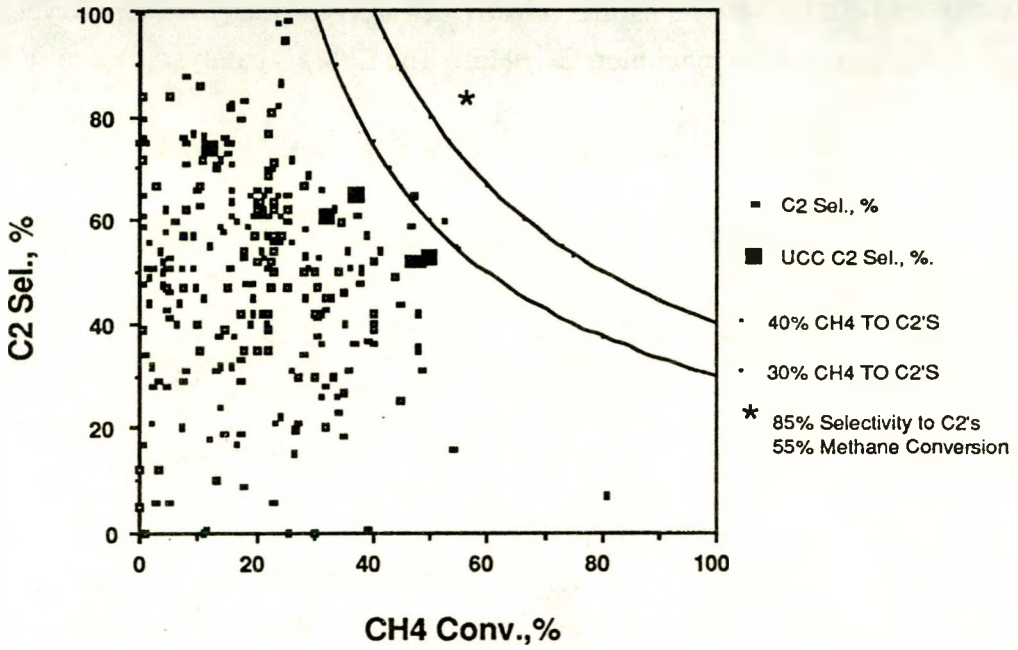
Table 31. Different Methane to Oxygen Ratios for $BaCO_3/Al_2O_3$ and Li/MgO Catalysts

Name	Catalyst	Temp	CH_4C	Sel	Yield	=/-	CH_4/O_2	CH_4 in	O_2 in	Time, h	GHSV	ECl
32-135	Li/MgO	720	37.91	51.8	19.31	1.18	1.98	9.509	4.8	1	9600	0
32-135	Li/MgO	700	30.5	51.1	15.4	1.0	2.0	9.5	4.8	68	4800	0
33-7	Ba/Al_2O_3	750	45.2	43.4	19.4	3.1	2.0	9.4	4.8	289	1667	50
32-135	Li/MgO	700	21.5	49.1	10.5	0.7	2.2	10.1	4.6	190	4800	0
33-74	Ba/Al_2O_3	750	43.0	46.4	19.7	3.1	2.0	10.1	5.0	291	1116	4
33-74	Ba/Al_2O_3	750	39.5	42.8	16.9	3.6	2.1	20.6	9.6	359	1088	30
32-135	Li/MgO	700	28.9	45.1	12.9	1.1	2.1	19.6	9.3	175	4800	0
33-7	Ba/Al_2O_3	750	43.8	41.8	18.1	3.9	2.2	19.2	8.9	286	1667	50
32-135	Li/MgO	700	15.0	67.8	9.8	0.6	9.2	78.8	8.6	98	7200	0
33-74	Ba/Al_2O_3	750	11.0	70.9	7.5	0.8	8.1	79.6	9.9	410	2233	47
33-7	Ba/Al_2O_3	750	9.8	76.4	7.5	1.2	18.5	81.1	4.4	138	1667	17

Summary of Methane Coupling Catalyst Performance

Figure 52 below presents a modified plot of the type first presented by Jon McCarty of SRI[76]. These best literature combinations of selectivity and methane conversion are displayed along with some of the better yields from alkaline earth/chloride/metal oxide catalysts explored at UCC&P during research on the current DOE Contract. The literature data for this plot is taken from the best runs (366) of the references listed in Appendix H.

Figure 52. Literature and UCC&P Results for Methane Coupling



The two curves indicate 30% and 40% yields to C_2's from methane. The star represents 85% selectivity and 55% methane conversion, which might currently be economically competitive with existing technology for ethane/propane cracking on the Gulf Coast. Selectivity/conversion combinations per pass over several different types of catalysts provide results which are comparable to better literature results[29,43,45,48,77]. C_2 yields of 20-26% have been demonstrated. C_2 selectivities as high as 74% and C_2 yields as high as 26% have been achieved. Table 32 below presents the UCC&P data displayed in Figure 52 above.

Table 32. Selected Results in Figure 52

Reference	Catalyst	Temp	CH_4 C	Sel	Yield	=/-	GHSV
32-BKW-40	$SrCO_3/Al_2O_3$	760	12	74	9	1.4	2087
31-BKW-33	$CaCl_2/Al_2O_3$	700	37	65	23	6.0	2341
32-BKW-41	$BaCO_3/Al_2O_3$	800	50	53	26	6.8	2087
31-BKW-119	$BaCl_2/Al_2O_3$	750	48	52	24	15	878
31-BKW-118	$SrCl_2/Al_2O_3$	750	47	52	24	17	1171

It is concluded that UCC&P has provided catalysts which are comparable in selectivity, activity, and C_2 yield to the better literature catalysts, but which exhibit higher ethylene to ethane product ratios and longer catalyst lifetimes than have been reported.

Avoiding the Heterogeneous/Homogeneous Mechanism

The barium and strontium catalyst systems described above are thought to operate by the heterogeneous/homogeneous mechanism with creation of methyl radicals on the catalyst surface by hydrogen abstraction from methane, followed by release into the gas phase of the methyl radical, then coupling of two methyl radicals to form ethane. The product distribution for this mechanism is largely dictated by the gas phase chemistry. Two approaches are suggested to avoid the heterogeneous/homogeneous mechanism in order to achieve higher C_2 selectivity/methane conversion combinations. One approach is to reduce the reaction temperature such that little gas phase chemistry will occur. This requires more active catalysts. The other approach is to change the gas phase chemistry to depart from the typical combustion reaction network.

Silver Catalysts

To increase the surface contribution of the reaction, one may increase the surface reaction rate relative to the reaction rates of gas phase reactions. This may be accomplished by increasing rates of reaction steps on the catalyst surface, or decreasing the rates of the gas phase reactions (operating at lower temperatures). Barium peroxide was reported[52] to convert methane to C_2's at temperatures below 400 °C. Certain other

metals activate hydrocarbons unselectively at low temperatures, e.g., silver, palladium, and platinum.

Catalysts were prepared containing silver, which is known to activate hydrocarbons unselectively at relatively low temperatures (compared to the typical temperatures of 700-950 °C used for methane coupling). Selective methane coupling activity is obtained in the presence of other catalyst components, such as alkali and alkaline earth components, and in the presence of chloride, despite the presence of the unselective metal component. The catalysts can be operated at relatively low temperature to effect methane coupling. Moreover, the use of the lower temperature reduces the homogeneous reaction rate in favor of the heterogeneous reactions.

A low temperature catalyst containing 9% silver, 5% barium chloride, and α-alumina (31-BKW-2) exhibited C_2 yields as high as 10% at 650 °C. Without the barium chloride (30-BKW-123), complete oxygen conversion occurred at temperatures of 300-500 °C, with methane converted only to carbon oxides. Examples of results are shown in Table 33. The two catalysts containing barium have different levels of barium and were prepared using different methods of silver deposition.

Table 33. Low Temperature Catalysts

Catalyst	Ref	T,°C	CH_4 Conv.	C_2 Sel.	C_2 Yield	GHSV	=/-	ECl
Ag/α-alumina	30-123	425	25	-	-	1636	-	50
Ag/ $BaCl_2/Al_2O_3$	31-2	650	32	32	10	682	0.8	50
Ag/ $BaCl_2/Al_2O_3$	34-63	670	17	25	4.5	1263	0.6	5

The catalyst with undoped silver resulted in methane oxidation to CO_2 at 425 °C, but it was necessary to raise the temperature to 650 °C to obtain high methane conversions with the doped catalyst. Lower levels of dopants were of interest in hopes of obtaining activity at lower temperatures, while retaining or improving the C_2 selectivity observed at 650-700 °C. Catalysts with a variety of dopants were made and tested for methane coupling activity. Catalyst preparation methods for catalyst containing silver are described in detail in Appendix C and catalyst compositions are described in Appendix D. With low levels of Pr (34-BKW-6 and 7), Bi (34-BKW-10), Ba (34-BKW-11,14), and

K (34-BKW-15) dopants, methane conversions were high, and C_2 selectivities were low, as they had been without dopants. For example, in reaction 34-BKW-6, at 425 °C, 98% oxygen conversion and 26% methane conversion to carbon dioxide were observed using 10% methane and 5% oxygen, with a space velocity of 2341 h^{-1}. The catalyst for this reaction contained 0.1% praseodymium. Addition of 10 ppm of ethyl chloride in the feed gas to this reaction at 400 °C resulted in an initial increase in methane conversion from 15 to 16%, followed by a drop in methane conversion to 4%. No significant amounts of C_2 products were produced with any of these catalysts under any conditions, even at 700 °C, where C_2's are produced to some extent without catalysts in gas phase reactions. It is concluded that these silver catalysts with low levels of modifiers not only oxidize methane efficiently to CO_2, but they also efficiently oxidize intermediates (e.g., radicals) and products (e.g., ethylene) of methane oxidation to CO_2.

The catalysts for reactions 34-BKW-6, 7, 10, 11, 14, and 15 were made using a different method of silver deposition on alumina. Nitrates were used as dopants in place of chloride, and a different level of silver was used (see Appendices C and D).

Additional catalysts were prepared (34-BKW-36 and 45) with the same method of silver deposition, but with different levels of dopant, using barium and calcium chlorides rather than nitrates. Unusually high C_3 selectivities (e.g., 18%, with C_2/C_3 product ratios of 1.4) were obtained with the $BaCl_2$/Ag/α-alumina catalyst. C_2/C_3 product ratios are normally around 15-20. Also, the C_3 product was all propane rather than propylene, which is usually observed for oxidative methane coupling. For example, Table 34 below shows that propylene ($C_3^=$) to propane (C_3^-) ratios are between 0.5 and 2 in reactions 32-BKW-135, with a Li/MgO catalyst and in reaction 33-BKW-6, with a Ba/Al_2O_3 catalyst, using 10% methane and 5% oxygen. In contrast, the catalyst with silver (34-BKW-63) shows no propylene, but only propane as product. Over the two catalysts without silver, the C_2/C_3 product ratios are 18-20, whereas almost as much propane as C_2's is produced in reaction 34-BKW-36.

Table 34. C_3 Products

Ref	Cat	T, °C	CH_4C	C_2Yield	C_2 Sel	=/–	$C_3^=/C_3^-$	C_3Sel	GHSV	Time, m	C_2/C_3	ECl
34-63	$Ba/Ag/Al_2O_3$	670	17	4.5	25	0.6	0	18	1263	255	1.4	5
32-135	Li/MgO	720	36	19	52	1.1	1.4	2.9	9600	665	18.2	0
33-6	Ba/Al_2O_3	750	39	20	52	2.4	0.7	2.6	2182	2590	20	10

Propylene is expected from the normal heterogeneous/homogeneous methane coupling mechanism. Propylene formation has been proposed to result from methyl radical reaction with ethylene in the gas phase[59,78]. It is likely that the propane in reaction 34-BKW-63 results from a mechanism other than the normal heterogeneous/homogeneous mechanism of methane coupling. Release of a significant amount of methyl radicals from the catalyst surface in the presence of product ethylene should result in some propylene. The absence of propylene therefore suggests that this does not occur. The presence of propane without propylene is consistent with a mechanism of conversion of methane to ethane followed by coupling of ethyl and methyl radicals, all on the catalyst surface. One might argue that the gas phase reaction product distributions (higher C_3's compared with C_2's) are significantly changed at 650 °C, or that propylene is selectively burned at 650 °C, but it is believed that these results demonstrate the principle of enhanced surface reaction during methane coupling.

Since these results were obtained, Matsuhashi[79] reported that a Na/ZrO_2 catalyst gives C_3 hydrocarbons as the main products during the oxidative coupling of methane. Their catalyst produced more C_3 than C_2 products with the C_3 hydrocarbons being 77% propane and 23% propylene. Another reference[39] reports high C_3 and C_4 yields with bivalent metal halides catalysts [46.8% of the hydrocarbons (38.6% overall selectivity including carbon oxides) are butenes over $BaBr_2$/pumice and 24.1% of the hydrocarbons (14.3% overall selectivity) are butenes with $CaBr_2$/MgO].

Silver catalysts were made containing lanthanum oxide, because one patent example[39] claimed a Ag/La_2O_3 (unsupported) catalyst among catalysts for methane conversion including Group IIA, IIIA, lanthanide series or mixtures of these components. It was desired to determine if the presence of La in catalysts containing silver would provide any advantage over silver catalysts not containing lanthanum. Results for methane coupling over catalysts containing silver with and without La are summarized in

Table 35 below. The results show that C_2 selectivities and C_2 yields are similar for silver catalysts with and without La.

Table 35. Silver Catalysts for Methane Coupling

Ref	Cat	T, °C	CH_4C	C_2 Yield	C_2 Sel	=/–	GHSV	Time, m	ECl
34-36	$Ba/Ag/Al_2O_3$	670	17	4.5	25	0.6	1263	205	5
34-37	$Ba/La/Ag/Al_2O_3$	670	16	4.5	28	0.6	1263	290	5
34-44	$Ba/La/Ag/Al_2O_3$	670	27	4.1	15	0.6	1263	325	5
34-50	$Ba/Ag/Al_2O_3$	675	23	6.6	29	0.6	1171	235	5
		675	21	6.5	30	0.7	1171	4060	500
34-51	$Ba/La/Ag/Al_2O_3$	675	27	7.2	27	0.6	1171	280	5
		675	27	8.2	30	0.8	1171	4105	500

Catalysts were prepared with barium chloride, using one method of silver deposition for catalysts in reactions 34-BKW-36, 37, and 44, and another method of silver deposition to prepare the catalysts used in reactions 34-BKW-50 and 51. These two types of silver catalysts contain different amounts of silver (see Appendices C and D). In reactions 34-BKW-50 and 51, 500 ppm ethyl chloride were added in the gas feed near the end of the runs (675 °C). The methane conversion, C_2 selectivity, and C_2 yield were rapidly rising when the runs were stopped. Higher C_2 yields might be expected from lined-out reactions with optimized ethyl chloride levels.

Figure 53 shows methane conversion, C_2 selectivity, C_2 yield, and ethylene to ethane product ratio for the oxidation of methane at 650 °C over a 17% $SrCl_2$/9% Ag/Al_2O_3 catalyst. As in the examples above, C_2 products can be obtained at lower temperatures with these catalysts containing silver than with typical literature methane coupling catalysts. The rates to C_2 products, the C_2 yield (nearly 9%), and the C_2 selectivity (45%) are higher using 500 ppm ethyl chloride in the feed gas rather than 10 or 50 ppm ethyl chloride with this catalyst.

Figure 53. 17% $SrCl_2$/9% Ag/Al_2O_3, 36-BKW-41

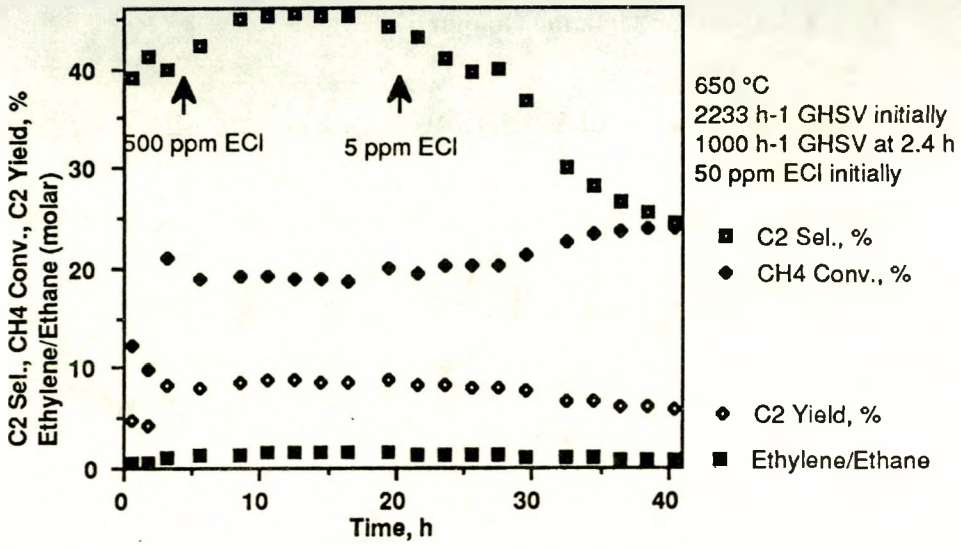
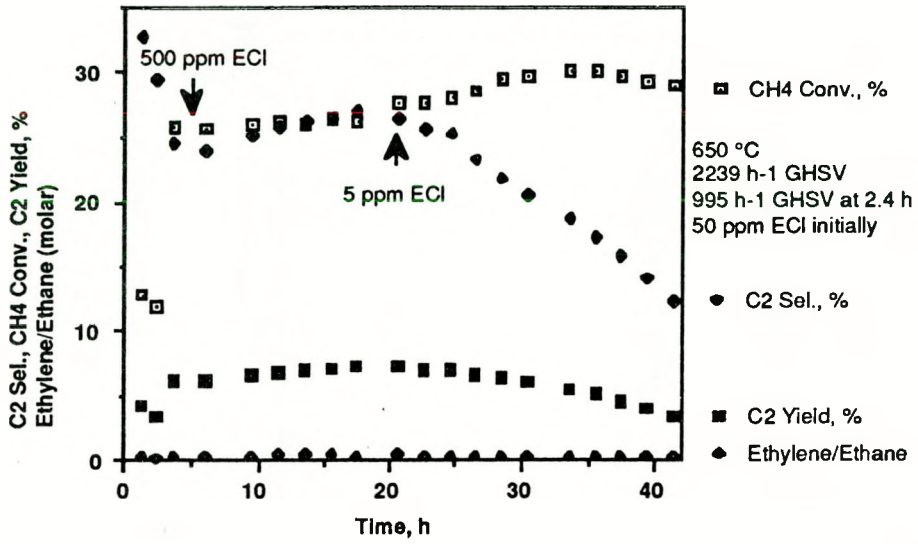


Figure 54 shows the same parameters for a 6% $SrCl_2$/9% Ag/Al_2O_3 catalyst (with C_2 yields of over 7% and C_2 selectivities of only about 25%). No propylene is produced in these reactions, and the C_2/C_3 product ratios vary from 6-25 on a molar basis.

Figure 54. 6% $SrCl_2$/9% Ag/Al_2O_3, 36-BKW-42



C_2 yields and selectivities are higher on the catalyst with a higher level of strontium chloride.

For both catalysts with 500 ppm ethyl chloride in the feed gas, Figures 55 and 56 show relatively constant rates to products over periods of about 10 hours (as long as these conditions were used). It may be seen that the C_2 selectivities and yields are higher for the catalyst with the higher level of strontium chloride, not because C_2's are produced at a higher rate on the catalyst with 17% strontium chloride, but rather because the catalyst with 6% strontium chloride produces such high levels of carbon dioxide.

Figure 55. 17% $SrCl_2$/9% Ag/Al_2O_3, 36-BKW-41

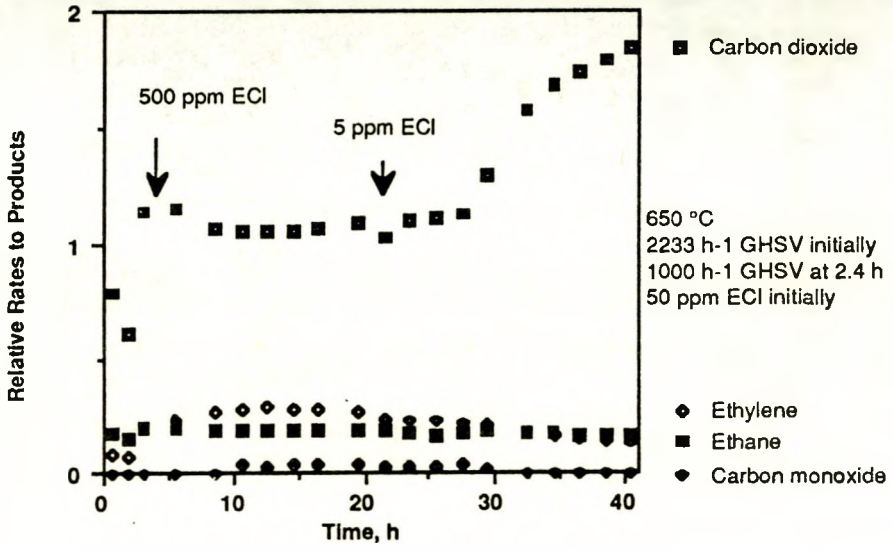
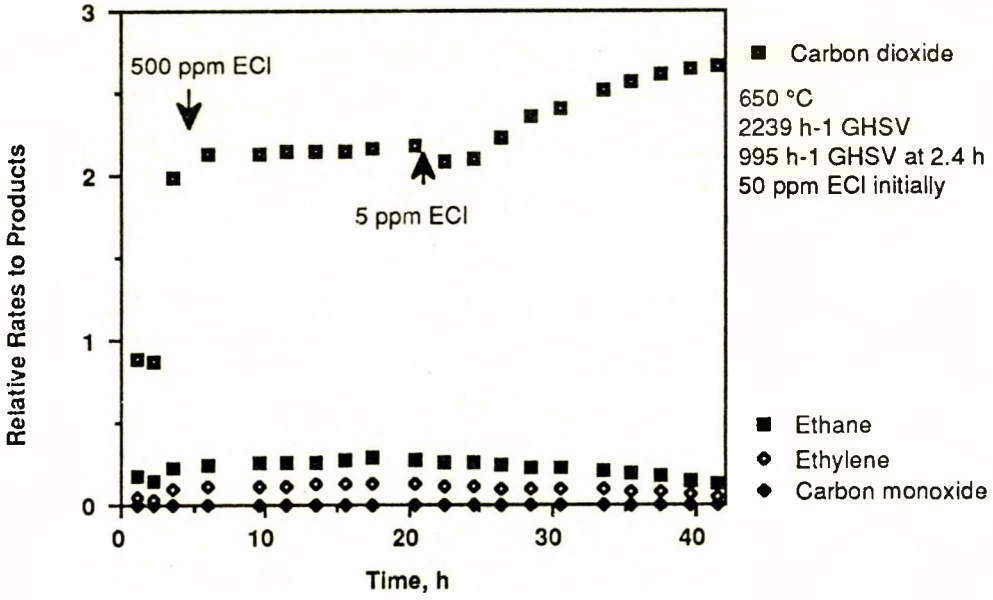


Figure 56. 6% $SrCl_2$/9% Ag/Al_2O_3, 36-BKW-42



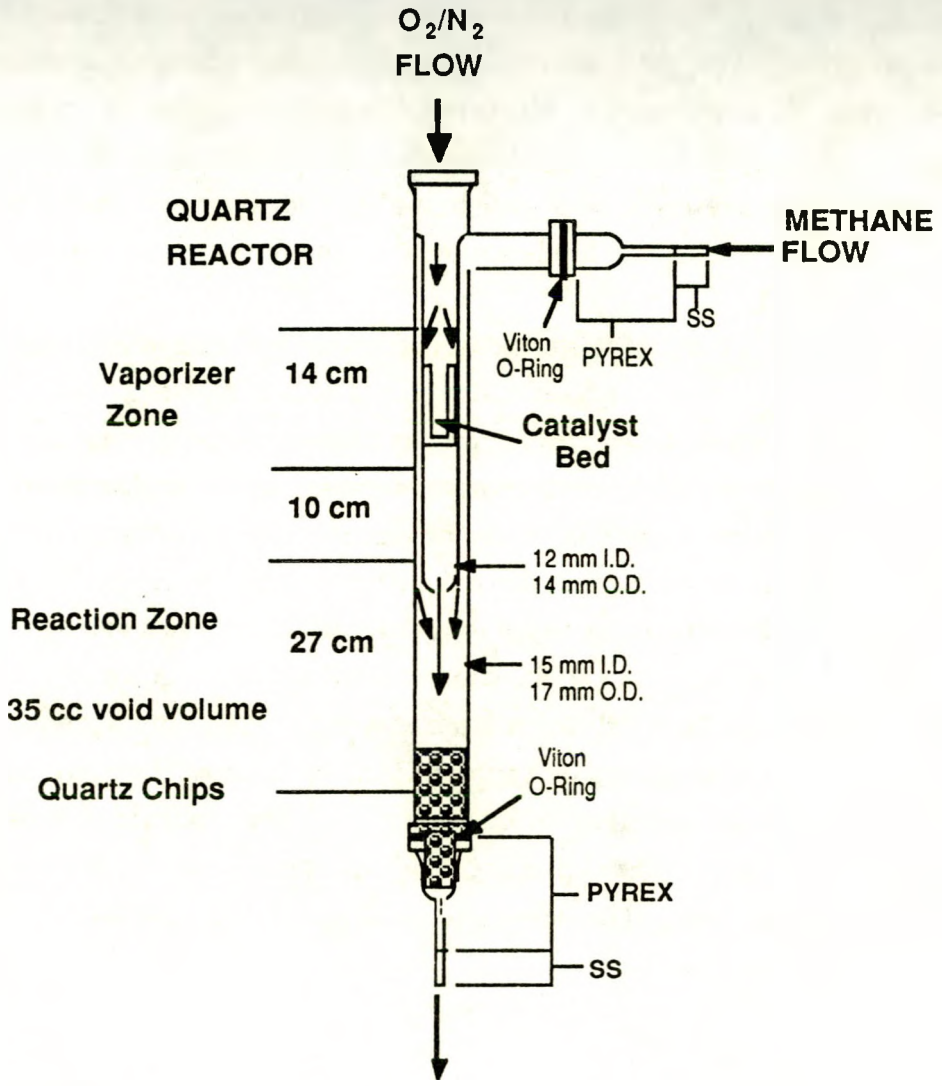
Vapor Phase Catalysts

The second approach suggested to avoid the heterogeneous/homogeneous mechanism is to change the gas phase chemistry to depart from the typical combustion reaction network. As an example, a volatile metal complex is oxidized to some state, for instance a superoxide, which abstracts a hydrogen atom from methane. The complex does not have as large a reservoir of oxygen to further oxidize the new methyl radical, as an oxidized surface would. Methyl radicals therefore couple in the gas phase rather than being further oxidized.

Alternately, volatile complexes could be used to quench the hydroperoxides which convert methane coupling intermediates and products to carbon oxides. Volatile catalysts could also be used to increase the rate of hydrogen abstraction and shift the gas phase reaction away from the typical heterogeneous/homogeneous product distribution, as halogen radicals were shown to do in producing higher ethylene to ethane product ratios.

The reactor used for vapor phase catalyst studies is shown in Figure 57. Oxygen and nitrogen are introduced into the top of the reactor which is heated in the vaporizer zone by one oven. The catalyst or additive to be volatilized is in a quartz cup within the vaporizer zone. Methane is added so that it mixes with the oxygen/nitrogen/vapor phase catalyst mixture in a reactor heated by a second oven. In this way, reactions may be conducted with or without volatile catalysts present, since the vaporizer zone oven can be turned on or off as desired. When operating with vapor phase catalysts, the volatile catalyst components are trapped in the cool quartz chips located in the bottom of the reactor.

Figure 57. Vapor Phase Catalytic Reactor



Results are shown in Table 36. Methane conversion is decreased significantly by addition of volatile CsCl to a methane oxidation reaction in an empty, heated reactor space. Since the methane is essentially all converted to carbon oxides under these conditions, the volatile catalyst reduces the rate of homogeneous methane conversion to carbon oxides. This is shown for temperatures of 650 and 750 °C. The effect can be shown by either adding the vapor phase catalyst, which results in a drop in methane conversion, or by stopping volatile catalyst addition, which results in an increase in methane conversion, as shown in Table 36. Results for LiCl were similar to those

obtained with CsCl. Experimental conditions and results for all vapor phase catalysts are shown in Tables F4 and F5 of Appendix F.

Table 36. Vapor Phase CsCl Catalyst

Vaporizer Zone T, °C	Reaction Zone T, °C	CH_4 Conv., %
196	650	5
600	650	0.8
650	750	4
226	750	15

The effect of volatile metal/salts on the homogeneous methane conversion was studied in the presence of a catalyst. Catalyst conditions and volatile chloride levels were not optimized, but results in Table 37 show an increase in selectivity to C_2's and a decrease in CO_2 formation upon addition of volatile catalyst to a methane coupling reaction over a used $BaCO_3/Cl/\alpha\text{-}Al_2O_3$ catalyst. This is interpreted as a reduction in the gas phase conversion of methane to carbon oxides, allowing the methane which would have reacted in the gas phase to react on the catalyst surface to produce C_2's. These results demonstrate the concept of changing the gas phase chemistry during methane oxidation with volatile catalysts, promoters, or inhibitors.

Table 37. Vapor Phase CsCl Over 4 g of $BaCO_3/Cl/\alpha\text{-}Al_2O_3$ Catalyst

Vaporizer T, °C	Reaction T, °C	CH_4 Conv. %	C_2 Sel. %	CO_x Sel. %
160 sccm feed gas flow rate, 0 ppm ECl				
185	750	21	46	51
750	750	21	53	44
80 sccm feed gas flow rate, 40 ppm ECl				
188	750	39	28	70
750	750	36	38	60

Metals in Activated States

A molecular orbital study of CH activation of methane by a Bi_2O_3 surface concluded[80] that barriers to the formation of surface OH^- and gas-phase methyl radicals decrease as the bismuth oxidation state increases. This is because the radical electron from hydrogen is promoted by σ-bond formation to successively lower-energy bismuth orbitals as the state of bismuth oxidation increases. Experimental results confirmed this trend. This trend, lowering of the activation energy for the formation of metal hydroxide by abstraction of hydrogen radical from methane, is predicted to apply to other metal oxides as well as to bismuth. Indeed, in literature examples where methane is fed in the absence of oxygen, the catalysts are stated to lose activity as the catalyst oxidation state becomes lower prior to catalyst regeneration in oxygen, even when an excess of available oxygen exists for reaction.

One idea for methane coupling proposed[81] was the study of catalysts in which well-defined, stable lattice structures stabilize unusual oxidation or coordination states of metals. High oxidation states and configurations with unpaired electrons are particularly desirable, as described above. Two of the classes of catalysts proposed[81] for these studies were perovskites and metal/molecular sieves. The study of perovskites is reported below in the KDC Laboratory Section.

Metal Molecular Sieve Catalysts

Metals in unusual oxidation states have been found to be stable in molecular sieves. Zeolites act as a solid matrix stabilizing odd electron states including Cu^{+}, Rh^{2+}, and Co (0) [82]. Many atypical metal oxidation states were detected by esr because of unpaired electrons. These materials might show activity for abstracting hydrogen from methane to form the methyl radical necessary for coupling to C_2's. Ions in molecular sieves detected by esr include Pd(I), $4d^9$; Pd(III), $4d^7$; Co^{2+}, d^7; Ni^{+}, d^9; and Cr^{5+}, d^1 [83]. Gallium promoted zeolites and crystalline galloaluminosilicates have been found[72-75] to efficiently convert alkanes to aromatics. In one of the patents published in this area[72], methane was converted to aromatics. It is thought that the gallium is in an environment in which it is particularly reactive for the activation of alkanes, since the conversion of methane selectively to aromatics can not be accomplished with gallium alone or with the sieve alone. Clearly, the environment in a zeolite is capable of supporting highly active states of metals. The zeolites in the reported patents have large pores. If small pore molecular sieves were substituted for the reported medium-pore materials, one might be able to effect the selective conversion of methane to light olefins including ethylene.

Other metal loaded molecular sieves have been reported to be highly active and selective in reactions involving hydrogen abstraction. A cesium-exchanged zeolite was found[84-89] to catalyze the alkylation of toluene with methanol to give styrene and ethylbenzene. It is likely that this reaction has hydrogen or proton abstraction as an essential step, followed by dehydrogenation of the alkylated product, ethyl benzene, to styrene. Similar catalysts prepared with smaller pore molecular sieves are of direct interest for methane coupling.

Molecular sieves with metals in the framework were of particular interest because of the possibility that metal ions locked into these structures might be stabilized in unusually active forms by being stabilized in unusual oxidation or coordination states. Available framework metal molecular sieves were therefore tested for methane coupling. Those of most interest contain metal ions which are components of methane coupling catalysts reported in the literature to be good (e.g., manganese).

Molecular sieve materials tested included those containing manganese, magnesium, cobalt, and phosphorus. These are listed in Appendix C and D. All were unselective, and some (MAPO 34, 29-BKW-147, MAPO 36, 30-BKW-80, and the highly acidic molecular sieve, 30-BKW-95) were surprisingly unreactive (may have quenched the

homogeneous reaction). Those catalysts examined by powder x-ray diffraction were found to have been unstable under reaction conditions, having lost crystallinity (ALPO-5, SAPO-5, MAPO-36, and the highly acidic molecular sieve).

No selectivities to C_2's above 30% were obtained using these molecular sieves as catalysts with 10% oxygen, 5% oxygen, and balance nitrogen, at 11 psig and space velocities of 1875 to 5455 h^{-1}. With the exception of the highly acidic molecular sieve, methane oxidation began at 600 or 700 °C. Methane conversions varied from 4.4% to 27% at 700 °C. The highly acidic molecular sieve was tested first at 250 °C, but even at 700 °C, methane conversion was less than 4% (which is comparable to or lower than control levels). Catalysts containing Mn and Co exhibited low C_2 selectivities (3-23%) at methane conversions varying from 13-27% at 700-800 °C. The highest C_2 yield obtained with any of the molecular sieves tested was 3.5% (28.5% C_2 selectivity). A summary of results is presented in Table F6 of Appendix F.

Base Catalysts - Hydrotalcites

Hydrotalcites are interesting layered, basic inorganic materials containing magnesium and aluminum cations, and hydroxide and carbonate anions, usually also containing water. It was thought that these materials would be a good starting material for catalysts and supports. The elemental composition of the materials used were:

$$Mg_6Al_2(OH)_{16}(CO_3^{=})\cdot\sim 4H_2O$$

The Mg/Al ratio of the bulk compounds is approximately 3. The surface compositions of the hydrotalcites are described in Procedure R of Appendix C.

A uniform and pure MgAl oxide was of interest, since different supports have been observed to produce catalysts with widely different methane coupling abilities, and because this material might be a precursor to materials with finely dispersed metal ions. Three samples of hydrotalcites were heated at 450 °C for 18 hours in air, heated at 850 °C for 4 hours in air, then tested for methane coupling activity (33-BKW-33, 34, and 39). Upon heating these materials at 450 °C, they lose carbon dioxide to produce $Mg_6Al_2O_8(OH)_2$. Further heating results in $MgAl_2O_4$ (spinel). The resulting materials were highly active but unselective for the conversion of methane to C_2's.

Three samples of hydrotalcites which had been heated to only 450 °C were doped with $BaCO_3$, then heated at 850 °C for 4 hours. These were also tested for methane

coupling activity (33-BKW-42, 43, and 48), and were also found to be highly active but unselective for the conversion of methane to C_2's. Results for hydrotalcite catalysts are summarized in Table F7 of Appendix F.

KDC Laboratory

Homogeneous Methane Oxidation

Recently, literature reports have addressed the question of the importance of the homogeneous oxidation of methane during catalytic oxidative coupling studies. Yates and Zlotin[90] studied methane coupling over lithium/magnesium oxide (Li/MgO) catalyst at atmospheric pressure and reported the formation of significant quantities of ethane and ethylene in the absence of a catalyst. They concluded that Li/MgO was mainly a combustion catalyst that produced more C_2's than the homogeneous reaction but at the cost of converting carbon monoxide to carbon dioxide. Hutchings, Scurrell, and Woodhouse[91] compared the homogeneous gas phase oxidation of methane to the reaction over Li/MgO at elevated pressures. At 520 °C and 5.8 atmospheres, they found that the catalyst appeared to have only limited effects. It enhanced the production of carbon oxides and hydrogen without significantly affecting the production of C_2's. Wolf and Lane[10] reported that at one atmosphere significant homogeneous gas phase oxidative coupling of methane occurred under certain experimental conditions. For a methane conversion of 2%, a hydrocarbon (C_{2+}) selectivity of 65% was reported. When the methane conversion was increased to 32%, a C_{2+} selectivity of 30% resulted with a C_{2+} yield of 9.6%. Fujimoto and coworkers[92,93] reported that the noncatalytic oxidative coupling reaction of methane was enhanced under pressurized conditions (up to 15.8 atm) in a temperature range from 650 to 800 °C. However, the best C_2 yields reported were less than 6%.

In order to measure the extent of the uncatalyzed homogeneous methane oxidation and the effects of experimental variables on the homogeneous oxidation a statistically designed set of 19 experiments was performed. Experimental independent variables of interest were:

VARIABLE	RANGE	CENTER VALUE
T = Reactor temperature (°C)	(650 - 850)	750
P = Reactor pressure (psig)	(5 - 15)	10
M = Methane/oxygen (molar ratio)	(2 - 15)	8.5
F = Flow rate in reactor (cc/min)	(100 - 300)	200

Additional experiments were also carried out to measure the effects of surface area on the extent of the homogeneous reaction.

Experiments were carried out in random order with the exceptions that centerpoint values were used for the first, last, and middle experiments. A quartz reactor packed with 20 to 40 mesh washed quartz chips was used for all experiments. A complete description of the experimental procedure is presented in Appendix A. The reported temperatures are the values measured at the center of the tube furnace. The methane/oxygen mole ratio defined the reactant stream composition since only air (N_2/O_2 mole ratio = 3.8) and methane were mixed to form the reactant stream. The measured void volume in the heated region of the packed reactor was 25.1 cc. A summary of all experimental results from the statistically designed set is presented in Table F8 of Appendix F.

High C_2 selectivities (51-59%) were obtainable; however, the high selectivities occurred only for low methane conversions (<5%). For higher methane conversions (>35%), the best C_2 selectivity observed was only 25%.

High ethylene to ethane product ratios (4-10) were obtained for runs at high temperatures (850 °C) and long residence times (14-15 seconds). This was expected since these conditions favor the homogeneous conversion of ethane (formed by the coupling of methyl radicals) to ethylene.

The highest C_2 yield observed in the experimental set was 8.6%. This result is in agreement with a maximum C_{2+} yield of 9.3% reported by Wolf and Lane[10] for the homogeneous oxidation of methane. Higher products have not been reported in the literature and it will be difficult, if not impossible, to obtain higher values from the homogeneous oxidation reaction alone.

Statistical analyses of the results were performed and regression models were developed. Many of the statistical models omit experimental variables, such as residence time and pressure, due to the fact that the extent of reaction went from almost no reaction at 650 °C to substantial reaction (complete O_2 conversion in many cases) at 850 °C, which caused the observed temperature effect to swamp the effects of variables of lesser importance. For this reason, models that omit experimental variables should be

considered correct only if the omitted variables are assigned the values at the midpoint temperature (750 °C). For example, the equation for CH_4 conversion (C-conv) is correct for a pressure of 10 psig and a residence time of 9.3 seconds.

A summary of the models in exponential form follows.

Independent Variables: Centered variables obtained by subtracting the midpoints of the ranges

T* = (Temperature in °C) - (750)

P* = (Pressure in psig) - (10)

M* = (Methane/oxygen molar ratio) - (8.3)

R* = (Residence time in seconds) - (9.3)

Dependent Variables:

C-conv = CH_4 conversion in %

O-conv = O_2 conversion in %

C_2-sel = C_2 selectivity in %

C_3-sel = C_3 selectivity in %

C_2 yield = (CH_4 conversion X C_2 selectivity) in %

(=/-) = Ethylene to ethane molar ratio

Models:

$$\text{C-conv} = 2.52 \cdot e^{0.017T^*} \cdot e^{-0.1606M^*}$$

As expected, methane conversion increases exponentially with temperature and decreases with methane/oxygen ratio. The model is unbounded (no upper limit) since methane was the excess reagent in all experiments.

$$\text{O-conv} = \frac{100}{1 + 5.51 \cdot e^{-0.03246T^*}}$$

Oxygen conversion increases exponentially with temperature towards its upper limit (100%).

$$C_2\text{-sel} = \frac{}{1 + 1.79 \cdot e^{-0.10338M^*} \cdot e^{0.07329R^*} \cdot e^{0.008M^*R^*}}$$

C_2 selectivity increases with methane/oxygen ratio and decreases with residence time. The reduction with residence time is due to the further reaction of the C_2 products. It is interesting that the model is not a function of temperature since C_2 selectivity increases with temperature in catalytic methane partial oxidation studies.

$$C_3\text{-sel} = 0.69 \cdot e^{0.01515T^*} \cdot e^{0.0009055T^*M^*}$$

$$C_2 \text{ yield} = 0.93 \cdot e^{0.01532T^*} \cdot e^{-0.077275M^*}$$

The C_2 yield is a function of temperature and methane to oxygen ratio similar to the model for methane conversion (C-conv).

$$(=/-) = 0.58 \cdot e^{0.01942T^*}$$

The temperature effect on the ethylene to ethane product ratio is much greater than any of the other variables; thus, it masks their effects.

The study showed that the homogeneous gas phase oxidation of methane was too large to allow the separation of catalytic effects from gas phase effects at temperatures above 800 °C using the study's experimental conditions. For studies in this high temperature region, the residence times of reactants and products in the heated region must be lowered (less gas phase oxidation) by either increasing the reactant flow rate or by using reactors with smaller void volumes.

Since the models showed no sensitivities of dependent variables to pressure, the effect of reactor pressure on the extent of homogeneous reaction was further examined by running pressures of 5 psig and 15 psig at 750 °C and 800 °C (2:1 ratio of CH_4:O_2; reactor filled with 20 to 40 mesh quartz chips). The residence times were 7.2 seconds at 750 °C and 4.8 seconds at 800 °C. Residence times were chosen to give similar CH_4 conversions at 5 psig (CH_4 conversions approximately 13%) and were adjusted by changing flow rates. The expected trend that increasing the pressure results in a greater rate of the homogeneous reaction of methane was clearly seen. When the pressure was

increased from 5 psig to 15 psig, the CH_4 conversions increased from 13% to 36% at both temperatures (O_2 conversions from 26% to 84-88%) The C_2 selectivity decreased (35-37% to 20-23%) with the increasing conversion while the ethylene to ethane product ratio increased (1.3-1.5 to 2.8-3.1).

The pressure effect seems independent of temperature at 750 °C and 800 °C. Even though residence times were chosen to give equal CH_4 conversions at 5 psig, it is surprising how closely the CH_4 conversion and C_2 selectivity match for the two temperatures when the pressure increases from 5 psig to 15 psig. The C_2 selectivities (20% versus 23%) and ethylene to ethane product ratios (2.8 versus 3.1) were slightly larger for a given methane conversion at the higher temperature.

Experiments were carried out using unpacked reactors to study the effect of the quartz surface on the extent of the uncatalyzed reaction. For the study, experimental conditions were chosen to match those of three runs in the designed sequence (Experiments 8, 14, and 19) except that the flow rates were increased to give the same residence times as the corresponding quartz packed reactor experiments. The results indicate that the quartz surface inhibits the uncatalyzed reaction. At 850 °C ($CH_4/O_2/N_2$ = 2.1/1/3.8; residence time = 4.8 sec), the CH_4 conversion decreased from 43% to 35% and at 750 °C ($CH_4/O_2/N_2$ = 8.2/1/3.8; residence time = 7.3 sec) it decreased from 3.4% to 2.1% when a quartz packed reactor was used in place of an empty reactor. The very large effect seen at 650 °C ($CH_4/O_2/N_2$ = 2.1/1/3.8; residence time = 14.4 sec) was unexpected. The CH_4 conversion decreased from 30% with the empty reactor to 3.3% with the quartz-filled reactor.

It is known that the homogeneous gas phase oxidation of methane proceeds by a complex chain branching free radical mechanism. The observed inhibition of the uncatalyzed reaction by the quartz surface could be explained by a surface reaction of a chain branching intermediate, such as $HO_2\bullet$ or H_2O_2, resulting in chain termination. The greater effect at lower temperatures (650 °C) could be due to more efficient surface chain termination or to more importance in the branching mechanism of the terminating species at the lower temperature relative to other reactions.

This study shows the homogeneous gas phase oxidation of methane can be significant under certain experimental conditions. However, C_2 yields greater than 10% are probably not possible from the homogeneous reaction alone. Also, the extent of the homogeneous reaction can be greatly diminished by the quartz reactor surface, especially at temperatures less than 700 °C. It is important to note that the purity and source of the

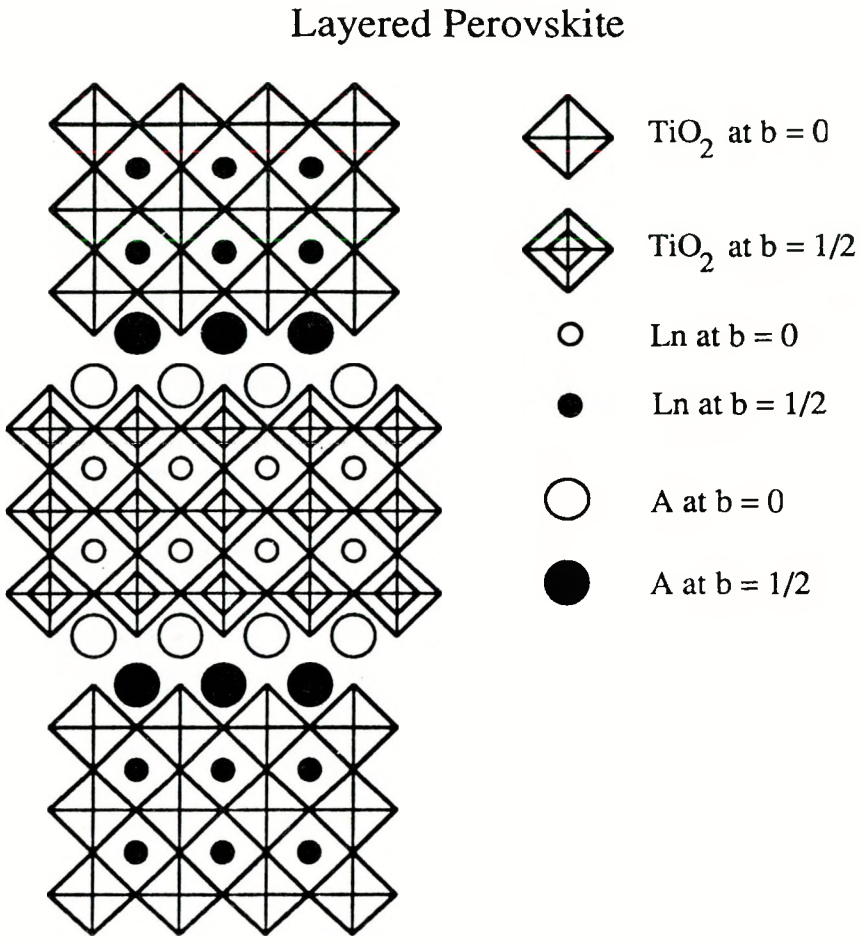
quartz can result in entirely different results since other quartz chips have been tested which increase the homogeneous oxidation reaction.

Layered Perovskites ($A_2Ln_2Ti_3O_{10}$)

Alkali doped lanthanide oxides have been reported to be very active catalysts for the oxidative coupling of methane. These materials are operated at high temperatures (usually 800 °C) and prepared using slurry or incipient wetness techniques. The high temperatures cause the loss of alkali components during reaction while the preparation methods result in catalysts in which the dispersion and location of the alkali components are not readily controlled. In order to alleviate some of these problems, layered perovskites containing layers of alkali ions dispersed and sandwiched between lanthanide perovskite layers were tested as methane coupling catalysts.

Layered perovskites of the form $A_2Ln_2Ti_3O_{10}$ (A=K,Rb; Ln=La,Nd,Sm,Gd,Dy) were first synthesized by J. Gopalakrishnan and V. Bhat[94]. These materials were prepared with the objective of forming Ruddlesden-Popper type layered oxides (with the general formula $A_2[A_{n-1}B_nO_{3n+1}]$, where $[A_{n-1}B_nO_{3n+1}]$ perovskite type slabs of n octahedra in thickness are interleaved by A cations) capable of exhibiting ion exchange and intercalation behavior. These materials are composed of three octahedra-thick perovskite slabs $[Ln_2Ti_3O_{10}]$ separated by alkali metal ions (Figure 58).

Figure 58. Structure of $A_2Ln_2Ti_3O_{10}$



In this structure the alkali and lanthanide species are in close contact with the lanthanide species in a perovskite environment. Potassium ions of $K_2Ln_2Ti_3O_{10}$ are easily exchanged with Na^+ or Li^+ by treating with molten alkali-metal nitrates.

Layered perovskites are prepared by grinding together appropriate mixtures (correct molar ratios of metals) of alkali carbonate, lanthanide oxide, and titanium dioxide and heating in air at 1000 °C for 8-12 hours. Mixtures are then reground and heated in air at 1000 °C for another 8-12 hours. Excess alkali carbonate (~20 mol%) is initially added to compensate for loss due to volatilization. More alkali is added after the first heating.

The layered perovskite $Na_2La_2Ti_3O_{10}$ is prepared by ion exchange of $K_2La_2Ti_3O_{10}$ in molten $NaNO_3$. Detailed preparation procedures are given in Appendix C.

Layered perovskites prepared include $K_2La_2Ti_3O_{10}$, $K_2Nd_2Ti_3O_{10}$, $K_2Sm_2Ti_3O_{10}$, $K_2Dy_2Ti_3O_{10}$, $K_2Gd_2Ti_3O_{10}$, $Rb_2La_2Ti_3O_{10}$, and $K_2Ce_2Ti_3O_{10}$, which had powder

x-ray diffraction patterns consistent with the structure reported for $K_2La_2Ti_3O_{10}$. Diffraction patterns were not obtained for $Na_2La_2Ti_3O_{10}$ or $K_2Pr_2Ti_3O_{10}$, which were also prepared.

These catalysts (1.0-4.0 g) were tested with flow rates of 50-200 ccm, a reactor pressure of 5 psig, and a $CH_4/O_2/N_2$ ratio of 2/1/3.8. A complete description of the experimental procedure is given in Appendix A.

The highest C_2 yield and selectivity to C_2's were obtained for $K_2La_2Ti_3O_{10}$, with a 39% methane conversion, a 42% selectivity to C_2's and a 16.4% C_2 yield, at 800 °C.

The following table (Table 38) gives comparative results for the materials prepared.

Table 38. Methane Coupling Results for $A_2Ln_2Ti_3O_{10}$ Layered Perovskites

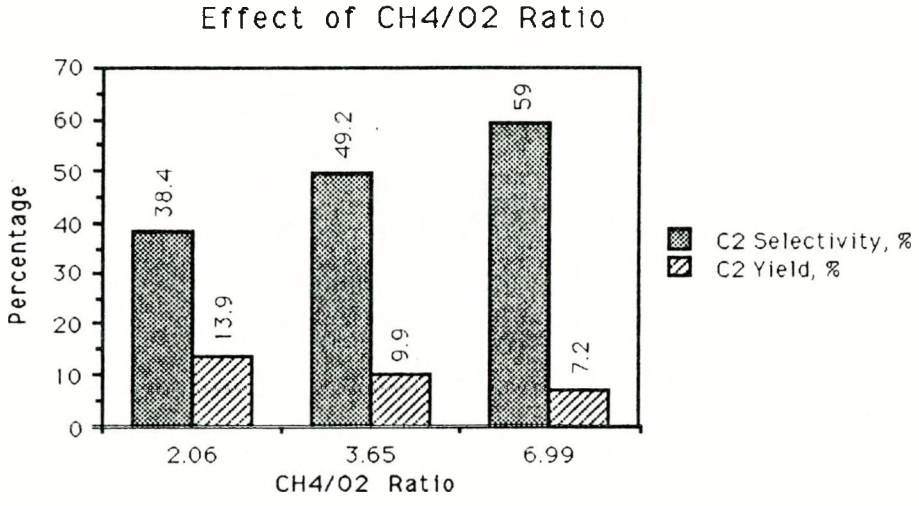
Catalyst	GHSV (h^{-1})	CH_4 Conv.	C_2 Yield	T(°C)
$K_2La_2Ti_3O_{10}$	3000	39% (42)*	16.4%	800
$K_2Nd_2Ti_3O_{10}$	3750	26% (24)	6.3%	800
$K_2Sm_2Ti_3O_{10}$	3000	25% (23)	5.8%	801
$K_2Dy_2Ti_3O_{10}$	3430	25% (16)	3.9%	800
$K_2Gd_2Ti_3O_{10}$	1770	29% (20)	5.7%	800
$Rb_2La_2Ti_3O_{10}$	4500	21% (31)	6.6%	807
$Na_2La_2Ti_3O_{10}$	4620	35% (28)	9.8%	800
$K_2Pr_2Ti_3O_{10}$	3430	34% (40)	13.2%	800
$K_2Ce_2Ti_3O_{10}$	571	29% (33)	9.6%	800

*: C_2 selectivity,%, given within parenthesis

Catalysts were prepared and tested to determine if alkali doping (20 wt% Na_2CO_3, 36 wt% K_2CO_3, and 40 wt% Li_2CO_3) of the $K_2La_2Ti_3O_{10}$ layered perovskite would improve the catalytic performance. The alkali dopings had little effect on the C_2 selectivities (C_2 selectivity ranges from 38-41%) but did result in decreased activity especially for the Na and Li dopants. These results were expected since the layered structure has alkali ions (K^+) associated in the structure with the active lanthanide species. Additional alkali doping should not affect the C_2 selectivity since the lanthanide species already have alkali ions in close proximity and could decrease activity due to the coating of the active surface with the alkali dopant.

The effects of changing the CH_4/O_2 ratio on the coupling process were determined for $K_2La_2Ti_3O_{10}$, $Rb_2La_2Ti_3O_{10}$, and $Na_2La_2Ti_3O_{10}$. Figure 59 depicts the effects observed on the C_2 selectivity and C_2 yield at different CH_4/O_2 ratios for $K_2La_2Ti_3O_{10}$ (T = 800 °C; GHSV = 3640 h^{-1}). As expected, higher CH_4/O_2 ratios resulted in higher C_2 selectivities but lower C_2 yields due to the decreased CH_4 conversions.

Figure 59. Effect of CH_4/O_2 Ratio on C_2 Selectivity and C_2 Yield



For all three catalysts, the CH_4 conversion, C_2 yield, ethylene to ethane product ratio, and CO_2/CO ratio decreased while the O_2 conversion and C_2 selectivity increased with increasing CH_4/O_2 ratio.

The effects of changing the amount of diluent in the feed stream (changing the partial pressures of the reactants) were measured for the $K_2Pr_2Ti_3O_{10}$ and $K_2Ce_2Ti_3O_{10}$ layered perovskites. In the experiment, the feedstream composition of $CH_4/O_2/N_2$ was changed from 2/1/3.8 to 2.1/1/18 (T = 800 °C; GHSV = 3070 h^{-1} for $K_2Pr_2Ti_3O_{10}$ and 1540 h^{-1} for $K_2Ce_2Ti_3O_{10}$). This resulted in a change of the partial pressures of CH_4/O_2 from 5.8 psia/2.9 psia to 2.0 psia/0.94 psia. The lowering of the partial pressures by increasing the diluent resulted in a slight decrease in the methane conversion but a significant increase in the C_2 selectivity. For $K_2Pr_2Ti_3O_{10}$, the CH_4 conversion decreased from 23.7% to 22.0% while the C_2 selectivity increased from 29% to 37%. For $K_2Ce_2Ti_3O_{10}$, the CH_4 conversion decreased from 28.9% to 27.4% while the C_2 selectivity increased from 33% to 41%. Since it is impossible to separate the contribution

of the gas phase homogeneous reaction from the heterogeneous reaction, it is unclear if the effects noted are due to changes in the catalytic heterogeneous reaction. However, the results show that the amount of diluent does affect the overall results.

The effects of changing the temperature on the coupling process were also determined for $K_2La_2Ti_3O_{10}$, $Rb_2La_2Ti_3O_{10}$, and $Na_2La_2Ti_3O_{10}$. For each catalyst, increasing temperature results in both increased CH_4 conversion and increased C_2 selectivity. Also, O_2 conversion, ethylene to ethane product ratio, and CO_2/CO ratio increased with increasing temperature.

Increasing CH_4 and O_2 conversions with increasing temperature is expected since higher temperatures increase the rate of the reaction and there is no equilibrium attained between the reactants and products. The increased ethylene to ethane product ratio with increased temperature is due to increased rates for the ethane -----> ethylene conversion. This reaction occurs primarily in the gas phase through an ethyl radical, $C_2H_5^{\bullet}$, intermediate formed by the abstraction of a hydrogen atom from ethane by either an oxygen molecule, a methyl radical, or the catalyst surface.

The increased C_2 selectivity with increasing temperature is due to the heterogeneous/homogeneous nature of the catalytic process. Higher temperatures shift the

$$CH_{3(ad)}^{\bullet} \text{ -----> } CH_{3(g)}^{\bullet} \quad \text{and the} \quad CH_{3(g)}^{\bullet} + O_{2(g)} \text{ ------> } CH_3O_{2(g)}^{\bullet}$$

equilibria towards the $CH_{3(g)}^{\bullet}$ radicals which couple in the gas phase to form ethane. Also, literature studies on the kinetics of the catalytic methane coupling reaction report that C_2 formation has a higher activation energy than CO_x formation. Thus, higher temperatures would be favorable to the formation of C_2's.

Layered perovskites of the form $A_2Ln_2Ti_3O_{10}$ represent a new type of methane coupling catalyst in which the alkali dopant is part of the crystal structure of the material. They give coupling results comparable to many of the reported literature methane coupling catalysts and show trends for increasing temperatures and CH_4/O_2 reactant ratios consistent with those reported in the literature.

Low Temperature Catalysts

For a methane oxidative coupling process to be commercially attractive, good rates of conversion of methane with high selectivities to higher hydrocarbons (C_2

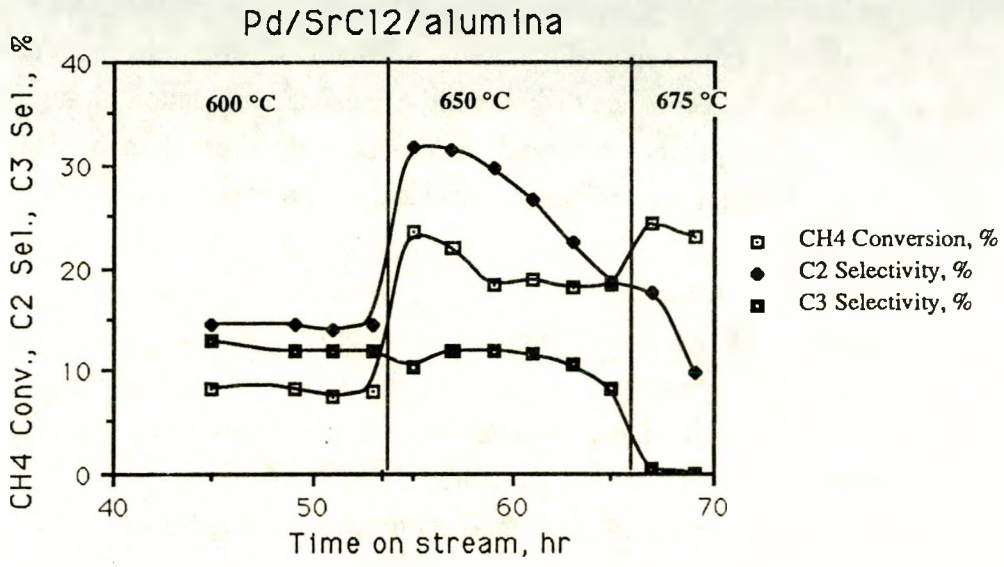
hydrocarbons) are required. Thus, catalytic processes are a requirement if methane oxidative coupling process are to become commercially attractive. At present, catalytic methane oxidative coupling processes require fairly high temperatures (in excess of 700 °C) which necessitate special materials of reactor construction, cause catalyst stability problems, and enhance the unselective gas phase oxidation of the reactants and products. Lower temperature catalysts could remove these problems as well as result in a shift from the heterogeneous/homogeneous catalytic process to one that is mainly heterogeneous. Such a low temperature catalyst must exhibit reasonable activity at the lower temperature while maintaining high C_2 selectivities.

With this reasoning, mixed catalysts were prepared and tested in which one component which exhibited good C_2 selectivities was doped with additives that enhanced activity. The catalysts were prepared using an incipient wetness or slurry technique. Detailed preparation procedures are given in Appendix C.

Catalytic tests were performed in a quartz reactor using flow rates of 50-100 ccm, a reactor pressure of 5 psig, and a $CH_4/O_2/N_2$ ratio of approximately 2/1/18. A complete description of the experimental procedure is given in Appendix A.

The first series of catalysts consisted of Pt or Pd doped Na_2CO_3/CaO catalysts. This series was found to show very high activities; but, it was concluded that control of the total oxidation by the additives (Pt or Pd) was not sufficient to result in an improved catalyst. Subsequently, Pd and Pt doping of $SrCl_2$/α-alumina was performed. The following graph shows the results obtained using a Pd/$SrCl_2$/α-alumina catalyst (Pd/Sr/Al molar ratio = 1/25/300). Reaction conditions: GHSV = 750 h^{-1}; $CH_4/O_2/N_2$ = 2.0/1/18.

Figure 60. Methane Coupling Results for $Pd/SrCl_2$/alumina



Similar results were obtained with a $Pt/SrCl_2/\alpha$-alumina catalyst. Although, the C_2 selectivity shown is much lower than for $SrCl_2/\alpha$-alumina, the fact that an unusually high C_3 selectivity is obtained is very important (C_2/C_3 ratios are normally around 15-20). Also, the C_3 product in this case was all propane instead of propylene which is usually observed for oxidative methane coupling catalysts. These differences indicate that a heterogeneous reaction is likely involved in the formation of the C_3 product which represents a change in the normally observed heterogeneous/homogeneous mechanism. Since these results, Matsuhashi, Sakurai, and Arata[79] have reported that Na/ZrO_2 gives C_3 hydrocarbons as main products during the oxidative coupling of methane. Their catalyst produced more C_3 than C_2 products with the C_3 hydrocarbons being 77% propane and 23% propylene.

As a follow-up to the Pd result, additional members of the Group VIII elements were used as additives for the $SrCl_2/\alpha$-alumina catalyst. The first member tested was cobalt, chosen because of its ability to activate molecular oxygen. Figures 61 and 62 show the catalytic difference between $SrCl_2/\alpha$-alumina (molar ratio Sr/Al = 1/50) and $Co/SrCl_2/\alpha$-alumina (molar ratio Co/Sr/Al = 1/9/204). Reaction conditions: $CH_4/O_2/N_2$ = 2.2/1/18-20; GHSV = 1500 h^{-1}.

Figure 61. Methane Coupling Results for $SrCl_2$/alumina

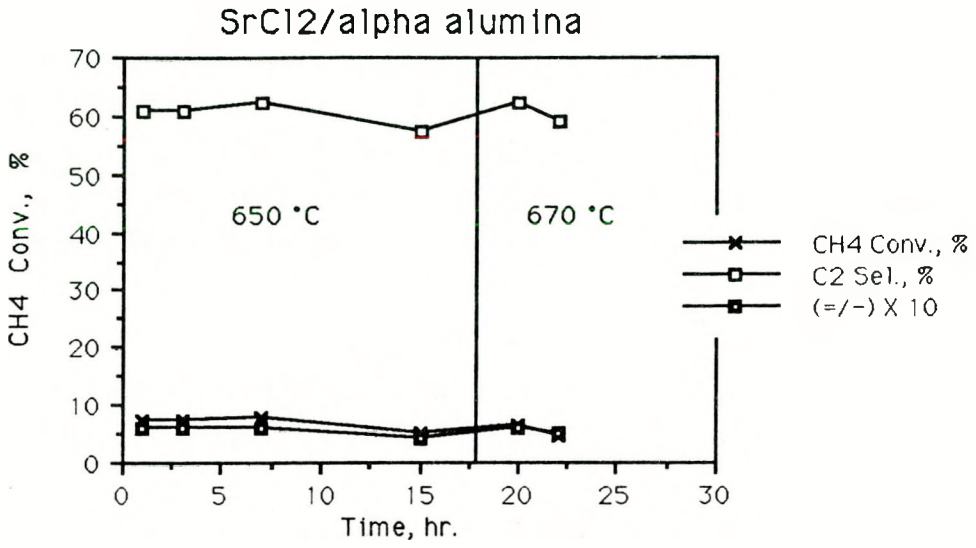
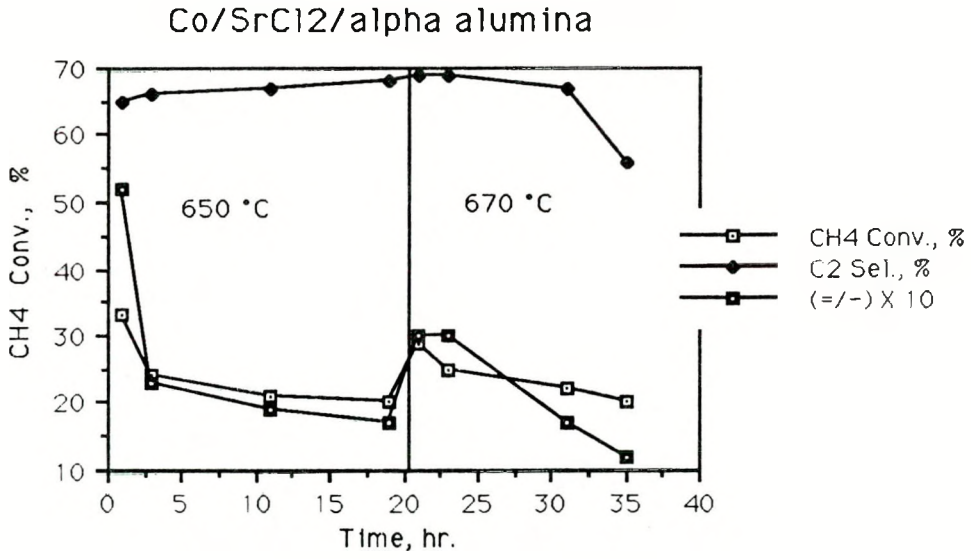


Figure 62. Methane Coupling Results for Co/$SrCl_2$/alumina



The addition of cobalt to the $SrCl_2$/α-alumina catalyst resulted in an increase in the CH_4 conversion and in the ethylene to ethane product ratio while maintaining the high C_2 selectivity. The deactivation observed for all of the chloride catalysts is due to the loss of chloride (exact mechanism unknown) from the catalyst. Based on previous work with

chloride systems, the deactivation should be preventable through the addition of volatile chloride containing species, such as ethylene chloride, to the reactant stream. It should be noted that results comparable to those for the $Co/SrCl_2/\alpha$-alumina catalyst can be obtained with the $SrCl_2/\alpha$-alumina catalyst at higher temperatures (50-100 °C higher).

Results similar to these have been reported by Larkins and Nordin[11] for the doping of Li/MgO with transition metals. Addition of two mole% Zn, Cu, Ni, Co, Fe, Mn, and Cr-oxide to Li/MgO increased the methane conversion at 800 °C while maintaining high C_2 selectivities. The addition of Mn resulted in comparable activity at 750 °C to the undoped catalyst at 800 °C.

Other catalysts were prepared by the addition of transition metals to the $SrCl_2/\alpha$-alumina catalyst. Results for these materials are presented in Table 39 below. Reaction conditions: $CH_4/O_2/N_2$ = 2.0-2.2/1/18-20; GHSV = 600-1700 h^{-1}; T = 650 °C.

Table 39. Methane Coupling Results for Low Temperature Catalysts

Catalyst*	CH_4 Conv. %	C_2 Sel. %	C_2 Yield %
$SrCl_2/\alpha$-alumina (1/50)	7.5	61	4.6
Pd/ $SrCl_2/\alpha$-alumina (1/25/300)	18	30**	5.4
Co/ $SrCl_2/\alpha$-alumina (1/9/204)	24	66	16
Ni/ $SrCl_2/\alpha$-alumina (1/9/200)	19	70	13
Fe/ $SrCl_2/\alpha$-alumina (1/9/206)	5.1	5.3	0.3
Cu/ $SrCl_2/\alpha$-alumina (1/14/323)	3.7	0.2	0
Rh/ $SrCl_2/\alpha$-alumina (1/17/198)	36	51	18
Co/α-alumina (1/225)	19	0.4	0.1

* : Molar ratio of metals given in parentheses.

** : High C_3 selectivity noted. (All propane)

The results show that the addition of Co, Ni, or Rh to $SrCl_2$/alumina catalysts enhance the activity while maintaining good C_2 selectivity. Addition of Pd or Pt results in decreased C_2 selectivity; however, unusually large C_3 selectivities are observed. Addition of Fe or Cu results in almost total loss of C_2 selectivity.

Double Perovskite Catalysts

Since the pioneering work at UCC&P[4] almost all of the literature studies dealing with the oxidative coupling of methane have utilized the concurrent feed (cofeed) of methane and oxygen. The main exceptions are the numerous works reported by Atlantic Richfield Company (ARCO) which uses a sequential or pulse flow of reactants like that reported by UCC&P. In the sequential technique, the catalyst is first oxidized by the passage of air or oxygen over the catalyst. The system is then flushed with an inert gas and methane is passed over the catalysts. The sequence can then be repeated. In the ARCO work, manganese-silica catalysts[5] were reported to give the best C_2 yields. The effects of alkali or alkaline doping of the manganese-silica catalysts[6] were studied. Alkali- and alkaline-doping, especially Na, increased the yields of higher hydrocarbons. A 15% Mn - 5% $Na_4P_2O_7$ - silica catalyst repeatedly gave 17% yields of higher hydrocarbons for 2 minutes at 850 °C. The beneficial effect of sodium addition was thought to be due to increased surface basicity, reduction of surface area, and a specific sodium-manganese interaction.

Most of the work reported by ARCO used transition metal oxides supported on silica. Only in a few cases were dopants added to the catalysts, such as the studies on Mn/silica, CeO_2, and Pr_6O_{11}.

In a recent article, Otsuka[95] proposed that the active species in a Li/NiO coupling catalyst was the complex oxide $LiNiO_2$. The oxidative coupling of methane was thought to proceed through the following redox cycle:

$$2LiNO_2 + 2CH_4 = Li_2O + 2NiO + C_2H_6 + H_2O$$
$$Li_2O + 2NiO + 1/2O_2 = 2LiNiO_2$$

If such a cycle is occurring, this catalyst should give even better coupling results when studied using the sequential technique. Also, if this is the active species for Li/NiO it is possible that other alkali-doped coupling catalysts react by similar mechanisms; thus, they too should give good results using the sequential technique.

A double perovskite, $LaCaMnCoO_6$, was tested as a coupling catalyst due to its unique structure and redox properties. Synthesis of $LaCaMnCoO_6$ was first reported in 1988[96]. Details on the synthesis of undoped and alkali doped $LaCaMnCoO_6$ are given in Appendix C. The material was an ordered perovskite showing multiple occupation of both A (La and Ca) and B (Mn and Co) sublattices. X-ray diffraction patterns suggested

the crystalline material possessed some ordered domains, while in other areas the cations were distributed at random. For the ordered domains, the most probable structural model was an ABO_3 perovskite-type structure in which Mn^{4+} and Co^{3+} ions occupied B positions in adjacent ABO_3 units while La^{3+} and Ca^{2+} ions alternate in the A positions. The material has a unique redox property in that two ions in the structure undergo reduction.

$$LaCaMn^{4+}Co^{3+}O_6 + H_2 \text{ ----------> } LaCaMn^{3+}Co^{2+}O_5 + H_2O$$

This makes the material of interest as a methane coupling catalyst for sequential studies.

In order to carry out sequential studies, one of the reactor units was modified such that the product stream could be collected in gas sampling bags directly after exiting the reactor. Product samples were collected during timed intervals and analyzed using the same analytical GC procedure employed in the cofeed studies. A detailed description of the experimental procedure is given in Appendix B.

The $LaCaMnCoO_6$ catalyst was very active in the sequential mode but gave low C_2 selectivities (<2%) at 800 and 850 °C (Table 40). Note: In the tables that follow, =/- represents the ethylene to ethane molar ratio.

Table 40. Sequential Mode Results for $LaCaMnCoO_6$

Temp. (°C)	GHSV (H^{-1})	Collection (min.)	CH_4 Conv.%	C_2 Sel.%	C_2 Yield%	=/-
Regenerated: 850 °C; Air = 100 ccm; 1 hour						
850	529	0 - 2.5	28.65	1.05	0.3	0.62
Regenerated: 800 °C; Air = 100 ccm; 1 hour						
800	529	0 - 2.5	13.73	0.34	0.05	0.52

Sodium doping (Na_2CO_3) of $LaCaMnCoO_6$ drastically changed its catalytic properties for methane coupling (Table 41).

Table 41. Sequential Mode Results for 20 wt% Na_2CO_3/$LaCaMnCoO_6$

Temp. (°C)	GHSV (H^{-1})	Collection (min.)	CH_4 Conv.%	C_2 Sel.%	C_2 Yield%	=/-
Pretreatment: 800 °C; Air = 100 ccm; overnight						
800	174	0 - 2	10.63	88.57	9.42	1.65
800	174	2 - 5	7.61	85.47	6.50	1.63
800	174	5 - 10	6.92	78.39	5.43	1.68
Regenerated: 800 °C; Air = 200 ccm; 2 hour						
800	523	0 - 2	7.30	90.59	6.62	1.07
800	523	2 - 10	5.43	85.32	4.64	0.97
Regenerated: 850 °C; Air = 50 ccm; 3 days						
850	174	0 - 2	10.04	80.27	8.06	1.76
850	174	2 - 5	6.06	60.87	3.69	1.24
850	174	5 - 10	4.23	24.99	1.06	0.65

$LaCaMnCoO_6$ gave very low C_2 selectivities with high activity in the sequential mode; but, Na_2CO_3 doped $LaCaMnCoO_6$ gave very high C_2 selectivities at lower CH_4 conversions.

Other alkali dopants were added to $LaCaMnCoO_6$ to determine if better methane coupling catalysts would result. Alkali dopants used included K_2CO_3, Li_2CO_3, Rb_2CO_3, and Cs_2CO_3. Representative results obtained in the sequential mode with these catalysts are presented in Tables 42-45.

Table 42. Sequential Mode Results for 24 wt% K_2CO_3/LaCaMnCoO$_6$

Temp. (°C)	GHSV (H^{-1})	Collection (min.)	CH_4 Conv.%	C_2 Sel.%	C_2 Yield%	=/-
Pretreatment: 800 °C; Air = 50 ccm; overnight						
800	222	0 - 2	6.81	75.48	5.14	0.61
800	222	2 - 5	5.38	68.43	3.68	1.02
800	222	5 - 10	3.82	45.18	1.73	0.89
Regenerated: 800 °C; Air = 175 ccm; 5 hours						
800	667	0 - 2	4.70	83.17	3.91	0.77
800	667	2 - 5	3.24	54.07	1.75	0.63
Regenerated: 850 °C ; Air = 50 ccm; overnight						
850	222	0 - 2	5.94	66.33	3.94	0.72
850	222	2 - 5	4.36	62.73	2.73	0.91
850	222	5 - 10	2.39	31.78	0.76	0.97
Regenerated: 850 °C; Air = 200 ccm; 2 hour						
850	667	0 - 2	7.26	76.94	5.58	0.96
850	667	2 - 5	3.89	43.18	1.68	0.75
850	667	5 - 10	18.01*	1.29	0.23	0.78

* Detectable amounts of hydrogen present in the 5 to 10 min. sample

Table 43. Sequential Mode Results for 15 wt% Li_2CO_3/LaCaMnCoO$_6$

Temp. (°C)	GHSV (H^{-1})	Collection (min.)	CH_4 Conv.%	C_2 Sel.%	C_2 Yield%	=/-
Pretreatment: 800 °C; Air = 200 ccm; 2 hours						
800	263	0 - 2	9.83	88.20	8.67	1.44
800	263	2 - 5	5.18	92.50	4.80	0.89
800	263	5 - 10	1.89	91.60	1.73	0.56
Regenerated: 800 °C; Air = 200 ccm; 3 hours						
800	789	0 - 2	8.49	89.29	7.58	1.01
800	789	2 - 5	3.50	95.82	3.35	0.58
800	789	5 - 10	1.84	93.06	1.72	0.41
Regenerated: 850 °C; Air = 100 ccm; overnight						
850	263	0 - 2	10.11	89.72	9.08	1.36
850	263	2 - 5	4.94	90.63	4.48	1.03
850	263	5 - 10	3.14	89.61	2.81	0.86
Regenerated: 850 °C; Air = 100 ccm; 4 hours						
850	789	0 - 2	7.88	91.21	7.19	1.15
850	789	2 - 5	3.84	94.47	3.63	0.78
850	789	5 - 10	1.79	89.97	1.61	0.45

Table 44. Sequential Mode Results for 48 wt% Rb_2CO_3/LaCaMnCoO$_6$

Temp. (°C)	GHSV (H^{-1})	Collection (min.)	CH_4 Conv.%	C_2 Sel.%	C_2 Yield%	=/-
Regenerated: 700 °C; Air = 200 ccm; Overnight						
700	2000	0 - 1	3.87	92.03	3.56	0.24
700	2000	1 - 3	2.27	94.31	2.14	0.19
700	2000	3 - 10	1.34	90.32	1.21	0.15
Regenerated: 750 °C; Air = 200 ccm; 4 hours						
750	2000	0 - 1	4.20	96.18	4.04	0.27
750	2000	1 - 3	2.25	96.38	2.17	0.21
750	2000	3 - 10	1.27	93.03	1.18	0.19

Table 45. Sequential Mode Results for 51 wt% Cs_2CO_3/LaCaMnCoO$_6$

Temp. (°C)	GHSV (H^{-1})	Collection (min.)	CH_4 Conv.%	C_2 Sel.%	C_2 Yield%	=/-
Regenerated: 700 °C; Air = 200 ccm; 3 hours						
700	1429	0 - 1	1.74	81.50	1.42	0.16
700	1429	1 - 3	0.84	71.35	0.60	0.08
700	1429	3 - 10	0.52	58.93	0.31	0.08
Regenerated: 725 °C; Air = 200 ccm; 3.5 hours						
725	1429	0 - 1	1.82	78.52	1.43	0.12
725	1429	1 - 3	1.06	65.99	0.70	0.17
725	1429	3 - 10	0.53	47.98	0.25	0.06
Regenerated: 750 °C; Air = 200 ccm; 4 hours						
750	1429	0 - 1	1.77	81.36	1.44	0.18
750	1429	1 - 3	0.74	69.57	0.52	0.10
750	1429	3 - 10	0.52	62.27	0.32	0.11

K_2CO_3 doping resulted in lower CH_4 conversions and lower C_2 selectivities than Na_2CO_3 doping. Li_2CO_3 doping resulted in lower activity but higher C_2 selectivity than Na_2CO_3 doping. For example, at 800 °C and 50 ccm of CH_4 (10 g catalyst), the Li_2CO_3 doped catalyst gave CH_4 conversions/C_2 selectivities of 9.8%/88% and 5.2%/93% for collection times of 0 to 2 and 2 to 5 minutes. For the same conditions and time intervals, the Na_2CO_3 doped catalyst gave CH_4 conversions/C_2 selectivities of 10.6%/89% and 7.6%/85% while the K_2CO_3 doped catalyst gave values of 6.8%/75% and 5.4%/68%.

The effect of using a diluted CH_4 stream in the sequential mode was studied with the Li_2CO_3/LaCaMnCoO$_6$ catalyst. At 725 °C and 150 ccm of CH_4, the Li_2CO_3 doped catalyst gave CH_4 conversions/C_2 selectivities of 3.0%/66%, 2.6%/50%, and 1.2%/87% for collection times of 0 to 2, 2 to 5, and 5 to 10 minutes. For the same conditions and time intervals, a reactant stream of 20% CH_4/80% N_2 gave CH_4 conversions/C_2 selectivities of 18.2%/49%, 12.4%/51%, and 8.1%/66%. The use of the diluted reactant stream gave higher C_2 yields due to the higher conversion but the C_2 selectivities were less. Since the total amount of CH_4 reacted in both cases was approximately the same, the undiluted case gave the better overall results.

To determine if large amounts of C_{3+} hydrocarbons were formed during the sequential mode experiments, gaseous samples of products collected using the 20 wt%

$Na_2CO_3/LaCaMnCoO_6$ catalyst (T = 800 °C; GHSV = 1380 h^{-1}) were analyzed by GC/MS. Table 46 gives the relative amounts of higher hydrocarbons in the gaseous product.

Table 46. GC/MS Analysis of Gaseous Product*

Interval (min)	Ethane	Ethylene	Propane	Propylene
0 - 1	100	24	3.2	1.9
1 - 3	100	24	2.6	1.3
3 - 10	100	20	1.6	1.0

Butadiene	Butenes	Pentene	C_5-Olefins	Benzene
4.5	0.60	0.25	0.23	0.29
1.7	**	**	**	**
1.1	**	**	**	**

*: Relative amounts based on an assigned value of 100 for for ethane.
**: Levels too low for detection.

The results shows that most of the higher hydrocarbons formed by the coupling of methane are C_2's with C_3's and C_4's being next in abundance. Only small amounts of hydrocarbons greater than C_4 are detected.

One trend reported[97] with all of the literature sequential mode catalysts is that the C_{2+} selectivity increases as the methane coupling catalyst is reduced (methane conversion decreases). Thus, initially when the methane conversion is greatest the C_{2+} selectivity is at its minimum. This trend is not observed with the alkali doped double perovskite $LaCaMnCoO_6$. Both the CH_4 conversions and C_2 selectivities are highest during the early stages of the catalyst reduction resulting in greater yields of C_{2+} products.

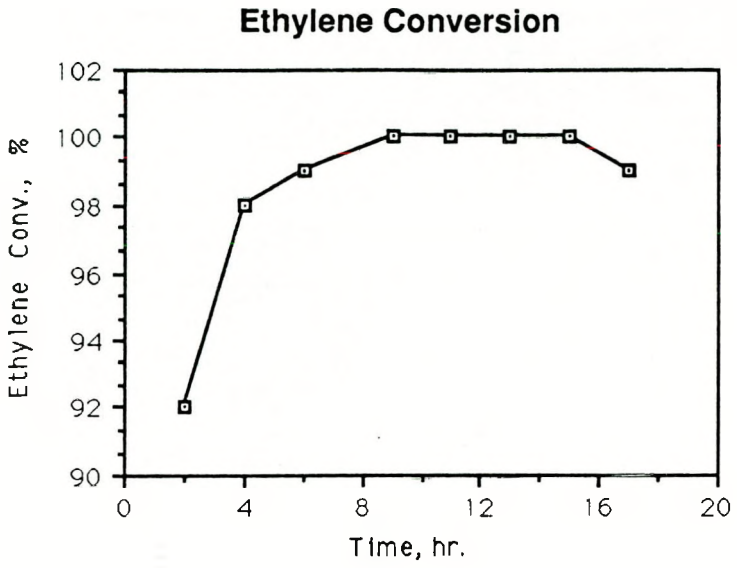
Alkali carbonate doped $LaCaMnCoO_6$ represents a unique class of sequential mode coupling catalysts. These catalysts shows very high C_{2+} selectivities and exhibit the unique characteristic that the CH_4 conversions and C_2 selectivities are highest during the early stages of the catalyst operation.

Oligomerization

The ability to integrate a methane oxidative coupling reaction directly to an olefin oligomerization reaction would result in a process for the conversion of methane to liquid hydrocarbon products without any intermediate steps, such as separations or compression. This ability would also improve the economic viability of a methane to liquid hydrocarbons process since the separations part of the system could be simplified. Studies were performed to explore the oligomerization of methane coupling products (ethylene) to liquid hydrocarbons and determine the feasibility of integrating the methane coupling reaction directly to an oligomerization reaction.

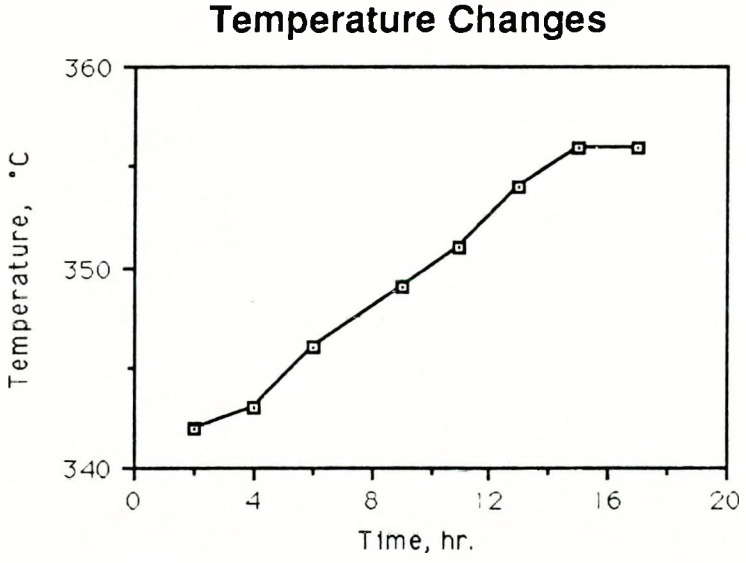
Experiments were carried out using a reactant stream composed of 66% ethylene, 24% ethane, and 10% nitrogen with LZ-105-6/alumina (ZSM-5 type material) as the olefin oligomerization catalyst. This material was chosen due to its availability and the numerous reports in the literature on the use of ZSM-5 as an oligomerization catalyst. Powder x-ray diffraction analyses of fresh and used LZ-105-6/alumina catalysts gave patterns consistent with that reported for HZSM-5[98]. A conventional continuous flow, high pressure stainless steel reactor was used for the study. Gaseous reactants and products were analyzed using an online GC and the liquid products were collected in a cooled trap for GC/MS analyses. The figures below show the ethylene conversion, oligomerization catalyst temperature (center of bed), and % reacted ethylene accounted for in the gas phase products when the reaction was carried out at 200 psig, 100 ccm, and 350 °C with 5 grams of catalyst. The temperature was chosen to ensure high ethylene conversion when the oligomerization and methane coupling reactions were integrated (very low ethylene pressure). At this temperature, the formation of aromatics as well as aliphatic hydrocarbons is expected[98].

Figure 63. Ethylene Conversion Over Oligomerization Catalyst



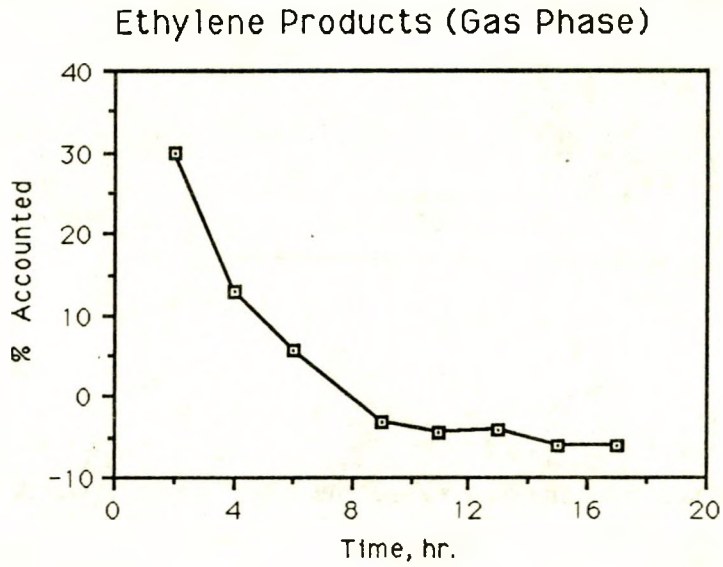
The graph shows that the ethylene conversion is nearly complete during the eighteen hour run. The decrease in conversion at the end of the run is due to coking of the catalyst.

Figure 64. Temperature of Oligomerization Catalyst



The catalyst temperature profile (center of catalyst bed) shows a gradual increase in temperature to a maximum at the end of the run. In another run, a drop in temperature was observed after the maximum. This profile corresponds to a slight hotspot moving through the catalyst bed as the catalyst deactivates (cokes).

Figure 65. Gaseous Products During Ethylene Oligomerization



The graph shows that most of the reacted ethylene is not converted into gaseous products. The negative values are due to the reaction of ethane with a product or intermediate formed during the ethylene oligomerization. Runs using only ethane in the reactant stream showed no ethane conversion.

GC/MS analysis of the resulting liquid hydrocarbon product is given in Table 47. The liquid composition was found to be very complex (>200 peaks in the GC scan), thus results were obtained assuming the same response factor for all components. This assumption causes a ±10% uncertainty in the results.

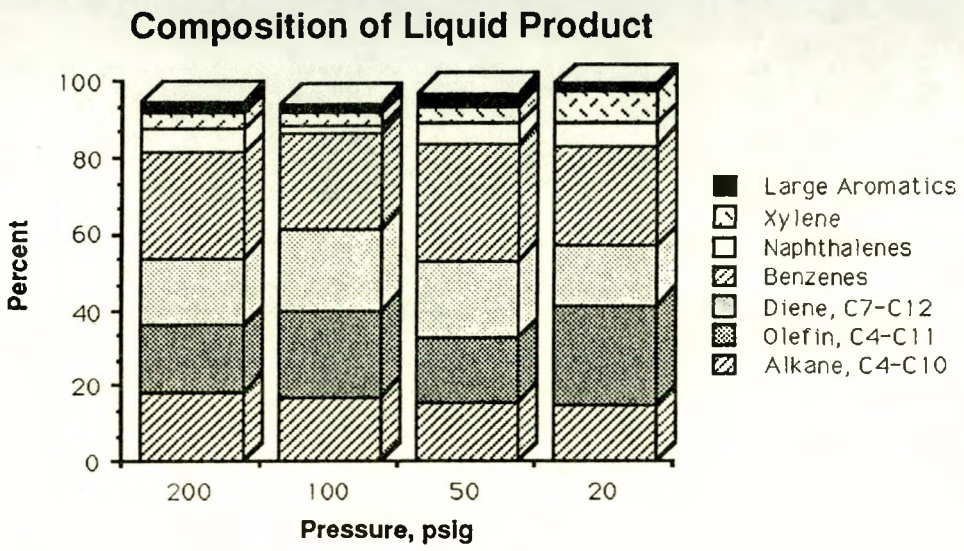
Table 47. Composition of Liquid Hydrocarbon Product

	LIQUID PRODUCT DISTRIBUTION (Wt %)
Alkane (C_4 - C_{10})	18%
Olefin (C_4 - C_{11})	18%
Diene (C_7 - C_{12})	18%
Benzene (Substituted)	27%
Naphthalene (Substituted)	6.5%
Xylene	4.3%
Styrene (Substituted)	1.3%
Tetralin (Substituted)	0.9%
Large aromatics	2.7%

The analysis shows the formation of a large aromatic fraction consistent with the high temperature used for the oligomerization reaction. The absence of any long chain aliphatics (greater than C_{12}) is thought due to the experimental conditions chosen for the study.

Additional experiments were performed to determine the effect of lowering reactor pressure on the product distribution. Figure 66 shows the composition of the liquid products obtained using experimental conditions as before except for changing pressure. Note that since the flow rate was held constant, the contact time also changed in these experiments.

Figure 66. Effect of Reaction Pressure on Liquid Product Composition



Surprisingly, the composition of the liquid does not vary greatly as the pressure is lowered from 200 to 20 psig. These results were encouraging since the methane coupling reaction to integrate with the oligomerization reaction can be operated at 20 psig.

Experiments at 20 psig were run in which the effluent from a methane coupling reactor was passed into an oligomerization reactor containing 5g of the LZ-105-6/alumina catalyst at 350 °C. Three different methane coupling catalysts were utilized: (reactant feed of $CH_4/O_2/N_2$ = 8.2/1/0.6).

- 4.77 wt% $BaCO_3$/α-alumina (ECl = 20ppm); 750 °C; GHSV = 606 h^{-1}
- $K_2La_2Ti_3O_{10}$; 800 °C; GHSV = 1710 h^{-1}
- 11.5 wt% Li_2CO_3/MgO; 720 °C; GHSV = 1930 h^{-1}

For the $BaCO_3$/α-alumina and $K_2La_2Ti_3O_{10}$ runs all the water of the coupling reaction was passed into the oligomerization reaction zone. This was accomplished using a single straight tube, quartz reactor passing through two furnaces. In the Li_2CO_3/MgO run, the coupling reactor effluent was passed through a cold trap before entering the oligomerization reactor resulting in the removal of approximately 99% of the water. For

this run, separate quartz reactors were used. GC/MS results for the hydrocarbon liquids formed in the integrated processes are given in Table 48. As before, there is a ±10% uncertainty in the results.

Table 48. Liquid Product Distribution for Integrated Runs*

PRODUCT	20 psig**	$BaCO_3$	$K_2La_2Ti_3O_{10}$	Li/MgO	20 psig***
Alkane C_4 - C_{10}, %	15	0	0	0.1	0.3
Olefin C_4 - C_{11}, %	26	0.01	0	0.2	0.7
Diene C_7 - C_{12}, %	16	0	0	0.01	0
Benzene (Substituted), %	26	38	27	49	45
Naphthalene (Substituted), %	5.6	23	45	6.8	7.0
Xylene, %	8.5	19	18	35	31
Styrene (Substituted), %	0.9	9.1	1.4	1.7	0.8
Tetralin (Substituted), %	0.1	1.5	3.7	1.0	0
Large aromatics, %	1.8	4.0	5.3	4.5	15

*: Distribution given in weight %.

**: Oligomerization run using reactant stream containing 66% ethylene.

***: Oligomerization run using reactant stream containing 9.5% ethylene.

The integrated process gives a product mix entirely different from that obtained for the ethylene-ethane-nitrogen (2.7/1/0.4) mixture at 20 psig. None of the aliphatic C_4-C_{12} products are observed. The main products are substituted benzenes, substituted naphthalenes, and xylene. To determine if the low partial pressure of ethylene present in the methane coupling effluent was responsible for the shift in product distribution, an oligomerization run was performed using a reactant stream comprising 9.5% ethylene, 5.2% ethane, and 85.3% nitrogen. The resulting liquid composition is given in the table above. The results for the 9.5% ethylene run agrees closely with those for the Li_2CO_3/MgO run indicating that the shift to aromatics is due to the low ethylene partial pressure produced in the coupling reaction.

Methane coupling products from low pressure reactions can be oligomerized to liquid hydrocarbons without separation and/or compression of the product stream. However, the formation of particular hydrocarbon fractions requires higher ethylene pressures in the oligomerization reaction and/or separation of some components from the product stream.

NEK Laboratory

The NEK laboratory reactor system containing two reactors is shown in Figure B5 of Appendix B. This was used to investigate the effects of pressure and steam as a diluent on the methane coupling reaction. Very little work has been reported in the literature in which steam is used as a diluent in the methane coupling reaction. In two ARCO patents[99,100], it is claimed that steam increases the C_{2+} hydrocarbon selectivity and activity when operating in a cofeed mode and increases the C_{2+} hydrocarbon selectivity when operating in the sequential feed mode. The best result reported for the cofeed mode is 93% selectivity to C_{2+} hydrocarbons, with an ethylene to ethane product ratio of less than 1, at 10% methane conversion using a CH_4:O_2 ratio of 16 and 44 mole % steam. The best result reported for the sequential feed mode is 88% selectivity to C_{2+} hydrocarbons at 20% methane conversion with 20 mole % steam in the methane feed.

One ARCO patent[101] reported catalyzed methane coupling at pressures above 25 psig. It was reported that the ratio of the yield of C_{3+} hydrocarbons to the yield of C_{2+} hydrocarbons increases with increasing pressure for the methane coupling reaction under sequential feed conditions in the presence of reducible metal oxides. Decreasing the space velocity is also shown to increase this ratio. The interior walls of the stainless steel tube were treated with potassium pyrophosphate to control coke formation catalyzed by the reactor wall. Typical example conditions are 700-800 °C, 400 to 3100 methane gas hourly space velocities and 100 psig. Increasing the pressure from atmospheric to 100 psig is shown to increase the methane conversion by 5 fold and increase the selectivity to C_{3+} hydrocarbons by 20 fold; however, no comparative data on the C_{2+} selectivity were given.

Reactor Validation

Barium carbonate on 30/60 mesh, Norton SA5451 alumina catalyst was prepared using a slow stirring rate. It was evaluated in runs 33-NEK-40 and 33-NEK-42, as shown in Tables F9 and F10 and in Figures F1 and F2 of Appendix F. At a time of 71 hours on stream, the detectability of the carbon oxides was improved by reducing the range on the TCD from 0.5 mV to 0.05 mV, and by recalibrating the GC.

The results of these two runs show fairly good reproducibility between the two different reactors under the startup conditions (750 °C, 2228 h^{-1}, 11 psig, 10:5:85 CH_4:O_2:inert gas and about 8 ppm ECl), as shown below:

	CH_4 conv.	C_2 Sel.	Yield
33-NEK-40	34.2%	52.3%	16.5%
33-NEK-42	32.9%	59.2%	17.3%

The differences between the two runs may be due to any of the following:

1) the longer furnace and reactor of reactor 2 vs 1;

2) differences in the packing of the catalyst bed; and

3) differences in the temperature profiles along the length of the reactors.

Bearing in mind that the purpose of this work is to evaluate the effect of diluent and pressure on catalyst performance rather than to discern small differences between two catalysts, these reactor systems were considered adequate.

Steam

The initial experiments to investigate the effect of steam were carried out during the latter portion of the runs used to validate the reactors (see Figures F1 and F2 and Tables F9 and F10 of Appendix F). At 186 HOS (hours on stream), 8.5% steam was introduced into the feed, while at the same time the argon flow was decreased by 10%, such that the total flow rate remained constant. Initially, the selectivity to C_2 hydrocarbons decreased and the CH_4 conversion was unchanged. At 216 HOS, the amount of steam in the feed was doubled, and again the argon flow was reduced to maintain a constant total flow rate. The effect on the C_2 hydrocarbon selectivity was the same, and the CH_4 conversion decreased. At about 230 HOS, the selectivity to CO started to increase and the selectivity to CO_2 started to decrease, although no change in reaction conditions was made at this time. The run in reactor 2, 33-NEK-42, was terminated at 228 HOS due to an unplanned shutdown. At 256 HOS, the furnace temperature on reactor 1, 33-NEK-40, was increased to 770 °C; however, this had little apparent effect on the continuing declining catalyst performance.

The next runs were carried out on a barium chloride on alumina catalyst rather than the barium carbonate catalysts, because it was expected that the chloride catalysts would show stable performance after only a few hours, rather than 24 hours required by the

carbonate based catalysts. In addition, the alumina used was changed from the 30/60 mesh Norton SA5451 to 14/30 mesh Norton SA5402 (a sufficient quantity of 14/30 mesh Norton SA5451 was not available) in order to try to reduce the pressure drop through the catalyst bed. Results are shown in Tables F11-F14 and Figures F3-F6 of Appendix F. The lower space velocities required with barium chloride catalysts in order to obtain performance similar to that obtained with barium carbonate catalysts required additional inert gas to be added to the stream after it left the reactor, but prior to the low flow sensor (to avoid shut down due to safety features). During unattended operation, argon (helium for run 33-NEK-122) was added, while during attended operation it was not. This should have had no effect on the results since the nitrogen fed to the reactor with the ethyl chloride was used as an internal standard; however, in practice, slight changes were observed. This is probably because the GC was operating close to the detection limits for carbon oxides. For each run in Tables F11-F14 of Appendix F, results reported were obtained under the same mode of operation whenever possible.

In run 33-NEK-86, Figure F4 and Table F12 of Appendix F, 2.1% steam was introduced at 24 HOS. The catalyst performance changed dramatically with the CO selectivity increasing and the CO_2 selectivity and methane conversion decreasing as shown in the Figure F4 of Appendix F. In addition, the ethylene to ethane product ratio decreased from 8.75 to 5.16. It is believed that these changes in catalyst performance are not due to the presence of steam in the feed, but rather to a gradual change which takes place in the catalyst over a long period of time, as will be discussed later. Further increases in steam concentration to 4.3 and 6.5% resulted in little change in performance. Increasing the steam concentration to 10.8% was detrimental to catalyst activity. Finally, increasing the steam concentration to 28.8% significantly affected the product distribution by increasing the carbon oxides at the expense of the C_2 hydrocarbons, and in addition, reduced the ethylene to ethane product ratio.

In the other two runs (33-NEK-70 and 33-NEK-110, Tables F11 and F13, and Figures F3 and F5 of Appendix F) in which steam was fed to barium chloride on alumina catalysts, methane was used as the diluent rather than argon or helium. Since the methane concentration changes each time the steam concentration changes, the changes in the C_{2+} hydrocarbon yields and methane conversions do not reflect changes in catalyst performance due to changing the steam concentration. It is more useful to compare rates to C_{2+} hydrocarbons in these cases.

The addition of steam and decrease in methane concentration in runs 33-NEK-70 and 33-NEK-110 resulted in decreased selectivity and rate to C_{2+} hydrocarbons. The

effect is quite small with 5% steam, but becomes more dramatic with increasing amounts of steam. When the steam concentration was increased from 15% to 42.2%, the ratio of ethylene to ethane increased from 1.4 to 2.4, as shown in Table F13 of Appendix F. It is believed that this is due to the lower concentration of methane present, rather than to the increase in steam concentration, as the opposite effect is observed in Table F11 of Appendix F when the methane concentration was increased from 10% to 70%.

One of the main reasons for pursuing chloride-based catalysts instead of the carbonate-based ones was that they were expected to give stable performance after a short activation period. Instead, as shown in Table F14 and Figure F6 of Appendix F for run 33-NEK-122, the performance of a barium chloride-based catalyst changed gradually between 25 and 65 HOS even though there was no change in reaction conditions. The instability of the catalyst performance may be due to using an unoptimized level of ethyl chloride. It was decided to return to studying carbonate catalysts, which operate at a higher space velocity, since chloride catalysts were not stable.

A barium carbonate on Norton SA5402 alumina catalyst was prepared and evaluated in run 33-NEK-132 (Table F15 and Figure F7 of Appendix F).
The C_2 yield was very low compared with the earlier barium carbonate runs and was unaffected by increasing the ethyl chloride level from 7.5 to 30 ppm. C_2 yields of greater than 10% were not achieved in the NEK laboratory with catalysts on Norton SA5402 alumina (see table below and Table F16 and Figure F8 of Appendix F). It is now known that Ba catalysts on Norton SA5402 alumina require higher levels of ethyl chloride than were used in these experiments in order to obtain high C_2 yields (see BKW Laboratory Section above).

In addition to the type of alumina, the particle size of the alumina appeared to affect the catalyst performance. Smaller particle size alumina resulted in a more active barium carbonate (4.77 wt %) catalyst as shown below for 10% methane, 5% oxygen, 85% helium + nitrogen, and 7.5 ppm ethyl chloride at 750 °C, 11 psig, and a space velocity of 2228 h^{-1}:

Ref	Mesh size	HOS	C conv	C_2 Sel	Yield	=/-
34-NEK-34	14/30	16	27.3	38.1	10.0	1.47
34-NEK-40	40/60	22	44.5	36.3	15.7	2.57

The catalyst on the 40/60 mesh Norton SA5451 alumina resulted in 100% oxygen conversion at the beginning of the run.

Another batch of the 40/60 mesh catalyst was tested in Run 34-NEK-58 (Table F16 and Figure F8 of Appendix F). This run was started with 30% methane and then the helium diluent was replaced with steam. This was Run 34-NEK-58 (Table F16 and Figure F8 of Appendix F). Concurrently with raising the methane concentration to 30%, the oxygen concentration was increased to 10%; however, it was found that a hotspot formed in the catalyst bed. The reaction could not be controlled with this feed composition even at much lower temperatures, thus the oxygen concentration was lowered to 5%. The temperature was lowered from 750 to 730 °C in order to avoid 100% conversion. This catalyst was prepared by the dry mix method and is not quite as selective to C_{2+} hydrocarbons as one prepared by a slurry method (see Table F17 and Figure F9 of Appendix F); however, the effect of replacing the helium diluent was investigated nonetheless.

First, 40% steam was introduced for a short period of time, followed by 62% steam. The 40% steam had little effect on the results, however, this may be because the steam had not actually gotten to the catalyst in the short period of time allotted. Increasing the steam level to 62% had a definite negative effect on methane conversion, C_2 selectivity and ethylene to ethane product ratio. The C_{2+} hydrocarbon selectivity decreased, while the selectivity to carbon monoxide increased, with little change in the selectivity to carbon dioxide. It was observed that introducing steam reduces the temperature of the catalyst bed. In order to determine if this was contributing to the reduced catalyst activity, the reactor temperature was increased to 750, 760 and finally to 770 °C. The initial increase to 750 °C resulted in an initial increase in the C_2 selectivity, the methane conversion, the ethylene to ethane product ratio and the rate to C_2 hydrocarbons; however, the activity was decreasing and the selectivity was shifting toward carbon oxides with time. These same trends were better observed when the system was run for longer times at 760 °C and 770 °C. When the steam was replaced with helium at 750 °C, the activity, C_2 selectivity and the ethylene to ethane product ratio all decreased quite dramatically.

Another run (34-NEK-70, Table F17 and Figure F9 of Appendix F) was carried out which was very similar to the above run except that the steam was introduced earlier and the GC data was collected continuously. The results are qualitatively very similar to the results from run 34-NEK-58. Because the GC data was collected continuously, it is seen that the ethylene to ethane product ratio did initially increase from 2 (prior to steam) to 3, but then it slowly decreased to about 1 after close to 25 hours.

Although Figure F8 of Appendix F shows that the catalyst activity, as reflected by the methane conversion, is quite stable under the various conditions of operation through almost 70 hours of operation, Figure F9 of Appendix F shows that the methane conversion starts to decrease upon introduction of steam at only 45 hours on stream. This might be due to a change in the required amount of ECl in the presence of steam. This hypothesis was tested by nearly tripling the ECl level at 117 HOS. This increased the C_2 selectivity and the ethylene to ethane product ratio, but catalyst deactivation continued.

Replacing the steam with helium towards the end of the run once again had an immediate and negative impact on the activity and ethylene to ethane product ratio. This indicates that steam is actually beneficial to catalyst performance. This is indeed shown in Figure F9 of Appendix F for the first couple of data points after steam is introduced; however, this improved performance is lost as the catalyst deactivates.

In order to determine if a much higher ethyl chloride level introduced concurrently with the steam would help stabilize the catalyst, a final run was carried out as shown in Table F18 and Figure F10 of Appendix F.

This catalyst was prepared by loading barium hydroxide onto Norton SA5451 alumina using the incipient wetness method. The catalyst evaluation began with 10% methane and 5% oxygen so that this catalyst could be compared with the barium carbonate catalyst prepared by the slurry method. The first two lines of results in the table below, in which a barium carbonate catalyst was used in run 34-NEK-70 and the barium hydroxide one for run 34-NEK-100, show that these two catalysts perform very similarly.

Ref	CH_4	ECL	Steam	HOS	C conv	C_2 Sel	Yield	=/-
34-NEK-70	9	8	0	23	43.8	35.3	15.1	2.9
34-NEK-100	9	8	0	18	45.3	36.5	15.5	3.0

At about 20 HOS the feed to the barium hydroxide loaded catalyst was changed to 65% steam, 30% methane, 5% oxygen, and 500 ppm of ethyl chloride. The data in Figure F10 of Appendix F show that even with 500 ppm ethyl chloride in the feed gas, the rate to C_2 hydrocarbons and the methane conversion decline steadily after initially increasing. In the presence of steam, with high ECl, the carbon dioxide selectivity increases at the expense of the carbon monoxide selectivity and the selectivity to C_2 hydrocarbons remains fairly constant, while with low ECl, the selectivity to C_2 hydrocarbons decreases dramatically, while the carbon monoxide selectivity increases.

A methane conversion of 8% and a 57% selectivity to C_2 hydrocarbons was obtained with 65% steam, 30% methane, 5% oxygen, and 500 ppm ECl. No attempt was made to optimize process variables, but the C_2 selectivity and methane conversion were constant at these levels for 20 hours.

The effect of using steam may initially be to improve catalyst performance, however the performance of barium on alumina catalysts degrade with time in the presence of steam under the conditions used. Each time that the steam was replaced with inert gas at the end of a run, the performance with the steam was better than without. It is likely that feeding steam to these barium on alumina catalysts changes the level of ECl required for optimum performance, although attempts to vary the ECl level to obtain stable performance were unsuccessful.

High Pressure

The quartz reactor used in the above experiments was designed for use at atmospheric to 25 psig pressure. In all cases, except one, it was operated at 11 psig outlet pressure. The only exception was one run in which the pressure was increased to 16 psig, shown in Table F11 and Figure F3 of Appendix F. In this case the small variation in the pressure did not noticeably affect results.

In order to operate the system at higher pressures, the sheathed reactor, shown in Figure B20 of Appendix B, was used since it could be operated at pressures up to 250 psig. The reactor was filled with quartz chips as shown in configuration A (see Figure B21 of Appendix B) and a designed set of experiments was run to determine the amount of reaction occurring without any catalyst. These runs, shown in Table F19 and Figure F11 of Appendix F, show that 18-38% of the methane is converted to C_2 hydrocarbons with a selectivity of between 16 and 24%. Although the void volume of this reactor, packed using configuration A, is very similar to that of the quartz reactor used in other experiments discussed above, the residence time at 200 psig is about 18 times longer than it is at 11 psig.

The void volume of this reactor was minimized by using packing configuration B (see Figure B21 of Appendix B), and a barium carbonate on alumina catalyst was evaluated as shown in Table F20 and Figure F12 of Appendix F. A two level fractional factorial designed set of experiments with center points was run during 88.6 to 255 HOS to evaluate the effect of pressure (100-200 psig), temperature (700-750 °C), space velocity (4456-8912 h^{-1}), and ECl level (30-60 ppm). The feed composition, with the

exception of the ECl level, was 30% methane, 5% oxygen, and the balance helium and nitrogen, and was the same throughout the designed set.

The results of the designed set and of the regression analysis are summarized in Table F21 of Appendix F. In general, the results at any one set of conditions in the designed set were quite stable. The exceptions to this were experiments #6 and #4, which were the only two experiments with both a low ECl level and a high flow. The catalyst performance is apparently not stable under these conditions; however, the performance is not permanently affected, since the center point data is quite reproducible.

The regression analysis shows that increasing the pressure increases the selectivity to CO and decreases the selectivity to C_2 hydrocarbons and CO_2, the yield and rate to C_2 hydrocarbons, the ratio of CO_2/CO and the ratio of C_2/C_1 hydrocarbons. In addition, some of the other variables significantly affected some of the measures of performance, as shown in Table F21 of Appendix F. It should be noted that since this is a fractional factorial, the ECl level is confounded with the three factor interaction among temperature, pressure, and flow. A nearly 50% selectivity to C_2 hydrocarbons was obtained at 17% methane conversion at a pressure of 100 psig. The homogeneous reaction is considered to be large under these conditions.

SUMMARY:

Studies showed that the homogeneous gas phase oxidation of methane can be significant under certain experimental conditions. High C_2 selectivities (51-59%) were obtainable in the gas phase oxidation; however, the high selectivities occurred only for low methane conversions (<5%). For higher methane conversions (>35%), the best C_2 selectivity observed was only 25%. High ethylene to ethane ratios (4-10) were obtained for runs at high temperatures (850 °C) and long residence times (14-15 seconds). The highest C_2 yield observed was 8.6%. The extent of the homogeneous reaction was greatly diminished by a quartz surface, especially at temperatures less than 700 °C.

Methane coupling catalysts were provided which are comparable in selectivity, activity, and C_2 yield to the better literature catalysts, but which provide hundreds of hours of stable operation in the oxidation of methane to C_2's with high ethylene to ethane product ratios (2.5-10 or more). These catalysts contain alkaline earth components and require the presence of halides, either as a catalyst component or as a periodic or continuous additive to the catalyst. The chloride appears to serve three distinct roles, resulting in suppression of carbon dioxide formation, increased rates to C_2 products, and

in higher ethylene to ethane product ratios. Acidic supports result in higher ethylene to ethane product ratios. As an example, after over 350 hours of methane coupling with a 5 weight percent barium carbonate on titanium dioxide catalyst (with ethyl chloride in the feed gas), a C_2 yield of 22%, a C_2 selectivity of 58%, and an ethylene to ethane product ratio of 8 are obtained.

Other classes of catalysts have been tested. Some of these were less promising, although the concepts, such as that of locking an active metal into an unusual coordination or oxidation state within a framework, remain viable and interesting. Those catalysts tested within the catalyst classes of framework metal molecular sieves, hydrotalcites, simple perovskites, catalysts based on Pr/Ce oxygen carriers, catalysts containing Fe and Cu, and superacids showed no advantages over literature catalysts.

Other catalysts were novel and have process advantages. These include layered perovskite catalysts, a unique class of sequential mode double perovskite coupling catalysts, catalysts containing silver, catalysts containing certain Group VIII metals, and vapor phase catalysts. Layered perovskites of the form $A_2Ln_2Ti_3O_{10}$ (A = K, Rb, Na; Ln = La, Nd, Sm, Dy, Gd, Pr, Ce) represent a new type of methane coupling catalyst in which the alkali dopant is part of the crystal structure. Alkali carbonate doped $LaCaMnCoO_6$ catalysts showed very high C_{2+} selectivities and exhibited the unique characteristic that the CH_4 conversions and C_2 selectivities were highest during the early stages of the catalyst reduction cycle. Catalysts containing $SrCl_2$, α-alumina, and Co, Ni, or Rh showed C_2 selectivities of 50-70% and C_2 yields of 13-18% at 650 °C.

Catalysts containing silver and Pd or Pt operate at lower temperatures than most methane coupling catalysts and show unusually high C_3 selectivities, demonstrating the concept of enhanced surface reactions, a move away from the heterogeneous/ homogeneous mechanism with the apparent C_2 yield barrier. Another way to avoid this barrier, that of changing the chemistry in the vapor phase, was proposed and explored. This concept was successfully demonstrated with vapor phase catalysts.

Process studies included studies of steam as diluent and, to a limited extent, the effect of pressure. In general, the effect of using steam on the performance of a barium on alumina catalyst was to initially improve the catalyst performance. The best result obtained with a steam diluent (65% steam, 30% methane, 5% oxygen, and 500 ppm ECl) was 8% methane conversion and 57% selectivity to C_2 hydrocarbons, without any optimization. C_2 selectivity and methane conversion were constant at these levels for 20 hours. Pressure studies indicated that increasing the pressure increases the selectivity to CO and decreases the selectivity to C_2 hydrocarbons and CO_2.

Methane coupling with an alkaline earth catalyst was demonstrated with a model processed natural gas mixture. Methane coupling products from low pressure coupling reactions (<25 psig) were oligomerized to liquid hydrocarbons without separation and/or compression of the product stream. The integrated process gave substituted benzenes, substituted napthalenes, and xylenes as the main products. To obtain particular hydrocarbon fractions, higher ethylene pressures in the oligomerization reaction and/or separation of some components from the product stream would be required.

TASK 2: Process Conceptualization

INTRODUCTION:

This portion of the program covers all of the engineering studies. Engineering participation in economic evaluation, process conceptualization, and experimental design is expected to speed up the development of a commercially attractive process.

The Comparison Case consists of the conversion of methane to synthesis gas followed by conversion of the synthesis gas to methanol. Methanol will be converted to liquid hydrocarbon fuels via olefins. All of the components of this technology have been demonstrated on a commercial or pilot scale. Case 1 consists of the conversion of methane to ethylene. Case 2 is the conversion of methane directly to C_2's and then to liquid hydrocarbon fuels. These two cases address the primary interests of UCC&P and DOE, respectively.

The purposes of the Task 2 engineering program have been to compare the economics of making gasoline and distillate fuels from methane, through olefins produced via methane coupling with a route utilizing synthesis gas and methanol as intermediates; and to provide economic direction to the methane coupling catalyst research program by quantifying the economic sensitivities to key process variables. Described herein is the impact of the following process variables on the process economics:

- Yield to C_2's versus selectivity to C_2's versus methane conversion based on an extrapolation of the results obtained from an experimental catalyst system
  - reactor diluents: nitrogen, steam, and methane
  - methane/oxygen feed ratio (1-10)
  - co-feed versus sequential feed

- Oxygen concentration in the reactor feed (5-11%)
- Ethylene to ethane production ratio (1-10)
- Fate of co-product ethane (crack versus sell)
- Reactor pressure and temperature (80-240 psig and 625-825 °C)
- Selectivity to C_2's and methane conversion for a hypothetical catalyst system.

Technology is currently available for the conversion of methane to liquid fuels based upon a four step process in which methane is successively converted to syn-gas, methanol, olefins and, finally, to gasoline and distillate products. Syn-gas production is accomplished by steam reforming of natural gas and ICI's low pressure methanol process is used to convert the syn-gas to methanol. Methanol is then converted to low molecular weight olefins via UOP's MTO process, and Mobil's Olefins to Gasoline and Distillate (MOGD) process is used for the final conversion of olefins to liquid fuels. All of these process steps have been demonstrated to be feasible or have already been commercialized; therefore, they establish a benchmark (Comparison Case) against which to compare the results from the present research in which methane is converted to liquid fuels in a three-step process involving the oxidative coupling of methane, the cracking of by-product ethane, followed by the oligomerization of the resulting crude ethylene stream to produce gasoline and distillate (Case 2).

RESULTS AND DISCUSSION

Comparison of Methane Coupling and Conventional Routes to Fuels

Methane Coupling Simplified Block Diagram

The Simplified Block Diagram for the methane coupling process is shown in Exhibit 1 of Appendix I integrated with the Mobil Olefins to Gasoline and Distillates (MOGD) oligomerization process. The material balance for this process configuration is contained in Exhibit 2 of Appendix I.

Fresh methane and oxygen mixed with recycle methane (streams 1, 2, and 11, respectively) enter the Catalytic Reactor System. There, the combined feed (stream 3) is brought up to the reactor operating conditions of 725 °C at 50 psig. To do so, the feed is first heated by cross-exchanging with the hot reactor product stream, followed by additional heating with a direct gas-fired heater. The reactors themselves are a series of shell-and-tube heat exchangers, the tubes are packed with catalyst for contact with the process. On each pass, 18.4% of the methane in the feed is converted to products, with an assumed 76.7% selectivity to ethylene and ethane. The balance of the methane that is converted forms carbon monoxide and dioxide, propylene, and propane.

The exothermic heat of reaction in the oxidative coupling reactors is removed as superheated 600 psig steam, which is generated on the shell sides of the reactors. This is accomplished by spraying in a mist of hot 600 psig condensate. This superheated steam is used to drive condensing turbines in the compression and refrigeration portions of the process.

The reactor product gas (stream 4) is cooled first in the feed cross-exchanger, and then is further cooled in a second exchanger to produce hot 600 psig condensate. The cooled reactor product gas then enters the Quench System. This is a large water-cooled partial condenser which cools the gas down to ambient temperature, and removes most of the water of reaction (stream 5). From there, the product gas (stream 6) enters the Compression System.

The Compression System consists of four stages of centrifugal compression. The first stage operates at a suction pressure of about 16 psig, and handles only the Steam Cracker System product gas. The Catalytic Reactor product is combined with the Steam Cracker product at the second stage, which operates at a suction pressure of 40 psig. Water is condensed out of the process stream at each of the compressor intercoolers. The discharge pressure from the fourth stage of the Compression System is 300 psig.

The compressed product gas (stream 8) then enters the Acid Gas Removal System, which consists of a standard amine-scrubbing system for removal of carbon dioxide from the product gas. This is followed by a molecular sieve dryer system which removes the last traces of moisture from the product gas.

The compressed, scrubbed, and dried product gas (stream 10) is ready for processing in the Cold Box System. The Cold Box feed first enters a series of refrigerated partial condensers, which remove successively larger portions of the stream as liquid. The last of these partial condensers operates at a temperature of -105 °C (-160 °F). These liquid fractions are richer in C_2 and heavier hydrocarbons than the

remaining vapor, and are fed to a methane column for removal of the light components. The vapor that is left after the final partial condenser then is combined with the vapor off the top of the methane column for further processing in a series of centrifugal expanders. Separators following each of these expanders collect liquids which are rich in C_2's and heavier hydrocarbons. These liquids are recycled to the methane column. The process temperature reaches -133 °C after the combined vapor has been expanded down to 80 psig. Ten percent of this material is removed as a purge from the process, while the rest is recycled back to the catalytic reaction system (stream 11). The purge gas (stream 12) is then expanded down to 5 psig before it is released from the process. Both the purge and recycle gas streams are heated back up to ambient temperature by cross-exchange with the gas entering the Cold Box System. This reduces the load on the Refrigeration System.

The bottoms product from the methane column in the Cold Box System (stream 13) consists of C_2 and heavier hydrocarbons. This is fed directly to the MOGD System where the ethylene, propylene, and a substantial portion of the C_4's are converted to gasoline and distillate fuels.

Ethane (stream 14) passes through the MOGD System essentially unconverted, and is returned to a conventional Steam Cracker System. About 55% of the ethane that enters the cracking furnaces is converted, with an 85% selectively to ethylene. The rest of the ethane that is converted forms hydrogen, methane, carbon monoxide and dioxide, propylene, and heavier hydrocarbons. The cracked gas (stream 16) exits the furnaces directly into transfer line exchangers which cool the gas and produce dilution steam for the furnaces.

The furnace gas then enters a Quench System where it is further cooled by direct contact with cold water in a large column. The quenched gas (stream 18) then enters the Compression System, where it is combined with the product from the oxidative coupling Catalytic Reaction System.

Synthesis Gas/Methanol Process Simplified Block Diagram

The existing technology for producing liquid fuels from methane proceeds through synthesis gas and methanol as intermediates. The economics of producing liquid fuel by this route have been determined for comparison with the methane coupling technology.

Exhibit 3 of Appendix I is the Simplified Block Diagram for this Synthesis Gas/Methanol Process. A detailed description of this process, its material balance, and its economics is contained in the Comparison Case Section (below) and in Appendix J.

Methane is first converted to synthesis gas in the Steam Reforming section of the process. The process information for this portion of the process is per SRI's formulation of an integrated methanol process[102]. A large excess of water is used in this system, which is recovered for recycle by condensing it away from the synthesis gas in a heat-integrated quench step.

The synthesis gas is then compressed for delivery to the Methanol Synthesis section of the process. This section is patterned after ICI's low-pressure process by SRI[102]. The methanol is condensed away from the unreacted synthesis gas in the second quench step. The methanol goes on to the MTO (Methanol to Olefins) section, while the unreacted synthesis gas is recycled to the Methanol Synthesis section.

UOP's MTO process[103] makes both DME (dimethyl ether) and mixed olefins. The unreacted methanol is recovered in a third quench step. The DME is removed in a water absorber, and is recycled back to the the Methanol Column. The water of reaction is removed by the Methanol Column as the bottoms product, and the make is a mixture of methanol, DME, and water, which is recycled to the MTO reactor. The DME is recycled to extinction by converting it to additional product. The DME Absorber overhead stream contains the mixed olefins product.

The MOGD system[104] produces gasoline and distillate fuels at a ratio of six to one. A small amount of light hydrocarbons are removed as a purge and used as fuel.

Gasoline and Distillate Economics

Exhibit 4 of Appendix I summarizes the economics of making gasoline and distillate fuels via methane coupling versus the Synthesis Gas and Methanol route. A more detailed description of these process economics is contained in the Comparison Case Section (below) and in Appendix J.

The methane coupling facility does not include the Refining System equipment that would be needed to produce high-purity ethylene, but rather is integrated with the MOGD process per the methane coupling Simplified Block Diagram. Both cases are cast on the basis of 1989 US Gulf Coast construction and operating costs, with methane purchased at the Intrastate Delivered price of $2.15/MMBtu (5.1 ¢/lb).

The two routes are similar in that most of the Total Fixed Investment is in the methane conversion portion of the processes. The MTO investment is a relatively small component of the Synthesis Gas and Methanol route ISBL investment, and the MOGD investment is a relatively small component of the Total Fixed Investment for both routes.

Overall, the investment costs for the two routes are about equal: the difference between them is well within the ±25% investment estimate accuracy.

The Operating Cost advantage that is shown for the Synthesis Gas and Methanol route is thought to be real. The selectivity to C_2's for the methane coupling route is only about 77%, versus nearly 100% for the competition. This difference in methane efficiency translates directly into a slight but real cash cost advantage for the Synthesis Gas and Methanol route.

Therefore, this route has a slightly lower Required Sales Price to produce a 10% ROIAT: $1.94/gallon versus $2.09/gallon via methane coupling. This difference is slight when compared to the current wholesale price of liquid fuels of less than $0.60/gallon. But a low-cost source of methane (such as at a remote location) would make the cost of producing liquid fuels via either of these processes more competitive overall. This would also diminish the impact of the lower methane usage for the Synthesis Gas and Methanol route. Therefore, these two technologies are essentially equivalent economically.

This result is viewed as encouraging, given the early state of development of oxidative coupling catalysis. The Synthesis Gas and Methanol route has had the benefit of many years of development and commercial practice. The economics of this route are not likely to be improved significantly by further research. In contrast, methane coupling is a comparatively young technology with no current commercial applications. Therefore, it is reasonable to expect that further research might incrementally improve the performance of the current catalyst systems, or lead to the discovery of novel catalyst systems with greatly improved performance.

Methane Coupling Sensitivity Studies

Sensitivity to Reactor Diluent

Methane coupling cases using different diluents were examined to determine the effect of the different diluents on the process economics. Results are summarized in Table 49 and described in more detail below:

Table 49. Reactor Diluent Cases and Co-feed versus Sequential Feed Cases

Case	A1.1b	A1.2a	A1.3b	A1.4b
Diluent	Nitrogen	Methane	Steam	None
Feed System	Co-feed	Co-feed	Co-feed	Sequential
Reactor Type	Fixed-bed	Fixed-bed	Fixed-bed	Fluidized-bed
CH_4 Conversion, %	45	18	45	24
Selectivity to C_2's, %	50	77	50	62
C_2 Yield, %	22	14	22	15
Total Fixed Investment	710	530	560	530
Total Cash Cost, ¢/lb	21.2	13.7	20.8	12.6
ROIAT, %	3.0	13.9	5.6	15.0

Methane Coupling Process Simplified Block Diagram

Exhibit 5 of Appendix I summarizes the process arrangement that has been used for the methane coupling sensitivity studies. It contains a Refining System to produce high-purity ethylene. The material balances for the Nitrogen, Methane, and Steam Diluent cases and the Sequential Feed case are contained in Exhibits 6, 7, 8, and 9 of Appendix I, respectively.

In the Catalytic Reactor System, fresh and recycle methane (streams 1 and 11, respectively) and any steam diluent are contacted with either air or oxygen (stream 2) to conduct the oxidative coupling reaction. In the Co-feed cases, air or oxygen is mixed with the fresh and recycle methane in the inlet to the reactor preheater. Air is fed separately to the Catalytic Reactor in the Sequential Feed case, and the spent nitrogen is exhausted to the atmosphere after heat recovery.

Both fixed-bed and fluidized-bed reactor systems have been evaluated. The fixed-bed reactor system consists of a series of shell-and-tube heat exchangers, the tubes packed with a supported catalyst. It has been assumed that stainless steel tubes would provide sufficient corrosion resistance. The large exothermic heat of reaction dominates the reactor design by requiring that a large heat transfer area be provided. In the fixed bed reactor system the reaction heat is removed as superheated 600 psig steam, which is

generated on the shell sides of the reactors. This is accomplished by spraying in a mist of hot 600 psig condensate which vaporizes instantly and superheats rapidly to near the process-side temperature. This superheated steam is used to drive condensing turbines in the Compression and Refrigeration portions of the process.

Alternately, a dilute-phase co-current down-flow reactor design has been used as the model for the fluidized-bed reactor system in this evaluation. The advantage of this system over more conventional fluidized-bed designs is the large catalyst-to-process flow ratios and the short contact times that are made possible. All of the reactor system vessels are constructed of refractory-lined steel, which confers both temperature and corrosion/erosion resistance. In this system, the large exothermic heat of reaction is removed by spraying hot condensate directly onto the catalyst solids as they exit the bottom of the reactor vessel. The condensate flashes explosively, generating low-pressure superheated steam and propelling the solids up a riser tube to the top of the reactor vessel. This superheated steam is then separated from the catalyst and used to drive condensing turbines elsewhere in the process.

Whether fixed-bed or fluidized-bed, the reactor feed (stream 3) is brought up to the reactor operating temperature by first cross-exchanging with the hot reactor product stream, followed by additional heating with a direct gas-fired heater. Only a portion of the methane that is fed is converted on each pass, but typically with a fairly high selectivity to ethylene and ethane. The balance of the methane that is converted forms carbon monoxide and dioxide, and C_3 and heavier hydrocarbons.

The reactor product gas (stream 4) is cooled first in the feed cross-exchanger, and then is further cooled in a second exchanger to produce hot condensate. The cooled reactor product gas then enters the Quench portion of the process. This is a large water-cooled partial condenser which cools the gas down to ambient temperature, and removes most of the water of reaction as a liquid (stream 5). From there, the product gas (stream 6) enters the Compression System.

The Compression System consists of four stages of centrifugal compression. The first stage operates at a suction pressure of about 16 psig, and handles only the Steam Cracker System product gas. The Catalytic Reactor product mixes with the Steam Cracker product at the second stage, which operates at a suction pressure of 40 psig. Water is condensed out of the process stream at each of the compressor intercoolers. The discharge pressure from the fourth stage of the Compression System is 300 psig. The compressed product gas (stream 8) then enters the Acid Gas Removal System, which consists of a standard amine-scrubbing system for removal of carbon dioxide from the

product gas. This is followed by a molecular sieve dryer system which removes the last traces of moisture from the product gas. The compressed, scrubbed, and dried product gas then is ready for processing in the Cold Box System.

The Cold Box feed first enters a series of refrigerated partial condensers, which remove successively larger portions of the stream as liquid. The last of these partial condensers operates at a temperature of less than -95 °C (-140 °F). These liquid fractions are richer in C_2 and heavier hydrocarbons than the remaining vapor, and are fed to a Methane Column for removal of the light components. The vapor that is left after the final partial condenser then is combined with the vapor off the top of the Methane Column for further processing in a series of centrifugal expanders. Separators following each of these expanders collect liquids which are rich in C_2's and heavier hydrocarbons. These liquids are recycled to the Methane Column. A portion of the remaining vapor is removed as a purge from the process, while the rest (stream 11) is recycled back to the Catalytic Reactor System. The purge gas (stream 12) is then expanded down to 5 psig before it is released from the process. Both the purge and recycle gas streams are heated back up to ambient temperature by cross-exchanging with the gas entering the Cold Box System. This cross-exchanging reduces the load on the Refrigeration System.

The bottoms product from the Methane Column in the Cold Box System (stream 13) consists of C_2 and heavier hydrocarbons. This is fed to a two-column Refining System for making high-purity ethylene. The De-ethanizer separates the C_3 and heavier hydrocarbons (stream 14) from the ethylene and ethane. The overhead make stream from the De-ethanizer (stream 15) is fed to the Ethylene Column. This column employs a vapor recompression system to reduce the refrigeration load on the column condenser. High purity ethylene (stream 16) is produced as the overhead product, while the bottoms product (stream 17) is ethane containing less than 1% ethylene.

This ethane is returned to a conventional Steam Cracker System. About 55% of the ethane that enters the cracking furnaces is converted, with an 85% selectively to ethylene. The rest of the ethane that is converted forms hydrogen, methane, carbon monoxide and dioxide, propylene and heavier hydrocarbons. The cracked gas (stream 18) exits the furnaces into transfer line exchangers which cool the gas and produce dilution steam for the furnaces.

The cracked gas then enters a Quench System where it is further cooled by direct contact with cold water in a large column. The quenched gas (stream 20) then enters the Compression System, where it is combined with the product from the Catalytic Reaction System.

Reactor Diluent Case Descriptions

Exhibit 10 of Appendix I summarizes the four methane coupling reactor diluent cases that have been evaluated. It has been assumed that the maximum amount of oxygen that can be present in the reactor feed is about 10-11% by volume, determined by the explosive limits for the mixture. However, the oxidative coupling reaction consumes only two moles of methane per mole of oxygen. The methane conversion per pass is thereby limited to less than 25% if only methane and oxygen are reacted with an initial oxygen concentration of 10-11%. Injecting additional oxygen in between reactor stages only leads to the unselective combustion of the C_2's with little additional C_2 formation. Therefore, the incentive for adding a diluent is to allow the methane conversion per pass to be increased above what would be possible by feeding methane and oxygen alone.

The Nitrogen Diluent case is the logical starting point for these sensitivity studies since most of the laboratory studies on methane coupling are conducted in nitrogen. The catalyst performance which is reflected in Exhibit 10 of Appendix I for the Nitrogen Diluent case is based on extrapolated UCC&P laboratory results with a barium on alumina catalyst with ethyl chloride (ECl) added as a promoter at atmospheric pressure. It has been assumed that the reactor pressure can be increased to 50 psig without major impact on the catalyst selectivity. The ratio of methane to oxygen in the feed for this case is 2, which was the mid-point of the range studied. The selectivity to C_2's is only 50% for this case, but the methane conversion is 45%, giving a yield to C_2's of 22%. This performance is competitive with any other oxidative coupling catalyst described in the literature. The reactor type is the fixed-bed system described in the previous discussion of the Simplified Block Diagram. An advantage of the Nitrogen Diluent case is that the oxygen can be added to the process in the form of air. This eliminates the need for an Air Separation system, which is both a high investment and a high operating cost item.

The Methane Diluent case described in Exhibit 10 of Appendix I covers the case wherein only methane and oxygen are fed to the catalytic reactor at an initial oxygen concentration of 10-11%. Since the methane is in vast excess to its requirements in the reaction, this excess methane essentially becomes the diluent. The catalyst performance for this case is based on extrapolated UCC&P laboratory results from the same barium catalyst that was used for the Nitrogen Diluent case.

The result obtained after 8300 minutes of time on-stream of reaction 33-BKW-7 was used as the basis for Case Al.2a. At this time analyses indicated a C_2 selectivity of 76.39%, a methane conversion of 9.84%, an oxygen conversion of 99.6%, and an

ethylene to ethane product ratio of 1.24. The space velocity was 1667 h^{-1} and the temperature was 750 °C, with the reactor pressure 11 psig (1.76 kPa). The oxygen fed was 4.83%, with 89.2% methane fed and 5.55% nitrogen fed. Products (relative moles) were:

CH_4	80.52
CO	0.269
CO_2	1.28
C_2H_4	1.90
C_2H_6	1.54
C_3H_6	0.13
C_3H_8	0.05

It was assumed that if the feed oxygen level were doubled, at 100% oxygen conversion, the methane conversion would double. It was assumed that the pressure could be changed to 50 psig (438 kPa).

A decrease in the methane to oxygen feed ratio would result in a decrease in selectivity, but the space velocity would be raised from 1667 to 3400 h^{-1} to counteract this. The ethyl chloride level in the feed gas was assumed to be 50 ppm rather than the 17 ppm of the example, since better results were obtained with high methane levels using 50 ppm in reaction 33-BKW-7. The C_2H_4/C_2H_6 product ratio was assumed to be 3, rather than 1.2, since a higher ECl level was assumed. The reactor type is fixed-bed. The methane-to-oxygen feed ratio is 7. Note that while the conversion per pass for this case is lower than that for the Nitrogen Diluent case, the selectivity to C_2's is higher. However, the overall effect is a yield-to-C_2's of only 14%.

The Steam Diluent case considers an alternative to nitrogen as a diluent in the methane coupling process. The catalyst performance for this case has been assumed to be identical to that for the Nitrogen Diluent case for lack of better information. The primary incentive of steam versus nitrogen as a diluent is that almost all of the steam will condense in the Quench step following the Catalytic Reactor, and will not have to be handled in the downstream Compression and Separation Systems. There is some precedent for using steam as a diluent also, since most hydrocarbon cracking operations use steam as a diluent to limit coke formation on the furnace tubes.

For the Nitrogen, Methane, and Steam Diluent cases, all of the reactants are mixed at the inlet to the fixed-bed catalytic reactor and enter all at the same time, which is referred to as the Co-feed system.

In the Sequential Feed system, the methane and oxygen are introduced to the reactor separately, rather than together. This allows the methane conversion per pass to be increased without a diluent, avoiding the explosive mixture limitations of the Co-feed cases. To do this, the catalyst is oxidized with air in one step, and then reduced in a separate step via the coupling reaction by contacting it with methane. The conversion per pass in this system is limited only by the relative proportions of methane and catalyst present and by the methane residence time in this second reaction zone. The catalyst performance data depicted in Exhibit 10 of Appendix I for the Sequential Feed case is based on literature results[6,97] for an ARCO catalyst system. A 24% methane conversion per pass and 62% selectivity to C_2's have been assumed, giving a 15% yield. Note that this case makes much more heavy C_4's+ hydrocarbons than the Co-feed cases. The fluidized-bed reactor design has been assumed for this case, allowing the sequential reaction to be carried out by feeding the methane and air separately but continuously to different points in the catalyst cycle. A fixed-bed Sequential Feed process is felt to be impractical.

The oxygen conversion in the Catalytic Reactor has been assumed to be 100% for all cases, versus actual laboratory oxygen conversions of 75 to 95%. It has been assumed that half of the hydrogen and carbon monoxide that enter the Reactor via the methane recycle stream are converted to water and carbon dioxide, respectively. All of the C_2's that are recycled to the Reactor are assumed to be destroyed (burned). Therefore, C_2 recycle is minimized.

All of these cases assume that the ratio of ethylene to ethane in the Catalytic Reactor product is about 3/1. Laboratory studies indicate that using ethyl chloride (ECl) as a promoter can produce this relatively high ratio versus the more typical ethylene to ethane product ratio of 1/1 that has been reported in the literature without a promoter. Sensitivity studies indicate that achieving this relatively high ratio is important economically, but that still higher ratios are less important. The economic significance of the ethylene to ethane product ratio should not be ignored, even though assuming about the same ratio for each of these cases eliminates this variable from this sensitivity analysis.

Reactor Diluent Investment Costs

Exhibit 11 of Appendix I summarizes the results of the investment estimates that have been prepared for the four methane coupling cases. In each case, facilities are

included to produce refined ethylene, but not gasoline and distillate fuel via the MOGD Process. The inherent assumption is that the process that is best for producing ethylene will also be the best for making liquid fuels.

All the ISBL (Inside Battery Limits) investment figures are of ±25% quality. They have been built-up from discrete, individual equipment sizes and costs, and have only been grouped into process systems to facilitate comparisons among the cases. They are based on 1989 US Gulf Coast non-union construction costs, and include a 15% contingency. The OSBL (Outside Battery Limits) investment has been estimated as 40% of the combined ISBL plus Air Separation investment.

The Nitrogen Diluent case has by far the highest investment cost of the group. Compared to the other cases, this case is more costly in the Compression, Acid Gas Removal, Cold Box, and Refrigeration Systems. These systems are all involved in maintaining the large nitrogen diluent cycle, and in separating the excess nitrogen from the unreacted methane. Therefore, while using nitrogen as a diluent may be logical for laboratory studies, a Nitrogen Diluent full-scale facility is impractical due to the high investment cost.

The Methane and Steam Diluent and the Sequential Feed cases all have about the same investment cost, well within the ±25% investment estimate accuracy.

The cost of the Catalytic Reactor System is most closely related to the amount of heat released in the reaction step. The heat released by the oxidative coupling reaction is much less than that for the non-selective burning reaction. Therefore, the Methane Diluent case has the lowest Catalytic Reactor investment, since it has the highest selectivity to C_2's, and hence the lowest amount of carbon monoxide and dioxide formed via the burning reaction.

Note that whether a case allows feeding air versus oxygen is not a significant distinguishing feature among these cases. This is because the Air Compression Systems for delivering air to the Catalytic Reactor are almost equal in cost to the Air Separation Systems.

Reactor Diluent Economics

Exhibit 12 of Appendix I summarizes the economics of the four methane coupling cases. Consistent with the investment estimates, these economics have been cast on the basis of producing ethylene for sales.

The Total Fixed Investment for each case is from Exhibit 11 of Appendix I. The Working Capital is an estimate of the value of the inventory and accounts receivable that would be involved in a methane coupling operation. The Total Utilized Investment is the sum of the Total Fixed Investment and the Working Capital.

All of the Operating Costs in Exhibit 12 of Appendix I have been expressed in terms of $MM (millions of dollars) for a unit producing one billion pounds per year of ethylene. Methane is by far the largest Operating Cost component. It has been assumed for this analysis that methane is being purchased at the 1989 average US Gulf Coast Intrastate Delivered price of $2.15 per MMBtu, or 5.1 ¢/lb. The Methane Diluent case has the lowest methane usage due to its high selectivity to C_2's.

The By-Product Credits are the sum of the values of the C_3 and heavier co-products, plus the fuel value of the lights purge stream. The Nitrogen Diluent case has a lower By-Product Credit than the others since the fuel value of its lights purge stream is extremely low. On the other hand, the economics of the Sequential Feed case is most sensitive to the By-Product Credits, because of the large amount of C_4 and heavier materials produced in this process.

The Utilities requirements for the methane coupling cases are mostly the fuel to fire the Catalytic Reactor preheaters, plus the electrical power to drive the Compression, Refrigeration, and Air Separation or Air Compression Systems. However, it has been found that the fuel requirements can usually be satisfied by the inerts purge stream from the Cold Box. Likewise, credit has been taken for the steam that is produced in the Catalytic Reactor Systems, which is used in turbine drivers and offsets the electrical requirements.

The Steam Diluent case is distinguished by its high utility cost, since most of the steam generated in the Catalytic Reactor System must be used as diluent, rather than as motive steam in turbines elsewhere in the process. On the other hand, the Sequential Feed case is distinguished by its low utility cost. The absence of a diluent that characterizes this case causes the Compression and Refrigeration System operating costs to be low. Also, air is used to oxidize the catalyst, which eliminates the high operating cost for the Air Separation System.

The Fixed Costs are mostly the cost of maintenance, which is assumed to be an annual percentage of the Total Fixed Investment. Operating labor is also included.

The Total Cash Cost is the sum of the Variable and Fixed Operating Costs. This represents the net cost of producing the product, and does not include any ex-plant costs such as distribution, or any marketing, sales, or technical staff support costs.

The ROIAT (Return on Investment After Tax) for each case is based on a 1989 average sales price of $0.32/lb for ethylene. ROIAT is the ratio of the NIAT (Net Income After Tax) to the Total Utilized Investment. NIAT is sales income minus cash cost, depreciation, and taxes.

ROIAT can be thought of as the first year's "interest rate" that the facility investment would return to the owners, assuming capacity operation. In this light, the returns from the Nitrogen and Steam Diluent cases are clearly unacceptable. The Methane Diluent case and the Sequential Feed cases are approximately equal on an ROIAT basis, both generating an acceptable return.

These returns are all likely to decrease over the next few months as the price of ethylene returns to more historical levels. As this happens, however, the cases should retain their current relative economic ranking, with the Methane Diluent and Sequential Feed Cases being clearly superior to either the Nitrogen or Steam Diluent cases.

Referring back to Exhibit 10 of Appendix I, note that the yield-to-C_2's for both the Methane Diluent and the Sequential Feed cases are lower than the yields for the Nitrogen and Steam Diluent cases. But Exhibit 12 of Appendix I shows that the Methane Diluent and the Sequential Feed cases have better economics.

The key to understanding this apparently contradictory result is to note that the cases with the lower cash costs have the better economics, and that methane cost is the largest single component of the cash cost. The low methane cost in the Methane Diluent case is due to its high selectivity to C_2's. The Sequential Feed case has not only high selectivity to C_2's, but also high by-product credits and low utility costs. The benefits of higher methane conversion and yield-to-C_2's that characterize the Nitrogen and Steam Diluent cases are more than offset by the costs of their lower selectivity to C_2's. Therefore, yield-to-C_2's is not a good general predictor of economics.

While the Methane Diluent and Sequential Feed cases are economically equivalent, other factors tip the balance of this overall analysis in favor of the Methane Diluent case. The non-economic factors in favor of the Methane Diluent case are:

- The Methane Diluent case is based on extrapolated laboratory catalyst results, while the Sequential Feed case is based solely on literature catalyst results.

- The Sequential Feed case requires a fluidized-bed reactor design, which is inherently more risky from an engineering standpoint than the fixed-bed reactor design which the Methane Diluent case allows.

- The low cash cost for the Sequential Feed case is due in part to its high co-product credits, based on the presumption of a ready customer for the heavy C_4's+ hydrocarbons stream. No such presumption is necessary for the Methane Diluent case.

Therefore, the Co-feed Methane Diluent case is preferred over the more technically and commercially risky Sequential Feed case.

Sensitivity to Methane/Oxygen Ratio

Nitrogen Diluent Cases

Three Nitrogen Diluent cases have been evaluated, each at a different methane/oxygen ratio in the reactor feed. All are based on an oxygen concentration in the feed to the reactor of 11.2%. These are summarized below:

Case	A1.1d	A1.1b	A1.1c
CH_4/O_2 Ratio	1	2	4
CH_4 Conversion, %	73	45	26
Selectivity to C_2's, %	33	50	59
Yield to C_2's, %	24	22	15
Total Fixed Investment, $MM	833	710	697
Total Cash Cost, ¢/lb	26.5	21.3	19.7
ROIAT, %	-1.9	2.9	4.7

Exhibit 13 of Appendix I summarizes the results of the investment estimates for the Nitrogen Diluent cases. Note that the Total ISBL (inside battery limits) investment for the cases decreases as the methane to oxygen ratio in the feed to the catalytic reactor system increases. This results from the fact that increasing the methane to oxygen ratio decreases the methane conversion, but increases the selectivity to C_2's. The design of the Catalytic Reactor System is dominated by the need to remove the heat of reaction, which decreases with increasing selectivity. Increasing selectivity also reduces the air requirements for the process, and hence, the size of the Air Compression System. This

trend overwhelms the tendency of decreasing methane conversion to increase the costs of the Steam Cracking, Cold Box, and Refrigeration Systems.

Exhibit 14 of Appendix I summarizes the economics for the Nitrogen Diluent cases. Note that the total cash cost decreases with increasing methane to oxygen ratio, due to the previously noted effect of this variable on the selectivity to C_2's, and hence the overall methane usage. This trend overwhelms the tendency of decreasing methane conversion to increase the utility costs. With both the investment and the cash cost decreasing with increasing methane to oxygen ratio, the sensitivity of the resultant ROIAT (return on investment after tax) to this variable is significant.

However, it is not possible to increase the methane to oxygen ratio beyond 4 and still feed air to the process. Beyond this limit, purified oxygen would have to be fed instead, and much of the advantage of the Nitrogen Diluent case would be lost. At a methane to oxygen ratio of 7, the process arrangement and economics would be identical to the Methane Diluent case (Case A1.2a).

Methane Diluent Case

Only one Methane Diluent case is possible if the oxygen concentration in the feed to the reactor is held at 11.2%:

Case	A1.2a
CH_4/O_2 Ratio	7
Methane conversion, %	18
Selectivity to C_2's, %	77
C_2 yield, %	14
Total Fixed Investment, $MM	530
Total Cash Cost, ¢/lb	13.7
ROIAT, %	13.9

The investment estimate and economics for this case are summarized in Exhibits 11 and 12 of Appendix I, respectively.

Steam Diluent Cases

Three Steam Diluent cases have been evaluated, each at a different methane to oxygen ratio in the reactor feed. All are based on a oxygen concentration in the feed to the reactor of 11.2%. The methane conversion and selectivity to C_2's for these cases have been assumed to be equal to those for the Nitrogen Diluent cases. The Steam Diluent cases are summarized below:

Case	A1.3d	A1.3b	A1.3c
CH_4/O_2 Ratio	1	2	4
CH_4 Conversion, %	73	45	26
Selectivity to C_2's, %	33	50	59
Yield to C_2's, %	24	22	15
Total Fixed Investment, $MM	679	561	556
Total Cash Cost, ¢/lb	30.8	20.8	16.9
ROIAT, %	-4.6	5.6	9.7

Exhibit 15 of Appendix I summarizes the results of the investment estimates for the Steam Diluent cases. Note that the Total ISBL (inside battery limits) investment for the cases reaches a minimum at a methane to oxygen ratio of 2, but generally decreases with increasing methane to oxygen ratio. This results from the fact that increasing the methane to oxygen ratio decreases the methane conversion, but increases the selectivity to C_2's. The design of the Catalytic Reactor System is dominated by the need to remove the heat of reaction, which decreases with increasing selectivity. This trend is countered by the tendency of decreasing methane conversion to increase the costs of the Steam Cracking, Compression, Cold Box, and Refrigeration Systems.

Exhibit 16 of Appendix I summarizes the economics for the Steam Diluent cases. Note that the Total Fixed Investment decreases with increasing methane to oxygen due to the previously noted effect of this variable on the selectivity to C_2's, and hence the cost of the Oxygen Plant (Air Separation Unit). Note also that the total cash cost decreases with increasing methane to oxygen ratio, due to the decrease in both the overall methane usage and the utility costs. The utility costs decrease with increasing methane to oxygen ratio due to the declining demand for steam diluent, allowing more of the reaction steam to be

used in driving the Compression and Refrigeration System turbines. With both the investment and the cash cost decreasing with increasing methane to oxygen ratio, the sensitivity of the resultant ROIAT to this variable is significant.
However, as the methane to oxygen ratio is increased beyond 4, the process arrangement and economics approach that of the Methane Diluent case (Case A1.2a).

Sequential Feed Cases

Four Sequential Feed cases have been evaluated, each assuming a different methane conversion. Each case assumes 100% conversion of the oxygen used to reoxidize the catalyst, resulting in four CH_4/O_2 ratios. All are based on ARCO literature catalyst results. Results are summarized below:

Case	A1.4c	A1.4b	A1.4d	A1.4e
CH_4/O_2 Ratio	2	5	7	10
CH_4 Conversion, %	45	24	20	16
Selectivity to C_2's, %	42	63	67	72
Yield to C_2's, %	19	15	14	12
Total Fixed Investment, $MM	587	532	554	579
Total Cash Cost, ¢/lb	16.3	12.6	13.3	13.9
ROIAT, %	9.5	15.0	13.5	12.1

Exhibit 17 of Appendix I summarizes the results of the investment estimates for the Sequential Feed cases. Note that the Total ISBL (inside battery limits) investment for the cases goes through a minimum at a methane to oxygen ratio of 5. This results from the fact that increasing the methane to oxygen ratio decreases the methane conversion, but increases the selectivity to C_2's. Increasing selectivity reduces the air requirements for the process, and hence, the size of the Air Compression System. This trend is countered by the tendency of decreasing methane conversion to increase the costs of the Compression, Cold Box, and Refrigeration Systems.

Exhibit 18 of Appendix I summarizes the economics for the Sequential Feed cases. Note that the total cash cost also goes through a minimum at a methane to oxygen ratio of 5, due to the previously noted effect of this variable on the selectivity to C_2's and methane

conversion. Increasing the selectivity to C_2's decreases the overall methane usage, but this trend is countered by the tendency of decreasing methane conversion to increase the utility costs. With both the investment and the cash cost reaching their minimums at a methane to oxygen ratio of 5, the resultant ROIAT reaches its maximum at this point as well.

Summary of Economic Sensitivity to Methane/Oxygen Ratio

Exhibits 19 and 20 of Appendix I summarize the results of the sensitivity studies conducted on reactor diluent and methane/oxygen ratio described above. The top graph in Exhibit 19 of Appendix I shows how the Total Fixed Investment for the four diluent systems compare among themselves, and how each varies with methane to oxygen ratio. The Nitrogen Diluent cases require much more investment than any of the others. This is due to the high cost of compressing the nitrogen diluent from the catalytic reactor pressure up to the operating pressure of the recovery and refining systems, plus the high cost of separating this nitrogen from the unreacted methane. The investment for the methane and Steam Diluent cases and the Sequential Feed cases are all approximately equal to each other, differing by less than the ±25% investment accuracy.

The bottom graph in Exhibit 19 of Appendix I shows how the Total Cash Cost for the four diluent systems compare among themselves, and how each varies with methane to oxygen ratio. Both the Nitrogen and Steam Diluent cases have a higher cash cost than either the Methane Diluent or the Sequential Feed cases. These cases have a higher methane usage due to their lower selectivity to C_2's. The Total Cash Cost for the Methane Diluent and the Sequential Feed cases are approximately equal to each other.

Exhibit 20 of Appendix I shows how the resulting ROIAT for the four diluent systems compare among themselves, and how each varies with methane to oxygen ratio. With their higher selectivity to C_2's, both the Methane Diluent and the Sequential Feed cases have a higher ROIAT than the Nitrogen or Steam Diluent cases. But the Nitrogen and Steam Diluent cases had a higher overall yield to C_2's. Again, yield-to-C_2's is not a good general indicator of economics. Rather, selectivity to C_2's appears to be the more reliable economic indicator.

Sensitivity to Oxygen Concentration in the Reactor Feed

Two Methane Diluent cases have been evaluated, differing in the oxygen concentration in the feed to the catalytic reactor:

Case	A1.2a	A1.2b
Oxygen concentration in Rx feed, %	11.2	5.2
Methane conversion, %	18	10
Selectivity to C_2's, %	77	87
C_2 yield, %	14	9
Total Fixed Investment, $MM	530	666
Cash Cost, ¢/lb ethylene	13.7	16.6
ROIAT, %	13.9	7.5

Exhibit 21 of Appendix I summarizes the results of the investment estimates for these cases. Note that the Total ISBL (inside battery limits) investment increases as the oxygen concentration in the feed to the catalytic reactor system decreases. This results from the fact that increasing the methane to oxygen ratio increases the selectivity to C_2's, but decreases the methane conversion. The design of the Catalytic Reactor System is normally dominated by the total heat of reaction, but in this instance is affected more strongly by the feed preheat and product quench heat loads. Decreasing methane conversion also increases the cost of the Compression, Acid Gas Removal, Cold Box, and Refrigeration Systems.

Exhibit 22 of Appendix I summarizes the economics for these cases. Note that the total cash cost increases with decreasing oxygen concentration, due to the previously noted effect of this variable on the methane conversion, and hence the total utilities cost. This trend overwhelms the tendency of increasing selectivity to C_2's to decrease the overall methane usage. With both the investment and the cash cost increasing with decreasing oxygen concentration, the sensitivity of the resultant ROIAT to this variable is significant.

In the section of this report dealing with the effect of reactor diluents, it is shown that selectivity to C_2's is the most reliable economic indicator, so long as the oxygen concentration in the feed to the reactor is held at a fixed value. Comparing Case A1.2a to

A1.2b; however, it is seen that a lower oxygen concentration increases the selectivity to C_2's, but has a detrimental effect on the economics. Therefore, the economics strongly favor maximizing the concentration of oxygen in the reactor feed. For this study, it has been assumed that this maximum concentration is about 11.2%, due to the explosive limits of the mixture. Obviously, determining precisely maximum limit for this variable is of prime importance from both an economic and a safety standpoint.

Sensitivity to Ethylene to Ethane Product Ratio

Three Sequential Feed cases have been evaluated, differing in the ratio of ethylene to ethane that is produced in the Catalytic Reactor System:

Case	A1.4b.4	A1.4b	A1.4b.5
Ethylene to Ethane Product Ratio	1/1	3.35/1	10/1
Total Fixed Investment, $MM	603	532	494
Cash Cost, ¢/lb ethylene	13.9	12.6	12.1
Return on Investment After Tax, %	11.4	15.0	17.0

Exhibit 23 of Appendix I summarizes the investment estimates for these cases. As the ethylene to ethane product ratio increases from 1 to 3.35, the costs for the Steam Cracking, Compression, and Refrigeration Systems decrease substantially. But the improvement in these areas is less significant as the ethylene to ethane product ratio increases further to 10/1.

Exhibit 24 of Appendix I summarizes the economics for these cases. While the raw material cost and the co-product credits are unaffected by this variable, the utility costs are sensitive to ethylene to ethane product ratio below 3.35, but not above. Overall, both cash cost and investment decrease with increasing ethylene to ethane product ratio, and the ROIAT increases accordingly. But the "point of diminished return" for this variable is at about 3-4 versus the typical level of 1. The economic significance of ethylene to ethane product ratios higher than 3.35 is marginal.

Sensitivity to the Fate of Co-Product Ethane

Two Sequential Feed cases have been evaluated, differing on whether the co-product ethane is sold externally or consumed within the process by cracking it:

Case	A1.4b.3	A1.4b
Fate of Co-Product Ethane	Sold	Cracked
Total Fixed Investment, $MM	557	532
Cash Cost, ¢/lb ethylene	13.5	12.6
Return on Investment After Tax, %	13.1	15.0

Exhibit 25 of Appendix I summarizes the investment estimates for these two cases. Selling the co-product ethane allows the Steam Cracking portion of the unit to be deleted, but the parts that remain must be made bigger to make up for the ethylene that was lost. The net effect is that the process investment increases.

Exhibit 25 of Appendix I summarizes the economics of these two cases. The ethane co-product credits do not make up for the extra methane that must be consumed if the ethane is sold, causing the ethylene cash cost to be higher if the ethane is sold externally. Ethane is more valuable if it is retained and cracked within the process than if it is sold externally as a co-product.

Sensitivity to Reactor Temperature and Pressure

These sensitivities are centered on the original Base Case (Case 1.0.0). Exhibit 27 of Appendix I shows the Simplified Block Diagram for Case 1.0.0, and Exhibit 28 of Appendix I shows the overall material balance. This is a Methane Diluent case based on the following assumptions regarding the Catalytic Reactor System operating conditions and product mix:

		Selectivity to, %	
Methane/oxygen ratio	9/1	C_2H_4	47.3
Rx Pressure, psig	150	C_2H_6	38.1
Rx Temperature, °C	725	C_3H_6	4.6
Methane Conversion, %	22.4	C_3H_8	2.8
Yield to C_2's, %	19	C_4's +	0.2
		CO_2	6.1
		CO	1.0

Reactor Temperature Cases

Case	1.0.3	1.0.0	1.0.4
Reactor Temperature, °C	625	725	825
Total Fixed Investment, $MM	527	538	561
Cash Cost, ¢/lb ethylene	12.7	12.7	12.9
Return on Investment After Tax, %	14.8	14.4	13.5

Exhibits 29 and 30 of Appendix I summarize the investment estimates and economics for the reactor temperature sensitivity cases. Assuming that by using different catalysts the same product mix could be obtained at a range of temperatures, then the catalyst that allowed the lowest temperature would be economically preferred. This arises entirely from the fact that the Catalytic Reactor System would become less costly to build as its design temperature was reduced. Note that the cash cost is not significantly affected by changes in the reactor operating temperature. With the impact of lower

reactor cost diluted by the investment for the rest of the process, the overall sensitivity of the economics to reactor operating temperature is not very significant in the range of 625-825 °C.

Reactor Pressure Cases

Case	1.0.1	1.0.0	1.0.2
Reactor Pressure, psig	80	150	240
Total Fixed Investment, $MM	547	538	525
Cash Cost, ¢/lb ethylene	13.5	12.7	12.1
Return on Investment After Tax, %	13.3	14.4	15.6

Exhibits 31 and 32 of Appendix I summarize the investment estimates and economics for the reactor pressure sensitivity cases. Assuming that changing the reactor operating pressure would not have any significant effect on the product mix, then the impact of this variable is on the investment cost of the Catalytic Reactor System, and on both the investment cost and the operating cost of the Compression System. As the pressure is increased, the higher investment cost of the Reactor System is mostly offset by the lower investment cost for the Compression System, so that the overall effect of this variable on investment is small. However, as the reactor pressure is increased, the utility cost drops due to the lower operating cost for the Compression System. Therefore, the economics favor a higher reactor operating pressure in the range of 80-240 psig.

Hypothetical Catalyst Performance Economics

Exhibit 33 of Appendix I summarizes the economics of hypothetical or future catalyst systems as a function of the methane conversion and selectivity to C_2's using the current technology as the starting point. The current technology is represented by the Methane Diluent case, which has been shown earlier to be the best of the methane coupling systems that have been considered.

The graph in the upper left corner of Exhibit 33 of Appendix I shows how the TFI (Total Fixed Investment) could be reduced from that required for the current technology. If catalyst improvements could be made that would allow the methane conversion to be

increased while retaining the current or higher selectivity to C_2's, then the TFI could be reduced from the current $530MM to less than $400MM.

The graph in the upper right corner of Exhibit 33 of Appendix I shows how the Cash Cost to ethylene could be reduced below that for the current technology. The strong effect of selectivity to C_2's on the Cash Cost is evident. Even at today's conversion per pass of only 18%, increasing the selectivity to C_2's to 85% would have almost as great an effect on the Cash Cost to ethylene as would increasing the conversion to 55% at 77% selectivity. Overall, catalyst improvements have the potential for reducing the cash cost from the current 13.7 ¢/lb to less than 11.5 ¢/lb.

The large graph at the bottom of Exhibit 33 of Appendix I shows how the ROIAT for a methane coupling facility could be improved over that for current technology. The horizontal dashed line at an ROIAT of 25% represents the minimum return that methane coupling would have to offer to attract investment. Any new process must have compelling economics versus the alternatives to justify taking on the associated technical and financial risk. Note that even a methane conversion of 55% does not bring the return up to the economic threshold if the selectivity is 77%. On the other hand, if the selectivity to C_2's could be improved to 85%, then a conversion per pass of 37% or more would generate sufficient return versus the alternatives to attract attention.

This goal is regarded as attainable long-term. Therefore, given sufficient time and resources, future catalyst improvements should confer superior economics to the methane coupling process.

In order to assure a substantial economic incentive in its favor, the most conservative methane coupling catalyst performance target would be 55% methane conversion and 85% selectivity to C_2's at current operating conditions.

Comparison Case

The process sequence for the conversion of methane to methanol is shown in Figures J1, J2, and J3 of Appendix J and the accompanying material balance is given in Table J1 of Appendix J. The information is based upon SRI International's[102] formulation of an integrated process to produce syn-gas from methane by steam reforming of natural gas followed by ICI's low pressure process for the conversion of syn-gas to methanol. Natural gas feed is desulfurized with activated carbon in M-101 and M-102, preheated to 88 °C in E-110 by heat exchange with the reformer product and then contacted with hot water at 204 °C in a countercurrent packed scrubber (C-101) which

provides about 50% of the required reformer steam. The exit gas from C-101 at 320 psia and 199 °C is blended with exhaust steam at 350 psia and 354 °C from the recycle gas compressor (K-202) in the methanol synthesis section and sent to E-101 where the reformer reactants are preheated to 538 °C; the reaction is then carried out in the radiant section of the reforming furnace (F-101). The furnace exit gas at 295 psia and 871 °C is cooled initially to 538 °C by generating 1100 psia steam in E-105 and then to 218 °C by generating 200 psia steam in E-106. Additional process to process heat exchange in E-107, E-108, E-109, and E-110 and final cooling in E-111 serves to condense almost all of the steam from the reaction product before it is sent to the methanol synthesis section at 240 psia and 38 °C (Stream 13). The condensate thus produced is blended with fresh demineralized water and, after being preheated by the methanol converter product in E-205, is either recycled to the feedstock water saturator (Stream 21) or is used as feed for generating 1100 psia steam (Stream 10).

Most of the fuel for the reforming furnace is supplied by a purge from the methanol synthesis section (Stream 7), with the balance being supplied by natural gas (Stream 3). The blended fuel is preheated to 88 °C in E-109 by heat exchange with the reformer product and then is mixed with hot air at 266 °C prior to entering the reformer furnace. The hot flue gases from the combustion reaction leave the radiant section of the reformer at 927 °C and are cooled to 127 °C in the convective section by preheating the reformer feed in E-101, raising 1100 psia steam at 538 °C in E-102 and E-103 and preheating the air required for combustion in E-104. The superheated steam generated by E-102 drives the turbines for compressors K-201 and K-202 in the methanol synthesis section. K-201 is driven by a condensing turbine with an exhaust pressure of 1.3 psia while K-202 is driven by a back-pressure turbine which exhausts steam at 350 psia to the reformer furnace.

In the methanol synthesis section, K-201 raises the pressure of the syn-gas from 240 psia to 1500 psia while K-202 boosts the pressure of the recycle gas from the methanol converter from 1350 psia to 1500 psia. The total feed to the reactor at 57 °C is preheated to 132 °C in E-202 by heat exchange with the synthesis product. Part of the reactor feed (Stream 16) is further heated to 243 °C in E-203 and sent to the methanol converter while the rest of the feed (Stream 15) is used as a "cold-shot" for controlling the temperature of the reactor. This is achieved by injecting portions of the gas mixture into the catalyst at three levels through specially designed distributor lozenges.

Crude product from the reactor emerges at 271 °C and is split into two streams for heat recovery. The first stream is cooled to 160 °C in E-203 while the second is cooled

initially to 235 °C in E-204 and then to 179 °C in E-205 by preheating the water in the reforming heat recovery section. These two streams are then recombined and cooled from 167 °C to 93 °C in E-202 by preheating the feed to the reactor. Further cooling of the reaction product to 82 °C is accomplished in E-206 by heating the purge stream during its expansion through the gas turbine (K-204). Final cooling to 38 °C occurs against cooling water in E-207 where most of the water and methanol condenses and is withdrawn as product from V-201 through the liquid turbine drive (K-203) which recovers drive-shaft energy by reducing the pressure from 1350 psia to 100 psia. Most of the vapor from V-201 is compressed from 1350 psia to 1500 psia and recycled to the methanol converter but a small portion is withdrawn as a purge and expanded to 90 psia through a gas turbine (K-204). Methanol is recovered from the purge gas by scrubbing with water in C-201 and the exit from the expander (Stream 7) is recycled to the reformer as fuel. The condensate from K-203 and the scrubber water tails from C-201 are then combined to form a crude methanol product (Stream 19) which is sent to storage.

The crude methanol product contains 18.3 wt% water and can be fed directly to UOP's process for converting methanol to olefins. The flowsheet for this process is shown in Figures J4 and J5 of Appendix J and the material balance is given in Table J2 of Appendix J. The crude feed is preheated to 200 °C in E-102 and mixed with a recycle stream (Stream 2) containing water, methanol, and dimethyl ether which has been preheated to 350 °C in E-101 prior to entering the fluidized bed reactor (R-101). The reactor effluent at 60 psia and 400 °C is cooled by process to process heat exchange in E-101, E-102, and E-103 and final cooling to 43 °C is effected with cooling water in E-104. Most of the water and methanol and some of the dimethyl ether in the reaction product condenses and the condensate (Stream 9) is sent to C-101 where methanol and dimethyl ether are recovered for recycle to the reactor along with the diluent steam needed for the reaction (Stream 2). The tails from C-101 furnishes the scrubber water required for C-201 (Stream 14) and provides a purge for removing the water generated by the reaction (Stream 15).

The vapor from the effluent separator at 46 psia and 43 °C (Stream 4) is compressed to 130 psia in three stages of compression by K-201 where some of the methanol, dimethyl ether, and water condenses and is recycled (Stream 10) to V-101. The residual methanol and dimethyl ether in the compressed vapor is recovered by scrubbing with water in C-201 while the carbon dioxide is removed by a conventional acid gas removal system (C-202 and C-203). The overhead vapor from C-202 is further compressed by K-201 to 650 psia and then cooled to 18 °C in order to liquefy the hydrocarbon product.

The bulk of the water in the product is removed by decantation in V-204 while the residual water is removed via molecular sieve dryers (C-204 and C-205).

Mobil's Olefins to Gasoline and Distillate (MOGD) process is used to convert olefins to liquid fuels with a distillate to gasoline ratio of six to one. The flowsheet for the process is shown in Figure J6 in Appendix J and the material balance is given in Table J3 of Appendix J. The olefins feed to the reactor at 650 psia and 18 °C is blended with the liquid overhead product from the debutanizer column (C-101) at 18 °C and a gasoline recycle stream from the splitter tower (C-103) at 65 °C to form a mixture (Stream 4) which is then preheated to 132 °C by the splitter tower partial condenser (E-112). The reactor feed is heated further to 145 °C in E-109 by heat exchange with the splitter tower tails stream and the final preheat to reaction conditions (600 psia and 235 °C) is achieved by heat exchange with the hot reaction product in E-101, E-102, and E-103. The temperature rise across each reactor bed is about 23 °C and the final reaction product leaving E-103 is at 525 psia and 209 °C. Additional cooling of the product stream is achieved by supplying heat to the deethanizer column reboiler (E-107), after which it enters the debutanizer column as a two phase mixture at 255 psia and 194 °C.

The debutanizer column removes most of the C_4 and lighter components overhead, leaving the gasoline (C_5-C_{10}) and distillate (C_{11}-C_{20}) fractions in the tails. The liquid overhead product (Stream 2) is predominately a C_3-C_4 stream and it is recycled to the reactor in order to facilitate control of the heat release from the reaction system. The vapor overhead product at 248 psia and 18 °C is a mixture of C_1-C_4's which is compressed to 485 psia and 57 °C by K-101 before entering the deethanizer column. The tails stream from this column at 487 psia and 102 °C is a mixture of C_3-C_4's which is sold as LPG while the overhead vapor product at 480 psia and -14 °C is a mixture of C_1-C_3's which is used as fuel gas for the dowtherm furnace.

The tails stream from the debutanizer column at 256 psia and 245 °C is fed to the splitter tower where gasoline is recovered overhead and distillate is removed as a tails stream. Part of the gasoline is recycled to the reactor in order to control the product mix at a six to one ratio of distillate to gasoline; the remainder is taken as a product stream. The distillate product leaving the column at 26 psia and 261 °C is cooled to 152 °C in E-109 by preheating the reactor feed; final cooling to 43 °C is accomplished with cooling water in E-110.

Case 2

The flowsheet for the MOGD process for Case 2 is basically the same as for the Comparison Case (See Figure J6 of Appendix J) except that the overhead product from the debutanizer column is all liquid, which eliminates the need for the deethanizer column feed compressor (K-101). Also, the dual cooling water and refrigerated condenser arrangement on the debutanizer column has been replaced with a single refrigerated condenser. With regard to operating conditions, the only major changes are an increase in the head pressure of the debutanizer column to 295 psia (from 248 psia) and a decrease in the head pressure of the deethanizer column to 345 psia (from 480 psia). Also, the overhead vapor product from the deethanizer column (Stream 10) is now recycled to an ethane cracker rather than to the fuel gas system. The material balance for this case is shown in Table J4 of Appendix J.

Economic Analysis

Comparison Case

The raw materials, utilities, and period costs, along with their usage and cost basis, are shown in Table J5 of Appendix J for the conversion of methane to methanol based upon a total production of 3320 metric tons per day of methanol from two parallel operating units. Similar data is displayed in Table J6 of Appendix J for the production of one billion pounds per year of mixed olefins from methanol and in Table J7 of Appendix J for the final production of 10,600 barrels per day of gasoline and distillate. These costs are summarized in Table J8 of Appendix J for the overall process.

The inside battery limits (ISBL) and outside battery limits (OSBL) investment estimates for each section of the overall process are given in Table J9 of Appendix J. Based upon a 1989 US Gulf Coast location, the total fixed investment is $490.9MM, of which 75% is attributable to the conversion of methane to methanol. Also shown in the table are the details of an economic analysis which indicates that an average sales price of $1.94/gallon of gasoline and distillate will be required in order to achieve a ten percent after tax return on investment.

The effect of the cost of methane and the required return on investment upon the economics is shown in Figure J7 of Appendix J. If the methane is considered to be free, then a sales price of $1.38/gallon will be sufficient to generate a ten percent after tax

return on investment. If it is assumed that no profit from the venture is required, then the sales price decreases further to $0.78/gallon. However, this still exceeds the present price of about $0.53/gallon from the current oil based route and so existing technology for the conversion of methane to liquid fuels is clearly not competitive in the present pricing environment.

There are indications in the literature that some improvements to the Comparison Case may be achievable by reducing the consumption of methane and/or by decreasing the total fixed investment for the conversion of methane to methanol. For example, Lurgi's[105] low pressure methanol process claims a methane consumption which is about 14% lower than in the present analysis and Korchnak[106] has reported a 25% reduction in investment using a "Catalytic Partial Oxidation and Methanol Synthesis" scheme instead of the conventional "Steam Reforming and Methanol Synthesis" process. Assuming that both of these improvements could be achieved simultaneously, the total fixed investment would be reduced to $398.9MM and the average sales price required for a ten percent after tax return on investment would be $1.63/gallon. For the free methane-no profit scenario, the liquid fuels sales price would be $0.66/gallon. The details of the economic analysis for this Hypothetical Case are given in Table J10 of Appendix J and the impact of the cost of methane and the required return on investment upon the results are shown in Figure J8 of Appendix J.

Case 2

The raw materials, utilities, and period costs, along with their usage and cost basis, are shown in Table J11 of Appendix J for the conversion of methane to olefins based upon the production of one billion pounds per year of mixed olefins. Similar data is displayed in Table J12 of Appendix J for the final production of 10,600 barrels per day of gasoline and distillate and the overall process product cost summary is shown in Table J13 of Appendix J.

The inside battery limits (ISBL) and outside battery limits (OSBL) investment estimates for each section of the overall process are given in Table J14 of Appendix J along with the details of a return on investment analysis. Based upon a 1989 Gulf Coast location, the total fixed investment is $538.1MM and an average sales price of $2.09/gallon of gasoline and distillate will be required in order to achieve a ten percent after tax return on investment. The impact of the cost of methane and the required return on investment upon the results are shown in Figure J9 of Appendix J.

The total fixed investment for Case 2 is about ten percent higher than for the Comparison Case but this is well within the accuracy of the estimates so it is difficult to tell if this difference is really significant. However, there is a definite advantage for the Comparison Case within regard to methane usage since about 95% of the available methane is converted to liquid fuels versus only about 75% for the methane coupling route. A comparison of Tables J8 and J13 of Appendix J indicates that this single factor accounts for most of the difference in product cost between the two processes. On balance, the two processes are judged to be roughly equivalent but the scope for improvement for Case 2 is probably greater since it is still in the very early stages of development. For example, the C_2 yield from the methane coupling reaction is only about fourteen percent in the present analysis whereas a yield approaching thirty percent should be achievable on a theoretical basis. Improvements of this magnitude would dramatically reduce the required investment.

SUMMARY:

The key directions given to the catalyst screening program by the Task 2 Engineering Program are that yield to C_2's is not a good general predictor of economic performance, and that high selectivity to C_2's is more critical than high methane conversion. These conclusions stem from the finding that the Methane Diluent case (where no diluent is added, but high methane to oxygen ratios are used) is favored economically to any of the Nitrogen and Steam Diluent cases. Compared to any other diluent, methane provides the maximum selectivity to C_2's, the minimum methane conversion, the minimum C_2 yield, and the best economics. These conclusions are further reinforced by the finding that for both Nitrogen and Steam Diluent cases, the economics improve with increasing methane/oxygen feed ratio, which increases selectivity to C_2's at the expense of lower methane conversion and C_2 yield.

The best of the Sequential Feed cases have similar economics to the Co-feed Methane Diluent case. However, the Sequential Feed cases are based on literature results versus extrapolation of actual laboratory results for the Co-feed cases; they require a fluidized-bed reactor design, while Co-feed cases can use fixed-bed reactors; and they require a ready customer for the heavy co-products which are produced. Therefore, the Co-feed Methane Diluent case is preferred over the more technically and commercially risky Sequential Feed cases.

The economics favor the maximum concentration of oxygen in the reactor feed, up to the explosive limits of the mixture, in spite of the higher selectivity to C_2's that result from lower oxygen concentrations. Increasing ethylene to ethane production ratio is important economically up to a level of 3 - less so above this level. The best way to handle any level of co-product ethane is to provide conventional steam cracking hardware to convert it to additional ethylene within the process. All other things being equal, the economics favor a lower reactor temperature and a higher reactor pressure. However, the impact of reactor pressure on the selectivity to C_2's has not been considered in this evaluation.

Hypothetical catalyst improvements that would allow both the selectivity to C_2's and the methane conversion to be increased from their current levels would greatly improve the economics of the resulting oxidative coupling process. Such improvements have the potential to reduce the Total Fixed Investment by 30%, and the Cash Cost by 17%. Given sufficient time and resources, future catalyst improvements should confer superior economics to the methane coupling process.

The best process configuration for oxidatively coupling methane to ethylene based on extrapolated catalyst results using a barium on alpha-alumina catalyst with low levels of ethyl chloride in the methane feed gas and a reactor pressure of 50 psig is with a fixed bed reactor, no added diluent (methane diluent), a methane to oxygen feed ratio of 7, a reactor temperature of 725 °C, and co-product ethane cracked to ethylene. The methane diluent case assumes a methane conversion of 18.4%, a selectivity to C_2's of 76.7%, and an ethylene to ethane production ratio of 3, based on extrapolated laboratory results. The Total Fixed Investment for this cases would be $482MM for a plant producing one billion pounds per year olefins, and the Cash Cost per pound of olefins would be 12.4 ¢.

The Comparison Case is based upon a total production of 3320 metric tons per day of methanol in two parallel operating units followed by single train MTO and MOGD facilities which produce a final product of 10,600 barrels per day of gasoline and distillate. The total fixed investment is $491MM, the total cash cost/lb is 13.6 ¢, and a sales price of $1.94/gallon of gasoline and distillate products will be required in order to generate a ten percent after tax return on investment based upon a natural gas cost of $2.15/MMBTU. For the same liquid fuels production rate, the total fixed investment for Case 2 is $538MM, the total cash cost/lb is 12.8 ¢, and the required sales price is $2.09/gallon. Thus, within the error of the estimates, both methane based routes to liquid fuels are judged to be about equal but the scope for improvement of the methane coupling process is probably greater since it is still in the very early stages of development.

However, enormous technological breakthroughs would be required for either process to be competitive with the present oil based route which currently produces liquid fuels at an average sales price of about $0.53/gallon.

The economics of producing gasoline and distillate fuels via methane coupling are equivalent to those for making these materials via the synthesis gas and methanol route. This result is viewed as encouraging, given the early state of development of oxidative coupling catalysis. Given sufficient time and resources, future generations of catalysts or catalyst improvements should confer superior economics to the methane coupling process.

REFERENCES:

1. C. A. Jones, J. J. Leonard, and J. A. Sofranko, *Energy and Fuels*, **1**, 12 (1987).

2. F. M. Dautzenberg, R. L. Garten, and G. Klingman, "Fuels from Remote Natural Gas: Defining the Research and Development Challenge," paper presented at ACS 21st Symposium, Mares Island, Florida (1986).

3. S. A. Tabak, "Production of Synthetic Diesel Fuel From Light Olefins," 1984 AIChE National Meeting, Philadelphia, 1984.

4. G. E. Keller and M. M. Bhasin, *J. Catal.*, **73**, 9 (1982).

5. J. A. Sofranko, J. J. Leonard, and C. A. Jones, *J. Catal.*, **103**, 302 (1987).

6. C. A. Jones, J. J. Leonard, and J. A. Sofranko, *J. Catal.*, **103**, 311 (1987).

7. W. Hinsen and M. Baerns, *Chemiker Zeitung*, **107**, 223 (1983).

8. W. Hinsen, W. Bytyn, and M. Baerns, *Proc. 8th Int. Congr. Catal.*, **3**, 81 (1984).

9. J. A. Sofranko, C. A. Jones, J. J. Leonard, A. M. Gaffney, and H. P. Withers, *Petr. Div. Preprints* **32**, 763 (1987).

10. G. S. Lane and E. E. Wolf, *J. Catal.*, **113**, 144 (1988).

11. F. P. Larkins and M. R. Nordin, "Studies in Surface Science and Catalysis: #36," Methane Conversion Symposium, 409, Auckland, New Zealand, April 26-30, 1987.

12. Research is currently being carried out in several countries including Canada, China, The Netherlands, France, Germany, England, Japan, United States, USSR, South Africa, and Australia.

13. Companies with patents in the area include Phillips Petroleum, Standard Oil, Atlantic Richfield, Idemitsu Kosan, Exxon, Akzo GmbH, W. R. Grace, Chevron, Johnson Matthey, and Amoco.

14. Research is currently being carried out at several academic sites including Texas A&M University (USA), Tokyo Institute of Technology (Japan), University of Twente (The Netherlands), Macquarie University (Australia), University of Mar del Plata (Argentina), and USSR Academy of Sciences (USSR).

15. Research is currently being carried out at governmental laboratories including Lawrence Livermore National Laboratory, Los Alamos National Laboratory, Morgantown Energy Technology Center, and Sandia National Laboratory.

16. D. J. Driscoll, W. Martin, J.-X. Wang, and J. H. Lunsford, *J. Am. Chem. Soc.*, **107**, 58 (1985).

17. K. D. Campbell, E. Morales, and J. H. Lunsford, *J. Am Chem. Soc.*, **109**, 7900 (1987).

18. K. D. Campbell, H. Zhang, and J. H. Lunsford, *J. Phys. Chem.*, **92**, 750 (1988).

19. K. D. Campbell and J. H. Lunsford, *J. Phys. Chem.*, **92**, 5792 (1988).

20. J. B. Kimble and J. H. Kolts, *Energy Progress*, **6**, 226 (1986).

21. K. Otsuka, K. Jinno, and A. Morikawa, *J. Catal.*, **100**, 353 (1986).

22. N. W. Cant, C. A. Lukey, P. F. Nelson, and R. J. Tyler, *J. Chem. Soc., Chem. Commun.*, 766 (1988).

23. A. Ekstrom and J. A. Lapszewicz, *J. Chem. Soc., Chem. Commun.*, 797 (1988).

24. J. B. Kimble and J. H. Kolts, Fall A.C.S. Meeting, 1988.

25. J. A. Labinger, *Catal. Letters*, **1**, 371 (1988).

26. J. G. McCarty, A-B. McEwen, and M. A. Quinlan, Proceedings of International Symposium, "New Developments in Selective Oxidation," Rimini, Italy, 1989.

27. S. J. Korf, J. A. Roos, J. M. Diphoorn, R. H. J. Veehof, J. G. van Ommen, and J. R. H. Ross, *Catalysis Today*, **4**, 279 (1989).

28. V. R. Choudhary, S. T. Chaudhari, A. M. Rajput, and V. H. Rane, *J. Chem. Soc. Chem. Comm.*, 555 (1989).

29. T. Ito, J.-X. Wang, C.-H. Lin, and J. H. Lunsford, *J. Am. Chem. Soc.*, **107**, 5062 (1985).

30. C. A. Jones and J. A. Sofranko, U. S. Patent 4,523,050 to ARCO, June 11, 1985.

31. C. A. Jones, J. J. Leonard, J. A. Sofranko, H. P. Withers, E. W. Breder, Jr., M. F. L. Johnson, and J. A. Jaecker, U. S. Patent 4,629,718 to ARCO, December 16, 1986.

32. A. M. Gaffney, U. S. Patent 4,499,324 to ARCO, February 12, 1985.

33. R. F. Hicks, International Patent #WO 86/07351, PCT/US86/01254 to W. R. Grace, December 18, 1986.

34. A. M. Gaffney, U. S. Patent 4,499,323 to ARCO, February 12, 1985.

35. B. K. Warren, K. D. Campbell, J. L. Matherne, and G. L. Culp, "Direct Conversion of Methane to C_2's and Liquid Fuels," Indirect Liquefaction Contractors' Review Meeting Proceedings, November 15-17, 1988, pp 117-204, U. S. Department of Energy, Pittsburgh Energy Technology Center (National Information Service U. S. Dept. of Commerce, Springfield, VA 22161).

36. B. K. Warren and K. D. Campbell, "Direct Conversion of Methane to C_2's and Liquid Fuels - Chemistry;" and J. L. Matherne, and G. L. Culp, "Direct Conversion of Methane to C_2's and Liquid Fuels - Process Economics;" Indirect Liquefaction Contractors' Review Meeting Proceedings, November 13-15, 1989, U. S. Department of Energy, Pittsburgh Energy Technology Center (National Information Service U. S. Dept. of Commerce, Springfield, VA 22161).

37. J. B. Kimble and J. H. Kolts, EP 210383 to Phillips, Dec. 12, 1986 (JP 61,282,322, U. S. Appl. 742,335, June 7, 1985).

38. N. W. Cant, C. A. Lukey, P. F. Nelson, and R. J. Tyler, *J. Chem. Soc., Chem. Commun.*, 776 (1988).

39. Ger. Patent No. 3,503,664 to AKZO, GmbH, Wuppertal, appl. Feb. 4, 1985. = EP 194425; = Australia 86-212857-33 (Feb. 4, 1985).

40. J. B. Kimble and J. H. Kolts, U. S. Patent 4,654,460, to Phillips, June 7, 1985. =J. B. Kimble and J. H. Kolts, EP 206,043 to Phillips, Nov. 30, 1986.

41. J. A. Sofranko and C. A. Jones, U. S. Patent 4,544,784 to ARCO, Oct. 1, 1985.

42. C. A. Jones, J. J. Leonard, J. A. Sofranko, and H. P Withers, U. S. Patent 4,634,800 to ARCO, (1987).

43. K. Otsuka and T. Komatsu, *J. Chem. Soc., Chem. Comm.*, 388 (1987).

44. K. Otsuka, Q. Liu, and A. Morikawa, *Inorg. Chim. Acta,* 118, L23 (1986).

45. K. Otsuka, Q. Liu, and A. Morikawa, *J. Chem. Soc., Chem. Comm.*, 586 (1986).

46. K. Otsuka, M. Hatano, Q. Liu, and A. Morikawa, 903 (1986).

47. K. Otsuka and T. Komatsu, *Chem. Soc. Japan, Chem. Lett.,* 1955 (1986).

48. K. Otsuka, M. Hatano, and T. Komatsu, *Studies in Surface Science and Catalysis,* **36,** Methane Conversion Symposium, 383, Auckland, April, 1987.

49. K. Otsuka, Sekiyu Giakkaishi, **30**, 385 (1985).

50. K. Otsuka, Q. Liu, M. Hatano, and A. Morikawa, *Chem. Lett.,* 467 (1986).

51. K. Otsuka, M. Hatano, Q. Liu, and A. Morikawa, "VIII Japan-USSR Catalytical Seminar; Catalysis by New Materials," Tokyo, p. 1 (1986).

52. K. Otsuka, A. A. Said, K. Jinno, and T. Komatsu, *Chem. Letters*, 77 (1987).

53. K. Aika, T. Moriyama, T. Takasaki, and E. Iwamatsu, *J. Chem. Soc., Chem. Commun.,* 1210 (1986).

54. R. F. Hicks, WO 86/07351 to W. R. Grace & Co., Dec. 18, 1986 (priority June 14, 1985).

55. R. D. Goodenaugh and V. A. Stenger, in *Comprehensive Inorganic Chemistry*, eds., J. C. Bailar, H. J. Emelius, R. Nyholm, and A.-F. Trotman-Dickenson, Chapter 10. Pergamon Press, New York, 1975.

56. S. Ahmed and J. B. Moffat, *Appl. Catal.*, **58**, 83 (1990); *ibid., J. Catal.*, **121**, 408 (1990).

57. M. C. Kung, K. T. Nguyen, D. Patel, and H. H. Kung, in Catalysis of Organic Reactions, D. W. Blackburn--ed., Chapter 18, Marcel Dekker, New York (1990); K. T. Nguyen and H. H. Kung, *J. Catal.*, **122**, *in press* (1990).

58. C. F. Cullis and B. M. Willatt, *J. Catal.*, **86**, 187 (1984).

59. J. A. Labinger and K. C. Ott, *J. Phys. Chem.*, **91**, 2682 (1987).

60. M. Baerns and W. Bytyn, *Appl. Catal.* **28**, 199 (1986).

61. J. A. S. P. Carreiro and M. Baerns, *React. Kinet. Catal. Lett.*, **35**, 349 (1987).

62. J. A. S. P. Carriero, G. Follmer, L. Lehman, and M. Baerns, *Proc. 9th Int. Congr. on Catal. Calgary*, Vol. 2: C1 Chemistry, p. 891.

63. J. A. S. P. Carriero and M. Baerns, *J. Catal.* **117**, 258 (1989).

64. J. A. S. P. Carreiro and M. Baerns, *J. Catal.* **117**, 396 (1989).

65. M. Baerns, *Catal. Today*, **1**, 357 (1987).

66. G. Follmer, L. Lehmann, and M. Baerns, *Catal. Today*, **4**, 323 (1989).

67. S. J. Korf, J. A. Roos, J. M. Diphoorn, R. H. J. Veehof, S. G. van Ommen, and J. R. H. Ross, ACS Los Angeles Meeting, Symposium 33, 437 (1988).

68. G. Follmer, L. Lehmann, and M. Baerns, ACS Los Angeles Meeting, Symposium 33, 453 (1988).

69. U. S. Patent 4,172,810, to Exxon Research and Engineering Co., October 30, 1979; U. S. Patent 4,205,194, to Exxon Research and Engineering Co., May 27, 1980; and U. S. Patent 4,239,658, to Exxon Research and Engineering Co., December 16, 1980.

70. I. T. Ali Emesh and Y. Amenomiya, *J. Phys. Chem.*, **90**, 4785 (1986).

71. I. Matsuura, T. Doi, and Y. Utsumi, *Chem. Letters*, 1473 (1987).

72. EP 0,093,543, to British Petroleum Company, April 21, 1983.

73. M. T. Barlow, WO 84/03879 to British Petroleum Company, October 11, 1984.

74. U. S. Patent 4,350,835 to Mobil, September 21, 1982.

75. U. S. Patent 4,392,989 to Mobil, September 21, 1982.

76. J. G. McCarty, M. A. Quinlan, and K. M. Sancier, "Oxidative Methane Dimerization by Basic Oxide Catalysts," paper presented at 1988 AIChE Spring National Meeting, New Orleans, 1988.

77. I. Matsuura, Y. Utsumi, M. Nakai, and T. Doi, *Chem. Letts.*, 1981 (1986).

78. J. W. M. H. Geerts, J. M. N. van Kasteren, and K. van der Wiele, *Catal. Today*, **4**, 453 (1989).

79. H. Matsuhashi, K. Sakurai, and K. Arata, *Chem. Letters*, 585 (1989).

80. S. P. Mehandru, A. B. Anderson, and J. F. Brazdil, *J. Chem. Soc., Faraday Trans.*, **83**, 463 (1987).

81. B. K. Warren, "Direct Conversion of Methane to C_2's and Liquid Fuels," Research Proposal from Union Carbide Corporation in response to PRDA RA22-87PC79803, June 1, 1987.

82. Y. Ben Taarit and M. Che, "Catalytic Reactions Induced by Transition Complexes Solvated in Zeolite Matrices: Oxidation, Carbonylation, and Related Reactions," in Studies in Surface Science and Catalysis, 5 (Catalysis by Zeolites), Elsevier Scientific Publishing Co., Amsterdam, pp. 167-193, 1980, and 76 references therein.

83. J. C. Vedrine, "Electron Spin Resonance," in Characterization of Heterogeneous Catalysts, F. Delaney, ed., Marcel Dekker, Inc., New York, Chapter 8, 1984.

84. A. Yashima, K. Sato, T. Hayasaka, and N. Hara, *J. Catal.*, **26**, 303 (1972).

85. Japanese Patent 57068144, to Ube Industries, April 26, 1982.

86. H.-C. Liu and R. J. Spohn, U. S. Patent, 4,449,317 to Exxon Research & Engineering Co., July 2, 1984.

87. M. L. Unland and G. E. Barker, U. S. Patent 4,140,726 to Monsanto Co., February 20, 1979.

88. M. L. Unland and G. E. Barker, U. S. Patent 4,115,424 to Monsanto Co., September 19, 1978.

89. M. L. Unland and G. E. Barker, *Chem. Ind.*, **5**, 51 (1981).

90. D. J. C. Yates and N. E. Zlotin, *J. Catal.*, **111**, 317 (1988).

91. G. J. Hutchings, M. S. Scurrell, and J. R. Woodhouse, *J. Chem. Soc., Chem. Commun.*, 253 (1988).

92. K. Asami, K. Omata, K. Fujimoto, and H. Tominage, *J. Chem. Soc., Chem. Commun.*, 1287 (1987).

93. K. Asami, K. Omata, K. Fujimoto, and H. Tominage, *Energy & Fuels*, **2**, 574 (1988).

94. J. Gopalakrishnan and V. Bhat, *Inorg. Chem.*, **26**, 4299 (1987).

95. M. Hatano and K. Otsuka, *Inorg. Chim. Acta*, **146**, 243 (1988).

96. M. Vallet-Regi, E. Garcia, and J. M. Gonzalez-Calbet, *J. Chem. Soc. Dalton Trans.*, 775 (1988).

97. J. A. Sofranko, J. J. Leonard, C. A. Jones, A. M. Gaffney, and H. P. Withers, *ACS:Petr. Div. Preprints*, **32**, 763 (1987).

98. U. S. Patent 3,775,501 to Mobil, November 1973.

99. D. W. Layshon, U. S. Patent 4,801,762 to ARCO, January 31, 1989.

100. A. M. Gaffney, U. S. Patent 4,788,372 to ARCO, November 29, 1988.

101. C. A. Jones, J. J. Leonard, and J. A. Sofranko, U. S. Patent 4,554,395 to ARCO, November 19, 1985.

102. SRI International, PEP Report No. 148, "Costs of Synthesis Gases and Methanol," February, 1983.

103. S. W. Kaiser, U.S. Patent No. 4,499,327 to Union Carbide Corporation, February 12, 1985.

104. H. Owen, et al, U. S. Patent No. 4,456,779 to Mobil Oil Corporation, June 26, 1984.

105. Hydrocarbon Processing, November, 1987, p. 78.

106. J. Korchnak, "Advances in Methane Technology," paper presented at the Auckland Methane Conversion Symposium, Auckland, New Zealand (April 26-30, 1987).

VI. APPENDICES

Appendix A. KEY TO TABLES AND TERMS

The following symbols are used in the key:

$n(i)_r$: relative molar amount of component "i" in the reactant stream (see Experimental Section).

$n(i)_p$: relative molar amount of component "i" in the product stream after correction for volume changes with nitrogen as an internal standard (see Experimental)

f(i) : number of carbon atoms per molecule of component "i".

Ref, #-KDC-X-#, #-BKW-#, or #-#	UCC&P notebook reference ID number. For #-#, the three letter sequence would be the same as the section in which this reference appears, e.g., 29-95 in the BKW Laboratory Section of the Results and Discussion Section refers to reference 29-BKW-95.
Catalyst (Cat)	UCC&P code number for catalyst or chemical composition.
Weight (Wt)	Weight of catalyst sample (g).
Volume	Volume of catalyst before dilution with quartz beads (cc).
$CH_4/O_2/N_2$	Mole ratios of reactants in feed stream.
Flow (ccm)	Total reactant flow rate (cc/min at ambient conditions for BKW and KDC laboratories and at STP for NEK laboratory).
Temperature (Temp)	Temperature of the catalyst bed (°C).
Time	Time since reactant flow was started (minutes, unless hours indicated).
CH_4 Conv. (CH_4 C or CC)	Mole % of methane reacted, also referred to as activity. $= \{[n(CH_4)_r - n(CH_4)_p]/n(CH_4)_r\} \times 100$
O_2 Conv. (O_2 C)	Mole % of oxygen reacted. $= \{[n(O_2)_r - n(O_2)_p]/n(O_2)_r\} \times 100$
C Balance (C Bal)	Mole % carbon detected in the product stream compared to the reactant stream. $= \{[\Sigma f(i)n(i)_p]/n(CH_4)_r\} \times 100$; where the "Σ" is over all carbon containing components.

C_2 Selectivity (Sel)	Selectivity to ethane + ethylene expressed as a percent, based on methane reacted. $= \{2[n(C_2H_6)_p + n(C_2H_4)_p]\}/[\Sigma f(i)n(i)_p] \times 100$; where the "Σ" excludes CH_4
C_3 Selectivity	Selectivity to propane + propene expressed as a percent, based on methane reacted. $= \{3[n(C_3H_8)_p + n(C_3H_6)_p]\}/[\Sigma f(i)n(i)_p] \times 100$; where the "Σ" excludes CH_4.
C_2 Yield (or Yield)	Mole % of methane converted to C_2's, calculated as (CH_4 conversion) X (C_2 selectivity)/100.
Ethylene to Ethane (=/-)	Mole ratio of ethylene to ethane in the product stream.
CO_2/CO	Mole ratio of carbon dioxide to carbon monoxide in the product stream.
GHSV	Gas hourly space velocity ($cc_{gas}\ cc_{cat}^{-1}\ h^{-1}$ at ambient temperature and room pressure for KDC and BKW laboratories and at STP for NEK laboratory), as h^{-1}.
ECl	Ethyl chloride in the feed gas in parts per million.
Reactor or R	The type of a reactor - A, B, C, D, E, F, G, or H.
R#	R#3 and R#4 refer to the two reactors in the BKW laboratory.
Activity	Methane conversion.

Relative amounts of products in figures are in volume percentages of the outlet gas.

Appendix B. EXPERIMENTAL

Catalyst tests carried out under this contract are assigned notebook ID numbers which identify the appropriate researcher and the notebook reference of the experiment. Codes including the letters KDC indicate that work is done in the KDC laboratory. Codes including the letters BKW indicate that work is done in the BKW laboratory. Codes including the letters NEK indicate that work is done in the NEK laboratory.

The reactor systems consist of gas feed-mix systems, steam feed systems, tubular reactors, tubular furnaces, liquid collection vessels, and gas analyzers connected directly to the feed and product streams. These are illustrated in Figures B1 to B5 of this appendix. Reactions coded with BKW are run at about 11 psig (176 kPa). Reactions coded with KDC are usually run at 5 psig (135 kPa). Reactions coded with NEK are usually run at pressures of 3 to 20 psig (122 to 239 kPa).

Figures B6 to B15 of this appendix are drawings of Reactors A through H, S and V. These are all quartz reactors except for Reactor S, which is stainless steel. The temperature distribution of Reactor A is shown in Figure B16 and the oven configuration of Reactor V is shown in Figure B17.

Linde oxygen, nitrogen, air, and ultra high-purity methane are used in all experiments unless noted otherwise. CP Grade ethyl chloride from Linde at 2% by volume is mixed in methane by UCC&P's Automated Analytical Systems Gas Mixing Laboratory. Quartz wool is obtained from Alltech Company, and quartz chips are obtained from either National Scientific or Thomas Scientific.

In both KDC and BKW laboratories, the gas mixtures entering and exiting the reactor system are analyzed by gas chromatographic methods (GC) using Hewlett-Packard Model HP-5880A gas chromatographs equipped with thermal conductivity detectors. Ultrapure helium is used for GC analyses. Calibrations are done in the HP ESTD mode using calibration gases prepared by UCC&P's Automated Analytical Services group. Injections of calibration gases, product streams, and reactant streams are accomplished using a Valco valve with a fixed volume sample loop. Tables B1-B5 show the GC program conditions, run table, report table, calibration table, and calibration gas mixture contents for the BKW laboratory. Tables B6-B9 show the GC program conditions, run table, calibration table, and calibration gas mixture contents for the KDC laboratory. Figure B18 shows the valve system used to switch columns for analyses in the KDC laboratory. Figure B19 shows the valve switching schematic for the BKW laboratory. In both KDC and BKW laboratories, the components analyzed include methane, oxygen, nitrogen, ethane, ethylene, propane,

propene, carbon monoxide, and carbon dioxide. Analyses for C_4's is not necessarily carried out unless there are large amounts of C_3's. Carbon balance calculations indicate that other hydrocarbon products and oxygenates are not present in significant quantities; thus, analyses of heavier hydrocarbons and oxygenates are not performed during these screening experiments. Heavier hydrocarbons and oxygenates were analyzed by gas chromatography coupled with mass spectrometry, and by gas chromatography coupled with ir. These were not present in significant amounts.

In the NEK laboratory, products are analyzed with a Varian 3700 gas chromatograph equipped with 6.1 flame ionization and thermal conductivity detectors.

The numbers from the ESTD mode from reactant streams are used as read from the GC. The numbers as read from the GC for product components are adjusted to correct for volume changes by multiplying by nitrogen in the reactants divided by nitrogen in the products. The Key in Appendix A shows how these numbers are used.

Pore size distributions were measured by the BET method with a Micromeritics ASAP-2400 instrument. Analyses of percentages of various elements were accomplished by ICP.

BKW Laboratory

For all BKW laboratory results or in Tables and Figures, Appendix D describes catalyst compositions, and Appendix C describes catalyst preparation procedures. The key to abbreviations used in Tables or Figures, and to terms used in the Results and Discussion Section appears in Appendix A. Activity refers to methane conversion.

The reactor system in the BKW laboratory is shown in Figure B1 and contains two parallel reactors which may be fed with a variety of gases. It consists of a gas feed system, two tubular microreactors (a steam feed system to one of these), two Lindberg tube furnaces, two liquid collection systems, an on-line gas analyzer with a stream selector, and a separate liquids analyzer. All the lines to the reactors are made of 1/8" and 1/4" SS tubing unless otherwise stated. The tubular reactors are operated outside the hood behind a safety shield. Figure B4 shows modifications to the reactor system for vapor phase experiments.

All experiments in the BKW laboratory are done in the cofeed mode where methane and oxygen are simultaneously fed. Unless stated otherwise, 10% methane and 5% oxygen are fed. The balance gas is nitrogen, and in some cases, ethyl chloride is fed in parts per million (from a mixed gas with methane). Methane, oxygen, nitrogen, and other gases are fed through a feed system which controls flows with Brooks mass flow meters and which controls pressure with a Grove back pressure regulator. The Grove regulator sends excess

gases to a vent in the hood. The system is designed so that gas ratios may be set independently from flow rates and reactor pressures (controlled by GO Regulators after the reactors and collection pots), and flow rates with all of these parameters easily and independently changed. Relief valves are present between the gas regulators and the Brooks mass flow meters. A relief valve (vented to the hood) set at 25 psig is installed immediately before each quartz reactor so that the pressure in the reactor cannot exceed 25 psig. Low flow switches after the reactors and before the liquid traps activate an emergency shut down system which passes nitrogen over the reactors and turns off heaters if there is a leak or plug in the reactor.

Two Lindberg Mini-Mite, model 55035 tube furnaces (800 watts, 115 volts, 1100 °C maximum operating temperature) are used for heating the tubular microreactors. The entire cylindrical heated chamber is comprised of two halves, making up the split-hinge furnace design. Each half is a composite unit of a high temperature ceramic fiber insulation, and a helically coiled alloy heating element. The furnaces are equipped with a chromel-alumel (type K) thermocouple (centrally positioned within the heated region) which is used to measure the temperature of the furnace. The heated region is 31 cm long and the hottest point is 2 cm above the center of this region. Athena temperature controllers are used to control the furnace temperatures. The temperature controllers have built-in overtemp devices which turn the furnace off when the operating temperature exceeds the set temperature by 80 °C.

Two cold traps, cooled with a circulating cooling fluid (50/50 mixture of propylene glycol and water) pumped through coiled copper tubing by a Haake A81 refrigeration unit, are used in parallel for each reactor so that one cold trap can be removed and sampled while the other one is collecting product. These traps are located after the reactor outlet (after the low flow switches) and before the reactor back pressure regulator. Another trap is present in the line after the back pressure regulator. This third trap is not cooled.

Compounds which are not trapped are analyzed on an HP 5880A GC equipped with a thermal conductivity detector and column switching (including a molecular sieve column), utilizing four Valco valves and a 10-port stream selector, programmed to operate from the HP 5880A keyboard. Initial and final column temperatures of 85 °C and 170 °C are used for the analyses. Feed streams are periodically analyzed before, during, and after runs. Analyses of trapped liquids by gc-ms indicate only water. The water is acidic (<pH 3) by litmus paper. By ir, traces of carbonyls are detected.

Thermocouples, heating tape, and glass insulating tape are present on the steam feed system and lines before and after the reactors. Brooks mass flow meters are calibrated in

place. Quartz tubing used in the construction of reactors is obtained from National Scientific Company.

Reactors A, C, D, E, S, and V (Figures B6, B8, B9, B10, B14, and B15, respectively) are used in the BKW laboratory. Reactors are operated vertically as shown in Figure B6. The center of the catalyst bed is 18.5 cm above the bottom of the oven, or 31.25 cm above the bottom of the reactor (see Figure B16). When this point is heated to 802 °C under typical flow rates of gases, it is 800 °C at 2-2.5 cm above this point and 800 °C at 2 cm below this point. 5 cm below this point, it is 793 °C, and 10 cm below this point, it is 773 °C. 18.5 cm below this point (at the bottom of the heated portion of the reactor, the temperature is 645 °C. There is a significant temperature drop from the catalyst bed to the bottom of the reactor. The temperature profile for Reactor A shown in Figure B16 is the same for Reactors C, D, and E. The oven configuration for Reactor V is shown in Figure B17.

The top 30.5 cm of Reactor D is constructed of 0.9 cm i. d. quartz tubing (1.1 cm o. d.). This is connected to 26 cm of 3 mm i. d. (5 mm o. d.) quartz tubing to minimize void volume. It is 56.5 cm long. The bottom of the heated region of the reactor is 12.75 cm above the bottom of the reactor. The top of the heated region is 46.75 cm above the bottom of the reactor. The post-catalyst volume of the wider part of the reactor is packed with 20/40 or 14/30 mesh quartz chips, quartz wool, or both quartz chips and quartz wool in order to minimize the high temperature post-catalyst residence time of the products, and to hold the catalyst in place. The bottom end of the reactor is connected to 1.0 cm i. d. (1.2 cm o. d.) quartz tubing at a right angle to the reactor. The ends of the reactor are made of quartz "O"-ring joints (1.5 cm i. d. at the inlet; 0.9 cm i. d. at the outlet).

Supported catalysts are usually prepared using the incipient wetness technique. In this procedure, the amounts of components (usually 99.99+% purity from Aesar) required to give the desired loading are dissolved in a quantity of distilled water necessary to just fill the pores of the support. The solution is then added to the support particles. In some cases, if the dopants are not easily soluble, suspensions of the finely ground components are added to a mixture of water which is stirred with the support with heating (with or without vacuum) to distribute the material in and on the support. The resulting material is dried in a vacuum oven at 130 °C under a vacuum of 120-630 mm Hg (16-84 kPa) for 1 to 50 hours (usually 18-20 hours). Most dried catalysts are tested without further treatment. A few are first calcined in air. Metal or inorganic compound loadings are expressed as weight percent based on the weight of the support.

Catalysts for reactions coded BKW are not first preconditioned with oxygen. The reactors are filled with washed quartz chips above and below the catalyst bed. The catalyst bed is situated in the hottest part of the reactor. Tubing of 0.3 cm i. d. in Reactors D and E is not filled with quartz. Quartz wool is used to separate quartz chips from the catalyst bed and to hold quartz chips in the reactor. Undiluted catalysts of varying mesh sizes are used except in cases where the catalyst is only available as a fine powder. In these cases, it is diluted with quartz chips.

Charged reactors are flushed with nitrogen during heating. After the experiment the reactant flow is terminated and the reactor is flushed with nitrogen while cooling. The reactor is cleaned between experiments by thoroughly rinsing with acid followed by distilled water. New reactors are frequently used.

KDC Laboratory

The reactor system used for catalyst testing consist of a gas feed-mix system, a steam feed system, tubular reactors, Lindberg tube furnaces, liquid collection vessels, and a gas analyzer connected directly to the product streams.

Quartz reactors were used for all of the work except the high pressure ethylene oligomerization study. Quartz Reactor B (Figure B7), used for cofeed catalytic studies (layered perovskites and low temperature catalysts), was constructed of 1.5 cm i. d. quartz tubing (1.7 cm o. d.) with a thermocouple well positioned along the center of the reactor of 0.3 cm i. d. quartz tubing (0.5 cm o. d.) enlarging to 1.3 cm o. d. at the outlet end (26.7 cm) of the thermocouple well. All quartz tubing used in the construction of the reactor was obtained from National Scientific Company. The thermocouple well extended through the catalyst bed (into the preheater region) which allows the temperatures of the preheater, catalyst bed and post-catalyst region to be monitored. The reactor had a length of 55.9 cm and the thermocouple well extended 33.0 cm into the reactor. The ends of the reactor are made up of quartz "O"-ring joints (1.5 cm i. d. at inlet ; 0.9 cm i. d. at outlet) which allows easy placement of the reactor in the system. The joints were connected using FETFE "O"-rings obtained from Ace Glass Incorporated. The "O"-ring joints were supplied by Quartz Scientific Inc. A similar reactor was used for the homogeneous gas phase oxidation study except the thermocouple well was not enlarged at the outlet end.

The reactor was charged with catalyst by adding 20 to 40 mesh washed quartz chips around the enlarged thermocouple well (post-catalyst region), quartz wool, catalyst bed,

quartz wool, and either a solid 1.3 cm o. d. quartz rod with 20 to 40 mesh washed quartz chips around the outside or 20 to 40 mesh washed quartz chips (preheater region).

In cofeed studies, charged reactors were flushed with nitrogen during heating. The reactor temperature was raised to 450-500 °C and the catalyst was usually preconditioned with flowing air (100 cc/min) for 1 hour. After preconditioning the air flow was terminated, the reactant flow was started, and the reactor temperature was raised to the desired value. Product stream analysis was carried out at timed intervals using gas chromatography. After the experiment the reactant flow was terminated and the reactor was flushed with nitrogen while cooling. The reactor was cleaned between experiments by thoroughly rinsing with acid followed by distilled water.

Sequential mode studies were performed (double perovskites) using two reactors modified such that product gases exiting the reactor could be collected in gas sampling bags. Quartz Reactor F (Figure B11) was used for most experiments. Quartz Reactor G (Figure B12) was used for a few runs. Results from both reactors were the same. In a typical sequential experiment, a quartz reactor was charged with catalyst by adding quartz wool, catalyst, quartz wool, and 20 to 40 mesh washed quartz chips (preheater region). Quartz Reactor F (Figure B11) consisted of a 1.5 cm i. d. (1.7 cm o. d.) quartz tubing bulb (12 cm long) positioned in the center with a piece of 0.5 cm i. d. quartz (0.7 cm o. d.) that was 14.0 cm in length at the inlet end and a piece of 0.2 cm i. d. quartz (0.4 cm o. d.) that was 24.1 cm in length at the outlet end with quartz "O"-ring joints at each end. The reactor had a total length of 56.5 cm. The reactor was encased in a Lindberg oven for the mid-31 centimeters of its length.

Charged reactors were flushed with air while the reactor temperature was raised to the desired value. Then, the catalyst was conditioned with flowing air (100-250 cc/min) for 1-2 hours. After conditioning the air flow was stopped and the reactor was flushed with nitrogen. Nitrogen flow was stopped, methane flow was initiated, and samples of gaseous product were collected immediately after exiting the reactor using gas sampling bags. The product samples were obtained during timed intervals. The reactor was then flushed with nitrogen, the reactor temperature was set to the desired value, the catalyst was conditioned with air, and the process was repeated. Collected samples were analyzed using the same GC analysis employed for the cofeed studies. After the experiment, the reactor was flushed with nitrogen while cooling. The reactor was cleaned between experiments by thoroughly rinsing with acid followed by distilled water.

NEK Laboratory

The reactor system in the NEK laboratory consists of a feed system, two tubular reactors in high temperature tubular furnaces, two liquid condensers, and on-line gas chromatographic analysis of each off-gas. The only common components of the two reactor systems are the feed gas cylinders, the check valves and safety relief valves, and the gas sampling system for the GC analysis. Other components were constructed in duplicate and are identical, with the exception of the two different tubular furnaces. A schematic of the reactor system is shown in Figure B5. Typical reaction conditions are:

temperature	500 - 850 °C
pressure	3-20 psig
total gas flow rate	250 to 1200 sccm
amount of catalyst	3 to 20 cc
methane	20-90%
oxygen	3-14%
water	0-85%
argon or helium	balance

Each reactor has its own gas feed system allowing different compositions to be fed to each reactor. The feed rate to each reactor is determined by the sum of the flow rates of each of the feed gases and, if steam is cofed, its feed rate, in ccm. Flow rates are determined by settings on calibrated Brooks mass flow metering valves. The feed rate of water to the vaporizer is determined from the Gilson liquid pump setting and the calibration graph for that pump.

The vaporizer consists of a 1/2" diameter stainless steel tube partially filled with glass beads and heated with heat tapes to a temperature about 20 °C above that required to produce steam at the reaction pressure.

During start-up, the feed system is isolated from the tubular reactors and all the feed gases are vented to the hood using a GO back pressure regulator to regulate the pressure in the feed system. The feed gas composition can be determined gas chromatographically (after diluting with inert and passing through a condenser, if the diluent is steam). The total flow rate can be measured with a bubble meter when there is no steam in the feed. Otherwise the flow measured is that of the feed gases, minus the steam, plus the diluent.

Once the feed has been analyzed and the furnace is at reaction temperature, the inert gas purging the reactor is replaced with the feed gas. If the feed gas composition is changed, the catalyst can be purged with argon or helium while the feed is analyzed, or the feed composition is calculated based on the Brooks meter settings and calibration. The later method was generally preferred and resulted in carbon mass balances of between 96 and 103%, which is not significantly different from those obtained using the gas chromatographically determined feed compositions.

Quartz reactors I, J, and K were used in NEK laboratory. Reactors I and J were the same as Reactor B except that the overall length of Reactor I was 56 cm and of Reactor J was 61 cm. The reactors were constructed of 1.5 cm i. d. quartz tubing (1.7 cm o. d.) with a thermocouple well positioned along the center of the reactor. The thermocouple well was constructed from 3 mm i. d. quartz tubing (0.5 cm o. d.) which is enlarged to 1.3 cm o. d. at the outlet end (26.7 cm) of the thermocouple well. All of the quartz tubing used in the construction of the reactors was obtained from National Scientific Company. The thermocouple well runs the entire length of the catalyst bed. The ends of the reactors are made up of quartz "O"-ring joints (1.5 cm i. d. at inlet ; 0.9 cm i. d. at outlet) which allows easy placement of the reactor in the system. The joints were connected using FETFE "O"-rings obtained from Ace Glass Incorporated. The "O"-ring joints were supplied by Quartz Scientific Inc.

The high pressure Reactor K is shown in Figure B20. It consists of a quartz tube sheathed in a stainless steel tube. The stainless steel tube is equipped with a port to allow pressurization of the space between the quartz and the stainless steel tube, however, this was not done in practice because the quartz reactor withstood in excess of 200 psig pressure without fracturing. The Swagelok fittings were welded directly to the stainless steel tube and teflon ferrules were used to make the seal to the quartz tube. Two configurations were used to pack the high pressure reactor as shown in Figure B21.

Each reactor is charged with catalyst by adding 20 to 40 mesh washed quartz chips around the enlarged thermocouple well (post-catalyst region), quartz wool, catalyst, quartz wool, and 20 to 40 mesh washed quartz chips (preheater region). The catalyst beds in experiments coded with NEK were composed of 20 cc of catalyst, which was weighed prior to loading. The quartz chips were obtained from National Scientific Company. After loading the tubular reactors with catalyst they are placed horizontally into tubular furnaces. Two different solid shell tubular furnaces were used to allow comparison of their performance. Both are 1-1/4 inch i. d., solid shell tubular furnaces which are resistively

heated with a variable pitch along a length of 18 inches. The one supplied by ThermPro Inc. also has 8 tapped shunts which allows the resistance to be varied by the addition of resistors. The other, supplied by CM Furnaces, Inc., does not have this capability; however, both companies claim that their furnace will provide a 6 inch section heated to 900 °C ± 1 °C.

From the vaporizer to the furnace inlet and from the furnace outlet to the inlet of the condenser, everything, with the exception of the Heise pressure gauge in the gas feed system, which is connected through a water filled pigtail, is heated with heat tapes.

Thermocouples for temperature determination are positioned under the heat tapes at various locations, and inside the vaporizers and the tubular reactors. Three thermocouples are located along the length of the catalyst bed and the temperature reported is that of the thermocouple located at the center of the bed.

The steam diluent and liquid products are condensed at atmospheric pressure in a 2250 cc teflon-lined Hoke cylinder which is cooled to 5 °C with methanol using a Cole Parmer circulating refrigerated bath. When steam is used as the diluent, the offgas is diluted with inert gas prior to entering the condenser. Thus, even if the conversion of the oxygen is low, the oxygen concentration in the gas exiting the condenser will be below the flammable limit. The condenser is drained at least once a day when steam is being fed and less frequently when it is not. The frequency of collection depends on whether the liquid samples are being collected for analysis or to prevent the condenser from overflowing.

Slip steams from the product gas and the feed gas from the reactors are sent to a stream select/gas sampling box and then to the vent. The positions of the four eight-port stream select valves and the one Valco 10 port gas sampling valve in the stream select/gas sampling box are controlled by Computer Automated Laboratory System (CALS) software on a Hewlett Packard computer. The gas sampling valve, shown in Figure B22, is configured for injection of two, two-milliliter samples of one gas stream simultaneously onto two GC columns.

The product and feed gas samples are analyzed on two analytical columns, which are located in the oven of a Varian 3700 gas chromatograph equipped with a flame ionization detector and a thermal conductivity detector. Both detectors are operated simultaneously with the signal outputs going through separate digimetries to the CALS. Ethylene, ethane, and propylene/propane (unresolved) in the sample are separated using a 10 ft. by 1/8" stainless steel Porapak R column with an argon or helium carrier gas and a flame ionization detector. C_4 hydrocarbons could be qualitatively detected. The carbon oxides, nitrogen, oxygen, hydrogen, methane, and water are analyzed with a thermal conductivity detector

using a 10 ft. by 1/8" stainless steel column filled with Carbosieve S-II. Both columns are subjected to the same temperature program, starting at 50 °C for 10 minutes after injection, then heating at 30 °C/min to 200 °C and holding at that temperature for 16 minutes, for a total analysis time of 31 minutes. The response factors for all of the expected compounds were determined by calibrating with gas standards prior to the first run. These are updated periodically. The analytical procedures used are detailed in Tables B10 and B11.

Calibrations were done at two levels for each component by using the calibration gas mixture shown in for one level and the calibration gas mixture shown in Table B9 for the other. The response factors were determined using a piecewise linear curve forced through the origin.

Nitrogen, cofed with ethyl chloride, is used as an internal standard to correct the mole percents in the product gas analysis for any volume contraction which may have occurred due to the reaction.

All runs prior to 33-NEK-120 used argon for the GC carrier gas and for the diluent, when an inert gas diluent was used, and all runs after 33-NEK-120 used helium as diluent and GC carrier gas.

An additional calibration standard (33-NEK-45, Table B12) was used midway into runs 33-NEK-40 and 33-NEK-42. Starting with the run on 33-NEK-70 the GC calibration was derived from the results of running both 33-NEK-45 and a new standard, 33-NEK-95 (see Table B13). The GC calibration for methane was modified (33-NEK-120) to include a result for 100% methane in addition to the results for the two gas standards mentioned above, so that the factor used when methane was the diluent (i.e., at high methane concentration) would be more accurate.

Table B1. GC Program Conditions, BKW Laboratory

Detector: Thermal Conductivity
Helium flow rate = 24 cc/min
Oven Temperature Profile:
Initial Value = 85 °C
Initial Time = 18.00 minutes
Program Rate = 30.00 °C/minute
Final Value = 170 °C
Final Time = 12.00 minutes
Post Value = 160 °C
Post Time = 2.00 minutes

Stream Selector Temp. = 100 °C
Detector Temp. = 200 ° C
Valve Box Temp. = 125 °C
Threshold = 3
Peak Width = 0.04

Table B2. Run Table, BKW Laboratory

Run Time 0.01	Valve 1 on
Run Time 0.03	Valve 3 off
Run Time 3.49	Integration off
Run Time 3.50	Valve 3 on
Run Time 3.80	Integration on
Run Time 12.00	Valve 3 off
Run Time 12.00	Integration off
Run Time 12.30	Integration on
Run Time 15.00	Valve 1 off
Run Time 19.00	Valve 3 on
Run Time 19.00	Integration off
Run Time 21.25	Integration on
Run Time 21.26	Set Baseline

Table B3. Report Table, BKW Laboratory

6.64 BL Mode 0
9.23 BL Mode 1

Table B4. Calibration Table, BKW Laboratory

No.	Ret. Time	Amount	Amount/Area	Name
1	4.787	3.00000E+00	1.95696E-05	CO_2
2	8.120	1.00000+01	1.98561E-05	C_2H_4
3	10.500	8.00000E+00	1.80894E-05	C_2H_6
4	12.781	1.00000E+00	3.72597E-05	O_2
5	13.460	4.57051E+01	3.19513E-05	N_2
6	15.973	3.00000E+01	3.65960E-05	CH_4
7	17.806	3.00000E-01	3.50648E-05	CO
8	22.320	1.00000E+00	1.53205E-05	C_3H_6
9	23.680	5.00000E-01	1.36812E-05	C_3H_8

Calibration Parameters:
Reference Window = 5%
Non-reference Window = 5%
Uncalibrated Reference = 0

Table B5. Calibration Gas Mixture, BKW Laboratory

Source:

UCC&P, Automated Analytical Systems, Gas Mixing Laboratory,
Technical Center, South Charleston, WV 25303

Date: 12-14-1987
Cylinder Material: Stainless Steel
Cylinder Number: 396
Final Pressure - PSIA: 300
Dewpoint: - 3 °C
Contents:

Component	Actual Mole Percent
Propylene	1.00000
Methanol	0.10000
n-Butane	1000.0 PPM
Propane	0.50000
Carbon Monoxide	0.30000
Hydrogen	1000.0 PPM
Carbon Dioxide	3.00000
Oxygen	1.00000
Acetylene	500.0 PPM
Ethylene	10.00000
Ethane	8.00000
Methane	30.00000
Nitrogen	45.70510
cis-2-Butene	300.0 PPM
trans-2-Butene	300.0 PPM
1-Butene	300.0 PPM
Isobutane	539.0 PPM *
Isopentane	2.0 PPM *
2,2-Dimethylpropane	1.0 PPM *
Water	2.3 PPM *
Isobutylene	4.2 PPM *
1,3-.Butadiene	0.6 PPM *

* = Estimated Impurities

Table B6. GC Program Conditions, KDC Laboratory

TCD Detector
Helium flow rate = 24 cc/min
Oven temperature profile:
Initial value = 60 °C
Initial time = 6.00 minutes
Level 1
Program rate = 30.00 °C/min
Final value = 75 °C
Final time = 5.00 minutes
Level 2
Program rate = 30.00 °C/min
Final value = 135 °C
Final time = 25.00 minutes

Detector temperature = 190 °C

Table B7. Run Table, KDC Laboratory

Run Time	0.01	Valve 1 On
Run Time	0.01	Valve 2 Off
Run Time	0.01	Integration Off
Run Time	0.01	Attenuation 2*9
Run Time	0.02	Valve 3 Off
Run Time	0.02	Set Baseline
Run Time	0.05	Zero
Run Time	1.00	Valve 1 Off
Run Time	1.01	Integration On
Run Time	1.02	Set Baseline
Run Time	1.02	Peak Width 0.05
Run Time	6.59	Integration Off
Run Time	6.60	Valve 2 On
Run Time	6.61	Integration On
Run Time	6.62	Set Baseline
Run Time	6.62	Peak Width 0.05
Run Time	6.70	Attenuation 2*9
Run Time	19.00	Integration Off
Run Time	19.01	Valve 2 Off
Run Time	19.01	Valve 3 On
Run Time	19.05	Integration On
Run Time	19.10	Set Baseline
Run Time	30.12	Attenuation 2*4
Run Time	30.15	Zero

Table B8. Calibration Table, KDC Laboratory

No.	Ret. Time	Amount	Amount/Area	Name
1	8.800	4.00000E+00	5.07023E-06	O_2
2	10.740	6.69800E+01	5.22171E-06	N_2
3	14.990	2.00000E+01	5.31680E-06	CH_4
4	16.671	1.00000E+00	4.02221E-06	CO
5	19.835	2.00000E+00	4.20280E-06	CO_2
6	21.255	2.00000E+00	3.97724E-06	C_2H_4
7	22.012	2.00000E+00	3.74037E-06	C_2H_6
8	26.559	1.00000E+00	3.18254E-06	C_3H_6
9	27.272	1.00000E+00	3.37955E-06	C_3H_8

Calibration Parameters:
Reference Window = 5%
Non-reference Window = 5%
Uncalibrated Reference = 0

Table B9. Calibration Gas Mixture, KDC Laboratory

Source:

UCC&P, Automated Analytical Systems, Gas Mixing Laboratory,
Technical Center, South Charleston, WV 25303

Date: 8/13/87
Cylinder material: Carbon steel
Cylinder number: W-327699
Final pressure: 250 psia
Dewpoint: -46 °C

Contents are as follows:

Component	Actual Mole Percent
Propane	1.0000
Propylene	1.0000
Carbon monoxide	1.0000
Ethane	2.0000
Ethylene	2.0000
Carbon dioxide	2.0000
Methane	20.0000
Oxygen	4.0000
Nitrogen	66.9853
Isobutane	55.1 ppm*
n-Butane	7.0 ppm*
Hydrogen	82.4 ppm*
Water	2.1 ppm*

*: Estimated impurities.

Table B10. GC Program Conditions, NEK Laboratory

Injectors at 200°C
Detectors at 200°C

Detector: Thermal Conductivity
- Column = 10' x 1/8" stainless steel Carbosieve SII
- Carrier Gas flow rate = 23.5 cc/min
- Carrier Gas = Helium or argon
- Current = 72 ma
- Sensitivity = 36 x 0.05 mV

Detector: Flame Ionization Detector
- Column = 10' x 1/8" stainless steel Porapak R
- Carrier Gas flow rate = 24.0 cc/min
- Carrier Gas = Helium or argon
- Air flow rate about 300 cc/min
- Hydrogen flow rate about 30 cc/min
- Sensitivity = 16 x 10^{-10} amps/mV

Oven Temperature Program
- Initial Temperature = 50°C
- Hold time = 10 minutes
- Ramp rate = 10°C/min
- Final Temperature = 200°C
- Hold time = 16 minutes
- Cool down and stabilization time = 14 minutes

Stream select and sampling valve box at room temperature.
Flow to stream select and sampling valves is about 10 cc/min.

Table B11. Calibration Table, NEK Laboratory

Thermal Conductivity Detector:

No.	Ret. Time	Name
1	7.82	Hydrogen
2	11.1	Oxygen
3	11.6	Nitrogen
4	13.4	Carbon monoxide
5	19.1	Methane
6	22.7	Carbon dioxide
7	26.8	Acetylene

Flame Ionization Detector:

No.	Ret. Time	Name
1	9.16	Ethylene
2	10.4	Ethane
3	11.1	Acetylene
4	18.76	Propylene + Propane
5	20-21.5	Butane and butylenes

Table B12. Calibration Gas Mixture, NEK Laboratory

Source:

UCC&P, Automated Analytical Systems, Gas Mixing Laboratory, Technical Center, South Charleston, WV 25303

Date: 7-7-89
Cylinder Material: Stainless Steel DOT E4884
Cylinder Number: 720
Final Pressure: 250 psia
Estimated Dewpoint: -43°C

Contents:

Component	Actual Mole Percent
Isobutane	0.20000
N-Butane	1000.0 ppm
Acetylene	0.20000
Propane	0.25000
Propylene	0.50000
Hydrogen	0.20000
Carbon Monoxide	2.00000
Ethane	1.50000
Ethylene	2.00000
Methane	20.00000
Carbon Dioxide	6.00000
Nitrogen	5.00000
Oxygen	1.00000
Argon	61.04945
Isopentane	2.1 ppm*
2-2 Dimethylpropane	1.0 ppm*
Water	2.3 ppm*

* Estimated Impurities

Table B13. Calibration Gas Mixture, NEK Laboratory

Source:

UCC&P, Automated Analytical Systems, Gas Mixing Laboratory, Technical Center, South Charleston, WV 25303

Date: 7-27-89
Cylinder Material: Carbon Steel
Cylinder Number: 5368326
Final Pressure: 300 psia
Estimated Dewpoint: -50°C

Contents:

Component	Actual Mole Percent
Acetylene	0.10000
Propane	500 ppm
Propylene	0.10000
Hydrogen	1.00000
Carbon Monoxide	0.50000
Ethane	0.50000
Ethylene	1.00000
Methane	5.00000
Carbon Dioxide	1.00000
Nitrogen	1.00000
Oxygen	5.00000
Argon	84.74934
N-Butane	0.8 ppm*
Isobutane	1.0 ppm*
Water	2.1 ppm*

* Estimated Impurities

Figure B1. Reactor System, BKW Laboratory

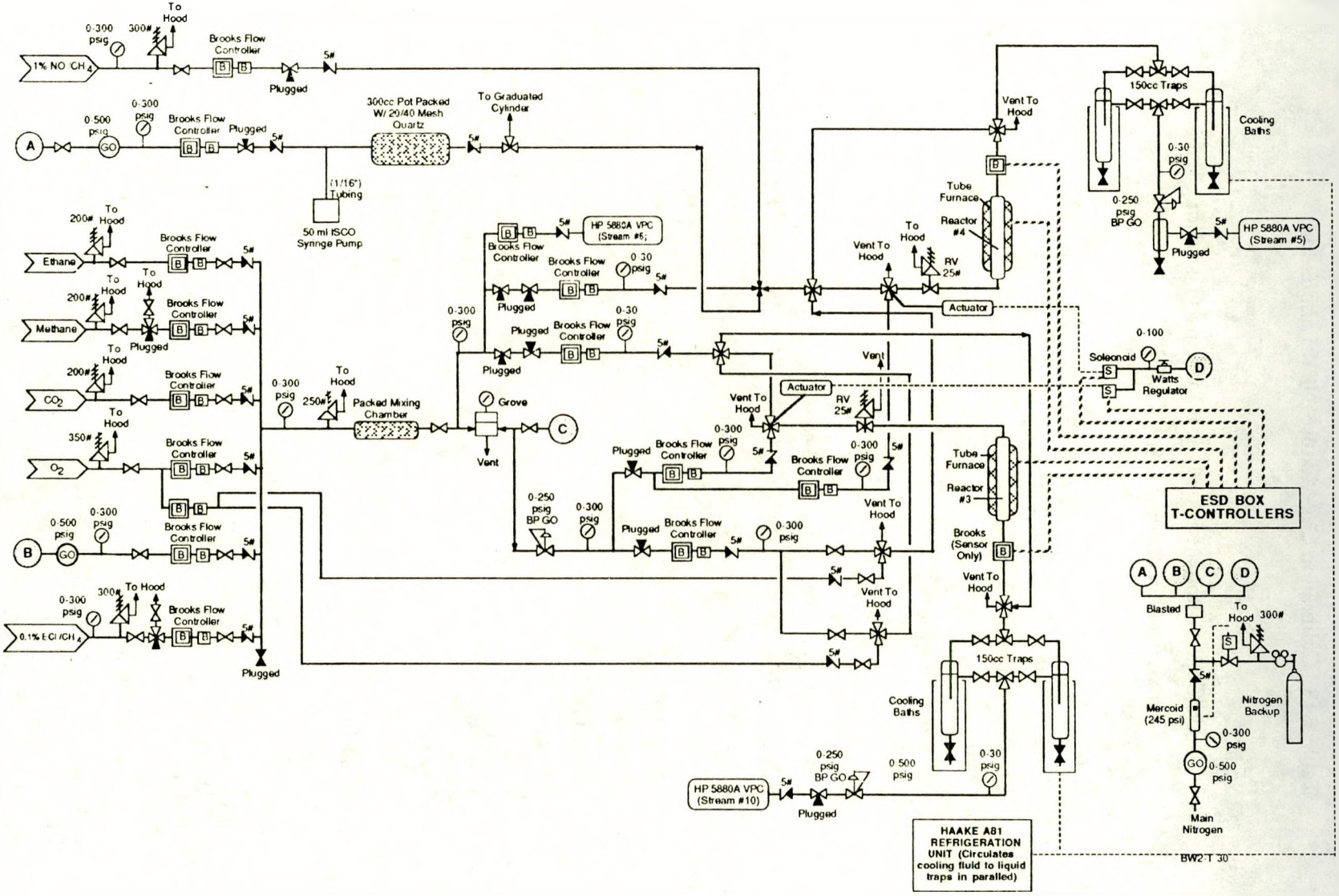


Figure B2. Reactor System, KDC Laboratory, Catalyst Tests 1-KDC-X-#

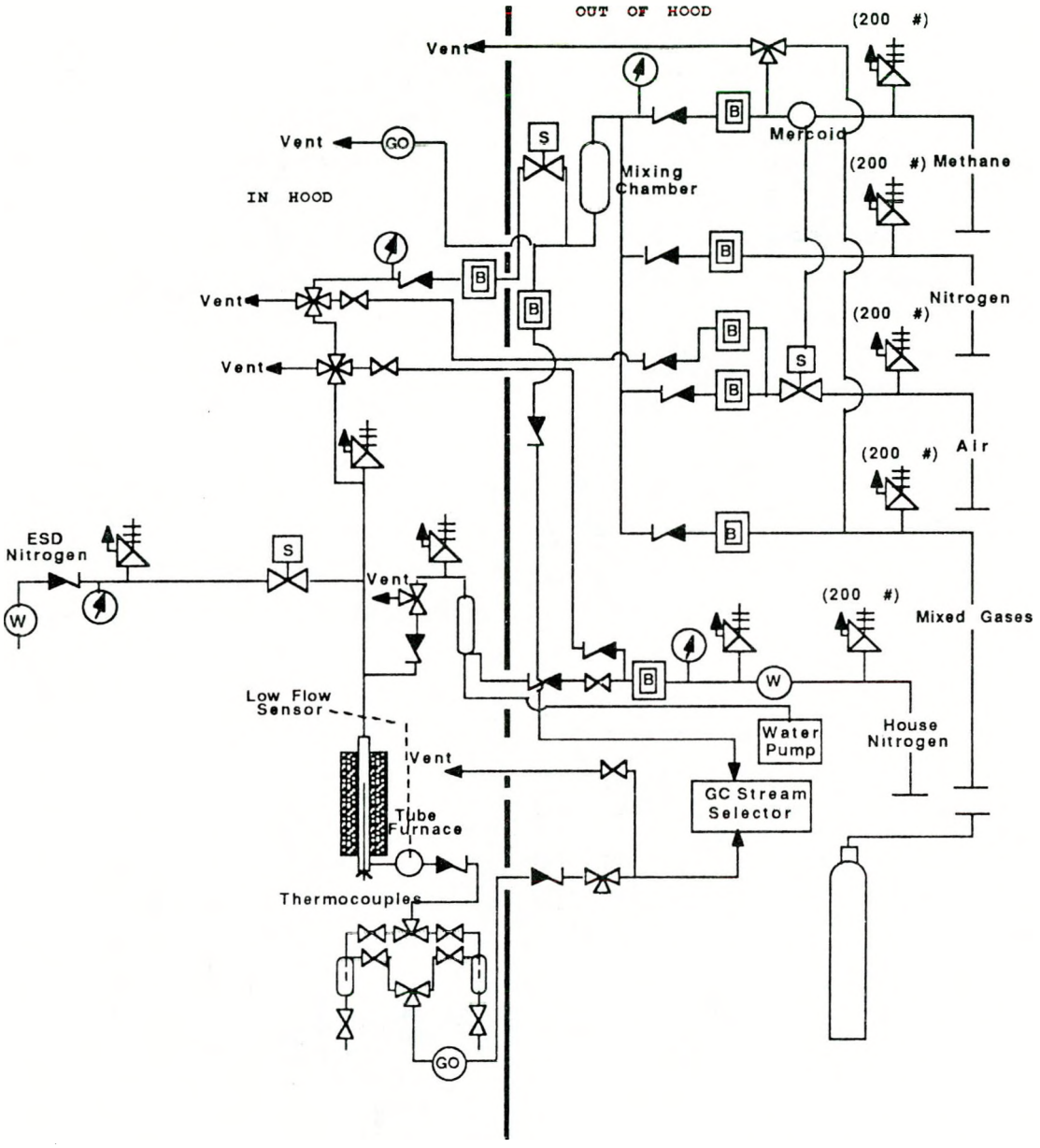


Figure B3. Reactor System, KDC Laboratory, Catalyst Tests 2-KDC-X-# thru 12-KDC-X-#

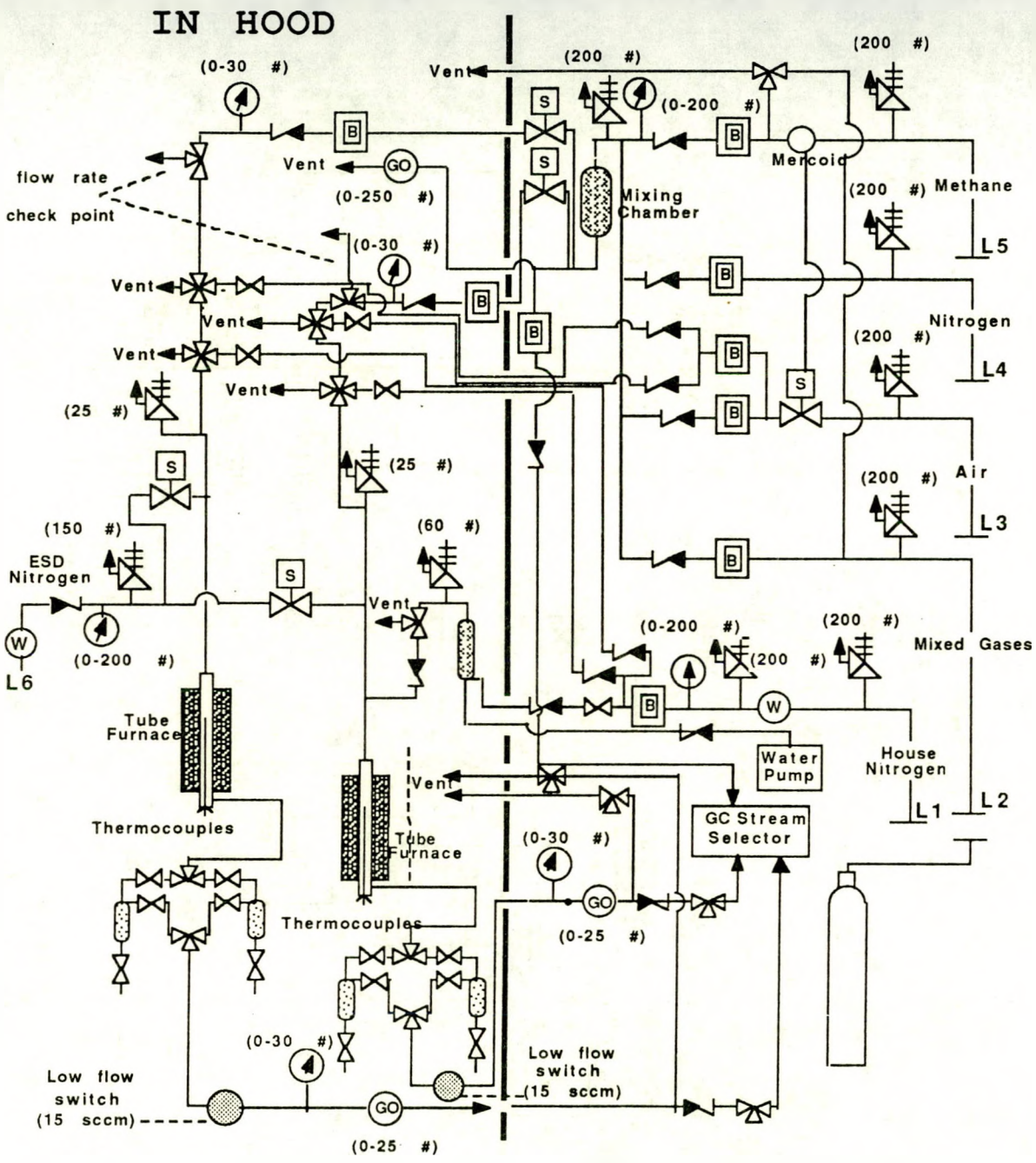


Figure B4. IR Reactor System, BKW Laboratory

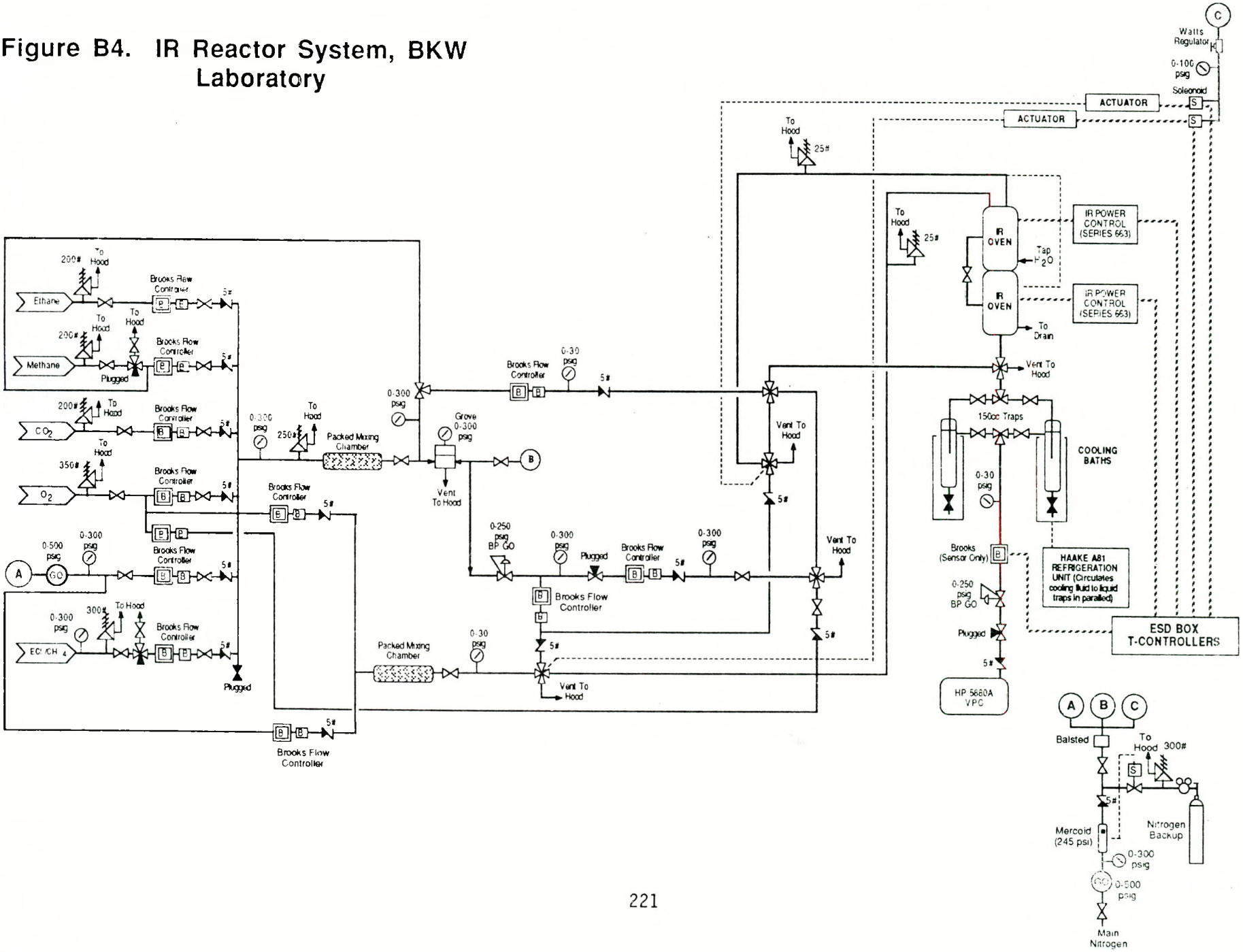


Figure B5. Reactor System, NEK Laboratory

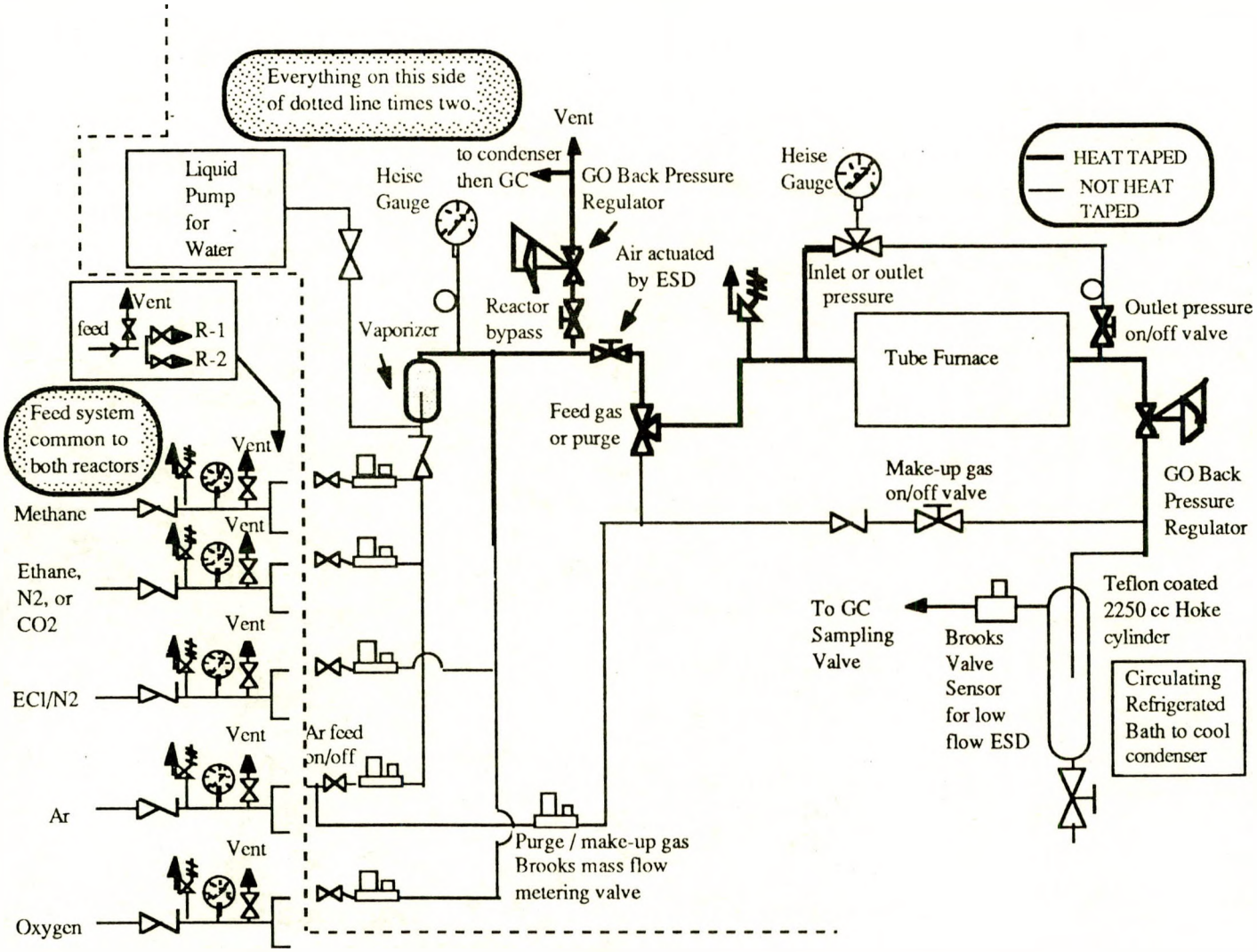
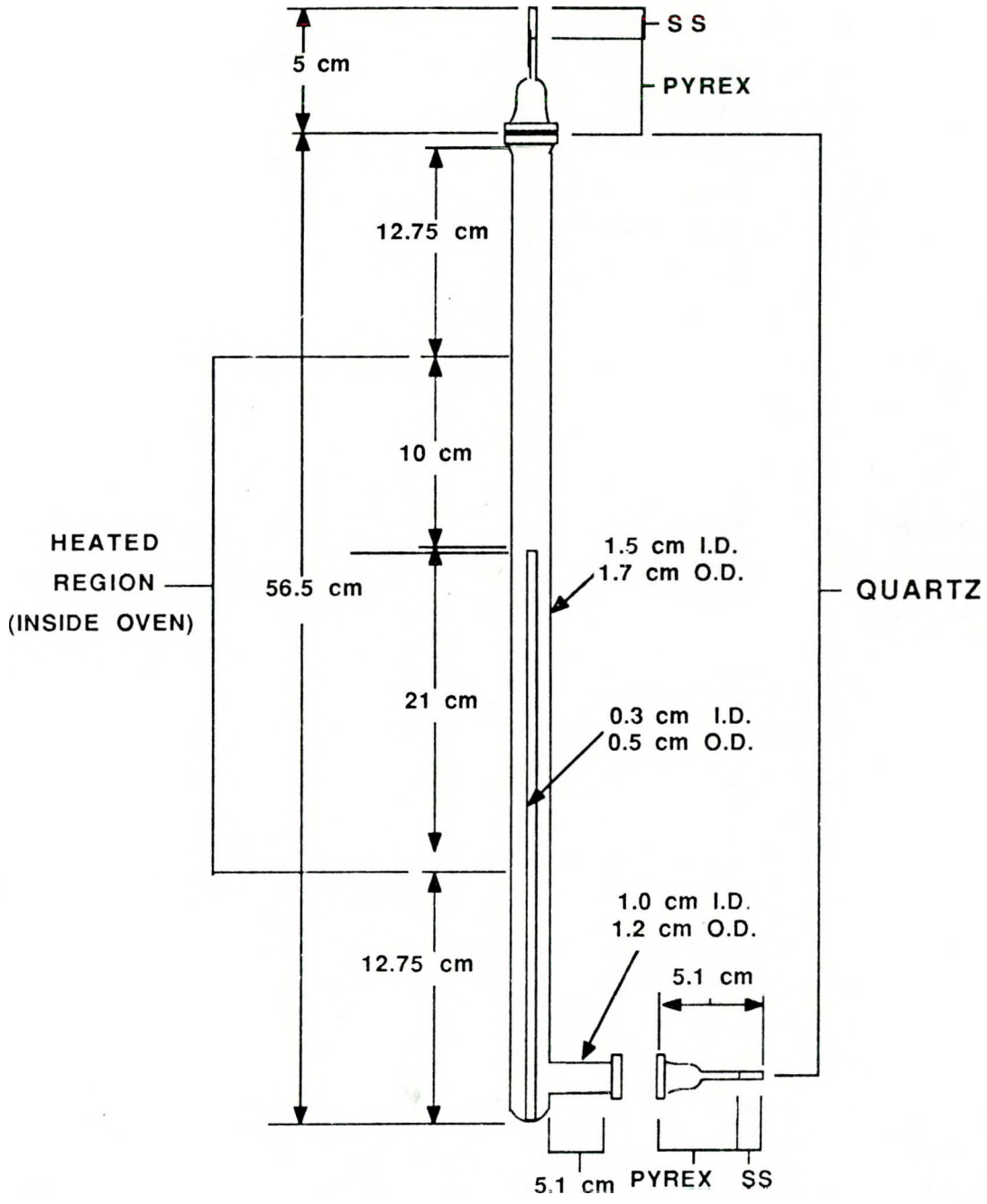
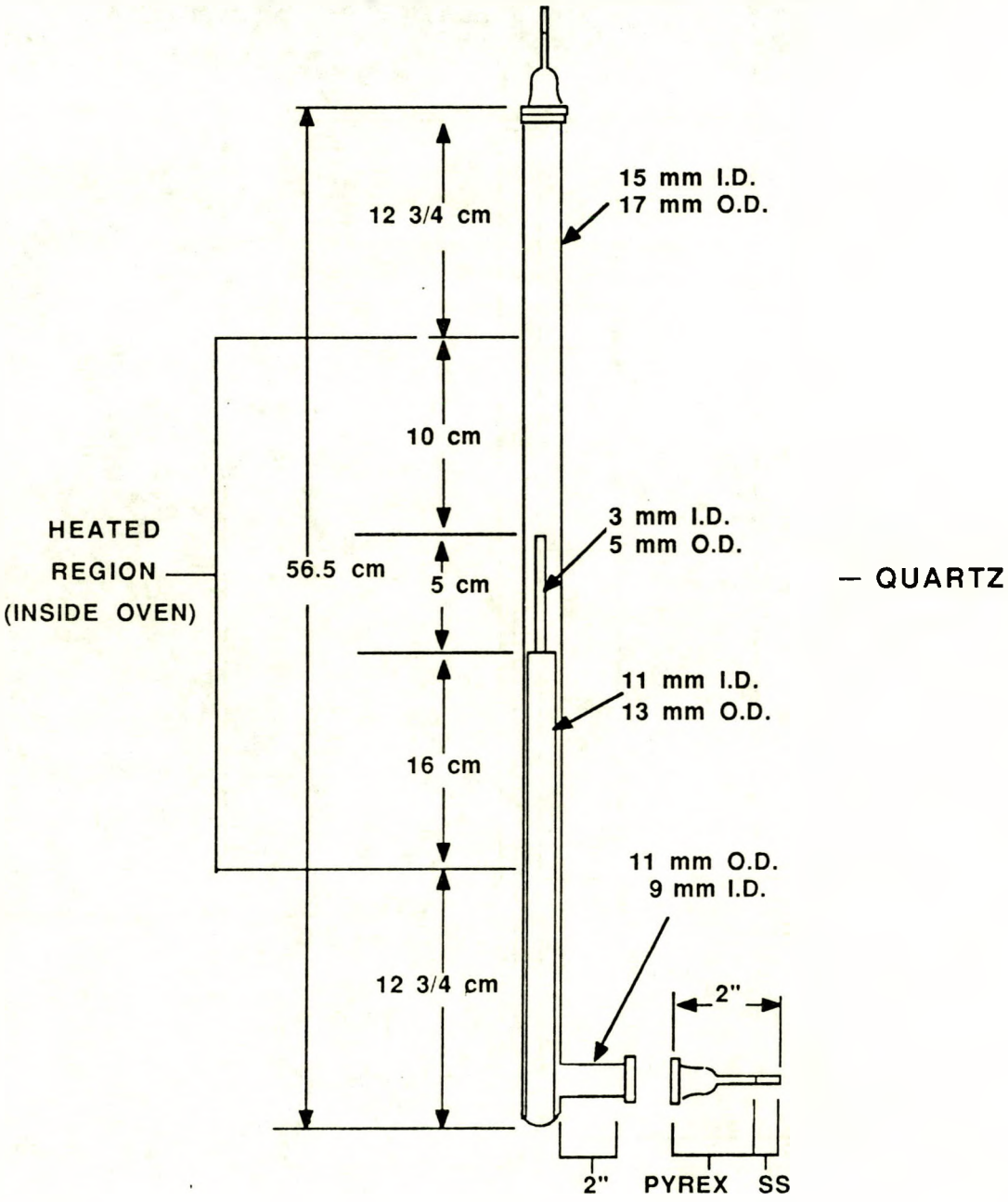


Figure B6. Quartz Reactor A



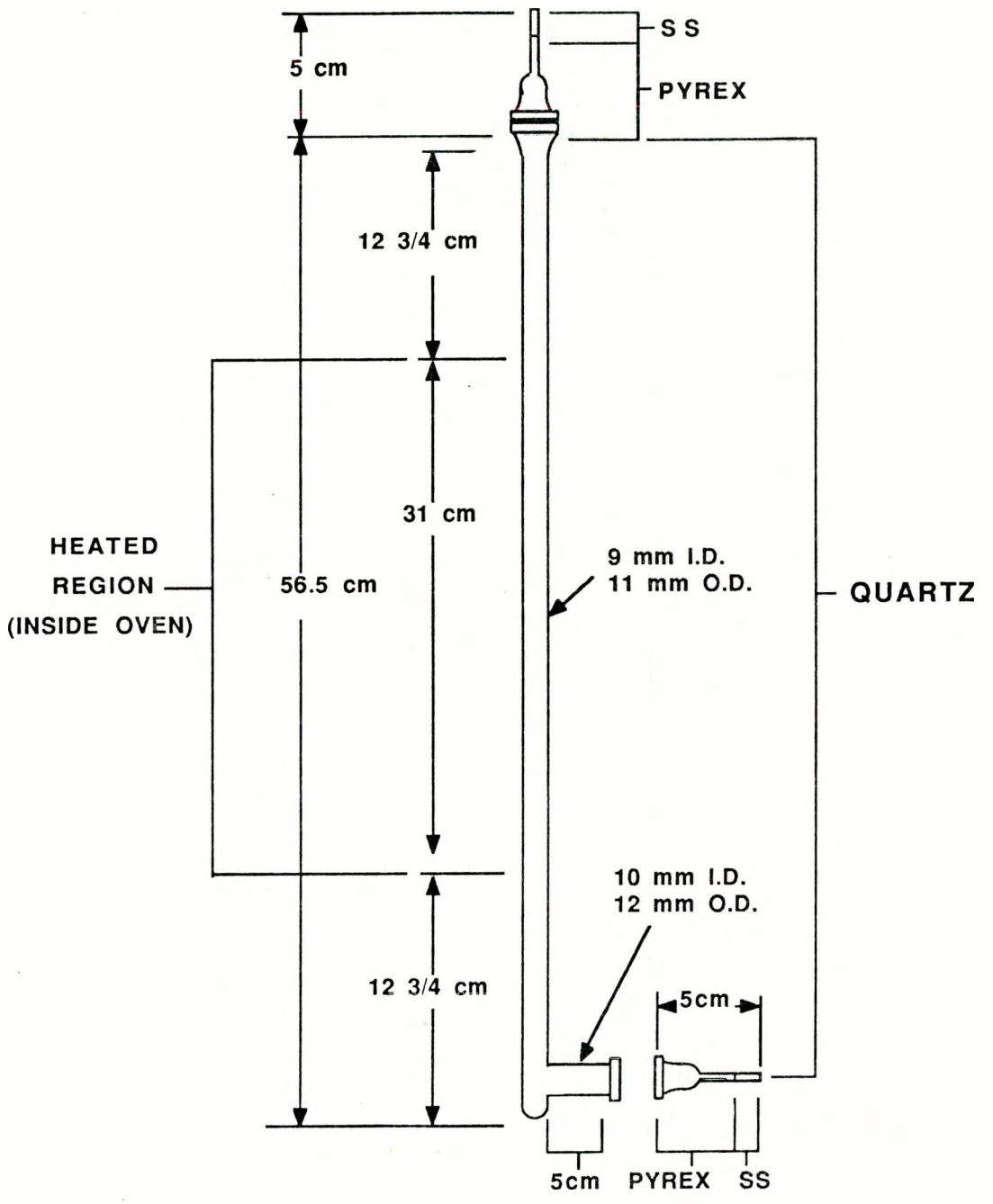
ALL O-RING CONNECTIONS
Not to scale

Figure B7. QUARTZ REACTOR B



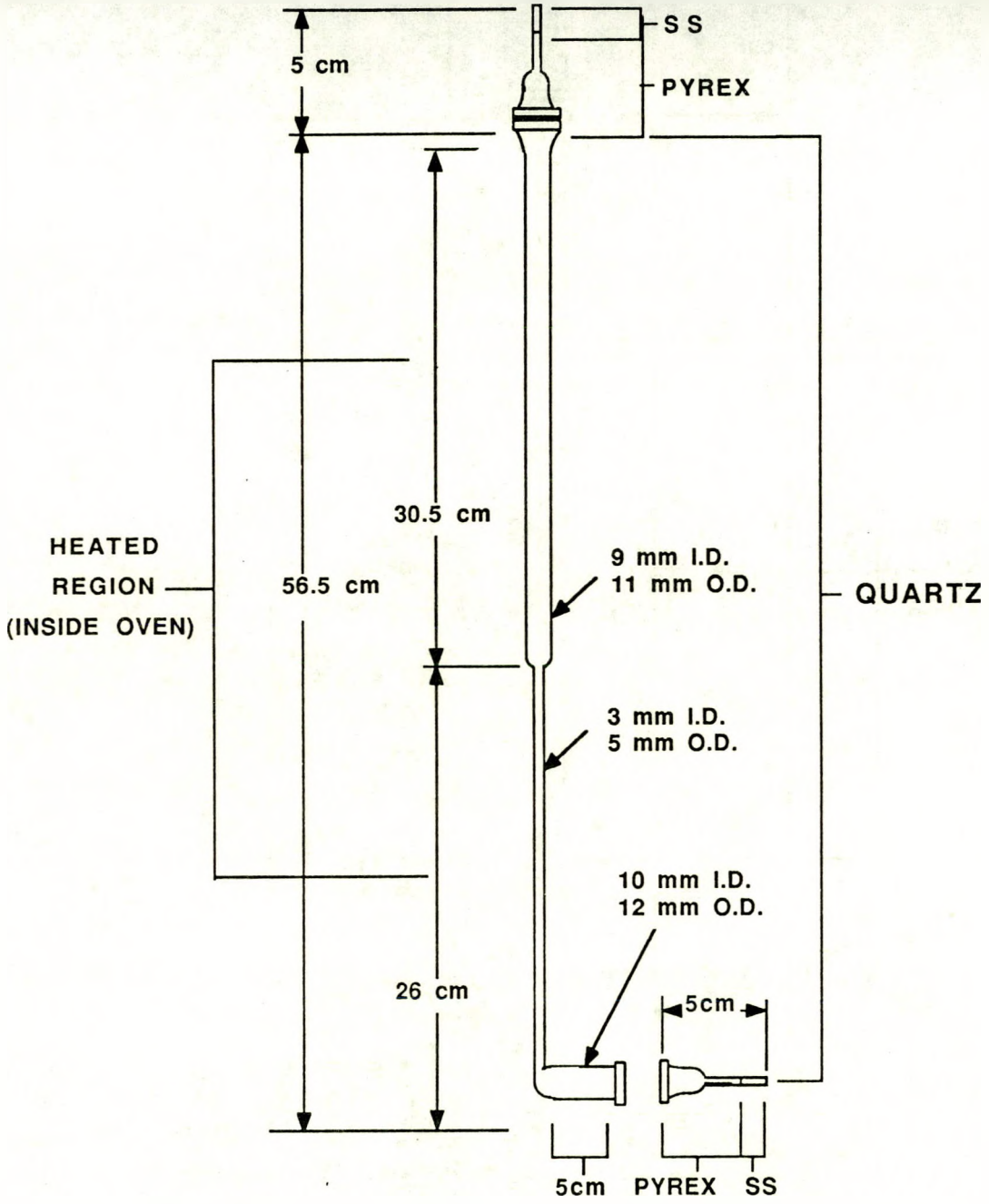
ALL O-RING CONNECTIONS
Not to scale

Figure B8. Quartz Reactor C



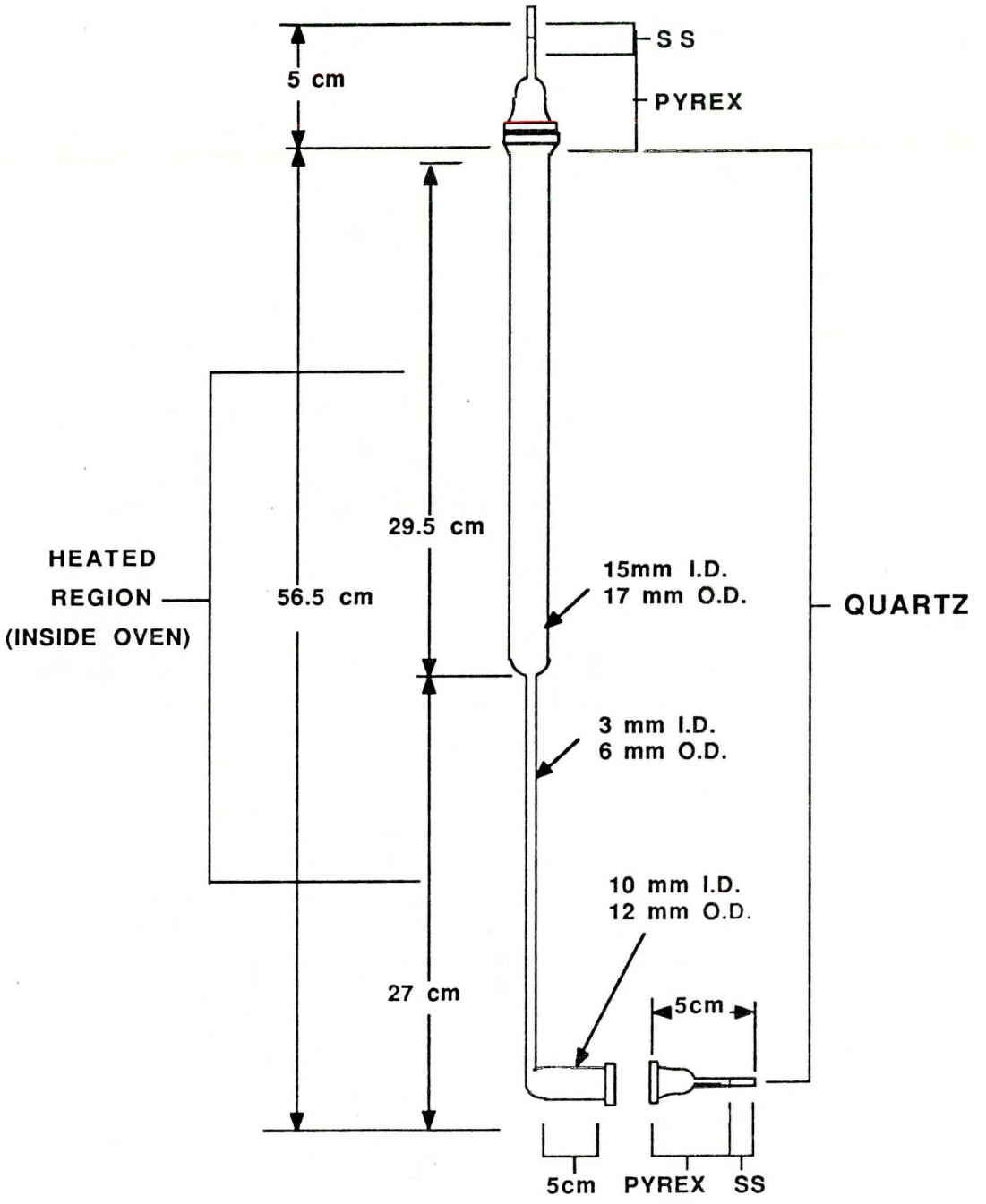
ALL O-RING CONNECTIONS
Not to scale

Figure B9. Quartz Reactor D



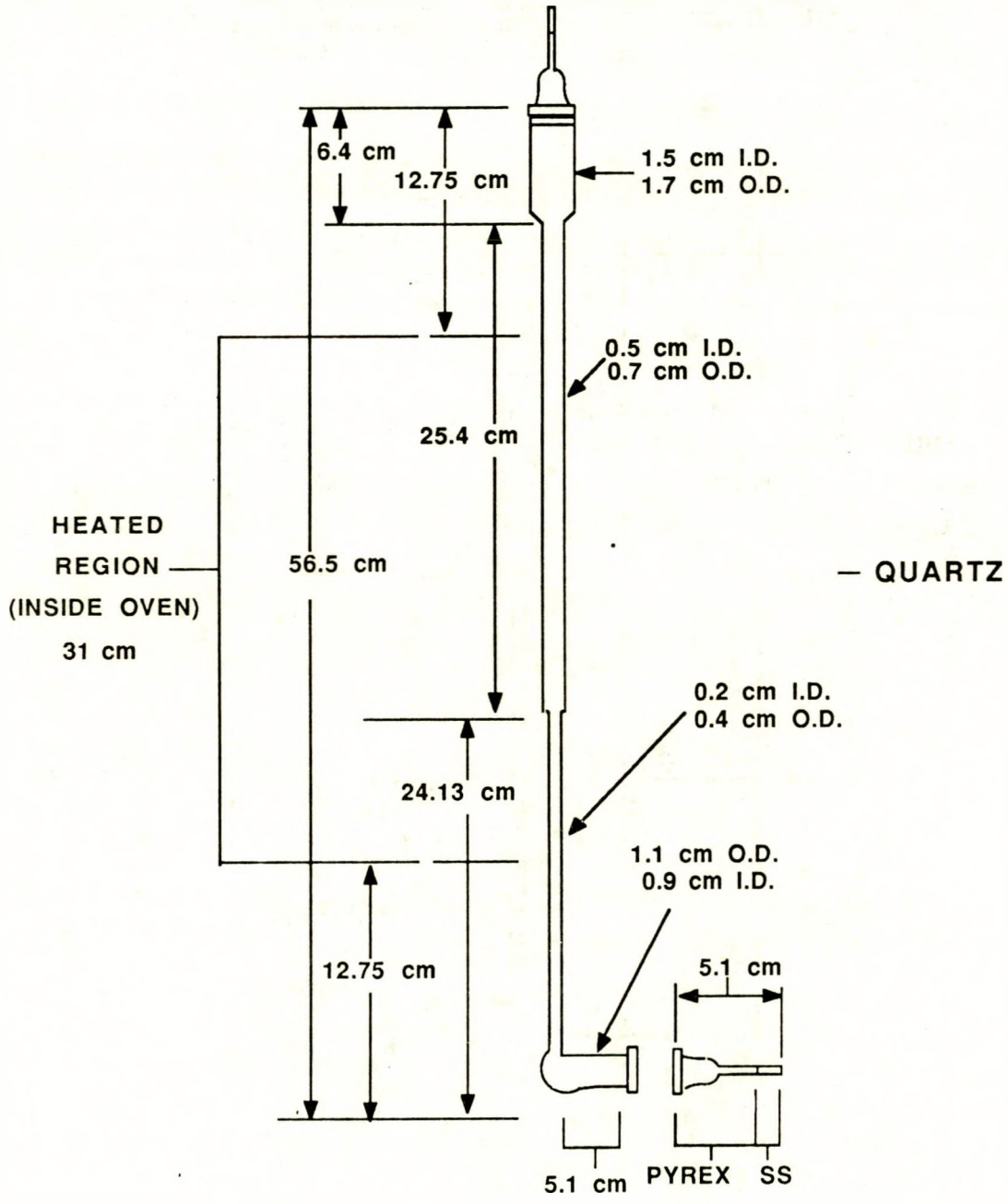
ALL O-RING CONNECTIONS
Not to scale

Figure B10. Quartz Reactor E



ALL O-RING CONNECTIONS
Not to scale

Figure B11. Quartz Reactor F



Drawing not to scale

Figure B12. Quartz Reactor G

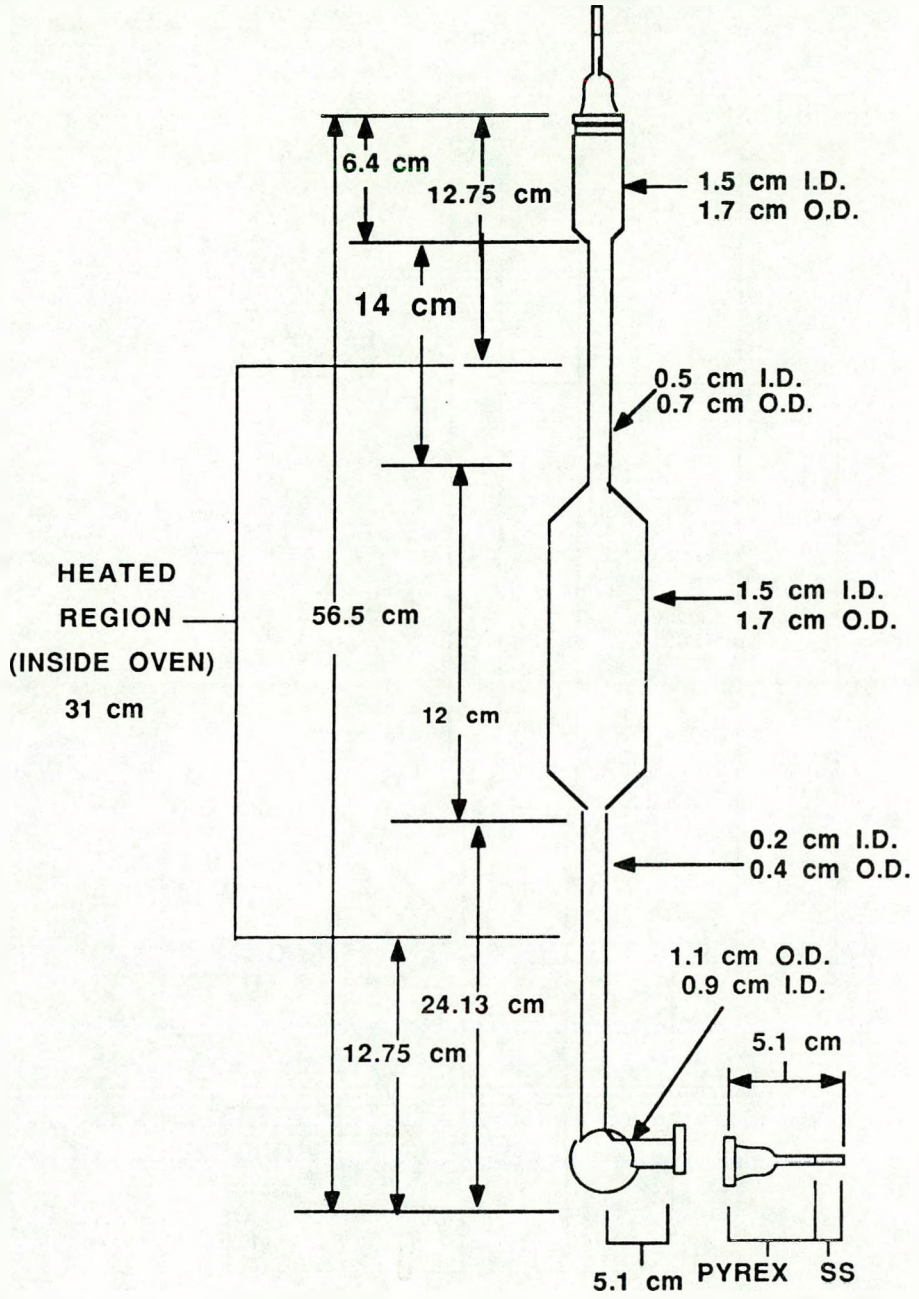


Figure B13. Quartz Reactor H

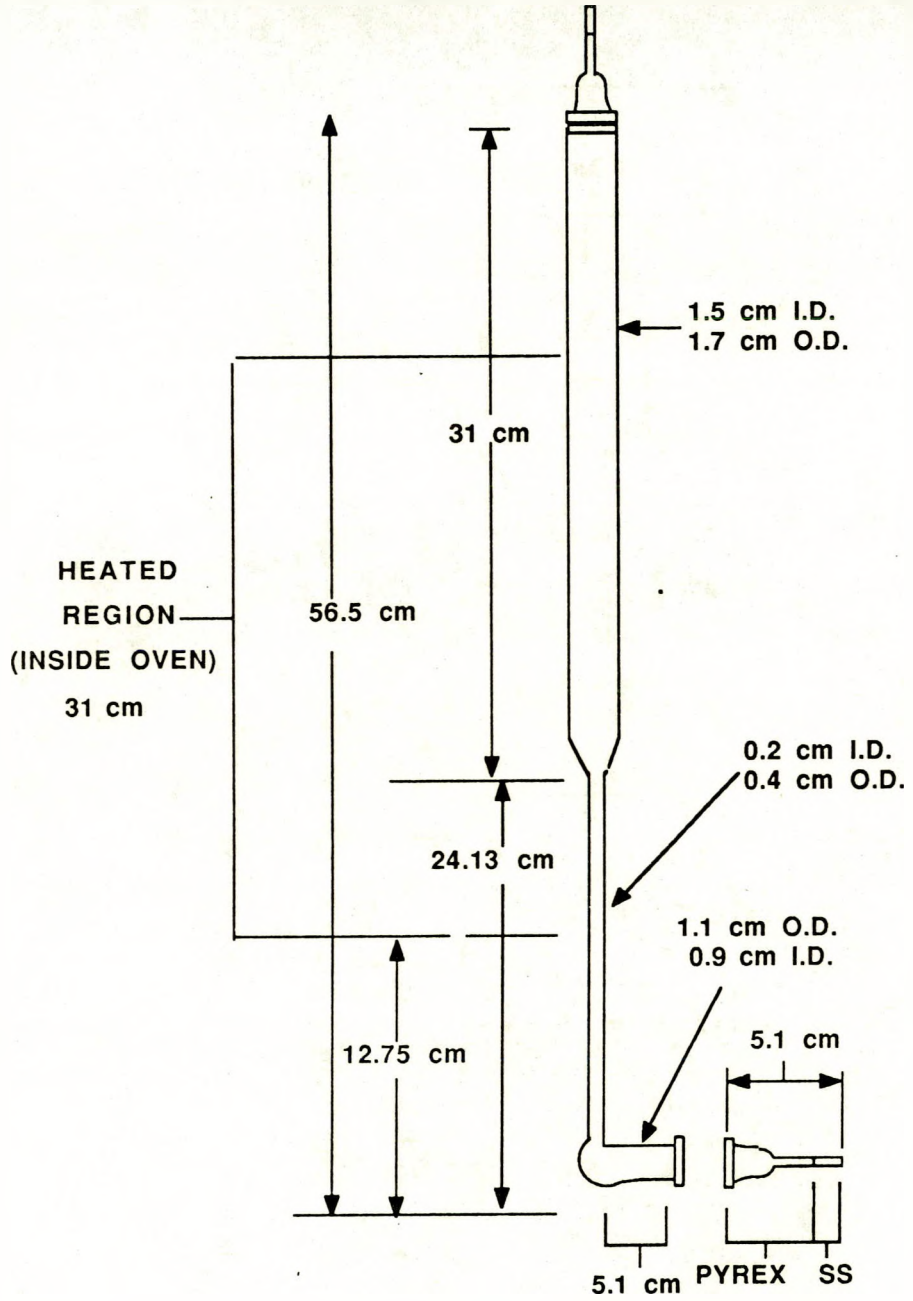


Figure B14. Stainless Steel Reactor S

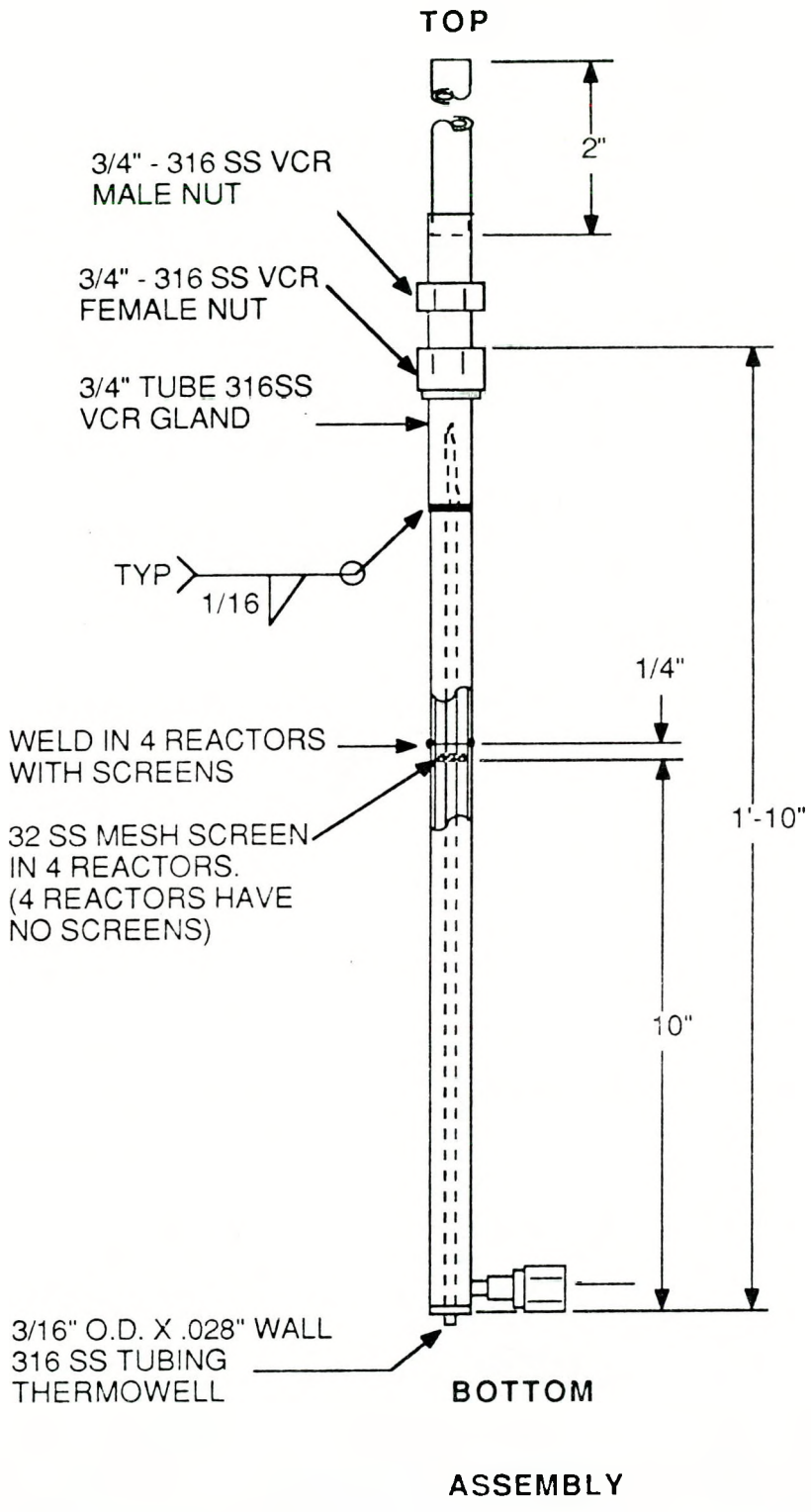


Figure B15. Vapor Phase Quartz Reactor V

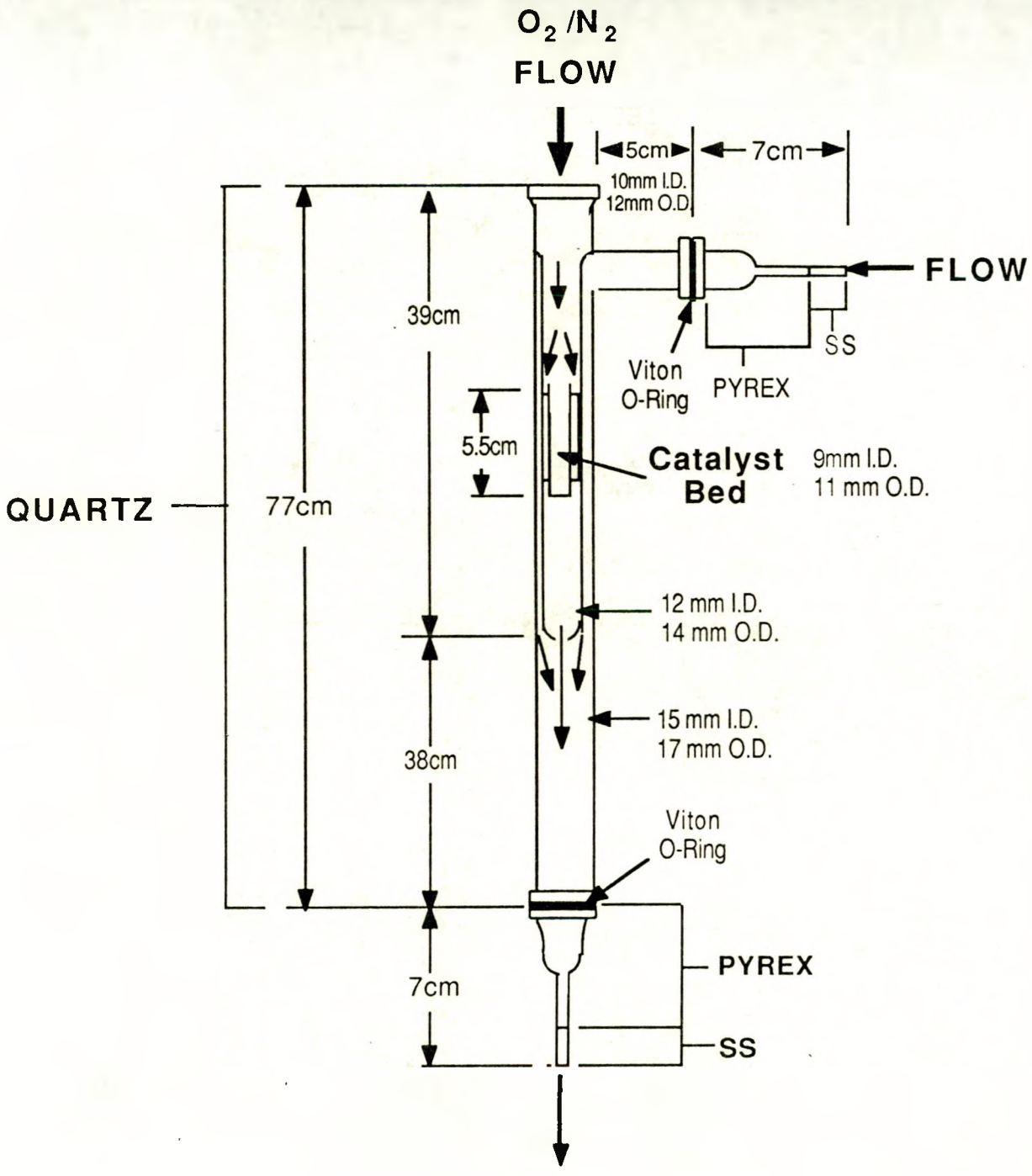
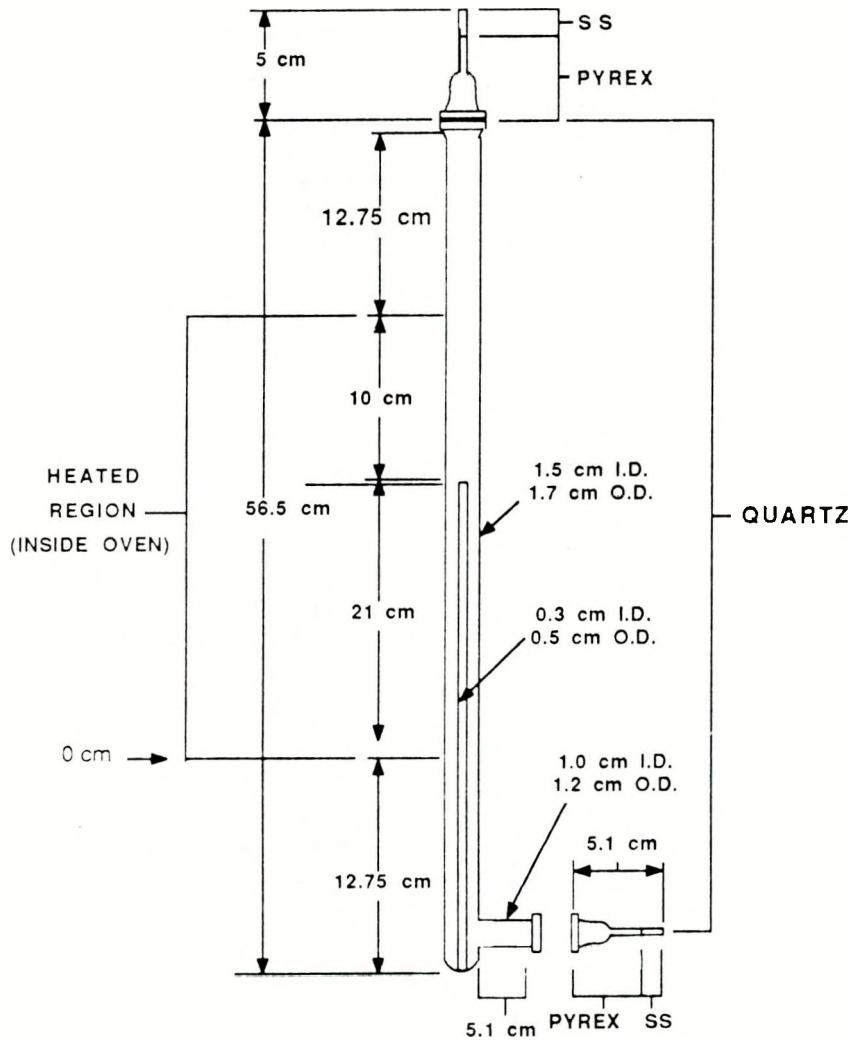


Figure B16. Quartz Reactor A, Temperature Profile

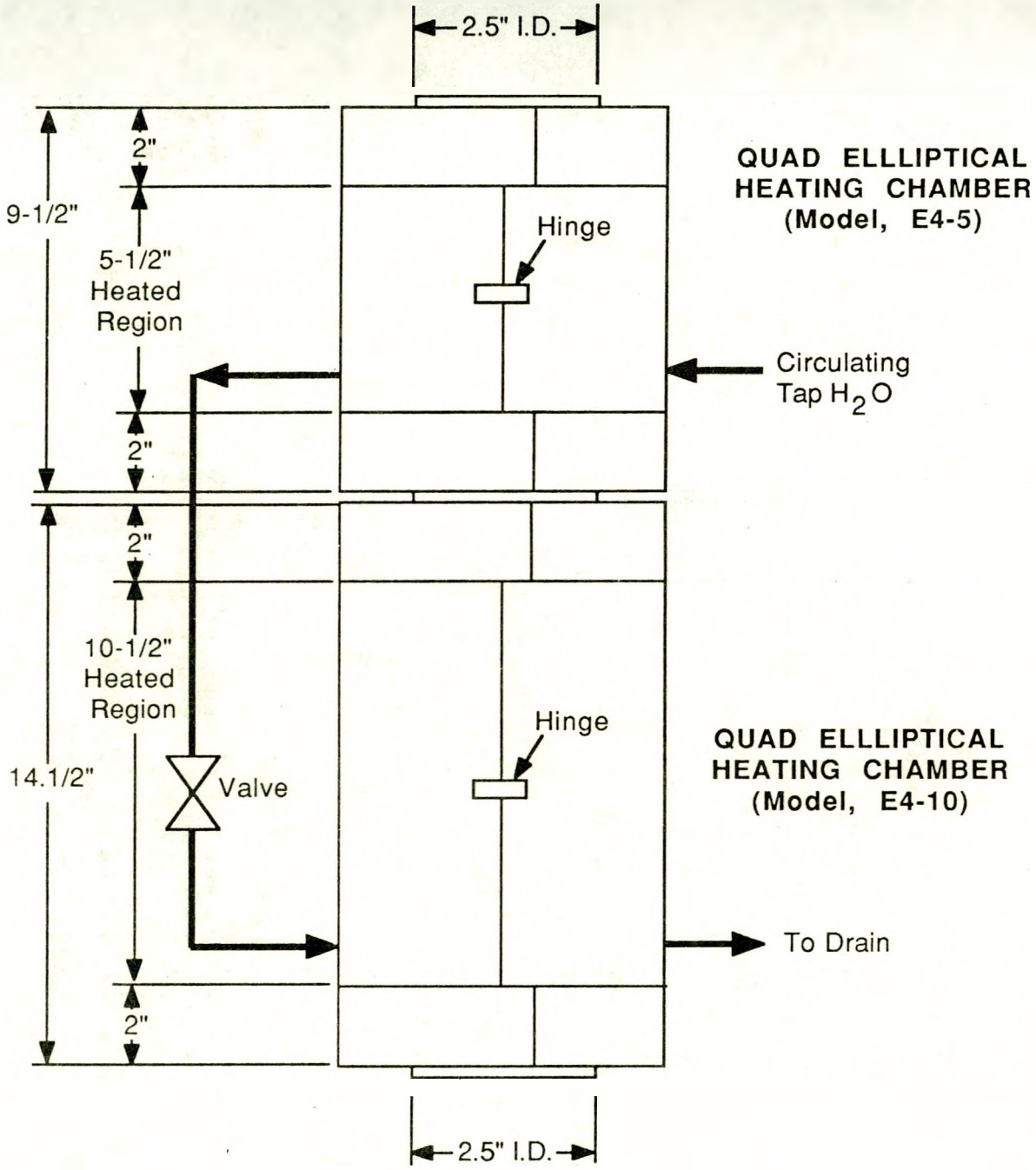


TEMPERATURE PROFILE

cm	°C	
21.0	800	Preheater Zone Thermocouple Position
20.5	800	
20.0	801	
19.5	801	
19.0	802	
18.5	802	Catalyst Bed Thermocouple Position
18.0	802	
17.5	801	
17.0	800	
16.5	800	
16.0	799	Post-Catalytic Volume Thermocouple Position
15.5	798	
15.0	797	
14.5	796	
14.0	795	
13.5	793	
13.0	791	
12.5	790	
12.0	788	
11.5	786	
11.0	784	
10.5	782	
10.0	779	
9.5	777	
9.0	775	
8.5	773	
8.0	772	
7.5	770	
7.0	766	
6.5	760	
6.0	755	
5.5	751	
5.0	746	
4.5	740	
4.0	733	
3.5	723	
3.0	714	
2.5	705	
2.0	694	
1.5	685	
1.0	674	
0.5	661	
0.0	645	

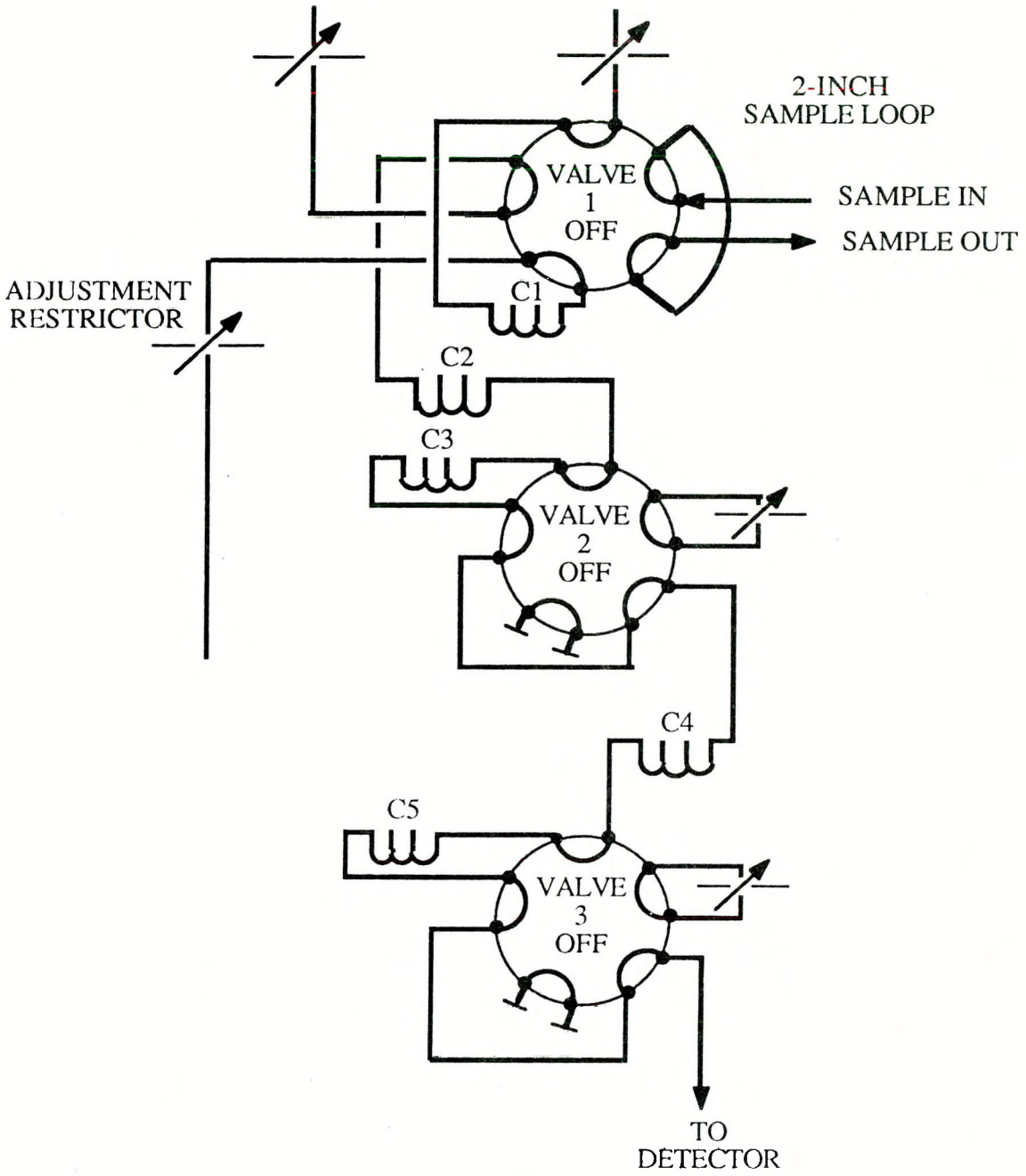
ALL O-RING CONNECTIONS
Not to scale
Reference 29-BKW-71

Figure B17. IR Ovens in Series, Used for Reactor V



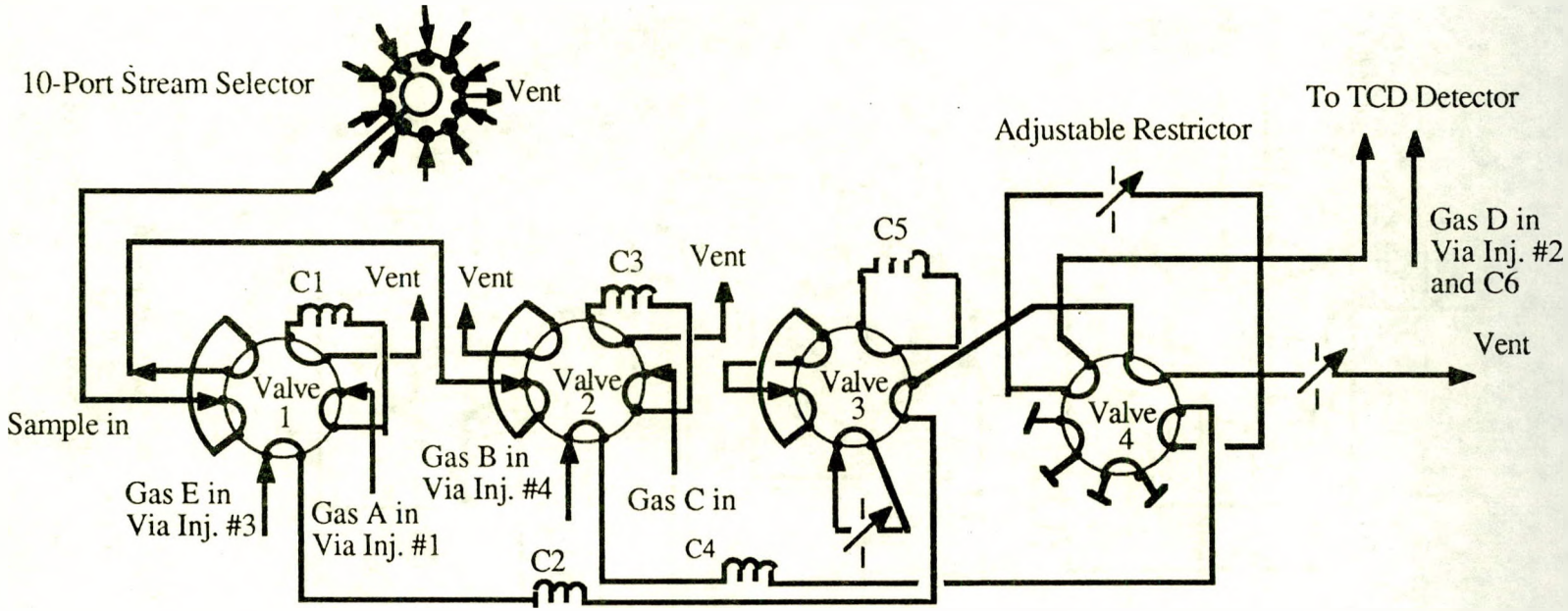
Heavy cast aluminum construction
Ovens containing four reflector
array with lamps

Figure B18. Valve Switching Schematic, KDC Laboratory



C1 = 24" x 1/8" SS CW 20M Chrom T 40/60
C3 = 13' x 1/8" SS Porapak Q 80/100
C5 = 15' x 1/8" SS 5A Molecular Sieve 60/80

Figure B19. Valve Switching Schematic, BKW Laboratory



Columns:

C1: 24" x 1/8" SS Poropak Q 80/100 mesh
C2: 13' x 1/8" SS Poropak Q 80/100 mesh
C3: 24" x 1/8" SS CW 20 m on Chromosorb T 40/60 mesh
C4: 16' x 1/8" SS UCON 75HB 90M on Chromosorb T 40/60 mesh
C5: 10' x 1/8" SS 5A Molecular Sieve 60/80 mesh
C6: 10' x 1/8" SS Tenax 60/80 mesh

Figure B20. Reactor K, High Pressure Reactor

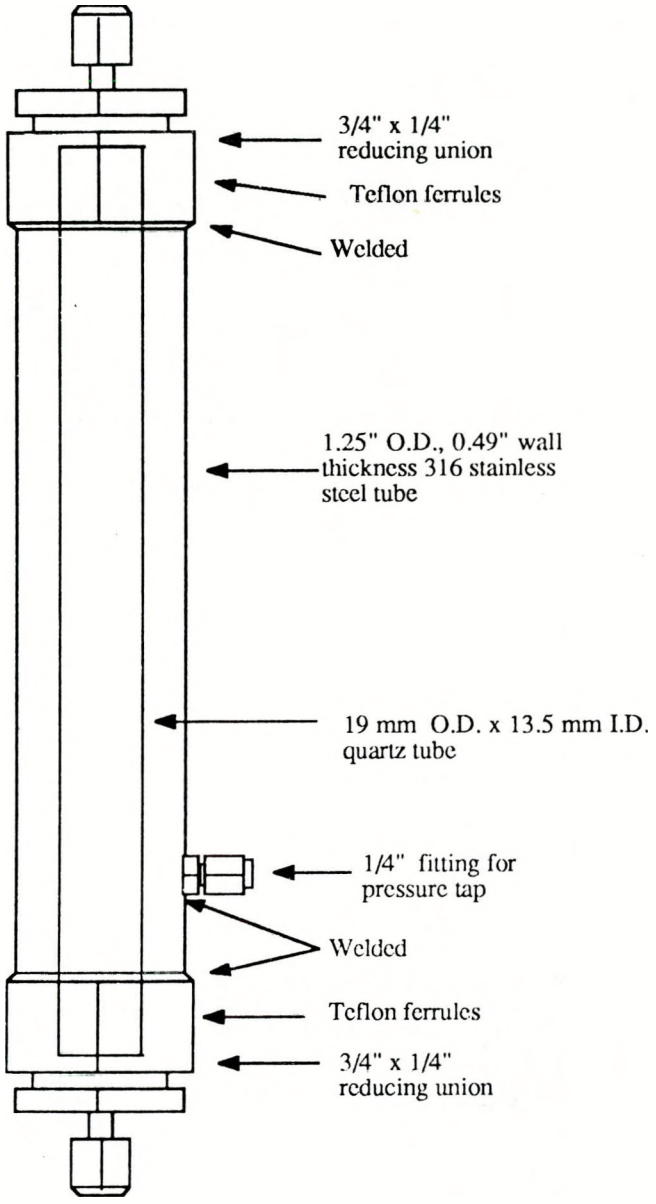
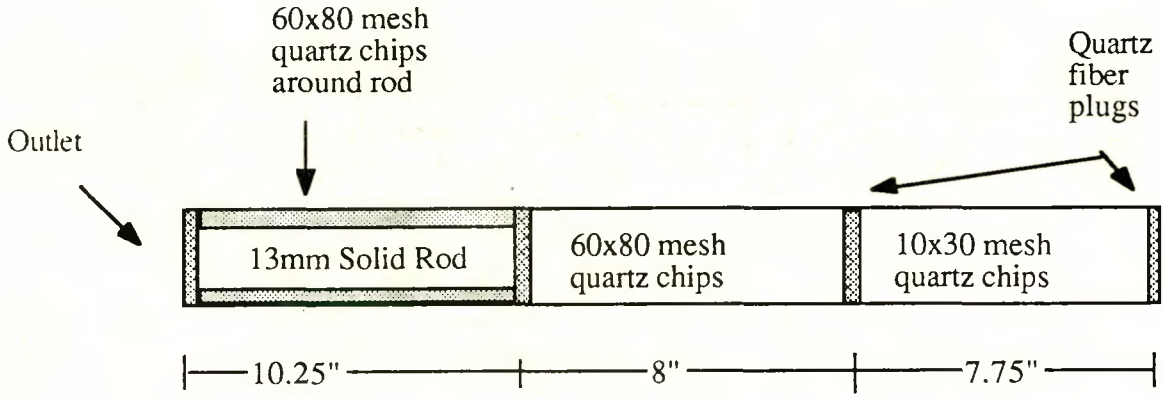
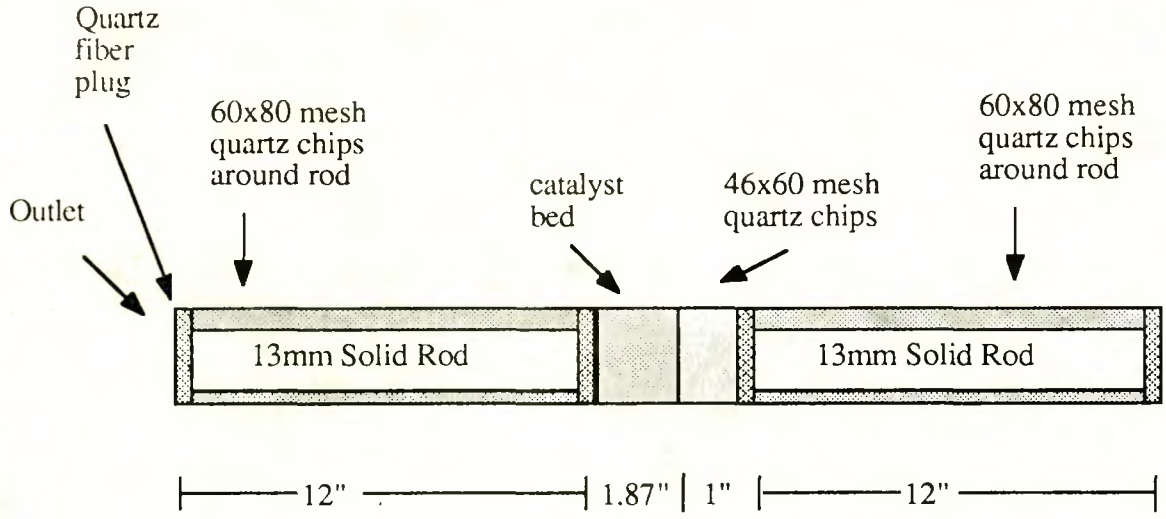


Figure B21. High Pressure Reactor Packing Configurations

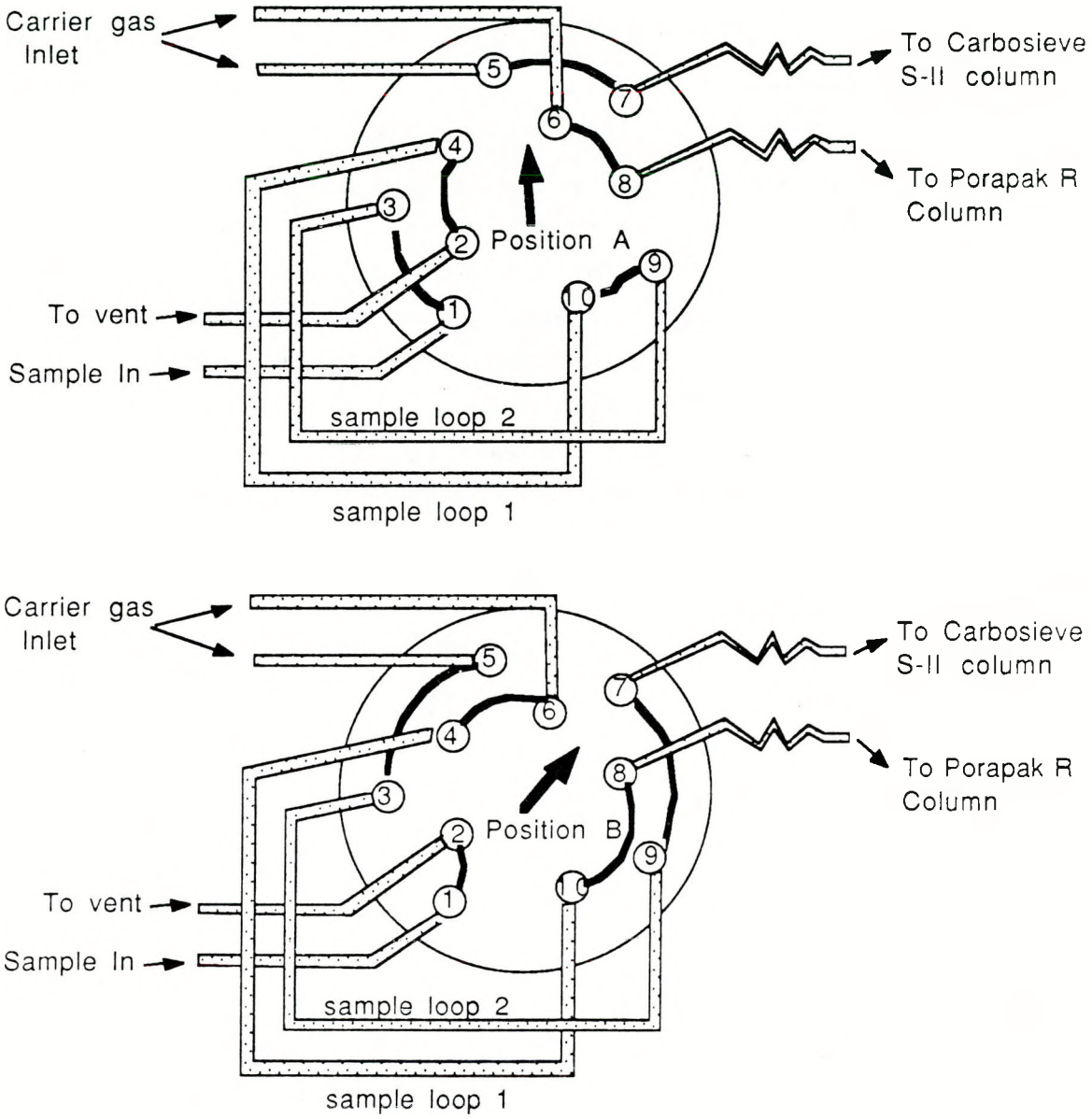


Configuration A



Configuration B

Figure B22. Valco Valves for simultaneous injection of one gas stream onto two GC columns, NEK Laboratory



Appendix C. CATALYST PREPARATION PROCEDURES

BKW Laboratory

Procedure A

In Procedure A, supported catalysts are prepared using the incipient wetness technique. In this procedure, the amounts of components required to give the desired loading are dissolved in a quantity of deionized, distilled water necessary to just fill the pores of the support. The solution is then added to the support particles. In some cases, if the dopants are not easily soluble, suspensions of the components are added to the support. The resulting materials is dried in a vacuum oven at 130 °C under a vacuum of 16-84 kPa for 1 to 50 hours (usually 18-20 hours). Most dried catalysts are tested without further treatment. Several were first calcined in air. In most cases, these are marked in Appendix D as procedure A(*). These were prepared in 15 gram batches prior to calcining, and 5.3 to 6 grams of materials was calcined, as indicated in Appendix D. Metal or inorganic compound loadings are expressed as weight percent based on 100 weight percent of the support.

Procedure A#3

Procedure A#3 is the same as Procedure A except that citric acid in water was used in place of water.

Procedure A#4

Procedure A#4 is the same as Procedure A except that the inorganic compound was stirred in water to form a solution or suspension. This was mixed with the support until the mixture was soaked up by the support.

Procedure A#5

Procedure A#5 is the same as Procedure A except that the metal salt was dissolved in the aqueous solution or suspension while heating slightly over hotplate until a clear aqueous solution or suspension of metal salt was observed. This was then added to the support.

Procedure A#6

Procedure A#6 is the same as Procedure A except that a purchased La/Nd nitrate (75/25) solution was used rather than dissolving a compound in water.

Procedure B

In Procedure B, supported catalysts were prepared by adding the proper amount of component(s) to a mixture of water which was stirred with the support, while heating in a glass container on a hotplate for 2 to 3 hours (or until almost no water was left), to distribute the material in and on the support. If the dopants were not easily soluble, they were finely ground first. Deionized, distilled water was used (50 mL unless stated otherwise). The resulting material was dried in a vacuum oven at 130 °C under a vacuum of 16-84 kPa for 1 to 50 hours (usually 18-20 hours). The dried catalysts were then calcined in air. Metal or inorganic compound loadings are expressed as weight percent based on the weight of the support.

Procedure B#1

Procedure B#1 is the same as Procedure B except that 30 mL of deionized, distilled water were used.

Procedure B#2

Procedure B#2 is the same as Procedure B except 100 mL of deionized, distilled water were used.

Procedure B#3

Procedure B#3 is the same as Procedure B except that 40 mL of deionized, distilled water were used.

Procedure B#4

Procedure B#4 is the same as Procedure B except that 70 mL of deionized, distilled water were used.

Procedure C

Silver/lactic acid solution preparation method (see Experimental Section).

Procedure E

The inorganic compound (6.21 grams) was dissolved in 11 grams of deionized, distilled water then dried in air for 3 hours at 130 °C and atmospheric pressure. The sample was further dried in air for 15 hours at 130 °C under vacuum.

Procedure F

Deionized, distilled water was added to wet the support then the mixture was stirred to form a paste. This was dried in air for 18 hours at 130 °C under vacuum.

Procedure G

A barium oxide·aluminum oxide (barium aluminate) catalyst ($3BaO{\cdot}Al_2O_3$, available from Alfa, Danvers, Massachusetts, Lot number K18G, 99.99 weight percent) is calcined at 850 °C for 2 hours. By powder x-ray analysis, phases of barium aluminate, barium oxide, and barium carbonate are present.

Procedure H

Powdered BaO (JM, lot #16962, technical grade, 88-94%) was heated in air for 4 hours at 850 °C in a zirconium crucible (from B-J Scientific Products, Inc., Albany, Oregon). This was crushed to 30/60 mesh (and used in 36-BKW-46).

Procedure I

In this procedure 80 g of $Ba(OH)_2{\cdot}8H_2O$ (Baker Analyzed Reagent, Lot #514157) were heated at 130 °C under a vacuum of 16-84 kPa for 18-20 hours in a zirconium crucible (B-J Scientific Products, Inc., Albany, Oregon). The resulting material was heated at 850 °C for 4 hours in air, then at 750 °C for 2 hours. The material was molten at 750 °C. Cooled material was crushed and meshed to 30 to 60 mesh.

Procedure P

Compound was stirred as a slurry and heated in water. The paste was dried in a vacuum oven at 130 °C under a vacuum of 16-84 kPa. The solid was then heated at 850 °C for 2 hours, prior to being chopped and sieved to 40/100 mesh.

Procedure R

Hydrotalcites ($Mg_6Al_2(OH)_{16}(CO_3^{=})\bullet\sim 4H_2O$) were prepared by W. T. Reichle of the Specialty Chemicals Division of UCC&P, at the Bound Brook, New Jersey Laboratory. The Mg/Al ratio of the bulk compounds is approximately 3. The surface composition of the hydrotalcites by ESCA for samples 16341-93A, 16341-94A, and 16341-95A by atomic percent are shown.

Sample	C	O	Mg	Al	Cl	Si	Na	Mg/Al
16341-93A	15	51	27	4.8	0.4	0.3	0.3	6.4
16341-94A	21	50	24	4.4	0.2	0.5	0.1	6.2
16341-95A	15.6	51.4	27.2	5.4	0.1	0.1	0.2	5.7

These samples were heated at 450 °C for 18 hours in air, then either heated at 850 °C for 4 hours in air (33-BKW-33, 34, and 39), or doped with barium carbonate using Procedure B, then heated at 850 °C for 4 hours in air (33-BKW-42, 43, and 48).

Procedure X

A 9 weight percent silver on alpha aluminum oxide catalyst is made by adding 600 grams of 88% aqueous lactic acid to a glass beaker and heating to 80 °C with stirring (30 minutes). Silver oxide (220 grams available from Ames Goldsmith Corporation, Glens Falls, New York) is slowly added, with stirring. The mixture is stirred an additional 30 minutes at 80-85 °C, then 10 milliliters of CP grade hydrogen peroxide from J. T. Baker are added. The clear solution is slowly added from a 1000 milliliter glass separatory funnel over a period of 5 minutes to 300 grams of Norton SA5502 (Sample number 82343) hollow cylinder supports. These are first evacuated under a vacuum of from less than 1kPa to 70 kPa pressure at 80 °C for 120 minutes in a 5.7 cm i. d. (5.9 o. d.) glass tube, which is 36 cm long. This tube is fitted with a stopcock on the bottom and on the top, through a

two-hole, black rubber, size 12 stopper, with a separatory funnel and a vacuum adapter. The glass tube is heated with a 6 foot Thermolyne heat tape, controlled by a Variac. The impregnating solution remains in the tube with the support at 81 °C for 60 minutes, then is drained. Recovered catalysts are placed in an oven at 60 °C and atmospheric pressure for 2 hours, then roasted on a moving belt at 500 °C using a forced air flow. The procedure for belt roasting catalysts which is used in General Procedures X and Y is described in M. M. Bhasin and G. H. Warner, "Silver Catalyst for the Manufacture of Ethylene Oxide and a Process for Preparing the Catalyst," U. S. Patent 4,419,276 to UCC&P. Hollow spheres are then ground to 30 to 60 mesh (U. S. Sieve Series) prior to evaluation or addition of other components. Components on silver catalysts in examples below are described by weight percent, based on the total catalyst weight.

Procedure Y

A 20 weight percent silver on an alpha aluminum oxide catalyst is made using the procedure described in M. M. Bhasin and G. H. Warner, "Silver Catalyst for the Manufacture of Ethylene Oxide and a Process for Preparing the Catalyst," U. S. Patent 4,419,276 to UCC&P. The silver oxide is available from either Ames Goldsmith Corporation, Glens Falls, New York, or Metz Metallurgical Co. Norton 5451 alpha aluminum oxide, 50 grams, Sample number 8883119, 30 to 60 mesh (U. S. Sieve Series) is used as support.

Procedure Z

A 16.9 weight percent silver/barium carbonate catalyst is made using Procedure Y except that barium carbonate is used instead of alpha aluminum oxide.

Examples

Procedure B ($BaCO_3$/MO Catalysts)

A 5 weight percent barium carbonate (3.5 weight percent barium) on alpha aluminum oxide catalyst (tested as 32-BKW-41) is prepared by the general procedure B set forth above using 0.75 grams of barium carbonate (from Johnson Matthey/AESAR Group, Seabrook, NH, Lot number S96252B, 99.997 weight percent) and 15 grams of alpha aluminum oxide (from Norton Company, Akron, OH, Sample number 8883118, Type SA

5451, B. E. T. surface area 0.27 square meters per gram). The catalyst particle size is 60 to 100 mesh (U. S. Sieve Series). Reactor D is used with 5.0 grams of catalyst.

A 5 weight percent barium carbonate (3.5 weight percent barium) on titanium dioxide catalyst (used in reaction 32-BKW-80) is prepared by the general procedure B set forth above using 0.3 grams of barium carbonate (from Johnson Matthey/AESAR Group, Seabrook, NH, Lot number S96252B, 99.997 weight percent) and 6.0 grams of titanium dioxide (from Johnson Matthey/AESAR Group, Seabrook, NH, Lot number S96579, 99.995 weight percent) except that 40 instead of 50 milliliters of water are used. The catalyst is calcined at 850 °C for 4 hours. The catalyst particle size is 60 to 100 mesh (U. S. Sieve Series).

Selected Silver Catalysts

Selected individual catalyst preparation procedures for silver catalysts follow. The first reference is that of the experiment testing the catalyst for methane coupling. The second reference (in parenthesis) is that of the catalyst preparation. Note that the percentages of components below are weight percentages based on the total catalyst weight. In Appendix D, weight percentages of metals are expressed as weight percent against 100 weight percent support (so they are higher, since the weight of the support is less than the weight of the total catalyst).

30-BKW-123 (30-BKW-115) A catalyst of 9 weight percent silver (calculated as elemental silver) on aluminum oxide is prepared by General Procedure X. Approximately 330.16 grams of catalyst are obtained.

34-BKW-32 (33-BKW-87) A catalyst of 20 weight percent silver (calculated as elemental silver) on aluminum oxide is prepared by General Procedure Y. Approximately 62.5 grams of catalyst are obtained. The catalyst particle size is 30 to 60 mesh (U. S. Sieve Series).

33-BKW-120 (33-BKW-119) A catalyst of 16.9 weight percent silver (calculated as elemental silver) on barium carbonate (from Johnson Matthey/AESAR Group, Seabrook, NH, Lot number S97090R, 99.997 weight percent) is prepared by General Procedure Z.

The catalyst is calcined at 800 °C for 4 hours. Approximately 18.82 grams of catalyst are obtained. The catalyst particle size is 30 to 60 mesh (U. S. Sieve Series).

34-BKW-6 (33-BKW-136A#1) A catalyst of 0.10 weight percent hydrated praseodymium nitrate (calculated as elemental praseodymium) and 20 weight percent silver on aluminum oxide is prepared by General Procedure Y followed by General Procedure A using 0.0185 grams of hydrated praseodymium nitrate (6 waters of hydration, from Johnson Matthey/AESAR Group, Seabrook, NH, Lot number 11240A, 99.99 weight percent) in 1.17 grams of deionized water and 6 grams of Catalyst VII. The catalyst is calcined at 800 °C for 4 hours. The catalyst particle size is 30 to 60 mesh (U. S. Sieve Series).

34-BKW-7 (33-BKW-136B#1) A catalyst of 0.01 weight percent hydrated praseodymium nitrate (calculated as elemental praseodymium) and 20 weight percent silver on aluminum oxide is prepared by General Procedure Y followed by General Procedure A using 0.00185 grams of hydrated praseodymium nitrate (6 waters of hydration, from Johnson Matthey/AESAR Group, Seabrook, NH, Lot number 11240A, 99.99 weight percent) in 1.17 grams of deionized water and 6 grams of Catalyst VII. The catalyst is calcined at 800 °C for 4 hours. The catalyst particle size is 30 to 60 mesh (U. S. Sieve Series).

34-BKW-10 (33-BKW-136C#1) A catalyst of 0.10 weight percent bismuth nitrate (calculated as elemental bismuth) and 20 weight percent silver on aluminum oxide is prepared by General Procedure Y followed by General Procedure A using 0.0139 grams of bismuth nitrate (from Johnson Matthey/AESAR Group, Seabrook, NH, Lot number S96494, 99.999 weight percent) in 2.17 grams of deionized water and 6 grams of Catalyst VII except that the solution is at a slightly elevated temperature such that it remains clear. The catalyst is calcined at 800 °C for 4 hours. The catalyst particle size is 30 to 60 mesh (U. S. Sieve Series).

34-BKW-11 (33-BKW-136D#1) A catalyst of 0.10 weight percent barium nitrate (calculated as elemental barium) and 20 weight percent silver on aluminum oxide is prepared by General Procedure Y followed by General Procedure A using 0.011 grams of barium nitrate (J. T. Baker Chemical Co., Phillipsburg, NJ, Lot number 43774, 99.3 weight percent) in 1.17 grams of deionized water and 6 grams of Catalyst VII. The catalyst is calcined at 800 °C for 4 hours. The catalyst particle size is 30 to 60 mesh (U. S. Sieve Series).

34-BKW-14 (33-BKW-136F#1) A catalyst of 1.0 weight percent barium nitrate (calculated as elemental barium) and 20 weight percent silver on aluminum oxide is prepared by General Procedure Y followed by General Procedure A using 0.11 grams of barium nitrate (J. T. Baker Chemical Co., Phillipsburg, NJ, Lot number 43774, 99.3 weight percent) in 1.17 grams of deionized water and 6 grams of Catalyst VII except that the solution is at a slightly elevated temperature such that it remains clear. The catalyst is calcined at 800 °C for 4 hours. The catalyst particle size is 30 to 60 mesh (U. S. Sieve Series).

34-BKW-15 (33-BKW-136I#1) A catalyst of 1.0 weight percent potassium nitrate (calculated as elemental potassium) and 20 weight percent silver on aluminum oxide is prepared by General Procedure Y followed by General Procedure A using 0.1551 grams of potassium nitrate (from Johnson Matthey/AESAR Group, Seabrook, NH, Lot number S95682, 99.999 weight percent) in 1.17 grams of deionized water and 6 grams of Catalyst VII. The catalyst is calcined at 800 °C for 4 hours. The catalyst particle size is 30 to 60 mesh (U. S. Sieve Series).

(34-BKW-23) A catalyst of 19 weight percent silver (calculated as elemental silver) on aluminum oxide is prepared by General Procedure Y. Approximately 61.89 grams of catalyst are obtained.

34-BKW-36 (34-BKW-24A#1) A catalyst of 3.5 weight percent barium chloride (calculated as elemental barium) and 18 weight percent silver on aluminum oxide is prepared by General Procedure Y followed by General Procedure A using 0.335 grams of barium chloride (from Johnson Matthey/AESAR Group, Seabrook, NH, Lot number S94730, 99.9999 weight percent) in 1.17 grams of deionized water and 6 grams of Catalyst XV. The catalyst is calcined at 800 °C for 4 hours. The catalyst particle size is 30 to 60 mesh (U. S. Sieve Series).

34-BKW-44 (34-BKW-24C#1) A catalyst of 3.4 weight percent barium chloride (calculated as elemental barium), 3.4 weight percent lanthanum oxide (calculated as elemental lanthanum) and 18 weight percent silver on aluminum oxide is prepared by General Procedure Y followed by General Procedure B using 0.335 grams of barium chloride (from Johnson Matthey/AESAR Group, Seabrook, NH, Lot number S94730, 99.9999 weight percent) and 0.262 grams of lanthanum oxide (from Johnson Matthey/

AESAR Group, Seabrook, NH, Lot number R3677, 99.99 weight percent) in 30 milliliters of deionized water and 6 grams of Catalyst XV. The catalyst is calcined at 800 °C for 4 hours. The catalyst particle size is 30 to 60 mesh (U. S. Sieve Series).

34-BKW-37 (34-BKW-24D#1) A catalyst of 3.5 weight percent barium chloride (calculated as elemental barium), 0.35 weight percent lanthanum oxide (calculated as elemental lanthanum) and 18 weight percent silver on aluminum oxide is prepared by General Procedure Y followed by General Procedure B using 0.335 grams of barium chloride (from Johnson Matthey/AESAR Group, Seabrook, NH, Lot number S94730, 99.9999 weight percent) and 0.0262 grams of lanthanum oxide (from Johnson Matthey/ AESAR Group, Seabrook, NH, Lot number R3677, 99.99 weight percent) in 30 milliliters of deionized and 6 grams of Catalyst XV. The catalyst is calcined at 800 °C for 4 hours. The catalyst particle size is 30 to 60 mesh (U. S. Sieve Series).

34-BKW-51 (34-BKW-41A#1) A catalyst of 4.1 weight percent barium chloride (calculated as elemental barium), 4.1 weight percent lanthanum oxide (calculated as elemental lanthanum) and 9 weight percent silver on aluminum oxide, Catalyst I, is prepared by General Procedure X followed by General Procedure B using 0.335 grams of barium chloride (from Johnson Matthey/AESAR Group, Seabrook, NH, Lot number S94730, 99.9999 weight percent) and 0.262 grams of lanthanum oxide (from Johnson Matthey/AESAR Group, Seabrook, NH, Lot number R3677, 99.999 weight percent) in 30 milliliters of deionized water and 6 grams of Catalyst I. The catalyst is calcined at 800 °C for 4 hours. The catalyst particle size is 30 to 60 mesh (U. S. Sieve Series).

34-BKW-50 (34-BKW-41B#1) A catalyst of 4.3 weight percent barium chloride (calculated as elemental barium) and 9 weight percent silver on aluminum oxide, Catalyst I, is prepared by General Procedure X followed by General Procedure A using 0.335 grams of barium chloride (from Johnson Matthey/AESAR Group, Seabrook, NH, Lot number S94730, 99.9999 weight percent) in 1.21 grams of deionized water and 6 grams of Catalyst I. The catalyst is calcined at 800 °C for 4 hours. The catalyst particle size is 30 to 60 mesh (U. S. Sieve Series).

34-BKW-45 (34-BKW-41C) A catalyst of 1.1 weight percent hydrated calcium chloride (calculated as elemental calcium) and 19 weight percent silver on aluminum oxide is prepared by General Procedure Y followed by General Procedure A using 0.353 grams of

hydrated calcium chloride (XH_2O waters of hydration, from Johnson Matthey/AESAR Group, Seabrook, NH, Lot number LV01629KV, 99.99+ weight percent) in 1.17 grams of deionized water and 6 grams of silver catalyst. The catalyst particle size is 30 to 60 mesh (U. S. Sieve Series).

Sources of Materials

Molecular Sieves

Elements contained in various molecular sieve catalysts tested include oxygen (O), aluminum (Al), phosphorus (P), cobalt (Co), magnesium (Mg), manganese (Mn), and/or silicon (Si). Abbreviations for these catalysts are followed by second abbreviations listing these elements in the Table below. All molecular sieves were powders. Catalysts were obtained from UCC&P's Molecular Sieves Department (prior to the formation of the joint venture UOP), and included:

29-BKW-142	MnAPSO-5	MnAlPSiO-5	U. S. Patent 4,686,092
29-BKW-143	CoAPSO-34	CoAlPSiO-34	U. S. Patent 4,744,970
29-BKW-146	MnAPSO-34	MnAlPSiO-34	U. S. Patent 4,686,092
29-BKW-147	MAPO-34	MgAlPO-34	U. S. Patent 4,567,029
29-BKW-151	CoAPSO-34	CoAlPO-34	U. S. Patent 4,567,029
30-BKW-66	AlPO4-5	AlPO4-5	U. S. Patent 4,310,440
30-BKW-67	SAPO-5	SiAlPO-5	U. S. Patent 4,440,871
30-BKW-80	MAPO-36	MgAlPO-36	U. S. Patent 4,567,029
30-BKW-95	highly acidic molecular sieve		

Metal Oxide Supports

Alpha-alumina supports were obtained from Norton, unless otherwise specified. Sample numbers are shown in tables in Appendix D, designating the type of alpha-alumina support. Metal oxides, unless specified, are also obtained from Johnson Matthey or AESAR, and are greater than 99.99% pure.

Magnesium oxide used for experiments conducted in 1988 was AESAR, 99.998% pure, with a water porosity of 6.21g H_2O/5g MgO powder. Although the magnesium oxide was a powder, the catalyst, derived from a dried paste, was sieved to the mesh indicated in Appendix D. Zirconium oxide, ZrO_2, was obtained from Johnson Matthey,

and was 99.9975% pure. MgO used in 32-BKW-134 and 135 was 3/16" pellets from Davison Chemicals.

Calcium oxide was 99.95% pure, phosphor grade from Johnson Matthey, lot #10923. Cerium oxide, CeO_2, was 99.99% pure, from Johnson Matthey, lot #R3843. Praseodymium oxide, Pr_6O_{11}, was 99.99% pure, from Johnson Matthey, lot #S70392, from Johnson Matthey. Zirconium oxide was from AESAR, lot #S96307. Zirconium oxide, ZrO_2, was obtained from Johnson Matthey, lot #S96307. Ga_2O_3 (36-BKW-21 and other reactions) was from JM, 99.999% pure, lot #S70392, and was sieved to 30/60 mesh. ZrO_2 (36-BKW-12, 13, 51 and other reactions) was from JM, 99.9975% pure, lot #S96307.

Silica supports used for reactions 32-BKW-110 and 111 were derived from Calsicat E-361P silica. This was washed with a warm oxalic acid solution to remove heavy metal impurities. The dried materials was sieved to 60 to 100 mesh. The surface area of the resulting materials was 95 m^2/g, and the pore volume was 1 cc/g.

Calcium aluminate, $CaAl_2O_4$, was lot #L28G, from Alfa, 99% pure. Magnesium aluminate, $MgAl_2O_4$, was prepared in another laboratory (55-WJB-101). Titania, TiO_2, was obtained from Johnson Matthey, lot #596579, 99.995% pure. Gallium oxide, Ga_2O_3, was obtained from Johnson Matthey, lot #570392, 99.999% pure.

Gamma-alumina used in 32-BKW-123 and 129 was SA6573, from Norton Co. The α-alumina samples used in 33-BKW-55 (SN:8855001), 33-BKW-55 (SN:8855011), 33-BKW-62 (SN:8855002), and 33-BKW-63 (SN:8855003) were obtained from Norton Co.

Norton TiO_2, sample number 88-55-004, 30/100 mesh, 0.6 m^2/g surface area, was used in catalysts for reactions 33-BKW-85 and 33-BKW-91 and for reactions with codes 30-BKW-XXX through 33-BKW-85 which used catalysts containing TiO_2. JM TiO_2, 30/60 mesh, 0.82 m^2/g surface area, lot #S96579, 99.995%, was used in catalysts for reactions 33-BKW-114 and 115 and 36-BKW-20, 26, 29, and 50

Catalyst Components

Alkaline earth salts and others salts, unless specified, were obtained from Johnson Matthey or AESAR, and are greater than 99.99% pure, unless specified. $BaCO_3$ was JM powder, 99.997% pure, lot #S96252B (for 33-BKW-85 and other reactions) and lot #S97090R for 33-BKW-91, 114, 115, 120, and 34-BKW-61 and 63. $SrCO_3$ was from

JM, 99.999% pure, lot #S96275. $BaCl_2$ was from JM (AESAR) that was used for all reactions except 33-BKW-81 was from lot #S94730, 99.999% pure.

Barium nitrate was from Baker, lot #43774, 99.3%. Bismuth nitrate was from JM (AESAR), 99.999% pure, lot #S96494. Potassium nitrate was from JM (AESAR), 99.999%. Praseodymium nitrate was from JM (AESAR), lot #11240A, 99.99% pure. Nickel chloride, $NiCl_2$, was obtained from AESAR, lot #S94654. Chromium chloride was obtained from AESAR, lot #16998. Gallium nitrate, $Ga(NO_3)_3 \cdot 6H_2O$ was obtained from Johnson Matthey, lot #S94730, 99.9999%. Alkaline earth salts were obtained from AESAR or Johnson Matthey, and were greater than 99.99% pure. Zirconium Chloride, $ZrCl_4$, was 99.5+% pure, from Johnson Matthey, lot #16965.

$SrCO_3$ was from JM, 99.999% pure, lot #S96275. The catalyst used in reaction 34-BKW-124 used BaO from JM, technical grade, powder, 88-94%, lot #16962. $SrCl_2$ for catalysts used in reactions 36-BKW-41 and 42 (and other reactions) was from JM, 99.9965% pure, lot #S94405. $Ba(OH)_2$ for the catalyst used in reaction 36-BKW-29 was Baker Analyzed Reagent $Ba(OH)_2 \cdot 8H_2O$, lot #514157.

KDC Laboratory

Low Temperature Catalysts

The low temperature catalysts were prepared using the general procedures given below.

Catalyst	Procedure	Dopant	Wt. % Dopant Based on Total Catalyst	Base Catalyst
1	KA	None	---	3 wt% $SrCl_2$/α-alumina
2	KD	$Pd(NO_3)_2$	0.66	11.6 wt% $SrCl_2$/α-alumina
3	KA & KB	$Co(NO_3)_2$	0.82	6.2 wt% $SrCl_2$/α-alumina
4	KA & KB	NiO	0.34	6.2 wt% $SrCl_2$/α-alumina
5	KA & KB	$FeCl_2$	0.56	6.2 wt% $SrCl_2$/α-alumina
6	KA & KB	$Cu(NO_3)_2$	0.53	6.2 wt% $SrCl_2$/α-alumina
7	KA & KB	$RhCl_3$	0.91	11.6 wt% $SrCl_2$/α-alumina
8	KC	$Co(NO_3)_2$	0.79	α-alumina

Procedure KA

The $SrCl_2$ is dissolved in just enough deionized water at room temperature to wet the α-alumina support (Norton Chemical SA-5402 30-60 mesh). The α-alumina support is added to the solution and mixed to assure total uptake of the liquid and even wetting of the alumina. The $SrCl_2$ and α-alumina support are provided in relative amounts to each other to provide the desired loading of alkaline earth metal component on the catalyst. The material is then dried in a vacuum oven at about 110 to 130 °C. Drying is usually complete in 4 to 6 hours; however, drying overnight does not effect performance. The catalyst is tested without further treatment.

Procedure KB

The selected transition metal component is dissolved in just enough deionized water at room temperature to wet the alkaline earth metal component/α-alumina catalyst prepared using procedure A. If the alkaline earth metal component is not soluble, dilute HCl solution is used as the dissolving media. The alkaline earth metal component/α-alumina catalyst is added to the solution and mixed to assure total uptake of the liquid and even wetting of the alumina. The transition metal component and alkaline earth metal component/α-alumina catalyst are provided in relative amounts to each other to provide the desired loading of transition metal component on the catalyst. The material is then dried in a vacuum oven at about 110 to 130 °C. Drying is usually complete in 4 to 6 hours; however, drying overnight does not effect performance. The catalyst is tested without further treatment.

Procedure KC

The selected transition metal component is dissolved in just enough deionized water at room temperature to wet the α-alumina support (Norton Chemical SA5402 30-60 mesh). The α-alumina support is added to the solution and mixed to assure total uptake of the liquid and even wetting of the alumina. The transition metal component and α-alumina support are provided in relative amounts to each other to provide the desired loading of transition metal component on the catalyst. The material is then dried in a vacuum oven at about 110 to 130 °C. Drying is usually complete in 4 to 6 hours; however, drying overnight does not effect performance. The catalyst is tested without further treatment.

Procedure KD

The $SrCl_2$ and noble metal component are dissolved in just enough deionized water at room temperature to wet the α-alumina support (Norton Chemical SA5402 30-60 mesh). The α-alumina support is added to the solution and mixed to assure total uptake of the liquid and even wetting of the alumina. The $SrCl_2$, noble metal component, and α-alumina support are provided in relative amounts to each other to provide the desired loading of $SrCl_2$ and noble metal component on the catalyst. The material is then dried in a vacuum oven at about 110 to 130 °C. Drying is usually complete in 4 to 6 hours; however, drying overnight does not effect performance. The catalyst is tested without further treatment.

Layered Perovskites

Preparations for the layered perovskite catalysts follow the procedure reported by J. Gopalakrishnan and V. Bhat[94].

Procedure KE

$K_2La_2Ti_3O_{10}$: A mixture of K_2CO_3, La_2O_3, and TiO_2 having the desired stoichiometric ratio was thoroughly ground in a mortar and placed in an alumina crucible. The mixture was heated in a muffle furnace in air at 800 °C for 4 hours then at 1000 °C for 4 hours. Then the mixture was cooled, an additional 20% excess of K_2CO_3 was added, the mixture was reground, and the mixture was heated once again in air at 800 °C for 4 hours then at 1000 °C for 4 hours. The resulting product was cooled, washed with deionized water (three times using 250 mL each time), and dried overnight in a vacuum oven at 130 °C.

Procedure KF

$K_2Nd_2Ti_3O_{10}$, $K_2Sm_2Ti_3O_{10}$, $K_2Dy_2Ti_3O_{10}$, $K_2Gd_2Ti_3O_{10}$, $K_2Pr_2Ti_3O_{10}$, and $K_2Ce_2Ti_3O_{10}$: All were prepared using the procedure for $K_2La_2Ti_3O_{10}$ with the corresponding lanthanide oxide substituted for La_2O_3.

Procedure KG

$Rb_2La_2Ti_3O_{10}$: Material was prepared using the procedure for $K_2La_2Ti_3O_{10}$ with Rb_2CO_3 substituted for K_2CO_3.

Procedure KH

$Na_2La_2Ti_3O_{10}$: 2 grams of $K_2La_2Ti_3O_{10}$ and 20 grams of $NaNO_3$ were mixed in an alumina crucible, covered, and heated in a muffle furnace at 300 °C for two days. The material was cooled, an additional 10 grams of $NaNO_3$ were added, and the mixture was heated again at 300 °C for 3 days. The resulting product was cooled, washed with deionized water until all nitrates were removed, and dried overnight in a vacuum oven at 130 °C.

Double Perovskites

Procedure KI

$LaCaMnCoO_6$: Preparation for the double perovskite catalyst follows the procedures reported by Maria Vallet-Regi, Ester Garcia, and José M. Gonzalez-Calbet[96] for double perovskites of the form $LaCaMnCoO_6$. Approximately 12.98g of $La(NO_3)_3$, 4.02g of $Co(NO_3)_2$, 7.36g of $CaCO_3$, and 4.60g of $MnCO_3$ are weighed into a 500 mL beaker containing a stirring bar and 100 mL of a saturated solution of citric acid is added with vigorous stirring. The solution is stirred until it is clear. Then, 53-60 mL ethylene glycol is added. The solution is then reduced in volume by evaporation. As the liquid evaporates the solution turns brown in color and becomes thick. If solids form at this point, 50 mL of the saturated citric acid solution are added. After evaporating to approximately 2/3 of the starting volume, the solution is placed in a vacuum oven at 130 °C for 8-15 hours. Then it is transferred to an alumina crucible and heated in a muffle furnace at 200 °C for 4-8 hours, 500-600 °C for 8-24 hours, and at 900-950 °C for 48-72 hours. Powder x-ray analysis of the resulting product agrees with patterns reported for $LaCaMnCoO_6$.

Procedure KJ

20 wt% Na_2CO_3/$LaCaMnCoO_6$: One part (usually 1g) by weight Na_2CO_3 and 4 parts (usually 4g) by weight $LaCaMnCoO_6$ are added to 150 mL deionized water. The mixture is evaporated with constant stirring to a thick paste. The resulting paste is then dried in vacuum oven at 110-130 °C. The resulting black solid is transferred to alumina crucibles and heated in a muffle furnace at 800 °C for approximately 24 hours. The resulting product was used without further treatment.

Procedure KK

24 wt% K_2CO_3/$LaCaMnCoO_6$; 15 wt% Li_2CO_3/$LaCaMnCoO_6$; 48 wt% Rb_2CO_3/$LaCaMnCoO_6$; and 51 wt% Cs_2CO_3-$LaCaMnCoO_6$: Catalysts were prepared using the same procedure given for 20 wt% Na_2CO_3/$LaCaMnCoO_6$ with the exceptions that the Rb_2CO_3/$LaCaMnCoO_6$ was only heated to 700 °C and the 51 wt% Cs_2CO_3/$LaCaMnCoO_6$ to 600 °C.

Other Preparations

Procedure KL

A high temperature migration technique was used to prepare some mixed oxides. Mixtures of metallic oxides, nitrates, and/or carbonates having the correct stoichiometric ratio of metals were ground to fine powders and placed in alumina crucibles. The crucibles were then heated in air at 900-1050 °C for 12 to 24 hours. The samples were then ground again, and the heating process was repeated. After three heating cycles, the samples were ground to powder and tested without further treatment.

Procedure KM

Literature catalysts reported as oxygen carriers, Pr-Ce oxides solid solution and Ag-Pr-Ce oxides solid solution, were prepared using a coprecipitation method. In the method, two aqueous solutions were used. Solution one consisted of nitrates of praseodymium, cerium, and silver (if desired) in amounts needed to give the desired composition. Solution two contained ammonium carbonate in an amount sufficient to precipitate all the metals as

carbonates. Solution one was then added dropwise to solution two with continuous stirring. The precipitate was separated by filtration and washed with deionized water. The solid was then dried in a vacuum oven at 110-130 °C and calcined at 750 °C for 2 hours.

Procedure KN

In a slurry technique, the required amounts of constituents needed to give the desired composition were added to 50-150 cc of distilled water. The mixture was evaporated with constant stirring until a thick slurry (paste) resulted. The paste was then dried in a vacuum oven at 110-130 °C.

Procedure KO

The oxide conducting material, $(Bi_2O_3)_{0.85}(La_2O_3)_{0.15}$, was prepared using a coprecipitation technique. In the technique, 50 mL of 10% HNO_3, 0.062 moles of $Bi(NO_3)_3 \cdot 5H_2O$, and 0.0109 moles of $La(NO_3)_3 \cdot 6H_2O$ were heated to 80 °C to dissolve the solids. Then the pH of the solution was adjusted from less than 1 to approximately 4 by the dropwise addition of concentrated NH_4OH. This resulted in the formation of a white solid. The liquid volume was reduced to about 20 cc by boiling and then dried in a vacuum oven. The resulting solid was calcined at 290 °C for 4 hours and 425 °C for 16 hours, ground to a fine powder, and calcined at 800 °C for 16 hours. The final product was a yellow solid.

Procedure KP

The V_2O_5/MgO catalyst was prepared by adding 16g of MgO to 1.03 liters of aqueous solution containing 0.5 wt% ammonium vanadate (NH_4VO_3) and 1 wt% ammonium hydroxide (NH_4OH) at 70 °C. The solution was evaporated to dryness at 70 °C using a purge of nitrogen. The resulting solid was calcined at 550 °C overnight.

Procedure KQ

Barium and strontium doped MgO were prepared by the slurry technique using a methanol/water mixture (11:1 volumetric ratio) as the dissolving media. Ion exchanging of Ba and Sr on MgO was carried out using the same solvent. In the ion-exchange process,

the MgO was mixed with the methanol/water solution containing the Ba or Sr for 2 hours and then filtered and washed with methanol. Materials were dried in a vacuum oven at 100-130 °C and calcined at 800 °C for 12-18 hours.

Procedure KR

A literature catalyst reported by ARCO, $Mn/Na_4P_2O_7$/silica, was prepared using an incipient wetness technique. In the incipient wetness procedure, the amounts of manganese acetate, $Mn(C_2H_3O_2)_2$, and sodium pyrophosphate, $Na_4P_2O_7$, required to give the desired metal and phosphorus loadings was dissolved in a quantity of distilled water necessary to just wet the silica (fill the void volume of the support). The silica was then added to the solution and thoroughly mixed to insure even wetting. The resulting material was dried in a vacuum oven at 110-130 °C overnight and then calcined at 800 °C for 16 hours.

Procedure KS

In an incipient wetness procedure, the amount of soluble dopant required to give the desired metal oxide loading was dissolved in a quantity of distilled water necessary to just wet the support (fill the void volume of the support). The support material was then added to the solution and thoroughly mixed to insure even wetting. The resulting material was dried in a vacuum oven at 110-130 °C.

Procedure KT

A literature catalyst reported by ARCO, $NaMnO_4/MgO$, was prepared using the reported preparation scheme.*

* (Sofranko, et al., *Petr. Div. Preprints*, **32**, 763 (1987).

Procedure KU

Doped mixed metal oxide catalysts were prepared by grinding to a fine powder the correct proportions of dopant (or dopant precursor) and mixed metal oxide necessary to give the desired dopant loading. The mixture was then heated to 800-900 °C for several hours and tested without further treatment.

NEK Laboratory

The barium chloride on alumina catalysts and most of the barium carbonate on alumina catalysts used in NEK's laboratory and reported herein were prepared by the slurry method described in Procedure B in the BKW laboratory section of this Appendix, above.

The barium acetate loaded catalyst was prepared by an incipient wetness method, in which the barium acetate was dissolved in sufficient distilled, deionized water to just wet the alumina support (i.e., fill the void volume), which was then added to the support and mixed to ensure wetting. This material was then dried for several hours at 80 °C, then at 110 °C, mixed and then calcined in air at 850°C for 4 hours. The barium hydroxide loaded catalyst was prepared by the same incipient wetness method, except that the barium hydroxide/water solution and the alumina support were heated to 80 °C prior to impregnation and the drying temperatures were 60 and 80 °C.

A third preparative method, called the dry mix method, was used for some of the barium carbonate loaded catalysts. It consisted of physically mixing the barium carbonate and alumina, and then calcining the mixture at 850 °C in air for 4 hours.

Appendix D. Catalyst Compositions and Preparation Procedures, BKW Laboratory

Ref. Run(Reactor #)	Catalyst	Wt. % Components	Moles/g Support	g/cc Catalyst	Mesh Prepared	Reference of Preparation	Date Run	Wt. % Metals	Preparation Procedure	g Support or * g Cat.
29-BKW-99(R#3)	NaCl / Al2O3, Norton SA 5551	3.85	0.000083	1.16	14/30	29-BKW-98A	3/30/88	1.57	A	30
29-BKW-101(R#4)	NaCl / Al2O3, Norton SA 5551	13.79	0.00274	1.16	14/30	29-BKW-98B	3/31/88	6.29	A	10
29-BKW-106(R#3)	KCl / Al2O3, Norton SA 5551	4.85	0.000084	1.16	14/30	29-BKW-77B	4/5/88	2.67	A	10
29-BKW-107(R#4)	CsCl / Al2O3, Norton SA 5551	7.06	0.000451	1.16	14/30	29-BKW-77D	4/5/88	5.99	A	10
29-BKW-110(R#3)	BaCl2 / Al2O3, Norton SA 5551	12.43	0.000682	1.16	14/30	29-BKW-77C	4/6/88	9.36	A#1	10
29-BKW-111(R#4)	LiCl / Al2O3, Norton SA 5551	2.82	0.000083	1.16	14/30	29-BKW-77E	4/6/88	0.47	A	10
29-BKW-114(R#3)	BaCl2 / Al2O3, Norton SA 5551	12.43	0.000682	1.16	14/30	29-BKW-77C	4/7/88	9.36	A#1	10
29-BKW-115(R#4)	LiCl / Al2O3, Norton SA 5551	2.82	0.000083	1.16	14/30	29-BKW-77E	4/7/88	0.47	A	10
29-BKW-118(R#3)	BaCl2 / Al2O3, Norton SA 5551	12.43	0.000683	1.16	14/30	29-BKW-120B	4/8/88	9.36	A#1	30
29-BKW-119(R#4)	NaCl / Al2O3, Norton SA 5551	3.85	0.000083	1.16	14/30	29-BKW-120A	4/8/88	1.57	A	30
29-BKW-124(R#3)	BaCl2 / Al2O3, Norton SA5551	1.41	0.0000086	1.16	14/30	29-BKW-121B	4/12/88	0.94	A	10
29-BKW-125(R#4)	BaCl2 / Al2O3, Norton SA5551	0.019	0.0000009	1.16	14/30	29-BKW-121D	4/12/88	0.0125	A	10
29-BKW-128(R#3)	BaCl2 / Al2O3, Norton SA5551	12.43	0.000682	1.16	14/30	29-BKW-121A	4/13/88	9.36	A#1	10
29-BKW-129(R#4)	BaCl2 / Al2O3, Norton SA5551	0.145	0.0000096	1.16	14/30	29-BKW-121C	4/13/88	0.095	A	10
29-BKW-132(R#3)	BaCl2 / Al2O3, Norton SA5551	1.41	0.0000086	1.16	100/140	29-BKW-131A	4/14/88	0.94	A	5
29-BKW-133(R#4)	BaCl2 / Al2O3, Aldrich	1.44	0.00007	1.16	100/140	29-BKW-131B	4/14/88	0.96	A	5
29-BKW-138(R#3)	BaCl2/ Al2O3, Norton SA5551	1.41	0.0000086	1.16	30/60	29-BKW-131C	4/15/88	0.94	A	10
29-BKW-142(R#3)	MnAPSO - 5			0.91	powder	10003-55-1-2C,SWK	4/18/88			
29-BKW-143(R#4)	CoAPSO - 34			0.5	powder	100058-5,SWK	4/18/88			
29-BKW-146(R#3)	MnAPSO - 34			0.56	powder	10024-61-1-3,SWK	4/19/88			
29-BKW-147(R#4)	MAPO - 34			0.71	powder	9688-68,SWK	4/19/88			
29-BKW-151(R#4)	CoAPO - 34			0.625	powder	9940-81,SWK	4/20/88			
29-BKW-152(R#3)	BaCl2/ Al2O3, Norton SA5551	1.41	0.0000086	1.16	30/60	29-BKW-131C	4/20/88	0.94	A	10
30-BKW-3(R#3)	BaCl2 / Al2O3, Norton SA5551	1.41	0.0000086	1.16	30/60	29-BKW-150A	4/21/88	0.94	A	10
30-BKW-5(R#4)	BaCl2 / Al2O3, Norton SA5551	1.41	0.0000086	1.16	60/100	29-BKW-150C	4/21/88	0.94	A	10
30-BKW-7(R#3)	BaCl2 / Al2O3, Norton SA5551	1.41	0.0000086	1.16	30/60	29-BKW-150B	4/22/88	0.94	A	10
30-BKW-9(R#4)	BaCl2 / Al2O3, Norton SA5551	1.41	0.0000086	1.16	30/60	29-BKW-150B	4/22/88	0.94	A	10
30-BKW-12(R#3)	BaCl2 / Al2O3, Norton SA3232	1.41	0.0000086	0.62	30/60	30-BKW-11A	4/27/88	0.94	A	10
30-BKW-13(R#4)	BaCl2 / Al2O3, Norton SA3235	1.41	0.0000086	0.66	30/60	30-BKW-11B	4/27/88	0.94	A	10
30-BKW-22(R#3)	BaCl2 / Al2O3, Norton SA5502	1.41	0.0000086	1.08	30/60	30-BKW-11C	4/28/88	0.94	A	10
30-BKW-23(R#4)	Pretzel "M" Salt (NaCl)	100		1.09		30-BKW-20	4/28/88			
30-BKW-28(R#3)	BaCl2 / Al2O3, Norton SA5551	1.41	0.0000086	1.16	140/200	29-BKW-150D	4/29/88	0.94	A	10
30-BKW-29(R#4)	NaCl / Al2O3, Norton SA5551	0.4	0.0000086	1.16	140/200	29-BKW-150E	4/29/88	0.158	A	10
30-BKW-36(R#3)	BaCl2 / Al2O3, Norton SA5551	1.41	0.0000086	1.16	60/100	29-BKW-150C	5/3/88	0.94	A	10
30-BKW-37(R#4)	BaCl2 / Al2O3, Norton SA5502	1.41	0.0000086	1.08	60/100	30-BKW-34A	5/3/88	0.94	A	5
30-BKW-44(R#3)	BaCl2 / Al2O3, Norton SA5551	0.146	0.000007	1.16	60/100	30-BKW-34C	5/6/88	0.096	A	5
30-BKW-45(R#4)	NaCl / Al2O3, Norton SA5551	0.4	0.0000083	1.16	60/100	30-BKW-34B	5/6/88	0.158	A	5
30-BKW-48(R#3)	Alberger Coarse Flake Salt (NaCl)	100		0.7		30-BKW-19	5/9/88			
30-BKW-52(R#3)	BaCl2 / Al2O3, Norton SA5551	5.033	0.00025	1.16	60/100	30-BKW-34F	5/10/88	3.5	A	10
30-BKW-53(R#4)	BaCl2 / Al2O3, Norton SA5551	0.507	0.0000245	1.16	60/100	30-BKW-34E	5/10/88	0.337	A	10
30-BKW-60(R#3)	BaCl2 / Al2O3, Norton SA5551	5.033	0.00025	1.16	30/60	30-BKW-34H	5/17/88	3.5	A	10
30-BKW-61(R#4)	BaCl2 / Al2O3, Norton SA5551	5.033	0.00025	1.16	30/60	30-BKW-34H	5/17/88	3.5	A	10
30-BKW-64(R#3)	RbCl / Al2O3, Norton SA5551	2.934	0.00025	1.16	30/60	30-BKW-34J	5/19/88	2.13	A	10
30-BKW-65(R#4)	CsCl / Al2O3, Norton SA5551	4.04	0.00025	1.16	30/60	30-BKW-34I	5/19/88	3.32	A	10
30-BKW-66(R#3)	AlPO4 - 5			0.31	powder	SWK	5/20/88		A	
30-BKW-67(R#4)	SAPO - 5			0.83	powder	SWK	5/20/88		A	
30-BKW-70(R#3)	LiCl / Al2O3, Norton SA5551	1.05	0.00025	1.16	30/60	30-BKW-68A	5/23/88	0.172	A	10
30-BKW-71(R#4)	CsCl / Al2O3, Norton SA5551	3.53	0.00025	1.16	30/60	30-BKW-68B	5/23/88	0.978	A	10
30-BKW-73(R#3)	KCl / Al2O3, Norton SA5551	1.31	0.00025	1.16	30/60	30-BKW-68B	5/24/88	0.178	A	10

Ref. Run(Reactor #)	Catalyst	Wt. % Components	Moles/g Support	g/cc Catalyst	Mesh Prepared	Reference of Preparation	Date Run	Wt. % Metals	Preparation Procedure	g Support or * g Cat.
30-BKW-74(R#4)	RbCl / Al2O3, Norton SA5551	2.934	0.00025	1.16	30/60	30-BKW-34J	5/24/88	2.13	A	10
30-BKW-80(R#4)	MAPO - 36			0.71	powder	10232-20,SWK	5/25/88		A	
30-BKW-83(R#3)	CsCl / Al2O3, Norton SA5551	4.04	0.00025	1.16	30/60	30-BKW-34I	5/26/88	3.32	A	10
30-BKW-86(R#3)	BaCl2 / ZrO2	5.033	0.00025	1.67	60/100	30-BKW-81A	5/27/88	3.5	A	10
30-BKW-87(R#4)	Ba3(PO4)2 / Al2O3, Norton SA5551	2.15	0.0000366	1.19	30/60	30-BKW-81B	5/27/88	1.5	A#2	5
30-BKW-93(R#4)	BaCl2 / Al2O3, Norton SA5502	5.033	0.000254	1.08	30/60	30-BKW-68D	6/2/88	3.5	A	5
30-BKW-95(R#3)	B(otf)3 / LZ10	7		0.33	powder	12957-19-3,SWK	6/3/88			
30-BKW-97(R#3)	BaCl2 / ZnO	5.033	0.00025	2.78	60/100	30-BKW-68E	6/6/88	3.5	A	10
30-BKW-100(R#3)	RbCl, BaCl2 / Al2O3, Norton SA5551	3.0689,5.033	262,0.000255	1.16	30/60	30-BKW-98A	6/7/88	2.24,3.32	A	5
30-BKW-101(R#4)	CsCl, BaCl2 / Al2O3, Norton SA5551	4.2237,5.033	262,0.000255	1.16	30/60	30-BKW-98B	6/7/88	3.48,3.32	A	5
30-BKW-106(R#3)	NaCl, BaCl2 / Al2O3, Norton SA5551	1.5089,5.033	262,0.000255	1.16	30/60	30-BKW-98C	6/8/88	0.602,3.32	A	5
30-BKW-107(R#4)	NaOH, BaCl2 / Al2O3, Norton SA5551	1.037,5.033	268,0.000255	1.16	30/60	30-BKW-98D	6/8/88	0.602,3.32	A	5
30-BKW-110(R#3)	KH2PO4, BaCl2 / Al2O3, Norton SA5551	3.419,5.033	0026,0.00025	1.16	30/60	30-BKW-98G	6/10/88	1.015,3.5	A	5
30-BKW-111(R#4)	KOH, BaCl2 / Al2O3, Norton SA5551	1.439,5.033	0026,0.00025	1.16	30/60	30-BKW-98F	6/10/88	1.015,3.5	A	5
30-BKW-118(R#3)	NaOH / Al2O3, Norton SA5551	1.037	0.00026	1.16	30/60	30-BKW-98H	6/14/88	0.606	A	5
30-BKW-119(R#4)	ZnCl2 / Al2O3, Norton SA5551	3.419	0.00026	1.16	30/60	30-BKW-98I	6/14/88	1.7	A	5
30-BKW-123(R#3)	Ag / Al2O3, Norton SA5502	9.13		1.14	cylindrical	30-BKW-115	6/16/88	10.05	X	300
30-BKW-129(R#4)	CaCl2.6H2O / Al2O3, Norton SA5551	5.267	0.000254	1.16	30/60	30-BKW-125A	6/20/88	1.016	A	5
30-BKW-132(R#3)	NaCl / Ga2O3	1.466	0.000254	1.25	30/60	30-BKW-125C	6/21/88	0.585	A	5
30-BKW-133(R#4)	BaCl2 / Ga2O3	5.033	0.000254	1.25	30/60	30-BKW-125B	6/21/88	3.5	A	5
30-BKW-134(R#3)	LiBO2 / Al2O3, Norton SA5502	1.244	0.000254	1.08	30/60	30-BKW-125E	6/22/88	0.172	B#1	5
30-BKW-135(R#4)	Li2B4O7 / Al2O3, Norton SA5502	4.123	0.000254	1.08	30/60	30-BKW-125F	6/22/88	0.353	B#1	5
30-BKW-136(R#4)	BaSO4 / Al2O3, Norton SA5502	5.607	0.000254	1.08	30/60	30-BKW-125D	6/22/88	3.5	B	5
31-BKW-1(R#3)	NaCl, Ag / Al2O3, Norton SA5502	1.5438,9.13	0.000268	1.08	30/60	30-BKW-122D	6/23/88	0.686,10.05	C(*) + A	(*5 g 30-BKW-115)
31-BKW-2(R#4)	BaCl2, Ag / Al2O3, Norton SA5502	5.285,9.13	0.000268	1.08	30/60	30-BKW-122C	6/23/88	4.08,10.05	C(*) + A	(*5 g 30-BKW-115)
31-BKW-7(R#3)	BaCl2 / Ga2O3	5.033	0.000254	1.25	60/100	30-BKW-125I	6/29/88	3.5	A	5
31-BKW-9(R#4)	KCl, Ag / Al2O3, Norton SA5502	1.96,9.13	0.000268	1.08	30/60	30-BKW-122A	6/29/88	1.17,10.05	C(*) + A	(*5 g 30-BKW-115)
31-BKW-11(R#3)	BaCl2 / SrCO3	5.033	0.000254		100/140	30-BKW-125G	7/1/88	3.5	A	3
31-BKW-13(R#4)	CaCl2.6H2O / Al2O3, Norton SA5502	5.267	0.000254	1.08	30/60	30-BKW-125H	7/1/88	1.016	A	5
31-BKW-16(R#3)	LiCl, Ag / Al2O3, Norton SA5502	1.125,9.13	0.000268	1.08	30/60	30-BKW-122B	7/5/88	0.207,10.05	C(*) + A	(*5 g 30-BKW-115)
31-BKW-17(R#4)	CsCl, Ag / Al2O3, Norton SA5502	4.319,9.13	0.000268	1.08	30/60	30-BKW-122E	7/15/88	3.96,10.05	C(*) + A	(*5 g 30-BKW-115)
31-BKW-20(R#3)	ZrCl4 / Al2O3, Norton SA5502	5.589	0.000254	1.16	30/60	31-BKW-15B	7/6/88	2.32	A	5
31-BKW-21(R#4)	CaCl2.6H2O/ZrO2	5.267	0.000254	1.67	30/60	31-BKW-15A	7/6/88	1.016	A	5
31-BKW-24(R#3)	BaCl2 / CaCO3	5.033	0.000254	1.22	140+	31-BKW-15C	7/7/88	3.5	A	5
31-BKW-25(R#4)	ZrO2	99.9975		1.67	30/60		7/7/88			
31-BKW-28(R#3)	SrCl2.6H2O / Al2O3, Norton SA5551	6.35	0.000254	1.16	30/60	31-BKW-26G	7/8/88	2.23	A	5
31-BKW-29(R#4)	(Citrate) BaCl2 / Al2O3, Norton SA5502	5.033	0.000254	1.08	30/60	31-BKW-26A	7/8/88	3.5	A#3	5
31-BKW-33(R#4)	CaCl2.6H2O / Al2O3, Norton SA5502	5.267	0.000254	1.08	60/100	31-BKW-26E	7/12/88	1.016	A#3	5
31-BKW-34(R#3)	BaCl2 / Al2O3, Norton SA5451	5.033	0.000254	1.09	60/100	31-BKW-26C	7/13/88	3.5	A#3	5
31-BKW-35(R#4)	BaCl2 / Al2O3, Norton SA5451	5.033	0.000254	1.09	30/60	31-BKW-26B	7/13/88	3.5	A#3	5
31-BKW-40(R#4)	CaCl2.6H2O / Ga2O3	5.267	0.000254	1.25	30/60	31-BKW-37A	7/14/88	1.016	A	5
31-BKW-41(R#3)	SrCl2.6H2O / Ga2O3	6.35	0.000254	1.25	30/60	31-BKW-37B	7/14/88	2.23	A	5
31-BKW-42(R#3)	CaCl2.6H2O / Al2O3, Norton SA5451	5.267	0.000254	1.09	60/100	31-BKW-37D	7/15/88	1.016	A	15
31-BKW-43(R#4)	CaCl2.6H2O / Al2O3, Norton SA5451	5.267	0.000254	1.09	30/60	31-BKW-37C	7/15/88	1.016	A	15
31-BKW-46(R#3)	BaCl2 / TiO2	5.033	0.000254	1.43	30/60	31-BKW-37E	7/18/88	3.5	A	5
31-BKW-47(R#4)	SrCl2.6H2O / Al2O3, Norton SA5451	6.35	0.000254	1.09	60/100	31-BKW-37F	7/18/88	2.23	A	5
31-BKW-52(R#3)	CaCl2.6H2O / Al2O3, Norton SA5451	5.267	0.000254	1.09	60/100	31-BKW-48B	7/20/88	1.016	A	15
31-BKW-53(R#4)	CaCl2.6H2O / Al2O3, Norton SA5451	5.267	0.000254	1.09	30/60	31-BKW-48A	7/20/88	1.016	A	15
31-BKW-58(R#3)	CaCl2.6H2O / Al2O3, Norton SA5502	5.267	0.000254	1.08	60/100	31-BKW-55A	7/25/88	1.016	A	10

Ref. Run(Reactor #)	Catalyst	Wt. % Components	Moles/g Support	g/cc Catalyst	Mesh Prepared	Reference of Preparation	Date Run	Wt. % Metals	Preparation Procedure	g Support or * g Cat.
31-BKW-59(R#4)	CaCl2.6H2O / Al2O3, Norton SA5502	5.267	0.000254	1.08	60/100	31-BKW-55A	7/25/88	1.016	A	10
31-BKW-62(R#3)	CaCl2.6H2O / MgO	5.267	0.000254	0.51	powder	31-BKW-48H	7/27/88	1.016	A#4	5
31-BKW-63(R#4)	CaCl2.6H2O / Al2O3, Norton SA5551	5.267	0.000254	1.16	60/100	31-BKW-55C	7/27/88	1.016	A	5
31-BKW-64(R#3)	CaCl2.6H2O / MgO	5.267	0.000254	0.51	powder	31-BKW-48H	7/27/88	1.016	A#4	5
31-BKW-66(R#3)	SrCl2.6H2O / MgO	6.35	0.000254	0.51	powder	31-BKW-48I	7/29/88	2.23	A#4	5
31-BKW-67(R#4)	BaCl2 / MgO	5.033	0.000254	0.51	powder	31-BKW-48G	7/29/88	3.5	A#4	5
31-BKW-76(R#3)	SrCl2 (dried 130 °C, 18 hrs)	99.9965		0.83	60/100		8/3/88			
31-BKW-77(R#4)	BaCl2 (dried 130 °C, 18 hrs)	99.9999		1.43	100/140		8/3/88			
31-BKW-83(R#3)	LiCl / MgO	1.063	0.000254	0.51	powder	31-BKW-80C	8/5/88	0.176	A#4	2
31-BKW-84(R#4)	Li2CO3 / MgO	0.9293	0.000127	0.51	powder	31-BKW-80A	8/5/88	0.177	B#2	5
31-BKW-86(R#3)	LaCl3 / Al2O3, Norton SA5451	5.874	0.000254	1.09	60/100	31-BKW-80K	8/9/88	3.53	A	5
31-BKW-87(R#4)	LaCl3 / Al2O3, Norton SA5451	5.874	0.000254	1.09	30/60	31-BKW-80J	8/9/88	3.53	A	5
31-BKW-92(R#3)	Ga2O3	99.999		1.25	30/60		8/11/88			
31-BKW-93(R#4)	TiO2	99.995		1.43	30/60		8/11/88			
31-BKW-96(R#3)	CaCl2.6H2O / TiO2	5.267	0.000254	1.43	30/60	31-BKW-55D	8/12/88	1.016	A	5
31-BKW-97(R#4)	SrCl2.6H2O / TiO2	6.35	0.000254	1.43	30/60	31-BKW-80F	8/12/88	2.23	A	5
31-BKW-102(R#3)	Ca(NO3)2.4H2O / Al2O3, Norton SA5502	5.66	0.000254	1.08	60/100	31-BKW-98A	8/16/88	1.024	A	5
31-BKW-103(R#4)	Ba(NO3)2.XH2O / Al2O3, Norton SA5502	6.23	0.000254	1.08	60/100	31-BKW-98B	8/16/88	3.49	A#5	5
31-BKW-112(R#3)	CeCl3.XH2O / Al2O3, Norton SA5451	5.89	0.000254	1.09	60/100	31-BKW-98C	8/19/88	3.56	A	5
31-BKW-113(R#4)	SrCl2.6H2O / CaO	6.35	0.000254	0.71	powder	31-BKW-80G	8/19/88	2.23	B#2	5
31-BKW-118(R#3)	SrCl2.6H2O / Al2O3, Norton SA5502	6.35	0.000254	1.08	60/100	31-BKW-55B	8/24/88	2.23	A	5
31-BKW-119(R#4)	BaCl2 / Al2O3, Norton SA5502	5.033	0.000254	1.08	60/100	31-BKW-26D	8/24/88	3.5	A#3	5
31-BKW-126(R#3)	SrCl2.6H2O / Al2O3, Norton SA5451 (800°C,1hr)	6.35	0.000254	1.09	60/100	31-BKW-122A	8/31/88	2.23	A(*)	* 5.3
31-BKW-127(R#4)	SrCl2.6H2O / Al2O3, Norton SA5451 (800°C,1hr)	3.279	0.000127	1.09	60/100	31-BKW-122B(#2)	8/31/88	1.114	A(*)	* 5.3
31-BKW-134(R#3)	SrCl2.6H2O / Al2O3, Norton SA5451 (800°C,1hr)	11.94	0.0005086	1.09	60/100	31-BKW-122H(#2)	9/6/88	4.45	A(*)	* 5.3
31-BKW-135(R#4)	SrCl2.6H2O / Al2O3, Norton SA5451 (900°C,1hr)	6.35	0.000254	1.09	60/100	31-BKW-122G	9/6/88	2.23	A(*)	* 6
32-BKW-1(R#3)	BaCl2 / CeO2	5.033	0.000254	2	powder	31-BKW-122E(#2)	9/15/88	3.5	A#4	2
32-BKW-2(R#4)	BaCl2 / Pr6O11	5.033	0.000254	1.67	powder	31-BKW-122F(#2)	9/15/88	3.5	A#4	2
32-BKW-6(R#3)	CeO2, Lot# R3843 (dried 130 °C)	99.99		2	powder	31-BKW-122E(#1)	9/20/88		F	2
32-BKW-7(R#4)	Pr6O11, Lot# R3485 (dried 130 °C)	99.99		1.67	powder	31-BKW-122F(#1)	9/20/88		F	2
32-BKW-12(R#3)	La,Nd nitrate (75/25) soln. / Al2O3, Norton SA5502	8.305,2.77		1.08	60/100	32-BKW-8A	9/23/88		A#6	5
32-BKW-13(R#4)	La,Nd nitrate (75/25) soln. / TiO2	7.33,2.436		1.22	60/100	32-BKW-8B	9/23/88		A#6	5
32-BKW-16(R#3)	MgCl2.6H2O / Al2O3, Norton SA5451	4.907	0.000254	1.09	60/100	31-BKW-98D	9/28/88	0.617	A#5	5
32-BKW-17(R#4)	SrCl2, Lot# S94313C (850 °C for 2 hours)	99.9965		1.28	60/100	31-BKW-122D(#2)	9/28/88		E(*)	* 5.8
32-BKW-22(R#3)	CrCl2 / Al2O3, Norton SA5451	3.03	0.000254	1.09	60/100	32-BKW-20B	9/30/88	1.32	A	10
32-BKW-23(R#4)	NiCl2.6H2O / Al2O3, Norton SA5451	5.7	0.000254	1.09	60/100	32-BKW-20A	9/30/88	1.492	A	10
32-BKW-28(R#3)	BaCl2 / CaAl2O4	5.024	0.000254	1.11	powder	32-BKW-20E	10/6/88	3.49	A#4	1
32-BKW-29(R#4)	CaAl2O4 (99% metal basis), (dried 130 °C)	99		1.11	powder	32-BKW-20C	10/6/88		F	1
32-BKW-36(R#3)	Ga(NO3)3.6H2O / Al2O3, Norton SA5451	6.1	0.000254	1.09	60/100	32-BKW-20F	10/11/88	1.768	A	5
32-BKW-37(R#4)	Ga(NO3)3.6H2O / MgO	6.1	0.000254	0.51	powder	32-BKW-20G	10/11/88	1.768	A#4	1
32-BKW-40(R#3)	SrCO3 / Al2O3, Norton SA5451	3.6	0.000254	1.09	60/100	32-BKW-20H	10/14/88	2.22	B	15
32-BKW-41(R#4)	BaCO3 / Al2O3, Norton SA5451	4.77	0.000254	1.09	60/100	32-BKW-20I	10/14/88	3.49	B	15
32-BKW-62(R#3)	BaCO3 / Al2O3, Norton SA5451(850 °C, 4hrs)	4.77	0.000254	1.09	60/100	32-BKW-20I(#1)	11/1/88	3.49	B(*)	(* 5 g of 32-BKW-20I)
32-BKW-63(R#4)	BaCO3 / Al2O3, Norton SA5451	4.77	0.000254	1.09	60/100	32-BKW-20I	11/1/88	3.49	B	15
32-BKW-80(R#3)	BaCO3 / TiO2 (850 °C, 4hrs)	4.76	0.000254	1.43	60/100	32-BKW-67A	11/22/88	3.49	B#3	6
32-BKW-81(R#4)	BaCO3 / Ga2O3 (850 °C, 4hrs)	4.76	0.000254	1.25	60/100	32-BKW-67B	11/22/88	3.49	B#3	6
32-BKW-94(R#3)	32-BKW-80(R#3) -- used catalyst						12/9/88			
32-BKW-105(R#3)	BaCl2 / MgAl2O4, 55-WJB-101 (850 °C, 2hrs)	5.02	0.000254	1.22	60/100	32-BKW-44G	12/16/88	3.49	A	5
32-BKW-110(R#3)	BaCl2 / SiO2, 55-WJB-100 (850 °C, 2hrs)	5.02	0.000254	0.45	60/100	32-BKW-106B	12/20/88	3.49	A	3

Ref. Run(Reactor #)	Catalyst	Wt. % Components	Moles/g Support	g/cc Catalyst	Mesh Prepared	Reference of Preparation	Date Run	Wt. % Metals	Preparation Procedure	g Support or * g Cat.
32-BKW-111(R#4)	BaCO3 / SiO2, 55-WJB-100 (850 °C, 2hrs)	4.77	0.000254	0.45	60/100	32-BKW-106A	12/20/88	3.48	B	3
32-BKW-116(R#3)	3BaO Al2O3 / Al2O3, Norton SA5451 (800 °C, 4hrs	4.53	0.000254	1.09	60/100	32-BKW-84A	12/27/88	3.48	G	10
32-BKW-117(R#4)	3BaO.Al2O3 (dried 850 °C, 4hrs)	99.99		0.71	powder	32-BKW-67C	12/27/88		F	10
32-BKW-120(R#4)	32-BKW-110(R#3) -- used catalyst						12/30/88			
32-BKW-122(R#3)	BaBr2.2H2O / Al2O3,Norton SA5451 (850 °C, 2hrs)	7.933	0.000254	1.09	60/100	32-BKW-118A	1/3/89	3.49	A	6
32-BKW-123(R#4)	gamma Al2O3, Norton SA6573	99.99		0.56	60/100		1/3/89			
32-BKW-128(R#3)	BaCO3 / ZrO2 (850 °C, 2hrs)	4.77	0.000254	2.63	60/100	32-BKW-118B	1/6/89	3.49	B	6
32-BKW-129(R#4)	BaCO3/gamma Al2O3,Norton SA6573 (850 °C, 2hrs	4.77	0.000254	0.63	60/100	32-BKW-118C	1/6/89	3.49	B	6
32-BKW-134(R#3)	Li2CO3 / MgO (600 °C, 12 hrs)	11.47	0.00175	0.5	30/60	32-BKW-132B	1/16/89	2.44	B#2(*)	(* 2.25 g of 32-BKW-132A)
32-BKW-135(R#4)	Li2CO3 / MgO (850 °C, 2 hrs)	11.47	0.00175	1	30/60	32-BKW-132C	1/16/89	2.44	B#2(*)	(* 2.25 g of 32-BKW-132A)
33-BKW-1(R#3)	BaCO3 / Al2O3, Norton SA5402 (600 °C, 16 hrs)	4.76	0.000254	1.14	60/100	32-BKW-132F(#1)	1/24/89	3.49	B#2(*)	(* 10 g of 32-BKW-132D)
33-BKW-2(R#4)	BaCO3 / Al2O3, Norton SA5402 (600 °C, 16 hrs)	29.87	0.00216	1.19	60/100	32-BKW-132G(#2)	1/24/89	29.65	B#2(*)	(* 10 g of 32-BKW-132E)
33-BKW-6(R#3)	BaCO3/Al2O3, SA5451 (600°C,14; 850°C,4)	4.76	0.000254	1.14	60/100	33-BKW-3A	1/27/89	3.49	B#2	6
33-BKW-7(R#4)	BaCO3/Al2O3, SA5451 (600°C,14; 850°C,4)	29.87	0.00216	1.11	60/100	33-BKW-3B	1/27/89	29.65	B#2	6
33-BKW-33(R#3)	MgAlOH hydrotalcite, 16341-93B-WTR (850 °C, 4)	100		0.366	60/100	33-BKW-15C	2/20/89		R	
33-BKW-34(R#4)	MgAlOH hydrotalcite, 16341-95B-WTR (850 °C, 4)	100		0.366	60/100	33-BKW-15D	2/20/89		R	
33-BKW-38(R#3)	BaF2 / Al2O3, Norton SA5451 (850 °C, 2 hrs)	4.26	0.000254	1.11	60/100	33-BKW-37A	2/23/89	3.49	A	6
33-BKW-39(R#4)	MgAlOH hydrotalcite, 16341-94B-WTR (850 °C, 4)	100		0.366	60/100	33-BKW-15E	2/23/89		R	
33-BKW-42(R#3)	BaCO3 / MgAlOH hydrotalcite, 93B (850 °C, 4 hrs)	4.76	0.000254	0.375	60/100	33-BKW-37B	2/28/89	3.49	R, B	3
33-BKW-43(R#4)	BaCO3 / MgAlOH hydrotalcite, 94B (850 °C, 4 hrs)	4.76	0.000254	0.375	60/100	33-BKW-37C	2/28/89	3.49	R, B	3
33-BKW-48(R#3)	BaCO3 / MgAlOH hydrotalcite, 95B (850 °C, 4 hrs)	4.76	0.000254	0.375	60/100	33-BKW-47A	3/3/89	3.49	R, B	3
33-BKW-49(R#4)	Ba(NO3)2 / Al2O3, Norton SA5451 (850 °C, 4 hrs)	6.22	0.000254	1.11	60/100	33-BKW-47B	3/3/89	3.49	B	6
33-BKW-54(R#3)	BaCl2 / Al2O3, SN:8855001 (850 °C, 2 hrs)	5.02	0.000254	1.22	18/60	33-BKW-51A	3/9/89	3.49	A	6
33-BKW-55(R#4)	BaCl2 / Al2O3, SN:8855011 (850 °C, 2 hrs)	5.02	0.000254	1.02	14/70	33-BKW-51D	3/9/89	3.49	A	6
33-BKW-62(R#3)	BaCl2 / Al2O3, SN:8855002 (850 °C, 2 hrs)	5.02	0.000254	0.98	18/60	33-BKW-51B	3/14/89	3.49	A	6
33-BKW-63(R#4)	BaCl2 / Al2O3, SN:8855003 (850 °C, 2 hrs)	5.02	0.000254	1.11	14/50	33-BKW-51C	3/14/89	3.49	A	6
33-BKW-66(R#3)	32-BKW-122(R#3) -- Used catalyst						3/17/89			
33-BKW-67(R#4)	BaCO3 / Al2O3, Norton SA5451 (850 °C, 4 hrs)	4.77	0.000254	1.16	60/100	33-BKW-64A(#1)	3/17/89	3.49	B(*)	(* 6 g of 33-BKW-64A)
33-BKW-74(R#3)	BaCO3 / Al2O3, Norton SA5451 (850 °C, 4 hrs)	4.77	0.000254	1.16	60/100	33-BKW-64A(#2)	3/22/89	3.49	B(*)	(* 6 g of 33-BKW-64A)
33-BKW-75(R#4)	BaCO3 (850 °C, 2 hrs)	99.997		1.16	40/100	33-BKW-15B	3/22/89		P	
33-BKW-81(R#4)	BaCl2 / Al2O3, Norton SA5451 (850 °C, 4hrs)	5.033	0.000254	1.11	60/100	33-BKW-79A	3/30/89	3.5	A(*)	(* 6 g of 31-BKW-48F)
33-BKW-85(R#4)	BaCO3 / TiO2, Norton 88-55-004 (850 °C, 4 hrs)	4.77	0.000254	1.32	30/100	33-BKW-79B(#1)	4/4/89	3.49	B#4(*)	(* 24 g of 33-BKW-79B)
33-BKW-91(R#3)	BaCO3 / TiO2, Norton 88-55-004 (850 °C, 4 hrs)	16.7	0.001	1.32	30/100	33-BKW-79C(#1)	4/18/89	13.95	B#4(*)	(* 24 g of 33-BKW-79C)
33-BKW-101(R#4)	33-BKW-85(R#4) -- Used catalyst						4/18/89			
33-BKW-114(R#3)	BaCO3 / TiO2 (850 °C, 4 hrs)	16.7	0.001	1.61	30/60	33-BKW-107B	4/28/89	13.95	B#3	18
33-BKW-115(R#4)	BaCO3 / TiO2 (850 °C, 4 hrs)	4.77	0.000254	1.61	30/60	33-BKW-107A	4/28/89	3.49	B#3	18
33-BKW-120(R#3)	Ag / BaCO3 (800 °C, 4 hrs)	16.9		1.22	30/60	33-BKW-119	5/5/89	20.33	Z	15.64
33-BKW-121(R#4)	50/50 BaCl2 / BaCO3 mixture (850 °C, 2 hrs)	99.999,99.997		2.375	30/100	33-BKW-15A	5/5/89	B#2 (melted when calcined)		
34-BKW-1(R#3)	32-BKW-63(R#4) -- used catalyst			1.33	60/100		5/16/89			
34-BKW-2(R#4)	32-BKW-63(R#4) -- used catalyst			1.33	60/100		5/16/89			
34-BKW-6(R#3)	Pr(NO3)3, Ag / Al2O3, SA5451 (800 °C, 4 hrs)	0.307,20	0.000007	1.22	30/60	33-BKW-136A(#1)	5/19/89	0.133,25.0	Y + A	(* 6 g of 33-BKW-87)
34-BKW-7(R#4)	Pr(NO3)3, Ag / Al2O3, SA5451 (800 °C, 4 hrs)	0.031,20	0.0000007	1.22	30/60	33-BKW-136B(#1)	5/19/89	0.013,25.0	Y + A	(* 6 g of 33-BKW-87)
34-BKW-10(R#3)	Bi(NO3)3, Ag / Al2O3, SA5451 (800 °C, 4 hrs)	0.23,20	0.0000047	1.22	30/60	33-BKW-136C(#1)	5/23/89	0.133,25.0	Y + A#5	(* 6 g of 33-BKW-87)
34-BKW-11(R#4)	Ba(NO3)2, Ag / Al2O3, SA5451 (800 °C, 4 hrs)	0.19,20	0.0000072	1.22	30/60	33-BKW-136D(#1)	5/23/89	0.133,25.0	Y + A	(* 6 g of 33-BKW-87)
34-BKW-14(R#3)	Ba(NO3)2, Ag / Al2O3, SA5451 (800 °C, 4 hrs)	1.87,20	0.0000728	1.22	30/60	33-BKW-136F(#1)	5/25/89	1.36,25.0	Y + A#5	(* 6 g of 33-BKW-87)
34-BKW-15(R#4)	KNO3, Ag / Al2O3, SA5451 (800 °C, 4 hrs)	2.52,20	0.000255	1.22	30/60	33-BKW-136I(#1)	5/25/89	1.366,25.0	Y + A	(* 6 g of 33-BKW-87)
34-BKW-18(R#3)	SrCO3 / Al2O3, Norton SA5451 (850 °C, 4 hrs)	6.97	0.000508	1.25	60/100	34-BKW-16A(#1)	5/26/89	4.45	B(*)	(* 6 g of 34-BKW-16A)
34-BKW-19(R#4)	SrCl2.6H2O / Al2O3, SA5451 (850 °C, 4 hrs)	11.94	0.0005086	1.14	60/100	34-BKW-16B	5/26/89	4.45	A(*)	(* 6 g of 31-BKW-122H#1)
34-BKW-32(R#3)	Ag / Al2O3, Norton SA5451 (800 °C, 4 hrs)	20		1.22	30/60	33-BKW-87A	6/16/89	25	Y	(* 5 g of 33-BKW-87)

Ref. Run(Reactor #)	Catalyst	Wt. % Components	Moles/g Support	g/cc Catalyst	Mesh Prepared	Reference of Preparation	Date Run	Wt. % Metals	Preparation Procedure	g Support or * g Cat.
34-BKW-36(R#3)	BaCl2, Ag / Al2O3, SA5451 (800 °C, 4hrs)	5.29,19.2	0.000268	1.32	30/60	34-BKW-24A(#1)	6/21/89	4.83,23.76	Y + A	(* 6 g of 34-BKW-23)
34-BKW-37(R#4)	BaCl2, La2O3, Ag / Al2O3, SA5451 (800 °C, 4 hrs)	5.29,0.43,19.2	68,0.0000134	1.32	30/60	34-BKW-24D(#1)	6/21/89	4.83,0.485,23.76	Y + B#1	(* 6 g of 34-BKW-23)
34-BKW-44(R#3)	BaCl2, La2O3, Ag / Al2O3, SA5451 (800 °C, 4 hrs)	5.29,4.18,19.2	268,0.000134	1.32	30/60	34-BKW-24C(#1)	6/23/89	4.84,4.91,23.76	Y + B#1	(* 6 g of 34-BKW-23)
34-BKW-45(R#4)	CaCl2.XH2O, Ag / Al2O3, Norton SA5451	5.56,19.2	0.000268	1.32	30/60	34-BKW-41C	6/23/89	1.411,23.76	Y + A	(* 6 g of 34-BKW-23)
34-BKW-50(R#3)	BaCl2, Ag / Al2O3, SA5502 (800 °C, 4 hrs)	5.29,9.13	0.000268	1.22	30/60	34-BKW-41B(#1)	6/26/89	4.90,10.05	X + A	(* 6 g of 30-BKW-115)
34-BKW-51(R#4)	BaCl2, La2O3, Ag / Al2O3, SA5502 (800 °C, 4 hrs)	5.29,4.18,9.13	268,0.000134	1.22	30/60	34-BKW-41A(#1)	6/26/89	4.91,4.96,10.05	X + B#1	(* 6 g of 30-BKW-115)
34-BKW-59(R#3)	SrCO3 / Al2O3, SA5451 (850 °C, 4 hrs)	6.97	0.000508	1.25	30/60	34-BKW-57A(#1)	7/7/89	4.45	B#3(*)	(* 3.5 g of 34-BKW-57A)
34-BKW-61(R#4)	BaCO3 / Al2O3, SA5451 (850 °C, 4 hrs)	9.107	0.000508	1.25	30/60	34-BKW-57B(#1)	7/7/89	6.98	B#3(*)	(* 3.5 g of 34-BKW-57B)
34-BKW-63(R#3)	BaCO3 / Al2O3, SA5451 (850 °C, 4 hrs)	9.107	0.000508	1.25	30/60	34-BKW-57B(#2)	7/11/89	6.98	B#3(*)	(* 6 g of 34-BKW-57B)
34-BKW-124(R#3)	BaO/Al2O3, Norton SA5451 (850 °C, 4 hrs)	3.74	0.000253	1.16	60/100	34-BKW-122D	10/20/89		B	7.5
34-BKW-125(R#4)	BaCO3/Al2O3, Norton SA5451 (850 °C, 4 hrs)	4.77	0.000253	1.16	60/100	34-BKW-122A	10/20/89		B	7.5
34-BKW-128(R#3)	BaCO3/Al2O3, SN:8855002 (850 °C, 4 hrs)	4.77	0.000253	1.09	18/60	34-BKW-127A	10/26/89		B	7.5
34-BKW-129(R#4)	BaCO3/Al2O3, SN:8855003 (850 °C, 4)	4.77	0.000253	1.28	14/50	34-BKW-122C	10/26/89		B	7.5
36-BKW-2(R#3)	BaCO3/Al2O3, Norton SA5502 (850 °C, 4)	25	0.001693	1.25	30/60	36-BKW-1A	11/2/89		B	7.5
36-BKW-3(R#4)	BaCO3/Al2O3, Norton SA5502 (850 °C, 4)	4.77	0.000253	1.25	30/60	36-BKW-122B	11/2/89		B	7.5
36-BKW-12(R#3)	BaCO3/ZrO2 (850 °C, 4)	15.06	0.000899	1.92	30/60	36-BKW-4C	11/9/89		B	7.5
36-BKW-13(R#4)	BaCO3/ZrO2 (850 °C, 4)	4.77	0.000253	2.17	30/60	36-BKW-4B	11/9/89		B	7.5
36-BKW-20	BaCO3/TiO2 30/60 (850 °C, 4)	9.11	0.000483	1.61	30/60	34-BKW-57-D#1	11/15/89		B	10
36-BKW-21	BaCO3/Ga2O3 (850 °C, 4)	4.77	0.000253	1.22	60/100	36-BKW-4A	11/15/89		B	7.5
36-BKW-26	SrCO3/TiO2 30/60 (850 °C, 4)	6.94	0.000253	1.56	30/60	34-BKW-57-C#1	11/20/89		B	10
36-BKW-29	Ba(OH)2•8H2O/TiO2 60/100 (850 °C, 4)	7.419	0.000254	1.43	60/100	36-BKW-28A	11/22/89		A	6*
36-BKW-41	SrCl2/Ag/Al2O3 5502 30/60	16.9, 9.1		1.39	30/60	36-BKW-35A	11/28/89		A*	*5g of 30-BKW-115
36-BKW-42	SrCl2/Ag/Al2O3 5502 60/100	6.34, 9.1		1.22	60/100	36-BKW-35B	11/28/89		X, A*	*5g of 30-BKW-115
36-BKW-46	BaO(JM Tech Grade) 30/60 (850 °C, 4)	100		2.38	powder	36-BKW-43A	11/30/89		H	25.35
36-BKW-47	Ba(OH)2•8H2O 30/60 (850 °C, 4)	100		2.08		36-BKW-15#1	11/30/89		I	
36-BKW-50	BaCO3/TiO2 (used 36-BKW-20)	9.1	0.000483	1.61	30/60	34-BKW-57C#1	12/4/89			
36-BKW-51	BaCO3/ZrO2 (used 36-BKW-13)	25	0.000169	2.17	30/60	36-BKW-4B	12/4/89			
A.) The loading of the catalyst is expressed as wt.% metal against 100 wt.% support (e.g. Al2O3, Ga2O3).										
B.) Mesh size shown refers to the mesh size of the catalyst when prepared and is not necessarily that which was run.										
C.) Refer to the Experimental Section (Appendix B) and Appendix C, Catalyst Preparation Procedures.										
E.) Grams/cc shown refers to the measured grams/cc of catalyst at the beginning of each run and after catalyst preparation.										
F.) Listed below are catalyst preparations referred to in the last column in some cases.										
	Li2CO3 / MgO (B. Bartley, 3/16 pellets)	11.47	0.00175		30/60	32-BKW-132A		2.44	B#2	5
	BaCO3 / Al2O3, Norton SA5402	4.76	0.000254		30/100	32-BKW-132D		3.49	B#2	12
	BaCO3 / Al2O3, Norton SA5402	29.87	0.00216		30/100	32-BKW-132E		29.65	B#2	12
	BaCO3 / Al2O3, Norton SA5451	4.77	0.000254		60/100	33-BKW-64A		3.49	B	15
	BaCl2 / Al2O3, Norton SA5451	5.033	0.000254	1.09	60/100	31-BKW-48F		3.5	A	15
	SrCl2.6H2O / Al2O3, Norton SA5451	11.94	0.0005086	1.09	60/100	31-BKW-122H(#1)		4.45	A	15
	BaCO3 / TiO2, SN:88-55-004	4.77	0.000254		30/100	33-BKW-79B		3.49	B#4	24
	Ag / Al2O3, Norton SA5451	20		1.28	30/60	33-BKW-87		25	Y	50
	Ag / Al2O3, Norton SA5451	19.2		1.28	30/60	34-BKW-23		23.76	Y	50

Appendix E. Catalyst Compositions and Preparation Procedures, KDC Laboratory

Catalyst Prep. Notebook Number	Preparation Method	Catalyst Components by Total Weight %	Catalyst Evaluation Notebook Numbers
1-KDC-X-8	KS	16.7% NaCl/alpha-alumina	1-KDC-X-9
1-KDC-X-14	KN	18% KNO3/BaCO3	1-KDC-X-16
			1-KDC-X-18
1-KDC-X-15	KN	16% NaNO3/BaCO3	1-KDC-X-22
1-KDC-X-33	KN	10% NaNO3/Nd2O3	1-KDC-X-38
			1-KDC-X-36
			1-KDC-X-46
			1-KDC-X-50
1-KDC-X-32	KN	8.3% LiNO3/Nd2O3	1-KDC-X-72
1-KDC-X-48	KN	10.9% Na2CO3/ 10.9% K2CO3/Nd2O3	1-KDC-X-52
			1-KDC-X-54
			1-KDC-X-64
1-KDC-X-49	KS	4.76%NaCl/alpha alumina	1-KDC-X-58
			1-KDC-X-60
			1-KDC-X-62
			1-KDC-X-80
1-KDC-X-56	KS	5% NaCl/silica	1-KDC-X-91
			1-KDC-X-92
1-KDC-X-57	KS	6% KCl/alpha alumina	1-KDC-X-87
			1-KDC-X-89
			1-KDC-X-98
1-KDC-X-82	KS	6.57% NaNO3/alpha alumina	1-KDC-X-83
			1-KDC-X-85
1-KDC-X-95	KL	BaPbO3	
1-KDC-X-96	KL	SrPbO3	
1-KDC-X-97	KS	5% NaCl/ gamma alumina	1-KDC-X-104
			1-KDC-X-110
1-KDC-X-109	KS	6.1% KCl/alpha alumina	1-KDC-X-115
1-KDC-X-112	KS	3.6% LiCl/alpha alumina	1-KDC-X-120
			1-KDC-X-122
1-KDC-X-113	KL	BaPbO3	1-KDC-X-130
1-KDC-X-114	KL	SrPbO3	1-KDC-X-126
			2-KDC-X-50
1-KDC-X-114	KL	SrPbO3	1-KDC-X-50
1-KDC-X-132	KS	3.9% CsCl/alpha alumina	1-KDC-X-133
2-KDC-X-72	KS	3.8% LaCl3/1.1% NaCl/ alpha alumina	2-KDC-X-77
2-KDC-X-68	KS	0.1% NaCl/5.0% LaCl3/ alpha alumina	2-KDC-X70
3-KDC-X-45	KE	K2La2Ti3O10	3-KDC-X-53
			3-KDC-X-69
			4-KDC-X-7
			4-KDC-X-88
3-KDC-X-46	KU	10% K2CO3/LaMnO3	3-KDC-X-61
3-KDC-X-51	KN	10% K2CO3/La[Mn.5Rh.5]O3	3-KDC-X-66
3-KDC-X-52	KN	10%K2CO3/KNbO(3-X)	
3 KDC-X-74	KL	K2La2Mn3O10	3-KDC-X-79
3-KDC-X-86	KE	K2La2Ti3O10	3-KDC-X-92
			4-KDC-X-15
3-KDC-X-87	KE	K2Sm2Ti3O10	3-KDC-X-96
3-KDC-X-88	KE	K2Nd2Ti3O10	3-KDC-X-89
3-KDC-X-95	KI	LaCaMnCoO6	3-KDC-X-103
3-KDC-X-112	KS	5% La2O3/alpha alumina (5551)	3-KDC-X-118
			4-KDC-X-49
3-KDC-X-113	KS	5% La(NO3)3/3.6% KNO3/alpha alumina (5551)	3-KDC-X-128
3-KDC-X-127	KI	LaCaMnCoO6	3-KDC-X-132
3-KDC-X-136	KU	10% K2CO3/LaFeO3	4-KDC-X-3

Catalyst Prep. Notebook Number	Preparation Method	Catalyst Components by Total Weight %	Catalyst Evaluation Notebook Numbers
4-KDC-X-14	KG	Rb2La2Ti3O10	4-KDC-X-23 4-KDC-X-36
4-KDC-X-22	KH	Na2La2Ti3O10	4-KDC-X-29
4-KDC-X-35	KN	10% K2CO3/ La2O3	4-KDC-X-41
5-KDC-X-1	KF	K2Dy2Ti301	4-KDC-X-66
5-KDC-X-2	KF	K2Gd2Ti3O10	4-KDC-X-70
5-KDC-X-3	KE	K2La2Ti3O10	6-KDC-X-10 6-KDC-X-29 7-KDC-X-10 7-KDC-X-30 8-KDC-X-15
5-KDC-X-4	KN	1.8% Li2CO3/ 1%Pt/alumina	
5-KDC-X-5	KN	3.35% Li2CO3/1%Pd/alumina	7-KDC-X-1
5-KDC-X-6	KN	1.3% Na2CO3/1%Pt/alumina	6-KDC-X-4
5-KDC-X-7	KN	3.3% Na2CO3/1%Pd/alumina	7-KDC-X-4
5-KDC-X-8	KN	21.7% Li2CO3/1%Pd/alumina	7-KDC-X-7
5-KDC-X-9	KN	21.7% Li2CO3/1%Pt/alumina	6-KDC-X-1 6-KDC-X-7
5-KDC-X-10	KN	35.5% Na2CO3/5% Pt/CaCO3	6-KDC-X-19
5-KDC-X-11	KN	35.5% Na2CO3/5%Pd/CaCO3	7-KDC-X-20
5-KDC-X-12	KS	0.71% Pd(NO3)2/10.7% SrCl2/alpha alumina (5402)	6-KDC-X-23
5-KDC-X-13	KS	0.71% Pd(NO3)2/10.7% SrCl2/alpha alumina (5451)	7-KDC-X-24
5-KDC-X-14	KI	LaCaMnCoO6	6-KDC-X-57
5-KDC-X-15	KT	11.1% NaMnO4/MgO	7-KDC-X-44 7-KDC-X-60
5-KDC-X-16	KS	0.52%Pd(NO3)2/10.7% SrCl2/alpha alumina (5402)	7-KDC-X-42
5-KDC-X-17	KI	LaCaMnCoO6	
5-KDC-X-18	KS	0.70% Pd(NO3)2/10% Ba(NO3)2/alpha alumina (5402)	6-KDC-X-47
5-KDC-X-19	KS	0.70% Pd(NO3)2/10.7% SrCl2/alpha alumina (5402)	7-KDC-X-51
5-KDC-X-20	KN	3% NaNO3/11.3% La(NO3)3/BaTiO3	6-KDC-X-53
5-KDC-X-21	KN	3.5% KNO3/11.3% La(NO3)3/BaTiO3	6-KDC-X-59 7-KDC-X-57
5-KDC-X-22	KR	34.5% Mn(CH3CO2)2/2.7% Na4P2O7/silica	6-KDC-X-63 6-KDC-X-61
5-KDC-X-23	KS	11.6% SrCl2/alpha alumina (5402)	7-KDC-X-23 11-KDC-X-91
5-KDC-X-24	KS	5.75% SrCl2/alpha alumina (5402)	7-KDC-X-24 12-KDC-X-40
5-KDC-X-25	KS	0.66% Pd(NO3)2/11.6% SrCl2/alpha alumina (5402)	6-KDC-X-65 8-KDC-X-60 9-KDC-X-95
5-KDC-X-26	KS	0.66% Pd(NO3)2/5.75% SrCl2/alpha alumina (5402)	6-KDC-X-84
5-KDC-X-27	KF	K2Ce2Ti3O10	6-KDC-X-75 7-KDC-X-83
5-KDC-X-28	KF	K2Pr2Ti3O10	6-KDC-X=81 7-KDC-X-77
5-KDC-X-29	KS	0.52% Pd(CH3CO2)2/11.6% SrCl2/alpha alumina (5402)	6-KDC-X-71
5-KDC-X-30	KS	0.52%Pd(CH3CO2)2/5.75% SrCl2/alpha alumina (5402)	7-KDC-X-73
5-KDC-X-31	KS	0.66% Pd(NO3)2/alpha alumina (5402)	
5-KDC-X-32	KI	LaCaMnCoO6	
5-KDC-X-33	KN	20% Na2CO3/K2La2Ti3O10	7-KDC-X-81
5-KDC-X-34	KJ	20% Na2CO3/ LaCaMnCoO6	6-KDC-X-79 8-KDC-X-57
5-KDC-X-35	KE	K2La2Ti3O10	6-KDC-X-90
5-KDC-X-36	KN	20% Na2CO3/K2La2Ti3O10	7-KDC-X-92
5-KDC-X-37	KJ	20% Na2CO3/ LaCaMnCoO6	6-KDC-X-95 12-KDC-X-67
5-KDC-X-39	KN	39.7% Li2CO3/K2La2Ti3O10	7-KDC-X-95

Catalyst Prep. Notebook Number	Preparation Method	Catalyst Components by Total Weight %	Catalyst Evaluation Notebook Numbers
5-KDC-X-40	KN	K2CO3/La2O3/TiO2 (molar ratio 2/2/3)	6-KDC-X-93
5-KDC-X-41	KN	36.2% K2CO3/K2La2Ti3O10	6-KDC-X-98
			6-KDC-X-129
5-KDC-X-42	KR	34.5% Mn(CH3CO2)2/2.7% Na4P2O7/silica	6-KDC-X-106
			7-KDC-X-108
			8-KDC-X-57
5-KDC-X-43	KI	LaCaMnCoO6	
5-KDC-X-45	KN	9.3% Sr(OH)2/Na4P2O7	7-KDC-X-115
			7-KDC-X-119
5-KDC-X-47	KN	K2CO3/La2O3/TiO2 (molar ratio 2/2/3)	7-KDC-X-123
5-KDC-X-48	KN	K2CO3/La2O3 (molar ratio 2/2)	6-KDC-X-113
			9-KDC-X-19
			9-KDC-X-28
5-KDC-X-49	KI	LaCaMnCoO6	6-KDC-X-115
			7-KDC-X-125
5-KDC-X-50	KL	K2Tb2Ti3O10	6-KDC-X-119
5-KDC-X-51	KL	K2[CaMn]Ti3O10	7-KDC-X-133
5-KDC-X-52	KI	LaCaMnCoO6	
5-KDC-X-53	KN	23.4% H3BO3/MgO	7-KDC-X-136
5-KDC-X-54	KN	30.8% H3BO3/Na4P2O7	
5-KDC-X-55	KN	10% H3BO3/Li4SiO4	6-KDC-X-122
			6-KDC-X-126
5-KDC-X-56	KK	24.4% K2CO3/LaCaMnCoO6	
5-KDC-X-57A	KQ	0.65% Ba(NO3)2/MgO	9-KDC-X-4
5-KDC-X-57B	KQ	Ba(NO3)2 (ion-exchange)/MgO	9-KDC-X-9
5-KDC-X-59A	KQ	0.53% Sr(NO3)2/MgO	8-KDC-X-4
			9-KDC-X-16
5-KDC-X-59B	KQ	Sr(NO3)2(ion-exchange)/MgO	
5-KDC-X-60	KL	K2Lu2Ti3O10	8-KDC-X-1
5-KDC-X-61	KL	K2Er2Ti3O10	8-KDC-X-21
5-KDC-X-62	KE	K2La2Ti3O10	8-KDC-X-7
5-KDC-X-63	KM	80 mole% Pr- 20 mole% Ce Oxide	8-KDC-X-11
5-KDC-X-64	KM	2.9 mole% Ag/ 77.7 mole% Pr-19.4 mole% Ce Oxide	9-KDC-X-24
			9-KDC-X-46
5-KDC-X-65	KN	20% Na2CO3/Ag- Pr-Ce Oxide	8-KDC-X-25
			9-KDC-X-38
5-KDC-X-66	KN	20% Na2CO3/Pr-Ce Oxide	8-KDC-X-33
			8-KDC-X-37
			9-KDC-X-34
			9-KDC-X-55
5-KDC-X-67	KP	20% V2O5/80% MgO	9-KDC-X-42
5-KDC-X-68	KK	14.7% Li2CO3/LaCaMnCoO6	8-KDC-X-42
			12-KDC-X-28
			12-KDC-X-30
5-KDC-X-69	KS	0.66% Pd(NO3)2/1.6% KCl/alpha alumina (5402)	9-KDC-X-64
5-KDC-X-70	KS	0.66%Pd(NO3)2/2.4% NaCl/alpha alumina (5402)	9-KDC-X-68
			9-KDC-X-70
5-KDC-X-71A	KS	14.4% BaCl2/alpha alumina (5402)	9-KDC-X-88
5-KDC-X-71B	KS	.66% Pd(NO3)2/14.4% BaCl2/alpha alumina (5402	9-KDC-X-73
			9-KDC-X-77
			9-KDC-X -86
5-KDC-X-72	KS	0.66% Pd(NO3)2/19.8% KCl/alpha alumina (5402)	9-KDC-X-80
5-KDC-X-73	Kn	20% Na2CO3/CeO2	8-KDC-X-49
5-KDC-X-74	KN	20% Na2CO3/Pr6O11	8-KDC-X-53
5-KDC-X-75	KO	(Bi2O3).85(La2O3).15	8-KDC-X-63
			9-KDC-X-99
5-KDC-X-76	KS	0.66% Pd(NO3)2/11.8% LaCl3/alpha alumina (5402)	9-KDC-X-92
5-KDC-X-77	KI	LaCaMnCoO6	

Catalyst Prep. Notebook Number	Preparation Method	Catalyst Components by Total Weight %	Catalyst Evaluation Notebook Numbers
5-KDC-X-78	KE	K2La2Ti3O10	9-KDC-X-105 11-KDC-X-124
5-KDC-X-79A	KS	5% Na2CO3/alpha alumina (5402)	9-KDC-X-123
5-KDC-X-79B	KS	1% Pd(NO3)2/5% Na2CO3/alpha alumina (5402)	8-KDC-X-79
5-KDC-X-80A	KS	5% NaCl/alpha alumina (5402)	9-KDC-X-128
5-KDC-X-80B	KS	7.4% Pd(NO3)2/5% NaCl/alpha alumina (5402)	8-KDC-X-84 9-KDC-X-90
5-KDC-X-81A	KA	3% SrCl2/alpha alumina (5402)	9-KDC-X-134
5-KDC-X-82	KO	(Bi2O3).85(La2O3).15	
5-KDC-X-83	KN	20% Na2CO3/CaCO3	11-KDC-X-14
5-KDC-X-84	KN	20% Na2CO3/5% Pd(NO3)2/CaCO3	
5-KDC-X-85	KN	20% Na2CO3/20 % V2O5/80% MgO	11-KDC-X-10
5-KDC-X-86	KN	20% Na2CO3/Bi2O3	
5-KDC-X-87A	KS	5% NaCl/8.8% SrCl2/alpha alumina (5402)	11-KDC-X-1
5-KDC-X-87B	KS	7.4% Pd(NO3)2/5% NaCl/8.8% SrCl2/alpha alumina (5402)	8-KDC-X-96
5-KDC-X-88	KA & KB	0.82% Co(NO3)2/6 2% SrCl2/alpha alumina (5402)	11-KDC-X-17 11-KDC-X-19 11-KDC-X-40 11-KDC-X-29 12-KDC-X-5 12-KDC-X-14
5-KDC-X-90	KN	5% Na2P4O7/LaCaMnCoO6	12-KDC-X-78
5-KDC-X-91	KA & KB	0.53% Cu(NO3)2/6 2% SrCl2/alpha alumina (5402)	11-KDC-X-23
5-KDC-X-93	KS	1.3% Co(NO3)2/8% BaCl2/alpha alumina (5402)	11-KDC-X-34 11-KDC-X-46
5-KDC-X-94	KC	0.79% Co(NO3)2/alpha alumina (5402)	11-KDC-X-84
5-KDC-X-96	KA & KB	0.91% RhCl3/6.2% SrCl2/alpha alumina (5402)	11-KDC-X-66 12-KDC-X-1
5-KDC-X-98	KS	0.64% Co(NO3)2/10% BaCO3/alpha alumina (5402)	11-KDC-X-57
5-KDC-X-99	KS	0.64% Co(NO3)2/10% BaCl2/alpha alumina (5402)	11-KDC-X-61 12-KDC-X-9
5-KDC-X-100	KJ	20% Na2CO3/LaCaMnCoO6	11-KDC-X-76 12-KDC-X-25
5-KDC-X-103	KK	24% K2CO3/LaCaMnCoO6	11-KDC-X-101 12-KDC-X-49
5-KDC-X-104	KN	41% CsCl/LaCaMnCoO6	12-KDC-X-60
5-KDC-X-105	KN	37.5% RbNO3/LaCaMnCoO6	11-KDC-X-110 12-KDC-X-54
5-KDC-X-106	KK	51% Cs2CO3/LaCaMnCoO6	11-KDC-X-115 12-KDC-X-55 12-KDC-X-69
5-KDC-X-107	KK	48% Rb2CO3/LaCaMnCoO6	12-KDC-X-62 12-KDC-X-75
5-KDC-X-108	KI	LaCaMnCoO6	
5-KDC-X-109	KJ	20% Na2CO3/LaCaMnCoO6	12-KDC-X-80 12-KDC-X-82
5-PCH-60	KL	LaAlO3	4-KDC-X-73
43-WJB-91	KL	LaCoO3	4-KDC-X-54
43-WJB-95B	KL	LaMnO3	3-KDC-X-5 3-KDC-X-13
43-WJB-123	KL	LaVO3	3-KDC-X-9
43-WJB-124	KL	La(.65)Sr(.35)MnO3	3-KDC-X-17
43-WJB-124	KL	LaSrMnO3	3-KDC-X-21
47-WJB-8	KL	SrLaRuO3	4-KDC-X-78
47-WJB-16	KL	BaFeO3	3-KDC-X-75
47-WJB-18	KL	SrMoO3	4-KDC-X-81 4-KDC-X-94

Catalyst Prep. Notebook Number	Preparation Method	Catalyst Components by Total Weight %	Catalyst Evaluation Notebook Numbers
47-WJB-29	KL	LaMnO(3-X)	3-KDC-X-9
47-WJB-36A	KL	BaTiO(3-X)	3-KDC-X-33
47-WJB-36B	KL	KNbO(3-X)	3-KDC-X-41
47-WJB-58	KL	La[Rh(.5)Mn(.5)]O3	3-KDC-X-27
			3-KDC-X-51
47-WJB-95B	KL	LaMnO3	3-KDC-X-5
			3-KDC-X-13
47-WJB-97	KL	SrCoO3	4-KDC-X-57
47-WJB-100	KL	La(.6)Sr(.4)CoO3	4-KDC-X-62
47-WJB-103	KL	BaWO3	4-KDC-X-45
47-WJB-105	KL	La(.2)Sr(.8)MoO3	4-KDC-X-82
47-WJB-136A	KL	LaFeO3	3-KDC-X-47
49-WJB-99-3	KL	LaIrO3	4-KDC-X-1
		empty reactor	2-KDC-X-62
		BaPbO3(Aesar)	2-KDC-X-44
		BaCoO3(Aldrich)	1-KDC-X-11
			1-KDC-X-13
			1-KDC-X-20
			2-KDC-X-53
		SrCoO3(Aldrich)	2-KDC-X-58
		Sm2O3(Aesar)	1-KDC-X-30
		Nd2O3(Aesar)	1-KDC-X-28
			1-KDC-X-34
			1-KDC-X-40
			1-KDC-X-44
		KCl(Aldrich)	1-KDC-X-124
		NaCl(aldrich)	1-KDC-X-126
		TiO2(Norton)	9-KDC-X-1
		MgO(Fisher)	9-KDC-X-13
		Li2AlO3(Strem)	9-KDC-X-103
		Na2SiO3(Strem)	11-KDC-X-7
		K2SiO3(Strem)	8-KDC-X-101
		quartz(National Scientific)	2-KDC-X-6
			6-KDC-X-40
			6-KDC-X-104
			7-KDC-X-38
		TiO2(Aesar)	7-KDC-X-90
		Li4SiO4(Strem)	7-KDC-X-98
			7-KDC-X-102
			11-KDC-X-105
			12-KDC-X-37
		La2O3(Aesar)	7-KDC-X-113
		MgO carrier(Norton)	7-KDC-X-130
		K2CO3(Aesar)	6-KDC-X-88
		Li2SiO3(Strem)	6-KDC-X-100
		BaTiO3(Aesar)	3-KDC-X-37
			3-KDC-X-114
		KNbO3(Aesar)	3-KDC-X-37
		LaFeO3(Alfa)	3-KDC-X-107
		MgO(Calsicat)	4-KDC-X-102
		Limgo(Calsicat)	4-KDC-X-103
		MgO(Alfa)	4-KDC-X-108
		MnO2/MgO(physical mix)	11-KDC-X-26
		Na2P4O7(MCB)	4-KDC-X-109
		5%Pd/CaCO3(aldrich)	4-KDC-X-114
		5%Pt/CaCO3(aldrich)	4-KDC-X-116
		1%Pd/alumina(aldrich)	4-KDC-X-126
		1%Pt/alumina(aldrich)	4-KDC-X-127

Catalyst Prep. Notebook Number	Preparation Method	Catalyst Components by Total Weight %	Catalyst Evaluation Notebook Numbers
		5%Pd/BaCO3(aldrich)	4-KDC-X-132
		5%Pd/BaSO4(aldrich)	4-KDC-X-133
		Na4SiO4(strem)	11-KDC-X-88
			11-KDC-X-94
		YBa2Cu3O7-5	11-KDC-X-120

Appendix F. TABLES AND FIGURES

Table F1. Methane Coupling in Quartz Reactor A, Empty or Packed with Quartz Chips*

Name	Catalyst	Temp	ccm	CH4 C	Sel	Yield	O2 C	=/-	CO2/CO	CH4/O2	CH4 in	O2 in	Time	C Bal
29 BKW 24 R#4	None	800	50	10.13	37.3	3.86	61	2.5	0.05	6.11	15.63	2.56	129	102
29 BKW 24 R#4	None	800	50	10.95	37.1	4.1	62	2.89	0.05	6.11	15.63	2.56	180	101
29 BKW 27 R#3	None	800	50	33.64	14.6	5.13	95	5.76	0.13	2.2	8.194	3.73	76	105
29 BKW 27 R#3	None	800	50	31.62	15	5.07	95	5.61	0.13	2.2	8.194	3.73	173	107
29 BKW 27 R#4	None	800	150	33.74	14.8	5.23	95	5.91	0.13	2.2	8.194	3.73	67	105
29 BKW 27 R#4	None	800	150	32.89	15.9	5.49	94	5.65	0.13	2.2	8.194	3.73	172	105
29 BKW 35 R#3	Quartz 20/40	900	50	36.93	10.8	4.03	98	20	0.1	2.55	8.283	3.25	60	101
29 BKW 35 R#3	Quartz 20/40	900	50	34.64	10.9	3.93	98	20.5	0.09	2.55	8.283	3.25	150	104
29 BKW 35 R#3	Quartz 20/40	800	50	9.56	34.3	3.29	24	1.55	0.09	2.55	8.283	3.25	285	100
29 BKW 35 R#3	Quartz 20/40	800	50	9.56	34.3	3.29	24	1.55	0.09	2.55	8.283	3.25	285	100
29 BKW 35 R#4	Quartz 20/40	900	50	36.55	10.9	4.09	98	17.9	0.09	2.55	8.283	3.25	60	103
29 BKW 35 R#4	Quartz 20/40	900	50	36.57	10.7	4	98	29.1	0.09	2.55	8.283	3.25	150	103
29 BKW 35 R#4	Quartz 20/40	800	50	8.8	34.9	3.1	22	1.57	0.05	2.55	8.283	3.25	285	101
29 BKW 35 R#4	Quartz 20/40	800	50	8.72	36	3.15	21	1.54	0.05	2.55	8.283	3.25	375	100
29 BKW 42 R#3	Quartz 20/40	600	50	***	5.01	0	3.5	0	***	2.37	8.609	3.64	60	101
29 BKW 42 R#3	Quartz 20/40	600	50	***	0	0	3.3	***	***	2.37	8.609	3.64	150	102
29 BKW 42 R#3	Quartz 20/40	700	50	0.85	36.1	0.31	6.5	0.16	0.21	2.37	8.609	3.64	240	99.9
29 BKW 42 R#3	Quartz 20/40	700	50	1.79	35	0.62	7.2	0.18	0.19	2.37	8.609	3.64	330	99.2
29 BKW 42 R#4	Quartz 20/40	600	50	0.41	12.5	0.05	2.6	***	***	2.37	8.609	3.64	60	99.6
29 BKW 42 R#4	Quartz 20/40	600	50	***	100	***	3.2	0.01	***	2.37	8.609	3.64	150	102
29 BKW 42 R#4	Quartz 20/40	700	50	***	33.2	0	5.8	0.01	0.07	2.37	8.609	3.64	240	101
29 BKW 42 R#4	Quartz 20/40	700	50	1.46	37.2	0.54	6.8	0.2	0.07	2.37	8.609	3.64	330	99.5
29 BKW 59 R#3	None	600	50	1.47	32	0.47	3.1	0.17	0.05	1.92	9.969	5.2	60	99.2
29 BKW 59 R#3	None	600	50	1.55	32.7	0.5	4.2	0.15	0.03	1.92	9.969	5.2	150	99.1
29 BKW 59 R#3	None	700	50	20.75	24.2	5.05	48	1.93	0.09	1.92	9.969	5.2	240	101
29 BKW 59 R#3	None	700	50	21.9	23.7	5.23	51	2.04	0.09	1.92	9.969	5.2	330	101
29 BKW 59 R#3	None	800	50	39.92	12	4.96	97	7.16	0.16	1.92	9.969	5.2	420	104
29 BKW 59 R#3	None	800	50	39.12	12.1	4.94	97	7.1	0.16	1.86	9.941	5.35	600	105
29 BKW 59 R#3	None	900	50	43.28	6.13	2.71	99	69.1	0.15	1.97	9.991	5.07	1680	102
29 BKW 59 R#3	None	900	90	43.01	6.12	2.69	99	62.1	0.15	1.97	9.991	5.07	1770	102
29 BKW 59 R#4	None	600	50	1.84	33.8	0.61	3.5	0.18	0.02	1.92	9.969	5.2	60	98.8
29 BKW 59 R#4	None	600	50	1.06	35.2	0.37	4	0.16	0.02	1.92	9.969	5.2	150	99.6
29 BKW 59 R#4	None	700	50	23.15	22.6	5.32	55	2.22	0.1	1.92	9.969	5.2	240	101
29 BKW 59 R#4	None	700	50	25.42	21.7	5.59	60	2.31	0.11	1.92	9.969	5.2	330	101
29 BKW 59 R#4	None	800	50	39.73	11.6	4.77	97	7.12	0.16	1.92	9.969	5.2	420	104
29 BKW 59 R#4	None	800	50	38.86	11.5	4.7	97	7.14	0.16	1.86	9.941	5.35	600	105
29 BKW 59 R#4	None	900	50	43.04	5.81	2.55	99	64.5	0.15	1.97	9.991	5.07	1680	102
29 BKW 59 R#4	None	900	50	42.71	5.75	2.52	99	79.5	0.15	1.97	9.991	5.07	1770	102

Table F1. Methane Coupling in Quartz Reactor A, Empty or Packed with Quartz Chips* (continued)

Name	Catalyst	Temp	ccm	CH4 C	Sel	Yield	O2 C	=/-	CO2/CO	CH4/O2	CH4 in	O2 in	Time	C Bal
29 BKW 62 R#3	Quartz, 14/30	600	50	0.15	0.83	0	***	37.3	5.24	2.02	10.01	4.97	60	100
29 BKW 62 R#3	Quartz, 14/30	600	50	***	0.26	0	***	0	10.48	2.02	10.01	4.97	150	101
29 BKW 62 R#3	Quartz, 14/30	700	50	0.51	12.3	0.06	0.7	0.19	0.54	2.02	10.01	4.97	240	101
29 BKW 62 R#3	Quartz, 14/30	700	50	0.84	16.3	0.14	***	0.25	0.42	2.03	10.08	4.97	690	99.9
29 BKW 62 R#3	Quartz, 14/30	800	50	7.94	27.4	2.16	17	1.32	0.1	1.96	10.07	5.14	3030	99.4
29 BKW 62 R#3	Quartz, 14/30	800	50	8.47	28.8	2.43	18	1.42	0.09	1.96	10.07	5.14	3120	99.7
29 BKW 62 R#3	Quartz, 14/30	900	50	43.96	8.28	3.73	99	41.5	0.14	1.93	10.18	5.27	4290	102
29 BKW 62 R#3	Quartz, 14/30	900	50	46.05	8.13	3.73	99	52.6	0.14	1.93	10.18	5.27	4380	99.7
29 BKW 62 R#4	Quartz, 14/30	600	50	0.16	***	0	***	0	3.83	2.02	10.01	4.97	60	100
29 BKW 62 R#4	Quartz, 14/30	600	50	***	***	0	***	***	3.05	2.02	10.01	4.97	150	101
29 BKW 62 R#4	Quartz, 14/30	700	50	1.28	16	0.2	-0.3	0.26	0.39	2.03	10.08	4.97	690	99.7
29 BKW 62 R#4	Quartz, 14/30	700	50	1.74	***	***	2	0	0.38	1.99	10.22	5.15	870	99
29 BKW 62 R#4	Quartz, 14/30	800	50	11.96	27.2	3.26	26	2.02	0.12	1.96	10.07	5.14	3030	100
29 BKW 62 R#4	Quartz, 14/30	800	50	14.04	27.5	3.86	30	2.27	0.12	1.96	10.07	5.14	3120	100
29 BKW 62 R#4	Quartz, 14/30	900	50	46.57	7.02	3.25	99	157	0.15	1.93	10.18	5.27	4290	99.6
29 BKW 62 R#4	Quartz, 14/30	900	50	45.98	6.92	3.18	99	278	0.14	1.93	10.18	5.27	4380	99.8
29 BKW 71 R#3	Quartz, 14/30	700	50	2.04	10	0.2	1.7	0.3	0.76	1.95	9.796	5.02	60	99.8
29 BKW 71 R#3	Quartz, 14/30	700	50	2.13	11.1	0.23	2	0.27	0.66	1.95	9.796	5.02	150	99.2
29 BKW 71 R#3	Quartz, 14/30	800	50	8.1	25.5	2.05	15	1.25	0.11	1.95	9.796	5.02	330	99.2
29 BKW 71 R#3	Quartz, 14/30	800	50	8.32	26.9	2.23	15	1.3	0.08	1.95	9.796	5.02	420	99.3
29 BKW 71 R#3	Quartz, 14/30	900	50	43.58	7.72	3.49	99	54.3	0.12	1.95	9.796	5.02	1590	104
29 BKW 71 R#3	Quartz, 14/30	900	50	43.71	7.75	3.52	99	55.8	0.12	1.95	9.796	5.02	1680	104
29 BKW 71 R#3	Quartz, 14/30	800	50	18.27	27.4	5.08	39	2.74	0.07	1.93	9.815	5.08	2850	102
29 BKW 71 R#3	Quartz, 14/30	800	50	17.83	28.3	5.08	36	2.58	0.07	1.93	9.815	5.08	2940	101
29 BKW 71 R#3	Quartz, 14/30	800	100	7.69	37.3	2.85	13	1.04	0.04	1.93	9.815	5.08	3030	99.5
29 BKW 71 R#3	Quartz, 14/30	800	100	7.87	37.2	2.91	12	1.04	0.04	1.93	9.815	5.08	3120	99.3

* Appendix A describes table headings and defines terms. Appendix B describes experimental procedures. Ccm refers to the flow rate in ccm, at ambient temperature and pressure.

*** Inaccurate due to small number, or not applicable.

Table F2. **Results From Reactor A Packed with Quartz and Alumina (29-BKW-71)***

Name	Time	CH4 C	O2 C	Sel.	Yield	Temp.	ccm	Res. Time	Void Vol., ccm
29 BKW 71 R#3	60	2.04	1.65	10	0.2	700	50	14.36756	23.41
29 BKW 71 R#3	150	2.13	1.98	11	0.23	700	50	14.36756	23.41
29 BKW 71 R#3	240	2.37	2.27	12	0.27	700	50	14.36756	23.41
29 BKW 71 R#3	330	8.1	15.2	25	2.05	800	50	13.05306	23.41
29 BKW 71 R#3	420	8.32	15.5	27	2.23	800	50	13.05306	23.41
29 BKW 71 R#3	960	9.3	18.7	29	2.75	800	50	13.05306	23.41
29 BKW 71 R#3	1140	9.52	18.9	30	2.85	800	50	13.05306	23.41
29 BKW 71 R#3	1320	9.82	19.5	30	2.96	800	50	13.05306	23.41
29 BKW 71 R#3	1590	43.58	99.4	7.7	3.49	900	50	11.95892	23.41
29 BKW 71 R#3	1680	43.71	99.3	7.8	3.52	900	50	11.95892	23.41
29 BKW 71 R#3	1770	43.93	99.3	7.8	3.52	900	50	11.95892	23.41
29 BKW 71 R#3	2850	18.27	38.6	27	5.08	800	50	13.05306	23.41
29 BKW 71 R#3	2940	17.83	35.9	28	5.08	800	50	13.05306	23.41
29 BKW 71 R#3	3030	7.69	12.7	37	2.85	800	100	6.526528	23.41
29 BKW 71 R#3	3120	7.87	12.1	37	2.91	800	100	6.526528	23.41
29 BKW 71 R#3	3210	8.26	12.4	37	3.04	800	100	6.526528	23.41
29 BKW 71 R#3	3300	9.58	14.5	37	3.5	800	100	6.526528	23.41
29 BKW 71 R#4	40	12.38	27.2	11	1.32	700	50	19.61501	31.96
29 BKW 71 R#4	130	10.96	23.4	11	1.16	700	50	19.61501	31.96
29 BKW 71 R#4	220	10.85	22.4	11	1.13	700	50	19.61501	31.96
29 BKW 71 R#4	760	26.55	69.5	18	4.74	800	50	17.8204	31.96
29 BKW 71 R#4	940	25.94	67.9	18	4.71	800	50	17.8204	31.96
29 BKW 71 R#4	1480	40.2	99.5	7.8	3.04	900	50	16.32666	31.96
29 BKW 71 R#4	1570	40.82	99.5	7.3	2.85	900	50	16.32666	31.96
29 BKW 71 R#4	2650	19.1	43.8	23	4.4	800	68	13.10324	31.96
29 BKW 71 R#4	2740	19.14	43.5	23	4.42	800	68	13.10324	31.96
29 BKW 71 R#4	2830	10.86	19.9	31	3.3	800	136	6.551619	31.96
29 BKW 71 R#4	2920	11.23	19.8	31	3.41	800	136	6.551619	31.96
29 BKW 71 R#4	3010	11.25	19.9	31	3.43	800	136	6.551619	31.96

* Appendix A describes table headings and defines terms. Appendix B describes experimental procedures. Ccm refers to the flow rate, in ccm at ambient temperature and pressure. R#3 contains quartz chips and R#4 contains alumina chips.

Table F3. Control Studies, Uncatalyzed Reactions*

Name	ECl	Temp	Ccm	CH4 C	Sel	Yield	O2 C	=/-	CO2/CO	CH4/O2	CH4 in	O2 in	C Bal	Time	Reactor
29 BKW 139 R#4	0	700	50	1.64	9.25	0.15	6.62	0.32	1.25	2	9.928	4.963	100.15	90	A
29 BKW 139 R#4	0	700	50	0.82	9.75	0.08	5.38	0.28	1.1	2	9.928	4.963	100.63	180	A
29 BKW 139 R#4	0	800	50	7.93	24.78	1.99	21.04	1.47	0.17	2	9.928	4.963	101.1	270	A
29 BKW 139 R#4	0	800	50	9.46	27.54	2.62	22.51	1.65	0.12	2	9.928	4.963	100.68	465	A
29 BKW 139 R#4	0	800	50	10.04	27.89	2.82	23.66	1.74	0.11	2	9.928	4.963	100.72	555	A
29 BKW 139 R#4	0	800	50	11.26	28.17	3.17	20.1	1.85	0.1	2.13	9.902	4.643	99.99	690	A
29 BKW 139 R#4	0	800	50	12.52	28.68	3.59	26.44	2	0.09	2.03	10.085	4.969	99.94	1020	A
29 BKW 139 R#4	0	800	50	12.39	28.52	3.56	27.26	2.06	0.09	2.03	10.085	4.969	100.78	1200	A
29 BKW 139 R#4	0	800	50	13.05	28.94	3.79	28.18	2.12	0.09	2.03	10.085	4.969	100.45	1380	A
29 BKW 139 R#4	0	800	50	13.75	28.65	3.96	28.33	2.19	0.09	2.05	10.053	4.892	100.39	1620	A
29 BKW 139 R#4	0	800	50	13.79	28.32	3.95	29.89	2.25	0.09	2.05	10.053	4.892	101.22	1995	A
29 BKW 139 R#4	0	800	50	15.06	28.42	4.3	34.43	2.3	0.09	1.96	9.999	5.103	100.39	2280	A
29 BKW 139 R#4	0	800	50	15.7	28.75	4.51	29.8	2.33	0.09	2.12	10.196	4.803	99.84	2460	A
29 BKW 139 R#4	0	800	50	15	28.44	4.31	30.27	2.36	0.09	2.12	10.196	4.803	101.09	2640	A
29 BKW 139 R#4	0	800	50	15.26	28.71	4.42	30.93	2.37	0.09	2.12	10.196	4.803	100.9	2820	A
29 BKW 139 R#4	0	800	50	15.69	28.63	4.52	34.53	2.38	0.09	2.04	9.937	4.883	100.6	3060	A
29 BKW 139 R#4	0	800	50	18.18	28.76	5.14	34.98	2.46	0.09	2.04	9.937	4.883	98.33	3240	A
29 BKW 139 R#4	0	800	50	20.09	28.37	5.51	35.81	2.45	0.09	2.04	9.937	4.883	96.6	3435	A
29 BKW 139 R#4	0	800	50	16.3	28.83	4.75	36.22	2.47	0.09	1.98	9.843	4.978	101.12	3720	A
29 BKW 139 R#4	0	800	50	16.99	28.82	4.92	35	2.49	0.09	2.04	9.902	4.859	100.53	3900	A
29 BKW 139 R#4	0	800	50	17.04	28.93	4.96	35.24	2.49	0.09	2.04	9.902	4.859	100.56	4080	A
29 BKW 139 R#4	0	800	50	17.04	28.76	4.92	35.32	2.48	0.09	2.04	9.902	4.859	100.47	4260	A
30 BKW 49 R#4	0	750	50	6.76	26.25	1.73	9.2	0.63	0.07	2.02	9.951	4.935	97.47	195	A
30 BKW 49 R#4	0	750	50	4.39	26.35	1.15	11.16	0.68	0.07	1.95	10.022	5.147	99.82	330	A
30 BKW 49 R#4	0	750	50	2.55	26.27	0.68	10.58	0.67	0.06	1.95	10.022	5.147	101.57	510	A
30 BKW 49 R#4	0	750	50	4.4	26.33	1.15	8.31	0.66	0.06	2.04	10.071	4.941	99.59	690	A
30 BKW 49 R#4	0	750	50	3.64	26.52	0.97	7.71	0.64	0.06	2.04	10.071	4.941	100.37	870	A
30 BKW 49 R#4	0	750	50	2.69	26.38	0.72	7.18	0.63	0.06	2.04	10.071	4.941	101.28	1050	A
30 BKW 49 R#4	100	750	50	8.69	28.99	2.49	15.45	1.34	0.05	1.96	9.984	5.083	98.96	1230	A
30 BKW 49 R#4	100	750	50	10.71	29.58	3.1	17.91	1.51	0.05	1.96	9.984	5.083	97.87	1320	A
30 BKW 49 R#4	100	750	50	12.53	29.18	3.54	20.36	1.6	0.05	1.96	9.984	5.083	96.73	1410	A
30 BKW 79 R#3	0	750	50	1.79	36.56	0.66	6.05	0.27	0.1	1.9	10.087	5.302	99.97	50	D
30 BKW 79 R#3	0	750	50	2.05	38.84	0.79	5.78	0.27	0.07	1.9	10.087	5.302	99.59	135	D
30 BKW 79 R#3	0	775	50	4.19	40.52	1.67	8.04	0.4	0.05	1.9	10.087	5.302	98.53	225	D
30 BKW 79 R#3	0	800	50	6.63	41.22	2.68	12.05	0.65	0.03	1.9	10.087	5.302	98.22	315	D
30 BKW 79 R#3	0	750	50	4.12	43.73	1.75	6.54	0.27	0.04	1.9	10.087	5.302	97.28	400	D
30 BKW 79 R#3	50	750	50	2.15	41.79	0.89	0	0.54	0.03	2.05	10.351	5.058	99.41	540	D
30 BKW 79 R#3	50	750	50	0.93	42.25	0.4	-0.04	0.53	0.03	2.05	10.351	5.058	100.59	720	D
30 BKW 79 R#3	50	750	50	1.97	43.34	0.85	2.45	0.49	0.03	2.03	10.349	5.092	99.57	900	D
30 BKW 79 R#3	50	750	50	1.32	42.99	0.57	1.48	0.49	0.02	2.03	10.349	5.092	100.27	1080	D
30 BKW 79 R#3	50	750	50	0.24	43.56	0.1	0.95	0.47	0.02	2.03	10.349	5.092	101.34	1260	D

Table F3. Control Studies, Uncatalyzed Reactions* (continued)

Name	ECl	Temp	Ccm	CH4 C	Sel	Yield	O2 C	=/-	CO2/CO	CH4/O2	CH4 in	O2 in	C Bal	Time	Reactor
30 BKW 82 R#4	50	750	50	7.22	27.98	2	15.61	0.97	0.09	1.97	10.312	5.232	98.87	60	E
30 BKW 82 R#4	50	775	50	13.49	29.56	3.9	25.63	1.69	0.06	1.97	10.312	5.232	97.83	150	E
30 BKW 82 R#4	50	775	50	15.4	30.08	4.49	27.83	1.8	0.06	1.97	10.312	5.232	96.83	240	E
30 BKW 82 R#4	50	800	50	27.18	23.59	6.26	54.74	3.43	0.08	1.97	10.312	5.232	97.69	330	E
30 BKW 82 R#4	50	750	50	12.77	33.2	4.01	18.97	1.17	0.04	1.97	10.312	5.232	94.53	420	E
30 BKW 82 R#4	50	750	50	8.25	33.42	2.75	13.85	1.24	0.04	2	10.25	5.118	99.91	555	E
30 BKW 82 R#4	50	750	50	6.51	34.09	2.25	13.7	1.2	0.01	2	10.25	5.118	101.43	735	E
30 BKW 82 R#4	50	750	50	6.81	33.99	2.34	14.64	1.13	0.04	2	10.167	5.094	101.13	915	E
30 BKW 82 R#4	50	750	50	5.34	34.07	1.87	13.61	1.11	0.03	2	10.167	5.094	102.59	1095	E
30 BKW 82 R#4	50	750	50	3.79	34.37	1.36	12.48	1.12	0.03	2	10.167	5.094	104.17	1275	E
30 BKW 82 R#4	0	750	50	9.92	35.06	3.38	12.78	1.05	0.03	2.04	10.376	5.085	97.3	1455	E
30 BKW 82 R#4	100	750	50	12.14	35.00	4.06	13.93	1.07	0.04	2.04	10.376	5.085	95.27	1545	E
30 BKW 82 R#4	100	750	100	8.31	41.79	3.28	5.49	0.48	0.02	2.04	10.376	5.085	94.42	1590	E
30 BKW 82 R#4	100	800	160	10.38	39.5	3.91	8.71	0.73	0.22	2.04	10.376	5.085	95.25	1640	E

* Appendix A defines terms and table headings. Reactors are illustrated in Appendix B, which also describes experimental procedures.

Table F4. Vapor Phase Reactions

Name	Wt	Catalyst	Temp	Ccm	CH4 C	Sel	Yield	O2 C	+/-	CO2/CO	CH4/O2	CH4 in	O2 in	C Bal	Time	GHSV	ECI
35 BKW 23 R#2	0.0	None (Control Run)	750	160	36.9	13.4	5.6	76	2.7	0.1	2.0	20.4	10.1	113	35	***	0
35 BKW 23 R#2	0.0	None (Control Run)	750	160	39.8	12.4	5.6	81	2.9	0.1	2.0	20.4	10.1	113	65	###	0
35 BKW 23 R#2	0.0	None (Control Run)	750	160	27.3	18.5	5.4	67	2.2	0.1	2.0	20.4	10.1	107	115	###	0
35 BKW 23 R#2	0.0	None (Control Run)	700	160	15.2	22.1	3.4	31	1.1	0.0	2.0	20.4	10.1	102	155	###	0
35 BKW 23 R#2	0.0	None (Control Run)	700	160	21.0	18.0	4.0	36	1.5	0.1	2.0	20.4	10.1	107	195	###	0
35 BKW 23 R#2	0.0	None (Control Run)	650	160	8.4	21.9	1.8	8	0.5	0.0	2.0	20.4	10.1	99	295	###	0
35 BKW 23 R#2	0.0	None (Control Run)	650	160	7.2	24.7	1.7	14	0.4	0.0	2.0	20.4	10.1	98	1230	###	0
35 BKW 23 R#2	0.0	None (Control Run)	650	160	9.0	22.9	2.0	11	0.5	0.0	2.0	20.4	10.1	97	1390	###	0
35 BKW 23 R#2	0.0	None (Control Run)	650	160	7.2	25.7	1.8	14	0.4	0.0	2.0	20.4	10.1	98	1420	###	0
35 BKW 23 R#2	0.0	None (Control Run)	650	160	7.7	22.5	1.7	10	0.5	0.0	2.0	20.4	10.1	99	1530	###	0
35 BKW 23 R#2	0.0	None (Control Run)	650	160	8.6	21.6	1.9	10	0.5	0.0	2.0	20.4	10.1	99	1560	###	0
35 BKW 23 R#2	0.0	None (Control Run)	650	160	5.7	25.0	1.4	17	0.4	0.0	2.0	20.4	10.1	99	1595	###	0
35 BKW 23 R#2	0.0	None (Control Run)	650	160	7.6	23.1	1.7	13	0.5	0.0	2.0	20.4	10.1	99	1620	###	0
35 BKW 23 R#2	0.0	None (Control Run)	650	160	11.2	20.0	2.2	8	0.6	0.0	2.0	20.4	10.1	99	1650	###	0
35 BKW 23 R#2	0.0	None (Control Run)	650	160	8.5	21.7	1.8	7	0.5	0.0	2.0	20.4	10.1	99	1675	###	0
35 BKW 23 R#2	0.0	None (Control Run)	650	160	6.0	24.3	1.5	13	0.4	0.0	2.1	20.4	9.9	99	1710	###	0
35 BKW 23 R#2	0.0	None (Control Run)	650	160	4.9	25.1	1.2	12	0.4	0.0	2.1	20.4	9.9	100	1795	###	0
35 BKW 26 R#2	5.0	CsOH.XH2O,100+	650	160	5.8	25.0	1.4	2	0.4	0.0	2.2	20.4	9.5	100	35	***	0
35 BKW 26 R#2	5.0	CsOH.XH2O,100+	650	160	6.4	22.9	1.5	0	0.5	0.0	2.2	20.4	9.5	102	80	***	0
35 BKW 26 R#2	5.0	CsOH.XH2O,100+	650	160	5.2	25.3	1.3	6	0.4	0.0	2.2	20.4	9.5	100	105	***	0
35 BKW 26 R#2	5.0	CsOH.XH2O,100+	650	160	3.1	37.6	1.1	-3	0.2	0.0	2.2	20.4	9.5	99	135	***	0
35 BKW 26 R#2	5.0	CsOH.XH2O,100+	650	160	3.5	31.6	1.1	-8	0.3	0.0	2.2	20.4	9.5	99	160	***	0
35 BKW 26 R#2	5.0	CsOH.XH2O,100+	650	160	1.2	43.0	0.5	1	0.2	0.0	2.2	20.4	9.5	100	190	***	0
35 BKW 26 R#2	5.0	CsOH.XH2O,100+	700	160	5.4	30.6	1.6	-9	0.5	0.0	2.2	20.4	9.5	100	215	***	0
35 BKW 26 R#2	5.0	CsOH.XH2O,100+	700	160	3.0	39.8	1.2	8	0.3	0.1	2.2	20.4	9.5	99	250	***	0
35 BKW 26 R#2	5.0	CsOH.XH2O,100+	700	160	3.3	33.0	1.1	-8	0.4	0.1	2.2	20.4	9.5	100	275	***	0
35 BKW 26 R#2	5.0	CsOH.XH2O,100+	700	160	2.8	33.2	0.9	3	0.3	0.1	2.2	20.4	9.5	100	310	***	0
35 BKW 26 R#2	5.0	CsOH.XH2O,100+	650	160	1.7	42.8	0.7	-9	0.2	0.1	2.1	20.1	9.7	100	1270	***	0
35 BKW 26 R#2	5.0	CsOH.XH2O,100+	650	160	2.5	38.0	0.9	###	0.2	0.0	2.1	20.1	9.7	99	1320	***	0
35 BKW 29 R#2	1.4	LiOH,100+	650	160	5.4	27.2	1.5	10	0.3	0.1	2.1	20.4	9.8	99	55	***	0
35 BKW 29 R#2	1.4	LiOH,100+	650	160	6.9	22.6	1.6	7	0.5	0.0	2.1	20.4	9.8	100	80	***	0
35 BKW 29 R#2	1.4	LiOH,100+	650	160	6.2	28.3	1.7	14	0.3	0.1	2.1	20.4	9.8	97	125	***	0
35 BKW 29 R#2	1.4	LiOH,100+	650	160	6.8	22.0	1.5	7	0.5	0.0	2.1	20.4	9.8	101	155	***	0
35 BKW 29 R#2	1.4	LiOH,100+	650	160	10.4	21.5	2.2	7	0.5	0.0	2.1	20.4	9.8	98	215	***	0
35 BKW 29 R#2	1.4	LiOH,100+	650	160	7.0	22.0	1.6	6	0.5	0.0	2.1	20.4	9.8	101	245	***	0
35 BKW 29 R#2	1.4	LiOH,100+	650	160	9.4	21.9	2.0	7	0.5	0.0	2.1	20.4	9.8	99	295	***	0
35 BKW 29 R#2	1.4	LiOH,100+	650	160	7.1	26.1	1.8	12	0.4	0.0	2.1	20.4	9.8	98	345	***	0
35 BKW 29 R#2	1.4	LiOH,100+	650	160	4.2	29.9	1.2	###	0.2	0.1	2.1	20.4	9.8	98	375	***	0
35 BKW 32 R#2	5.0	CsCl,100+	650	160	5.4	23.9	1.3	4	0.4	0.0	2.1	20.1	9.8	100	45	***	0
35 BKW 32 R#2	5.0	CsCl,100+	650	160	7.0	22.6	1.6	2	0.5	0.0	2.1	20.1	9.8	100	70	***	0
35 BKW 32 R#2	5.0	CsCl,100+	650	160	5.3	25.4	1.4	7	0.4	0.0	2.1	20.1	9.8	100	95	***	0
35 BKW 32 R#2	5.0	CsCl,100+	650	160	3.7	27.5	1.0	13	0.3	0.0	2.1	20.1	9.8	100	125	***	0
35 BKW 32 R#2	5.0	CsCl,100+	650	160	5.6	23.1	1.3	7	0.5	0.0	2.1	20.1	9.8	102	160	***	0
35 BKW 32 R#2	5.0	CsCl,100+	650	160	6.4	24.1	1.5	7	0.5	0.0	2.1	20.1	9.8	100	205	***	0

Table F4. Vapor Phase Reactions (continued)

Name	Wt	Catalyst	Temp	Ccm	CH4 C	Sel	Yield	O2 C	=/-	CO2/CO	CH4/O2	CH4 in	O2 in	C Bal	Time	GHSV	ECI
35 BKW 32 R#2	5.0	CsCl,100+	650	160	0.8	60.5	0.5	0	0.2	0.1	2.1	20.1	9.8	100	245	***	0
35 BKW 32 R#2	5.0	CsCl,100+	650	160	###	83.2	###	1	0.1	###	2.1	20.1	9.8	101	305	***	0
35 BKW 32 R#2	5.0	CsCl,100+	650	160	###	80.6	###	###	0.0	###	2.1	20.1	9.8	101	335	***	0
35 BKW 32 R#2	5.0	CsCl,100+	700	160	###	47.2	0.0	2	0.2	0.2	2.1	20.1	9.8	101	365	***	0
35 BKW 32 R#2	5.0	CsCl,100+	750	160	4.1	31.0	1.3	6	0.6	0.1	2.1	20.1	9.8	101	390	***	0
35 BKW 32 R#2	5.0	CsCl,100+	750	160	3.5	32.0	1.1	10	0.6	0.1	2.1	20.1	9.8	101	420	***	0
35 BKW 32 R#2	5.0	CsCl,100+	750	160	15.5	25.6	4.0	31	1.4	0.1	2.0	20.2	10.3	101	1400	***	0
35 BKW 32 R#2	5.0	CsCl,100+														***	0
35 BKW 35 R#2	2.0	LiCl,100+	650	160	3.2	42.6	1.3	7	0.2	0.0	2.0	20.1	9.9	98	55	***	0
35 BKW 35 R#2	2.0	LiCl,100+	650	160	3.1	28.6	0.9	2	0.2	0.0	2.0	20.1	9.9	99	85	***	0
35 BKW 35 R#2	2.0	LiCl,100+	650	160	1.4	64.3	0.9	###	0.1	0.1	2.0	20.1	9.9	99	125	***	0
35 BKW 35 R#2	2.0	LiCl,100+	650	160	0.6	50.1	0.3	###	0.2	0.1	2.0	20.1	9.9	100	155	***	0
35 BKW 35 R#2	2.0	LiCl,100+	650	160	###	64.6	###	6	0.1	0.0	2.0	20.1	9.9	101	185	***	0
35 BKW 35 R#2	2.0	LiCl,100+	750	160	12.5	22.2	2.9	18	1.5	0.0	2.0	20.1	9.9	106	220	***	0
35 BKW 35 R#2	2.0	LiCl,100+	750	160	12.9	22.4	3.0	22	1.7	0.0	2.0	20.1	9.9	104	265	***	0
35 BKW 35 R#2	2.0	LiCl,100+	850	160	30.4	3.8	1.2	96	6.2	1.7	2.0	20.1	9.9	103	300	***	0
35 BKW 35 R#2	2.0	LiCl,100+	800	160	29.1	3.7	1.1	95	3.5	1.9	2.0	20.1	9.9	103	345	***	0
35 BKW 35 R#2	2.0	LiCl,100+	750	160	27.6	3.5	1.0	93	1.7	2.6	2.0	20.1	9.9	101	430	***	0
35 BKW 35 R#2	2.0	LiCl,100+	750	160	30.8	2.9	0.9	94	1.6	2.5	2.0	20.1	9.9	102	520	***	0
35 BKW 37 R#2	5.0	CsCl,100+	650	160	###	6.8	0.0	8	0.0	3.2	2.0	20.1	10.3	101	35	***	0
35 BKW 37 R#2	5.0	CsCl,100+	650	160	0.3	7.3	0.0	9	0.0	2.6	2.0	20.1	10.3	100	65	***	0
35 BKW 37 R#2	5.0	CsCl,100+	650	160	0.5	9.2	0.0	3	0.0	12.3	2.0	20.1	10.3	100	100	***	0
35 BKW 37 R#2	5.0	CsCl,100+	700	160	1.7	14.5	0.2	10	0.2	0.8	2.0	20.1	10.3	100	130	***	0
35 BKW 37 R#2	5.0	CsCl,100+	700	160	1.9	14.3	0.3	7	0.2	0.6	2.0	20.1	10.3	100	160	***	0
35 BKW 37 R#2	5.0	CsCl,100+	700	160	2.3	17.0	0.4	7	0.2	0.6	2.0	20.1	10.3	99	190	***	0
35 BKW 37 R#2	5.0	CsCl,100+	750	160	4.0	21.9	0.9	17	0.5	0.2	2.0	20.1	10.3	100	220	***	0
35 BKW 37 R#2	5.0	CsCl,100+	750	160	3.8	23.0	0.9	10	0.4	0.2	2.0	20.1	10.3	100	340	***	0
35 BKW 37 R#2	5.0	CsCl,100+	750	160	3.1	21.4	0.7	12	0.4	0.2	2.0	20.1	10.3	101	3985	***	0
35 BKW 37 R#2	5.0	CsCl,100+	750	160	2.7	18.1	0.5	8	0.3	0.2	2.0	20.1	10.3	101	4150	***	0
35 BKW 37 R#2	5.0	CsCl,100+	750	160	3.5	17.8	0.6	3	0.3	0.2	2.0	20.1	10.3	100	4190	***	0
35 BKW 41 R#2	4.0	RuO2,powder	650	160	5.0	24.7	1.3	5	0.4	0.2	2.1	20.1	9.8	101	30	***	0
35 BKW 41 R#2	4.0	RuO2,powder	650	160	5.9	27.8	1.6	9	0.4	0.2	2.1	20.1	9.8	98	60	***	0
35 BKW 41 R#2	4.0	RuO2,powder	650	160	5.8	24.5	1.4	6	0.4	0.2	2.1	20.1	9.8	100	90	***	0
35 BKW 41 R#2	4.0	RuO2,powder	650	160	4.0	27.7	1.1	6	0.4	0.2	2.1	20.1	9.8	101	120	***	0
35 BKW 41 R#2	4.0	RuO2,powder	650	160	6.5	23.6	1.5	7	0.5	0.1	2.1	20.1	9.8	100	160	***	0
35 BKW 41 R#2	4.0	RuO2,powder	650	160	5.9	24.7	1.5	9	0.4	0.1	2.1	20.1	9.8	100	195	***	0
35 BKW 41 R#2	4.0	RuO2,powder	650	160	3.0	28.4	0.9	7	0.3	0.1	2.1	20.1	9.8	101	230	***	0
35 BKW 41 R#2	4.0	RuO2,powder	650	160	2.5	30.5	0.8	###	0.3	0.2	2.1	20.1	9.8	100	275	***	0
35 BKW 41 R#2	4.0	RuO2,powder	750	160	32.8	12.0	4.4	77	2.2	0.2	2.1	20.1	9.8	113	320	***	0
35 BKW 41 R#2	4.0	RuO2,powder	750	160	29.0	13.8	4.4	71	2.0	0.2	2.1	20.1	9.8	110	360	***	0
35 BKW 41 R#2	4.0	RuO2,powder	750	160	33.3	12.2	4.6	76	2.3	0.2	2.1	20.1	9.8	113	460	***	0
35 BKW 41 R#2	4.0	RuO2,powder	750	160	26.8	14.3	4.2	69	1.9	0.2	2.1	20.1	9.8	110	595	***	0
35 BKW 41 R#2	4.0	RuO2,powder	750	160	34.6	12.5	4.9	76	2.4	0.2	2.1	20.4	9.8	112	1310	***	0
35 BKW 41 R#2	4.0	RuO2,powder	750	160	27.3	17.1	5.0	62	2.1	0.2	2.1	20.4	9.8	107	1385	***	0

Table F4. Vapor Phase Reactions (continued)

Name	Wt	Catalyst	Temp	Ccm	CH4 C	Sel	Yield	O2 C	=/-	CO2/CO	CH4/O2	CH4 in	O2 in	C Bal	Time	GHSV	ECI
35 BKW 41 R#2	4.0	RuO2,powder	750	160	28.9	15.8	5.0	65	2.2	0.2	2.1	20.4	9.8	109	1435	***	0
35 BKW 44 R#2	5.0	CsCl,100+	750	160	34.7	13.9	5.5	78	2.8	0.1	2.0	20.2	10.2	114	45	***	0
35 BKW 44 R#2	5.0	CsCl,100+	750	160	34.2	13.8	5.4	79	2.8	0.1	2.0	20.2	10.2	115	70	***	0
35 BKW 44 R#2	5.0	CsCl,100+	750	160	5.7	29.9	1.7	16	0.8	0.1	2.0	20.2	10.2	101	100	***	0
35 BKW 44 R#2	5.0	CsCl,100+	750	160	9.6	27.5	2.7	18	1.4	0.1	2.0	20.2	10.2	101	150	***	0
35 BKW 44 R#2	5.0	CsCl,100+	750	160	9.9	28.3	2.8	23	1.5	0.1	2.0	20.2	10.2	101	190	***	0
35 BKW 44 R#2	5.0	CsCl,100+	750	160	17.2	20.5	3.7	40	2.7	0.1	2.0	20.2	10.2	106	270	***	0
35 BKW 44 R#2	5.0	CsCl,100+	750	160	21.8	18.1	4.2	45	3.1	0.1	2.0	20.2	10.2	106	310	***	0
35 BKW 44 R#2	5.0	CsCl,100+	750	160	9.7	28.4	2.8	18	1.0	0.1	2.0	20.2	10.2	101	5605	***	0
35 BKW 44 R#2	5.0	CsCl,100+	750	160	10.4	28.8	3.0	19	1.0	0.1	2.0	20.2	10.2	100	5900	***	0
35 BKW 47 R#2	4.0	BaCO3,Al2O3,5451,30/60	750	160	20.8	49.1	10.1	33	1.7	1.1	2.0	20.2	10.3	99	55	3000	0
35 BKW 47 R#2	4.0	BaCO3,Al2O3,5451,30/60	750	160	21.1	46.5	9.8	36	1.9	0.9	2.0	20.2	10.3	100	85	3000	0
35 BKW 47 R#2	4.0	BaCO3,Al2O3,5451,30/60	750	160	21.0	48.9	10.3	35	1.8	1.0	2.0	20.2	10.3	100	120	3000	0
35 BKW 47 R#2	4.0	BaCO3,Al2O3,5451,30/60	750	160	21.7	50.9	10.9	37	1.8	1.1	2.0	20.2	10.3	99	155	3000	0
35 BKW 47 R#2	4.0	BaCO3,Al2O3,5451,30/60	750	160	20.0	52.2	10.5	35	1.7	1.2	2.0	20.2	10.3	100	185	3000	0
35 BKW 47 R#2	4.0	BaCO3,Al2O3,5451,30/60	750	160	21.3	53.1	11.2	36	1.7	1.2	2.0	20.2	10.3	99	220	3000	0
35 BKW 47 R#2	4.0	BaCO3,Al2O3,5451,30/60	750	160	20.7	54.4	11.2	41	1.7	1.3	2.0	20.2	10.3	99	255	3000	0
35 BKW 47 R#2	4.0	BaCO3,Al2O3,5451,30/60	750	160	23.7	50.8	12.0	42	1.8	1.4	2.0	20.2	10.3	100	1155	3000	0
35 BKW 47 R#2	4.0	BaCO3,Al2O3,5451,30/60	750	160	23.2	50.2	11.8	43	1.8	1.4	2.0	20.2	10.3	101	1290	3000	0
35 BKW 47 R#2	4.0	BaCO3,Al2O3,5451,30/60	750	80	34.8	41.2	14.3	76	3.3	1.3	2.0	20.2	10.3	99	1355	1500	0
35 BKW 47 R#2	4.0	BaCO3,Al2O3,5451,30/60	750	80	39.6	33.8	13.7	65	4.1	1.2	2.0	20.2	10.3	102	1395	1500	0
35 BKW 47 R#2	4.0	BaCO3,Al2O3,5451,30/60	750	80	34.3	37.9	12.8	70	3.3	1.2	2.0	20.2	10.3	98	1440	1500	0
35 BKW 47 R#2	4.0	BaCO3,Al2O3,5451,30/60	750	80	41.0	29.8	12.0	70	4.6	1.0	2.0	20.2	10.3	98	1480	1500	0
35 BKW 47 R#2	4.0	BaCO3,Al2O3,5451,30/60	750	80	39.3	27.7	11.0	67	4.6	0.9	2.0	20.2	10.3	101	1520	1500	0
35 BKW 47 R#2	4.0	BaCO3,Al2O3,5451,30/60	750	80	41.4	28.7	12.0	69	4.8	1.0	2.0	20.2	10.3	101	1555	1500	0
35 BKW 47 R#2	4.0	BaCO3,Al2O3,5451,30/60	750	80	36.0	37.6	13.6	75	3.7	1.2	2.0	20.2	10.3	100	1605	1500	0
35 BKW 47 R#2	4.0	BaCO3,Al2O3,5451,30/60	750	80	40.5	36.1	14.7	64	3.8	1.4	2.0	20.2	10.3	100	1645	1500	0
35 BKW 47 R#2	4.0	BaCO3,Al2O3,5451,30/60	750	80	41.9	35.3	14.8	60	3.8	1.4	2.0	20.2	10.3	100	1690	1500	0
35 BKW 47 R#2	4.0	BaCO3,Al2O3,5451,30/60	750	80	40.5	36.1	14.6	57	3.6	1.4	2.0	20.2	10.3	100	1745	1500	0
35 BKW 47 R#2	4.0	BaCO3,Al2O3,5451,30/60	750	80	36.2	34.7	12.7	69	3.8	1.1	2.0	20.2	10.3	101	1800	1500	0
35 BKW 47 R#2	4.0	BaCO3,Al2O3,5451,30/60	750	80	39.8	27.7	11.3	66	4.7	1.0	2.0	20.2	10.3	102	1890	1500	0
35 BKW 47 R#2	4.0	BaCO3,Al2O3,5451,30/60	750	80	41.5	25.2	10.8	76	5.2	0.9	2.0	20.2	10.3	103	2655	1500	0

Appendix A and the Experimental Section describe Table headings and experimental procedures.

Numbers are too small for significant results.

*** Gas flow rate was 160 ccm (ambient conditions).

Reactor V was used for all experiments.

Reaction 35-BKW-47 contained CsCl in the Vaporizer and BaCO3/Al2O3 in the reactor (see Experimental Section, Discussion Section, and Appendix F).

Table F5. Vapor-Phase Catalysts

35-BKW-23, No Catalyst

Reactor Temp	Vaporizer Temp	Run Time (min)	% C Bal	CH4 Conv	O2 Conv	% CO2	% CO	% C2H6	% C2H4	Total C2 Sel	Total C1 Sel
750	232	115	106.7	27.27	66.93	0.377	5.557	0.213	0.467	18.47	80.58
700	218	195	106.5	20.99	36.06	0.247	4.467	0.207	0.313	18.03	81.70
650	203	1420	97.6	7.20	13.98	0.014	0.731	0.093	0.035	25.66	74.33
650	300	1560	99.1	8.63	9.57	0.028	1.214	0.113	0.058	21.62	78.38
650	500	1675	99.5	8.50	7.48	0.028	1.244	0.117	0.060	21.65	77.66
650	650	1980	99.5	6.63	10.55	0.020	0.949	0.102	0.044	23.05	76.27

35-BKW-26, CsOH

Reactor Temp	Vaporizer Temp	Run Time (min)	% C Bal	CH4 Conv	O2 Conv	% CO2	% CO	% C2H6	% C2H4	Total C2 Sel	Total C1 Sel
650	225	105	100.3	5.23	6.21	0.021	0.823	0.101	0.042	25.28	74.39
650	300	160	99.2	3.52	-8.38	0.009	0.365	0.069	0.017	31.61	68.39
650	400	190	100.0	1.23	0.94	0.004	0.143	0.047	0.008	43.01	56.99
700	400	215	100.3	5.36	-8.75	0.031	0.758	0.117	0.058	30.55	68.73
700	500	250	99.2	2.97	7.91	0.013	0.253	0.068	0.020	39.82	60.18
700	600	275	99.8	3.27	-7.69	0.023	0.388	0.075	0.026	32.98	66.79
700	650	310	99.6	2.84	3.47	0.020	0.308	0.063	0.019	33.23	66.77
650	225	1350	100.0	0.57	-0.05	0.003	0.036	0.032	0.004	65.14	34.86

35-BKW-29, LiOH

Reactor Temp	Vaporizer Temp	Run Time (min)	% C Bal	CH4 Conv	O2 Conv	% CO2	% CO	% C2H6	% C2H4	Total C2 Sel	Total C1 Sel
650	149	125	97.5	6.23	13.66	0.027	0.525	0.083	0.026	28.33	71.48
650	250	155	101.5	6.79	6.55	0.050	1.271	0.123	0.063	21.99	78.01
650	300	215	98.2	10.43	6.82	0.053	1.349	0.125	0.067	21.52	78.48
650	350	245	101.4	7.04	6.32	0.050	1.293	0.125	0.065	21.98	77.77
650	400	295	98.5	9.36	7.45	0.049	1.222	0.117	0.061	21.87	78.13
650	450	345	97.7	7.07	12.15	0.032	0.707	0.095	0.036	26.10	73.90
650	500	375	97.8	4.17	-3.32	0.029	0.257	0.050	0.011	29.85	70.14

Table F5. Vapor-Phase Catalysts (continued)

35-BKW-32, CsCl

Reactor Temp	Vaporizer Temp	Run Time (min)	% C Bal	CH4 Conv	O2 Conv	% CO2	% CO	% C2H6	% C2H4	Total C2 Sel	Total C1 Sel
650	196	95	99.9	5.34	7.44	0.023	0.771	0.096	0.039	25.35	74.35
650	300	125	100.2	3.72	12.96	0.014	0.513	0.083	0.026	27.50	66.08
650	400	160	101.6	5.57	6.69	0.031	1.069	0.112	0.054	23.08	76.24
650	500	205	100.3	6.36	7.18	0.026	0.998	0.112	0.051	24.10	75.90
650	600	245	99.8	0.77	-0.34	0.005	0.043	0.032	0.005	60.45	39.55
650	650	305	100.6	-0.48	1.27	0.004	0.000	0.009	0.000	83.21	16.79
700	650	365	101.0	-0.07	2.27	0.016	0.085	0.037	0.008	47.17	52.83
750	650	390	101.0	4.06	5.50	0.042	0.659	0.097	0.061	31.04	68.96
750	700	420	100.8	3.48	10.19	0.035	0.550	0.089	0.051	32.02	67.10
750	226	1400	101.5	15.49	31.34	0.134	2.463	0.188	0.266	25.58	73.15

35-BKW-35, LiCl

Reactor Temp	Vaporizer Temp	Run Time (min)	% C Bal	CH4 Conv	O2 Conv	% CO2	% CO	% C2H6	% C2H4	Total C2 Sel	Total C1 Sel
650	165	85	99.4	3.14	1.76	0.008	0.359	0.059	0.014	28.58	71.42
650	550	125	99.0	1.43	-1.42	0.002	0.030	0.025	0.003	64.25	35.75
650	600	155	100.1	0.64	-7.44	0.003	0.069	0.031	0.005	50.06	49.94
650	650	185	101.1	-0.70	6.21	0.001	0.027	0.022	0.003	64.60	35.40
750	750	220	105.7	12.46	17.82	0.104	2.704	0.162	0.247	22.17	76.09
850	850	300	103.3	30.36	96.25	4.481	2.634	0.020	0.120	3.75	95.57
800	800	345	102.6	29.09	94.58	4.351	2.349	0.029	0.101	3.72	95.57
750	183	1400	101.9	25.88	92.28	4.296	1.604	0.041	0.067	3.52	96.25

35-BKW-37, CsCl

Reactor Temp	Vaporizer Temp	Run Time (min)	% C Bal	CH4 Conv	O2 Conv	% CO2	% CO	% C2H6	% C2H4	Total C2 Sel	Total C1 Sel
650	183	65	100.2	0.25	8.51	0.063	0.024	0.003	0.000	7.28	92.73
650	650	100	100.0	0.48	3.11	0.084	0.007	0.005	0.000	9.24	90.76
700	650	130	100.1	1.65	10.18	0.129	0.170	0.021	0.004	14.46	85.53
700	700	160	99.9	1.85	7.47	0.110	0.187	0.021	0.004	14.28	85.72
700	750	190	99.3	2.30	6.75	0.097	0.172	0.023	0.005	16.98	83.02
750	750	3985	100.8	3.07	12.18	0.094	0.520	0.061	0.024	21.38	77.78
750	195	4190	100.0	3.50	2.65	0.091	0.489	0.048	0.016	17.84	82.16

Table F5. Vapor-Phase Catalysts (continued)

35-BKW-41, RuO_2

Reactor Temp	Vaporizer Temp	Run Time (min)	% C Bal	CH4 Conv	O2 Conv	% CO2	% CO	% C2H6	% C2H4	Total C2 Sel	Total C1 Sel
650	152	60	98.4	5.85	9.11	0.094	0.524	0.088	0.031	27.75	72.25
650	200	90	100.2	5.79	6.04	0.117	0.798	0.105	0.045	24.49	74.91
650	300	120	100.5	4.01	6.46	0.085	0.578	0.094	0.033	27.74	72.26
650	400	160	100.5	6.50	7.07	0.114	0.964	0.113	0.053	23.58	76.42
650	500	195	100.2	5.93	8.93	0.080	0.851	0.108	0.046	24.67	74.61
650	600	230	100.6	3.03	6.58	0.046	0.483	0.080	0.025	28.36	71.64
650	650	275	100.2	2.54	-5.16	0.053	0.326	0.066	0.017	30.45	69.55
750	650	360	110.2	28.95	70.71	1.289	5.821	0.194	0.380	13.79	85.42
750	750	1310	112.1	34.63	75.86	1.390	7.388	0.188	0.443	12.49	86.88
750	183	1475	113.2	28.59	68.50	1.139	6.477	0.203	0.447	14.50	84.97

35-BKW-44, CsCl

Reactor Temp	Vaporizer Temp	Run Time (min)	% C Bal	CH4 Conv	O2 Conv	% CO2	% CO	% C2H6	% C2H4	Total C2 Sel	Total C1 Sel
750	188	70	114.8	34.15	79.12	0.718	8.338	0.196	0.533	13.77	86.23
750	750	100	100.8	5.68	16.35	0.048	0.875	0.115	0.091	29.92	68.96
750	800	190	101.0	9.85	22.62	0.083	1.523	0.134	0.188	28.27	71.74
750	850	270	106.0	17.19	39.55	0.245	3.528	0.139	0.362	20.48	77.97
750	864	310	106.4	21.82	44.76	0.350	4.499	0.134	0.406	18.06	81.94
750	188	5975	101.0	10.46	16.63	0.082	1.596	0.161	0.170	27.55	71.03

Table F5. Vapor-Phase Catalysts (continued)

35-BKW-47, CsCl in Vaporizer and $BaCO_3/Al_2O_3$ in Reactor

Reactor Temp	Vaporizer Temp	Run Time (min)	% C Bal	CH4 Conv	O2 Conv	% CO2	% CO	% C2H6	% C2H4	Total C2 Sel	Total C1 Sel	ppm ECl
750	185	85	99.7	21.08	35.88	1.063	1.188	0.365	0.665	46.49	51.10	20
750	650	120	100.0	21.03	34.54	1.088	1.050	0.390	0.706	48.87	47.92	20
750	700	185	100.0	20.02	34.60	1.027	0.878	0.417	0.698	52.22	47.85	20
750	750	220	99.2	21.32	35.92	1.045	0.857	0.436	0.728	53.06	43.57	20
750	750	1290	101.2	23.16	42.94	1.441	1.007	0.466	0.846	50.17	47.01	20
750	750	1395	102.1	39.57	64.53	3.154	2.598	0.311	1.238	33.83	63.06	40
750	188	1440	98.2	34.26	69.97	2.238	1.927	0.322	1.051	37.90	57.75	40
750	188	1520	101.0	39.31	66.77	2.895	3.329	0.224	1.005	27.68	70.44	40
750	750	1605	100.2	36.04	74.71	2.674	2.163	0.330	1.191	37.60	60.02	40
750	850	1745	99.7	40.49	56.57	3.130	2.303	0.349	1.241	36.13	61.96	40
750	185	1800	101.1	36.16	69.25	2.776	2.428	0.303	1.126	34.66	63.39	40
750	185	2655	103.0	41.54	76.35	3.458	3.757	0.205	1.040	25.20	73.38	40
750	185	2720	101.7	41.25	74.15	3.246	3.635	0.202	0.993	25.09	72.60	10
750	185	2900	101.1	43.04	74.26	3.403	3.909	0.187	0.960	23.39	74.95	10
750	185	3055	104.2	41.54	72.43	3.444	4.064	0.185	0.946	22.48	75.01	20
750	750	3115	101.1	39.36	62.83	3.217	2.783	0.264	1.079	30.23	67.84	20
750	750	4590	100.5	28.31	49.98	2.127	1.784	0.344	0.752	35.18	63.12	20

Initial results at 160 sccm flow rate. After 1395 m, 80 sccm flow rate.

Table F6. Molecular Sieve Catalysts

Name	Wt	Catalyst	Temp	Ccm	CH4 C	Sel	Yield	O2 C	=/-	CO2/CO	CH4/O2	CH4 in	O2 in	C Bal	Time	GHSV	C	ECI	R
29 BKW 142 R#3	0.5	MnApso-5	700	50	20.9	3.1	0.7	69.1	0.8	0.99	2.1	9.6	4.6	103	45	5455	C	0	A
29 BKW 142 R#3	0.5	MnApso-5	700	50	19.6	2.8	0.6	64.8	0.7	0.89	2.1	9.6	4.6	103	195	5455		0	A
29 BKW 142 R#3	0.5	MnApso-5	700	50	18.6	3.3	0.6	60.4	0.6	0.69	2.1	10.1	4.8	102	1065	5455		0	A
29 BKW 143 R#4	0.5	CoApso-34	700	50	19.9	2.5	0.5	62.6	1.3	0.71	2.1	9.6	4.6	103	90	3000	C	0	A
29 BKW 143 R#4	0.5	CoApso-34	700	50	19.3	2.5	0.5	61.1	1.3	0.70	2.1	9.6	4.6	103	135	3000		0	A
29 BKW 143 R#4	0.5	CoApso-34	700	50	18.2	2.6	0.5	56.6	1.0	0.73	2.1	10.1	4.8	102	1110	3000		0	A
29 BKW 146 R#3	0.5	MnApso-34	700	50	26.3	5.5	1.5	85.1	2.1	0.48	2.1	10.1	4.8	104	30	3333	C	0	A
29 BKW 146 R#3	0.5	MnApso-34	700	50	26.8	3.3	0.9	83.4	1.0	0.56	2.1	10.1	4.8	102	120	3333		0	A
29 BKW 146 R#3	0.5	MnApso-34	700	50	24.0	3.1	0.8	80.2	1.0	0.59	1.9	10.2	5.3	103	1320	3333		0	A
29 BKW 147 R#4	0.5	MApo-34	700	50	3.1	15.5	0.5	4.7	0.3	0.54	2.1	10.1	4.8	99	75	4286	C	0	A
29 BKW 147 R#4	0.5	MApo-34	700	50	3.6	17.9	0.6	3.9	0.3	0.41	2.1	10.1	4.8	98	165	4286		0	A
29 BKW 147 R#4	0.5	MApo-34	800	50	10.8	27.5	3.0	23.2	1.7	0.11	2.1	10.1	4.8	100	450	4286	C	0	A
29 BKW 147 R#4	0.5	MApo-34	800	50	11.0	27.6	3.1	23.6	1.8	0.10	2.1	10.1	4.8	100	540	4286		0	A
29 BKW 147 R#4	0.5	MApo-34	800	50	12.1	28.5	3.5	30.4	2.0	0.09	1.9	10.2	5.3	101	1365	4286		0	A
29 BKW 151 R#4	0.5	CoAPO-34	700	50	6.2	22.7	1.5	27.6	2.4	0.73	2.0	10.1	5.1	108	30	3750	C	0	A
29 BKW 151 R#4	0.5	CoAPO-34	700	50	4.8	13.0	0.6	17.4	0.4	0.28	2.0	10.1	5.1	101	120	3750		0	A
29 BKW 151 R#4	0.5	CoAPO-34	800	50	19.0	22.5	4.3	47.0	2.7	0.15	2.0	10.1	5.1	101	405	3750	C	0	A
29 BKW 151 R#4	0.5	CoAPO-34	800	50	18.2	23.4	4.3	44.5	2.7	0.13	2.0	9.9	4.9	101	540	3750		0	A
29 BKW 151 R#4	0.5	CoAPO-34	800	20	24.8	17.9	4.5	63.9	3.6	0.17	2.0	9.9	4.9	102	1380	1500	C	0	A
30 BKW 66 R#3	0.5	AlPO4-5,powder	600	50	6.6	0.7	0.1	22.5	0.0	2.36	2.0	10.3	5.0	100	30	1875	C	0	C
30 BKW 66 R#3	0.5	AlPO4-5,powder	700	50	23.5	0.8	0.2	73.5	0.6	0.24	2.0	10.3	5.0	104	120	1875	C	0	C
30 BKW 66 R#3	0.5	AlPO4-5,powder	700	50	23.3	0.7	0.2	73.1	0.5	0.25	2.0	10.3	5.0	103	210	1875		0	C
30 BKW 66 R#3	0.5	AlPO4-5,powder	750	50	29.8	1.5	0.5	90.6	0.9	0.22	2.0	10.3	5.0	105	300	1875	C	0	C
30 BKW 66 R#3	0.5	AlPO4-5,powder	750	50	29.8	1.6	0.5	89.6	0.8	0.23	2.0	10.3	5.0	104	385	1875		0	C
30 BKW 66 R#3	0.5	AlPO4-5,powder	750	50	27.8	1.3	0.4	86.0	1.1	0.22	2.2	10.6	4.9	104	525	1875	C	50	C
30 BKW 66 R#3	0.5	AlPO4-5,powder	750	50	27.6	1.4	0.4	84.7	1.1	0.22	2.2	10.6	4.9	104	705	1875		50	C
30 BKW 66 R#3	0.5	AlPO4-5,powder	750	50	27.3	1.4	0.4	88.4	1.1	0.29	2.2	10.6	4.9	105	4125	1875		50	D
30 BKW 67 R#4	0.5	SAPO-5	600	50	2.3	2.3	0.1	8.8	0.0	11.39	2.0	10.3	5.0	100	75	5000	C	0	D
30 BKW 67 R#4	0.5	SAPO-5	700	50	14.4	0.6	0.1	58.3	0.1	35.11	2.0	10.3	5.0	100	165	5000	C	0	D
30 BKW 67 R#4	0.5	SAPO-5	750	50	20.1	1.4	0.3	76.6	0.1	2.94	2.0	10.3	5.0	101	255	5000	C	0	D
30 BKW 67 R#4	0.5	SAPO-5	750	50	19.8	1.5	0.3	73.8	0.1	2.13	2.0	10.3	5.0	101	345	5000		0	D
30 BKW 67 R#4	0.5	SAPO-5	750	50	17.7	1.4	0.3	71.9	0.1	1.32	2.0	10.3	5.0	103	435	5000	C	50	D
30 BKW 67 R#4	0.5	SAPO-5	750	50	19.4	1.3	0.3	67.1	0.3	0.76	2.2	10.6	4.9	101	570	5000		50	D
30 BKW 67 R#4	0.5	SAPO-5	750	50	18.4	1.7	0.3	61.9	0.3	0.41	2.1	10.6	5.1	102	1110	5000		50	D
30 BKW 80 R#4	0.5	MAPO-36,powder	600	50	0.9	8.8	0.1	5.6	0.0	###	1.9	10.1	5.3	100	45	4286	C	0	C
30 BKW 80 R#4	0.5	MAPO-36,powder	600	50	1.3	8.8	0.1	5.3	0.0	###	1.9	10.1	5.3	99	135	4286		0	C
30 BKW 80 R#4	0.5	MAPO-36,powder	700	50	4.4	9.1	0.4	12.4	0.3	1.73	1.9	10.1	5.3	98	225	4286	C	0	C
30 BKW 80 R#4	0.5	MAPO-36,powder	750	50	7.3	15.1	1.1	17.5	0.4	0.49	1.9	10.1	5.3	98	315	4286	C	0	C
30 BKW 80 R#4	0.5	MAPO-36,powder	750	50	6.2	16.1	1.0	14.7	0.7	0.30	2.1	10.4	5.1	101	405	4286	C	50	C
30 BKW 80 R#4	0.5	MAPO-36,powder	750	50	7.0	16.6	1.2	14.6	0.7	0.22	2.1	10.4	5.1	100	540	4286		50	C
30 BKW 80 R#4	0.5	MAPO-36,powder	750	50	4.8	17.4	0.9	15.3	0.7	0.19	2.0	10.3	5.1	102	1260	4286		50	C
30 BKW 95 R#3	0.5	Highly Acidic Molecular Sieve	250	50	-1.3	3.5	0.0	0.8	-0.3	###	2.0	10.1	5.2	101	50	2000	C	0	D
30 BKW 95 R#3	0.5	Highly Acidic Molecular Sieve	250	50	-0.6	25.1	-0.1	0.6	3.6	###	2.0	10.1	5.2	101	80	2000		0	D

Table F6. Molecular Sieve Catalysts (continued)

Name	Wt	Catalyst	Temp	Ccm	CH4 C	Sel	Yield	O2 C	=/-	CO2/CO	CH4/O2	CH4 in	O2 in	C Bal	Time	GHSV	C	ECI	R
30 BKW 95 R#3	0.5	Highly Acidic Molecular Sieve	295	50	-0.5	1.0	0.0	1.2	-0.5	###	2.0	10.1	5.2	101	125	2000	C	0	D
30 BKW 95 R#3	0.5	Highly Acidic Molecular Sieve	295	50	-0.1	2.4	0.0	0.7	-0.4	###	2.0	10.1	5.2	100	165	2000		0	D
30 BKW 95 R#3	0.5	Highly Acidic Molecular Sieve	500	50	0.2	3.0	0.0	1.3	-0.3	###	2.0	10.1	5.2	100	205	2000	C	0	D
30 BKW 95 R#3	0.5	Highly Acidic Molecular Sieve	500	50	0.2	19.7	0.0	1.2	153.0	###	2.0	10.1	5.2	100	240	2000		0	D
30 BKW 95 R#3	0.5	Highly Acidic Molecular Sieve	600	50	1.4	-0.4	0.0	5.0	0.8	###	2.0	10.1	5.2	99	315	2000	C	0	D
30 BKW 95 R#3	0.5	Highly Acidic Molecular Sieve	600	50	0.6	1.7	0.0	3.7	3.5	###	2.0	10.1	5.2	100	350	2000		0	D
30 BKW 95 R#3	0.5	Highly Acidic Molecular Sieve	700	50	2.7	11.1	0.3	9.4	0.2	1.68	2.0	10.1	5.2	99	500	2000	C	0	D
30 BKW 95 R#3	0.5	Highly Acidic Molecular Sieve	700	50	2.2	11.6	0.3	8.7	0.2	1.63	2.0	10.1	5.2	100	680	2000		0	D
30 BKW 95 R#3	0.5	Highly Acidic Molecular Sieve	700	50	2.6	13.8	0.4	4.1	0.2	0.72	2.0	10.1	5.0	99	3920	2000		0	D
30 BKW 95 R#3	0.5	Highly Acidic Molecular Sieve	700	50	3.5	11.1	0.4	8.6	0.6	0.97	2.0	10.3	5.1	99	4500	2000	C	50	D

* Appendix A and the Experimental Section describe Table headings and experimental procedures.
The C column shows a letter C whenever a process change was made. =/- is the ethylene to ethane molar ratio.

Inaccurate due to a small number, division by a small number, or not applicable.

Table F7. Hydrotalcite Catalysts

Name	Wt	Catalyst	Temp	Ccm	CH4 C	Sel	Yield	O2 C	=/-	CO2/CO	CH4/O2	CH4 in	O2 in	C Bal	Time	GHSV	ECI
33 BKW 33 R#3	1.5	MgAlOH,60/100	750	160	36.7	3.7	1.4	98	1.4	1.5	2.0	10.2	5.1	102	50	2341	0
33 BKW 33 R#3	1.5	MgAlOH,60/100	750	160	36.7	-0.1	0.0	97	0.0	1.5	2.0	10.2	5.1	101	120	2341	0
33 BKW 33 R#3	1.5	MgAlOH,60/100	700	160	26.7	0.4	0.1	62	0.9	0.9	2.0	10.2	5.1	102	210	2341	0
33 BKW 33 R#3	1.5	MgAlOH,60/100	700	160	26.3	0.3	0.1	63	0.0	0.9	2.0	10.1	5.1	102	390	2341	0
33 BKW 33 R#3	1.5	MgAlOH,60/100	700	160	26.2	0.6	0.2	62	0.6	0.9	2.0	10.1	5.1	103	795	2341	0
33 BKW 33 R#3	1.5	MgAlOH,60/100	700	160	25.7	0.5	0.1	61	0.7	0.9	2.0	10.2	5.0	103	1290	2341	0
33 BKW 33 R#3	1.5	MgAlOH,60/100	700	160	26.4	0.6	0.2	62	0.6	0.9	2.0	10.3	5.1	102	1380	2341	10
33 BKW 33 R#3	1.5	MgAlOH,60/100	700	160	26.6	0.6	0.2	62	0.6	0.9	2.0	10.3	5.1	102	1470	2341	10
33 BKW 34 R#4	1.5	MgAlOH,60/100	750	160	35.8	5.6	2.0	99	1.3	2.3	2.0	10.2	5.1	101	95	2341	0
33 BKW 34 R#4	1.5	MgAlOH,60/100	700	160	32.0	1.9	0.6	99	0.6	7.2	2.0	10.2	5.1	99	185	2341	0
33 BKW 34 R#4	1.5	MgAlOH,60/100	700	160	32.3	1.8	0.6	99	0.6	6.6	2.0	10.2	5.1	99	275	2341	0
33 BKW 34 R#4	1.5	MgAlOH,60/100	700	160	33.1	1.5	0.5	98	0.5	4.2	2.0	10.1	5.1	101	1040	2341	0
33 BKW 34 R#4	1.5	MgAlOH,60/100	650	160	21.6	0.1	0.0	68	0.0	14.4	2.0	10.2	5.0	100	1175	2341	0
33 BKW 34 R#4	1.5	MgAlOH,60/100	650	160	21.8	0.1	0.0	68	0.0	10.8	2.0	10.2	5.0	100	1265	2341	0
33 BKW 34 R#4	1.5	MgAlOH,60/100	650	160	24.1	0.3	0.1	67	0.5	9.8	2.0	10.3	5.1	98	1355	2341	10
33 BKW 34 R#4	1.5	MgAlOH,60/100	650	160	22.2	0.3	0.1	67	0.6	9.3	2.0	10.3	5.1	99	1425	2341	10
33 BKW 39 R#4	1.5	MgAlOH,60/100	750	160	35.8	3.2	1.2	93	1.3	1.3	2.0	10.5	5.2	103	200	2341	0
33 BKW 39 R#4	1.5	MgAlOH,60/100	750	160	36.0	3.2	1.2	93	1.3	1.3	2.0	10.5	5.2	103	290	2341	0
33 BKW 39 R#4	1.5	MgAlOH,60/100	750	160	35.4	3.4	1.2	92	1.2	1.3	2.0	10.6	5.2	103	605	2341	0
33 BKW 39 R#4	1.5	MgAlOH,60/100	750	160	34.8	3.5	1.2	90	1.3	1.3	2.0	10.5	5.2	103	1565	2341	0
33 BKW 39 R#4	1.5	MgAlOH,60/100	750	160	35.0	3.2	1.1	90	1.5	1.3	2.0	10.4	5.2	103	1685	2341	10
33 BKW 39 R#4	1.5	MgAlOH,60/100	750	160	36.1	3.0	1.1	90	1.7	1.3	2.0	10.4	5.2	102	1775	2341	10
33 BKW 39 R#4	1.5	MgAlOH,60/100	750	160	35.0	3.6	1.3	89	1.4	1.2	2.0	10.4	5.2	104	2270	2341	10
33 BKW 42 R#3	1.5	BaCO3,MgAlOH,60/100	750	160	34.7	5.8	2.0	99	1.4	2.4	2.0	10.3	5.2	102	40	2400	0
33 BKW 42 R#3	1.5	BaCO3,MgAlOH,60/100	725	160	33.0	1.7	0.6	92	0.9	2.0	2.0	10.3	5.2	102	100	2400	0
33 BKW 42 R#3	1.5	BaCO3,MgAlOH,60/100	725	160	33.1	1.7	0.6	91	0.9	2.0	2.0	10.3	5.2	102	210	2400	0
33 BKW 42 R#3	1.5	BaCO3,MgAlOH,60/100	725	160	32.5	1.4	0.5	89	0.9	1.9	2.0	10.4	5.2	102	1290	2400	0
33 BKW 42 R#3	1.5	BaCO3,MgAlOH,60/100	725	160	33.4	1.6	0.5	87	1.2	1.8	2.0	10.4	5.2	101	1470	2400	10
33 BKW 42 R#3	1.5	BaCO3,MgAlOH,60/100	725	160	33.6	2.0	0.7	86	1.3	1.6	2.0	10.4	5.2	102	1650	2400	10
33 BKW 42 R#3	1.5	BaCO3,MgAlOH,60/100	725	160	34.2	2.8	1.0	87	1.1	1.1	2.0	10.3	5.2	103	2640	2400	10
33 BKW 42 R#3	1.5	BaCO3,MgAlOH,60/100	725	160	34.2	2.7	1.0	87	1.2	1.1	2.0	10.3	5.2	104	3090	2400	200
33 BKW 42 R#3	1.5	BaCO3,MgAlOH,60/100	725	160	36.9	8.8	3.5	86	2.7	0.6	2.0	10.3	5.2	106	3270	2400	200
33 BKW 42 R#3	1.5	BaCO3,MgAlOH,60/100	725	160	38.8	11.2	4.6	90	2.8	0.6	2.0	10.2	5.2	106	170	2400	200
33 BKW 43 R#4	1.5	BaCO3,MgAlOH,60/100	750	160	34.9	4.2	1.5	99	1.3	2.2	2.0	10.3	5.2	102	75	2400	0
33 BKW 43 R#4	1.5	BaCO3,MgAlOH,60/100	725	160	33.2	1.5	0.5	91	0.8	1.9	2.0	10.3	5.2	102	130	2400	0
33 BKW 43 R#4	1.5	BaCO3,MgAlOH,60/100	725	160	33.1	1.4	0.5	90	0.8	1.8	2.0	10.3	5.2	102	255	2400	0
33 BKW 43 R#4	1.5	BaCO3,MgAlOH,60/100	725	160	32.3	1.1	0.4	86	0.9	1.7	2.0	10.4	5.2	102	1330	2400	0
33 BKW 43 R#4	1.5	BaCO3,MgAlOH,60/100	725	160	33.4	1.4	0.5	85	1.2	1.6	2.0	10.4	5.2	101	1515	2400	10

Table F7. Hydrotalcite Catalysts (continued)

Name	Wt	Catalyst	Temp	Ccm	CH4 C	Sel	Yield	O2 C	=/-	CO2/CO	CH4/O2	CH4 in	O2 in	C Bal	Time	GHSV	ECI
33 BKW 43 R#4	1.5	BaCO3,MgAlOH,60/100	725	160	33.2	1.7	0.6	85	1.3	1.5	2.0	10.4	5.2	102	1695	2400	10
33 BKW 43 R#4	1.5	BaCO3,MgAlOH,60/100	725	160	34.2	2.4	0.9	86	1.1	1.1	2.0	10.3	5.2	103	2595	2400	10
33 BKW 43 R#4	1.5	BaCO3,MgAlOH,60/100	725	160	35.1	4.5	1.7	86	2.1	1.0	2.0	10.3	5.2	104	3135	2400	200
33 BKW 43 R#4	1.5	BaCO3,MgAlOH,60/100	725	160	37.1	8.2	3.2	87	2.7	0.6	2.0	10.3	5.2	106	3315	2400	200
33 BKW 43 R#4	1.5	BaCO3,MgAlOH,60/100	725	160	38.2	9.7	4.0	89	2.8	0.6	2.0	10.2	5.2	106	4125	2400	200
33 BKW 48 R#3	1.5	BaCO3,MgAlOH,60/100	675	160	30.3	3.3	1.0	99	0.6	11.1	2.0	10.4	5.2	99	30	2400	0
33 BKW 48 R#3	1.5	BaCO3,MgAlOH,60/100	675	160	29.4	1.9	0.6	99	0.5	12.4	2.0	10.4	5.2	100	150	2400	0
33 BKW 48 R#3	1.5	BaCO3,MgAlOH,60/100	675	160	27.9	0.2	0.1	86	0.0	5.5	2.0	10.4	5.3	101	3750	2400	0
33 BKW 48 R#3	1.5	BaCO3,MgAlOH,60/100	675	160	31.8	0.7	0.2	85	1.0	5.5	2.0	10.4	5.1	97	3885	2400	10
33 BKW 48 R#3	1.5	BaCO3,MgAlOH,60/100	675	160	30.4	1.9	0.6	91	0.9	3.4	2.0	10.4	5.1	103	3970	2400	10
33 BKW 48 R#3	1.5	BaCO3,MgAlOH,60/100	675	160	33.3	1.8	0.6	93	0.6	1.9	2.0	10.4	5.1	103	4065	2400	10
33 BKW 48 R#3	1.5	BaCO3,MgAlOH,60/100	675	160	33.8	1.6	0.6	94	0.5	1.6	2.0	10.4	5.1	103	4140	2400	10
33 BKW 48 R#3	1.5	BaCO3,MgAlOH,60/100	675	160	33.2	1.1	0.4	89	0.5	1.3	2.0	10.3	5.1	104	4335	2400	2
33 BKW 48 R#3	1.5	BaCO3,MgAlOH,60/100	675	160	32.9	0.8	0.3	86	0.4	1.2	2.0	10.3	5.1	103	4425	2400	2
33 BKW 48 R#3	1.5	BaCO3,MgAlOH,60/100	675	160	25.8	0.3	0.1	66	0.6	1.0	2.0	10.3	5.1	104	5685	2400	2
33 BKW 48 R#3	1.5	BaCO3,MgAlOH,60/100	675	160	26.7	0.3	0.1	65	0.6	1.0	2.0	10.4	5.2	103	5955	2400	200
33 BKW 48 R#3	1.5	BaCO3,MgAlOH,60/100	675	160	27.0	0.4	0.1	64	0.6	0.9	2.0	10.4	5.2	103	6135	2400	200
33 BKW 48 R#3	1.5	BaCO3,MgAlOH,60/100	675	160	32.5	3.1	1.1	74	1.6	0.4	2.0	10.3	5.2	107	6720	2400	200

Appendix A and the Experimental Section describe Table headings and experimental procedures.
Reactor D was used for all experiments.

Table F8. Summary of Experimental Variables for Homogeneous Gas Phase Experiments

Experiment #	T (C)	P (psig)	CH4/O2 Ratio (mole/mole)	FR* (cc/min)	FR(reactor)** (cc/min)	Residence Time*** (sec)
1	750	10	8.36/1	100	208	7.25
2	850	15	14.3/1	164	311	4.84
3	850	15	14.3/1	56.9	108	14.0
4	850	15	2.09/1	163	309	4.87
5	850	15	2.03/1	55.7	106	14.3
6	850	5	15.2/1	108	309	4.88
7	850	5	14.7/1	35.9	103	14.7
8	850	5	2.09/1	110	315	4.79
9	850	5	2.01/1	36.1	103	14.6
10	750	10	8.29/1	100	208	7.25
11	649	15	14.3/1	202	315	4.79
12	649	15	14.6/1	67.1	105	14.4
13	649	15	2.05/1	201	313	4.81
14	649	15	2.06/1	67.1	105	14.4
15	649	5	14.6/1	133	312	4.82
16	649	5	14.7/1	43.5	102	14.7
17	649	5	2.00/1	133	312	4.82
18	650	5	2.00/1	43.8	103	14.6
19	749	10	8.14/1	100	208	7.25

*: Ambient conditions.
**: FR(reactor)= FR x (14.7/(P+14.7)) x ((T+273)/293)
***: Residence Time = [Void Volume/FR(reactor)] x 60; where, the void volume of the quartz bed is 25.1cc

Table F8. **Summary of Experimental Results for Homogeneous Gas Phase Experiments (Continued)**

Experiment #	CH4 Conv. (%)	O2 Conv. (%)	C2 Sele. (%)	C3 Sele. (%)	C2 Yield (%)	Ethylene/Ethane (mole/mole)	CO2/CO (mole/mole)	C Balance (%)
1	3.9	10.9	51.2	1.9	1.9	0.5	0.08	97.7
2	4.4	54.3	53.1	7.3	2.4	2.1	0.02	101.3
3	7.7	93.5	38.9	7.3	3.0	6.1	0.06	100.3
4	37.7	92.6	20.2	1.1	7.5	4.8	0.13	96.7
5	38.3	94.4	15.3	0.9	5.7	10.4	0.13	96.6
6	3.1	28.7	58.6	6.1	1.8	1.4	0.03	100.3
7	7.6	82.9	41.9	6.0	3.2	4.2	0.05	99.7
8	35.4	81.2	25.3	1.4	8.6	4.1	0.06	96.4
9	39.3	93.5	16.3	0.7	6.0	7.4	0.03	93.7
10	1.2	9.5	48.9	1.5	0.6	0.4	0.03	100.3
11	**	1.4	**	**	**	**	**	101.0
12	0.8	2.5	30.4	0.0	0.2	0.1	0.04	99.5
13	1.1	***	23.2	0.0	0.3	0.0	****	99.6
14	3.3	1.9	21.8	0.5	0.7	0.2	****	98.5
15	**	0.4	**	**	**	**	**	100.4
16	**	2.7	**	**	**	**	**	100.1
17	1.3	1.1	19.8	0.0	0.3	0.0	****	98.9
18	0.7	***	27.2	0.0	0.2	0.2	0.22	100.2
19	2.1	11.0	53.7	2.3	1.1	0.5	0	99.8

**: CH4 conversion too low for meaningful results.
***: O2 conversion too low for meaningful results.
****: CO2 amount too low for meaningful results.

Table F9. Results of Reactor Validation Runs

Run Reference: 33-NEK-40
Catalyst: 33-NEK-34-3 4.77wt% $BaCO_3$ on 30/60 mesh Norton SA5451 alumina. Prepared by the slurry method. Charged 15cc = 16.34g

	CONDITIONS								RESULTS,%**			
HOS*	O_2	N_2	CH_4	Steam	ECl(ppm)	Temp	GHSV	Press	C Conv	C2 Sel	Yield	C2=/C2
0.0	5.0	0.7	10	0.0	7	750	2228	11	35.2	55.1	17.5	1.96
44.8	5.0	**0.8**	10	0.0	**8**	750	2228	11	34.2	52.3	16.5	1.92
70.9	Changed range on TCD from 0.5 to 0.05 mV											
161.3	Purging with argon, while analyzing feed gas.											
164.5	**5.5**	**0.9**	**11**	0.0	**9**	750	2228	11	35.7	52.3	16.8	1.92
184.6	5.0	0.8	10	**8.5**	8	750	2228	11	34.7	44.7	14.4	1.89
190.0	Reprimed liquid pump, had not been pumping continuously											
216.0	5.0	0.8	10	**17.0**	8	750	2228	11	30.9	42.0	11.3	1.41
256.6	5.0	0.8	10	17.0	8	**770**	2228	11	20.7	43.6	8.3	1.24
315.0	System ESD'd											
334.0	5.0	0.8	10	17.0	8	770	2228	11	10.7	42.0	4.3	0.57
341.0	Shutdown											

* Time change was made or event occurred
** Just prior to next change

Table F10. Results of Reactor Validation Runs

Run Reference: 33-NEK-40
Catalyst: 33-NEK-34-3 4.77wt% $BaCO_3$ on 30/60 mesh Norton SA5451 alumina. Prepared by the slurry method. Charged 15cc = 16.34g

	CONDITIONS								RESULTS,%**			
HOS*	O_2	N_2	CH_4	Steam	ECl(ppm)	Temp	GHSV	Press	C Conv	C2 Sel	Yield	C2=/C2
0.0	5.0	0.7	10	0.0	7	750	2228	11	35.2	55.1	17.5	1.96
44.8	5.0	**0.8**	10	0.0	**8**	750	2228	11	34.2	52.3	16.5	1.92
70.9	Changed range on TCD from 0.5 to 0.05 mV											
161.3	Purging with argon, while analyzing feed gas.											
164.5	**5.5**	**0.9**	**11**	0.0	**9**	750	2228	11	35.7	52.3	16.8	1.92
184.6	5.0	0.8	10	**8.5**	8	750	2228	11	34.7	44.7	14.4	1.89
190.0	Reprimed liquid pump, had not been pumping continuously											
216.0	5.0	0.8	10	**17.0**	8	750	2228	11	30.9	42.0	11.3	1.41
256.6	5.0	0.8	10	17.0	8	**770**	2228	11	20.7	43.6	8.3	1.24
315.0	System ESD'd											
334.0	5.0	0.8	10	17.0	8	770	2228	11	10.7	42.0	4.3	0.57
341.0	Shutdown											

* Time change was made or event occurred
** Just prior to next change

Table F11. Test Results Using Steam as a Diluent

Run Reference: 33-NEK-70
Catalyst: 33-NEK-44 5.03 wt% $BaCl_2$ on 14-30 mesh Norton SA5402 alumina. Prepared by the slurry method. Charged 19.25cc = 19.87g

	CONDITIONS								RESULTS,%**				
HOS*	O_2	N_2	CH_4	Steam	ECl(ppm)	Temp	GHSV	Press	C Conv	C2 Sel	Yield	C2=/C2	Rate
0.0	5.2	22.6	9.5	0.0	225	750	814	11	47.0	41.1	19.2	7.42	63
22.9	**10.4**	22.6	**11.0**	0.0	225	750	814	11	34.2	38.8	13.5	4.64	93
24.8	GCs not working												
40.0	Restarted GCs												
43.8	10.4	**25.4**	11.0	0.0	**257**	750	814	11	38.3	38.2	13.8	4.65	91
47.0	**5.2**	**22.6**	**9.5**	0.0	**225**	750	814	11	37.2	41.7	15.5	5.70	51
64.8	5.2	22.6	9.5	0.0	225	**765**	814	11	43.8	42.1	17.6	7.22	54
71.9	5.2	22.6	9.5	0.0	225	**780**	814	11	45.3	35.4	15.9	8.22	52
155.0	Flame out on FID												
161.0	Flame on												
163.0	5.2	22.6	9.5	0.0	225	780	814	**16**	47.6	34.6	15.3	8.80	46
191.5	5.2	22.6	**72.2**	0.0	225	780	814	16	10.1	55.3	5.5	2.84	120
209.9	5.2	22.6	**69.8**	**2.4**	225	780	814	16	10.4	52.0	5.3	2.89	118
237.5	5.2	22.6	**67.4**	**4.8**	225	780	814	16	9.1	49.7	4.5	2.77	108
264.0	5.2	22.6	67.4	4.8	225	**750**	814	**11**	6.0	44.3	2.6	1.31	57
333.3	Shut down												

* Time change was made or event occurred
** Just prior to next change

Table F12. Test Results Using Steam as a Diluent

Run Reference: 33-NEK-86
Catalyst: 33-NEK-68A 5.03 wt% $BaCl_2$ on 14-30 mesh Norton SA5402 alumina. Prepared by the slurry method. Charged 22cc = 22.88g

	CONDITIONS								RESULTS,%**			
HOS*	O_2	N_2	CH_4	Steam	ECl(ppm)	Temp	GHSV	Press	C Conv	C2 Sel	Yield	C2=/C2
0.0	5.0	23.0	8.9	0.0	230	750	782	11	50.1	43.6	21.5	8.75
24.0	5.0	23.0	8.9	**2.1**	230	750	782	11	33.0	43.6	14.3	5.16
90.4	5.0	23.0	8.9	**4.3**	230	750	782	11	32.5	43.3	14.0	5.10
120.0	5.0	23.0	8.9	**6.5**	230	750	782	11	29.3	45.5	13.2	4.69
139.5	5.0	23.0	8.9	**10.8**	230	750	782	11	22.9	44.5	10.7	4.44
166.3	**5.6**	**28.8**	**11.2**	**28.8**	**290**	750	782	11	26.9	25.2	6.7	3.51
264.8	**5.0**	**23.0**	**8.9**	**10.8**	**230**	750	782	11	No data			
285.0	Reactor pressure at 18 psig, couldn't be reduced, shut down unit											

* Time change was made or event occurred
** Just prior to next change

Table F13. Test Results Using Steam as a Diluent

Run Reference: 33-NEK-110
Catalyst: 33-NEK-68B 5.03 wt% $BaCl_2$ on 14/30 mesh Norton SA5402 alumina. Prepared by the slurry method. Charged 22cc = 23.47g

	CONDITIONS								RESULTS,%**				
HOS*	O_2	N_2	CH_4	Steam	ECl(ppm)	Temp	GHSV	Press	C Conv	C2 Sel	Yield	C2=/C2	Rate
0.0	5.0	23.5	72.5	0.0	235	750	782	11	6.5	66.1	4.3	1.51	94
65.0	System was shutdown, ESD was activated, reactor temp was 441 C. Restarted unit.												
112.5	5.0	23.5	67.2	**5.0**	235	750	782	11	7.0	67.7	4.7	1.83[a]	90
144.0	Switch to helium carrier gas on GC												
162.4	5.0	23.5	**62.2**	**10.0**	235	750	782	11	7.7	63.6	4.8	1.62	78
233.0	Unit ESD'd. Temp = 600 °C. Restarted unit with He purge while analyzing feed gas.												
238.7	5.0	23.5	**57.2**	**15.0**	235	750	782	11	7.1	62.8	4.3	1.41	67
240.3	Switched feed to reactor.												
260.8	5.0	23.5	**30.0**	**42.2**	235	750	782	11	14.1	36.8	5.3	2.36	49
285.3	Shutdown.												

* Time change was made or event occurred
** Just prior to next change
[a] Higher ratio than for 0.0 HOS result is due to recalibrating with He, probably not due to steam.

Table F14. Test Results Using Steam as a Diluent

Run Reference: 33-NEK-122 **Helium as Diluent**
Catalyst: 33-NEK-68B 5.03 wt% $BaCl_2$ on 14/30 mesh Norton SA5402 alumina. Prepared by the slurry method. Charged 22cc = 23.36g

	CONDITIONS								RESULTS,%**				
HOS*	O_2	N_2	CH_4	Steam	ECl(ppm)	Temp	GHSV	Press	C Conv	C2 Sel	Yield	C2=/C2	Rate
0.0	4.6	22.5	8.5	0.0	225	750	782	11	31.7	48.7	15.1	6.05	
118.3	4.6	**18.2**	**10.0**	0.0	**182**	750	782	11	33.3	47.7	15.3	6.09	
141.0	Shutdown.												

* Time change was made or occurred
** Just prior to next change. CO2 concentration in off-gas less than detection limit after about 50 HOS; the concentration was estimated resulting in the stairstep selectivity observed in the graph.

Table F15. Test Results Using Steam as a Diluent

Run Reference: 33-NEK-132
Catalyst: 33-NEK-129 4.77 wt% $BaCO_3$ on 14/30 mesh Norton SA5402 alumina. Prepared by the slurry method. Charged 15cc = 17.81g

				CONDITIONS					RESULTS,%**			
HOS*	O_2	N_2	CH_4	Steam	ECl(ppm)	Temp	GHSV	Press	C Conv	C2 Sel	Yield	C2=/C2 Rate
0.0	9.6	0.8	89.6	0.0	8.3	750	2227	11	8.8	37.8	3.3	1.11
114.6	9.6	**1.5**	**88.5**	0.0	**15.0**	750	2227	11	8.3	38.4	3.2	1.10
142.5	9.6	**2.3**	**87.8**	0.0	**22.5**	750	2227	11	6.7	38.2	2.6	1.09
161.3	9.6	**3.0**	**87.0**	0.0	**30.0**	750	2227	11	6.2	38.2	2.4	1.07
183.9	9.6	**2.3**	**87.8**	0.0	**22.5**	750	2227	11	6.2	30.7	1.9	0.85
232.6	9.6	2.3	**29.9**	**57.9**	22.5	750	2227	11	12.7	24.2	3.0	1.20
238.3	Unit ESD'd. Restarted.											
239.3	Unit ESD'd. Restarted, again.											
239.8	9.6	2.3	**59.9**	**27.9**	22.5	750	2227	11	5.4	26.1	1.4	0.70
280.0	Shutdown.											

* Time change was made or event occurred
** Just prior to next change.

Table F16. Test Results Using Steam as a Diluent

Run Reference: 34-NEK-58
Catalyst: 34-NEK-44A & B 4.77 wt% $BaCO_3$ on 40/60 mesh Norton SA5451 Alumina. Prepared by the dry mix method. Charged 15cc = 16.37g

				CONDITIONS					RESULTS,%**			
HOS*	O_2	N_2	CH_4	Steam	ECl(ppm)	Temp	GHSV	Press	C Conv	C2 Sel	Yield	C2=/C2 Rate
0.0	5.0	0.8	9.4	0.0	8	750	2228	11	40.9	29.8	11.8	2.48
26.4	5.0	0.8	9.4	0.0	8	750	**3342**	11	36.6	33.2	12.2	2.23
44.4	**10.0**	**3.0**	**30.0**	0.0	**30**	750	3342	11	35.3	46.6	15.8	2.30
49.5	Varying temperature, in an attempt to quench hot spot. Unsuccessful.											
53.2	**5.0**	3.0	30.0	0.0	30	750	3342	11	No data			
53.4	5.0	3.0	30.0	0.0	30	**730**	3342	11	22.2	59.1	12.7	1.53
69.7	5.0	3.0	30.0	**40.0**	30	730	3342	11	22.4	60.7	13.0	2.09
73.9	5.0	3.0	**29.8**	**62.2**	30	730	3342	11	12.7	46.1	5.7	0.76
74.5	No GC data until 95.5 HOS											
97.2	5.0	3.0	29.8	62.2	30	**750**	3342	11	15.6	49.6	7.5	1.20
99.6	5.0	3.0	29.8	62.2	30	**760**	3342	11	12.4	47.3	5.7	1.02
117.4	5.0	3.0	29.8	62.2	30	**770**	3342	11	10.1	45.3	4.5	0.85
146.8	Pump reservoir dry since 137 HOS, added water and primed.											
165.0	5.0	3.0	29.8	**0.0**	30	750	3342	11	6.8	35.3	2.4	0.41
173.1	Shutdown.											

* Time change was made or event occurred
** Just prior to next change.

Table F17. Test Results Using Steam as a Diluent

Run Reference: 34-NEK-70
Catalyst: 34-NEK-64 4.77 wt% $BaCO_3$ on 40/60 mesh Norton SA5451 alumina. Prepared by the slurry method. Charged 15cc = 16.26g

	CONDITIONS								RESULTS,%**				
HOS*	O_2	N_2	CH_4	Steam	ECl(ppm)	Temp	GHSV	Press	C Conv	C2 Sel	Yield	C2=/C2	Rate
0.0	4.9	0.8	9.2	0.0	7.8	750	2228	11					
	Reactor ESD'd overnight. Back-pressure regulator was replaced. Unit was restarted at zero hrs.												
0.0	4.9	0.8	9.2	0.0	7.8	750	2228	11	43.8	35.3	15.1	2.86	
23.8	4.9	**3.0**	9.2	0.0	**30**	750	**3342**	11	42.2	40.7	17.3	2.80	
28.6	4.9	3.0	**30.0**	0.0	30	750	3342	11	21.2	64.4	13.9	1.98	
45.3	4.9	3.0	**29.8**	**62.2**	30	750	3342	11	9.5	47.5	4.6	1.05	
69.5	4.9	3.0	29.8	62.2	30	**770**	3342	11	8.5	49.1	4.3	1.06	
93.5	4.9	3.0	29.8	62.2	30	**790**	3342	11	9.5	48.7	4.7	1.35	
117.0	4.9	**8.0**	29.8	**57.2**	**80**	790	3342	11	11.0	52.7	5.8	1.32	
124.8	4.9	**8.7**	**29.6**	**56.8**	**87**	790	3342	11	7.0	48.9	3.5	0.92	
141.3	4.9	**8.0**	**30.2**	56.8	**80**	790	**2228**	11	9.0	47.0	4.2	1.22	
148.8	4.9	8.0	30.2	**0.0**	80	790	2228	11	5.9	45.5	2.7	0.82	
165.5	4.9	**3.0**	30.0	0.0	**30**	790	2228	11	6.6	41.0	2.7	0.81	
172.3	Shutdown.												

* Time change was made or event occurred
** Just prior to next change.

Table F18. Test Results Using Steam as a Diluent

Run Reference: 34-NEK-100
Catalyst: 34-NEK-85 4.16 wt% $Ba(OH)_2$ on Norton SA 5451 alumina 40/60 mesh. Prepared by incipient wetness. Charged 15cc = 15.67g.

	CONDITIONS								RESULTS,%**				
HOS*	O_2	N_2	CH_4	Steam	ECl(ppm)	Temp	GHSV	Press	C Conv	C2 Sel	Yield	C2=/C2	Rate
0.0	4.8	0.8	9.3	0.0	7.8	750	2133	11	45.3	36.5	15.5	3.0	132
19.6	4.8	**0.0**	**30.0**	**65.0**	**500**	750	**3200**	11	8.2	56.7	4.6	1.0	106
68.1	4.8	0.0	30.0	**0.0**	500	750	**2848**	11	4.7	57.8	2.7	1.0	107
75.6	Shutdown.												

* Time change was made or event occurred
** Just prior to next change.

Table F19. High Pressure Blank Run Results

Run Reference: 34-NEK-78 High pressure, blank design set.
Catalyst: None.

	CONDITIONS								RESULTS,%**		
GC#	O_2	N_2	CH_4	Steam	ECl(ppm)	Temp	Flow	Press	C Conv	C2 Sel	Yield
0.0	5.0	0	10.0	0	0	**700**	557	**100**	35.8	16.7	6.0
2.3	**7.5**	0	**30.0**	0	0	700	**1114**	100	19.3	24.6	4.9
5.5	7.5	0	30.0	0	0	700	**557**	**200**	18.1	13.3	2.5
22.0	**5.0**	0	**10.0**	0	0	700	**1114**	200	35.9	14.4	5.3
24.3	**7.5**	0	**30.0**	0	0	**750**	**557**	**100**	20.3	23.5	4.9
27.5	**5.0**	0	**10.0**	0	0	750	**1114**	100	34.3	20.4	7.0
30.5	5.0	0	10.0	0	0	750	**557**	**200**	38.2	12.3	4.6

* Time change was made or occurred
** Just prior to next change

Table F20. Results of Catalyst Evaluation at High Pressure

Run Reference: 34-NEK-96
Catalyst: 34-NEK-87 4.77 wt% $BaCO_3$ on 60/100 mesh Norton SA5451 alumina. Slurry. Charged 7.5cc= 8.6445g

	CONDITIONS								RESULTS,%**				
HOS*	O_2	N_2	CH_4	Steam	ECl(ppm)	Temp	GHSV	Press	C Conv	C2 Sel	Yield	C2=/C2	Rate
0.0	5.0	3.1	29.8	0.0	31	750	4456	200	15.7	30.2	4.8	2.5	288
19.5	Shut-off all feed gases and reduced furnace temp to 500C, while purging with 200 sccm He. Reactor remained at 500C for five days under He purge.												
19.5	Restarted feed to reactor utilizing the original set points.												
39.5	5.0	**9.0**	29.8	0.0	**90**	750	4456	200	15.8	29.8	4.7	2.4	284
47.0	5.0	9.0	29.8	0.0	90	750	4456	**150**	13.8	29.0	4.1	2.5	283
63.1	5.0	9.0	29.8	0.0	90	750	4456	**100**	14.8	32.9	5.0	2.8	325
71.4	5.0	**3.0**	29.8	0.0	**30**	750	4456	100	16.7	44.9	7.5	2.6	446
	The following sets of data comprise a "designed set of experiments" to investigate the effects of temp., pressure, space velocity, and ECl level.												
88.6	5.0	3.0	29.8	0.0	30	750	8912	100	17.3	48.1	8.3	2.4	969
128.2	5.0	**4.5**	29.8	0.0	**45**	**725**	**6684**	**150**	12.3	32.9	4.2	2.1	461
138.5	5.0	**6.0**	29.8	0.0	**60**	**700**	**8912**	**100**	18.5	46.2	8.3	1.6	862
149.6	5.0	6.0	29.8	0.0	60	700	**4456**	**200**	12.0	26.6	3.3	1.6	236
149.9	Shut-off feed and cooled reactor to 600C, while purging with He. Bldg ventilation to be turned off												
165.8	Started system heating to 725C, set flows for center pt.												
170.3	5.0	**4.5**	29.8	0.0	**45**	**725**	**6684**	**150**	12.4	34.6	4.4	2.1	470
181.8	5.0	**3.0**	29.8	0.0	**30**	**700**	**8912**	**200**	12.1	30.7	3.8	1.8	103
192.3	5.0	**6.0**	29.8	0.0	**60**	**750**	8912	200	13.7	32.7	4.6	2.6	635
207.8	5.0	**3.0**	29.8	0.0	**30**	750	**4456**	200	15.3	30.5	4.7	2.6	283
214.0	5.0	**6.0**	29.8	0.0	**60**	750	4456	**100**	14.2	43.2	6.3	2.7	426
229.8	5.0	**3.0**	29.8	0.0	**30**	**700**	4456	100	13.2	36.7	4.9	1.4	298
236.9	5.0	**4.5**	29.8	0.0	**45**	**725**	**6684**	**150**	12.8	34.2	4.5	2.1	470
254.8	5.0	**3.0**	29.8	0.0	**30**	**750**	**8912**	**100**	13.2	45.2	6.1	2.1	813
254.9	End "design set of experiments".												
258.5	5.0	**6.0**	29.8	0.0	**60**	750	8912	100	17.2	46.6	7.8	2.1	773
261.2	5.0	**6.0**	29.8	0.0	**260**	750	8912	100	18.4	43.4	7.7	2.8	740
285.0	5.0	**6.0**	29.8	0.0	**60**	750	8912	100	15.8	44.0	6.7	2.0	607
301.9	Shutdown.												

* Time change was made or occurred
** Just prior to next change

Table F21. Results from High Pressure Designed Set of Experiments, Run 33-NEK-96

Conditions					Selectivity,%			C2	C2			
Temp	Press	flow	ECL	C Conv	CO	CO2	C2	Yield	Rate	C2=/C2	CO2/CO	C2/C1
-1	-1	-1	-1	13.3	13.2	46.3	36.7	4.9	298	1.35	3.51	0.62
-1	-1	1	1	18.5	12.6	36.3	46.2	8.3	862	1.62	2.88	0.95
-1	1	-1	1	12	60.9	9.0	26.6	3.3	236	1.55	0.15	0.38
-1	1	1	-1	12.1	51.4	13.8	30.7	3.8	534	1.84	0.27	0.47
1	-1	-1	1	14.2	27.6	23.9	43.2	6.3	426	2.69	0.87	0.84
1	-1	1	-1	17.3	13.6	32.8	48.1	8.3	969	2.38	2.41	1.04
1	1	-1	-1	15.3	47.9	17.3	30.5	4.7	283	2.62	0.36	0.47
1	1	1	1	13.7	50.3	12.5	32.7	4.6	635	2.61	0.25	0.52
0	0	0	0	12.3	38.9	23.6	32.9	4.2	461	2.08	0.61	0.53
0	0	0	0	12.4	37.0	23.7	34.6	4.4	470	2.12	0.64	0.57
0	0	0	0	12.8	36.9	24.2	34.2	4.5	470	2.10	0.66	0.56

Correlations from Regression Analysis

Methane Conversion, %
Not correlated

CO Selectivity, %
= 35.34 + 17.95 (P) $R^2 = 90.43$

CO_2 Selectivity, %
= 23.93 - 10.84 (P) - 3.57 (ECl) $R^2 = 84.50$

C_2 Selectivity, %
= 36.22 - 6.71 (P) + 2.60 (flow) + 1.78 (T) $R^2 = 93.22$

C_2 Yield, %
= 5.27 - 1.41 (P) + 0.735 (flow) $R^2 = 72.34$

C_2 Rate, moles carbon in C_2 products/l catalyst/hr
= 517.4 + 219.5 (flow) - 108.4 (P) $R^2 = 90.08$

$C_2^=/C_2$ ratio
= 2.086 + 0.493 (T) $R^2 = 91.58$

CO_2/CO ratio
= 1.20 + 1.08 (T) $R^2 = 66.80$

C_2/C_1 ratio
= 0.64 - 0.20 (P) + 0.084 (flow) $R^2 = 83.86$

Pressure	+1 = 200 psig	-1 = 100 psig
Temperature	+1 = 750 °C	-1 = 700 °C
Flow	+1 = 557 sccm	-1 = 1114 sccm
ECl Level	+1 = 60 ppm	-1 = 30 ppm

Figure F1. Results of Reactor Validation Run 33-NEK-40

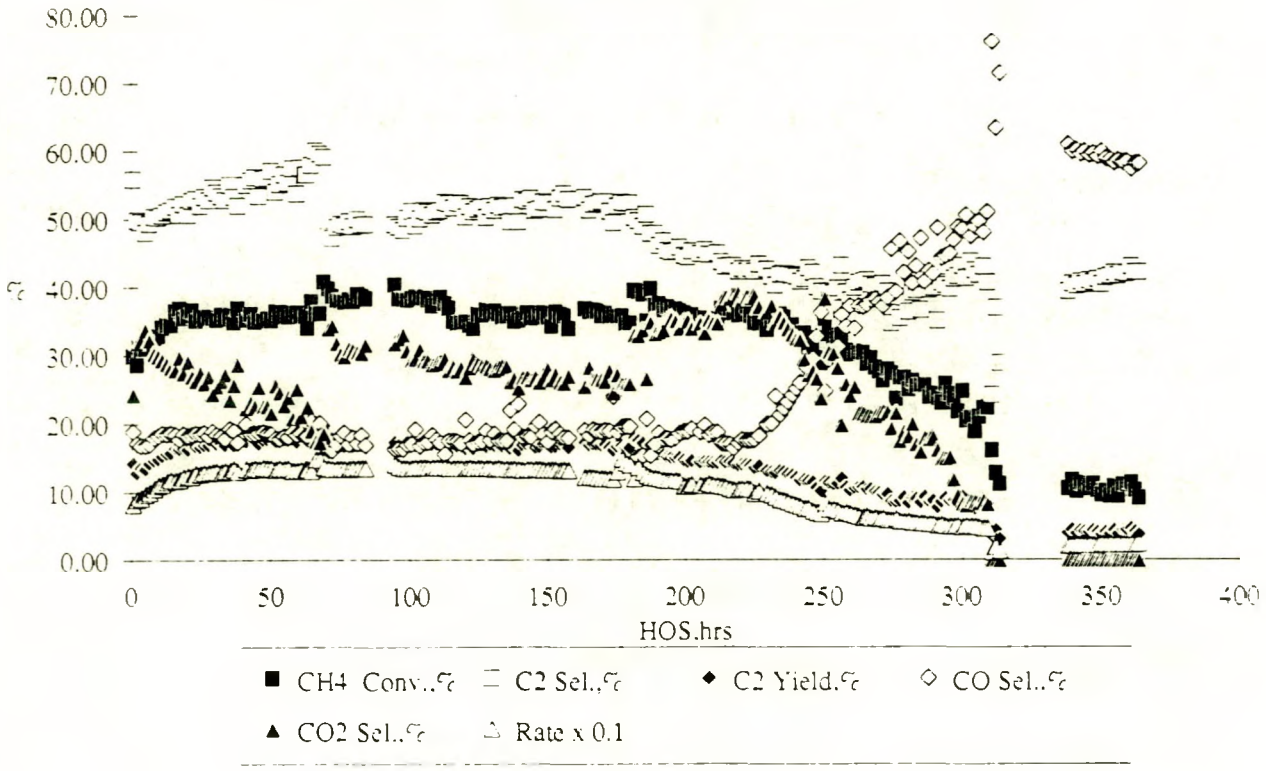


Figure F2. Results of Reactor Validation Run 33-NEK-42

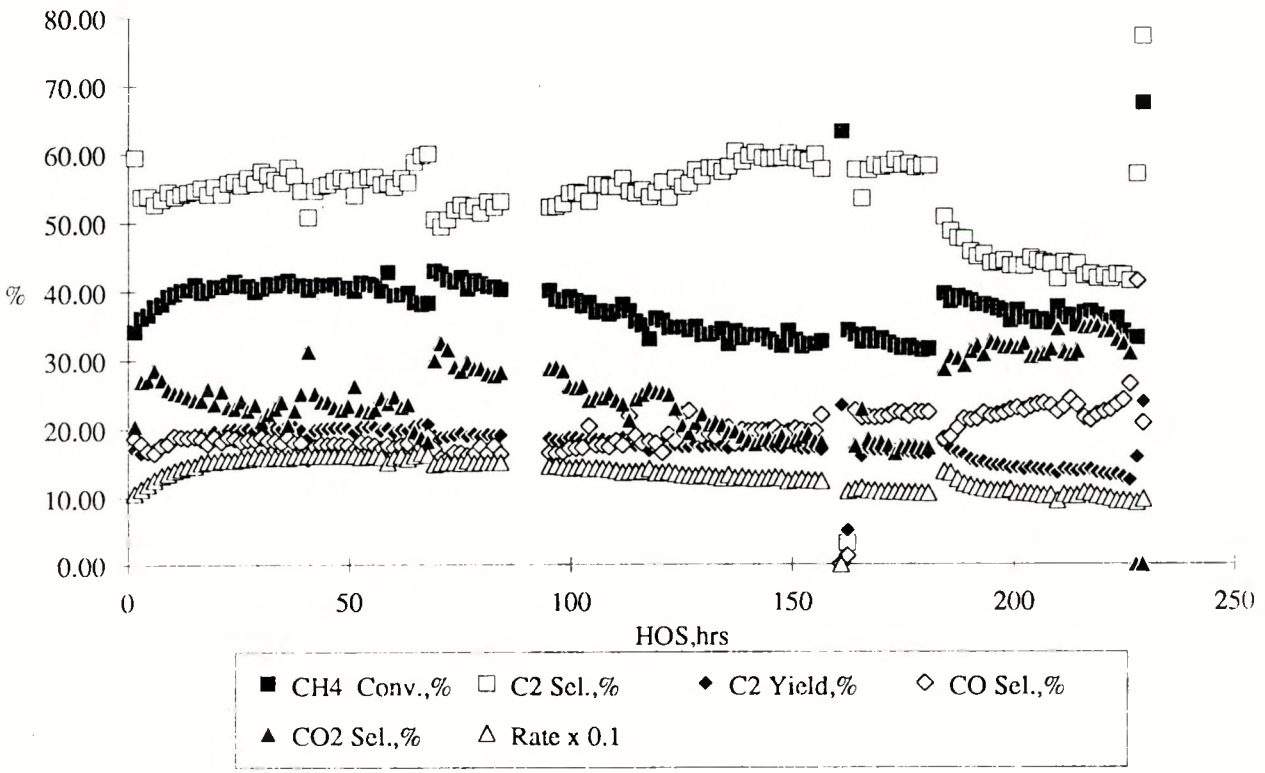


Figure F3. Test Results Using Steam as a Diluent

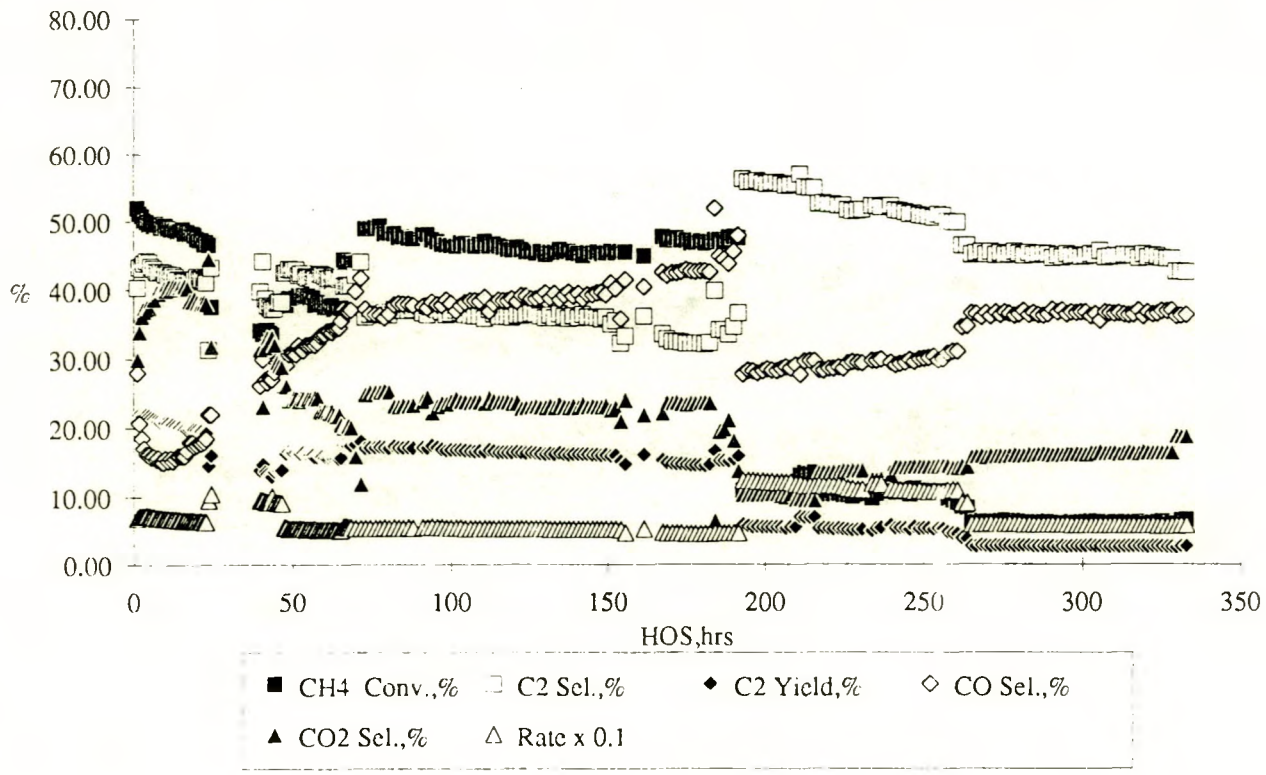


Figure F4. Test Results Using Steam as a Diluent

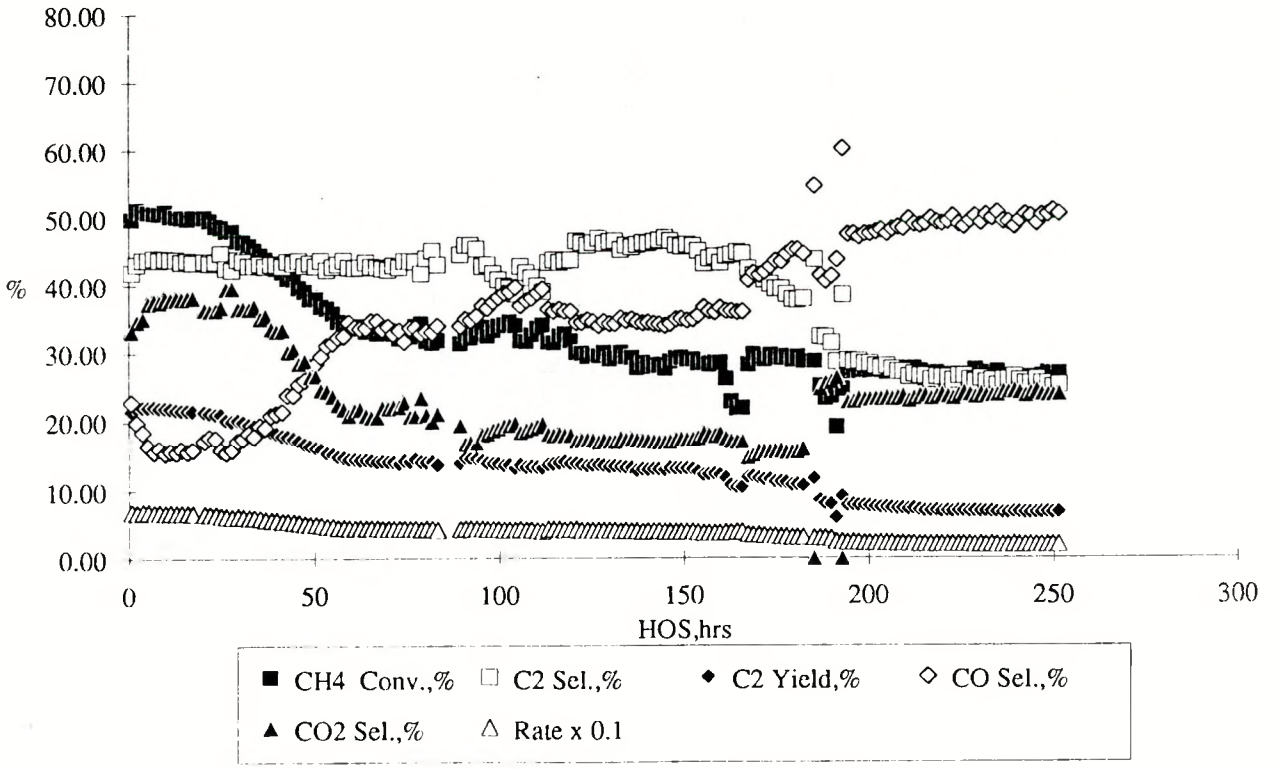


Figure F5. Test Results Using Steam as a Diluent

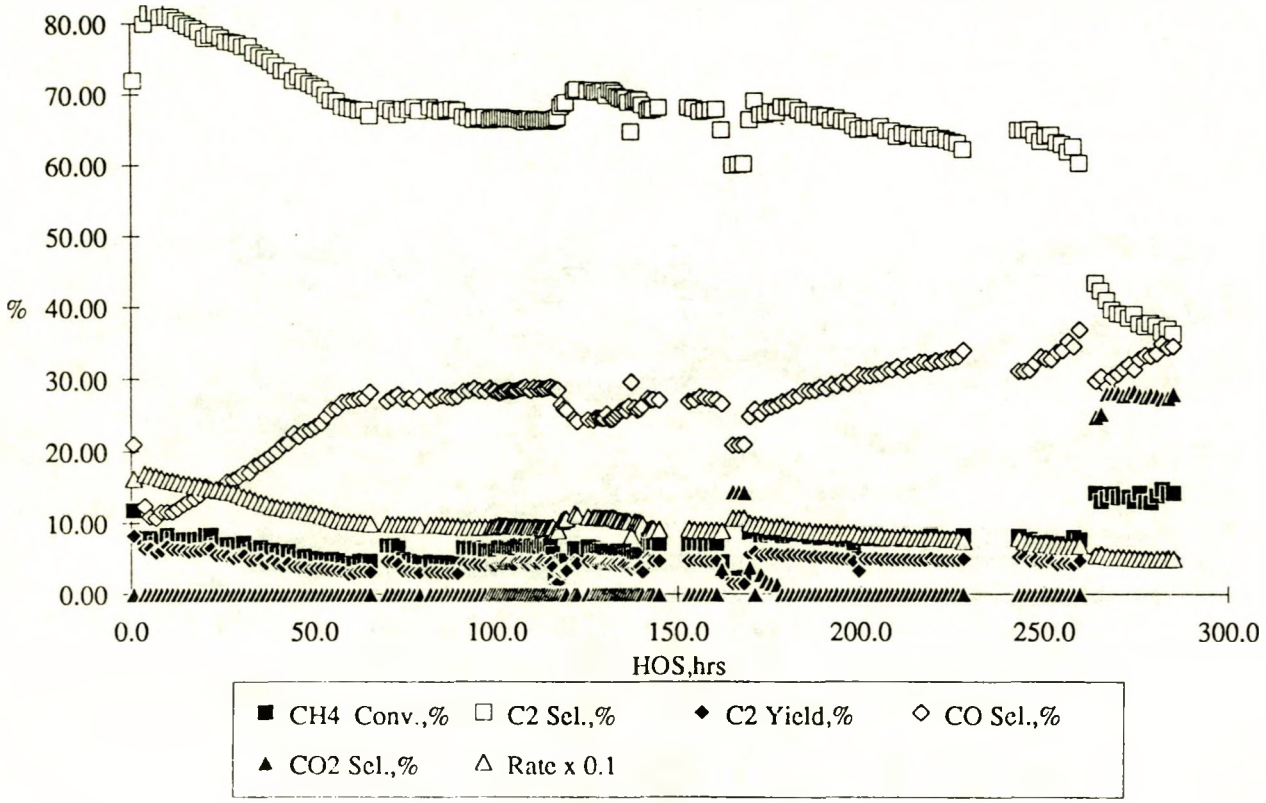


Figure F6. Test Results Using Steam as a Diluent

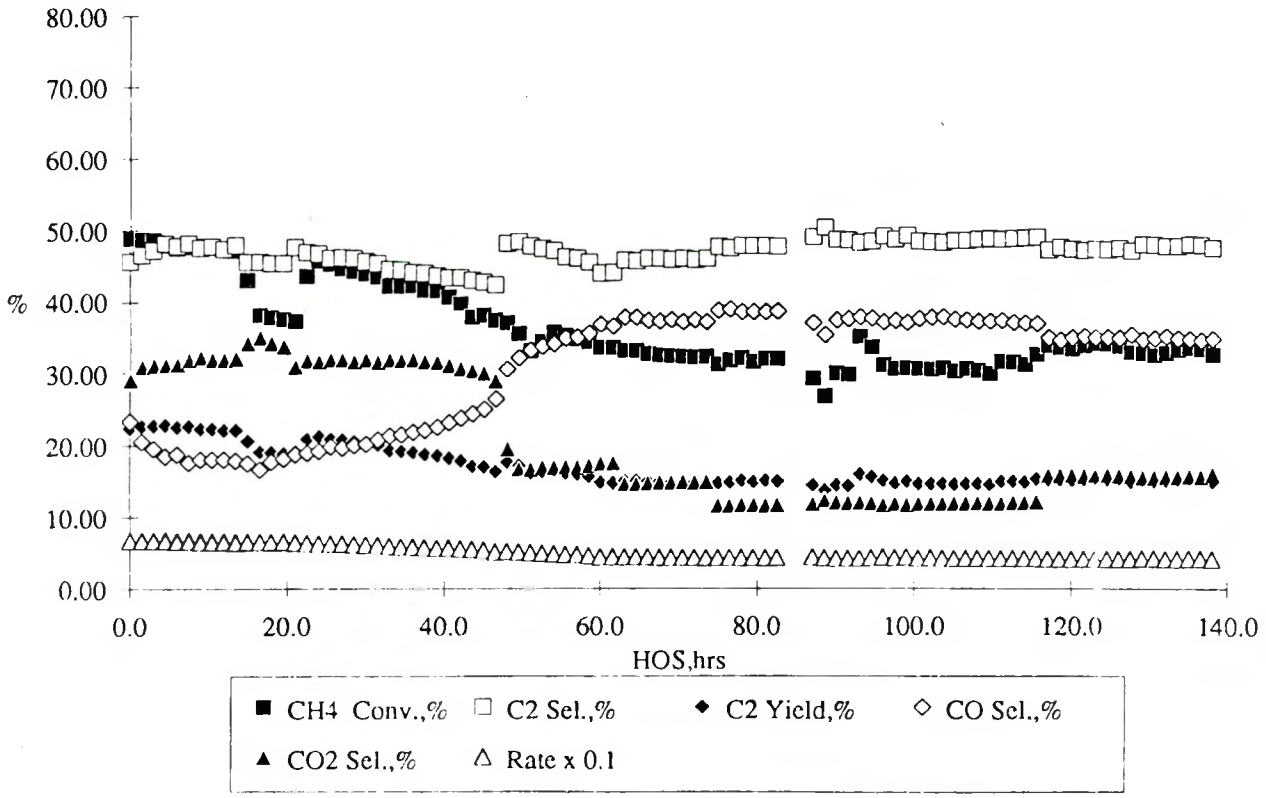


Figure F7. Test Results Using Steam as a Diluent

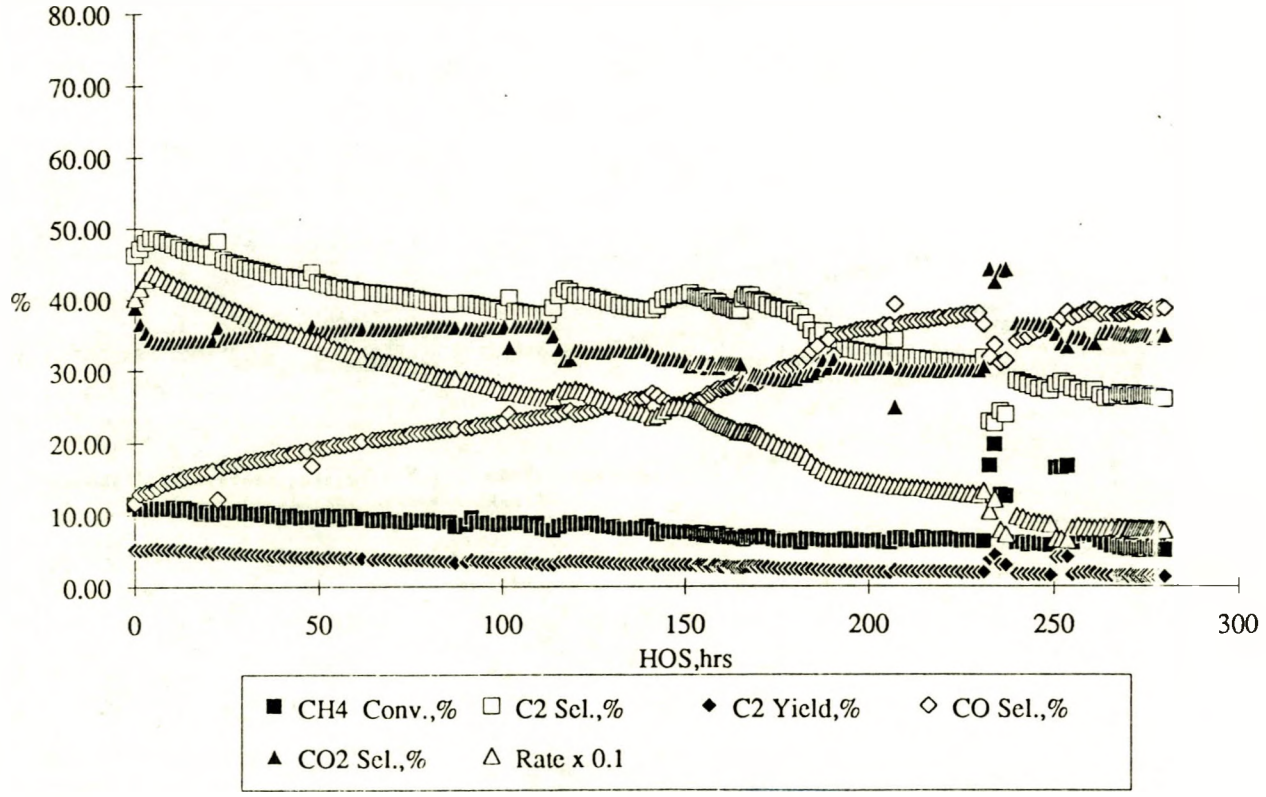


Figure F8. Test Results Using Steam as a Diluent

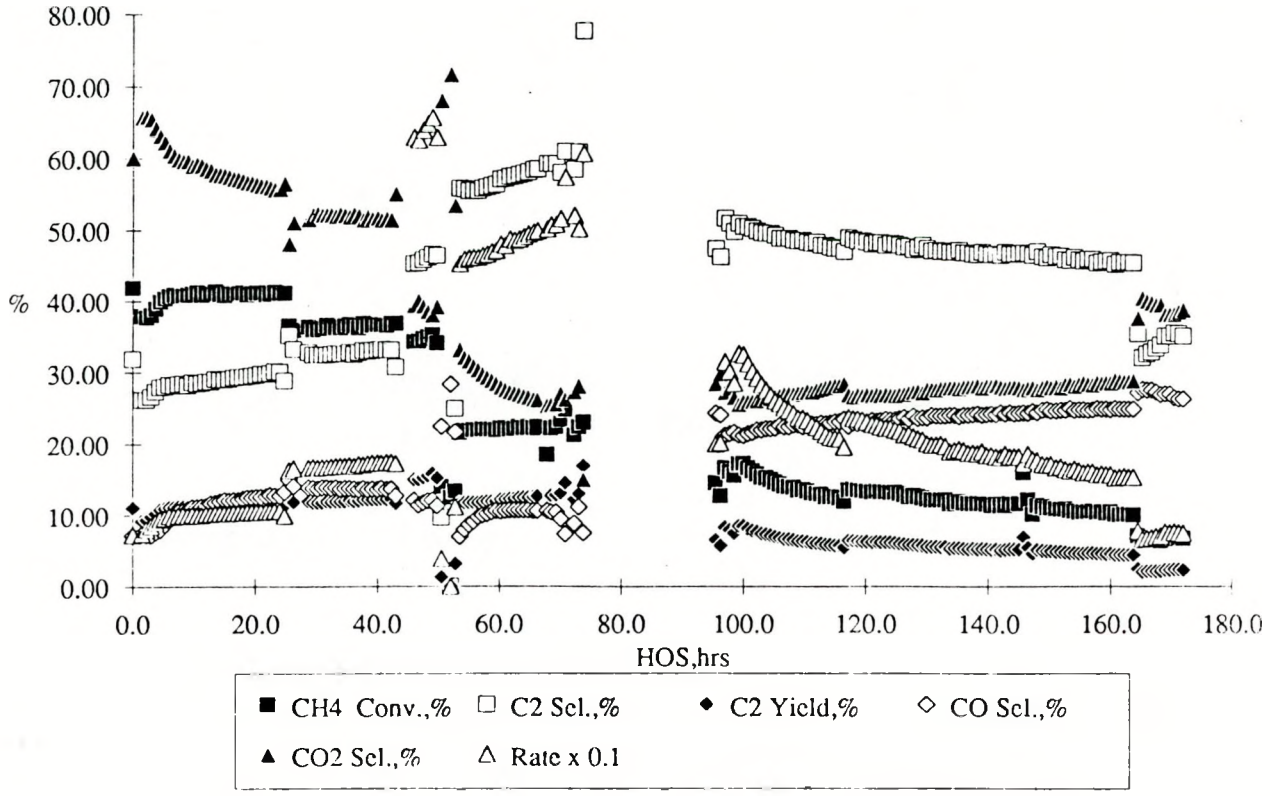


Figure F9. Test Results Using Steam as a Diluent

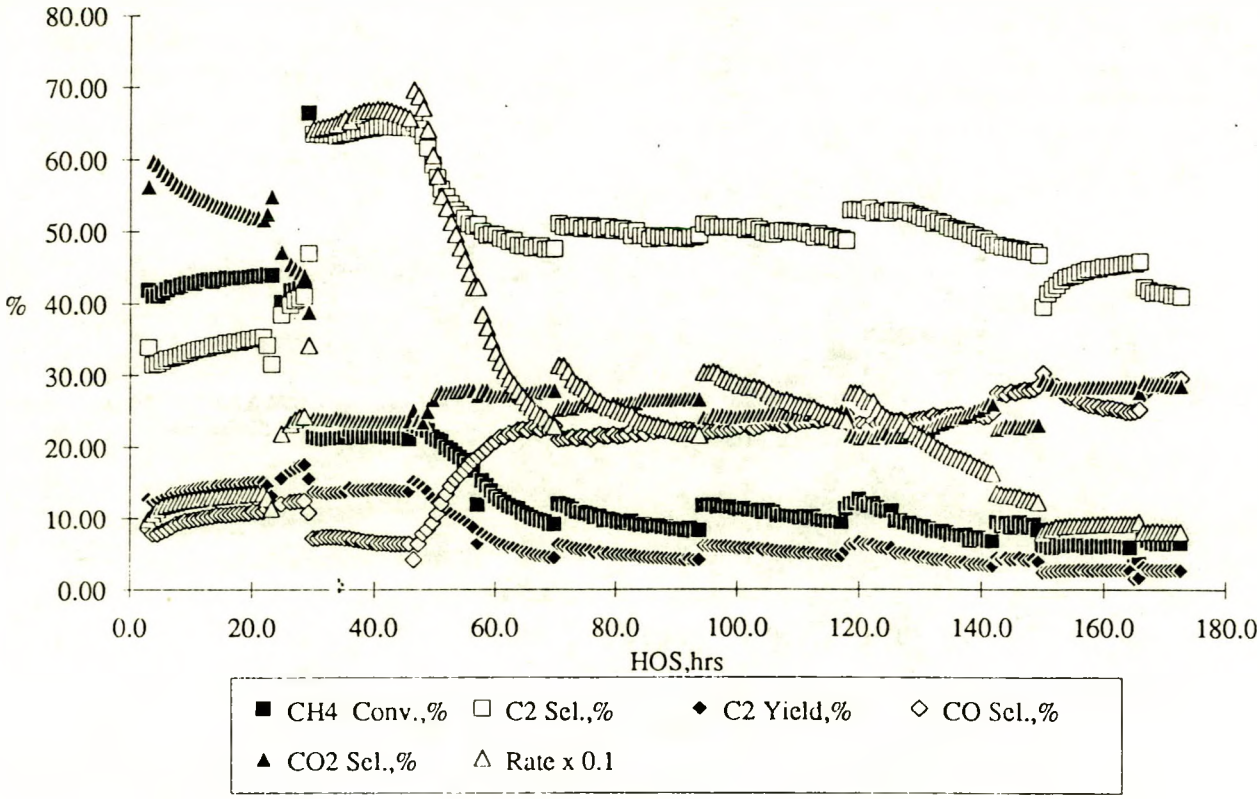


Figure F10. Test Results Using Steam as a Diluent

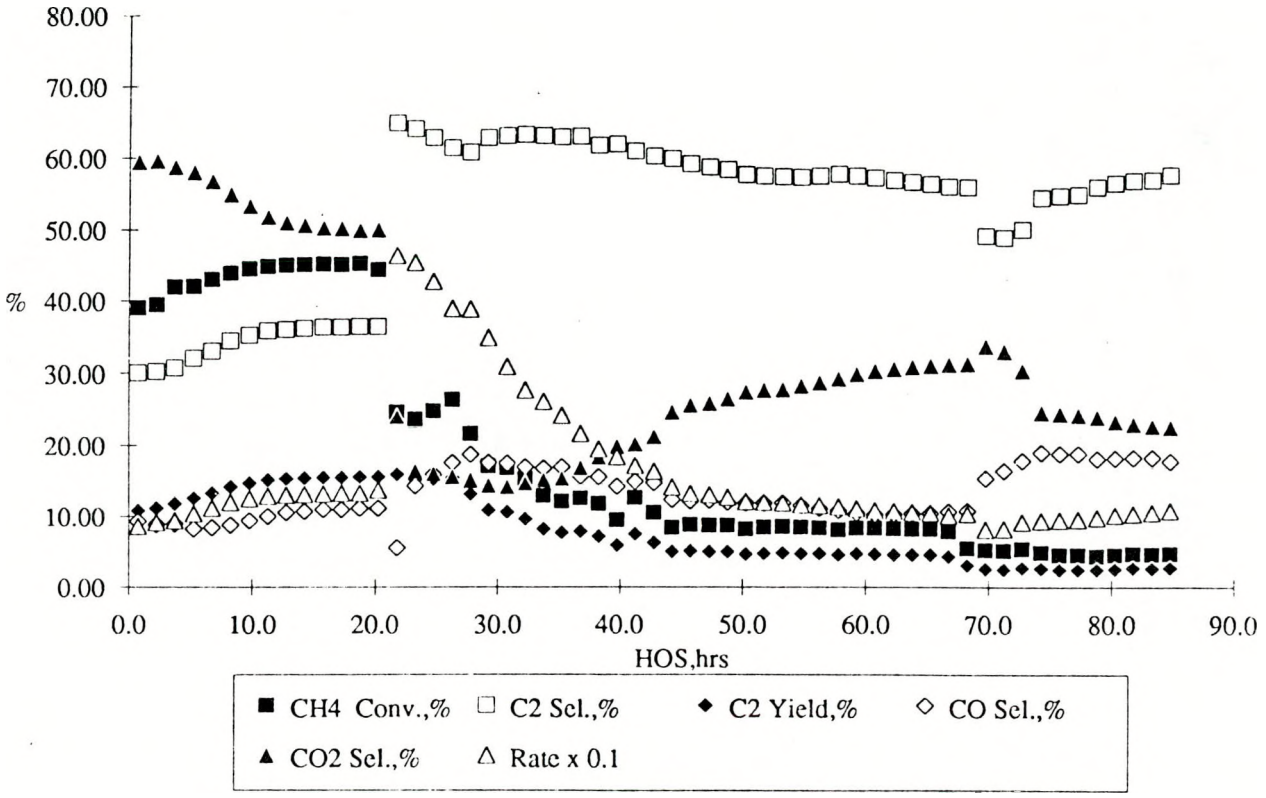


Figure F11. High Pressure Blank Run Results

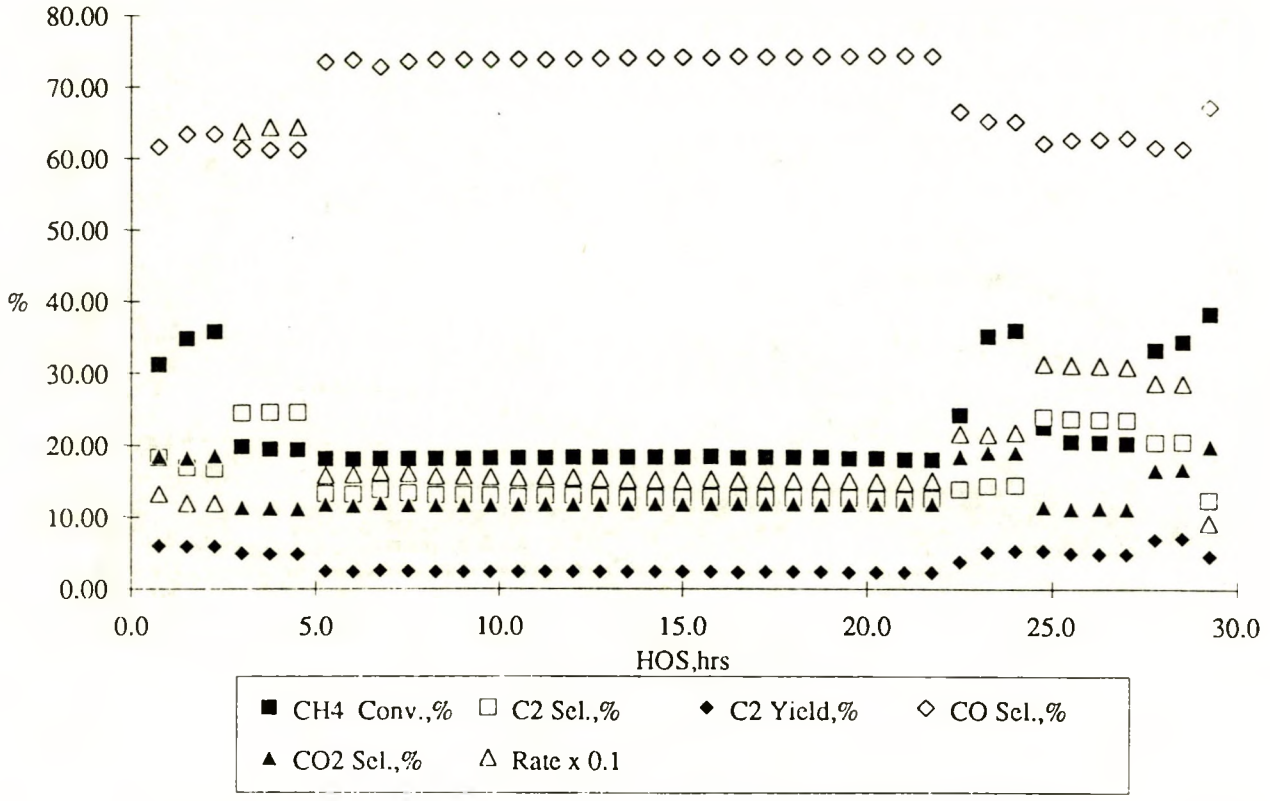
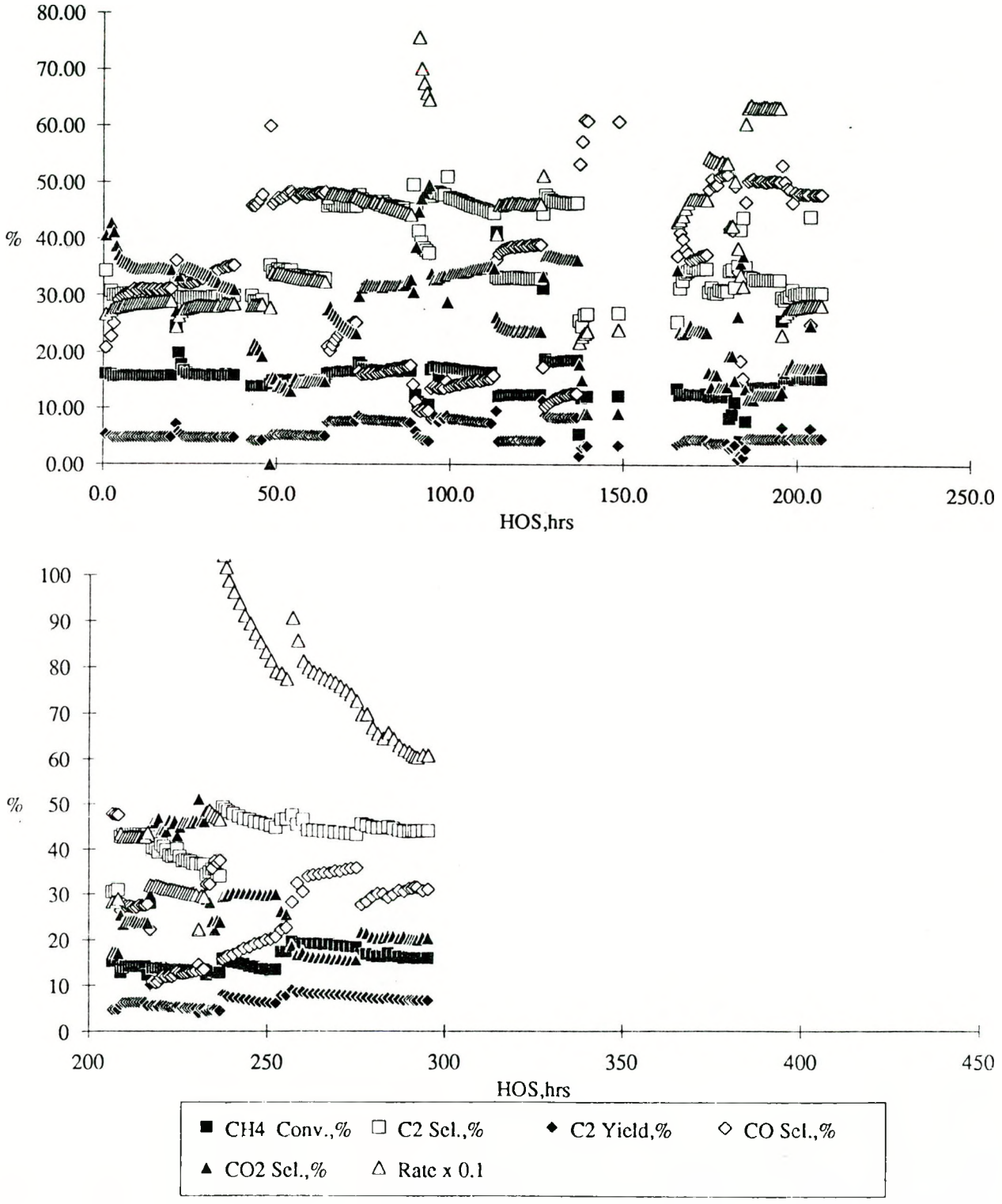


Figure F12. Results of Catalyst Evaluation at High Pressure, 34-NEK-96



Appendix G. EDS DATA - WEIGHT & ATOM PERCENT

Table G1. $BaCO_3/Al_2O_3$ Catalysts, 34-BKW-57 (fresh) and 34-BKW-63 (used)

	Weight%		Atom%	
34-BKW-57B2 (fresh)	Al	Ba	Al	Ba
Area 1 (500X)	11.64	33.57	64.76	36.24
Area 2 (500X)	23.20	57.61	77.50	22.50
Area 3 (500X)	11.95	33.82	64.19	33.88
Area 4 (500X)	17.25	44.86	66.12	33.88
34-BKW-63 (used)	Al	Ba	Al	Ba
Area 1 (500X)	22.96	28.12	80.56	19.44
Area 2 (500X)	31.53	16.01	90.90	9.10
Area 3 (500X)	22.23	25.81	81.38	18.62
Area 4 (500X)	16.82	15.10	84.97	15.03

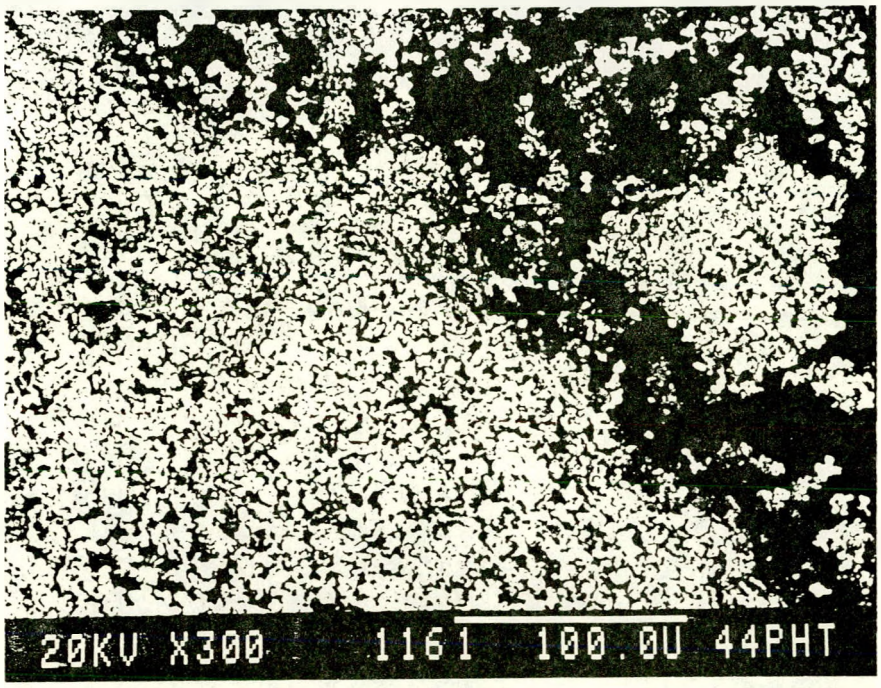
Table G2. Used BaO/Al_2O_3 (34-BKW-124) and $BaCO_3/Al_2O_3$ (34-BKW-125), EDS Results Catalysts

Weight %		Element			
		Al	Si	Cl	Ba
34-BKW-124	- Area 1 (500X)	15.71	0.00	0.19	2.44
	- Area 2 (500X)	27.40	0.00	1.81	20.36
	- Area 3 (500X)	32.10	0.00	1.12	12.52
	- Area 4 (500X)	14.55	0.00	0.10	3.28
	- Area 5 (500X)	18.24	0.00	0.14	4.44
		21.60	0.00	0.67	8.61
34-BKW-125	- Area 1 (500X)	10.40	0.00	0.22	2.80
	- Area 2 (500X)	7.50	0.00	0.21	2.16
	- Area 3 (500X)	21.83	0.00	0.51	5.77
	- Area 4 (500X)	25.69	0.00	0.73	4.62
	- Area 5 (500X)	25.04	0.00	0.18	2.32
		18.09	0.00	0.43	3.53

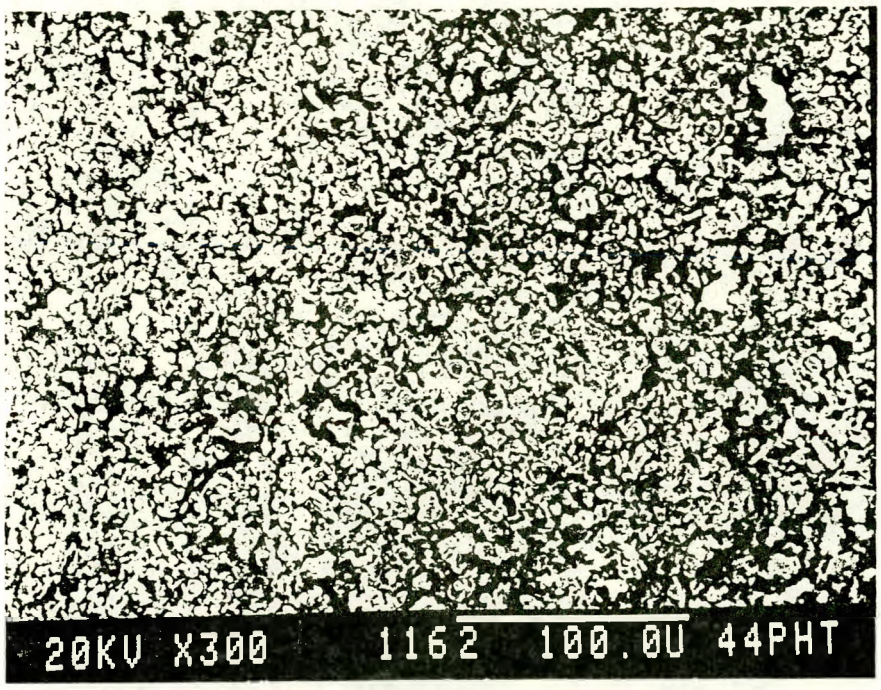
Atom %		Element			
		Al	Si	Cl	Ba
34-BKW-124	- Area 1 (500X)	96.15	0.00	0.89	2.95
	- Area 2 (500X)	83.52	0.00	4.25	12.23
	- Area 3 (500X)	90.60	0.00	2.43	6.96
	- Area 4 (500X)	95.26	0.00	0.51	4.23
	- Area 5 (500X)	94.88	0.00	0.57	4.55
		92.08	0.00	1.73	6.18
34-BKW-125	- Area 1 (500X)	93.51	0.00	1.53	4.96
	- Area 2 (500X)	92.70	0.00	2.03	5.27
	- Area 3 (500X)	93.45	0.00	1.69	4.86
	- Area 4 (500X)	94.58	0.00	2.07	3.35
	- Area 5 (500X)	97.69	0.00	0.53	1.78
		94.39	0.00	1.57	4.04

Electron Microscopy Skill Center
45PHT58
11/14/89

Figure G1. $BaCO_3/Al_2O_3$ Catalysts, 34-BKW-57 (fresh) and 34-BKW-63 (used)

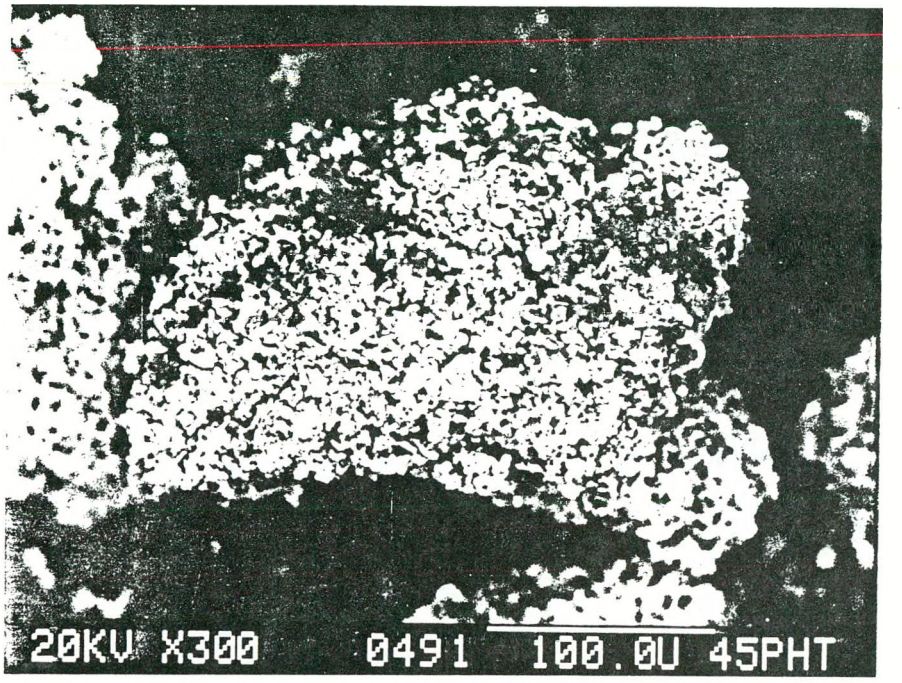


34-BKW-57, $BaCO_3/Al_2O_3$, 7% Ba BEI

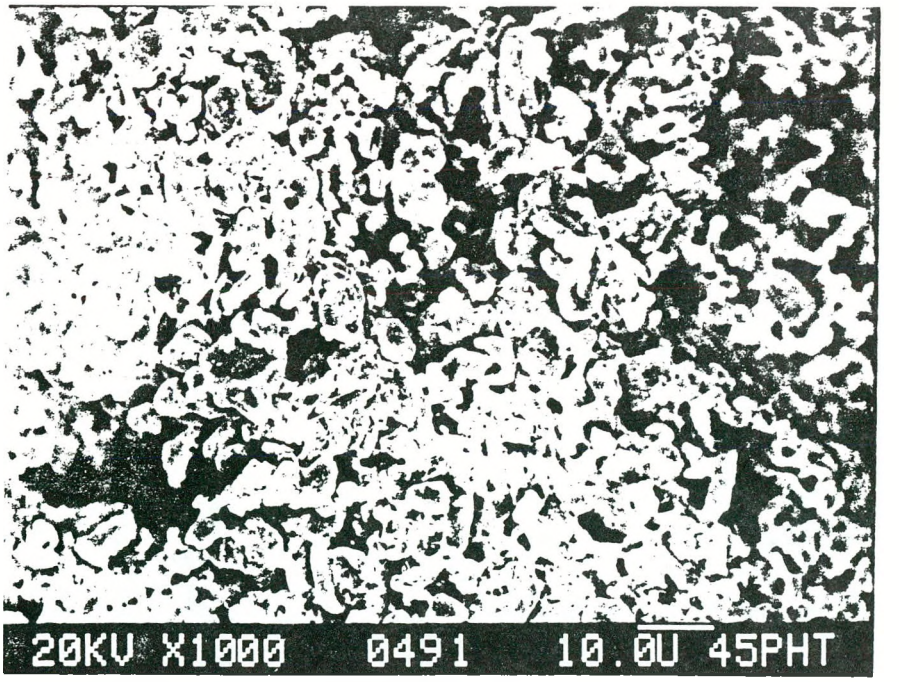


34-BKW-63, Used 34-BKW-57B BEI

Figure G2. Used BaO/Al_2O_3 Catalyst, 34-BKW-124

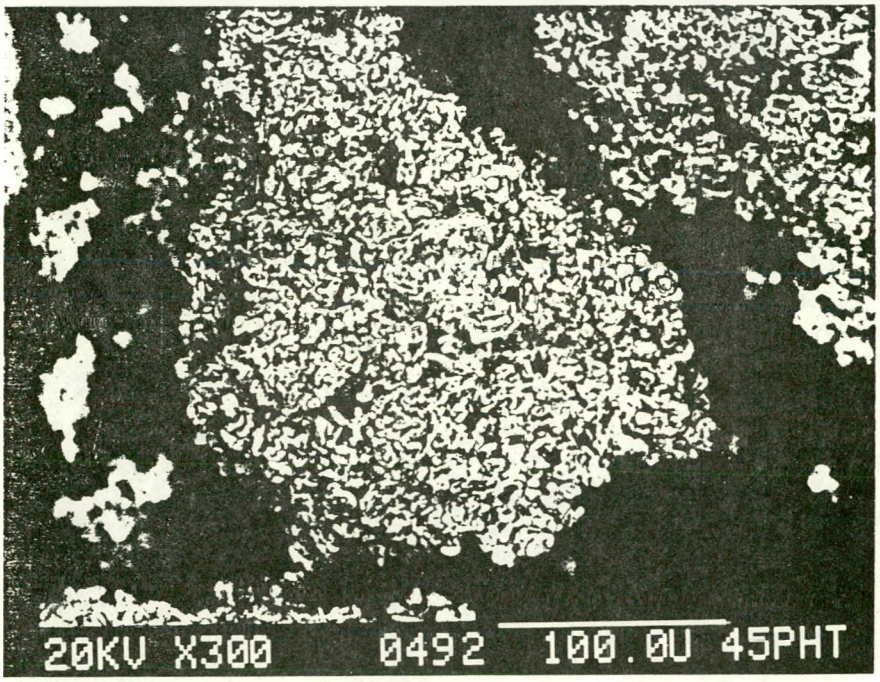


34-BKW-124, 3.7% BaO/Al_2O_3 BEI

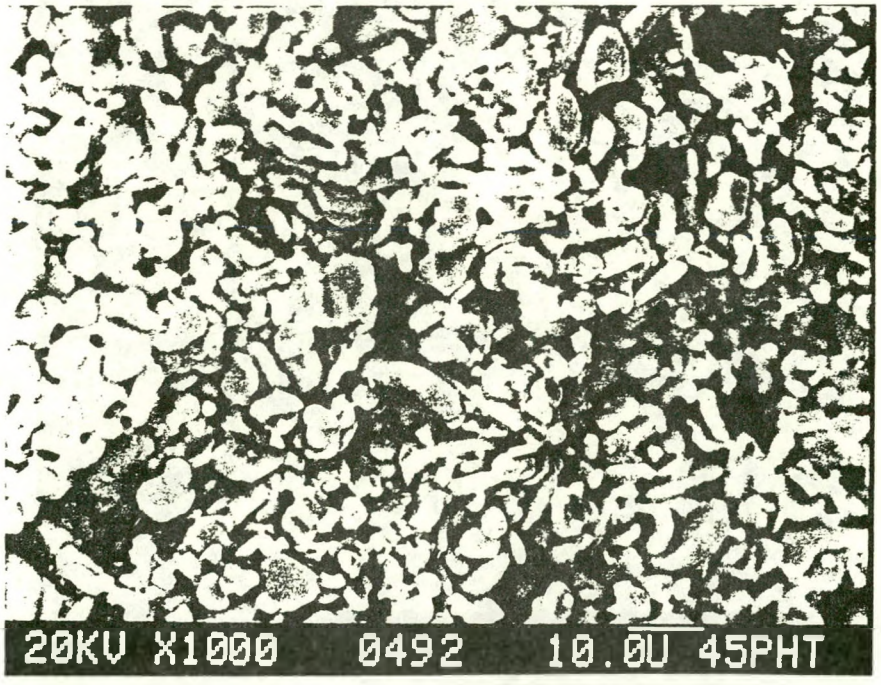


34-BKW-124, 3.7% BaO/Al_2O_3 BEI

Figure G3. Used $BaCO_3/Al_2O_3$ Catalyst, 34-BKW-125



34-BKW-125, 4.8% $BaCO_3/Al_2O_3$ BEI



34-BKW-125, 4.8% $BaCO_3/Al_2O_3$ BEI

Appendix H. REFERENCES FOR SELECTIVITY/CONVERSION PLOT

Ref.#	AUTHORS	TITLE	SOURCE	YEAR
1	**Standard Oil-** Fox, J.R. Curatolo, B.S. Pesa, F.A.	Conversion of Methane to Olefins and Hydrogen	US Patent: 4,450,310	1984
2	**Phillips Petrol.-** Kimble, J.B. Kolts, J.H.	Oxidative Coupling of Methane to Higher Hydrocarbons	Energy Progress Vol. 6, No. 4	1986
3	**Lunsford, J.H.** Lin, C.H. Wang, J.X. Campbell, K.D.	The Role of [M+O-] Centers (M+=Group IA Ion) in the Activation of Methane on Metal Oxides	Mater. Res. Soc. Symp. Proc., 111 p. 305	1988
4	Roos, J.A. Bakker, A.G. Bosch, H. van Ommen, J.G. **Ross, J.R.H.**	Selective Oxidation of Methane to Ethane and Ethylene Over Various Oxide Catalysts	Catal. Today 1, 133	1987
5	Lin, C.H. Ito, T. Wang, J.X. **Lunsford, J.H.**	Oxidative Dimerization of Methane over MgO and CaO Catalysts Promoted with Group IA Ions: Role of [M+O-] Centers	J. Am. Chem. Soc. 109, 4808	1987
6	Driscoll, D. Mariir, W. Wang, J.X. **Lunsford, J.H.**	Formation of Gas-Phase Methyl Radicals Over MgO	J. Am. Chem. Soc. 107, 58	1985
7	Ito, T. Wang, J.X. Lin, C.H. **Lunsford, J.H.**	Oxidative Dimerization of Methane over Li/MgO Catalyst	J. Am. Chem. Soc. 107, 5062	1985
8	Lin, C.H. Wang, J.X. **Lunsford, J.H.**	Oxidative Dimerization of Methane over Na/CaO	J. Catal. 111, 302	1988
9	Phillips Petrol.- Kolts, J.H. **Lunsford, J.H.**	Oxidative Conversion of Methane to Ethane and Ethylene by Contacting with Oxygen over Li/MgO	European Patent Appl.: # 0196541	1986
10	Iwamatsu, E. Moriyama,T. Takasaki,N. **Aika, K.**	Importance of the Specific Surface Area in Oxidative Dimerization of Methane over Promoted MgO	J. Chem. Soc., Chem. Commun. 19	1987

Appendix H. REFERENCES FOR SELECTIVITY/CONVERSION PLOT (continued)

Ref.#	AUTHORS	TITLE	SOURCE	YEAR
11	Moriyama, T. Takasaki, N. Iwamatsu, E. **Aika,K.**	Oxidative Dimerization of Methane over Promoted MgO. Important Factors.	Chem. Soc. Japan, Chem. Lett. 1165	1986
12	**Hutchings, G.J.** Scurrell, M.S. Woodhouse, J.R.	Comparison of Ethene and Ethane Selectivies over Li/MgO and MgO. Comments on the Role of Li.	J. Chem. Soc., Chem. Commun. 1862	1987
13	Campbell, K.D. Morales, E. **Lunsford, J.H.**	Gas-Phase Coupling of Methyl Radicals during the Catalytic Partial Oxidation of Methane	J. Am. Chem. Soc. 109, 7900	1987
14	Iwamatsu, E. Moriyama, T. Takasaki, N. **Aika, K.**	Oxidative Coupling of Methane over Na+ and Rb+ Added MgO Catalysts	J. Catal. 113, 25	1988
15	Wang, J.X. **Lunsford, J.H.**	Characterization of [Li+O-] Centers in Li/MgO Catalysts	J. Phys. Chem. 90, 5883	1986
16	**Yamagata, N.** Tanaka, K. Sasaki, S. Okazaki, S.	Oxidative Coupling of Methane over BaO Mixed with CaO and MgO	Chem. Soc. Japan, Chem. Lett. 81	1987
17	**Aika, K.** Moriyama, T. Takasaki, N. Iwamatsu, E.	Oxidative Dimerization of Methane over BaCO3, SrCO3 and these Catalyst Promoted with Alkali	J. Chem. Soc., Chem. Commun. 1210	1986
18	**Matsuura, I.** Doi, T. Utsumi, Y.	Oxidative Coupling of Methane Over a Li/BeO Catalyst	Chem. Soc. Japan Chem. Lett. 1473	1987
19	**ARCO-** Jones, C.A. Leonard, J.J. Sofranko, J.A.	Methane Conversion	US Patent # 4,443,646	1984
20	**Emesh, I.T.** Amenomiya, Y.	Oxidative Coupling of Methane over the Oxides of Groups IIIA, IVA, and VA Metals	J. Phys. Chem. 90, 4785	1986

Appendix H. REFERENCES FOR SELECTIVITY/CONVERSION PLOT (continued)

Ref.#	AUTHORS	TITLE	SOURCE	YEAR
21	**Keulks, G.W.** Yu, M.	Oxidative Coupling of Methane	React. Kinet. Catal. Lett. Vol. 35, 361	1987
22	**ARCO** Gaffney, A.M.	Methane Conversion	US Patent # 4,499,324	1985
23	**Phillips Petrol.-** Kimble, J.B. Kolts, J.H.	Methane Conversion	US Patent # 4,620,057	1986
24	**Otsuka, K.** Yokoyama, S. Morikawa, A.	Catalytic Activity and Selectivity Control for Oxidative Coupling of Methane by Oxygen Pumping Through Y2O3-stabilized ZrO2	Chem. Soc. Japan, Chem. Lett. 319	1985
25	Asami,K. Omata, K. **Fujimoto, K.** Tominaga, H.	Oxidative Coupling of Methane in the Homogeneous Gas Phase under Pressure	J. Chem. Soc., Chem. Commun. 1287	1987
26	**ARCO-** Jones, C.A. Leonard, J.J. Sofranko, J.A.	Methane Conversion	US Patent # 4,443,645	1984
27	**W. R. Grace-** Hicks, R.F. Cabic, E.J.	Methane Conversion to Hydrogen, Ethane etc. Using Catalyst Comprising Groups II, III and/or Lanthanide Metal Oxides with Promoter Metal Oxide	International Patent # WO 86/07351 PCT/US86/01254	1986
28	**ARCO-** Jones, C.A. Leonard, J.J. Sofranko, J.A.	Methane Conversion	US Patent # 4,443,648	1984
29	**Imai, H.** Tagawa, T. Kamide, N.	Oxidative Coupling of Methane over Amorphous Lanthanum Aluminum Oxides	J. Catal. 106, 394	1987
30	France, J.E. **Shamsi, A.** Ahsan, M.Q.	Oxidative Coupling of Methane Over Perovskite-Type Oxides	Energy & Fuel 2, 235	1988

Appendix H. REFERENCES FOR SELECTIVITY/CONVERSION PLOT (continued)

Ref.#	AUTHORS	TITLE	SOURCE	YEAR
31	Lin, C.H. Campbell, K.D. Wang, J.X. **Lunsford, J.H.**	Oxidative Dimerization of Methane over La2O3	J. Phys. Chem. 90, 534	1986
32	Wang, J.X. **Lunsford, J.H.**	Evidence for the Thermal Generation of Superoxide Ions on La2O3	J. Phys. Chem. 90, 3890	1986
33	**Otsuka, K.** Jinno, K. Morikawa, A.	Catalysts Active and Selective in Oxidative Coupling of Methane	Chem. Soc. Japan, Chem. Lett. 499	1985
34	**Otsuka, K.** Jinno, K. Morikawa, A.	Active and Selective Catalysts for the Synthesis of C2H4 and C2H6 via Oxidative Coupling of Methane	J. Catal. 100, 353	1986
35	Idemitsu Kosan Co. **Otsuka, K.** Morikawa, A.	Conversion of Methane to Higher Hydrocarbons by Contact with Rare Earth Catalyst in Presence of Oxygen	European Patent Application # 0189079	1986
36	**Phillips Petrol.-** Kolts, J.H. Kimble, J.B.	Catalyst for Oxidation of Methane to Ethylene and Ethane. Comprises La2O3 with a Halide or La-compound with Alkali Metal Compound	European Patent Application # 0206044	1986
37	**Machida, K.** Enyo, M.	Oxidative Dimerization of Methane over Cerium Mixed Oxides and its Relation with their Ion-Conducting Characteristics	J. Chem. Soc., Chem. Commun. 1639	1987
38	**Otsuka, K.** Shimizu, Y. Komatsu, T.	Ba Doped Cerium Oxides Active for Oxidative Coupling of Methane	Chem. Soc. Japan, Chem. Lett. 1835	1987
39	**Otsuka, K.** Komatsu, T.	Active Catalyst in Oxidative Coupling of Methane	J. Chem. Soc., Chem. Commun. 388	1987
40	**ARCO-** Jones, C.A. Leonard, J.J. Sofranko, J.A.	Methane Conversion	US Patent # 4,443,649	1984

Appendix H. REFERENCES FOR SELECTIVITY/CONVERSION PLOT (continued)

Ref.#	AUTHORS	TITLE	SOURCE	YEAR
41	**ARCO-** Jones, C.A. Sofranko, J.A.	Methane Conversion Process	US Patent # 4,523,050	1985
42	**ARCO-** Jones, C.A. Leonard, J.J. Sofranko, J.A.	Oxidative Conversion of Methane to Higher Hydrocarbons over Alkali-Promoted Mn/SiO2	J. Catal. 103, 311	1987
43	**Garcia, E.Y.** Rivera, G.L. Resasco, D.E.	Direct Catalytic Synthesis of Ethylene from Methane	React. Kinet. Catal. Lett. Vol. 28, 481	1985
44	**Exxon-** Mitchell,III,H.L. Waghorne, R.H.	Conversion of Low Molecular Weight Hydrocarbons to High Molecular Weight Hydrocarbons	US Patent #4,172,810 #4,205,194 4239658	1979 1980 1980
45	**Otsuka, K.** Liu, Q. Morikawa, A.	Active and Selective Catalysts in Oxidative Coupling of Methane. Nickel Oxides with Alkali Metals.	Inorg. Chim. Acta 118, L23	1986
46	**Baerns, W.** Bytyn, W.	Supported PbO Catalysts for the Oxidative Coupling of Methane-Effect of Surface Acidity	Appl. Catal. 28, 199	1986
47	**Asami, K.** Shikada, T. Fujimoto, K. Tominaga, H. Hashimoto, S.	Oxidative Coupling of Methane to Ethane and Ethylene over Supported PbO Catalysts	Ind. Eng. Chem. Res. 26, 1485	1987
48	**Asami, K.** Shikada, T. Fujimoto, K. Tominaga, H.	Oxidative Coupling of Methane Over Lead Oxide: Kinetic Study and Reaction Mechanism	Ind. Eng. Chem. Res. 26, 2348	1987
49	**Asami, K.** Shikada, T. Fujimoto, K. Tominaga, H. Hasimoto, S.	Selective Oxidative Coupling of Methane over Supported Lead Oxide	Chem. Soc. Japan, Chem. Lett. 1233	1986
50	Hinsen, W. Bytyn, W. **Baerns, M.**	Oxidative Dehydrogenation and Coupling of Methane	Proc. 8th Int. Congr. Catal. 3, 81	1984

Appendix H. REFERENCES FOR SELECTIVITY/CONVERSION PLOT (continued)

Ref.#	AUTHORS	TITLE	SOURCE	YEAR
51	Hinsen, W. **Baerns, M.**	Process for the Production of Ethane and Ethylene From Methane	US Patent # 4,608,449	1986
52	**Meng, H.** Sanger, A.R.	Direct Synthesis of Ethylene/Ethane From Methane	Appl. Catal. 32, 347	1987
53	**ARCO-** Jones, C.A. Leonard, J.J. Sofranko, J.A.	Methane Conversion	US Patent # 4,443,647	1984
54	Carreiro, J.A.S.P. **Baerns, M.**	Catalytic Conversion of Methane by Oxidative Coupling To C2+ Hydrocarbons	React. Kinet. Catal. Lett. Vol. 35, 349	1987
55	**ARCO-** Gaffney, A.M.	Methane Conversion	US Patent # 4,499,323	1985
56	**ARCO-** Jones, C.A. Leonard, J.J. Sofranko, J.A.	Methane Conversion	US Patent # 4,443,644	1984
57	**Otsuka, K.** Said, A.A.	Role of Lattice Oxygen Atoms in Partial Oxidations of Methane, Ethane and Ethylene over Sm_2O_3	Inorg. Chim. Acta 132, 123	1987
58	**Otsuka, K.** Komatsu, T.	High Catalytic Activity of Sm_2O_3 for Oxidative Coupling of Methane into Ethane and Ethylene	Chem. Soc. Japan, Chem. Lett. 483	1987
59	**Otsuka, K.** Jinno, K.	Kinetic Studies on Partial Oxidation of Methane over Sm_2O_3	Inorg. Chim. Acta 121, 237	1986
60	**Otsuka, K.** Liu, Q. Morikawa, A.	Selective Synthesis of Ethylene by Partial Oxidation of Methane over LiCl-Sm_2O_3	J. Chem. Soc., Chem. Commun. 586	1986
61	**Otsuka, K.** Liu, Q. Morikawa, A. Hatano, M:	Catalysts Active and Selective in Oxidative Coupling of Methane. Alkali-Doped Sm_2O_3	Chem. Soc. Japan, Chem. Lett. 467	1986

Appendix H. REFERENCES FOR SELECTIVITY/CONVERSION PLOT (continued)

Ref.#	AUTHORS	TITLE	SOURCE	YEAR
62	**ARCO-** Jones, C.A. Leonard, J.J. Sofranko, J.A.	Methane Conversion	US Patent # 4,444,984	1984
63	Keller, G.E. **Bhasin, M.M.**	Synthesis of Ethylene via Oxidative Coupling of Methane	J. Catal. 73, 9	1982
64	**ARCO-** Sofranko, J.A. Leonard, J.J. Jones, C.A.	Oxidative Conversion of Methane to Higher Hydrocarbons	J. Catal. 103, 302	1987
65	**ARCO-** Sofranko, J.A. Withers, Jr. H.P.	Methane Conversion	US Patent # 4,547,610	1985
66	**ARCO-** Sofranko, J.A. Leonard, J.J. Jones, C.A.	Methane Conversion	US Patent # 4,560,821	1985
67	**ARCO-** Sofranko, J.A. Leonard, J.J. Jones, C.A.	Methane Conversion	US Patent # 4,523,049	1985
68	**ARCO-** Sofranko, J.A. Jones, C.A.	Methane Conversion	US Patent # 4,499,322	1985
69	**ARCO-** Sofranko, J.A. Jones, C.A.	Methane Conversion	US Patent # 4,547,611	1985
70	**Otsuka, K.** Liu, Q. Hatano, M. Morikawa, A.	Synthesis of Ethylene by Partial Oxidation of Methane Over Oxides of Transition Metals with LiCl	Chem. Soc. Japan, Chem. Lett. 903	1986
71	**Standard Oil-** Brazdil, J.F. Grasselli, R.K. Bartek, J.P.	Conversion of Low M.W. Alkanes to Higher Hydrocarbons on Multicomponent Oxide Catalysts	European Patent Application # 0177327	1985

Appendix H. REFERENCES FOR SELECTIVITY/CONVERSION PLOT (continued)

Ref.#	AUTHORS	TITLE	SOURCE	YEAR
72	**Matsuura, I.** Utsumi, Y. Nakai, M. Doi, T.	Oxidative Coupling of Methane over Li-Promoted ZnO Catalyst	Chem. Soc. Japan, Chem. Lett. 1981	1986
73	Zhang, H.S. Wang, J.X. Driscoll, D.J. **Lunsford, J.H.**	Activation and Oxidative Dimerization of Methane over Li-Promoted ZnO	J. Catal. 112, 366	1988
74	**Otsuka, K.** Komatsu, T.	Conversion of Methane to Aromatic Hydrocarbons by Combination of Catalysts	Chem. Soc. Japan, Chem. Lett. 1955	1986
75	**Anderson, J.R.** Tsai, P.	Oxidation of Methane Over H-ZSM5 and Other Catalysts	Appl. Catal. p. 141	1985
76	**Shepelev, S.S.** Ione, K.G.	Catalytic Properties of Zeolites with Various Structures and Chemical Composition in the Preparation of Aromatics from Methane	React. Kinet. Catal. Lett. 23, 3	1983
77	**Aika, K.** Nishiyama, T.	Utilisation of CO2 in the Oxidative Coupling of Methane Over PbO-MgO and PbO-CaO	J. Chem. Soc., Chem. Commun. 70	1988
78	**ARCO-** Sofranko, J.A. Jones, C.A. Leonard, J.J. Gaffney, A.M. Withers, H.P.	Catalytic Oxidative Coupling of Methane Over Na-Promoted Mn/SiO2 and Mn/MgO	Petr. Div. Preprints 32, 763	1987
79	Lo, M.Y. Agarwai, S. **Marcelin, G.**	Oxidative Coupling of Methane Over K-Modified Antimony Oxide	Petr. Div. Preprints 32, 770	1987
80	**Standard Oil** Bartek, J.P. Hupp, J.M. Brazdil, J.F. Grasselli, R.K.	Oxidative Dimerization of Methane Over Pb-Mg Mixed Oxide Catalysts	Petr. Div. Preprints 32, 774	1987
81	**Shepelev, S.S.** Ione, K.G.	Preparation of Aromatic Hydrocarbons from Methane in the Presence of O2	React. Kinet. Catal. Lett. 23, 323	1983

Appendix H. REFERENCES FOR SELECTIVITY/CONVERSION PLOT (continued)

Ref.#	AUTHORS	TITLE	SOURCE	YEAR
82	Lane, G.S. **Wolf, E.E.**	Methane Utilization by Oxidative Coupling: A Study of Reactions in the Gas Phase	J. Catal. 113, 144	1988
83	Campbell, K.D. Zhang, H. **Lunsford, J.H.**	Methane Activation by the Lanthanide Oxides	J. Phys. Chem. 92, 750	1988
84	**Hutchings, G.J.** Scurrell, M.S. Woodhouse, J.R.	The Role Of Gas Phase Reaction in the Selective Oxidation of Methane	J. Chem. Soc., Chem. Commun. 253	1988
85	**Fujimoto, K.** Hashimoto, S. Asami, K. Tominaga, H.	Oxidative Coupling of Methane with Alkaline Earth Halide Catalysts Supported on Alkaline Earth Oxides	Chem. Soc. Japan, Chem. Lett. 2157	1987
86	Campbell, K.D. **Lunsford, J.H.**	The Contribution of Gas-Phase Radical Coupling in the Catalytic Oxidation of Methane	J. Phys. Chem. 92, 5792	1988
87	**Otsuka, K.** Nakajima, T.	Oxidative Coupling of Methane over Samarium Oxides using N2O as Oxidant	J. Chem. Soc., Faraday Trans. I 83, 1315	1987
88	**GRACE-** Deboy, J.M. Hicks, R.F.	Kinetics of the Oxidative Coupling of Methane over 1 wt% Sr/La2O3	J. Catal. 113, 517	1988
89	**Otsuka, K.** Nakajima, T.	Partial Oxidation of Methane Over Rare Earth Metal Oxides Using N2O and O2 as Oxidants	Inorg. Chim. Acta 120, L27	1986
90	Kastanas, G.N. Tsigdinos, G.A. **Schwank, J.**	Selective Oxidation of Methane Over Vycor Glass, Quartz Glass and Various Silica, Magnesia and Alumina Surfaces	Appl. Catal. 44, 33	1988
91	**Thomas, J.M.** Kuan, X. Stachurski, J.	Synthetic Kentrolite as a Catalyst for the Selective Oxidation of Methane to C2-Hydrocarbons	J. Chem. Soc., Chem. Commun. 162	1988
92	**BP Company** Hall, A.H.P. McCarroll, J.J.	Conversion of Methane to Aromatic Hydrocarbons Using an Aluminosilicate Catalyst in the Absence of Oxygen	European Patent Application #0216491	1986

Appendix H. REFERENCES FOR SELECTIVITY/CONVERSION PLOT (continued)

Ref.#	AUTHORS	TITLE	SOURCE	YEAR
93	**Standard Oil Co.** Velenyi, L.J.	Molybdenum-Tungsten-Containing Catalyst and Methane Conversion Process Using Same	US Patent #4,695,668	1987
94	**Standard Oil Co.** Brazdil, J.F. Teller, R.G. Bartek, J.P. Grasselli, R.K.	Methane Conversion Process Using Phosphate-Containing Catalyst	US Patent #4,665,259	1987
95	**ARCO** Mazurek, H.	Molten Salt Hydrocarbon Conversion Process Using Oxygen Containing Feed	US Patent #4,678,862	1987
96	**Hutchings, G.J.** Scurrell, M.S. Woodhouse, J.r.	Role of Surface O- in the Selective Oxidation of Methane	J. Chem. Soc., Chem. Commun. 1388	1987
97	Martin, G.A. **Mirodatos, C.**	Evidence of Carbene Formation in Oxidative Coupling of Methane Over Li/MgO	J. Chem. Soc., Chem. Commun. 1393	1987
98	Korf, S.J. Roos, J.A. deBruijn, N.A. van Ommen, J.G. **Ross, J.R.H.**	Influence of CO2 on the Oxidative Coupling of Methane Over Li/MgO	J. Chem. Soc., Chem. Commun. 1433	1987
99	Zhang, H.S. Wang, J.X. Driscoll, D.J. **Lunsford, J.H.**	Oxidative Dimerization of Methane Over Li/ZnO	ACS: Div. Fuel Chem. Vol. 32, #3, 242 194th National Meeting	1987
100	**Tyler, R.J.** Lukey, C.A.	Catalytic Partial Oxidation of Methane to Higher Hydrocarbons	ACS: Div. Fuel Chem. Vol. 32, #3, 249 194th National Meeting	1987
101	Iwamatsu, E. Moriyama, T. Takasaki, N. **Aika, K.**	Oxidative Coupling of Methane Over Promoted MgO Catalysts: Relation Between Activity & Specific Surface Area	Studies in Surface Science & Catalysis: #36 Methane Conversion Symp.: Auckland: April p. 373	1987

Appendix H. REFERENCES FOR SELECTIVITY/CONVERSION PLOT (continued)

Ref.#	AUTHORS	TITLE	SOURCE	YEAR
102	**Otsuka, K.** Hatano, M. Komatsu, T.	Synthesis of C2H4 by Partial Oxidation of CH4 Over Transition Metal Oxides with Alkali-Chlorides	Studies in Surface Science & Catalysis: #36 Methane Conversion Symp.: Auckland: April p. 383	1987
103	**Garnett, J.L.** Kennedy, E.M. Long, M.A. Than, C. Watson, A.J.	Catalytic Oxidation of Methane Over AlPO4(-5) and Metal Doped AlPO4(-5)	Studies in Surface Science & Catalysis: #36 Methane Conversion Symp.: Auckland: April p. 389	1987
104	Edwards, J.H. **Tyler, R.J.**	Production of Liquid Fuels Via the Catalytic Oxidation of Methane	Studies in Surface Science & Catalysis: #36 Methane Conversion Symp.: Auckland: April p. 395	1987
105	**Asami, K.** Hashimoto, S. Fujimoto, K. Tominaga, H.	Selective Oxidative Coupling of Methane to Ethane & Ethylene	Studies in Surface Science & Catalysis: #36 Methane Conversion Symp.: Auckland: April p. 403	1987
106	**Larkins, F.P.** Nordin, M.R.	Oxidative Dehydrogenation of Methane to Form Higher Hydrocarbons	Studies in Surface Science & Catalysis: #36 Methane Conversion Symp.: Auckland: April p. 409	1987
107	**Hutchings, G.J.** Scurrell, M.S. Woodhouse, J.R.	Effect of O3 versus O2 as Oxidants for Methane	Studies in Surface Science & Catalysis: #36 Methane Conversion Symp.: Auckland: April p. 415	1987
108	Roos, J.A. Korf, S.J. Bakker, A.G. de Bruijn, N.A. van Ommen, J.G. **Ross, J.R.H.**	Oxidative Coupling of Methane: Catalyst Requirements & Process Conditions	Studies in Surface Science & Catalysis: #36 Methane Conversion Symp.: Auckland: April p. 373	1987
109	**Chevron-** Devries, L. Ryason, P.R.	Conversions of Low M.W. Hydrocarbons to Higher M.W. Hydrocarbons Using a Metal Compound-Containing Catalyst (IV-B)	U.S. Patent # 4704487	1987

Appendix H. REFERENCES FOR SELECTIVITY/CONVERSION PLOT (continued)

Ref.#	AUTHORS	TITLE	SOURCE	YEAR
110	**Chevron-** Devries, L. Ryason, P.R.	Conversions of Low M.W. Hydrocarbons to Higher M.W. Hydrocarbons Using a Metal Compound-Containing Catalyst	U.S. Patent # 4704488	1987
111	**Chevron-** Devries, L. Ryason, P.R.	Conversions of Low M.W. Hydrocarbons to Higher M.W. Hydrocarbons Using a Metal Compound-Containing Catalyst	U.S. Patent # 4709108	1987
112	**Cant, N.W.** Lukey, C.A. Nelson, P.F. Tyler, R.J.	Rate Controlling Step in the Oxidative Coupling of Methane over Li/MgO Catalyst	J. Chem. Soc., Chem. Commun. 766	1988
113	**Ekstrom, A.** Lapszewicz, J.A.	Methane Adsorption on a Working Sm2O3 Catalyst and its Role in Hydrocarbon Formation during High Temperature Partial Oxidation	J. Chem. Soc., Chem. Commun. 797	1988
114	**Nagamoto, H.** Amanuma, K. Nobutomo, H. Inoue, H.	Methane Oxidation Over Perovskite-Type Oxide Containing Alkaline-Earth Metal	Chem. Soc. Jpn., Chem. Lett. 237	1988
115	Anpo, M. Sunamoto, M. Doi, T. **Matsuura, I.**	Oxidative Coupling of Methane over Ultrafine Crystalline MgO Doped with Li: Role of Lower Coordinative Sites Produced by Li-Doping	Chem. Soc. Jpn., Chem. Lett. 701	1988
116	Korf, S.J. Roos, J.A. de Bruijn, N.A. van Ommen, J.G. **Ross, J.R.H.**	Oxidative Coupling of Methane over Li/MgO Catalysts	Catal. Today 2, 535	1988
117	Kowalak, S. **Moffat, J.B.**	Partial Oxidation of Methane Catalyzed by H-Mordenite and Fluorinated Mordenite	Appl. Catal. 36, 139	1988
118	**Hutchings, G.J.** Scurrell, M.S. Woodhouse, J.R.	Direct Partial Oxidation of Methane: Effect of the Oxidant on the Reaction	Appl. Catal. 38, 157	1988

Appendix H. REFERENCES FOR SELECTIVITY/CONVERSION PLOT (continued)

Ref.#	AUTHORS	TITLE	SOURCE	YEAR
119	Bi, Y. **Zhen, K.** Jiang, Y. Teng, C. Yang, X.	Catalytic Oxidative Coupling of Methane over Alkali, Alkaline Earth and Rare Earth Metal Oxides	Appl. Catal. 39, 185	1988
120	**Yates, D.J.C.** Zlotin, N.E.	Blank Reactor Corrections in Studies of the Oxidative Dehydrogenation of Methane	J. Catal. 111, 317	1988
121	Tagawa, T. **Imai, H.**	Mechanistic Aspects of Oxidative Coupling of Methane over LaAlO3	J. Chem. Soc., Faraday Trans. I 84, 923	1988
122	**McCarty, J.G.** Quinlan, M.A. Sancier, K.M.	Oxidative Methane Dimerization by Basic Oxide Catalysts	Presentation to: 1988 AIChE Spring National Meeting New Orleans	1988
123	Carreiro, J.A. Follmer, G. Lehmann, L. **Baerns, M.**	Oxidative Coupling of Methane to C2+ Hydrocarbons: Performance of Pb Compounds & Alkali/Alkaline Earths Compounds	Proceedings 9th Int. Cong. on Catalysis: Calgary Vol. 2: C1 Chemistry p. 891	1988
124	**Mirodatos, C.** Martin, G.A.	Oxidative Coupling of Methane on Li/MgO: Kinetics & Mechanism Involving Carbenic Intermediates	Proceedings 9th Int. Cong. on Catalysis: Calgary Vol. 2: C1 Chemistry p. 899	1988
125	**Aika, K.** Nishiyama, T.	Simultaneous Process of Oxidative Coupling of Methane & Reverse Shift of CO2	Proceedings 9th Int. Cong. on Catalysis: Calgary Vol. 2: C1 Chemistry p. 907	1988
126	**Hutchings, G.J.** Woodhouse, J.R. Scurrell, M.S.	Partial Oxidation of Methane Using O3, N2O, & O2 as Oxidants: A Comparative Study	Proceedings 9th Int. Cong. on Catalysis: Calgary Vol. 2: C1 Chemistry p. 923	1988
127	van Kasteren, H. Geerts, J.W. **van der Wiele, K.**	Ethylene Synthesis by Catalytic Oxidation of Methane over Li/MgO: Interaction of Catalytic & Non-Catalytic Reaction Steps	Proceedings 9th Int. Cong. on Catalysis: Calgary Vol. 2: C1 Chemistry p. 930	1988
128	Doi, T. Utsumi, Y. **Matsuura, I.**	Active & Selective Catalysts in Oxidative Coupling of Methane: Li2O Mixed with ZnO & BeO	Proceedings 9th Int. Cong. on Catalysis: Calgary Vol. 2: C1 Chemistry p. 937	1988

Appendix H. REFERENCES FOR SELECTIVITY/CONVERSION PLOT (continued)

Ref.#	AUTHORS	TITLE	SOURCE	YEAR
129	Lane, G.S. **Wolf, E.E.**	Methane Conversion to Hydrocarbons Via Oxidative Coupling on Li2O/TiO2 Catalysts	Proceedings 9th Int. Cong. on Catalysis: Calgary Vol. 2: C1 Chemistry p. 944	1988
130	**Imai, H.** Tagawa, T. Kamide, N. Wada, S.	Preparation & Characterization of Lanthanum Aluminum Mixed Oxide Catalysts For Oxidative Coupling of Methane	Proceedings 9th Int. Cong. on Catalysis: Calgary Vol. 2: C1 Chemistry p. 952	1988
131	Ueda, W. **Thomas, J.M.**	Layered Bismuth Oxyhalides: A New Family of Methane Oxidation Catalysts	Proceedings 9th Int. Cong. on Catalysis: Calgary Vol. 2: C1 Chemistry p. 960	1988
132	Sinev, M.Y. Korchak, V.N. **Krylov, O.V.**	Mechanism of Oxidative Condensation of Methane Into C2 Hydrocarbons Over Oxide Catalysts	Proceedings 9th Int. Cong. on Catalysis: Calgary Vol. 2: C1 Chemistry p. 968	1988
133	**Johnson Matthey:** Shutt, E. Jenkins, J.W. Altena, A.S.	Oxidative Conversion of Methane to Ethylene and/or Ethane+ on Catalyst Containing Refractory Non-Reducible Metal Compounds Carrying Oxygen: Compounds of Boron or Phosphorus	European Patent Application #0256857	1987
134	Sinev, M.Y. Korchak, V.N. **Krylov, O.V.**	Kinetic Peculiarities of Oxidative Condensation of Methane on Oxide Catalysts in a Heterogeneous-Homogeneous Process	Kinetics & Catalysis 28(6), 1188	1987
135	Lo, Y.M. Agarwal, S.K. **Marcelin, G.**	Oxidative Coupling of Methane over Antimony-Based Catalysts	J. Catal. 112, 168	1988
136	**Ekstrom, A.** Lapszewicz, J.A.	Role of Oxygen in the Partial Oxidation of Methane over a Samarium Oxide Catalyst	J. Am. Chem. Soc. 110, 5226	1988
137	**GRACE-** DeBoy,J.M. Hicks, R.F.	Oxidative Coupling of Methane over Alkaline Earth Promoted La2O3	J. Chem. Soc., Chem. Commun. 982	1988

Appendix H. REFERENCES FOR SELECTIVITY/CONVERSION PLOT (continued)

Ref.#	AUTHORS	TITLE	SOURCE	YEAR
138	**Mirodatos, C.** Perrichon, V. Durupty, M.C. Moral, P.	Deactivation of Alkali Promoted Magnesia in Oxidative Coupling of Methane	Catalyst Deactivation 183	1987
139	Carreiro, J.A.S. **Baerns, M.**	Oxidative Methane Coupling Part 1: Alkaline Earth Catalysts	Submitted for publication.	1988
140	Carreiro, J.A.S. **Baerns, M.**	Oxidative Methane Coupling Part 2: Composite Catalysts of Basic Materials	Submitted for publication.	1988
141	Nelson, P.F. Lukey, C.A. **Cant, N.W.**	Isotopic Evidence for Direct Methyl Coupling and Ethane to Ethylene Conversion during Partial Oxidation of Methane over Li/MgO	J. Phys. Chem. 92, 6176	1988
142	Pitchai, R. **Klier, K.**	Partial Oxidation of Methane	Catal. Rev. - Sci. Eng. 28, 13	1986
143	**Scurrell, M.S.**	Prospects for the Direct Conversion of Light Alkanes to Petrochemical Feedstocks and Liquid Fuels	Appl. Catal. 32, 1	1987
144	Preub, U. **Baerns, M.**	Chemical Technology of Natural Gas - Its Present State & Prospects	Chem. Eng. Technol. 10, 297	1987
145	**Baerns, M.**	Oxidative Catalytic Methane Conversion	Catal. Today 1, 357	1987
146	**Lunsford, J.H.**	Direct Conversion of Methane to Methanol and Higher Hydrocarbons	Studies in Surface Science & Catalysis: #36 Methane Conversion Symp.: Auckland: April p. 359	1987
147	**Bhasin, M.M.**	Feasibility of Ethylene Synthesis Via Oxidative Coupling of Methane	Studies in Surface Science & Catalysis: #36 Methane Conversion Symp.: Auckland: April p. 373	1987
148	**Phillips Petrol.** Kimble, J.B. Kolts, J.H.	Feedstock conversion	European Patent # 210383	1987

Appendix H. REFERENCES FOR SELECTIVITY/CONVERSION PLOT (continued)

Ref.#	AUTHORS	TITLE	SOURCE	YEAR
149	**Yates, D.J.C.** Zlotin, N.E. McHenry, J.A.	Supported Lithium Tetraborate as a Catalyst for the Continuous Oxidative Dehydrogenation of Methane	Submitted for publication.	1988
150	**Yamaguchi, T.** Kadota, A. Saito, C.	Dehydrogenative Coupling of Methane by Use of Thermal Diffusion Column	Chem. Soc. Japan, Chem. Lett. 681	1988
151	**ARCO:** Jaecker, J.A. Johnson, M.F.L.	Hydroxylated Magnesia Support	U.S. Patent #4,613,718	1986
152	Driscoll, D.J. **Lunsford, J.H.**	Gas-Phase Radical Formation during the Reactions of Methane, Ethane, Ethylene, and Propylene over Selected Oxide Catalysts	J. Phys. Chem. 89, 4415	1985
153	Ito, T. **Lunsford, J.H.**	Synthesis of Ethane and Ethylene by Partial Oxidation of Methane over Li/MgO	Nature 314, 721	1985
154	Driscoll, D.J. Martir, W. Wang, J.X. **Lunsford, J.H.**	The Production of Gas Phase Methyl Radicals over Li/MgO	Adsorption & Catalysis on Oxide Surfaces	1985
155	Hatano, M. **Otsuka, K.**	Alkali Metal Doped Transition Metal Oxides Active for Oxidative Coupling of Methane	Inorg. Chim. Acta 146, 243	1988
156	**Imai, H.** Tagawa, T.	Oxidative Coupling of Methane over LaAlO3	J. Chem. Soc., Chem. Commun. 52	1986
157	Asami, K. Omata, K. **Fujimoto, K.** Tominaga, H.	Vapor-Phase Oxidative Coupling of Methane under Pressure	Energy & Fuels 2, 574	1988
158	**Labinger, J.A.** Ott, K.C.	Mechanistic Studies on the Oxidative Coupling of Methane	J. Phys. Chem. 91, 2682	1987

Appendix H. REFERENCES FOR SELECTIVITY/CONVERSION PLOT (continued)

Ref.#	AUTHORS	TITLE	SOURCE	YEAR
159	**Labinger, J.A.** Ott, K.C. Mehta, S. Rockstad, H.K. Zoumaian, S.	Oxidative Coupling of Methane: Role of Solid State Chemistry	J. Chem. Soc., Chem. Commun. 543	1987
160	**Otsuka, K.** Said, A.A. Jinno, K. Komatsu, T.	Peroxide Anions as Possible Active Species in Oxidative Coupling of Methane	Chem. Soc. Japan, Chem. Lett. 77	1987
161	**Ito, T.** Tashiro, T. Watanabe, T. Toi, K. Ikemoto, I.	Activation of Methane on the MgO Surface at Low Temperatures	Chem. Soc. Japan, Chem. Lett. 1723	1987
162	Suleimanov, A.I. Ismailov, E.G. Aliev, S.M. **Sokolovskii, V.D.**	Contribution of One-Electron Acceptor Centers to Oxidative Dimerization of Methane	React. Kinet. Catal. Lett. 34, 51	1987
163	**Sokolovskii, V.D.**	Reaction Mechanism and Principles of Choosing Catalysts for Selective Oxidation at C-H Bonds	React. Kinet. Catal. Lett. 32, 159	1986
164	Buevskaya, O.V. Suleimanov, A.I. Aliev, S.M. **Sokolovskii, V.D.**	Activation of Hydrocarbons in the Oxidative Dimerization of Methane Over Alkaline Earth Metals	React. Kinet. Catal. Lett. 33, 223	1987
165	Nersesyan, L.A. Vardanyan, I.A. Kegeyan, E.M. Margolis, L.Ya. **Nalbandyan, A.B.**	Heterogeneous-Homogeneous Oxidation of Methane	Doklady Akad. Nauk SSSr 220, 605	1975
166	Ungar, R.K. Zhang, X. **Lambert, R.M.**	High Selectivity Catalysts for the Oxidative Coupling of Methane-Complex Oxides with the Rock Salt Structure	Appl. Catal. 42, L1	1988
167	Amorebieta, V.T. **Colussi, A.J.**	Kinetics and Mechanism of the Catalytic Oxidation of Methane over Li/MgO	J. Phys. Chem. 92, 4576	1988

Appendix H. REFERENCES FOR SELECTIVITY/CONVERSION PLOT (continued)

Ref.#	AUTHORS	TITLE	SOURCE	YEAR
168	**ARCO-** Jones, C.A. Leonard, J.J. Sofranko, J.A.	Fuels for the Future: Remote Gas Conversion	Energy & Fuels 1, 12	1987
169	**Phillips Petrol.-** Kimble, J.B. Kolts, J.H.	Playing Matchmaker with Methane	Chemtech August	1987
170	**Akzo, GmbH**	Production of Ethylene-Ethane Mixtures	German Patent #3503,664	1985
171	**Phillips Petrol.:** Kimble, J.B. Kolts, J.H.	Contact Material or Catalyst for Oxid., Esp. Methane to Ethylene and Ethane. Comprises TiO2 or Alkali or Alkaline Earth Titanate.	European Patent #0206042	1986
172	**Phillips Petrol.:** Kimble, J.B. Kolts, J.H.	Converting Methane to Ethylene and Ethane by Reaction with Oxygen & Catalyst Containing Metals of Group IAa and/or IIA Phosphate and Optional Halide	European Patent #0206043	1986
173	**Phillips Petrol.:** Kolts, J.H. Guillory, J.P.	Oxidation Catalysts, Especially for Ethylene Production. Comprises Alkali and Alkaline Earth Metal Components	European Patent #205,765 or AU-A-54353/86	1986
174	**Phillips Petrol.:** Kolts, J.H. Kimble, J.B.	Oxidation Catalysts, Especially for Ethylene Production. Comprises Group IA Metal or Compounds, Zinc or Compounds, and Optional Chloride Ion or Tin	European Patent #216,984 or AU-A-54350/86	1987
175	**Phillips Petrol.:** Kolts, J.H. Kimble, J.B.	Converting Methane to Ethane or Ethylene. Catalyst Comprises Alkaline Earth Oxide Optional Mix with Alkali Metal Oxide, Tin & Compounds, or Chlorides	European Patent #0,198,251	1986
176	**Amoco Corp.:** Jezl, J.L. Michaels, G.O. Spangler, M.J.	Converting Lower Alkanes to Higher Hydrocarbons by Catalyzed Oxidative Coupling Followed by Oligmerization	International Patent # WO 86/05176 PCT/US86/00389	1986
177	**W.R. Grace** Deboy, J.M. Hicks, R.F.	Oxidative Coupling of Methane Over Alkali, Alkaline Earth, and Rare Earth Oxides	Ind. Eng. Chem. Res. 27, 1577	1988

Appendix H. REFERENCES FOR SELECTIVITY/CONVERSION PLOT (continued)

Ref.#	AUTHORS	TITLE	SOURCE	YEAR
178	Ueda, W. **Thomas, J.M.**	Bismuth-Rich Layered Solids as Catalysts for the Oxidation of Methane to Higher Hydrocarbons	J. Chem. Soc., Chem. Commun. 1148	1988
179	**Labinger, J.A.**	Oxidative Coupling of Methane: An Inherent Limit to Selectivity	Submitted for publication	1988
180	**Yamaguchi, T.** Saito, C.	Selective Synthesis of Ethylene by Dehydrogenative Coupling of Methane by Use of Thermal Diffusion Column	Bull. Chem. Soc. Jpn. 61, 2649	1988
181	**Lee, J.S.** Oyama, S.T.	Oxidative Coupling of Methane to Higher Hydrocarbons	Catal. Rev.-Sci. Eng. 30(2), 249	1988
182	Idemitsu Kosan: **Otsuka, K.** Morigawa, K. Ryu, T.	Production Method of Hydrocarbon	JP 62/205036	1987
183	Korf, S.J. Roos, J.A. Diphoorn, J.M. Veehof, R.H.J. van Ommen, J.G. **Ross, J.R.H.**	Selective Oxidation of Methane to Ethane and Ethylene over Doped and Un-doped Rare Earth Oxides	Submitted to Catalysis Today	1988
184	Korf, S.J. Roos, J.A. Veehof, R.H.J. van Ommen, J.G. **Ross, J.R.H.**	Kinetics of the Oxidation of Ethane and Ethylene over Li/MgO and Ca/Sm2O3 Catalysts in Relation to the Oxidative Coupling of Methane	Submitted to Catalysis Today	1988
185	Korf, S.J. Roos, J.A. Diphoorn, J.M. Veehof, R.H.J. van Ommen, J.G. **Ross, J.R.H.**	Effect of Promoters on the Behavior of Sm2O3 Catalysts for the Oxidative Coupling of Methane	Preprint: Div. Pet. Chem. ACS LA Meeting:Symposia 33, 437	1988
186	Kastanas, G.N. Tsigdinos, G.A. **Schwank, J.**	Effect of Small Amounts of Ethane on Selective Oxidation of Methane over Silicic Acid and Quartz	J. Chem. Soc., Chem. Commun. 1298	1988
187	**ARCO:** Withers, H.P.	Methane Conversion	US Patent # 4,489,215	1984

Appendix H. REFERENCES FOR SELECTIVITY/CONVERSION PLCT (continued)

Ref.#	AUTHORS	TITLE	SOURCE	YEAR
188	**ARCO:** Jones, C.A. Sofranko, J.A.	Methane Conversion	US Patent # 4,495,374	1985
189	**ARCO:** Sofranko, J.A.	Hydoxylated Magnesia Support	US Patent # 4,517,398	1985
190	**ARCO:** Maffia, G.J.	Natural Gas Conversion	US Patent # 4,533,780	1985
191	**ARCO:** Sofranko, J.A. Jones, C.A.	Methane Conversion	US Patent # 4,544,784	1985
192	**ARCO:** Withers, H.P. Sofranko, J.A.	Methane Conversion	US Patent # 4,544,785	1985
193	**ARCO:** Breder Jr., E.W. Jaecker, J.A.	Methane Conversion Using a Magnesia/Silica Support	US Patent # 4,544,786	1985
194	**ARCO:** Jones, C.A. Sofranko, J.A. Leonard, J.J.	Methane Conversion Process	US Patent # 4,547,607	1985
195	**ARCO:** Johnson, M.F.L.	Methane Conversion Using a Magnesia/Silica Support	US Patent # 4,547,608	1985
196	**ARCO:** Jones, C.A. Sofranko, J.A.	Methane Conversion	US Patent # 4,547,611	1985
197	**ARCO:** Jones, C.A. Sofranko, J.A. Leonard, J.J.	Methane Conversion	US Patent # 4,554,395	1985
198	**ARCO:** Jones, C.A. Sofranko, J.A. Leonard, J.J.	Two-Step Methane Conversion	US Patent # 4,567,307	1986

Appendix H. REFERENCES FOR SELECTIVITY/CONVERSION PLOT (continued)

Ref.#	AUTHORS	TITLE	SOURCE	YEAR
199	**ARCO:** Jaecker, J.A.	Preparative Process for Methane Conversion Agents	US Patent # 4,568,785	1986
200	**ARCO:** Withers, H.P.	Methane Conversion	US Patent # 4,593,139	1986
201	**ARCO:** Jones, C.A. Leonard, J.J. Sofranko, J.A. Withers, H.P. Breder Jr., E.W. Johnson, M.F.L. Jaecker, J.A.	Alkali Promoted Manganese Oxide Compositions Containing Silica and/or Alkaline Earth Oxides	US Patent # 4,629,718	1986
202	**ARCO:** Jones, C.A. Leonard, J.J. Sofranko, J.A. Withers, H.P.	Methane Conversion Process	US Patent # 4,634,800	1987
203	**ARCO:** Jones, C.A. Sofranko, J.A.	Alkali Promoted Manganese Oxide Compositions Containing Zirconium	US Patent # 4,650,781	1987
204	**ARCO:** Sofranko, J.A.	Alkali Promoted Manganese Oxide Compositions Containing Barium Carbonate	US Patent # 4,654,459	1987
205	**Phillips Petrol:** Kimble, J.B. Kolts, J.H.	Methane Conversion	US Patent # 4,650,460	1987
206	**ARCO:** Josefowicz, J.Y.	Reducible Metal Oxide Compositions Containing Zirconium Oxide, Yttrium Oxide and an Alkali Metal Component	US Patent # 4,656,155	1987
207	**ARCO:** Jones, C.A. Leonard, J.J. Sofranko, J.A.	Methane Conversion	US Patent # 4,665,260	1987
208	**ARCO:** Mazurek, H.	Hydrocarbon Conversion Process Using a Molten Salt	US Patent # 4,665,261	1987

Appendix H. REFERENCES FOR SELECTIVITY/CONVERSION PLOT (continued)

Ref.#	AUTHORS	TITLE	SOURCE	YEAR
209	**ARCO:** Withers, H.P. Jones, C.A. Leonard, J.J. Sofranko, J.A. Gaffney, A.M.	Methane Conversion Process	US Patent # 4,670,619	1987
210	**ARCO:** Jaecker, J.A.	Preparative Process for Methane Conversion Agents	US Patent # 4,743,575	1988
211	**Amoco:** Jezl, J.L. Michaels, G.O. Spangler, M.J.	Conversion of a Lower Alkane	US Patent # 4,751,336	1988
212	**ARCO:** Coughenour, G.E. Jubin Jr., J.C.	Chemical Conversion Process	US Patent # 4,754,095	1988
213	**National Dist. & Chemical Corp:** Murib, J.H. Kahn, J.H.	Process for Making Higher Hydrocarbons from Methane	US Patent # 4,769,507	1988
214	**ARCO:** Gastinger, R.G. Withers, H.P. Sofranko, J.A.	Alkali Promoted Manganese Oxide Compositions Containing Titanium	US Patent # 4,769,508	1988
215	**ARCO:** Josefowicz, J.Y.	Reducible Metal Oxide Compositions Containing Zirconium	US Patent # 4,769,509	1988
216	**Phillips Petrol:** Kimble, J.B. Kolts, J.H.	Composition of Matter	US Patent # 4,775,654	1988
217	**ARCO:** Sofranko, J.A. Gastinger, R.G. Jones, C.A.	Boron-Promoted Reducible Metal Oxides and Methods of their Use	US Patent # 4,777,313	1988
218	**W.R. Grace:** Hicks, R.F.	Catalyst for the Conversion of Methane	US Patent # 4,780,449	1988

Appendix H. REFERENCES FOR SELECTIVITY/CONVERSION PLOT (continued)

Ref.#	AUTHORS	TITLE	SOURCE	YEAR
219	**AKZO GmbH:** Wohlfahrt, K. Bergfeld, M. Zengel, H.	Oxidative Coupling of Methane to Ethane and Ethylene	AU-A-52925/86	1986
220	**AKZO GmbH:** Wohlfahrt, K. Bergfeld, M. Zengel, H.	Production of Ethylene and Ethane Mixtures	AU-A-54467/86	1986
221	**ARCO:** Gastinger, R.G. Jones, C.A. Sofranko, J.A.	Boron-Promoted Reducible Metal Oxide and Methods for their Use	European Patent Application # 253,522	1987
222	France, J.E. **Shamsi, A.** Headley, L.C. Ahsan, M.Q.	Oxidative Coupling Catalyst Research for Conversion of Natural Gas to Liquid Fuels	Energy Progress 8, 185	1988
223	Harris, K.D. Ueda, W. **Thomas, J.M.** Smith, G.W.	New Type of Catalyst for Selective Oxidation Derived from Bismuth Oxychloride	Angew. Chem. Int. Ed. Engl. 27, 1364	1988
224	**ARCO-** Gaffney, A.M. Jones, C.A. Leonard, J.J. Sofranko, J.A.	Oxidative Coupling of Methane over Sodium Promoted Praseodymium Oxide	J. Catal. 114, 422	1988
225	**Elkstrom, A.** Lapszewicz, J.A.	Investigation of the Mechanism of Partial Oxidation of Methane over Samaria Catalysts	Preprint: Div. Pet. Chem. ACS LA Meeting:Symposia 33, 430	1988
226	Erekson, E.J. **Lee, A.L.**	Coupling of Methane over Promoted Li-Mixed Oxide Catalysts	Preprint: Div. Pet. Chem. ACS LA Meeting:Symposia 33, 443	1988
227	**ARCO-** Gaffney, A.M. Jones, C.A. Leonard, J.J. Sofranko, J.A.	Oxidative Coupling of Methane over Sodium Promoted Praseodymium Oxide	Preprint: Div. Pet. Chem. ACS LA Meeting:Symposia 33, 445	1988
228	Follmer, G. Lehmann, L. **Baerns, M.**	Application of Laboratory Scale Fixed & Fluidized Bed Reactors in the Oxidative Coupling of Methane	Preprint: Div. Pet. Chem. ACS LA Meeting:Symposia 33, 453	1988

Appendix H. REFERENCES FOR SELECTIVITY/CONVERSION PLOT (continued)

Ref.#	AUTHORS	TITLE	SOURCE	YEAR
229	**Zhen, K.** Bi, Y. Yang, X.	Catalytic Oxidative Coupling of Methane	React. Kinet. Catal. Lett. 37, 133	1988
230	**Minachev, K.M.** Usachev, N.Y. Udut, V.N. Khodakov, Y.S.	Oxidative Condensation of Methane	Russian Chem. Reviews 57, 221	1988
231	Tagawa, T. **Imai, H.**	Activity & Selectivity of Oxidative Coupling of Methane over LaAlO3	React. Kinet. Catal. Lett. 37, 115	1988
232	Shigapov, A.N. Novozhilova, M.A. Vereshchagin, S. Anshits, A.G. **Sokolovskii, V.D.**	Peculiarties in Oxidative Conversion of Methane to C2 Compounds over CaO-CaCl2 Catalysts	React. Kinet. Catal. Lett. 37, 397	1988
233	Suleimanov, A.I. Aliev, S.M. **Sokolovskii, V.D.**	High Temperature Catalytic Synthesis of Higher Hydrocarbons from Methane	React. Kinet. Catal. Lett. 31, 285	1986
234	Doval, H.J.F. Scelza, O.A. **Castro, A.A.**	Methane Oligomerization on Supported Metallic Oxides	React. Kinet. Catal. Lett. 34, 143	1987
235	Krylov, O.V.	Free Radical Process In Heterogeneous Oxidation Catalysis	React. Kinet. Catal. Lett. 35, 315	1987
236	**Burch, R.** Squire, G.D. Tsang, S.C.	Comparative Study of Catalysts for the Oxidative Coupling of Methane	Appl. Catal. 43, 105	1988

Appendix I. PROCESS CONCEPTUALIZATION - METHANE TO C_2'S

Exhibit 1

Methane Coupling Process Simplified Block Diagram

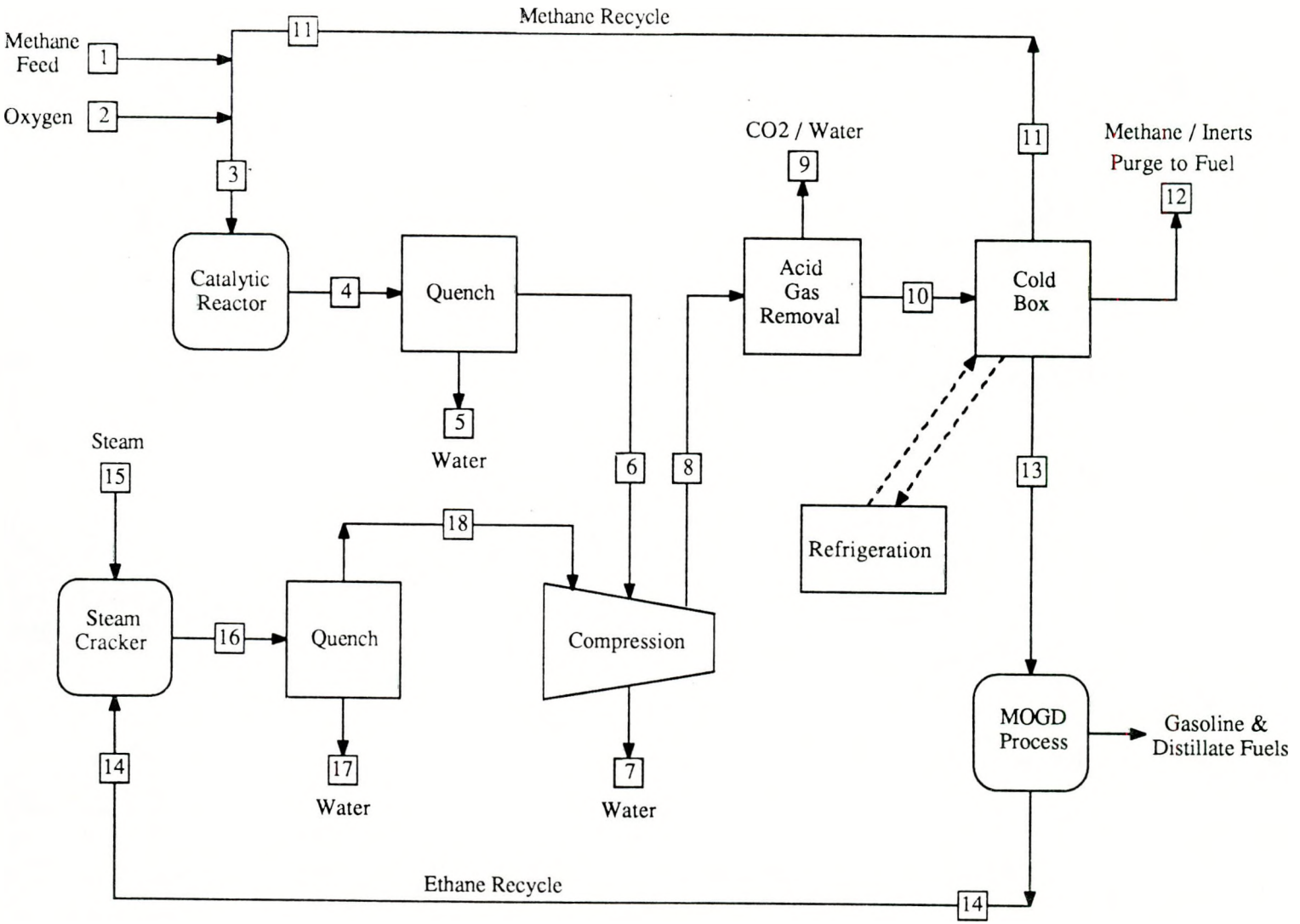


Exhibit 2

Methane Coupling Process Material Balance

Stream	1		2		3		4		5		Stream
Component	lb/hr	mol fr.	lb/hr	mol fr.	lb/hr	mol fr.	lb/hr	mol fr.	lb/hr	mol fr.	Component
H2					3366	0.0230	1683	0.0116			**H2**
N2	1726	0.0040	5941	0.0254	78408	0.0385	78408	0.0390			**N2**
O2			260052	0.9746	260697	0.1120	715	0.0003			**O2**
CO					15144	0.0074	16750	0.0083			**CO**
CO2	740	0.0011			740	0.0002	81235	0.0257	21	44 ppm	**CO2**
CH4	246697	0.9897			952257	0.8160	777051	0.6756	10	57 ppm	**CH4**
C2H4					3448	0.0017	91585	0.0455	4	13 ppm	**C2H4**
C2H6	2466	0.0053			2682	0.0012	34176	0.0159			**C2H6**
C3H6							6652	0.0022			**C3H6**
C3H8							2678	0.0008			**C3H8**
C4s											**C4s**
H2O							225805	0.1748	197271	0.9999	**H2O**
Total	**251629**	15537.7	**265993**	8339.0	**1316742**	72741.8	**1316738**	71689.8	**197306**	10951.6	**Total**

Stream	6		7		8		9		10		Stream
Component	lb/hr	mol fr.	lb/hr	mol fr.	lb/hr	mol fr.	lb/hr	mol fr.	lb/hr	mol fr.	Component
H2	1683	0.0137			3742	0.0296			3742	0.0307	**H2**
N2	78407	0.0461			78407	0.0447			78407	0.0463	**N2**
O2	715	0.0004			715	0.0004			715	0.0004	**O2**
CO	16750	0.0098			16824	0.0096			16824	0.0099	**CO**
CO2	81214	0.0304	7	113 ppm	81231	0.0295	81231	0.8470			**CO2**
CH4	777041	0.7974	3	133 ppm	778885	0.7747			778885	0.8026	**CH4**
C2H4	91581	0.0537	2	51 ppm	121735	0.0692			121735	0.0717	**C2H4**
C2H6	34175	0.0187			61900	0.0328			61900	0.0340	**C2H6**
C3H6	6652	0.0026			7239	0.0027			7239	0.0028	**C3H6**
C3H8	2678	0.0010			2784	0.0010			2784	0.0010	**C3H8**
C4s					1729	0.0005			1729	0.0005	**C4s**
H2O	28535	0.0261	25389	0.9997	6006	0.0053	6006	0.1530			**H2O**
Total	**1119431**	60738.1	**25401**	1409.7	**1161197**	62670.9	**87237**	2179.1	**1073960**	60491.8	**Total**

Exhibit 2

Methane Coupling Process Material Balance

Stream	11		12		13		14		15		Stream
Component	lb/hr	mol fr.	lb/hr	mol fr.	lb/hr	mol fr.	lb/hr	mol fr.	lb/hr	mol fr.	Component
H2	3366	0.0342	374	0.0364							**H2**
N2	70741	0.0517	7814	0.0548							**N2**
O2	645	0.0004	70	0.0004							**O2**
CO	15144	0.0111	1673	0.0117							**CO**
CO2											**CO2**
CH4	705559	0.9000	73214	0.8964	32	0.0003	32	0.0009			**CH4**
C2H4	3448	0.0025	29	0.0002	118271	0.6451	2320	0.0387			**C2H4**
C2H6	217	0.0001	1	7 ppm	61686	0.3139	61419	0.9554			**C2H6**
C3H6					7239	0.0263	48	0.0005			**C3H6**
C3H8					2784	0.0097	418	0.0044			**C3H8**
C4s					1729	0.0047	4	33 ppm			**C4s**
H2O									11555	1.0000	**H2O**
Total	**799120**	48865.1	**83175**	5091.1	**191741**	6535.3	**64241**	2138.0	**11555**	641.4	**Total**

Stream	16		17		18		Stream
Component	lb/hr	mol fr.	lb/hr	mol fr.	lb/hr	mol fr.	Component
H2	2059	0.2673			2059	0.3056	**H2**
N2							**N2**
O2							**O2**
CO	74	0.0007			74	0.0008	**CO**
CO2	23	0.0001			23	0.0002	**CO2**
CH4	1848	0.0301			1848	0.0345	**CH4**
C2H4	30157	0.2813	0.5	37 ppm	30156	0.3216	**C2H4**
C2H6	27726	0.2413	0.2	14 ppm	27726	0.2759	**C2H6**
C3H6	587	0.0037			587	0.0042	**C3H6**
C3H8	106	0.0006			106	0.0007	**C3H8**
C4s	1729	0.0081			1729	0.0092	**C4s**
H2O	11488	0.1669	8640	0.9999	2848	0.0473	**H2O**
Total	**75797**	3821.6	**8641**	479.6	**67156**	3342.0	**Total**

Exhibit 3

Synthesis Gas / Methanol Process Simplified Block Diagram

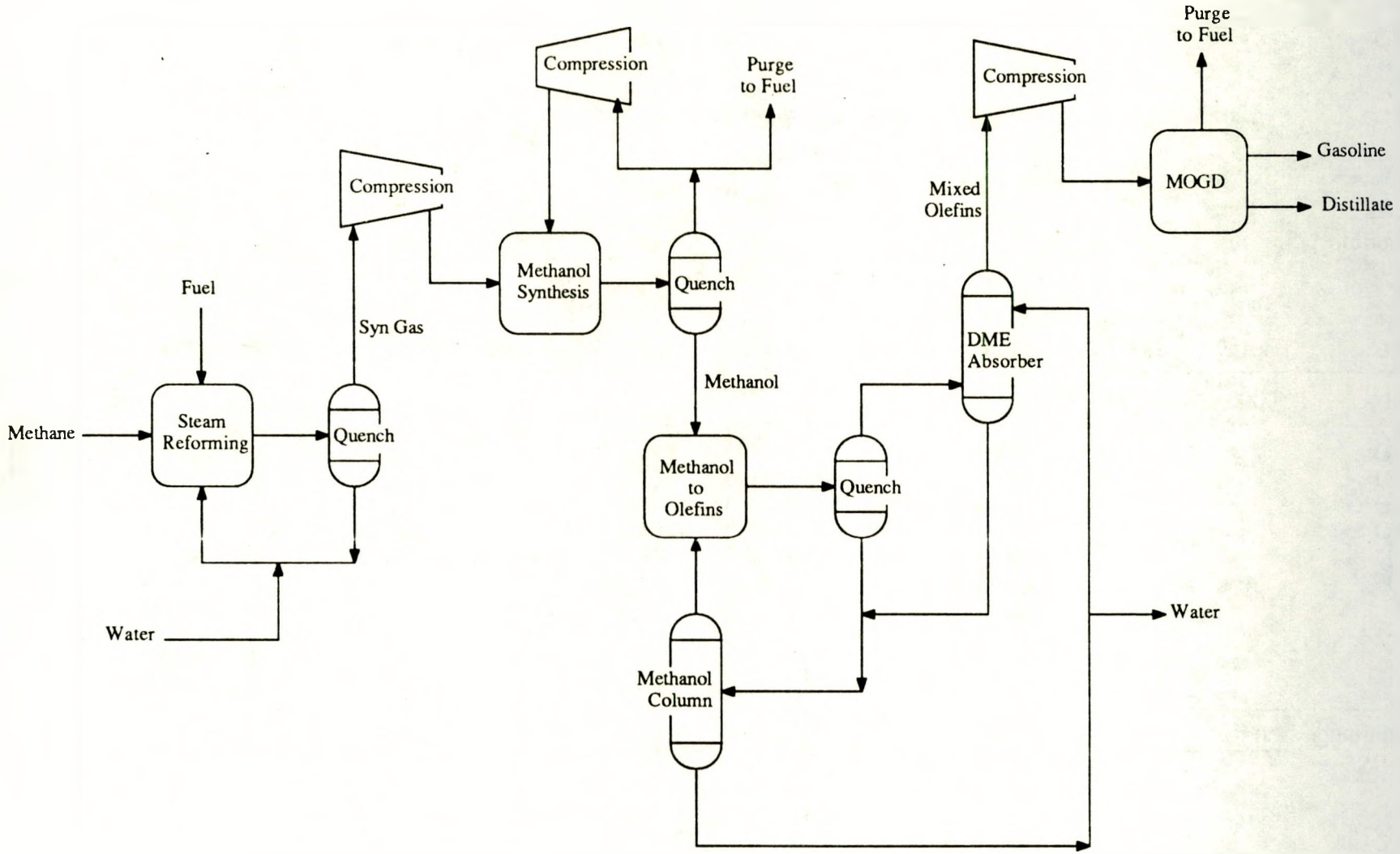


Exhibit 4

Gasoline & Distillate Economics

The two routes are equivalent.

	Methane Coupling	Synthesis Gas & Methanol
ISBL Investment	285	314
Air Separation Unit	61	--
MOGD	40	35
OSBL Investment	154	141
Total Fixed Investment	**540**	**490**
Working Capital	50	46
Total Utilized Investment	**590**	**536**
Operating Costs		
Methane	101	60
By-Product Credits	(26)	(2)
Utilities	23	28
Variable Cost	**98**	**88**
Fixed Cost	38	40
Total Cash Cost	**136**	**128**
Required Sales Price $/gal Product	**$2.09**	**$1.94**

All Costs are $MM/yr for a 10,600 bpd Unit
(1,000 MMppy olefins)
Required Sales Price generates a 10% ROIAT

Exhibit 5

Methane Coupling Process Simplified Block Diagram

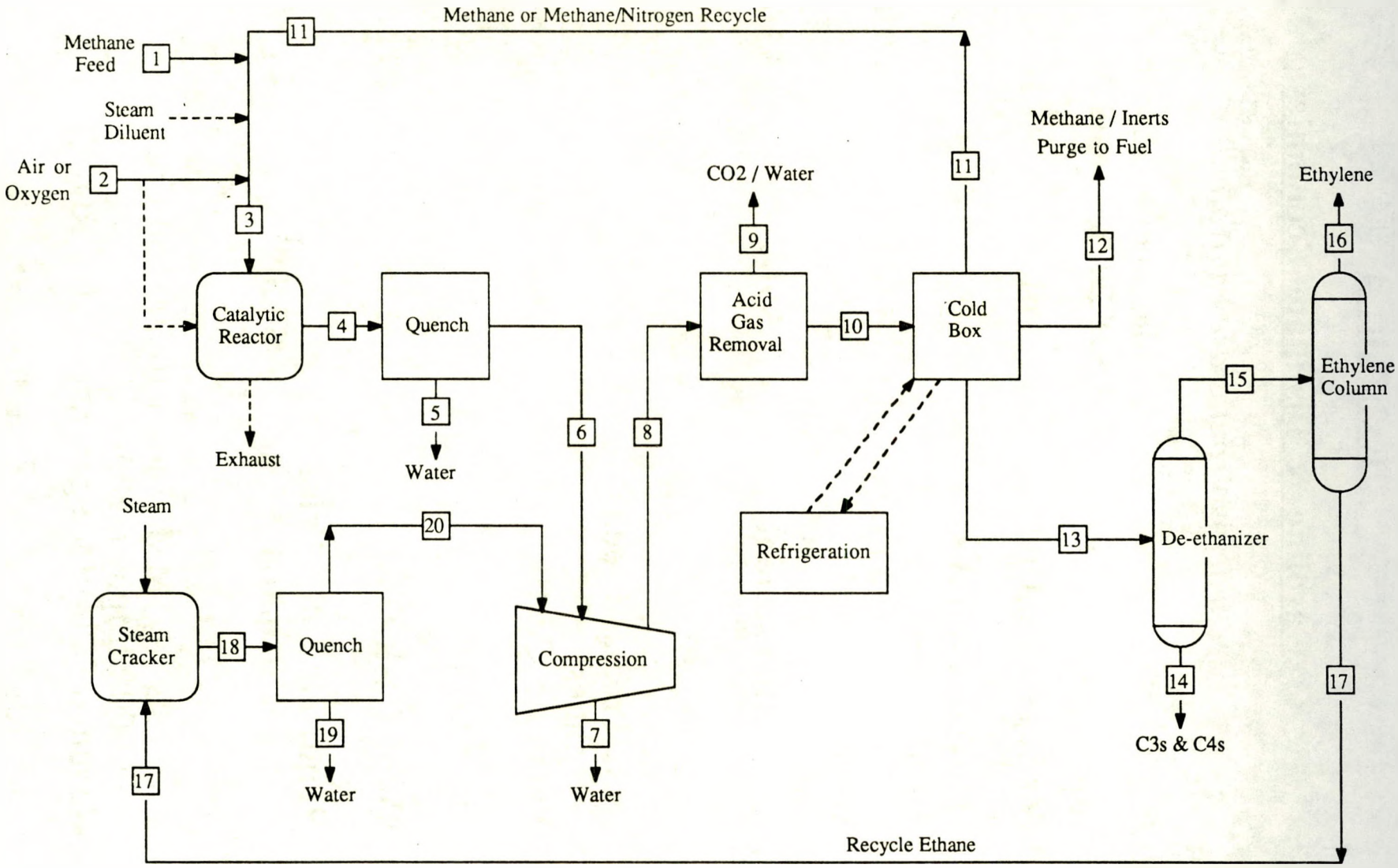


Exhibit 6

Nitrogen Diluent (Case A1.1b) Material Balance

Stream	1		2		3		4		5		Stream
Component	lb/hr	mol fr.	lb/hr	mol fr.	lb/hr	mol fr.	lb/hr	mol fr.	lb/hr	mol fr.	Component
H2					577	0.0016	291	0.0008			**H2**
N2	2367	0.0040	2082930	0.7909	3260180	0.6570	3260180	0.6556	15	28 ppm	**N2**
O2			629218	0.2091	629218	0.1110					**O2**
CO					35349	0.0071	91612	0.0184			**CO**
CO2	1014	0.0011			1014	0.0001	275867	0.0353	52	61 ppm	**CO2**
CH4	333236	0.9895			630826	0.2220	351430	0.1234	3	10 ppm	**CH4**
C2H4					2518	0.0005	97491	0.0196	3	6 ppm	**C2H4**
C2H6	3381	0.0054			3731	0.0007	32068	0.0060			**C2H6**
C3H6							5383	0.0007			**C3H6**
C3H8							1796	0.0002			**C3H8**
C4s											**C4s**
H2O							447289	0.1399	347102	0.9999	**H2O**
Total	**339998**	20991.4	**2712148**	94019.5	**4563413**	177151	**4563407**	177509	**347175**	19269.4	**Total**

Stream	6		7		8		9		10		Stream
Component	lb/hr	mol fr.	lb/hr	mol fr.	lb/hr	mol fr.	lb/hr	mol fr.	lb/hr	mol fr.	Component
H2	291	0.0009			2218	0.0070			2218	0.0074	**H2**
N2	3260160	0.7425	9	94 ppm	3260150	0.7450			3260150	0.7791	**N2**
O2											**O2**
CO	91611	0.0209			91680	0.0210			91680	0.0219	**CO**
CO2	275815	0.0400	31	196 ppm	275806	0.0401	275806	0.9167			**CO2**
CH4	351427	0.1398	2	33 ppm	353123	0.1409			353123	0.1474	**CH4**
C2H4	97488	0.0222	2	22 ppm	124035	0.0283			124035	0.0296	**C2H4**
C2H6	32068	0.0068			58011	0.0124			58011	0.0129	**C2H6**
C3H6	5383	0.0008			8063	0.0012			8063	0.0013	**C3H6**
C3H8	1796	0.0003			1899	0.0003			1899	0.0003	**C3H8**
C4s					1641	0.0002			1641	0.0002	**C4s**
H2O	73187	0.0259	64369	0.9997	10263	0.0036	10263	0.0833			**H2O**
Total	**4189226**	156740	**64413**	3574.3	**4186889**	156215	**286069**	6836.6	**3900820**	149379	**Total**

Exhibit 6

Nitrogen Diluent (Case A1.1b) Material Balance

Stream	11		12		13		14		15		Stream
Component	lb/hr	mol fr.	lb/hr	mol fr.	lb/hr	mol fr.	lb/hr	mol fr.	lb/hr	mol fr.	Component
H2	577	0.0046	1640	0.0100							**H2**
N2	1174880	0.6783	2085190	0.9186							**N2**
O2											**O2**
CO	35349	0.0204	56329	0.0248							**CO**
CO2											**CO2**
CH4	292591	0.2950	60565	0.0466	31	0.0003			31	0.0003	**CH4**
C2H4	2518	0.0015			121518	0.6649			121500	0.6864	**C2H4**
C2H6	350	0.0002			57661	0.2943	62	0.0101	57599	0.3036	**C2H6**
C3H6					8062	0.0294	5900	0.6846	2164	0.0082	**C3H6**
C3H8					1899	0.0066	1492	0.1652	407	0.0015	**C3H8**
C4s					1641	0.0045	1610	0.1401	27	0.0001	**C4s**
H2O											**H2O**
Total	**1506265**	61828.1	**2203724**	81036.2	**190812**	6515.0	**9064**	204.8	**181728**	6309.6	**Total**

Stream	16		17		18		19		20		Stream
Component	lb/hr	mol fr.	lb/hr	mol fr.	lb/hr	mol fr.	lb/hr	mol fr.	lb/hr	mol fr.	Component
H2					1927	0.2683			1927	0.3067	**H2**
N2											**N2**
O2											**O2**
CO					70	0.0007			70	0.0008	**CO**
CO2					22	0.0001			22	0.0002	**CO2**
CH4	31	0.0004			1699	0.0297			1699	0.0340	**CH4**
C2H4	120998	0.9986	503.0	0.0090	26550	0.2656		38 ppm	26550	0.3037	**C2H4**
C2H6	128	0.0010	57472.0	0.9603	25944	0.2422		15 ppm	25944	0.2768	**C2H6**
C3H6			2164	0.0258	2680	0.0179			2680	0.0204	**C3H6**
C3H8			407	0.0046	103	0.0007			103	0.0007	**C3H8**
C4s			27	0.0002	1641	0.0082			1641	0.0094	**C4s**
H2O					10695	0.1666	8039	0.9999	2656	0.0473	**H2O**
Total	**121157**	4319.2	**60573**	1990.4	**71331**	3562.9	**8040**	446.3	**63291**	3116.6	**Total**

Exhibit 7

Methane Diluent (Case A1.2a) Material Balance

Stream	1		2		3		4		5		Stream
Component	lb/hr	mol fr.	lb/hr	mol fr.	lb/hr	mol fr.	lb/hr	mol fr.	lb/hr	mol fr.	Component
H2					3526	0.0231	1764	0.0117			**H2**
N2	1800	0.0040	6183	0.0254	76489	0.0361	76489	0.0366			**N2**
O2			271269	0.9746	271269	0.1120					**O2**
CO					15804	0.0075	17483	0.0084			**CO**
CO2	771	0.0011			771	0.0002	84742	0.0258	22	44 ppm	**CO2**
CH4	257089	0.9897			994249	0.8188	811466	0.6781	10	55 ppm	**CH4**
C2H4					2487	0.0012	94436	0.0451	4	12 ppm	**C2H4**
C2H6	2571	0.0053			2731	0.0012	35586	0.0159			**C2H6**
C3H6							6940	0.0022			**C3H6**
C3H8							2794	0.0008			**C3H8**
C4s											**C4s**
H2O							235621	0.1753	205958	0.9999	**H2O**
Total	**262231**	16192.3	**277452**	8698.1	**1367326**	75692.1	**1367321**	74593.0	**205994**	11433.8	**Total**

Stream	6		7		8		9		10		Stream
Component	lb/hr	mol fr.	lb/hr	mol fr.	lb/hr	mol fr.	lb/hr	mol fr.	lb/hr	mol fr.	Component
H2	1764	0.0139			3915	0.0299			3915	0.0309	**H2**
N2	76489	0.0432			76489	0.0420			76489	0.0434	**N2**
O2											**O2**
CO	17483	0.0099			17560	0.0096			17560	0.0100	**CO**
CO2	84720	0.0305	10	153 ppm	84734	0.0296	84734	0.8959			**CO2**
CH4	811455	0.8008	5	198 ppm	813346	0.7794			813346	0.8061	**CH4**
C2H4	94432	0.0533	2	54 ppm	124059	0.0680			124059	0.0703	**C2H4**
C2H6	35585	0.0187			64540	0.0330			64540	0.0341	**C2H6**
C3H6	6940	0.0026			9743	0.0036			9743	0.0037	**C3H6**
C3H8	2794	0.0010			2913	0.0010			2913	0.0011	**C3H8**
C4s					1801	0.0005			1801	0.0005	**C4s**
H2O	29663	0.0261	27241	0.9996	4031	0.0034	4031	0.1041			**H2O**
Total	**1161325**	63159	**27258**	1512.7	**1203131**	65044.6	**88765**	2149.1	**1114366**	62895	**Total**

Exhibit 7

Methane Diluent (Case A1.2a) Material Balance

Stream	11		12		13		14		15		Stream
Component	lb/hr	mol fr.	lb/hr	mol fr.	lb/hr	mol fr.	lb/hr	mol fr.	lb/hr	mol fr.	Component
H2	3526	0.0344	392	0.0368							**H2**
N2	68507	0.0481	7615	0.0515							**N2**
O2											**O2**
CO	15804	0.0111	1743	0.0118							**CO**
CO2											**CO2**
CH4	737160	0.9045	76258	0.8998	33	0.0003			33	0.0003	**CH4**
C2H4	2487	0.0017	20	0.0001	121554	0.6367			121554	0.6629	**C2H4**
C2H6	160	0.0001			64376	0.3146	80	0.0099	64296	0.3271	**C2H6**
C3H6					9741	0.0340	7524	0.6648	2217	0.0081	**C3H6**
C3H8					2913	0.0097	2442	0.2059	471	0.0016	**C3H8**
C4s					1801	0.0047	1801	0.1194			**C4s**
H2O											**H2O**
Total	**827644**	50801.8	**86028**	5282.6	**200418**	6805.5	**11847**	268.9	**188571**	6536.6	**Total**

Stream	16		17		18		19		20		Stream
Component	lb/hr	mol fr.	lb/hr	mol fr.	lb/hr	mol fr.	lb/hr	mol fr.	lb/hr	mol fr.	Component
H2					2151	0.2688			2151	0.3072	**H2**
N2											**N2**
O2											**O2**
CO					78	0.0007			78	0.0008	**CO**
CO2					24	0.0001			24	0.0002	**CO2**
CH4	33	0.0005			1896	0.0298			1896	0.0340	**CH4**
C2H4	120943	0.9984	611	0.0098	29631	0.2661	1	37 ppm	29630	0.3041	**C2H4**
C2H6	143	0.0011	64153	0.9616	28955	0.2426		12 ppm	28955	0.2772	**C2H6**
C3H6			2217	0.0237	2803	0.0168			2803	0.0192	**C3H6**
C3H8			471	0.0048	119	0.0007			119	0.0008	**C3H8**
C4s					1801	0.0081			1801	0.0092	**C4s**
H2O					11906	0.1665	8945	1.0000	2961	0.0473	**H2O**
Total	**121119**	4317.9	**67452**	2218.7	**79364**	3969.9	**8946**	496.6	**70418**	3473.4	**Total**

Exhibit 8
Steam Diluent (Case A1.3b) Material Balance

Stream	1		2		3		4		5		Stream
Component	lb/hr	mol fr.	lb/hr	mol fr.	lb/hr	mol fr.	lb/hr	mol fr.	lb/hr	mol fr.	Component
H2					3115	0.0083	1564	0.0042			**H2**
N2	2137	0.0040	15166	0.0254	172747	0.0332	172747	0.0333	18	5 ppm	**N2**
O2			665520	0.9746	665520	0.1120					**O2**
CO					122272	0.0235	135376	0.0261	20	5 ppm	**CO**
CO2	916	0.0011			916	0.0001	344468	0.0423	1410	233 ppm	**CO2**
CH4	305388	0.9897			630400	0.2116	350319	0.1181	70	32 ppm	**CH4**
C2H4					12965	0.0025	108170	0.0208	69	18 ppm	**C2H4**
C2H6	3053	0.0053			4243	0.0008	32650	0.0059	8	2 ppm	**C2H6**
C3H6							5396	0.0007	3	1 ppm	**C3H6**
C3H8							1800	0.0002			**C3H8**
C4s											**C4s**
H2O					2034000	0.6080	2493680	0.7483	2471160	0.9997	**H2O**
Total	**311494**	19234.2	**680686**	21339.5	**3646178**	185700	**3646170**	184972	**2472758**	137213	**Total**

Stream	6		7		8		9		10		Stream
Component	lb/hr	mol fr.	lb/hr	mol fr.	lb/hr	mol fr.	lb/hr	mol fr.	lb/hr	mol fr.	Component
H2	1564	0.0162			3477	0.0347			3477	0.0414	**H2**
N2	172729	0.1291		14 ppm	172729	0.1239			172729	0.1480	**N2**
O2											**O2**
CO	135356	0.1012		15 ppm	135425	0.0972			135425	0.1161	**CO**
CO2	343058	0.1632	6	136 ppm	343049	0.1567	343049	0.9638			**CO2**
CH4	350249	0.4571	3	184 ppm	351934	0.4410			351934	0.5266	**CH4**
C2H4	108101	0.0807	3	89 ppm	134457	0.0963			134457	0.1150	**C2H4**
C2H6	32642	0.0227		9 ppm	58398	0.0390			58398	0.0466	**C2H6**
C3H6	5393	0.0027			8074	0.0039			8074	0.0046	**C3H6**
C3H8	1800	0.0009			1900	0.0009			1900	0.0010	**C3H8**
C4s					1622	0.0006			1622	0.0007	**C4s**
H2O	22524	0.0262	18684	0.9996	5273	0.0059	5273	0.0362			**H2O**
Total	**1173416**	47759.3	**18697**	1037.6	**1216338**	49748.8	**348322**	8087.5	**868016**	41661.3	**Total**

Exhibit 8

Steam Diluent (Case A1.3b) Material Balance

Stream	11		12		13		14		15		Stream
Component	lb/hr	mol fr.	lb/hr	mol fr.	lb/hr	mol fr.	lb/hr	mol fr.	lb/hr	mol fr.	Component
H2	3115	0.0480	363	0.0610							H2
N2	155444	0.1722	17288	0.2092							N2
O2											O2
CO	122272	0.1355	13159	0.1593							CO
CO2											CO2
CH4	325011	0.6288	26963	0.5697	31	0.0003			31	0.0003	CH4
C2H4	12965	0.0143	62	0.0007	121444	0.6662			121444	0.6879	C2H4
C2H6	1191	0.0012	1	11 ppm	57221	0.2929	62	0.0101	57159	0.3021	C2H6
C3H6					8075	0.0295	5906	0.6841	2169	0.0082	C3H6
C3H8					1900	0.0066	1504	0.1662	396	0.0014	C3H8
C4s					1624	0.0045	1607	0.1396	17	48 ppm	C4s
H2O											H2O
Total	**619998**	32219.9	**57836**	2949.9	**190295**	6497.8	**9079**	205.2	**181216**	6292.6	Total

Stream	16		17		18		19		20		Stream
Component	lb/hr	mol fr.	lb/hr	mol fr.	lb/hr	mol fr.	lb/hr	mol fr.	lb/hr	mol fr.	Component
H2					1913	0.2701			1913	0.3090	H2
N2											N2
O2											O2
CO					69	0.0007			69	0.0008	CO
CO2					22	0.0001			22	0.0002	CO2
CH4	31	0.0004			1686	0.0299			1686	0.0342	CH4
C2H4	121128	0.9986	316	0.0057	26359	0.2674		37 ppm	26359	0.3060	C2H4
C2H6	129	0.0010	57030	0.9635	25756	0.2438		12 ppm	25756	0.2789	C2H6
C3H6			2169	0.0262	1680	0.0114			1680	0.0130	C3H6
C3H8			396	0.0046	100	0.0006			100	0.0007	C3H8
C4s					1622	0.0082			1622	0.0094	C4s
H2O					10620	0.1678	7981	1.0000	2639	0.0477	H2O
Total	**121288**	4323.9	**59911**	1968.4	**69827**	3513.7	**7982**	443.0	**61845**	3070.7	Total

Exhibit 9
Sequential Feed (Case A1.4b) Material Balance

Stream	1		2		3		4		5		Stream
Component	lb/hr	mol fr.	lb/hr	mol fr.	lb/hr	mol fr.	lb/hr	mol fr.	lb/hr	mol fr.	Component
H2					3291	0.0249	1651	0.0135			**H2**
N2	2010	0.0040	1178854	0.7909	93637	0.0510	101751	0.0598			**N2**
O2			356112	0.2091							**O2**
CO					68422	0.0372	75906	0.0446			**CO**
CO2	861	0.0011			861	0.0003	119776	0.0448			**CO2**
CH4	287239	0.9897			930475	0.8841	707890	0.7266			**CH4**
C2H4					1789	0.0010	95887	0.0563			**C2H4**
C2H6	2871	0.0053			2968	0.0015	33016	0.0181			**C2H6**
C3H6							9009	0.0035			**C3H6**
C3H8							3144	0.0012			**C3H8**
C4s							18821	0.0055			**C4s**
H2O							28558	0.0261			**H2O**
Total	**292981**	18091.1	**1534966**	53211.2	**1101443**	65598.7	**1195409**	60729	**0**		**Total**

Stream	6		7		8		9		10		Stream
Component	lb/hr	mol fr.	lb/hr	mol fr.	lb/hr	mol fr.	lb/hr	mol fr.	lb/hr	mol fr.	Component
H2	1651	0.0135			3639	0.0289			3639	0.0303	**H2**
N2	101751	0.0598		8 ppm	101750	0.0582			101750	0.0611	**N2**
O2											**O2**
CO	75906	0.0446		9 ppm	75976	0.0435			75976	0.0456	**CO**
CO2	119776	0.0448	15	227 ppm	119742	0.0436	119742	0.9260			**CO2**
CH4	707890	0.7266	4	180 ppm	709628	0.7086			709628	0.7436	**CH4**
C2H4	95887	0.0563	2	56 ppm	123298	0.0704			123298	0.0739	**C2H4**
C2H6	33016	0.0181		9 ppm	59809	0.0319			59809	0.0334	**C2H6**
C3H6	9009	0.0035			11745	0.0045			11745	0.0047	**C3H6**
C3H8	3144	0.0012			3237	0.0012			3237	0.0012	**C3H8**
C4s	18821	0.0055			20487	0.0058			20487	0.0061	**C4s**
H2O	28558	0.0261	26132	0.9995	3917	0.0035	3917	0.0740			**H2O**
Total	**1195409**	60729.3	**26154**	1451.3	**1233228**	62422.6	**123659**	2938.2	**1109569**	59484.4	**Total**

Exhibit 9

Sequential Feed (Case A1.4b) Material Balance

Stream	11		12		13		14		15		Stream
Component	lb/hr	mol fr.	lb/hr	mol fr.	lb/hr	mol fr.	lb/hr	mol fr.	lb/hr	mol fr.	Component
H2	3291	0.0344	364	0.0366							**H2**
N2	91627	0.0688	10137	0.0733							**N2**
O2											**O2**
CO	68422	0.0514	7551	0.0546							**CO**
CO2											**CO2**
CH4	643236	0.8440	66157	0.8354	34	0.0003			34	0.0003	**CH4**
C2H4	1789	0.0013	13	0.0001	121487	0.6155			121487	0.6794	**C2H4**
C2H6	97	0.0001			59714	0.2822	199	0.0100	59515	0.3105	**C2H6**
C3H6					11743	0.0397	9501	0.3408	2242	0.0084	**C3H6**
C3H8					3237	0.0104	2869	0.0982	368	0.0013	**C3H8**
C4s					20483	0.0519	20483	0.5510			**C4s**
H2O											**H2O**
Total	**808462**	47507.6	**84222**	4936.2	**216698**	7036.0	**33052**	662.5	**183646**	6373.5	**Total**

Stream	16		17		18		19		20		Stream
Component	lb/hr	mol fr.	lb/hr	mol fr.	lb/hr	mol fr.	lb/hr	mol fr.	lb/hr	mol fr.	Component
H2					1988	0.2682			1988	0.3066	**H2**
N2											**N2**
O2											**O2**
CO					72	0.0007			72	0.0008	**CO**
CO2					23	0.0001			23	0.0002	**CO2**
CH4	31	0.0004			1754	0.0297			1754	0.0340	**CH4**
C2H4	120969	0.9985	518	0.0090	27420	0.2659		37 ppm	27420	0.3039	**C2H4**
C2H6	139	0.0011	59376	0.9610	26794	0.2424		12 ppm	26794	0.2771	**C2H6**
C3H6			2242	0.0259	2737	0.0177			2737	0.0202	**C3H6**
C3H8			368	0.0041	93	0.0006			93	0.0007	**C3H8**
C4s					1667	0.0081			1667	0.0092	**C4s**
H2O					11036	0.1666	8295	1.0000	2741	0.0473	**H2O**
Total	**121139**	4318.6	**62504**	2054.7	**73584**	3676.5	**8296**	460.5	**65288**	3216.0	**Total**

Exhibit 10

Reactor Diluent Case Descriptions

Using Nitrogen or Steam as a diluent gives high Yield-to-C_2's.

Case	A1.1b	A1.2a	A1.3b	A1.4b
Diluent	Nitrogen	Methane	Steam	None
Feed System		Co-feed		Sequential
Catalyst		UCC $BaCO_3/Al_2O_3/ECl$		Arco $Mn/Na/P/SiO_2$
Reactor				
Type		Fixed-Bed		Fluidized-Bed
Temperature, °C		750		850
Pressure, psig		50		50
GHSV, hr^{-1}		2133		1200
CH_4				
Conversion, %	45	18	45	24
Selectivity to:				
C_2H_4, %	39	58	39	48
C_2H_6, %	11	19	11	14
C_3H_6, %	2.2	4.3	2.2	4.6
C_3H_8, %	0.7	1.7	0.7	1.5
C_4's +, %	0.2	--	0.2	10
CO, %	15	3	15	11
CO_2, %	32	14	32	11
C_2 Yield, %	**22**	**14**	**22**	**15**

Exhibit 11
Reactor Diluent Investment Costs

Case Diluent	A1.1b Nitrogen	A1.2a Methane	A1.3b Steam	A1.4b Sequential
Coupling Reaction System	116	72	113	95
Steam Cracking System	25	28	25	26
Compression	149	81	48	77
Gas Pretreating	31	14	13	14
Cold Box & Methane Column	49	45	26	51
Refining	31	31	31	31
Refrigeration	39	45	38	49
Acetylene Hydrogenation	1	1	1	1
Air Compression System	66			36
Total ISBL	**507**	**317**	**295**	**380**
Air Separation Unit		62	105	
OSBL	203	151	160	152
Total Fixed Investment	**710**	**530**	**561**	**532**

All figures are $MM ± 25% for a unit producing 1,000 MMppy of ethylene.

Exhibit 12
Reactor Diluent Economics

Case Diluent	A1.1b Nitrogen	A1.2a Methane	A1.3b Steam	A1.4b Sequential
Total Fixed Investment	**710**	**530**	**561**	**532**
Working Capital	66	60	70	60
Total Utilized Investment	**776**	**590**	**631**	**592**
Operating Costs				
Methane	146	112	132	124
By-Product Credits	(12)	(44)	(22)	(53)
Utilities	26	29	56	15
Variable Cost	**160**	**97**	**166**	**86**
Fixed Cost	52	40	42	40
Total Cash Cost	**212**	**137**	**208**	**126**
ROIAT, %	**3.0**	**13.9**	**5.6**	**15.0**

All figures are $MM for a unit producing 1,000 MMppy of ethylene.
ROIAT is based on ethylene sales at $0.32/lb.

Exhibit 13
Nitrogen Diluent Investment Costs

Case	A1.1d	A1.1b	A1.1c
Methane / Oxygen Ratio	**1**	**2**	**4**
Coupling Reaction System	188	116	96
Steam Cracking System	21	25	30
Compression	119	149	128
Gas Pretreating	31	31	24
Cold Box & Methane Column	58	49	71
Refining	31	31	32
Refrigeration	31	39	54
Acetylene Hydrogenation	1	1	1
Air Compression System	115	66	49
Total ISBL	**595**	**507**	**485**
Air Separation Unit OSBL	238	203	194
Total Fixed Investment	**833**	**710**	**679**

All figures are $MM ± 25% for a unit producing 1,000 MMppy of ethylene.

Exhibit 14
Nitrogen Diluent Economics

Case	A1.1d	A1.1b	A1.1c
Methane / Oxygen Ratio	**1**	**2**	**4**
Total Fixed Investment	**833**	**710**	**679**
Working Capital	74	66	65
Total Utilized Investment	**907**	**776**	**744**
Operating Costs			
Methane	200	146	129
By-Product Credits	(8)	(12)	(19)
Utilities	11	26	36
Variable Cost	**203**	**160**	**146**
Fixed Cost	62	53	51
Total Cash Cost	**265**	**213**	**197**
ROIAT, %	**-1.9**	**2.9**	**4.7**

All figures are $MM for a unit producing 1,000 MMppy of ethylene.
ROIAT is based on ethylene sales at $0.32/lb.

Exhibit 15
Steam Diluent Investment Costs

Case	A1.3d	A1.3b	A1.3c
Methane / Oxygen Ratio	1	2	4
Coupling Reaction System	162	113	93
Steam Cracking System	20	25	30
Compression	55	48	62
Gas Pretreating	16	13	15
Cold Box & Methane Column	24	26	32
Refining	30	31	33
Refrigeration	33	38	45
Acetylene Hydrogenation	1	1	1
Air Compression System			
Total ISBL	**341**	**295**	**311**
Air Separation Unit	144	105	86
OSBL	194	160	159
Total Fixed Investment	**679**	**561**	**556**

All figures are $MM ± 25% for a unit producing 1,000 MMppy of ethylene.

Exhibit 16
Steam Diluent Economics

Case	A1.3d	A1.3b	A1.3c
Methane / Oxygen Ratio	**1**	**2**	**4**
Total Fixed Investment	**679**	**561**	**556**
Working Capital	87	70	65
Total Utilized Investment	**766**	**631**	**621**
Operating Costs			
Methane	183	132	122
By-Product Credits	(16)	(23)	(37)
Utilities	90	56	42
Variable Cost	**257**	**165**	**127**
Fixed Cost	51	43	42
Total Cash Cost	**308**	**208**	**169**
ROIAT, %	**-4.6**	**5.6**	**9.7**

All figures are $MM for a unit producing 1,000 MMppy of ethylene.
ROIAT is based on ethylene sales at $0.32/lb.

Exhibit 17
Sequential Feed Investment Costs

Case	A1.4c	A1.4b	A1.4d	A1.4e
Methane / Oxygen Ratio	2	5	7	10
Coupling Reaction System	113	95	100	104
Steam Cracking System	27	26	26	26
Compression	71	77	85	94
Gas Pretreating	15	14	16	17
Cold Box & Methane Column	39	51	52	58
Refining	31	31	31	31
Refrigeration	47	49	52	55
Acetylene Hydrogenation	1	1	1	1
Air Compression System	75	36	32	27
Total ISBL	**419**	**380**	**395**	**413**
Air Separation Unit OSBL	168	152	158	165
Total Fixed Investment	**587**	**532**	**554**	**579**

All figures are $MM ± 25% for a unit producing 1,000 MMppy of ethylene.

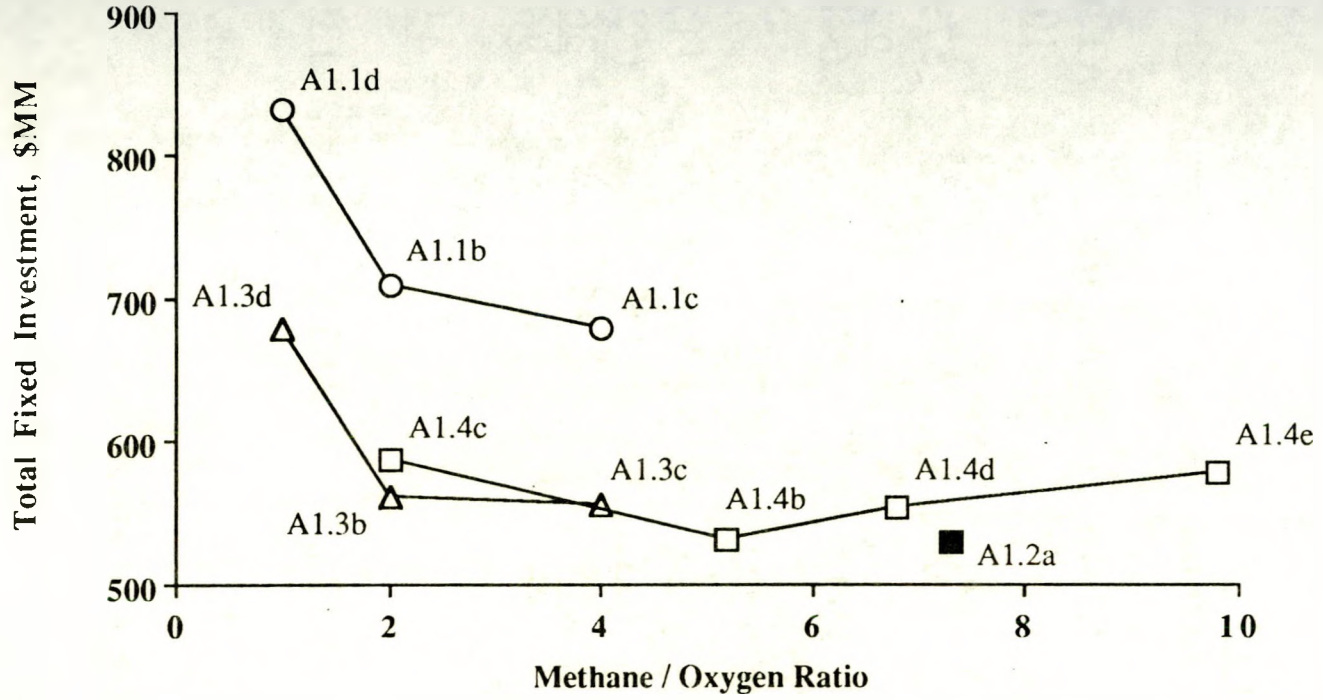
Exhibit 18
Sequential Feed Economics

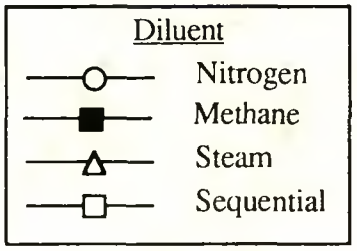
Case	A1.4c	A1.4b	A1.4d	A1.4e
Methane / Oxygen Ratio	**2**	**5**	**7**	**10**
Total Fixed Investment	**587**	**532**	**554**	**579**
Working Capital	66	60	61	62
Total Utilized Investment	**653**	**592**	**615**	**641**
Operating Costs				
Methane	164	124	119	112
By-Product Credits	(49)	(53)	(53)	(52)
Utilities	4	15	25	36
Variable Cost	**119**	**86**	**91**	**96**
Fixed Cost	44	40	42	43
Total Cash Cost	**163**	**126**	**133**	**139**
ROIAT, %	**9.5**	**15.0**	**13.5**	**12.1**

All figures are $MM for a unit producing 1,000 MMppy of ethylene.
ROIAT is based on ethylene sales at $0.32/lb.

Exhibit 19

Summary of Economic Sensitivity to Methane / Oxygen Ratio





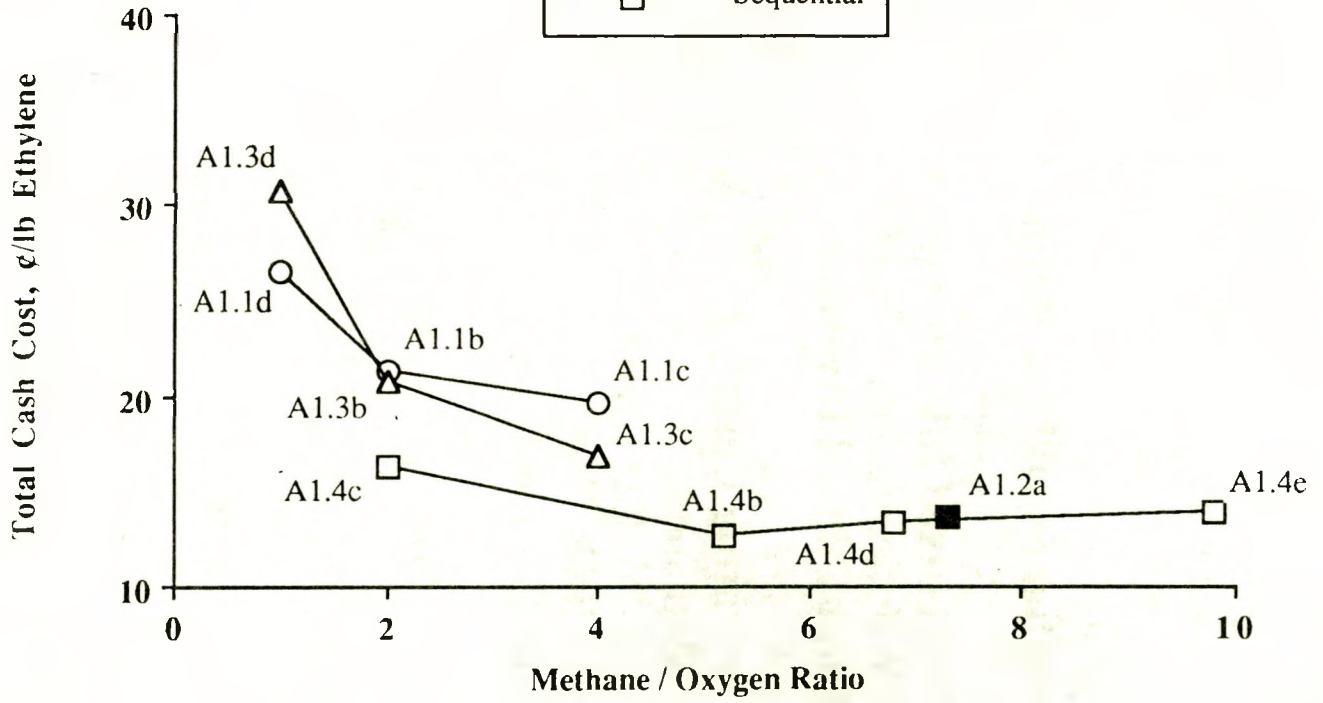


Exhibit 20

Summary of Economic Sensitivity to Methane / Oxygen Ratio

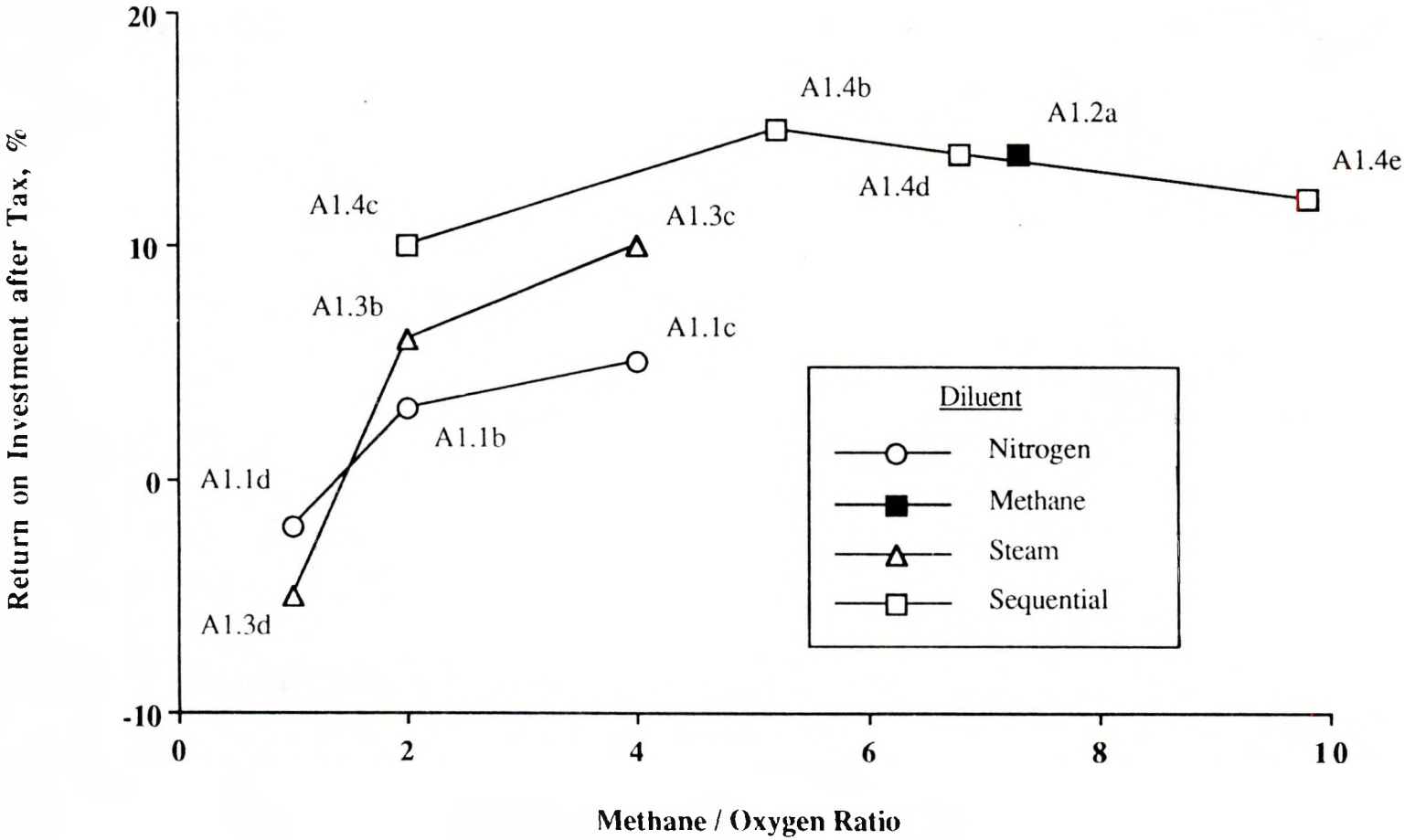


Exhibit 21
Rx Oxygen Concentration Investment Costs

Case	A1.2a	A1.2b
Rx Oxygen Concentration, %	11%	5%
Coupling Reaction System	72	101
Steam Cracking System	28	28
Compression	81	118
Gas Pretreating	14	22
Cold Box & Methane Column	45	65
Refining	31	31
Refrigeration	45	59
Acetylene Hydrogenation	1	1
Air Compression System		
Total ISBL	**317**	**425**
Air Separation Unit	62	50
OSBL	151	190
Total Fixed Investment	**530**	**666**

All figures are $MM ± 25% for a unit producing 1,000 MMppy of ethylene.

Exhibit 22
Rx Oxygen Concentration Economics

Case	**A1.2a**	**A1.2b**
Rx Oxygen Concentration, %	**11%**	**5%**
Total Fixed Investment	**530**	**666**
Working Capital	60	64
Total Utilized Investment	**590**	**730**
Operating Costs		
Methane	112	100
By-Product Credits	(44)	(41)
Utilities	29	58
Variable Cost	**97**	**117**
Fixed Cost	40	49
Total Cash Cost	**137**	**166**
ROIAT, %	**13.9**	**7.5**

All figures are $MM for a unit producing 1,000 MMppy of ethylene.
ROIAT is based on ethylene sales at $0.32/lb.

Exhibit 23
Ethylene / Ethane Ratio Investment Costs

Case	A1.4b.4	A1.4b	A1.4b.5
Ethylene / Ethane Ratio	1	3.35	10
Coupling Reaction System	100	95	94
Steam Cracking System	54	26	12
Compression	85	77	74
Gas Pretreating	15	14	13
Cold Box & Methane Column	53	51	46
Refining	31	31	31
Refrigeration	55	49	46
Acetylene Hydrogenation	2	1	1
Air Compression System	36	36	36
Total ISBL	**431**	**380**	**353**
Air Separation Unit OSBL	172	152	141
Total Fixed Investment	**603**	**532**	**494**

All figures are $MM ± 25% for a unit producing 1,000 MMppy of ethylene.

Exhibit 24
Ethylene / Ethane Ratio Economics

Case	A1.4b.4	A1.4b	A1.4b.5
Ethylene / Ethane Ratio	**1**	**3.35**	**10**
Total Fixed Investment	**603**	**532**	**494**
Working Capital	62	60	59
Total Utilized Investment	**665**	**592**	**553**
Operating Costs			
Methane	128	124	123
By-Product Credits	(56)	(53)	(51)
Utilities	22	15	12
Variable Cost	**94**	**86**	**84**
Fixed Cost	45	40	37
Total Cash Cost	**139**	**126**	**121**
ROIAT, %	**11.4**	**15.0**	**17.0**

All figures are $MM for a unit producing 1,000 MMppy of ethylene.
ROIAT is based on ethylene sales at $0.32/lb.

Exhibit 25
Fate of Co-Product Ethane Investment Costs

Case Fate of Co-Product Ethane	A1.4b.3 Sold	A1.4b Cracked
Coupling Reaction System	115	95
Steam Cracking System		26
Compression	86	77
Gas Pretreating	17	14
Cold Box & Methane Column	55	51
Refining	28	31
Refrigeration	53	49
Acetylene Hydrogenation	1	1
Air Compression System	43	36
Total ISBL	**398**	**380**
Air Separation Unit OSBL	159	152
Total Fixed Investment	**557**	**532**

All figures are $MM ± 25% for a unit producing 1,000 MMppy of ethylene.

Exhibit 26
Fate of Co-Product Ethane Economics

Case	A1.4b.3	A1.4b
Fate of Co-Product Ethane	**Sold**	**Cracked**
Total Fixed Investment	**557**	**532**
Working Capital	65	60
Total Utilized Investment	**622**	**592**
Operating Costs		
Methane	153	124
By-Product Credits	(72)	(53)
Utilities	12	15
Variable Cost	**93**	**86**
Fixed Cost	42	40
Total Cash Cost	**135**	**126**
ROIAT, %	**13.1**	**15.0**

All figures are $MM for a unit producing 1,000 MMppy of ethylene.
ROIAT is based on ethylene sales at $0.32/lb.

Exhibit 27

Methane Coupling Process Simplified Block Diagram

Base Case

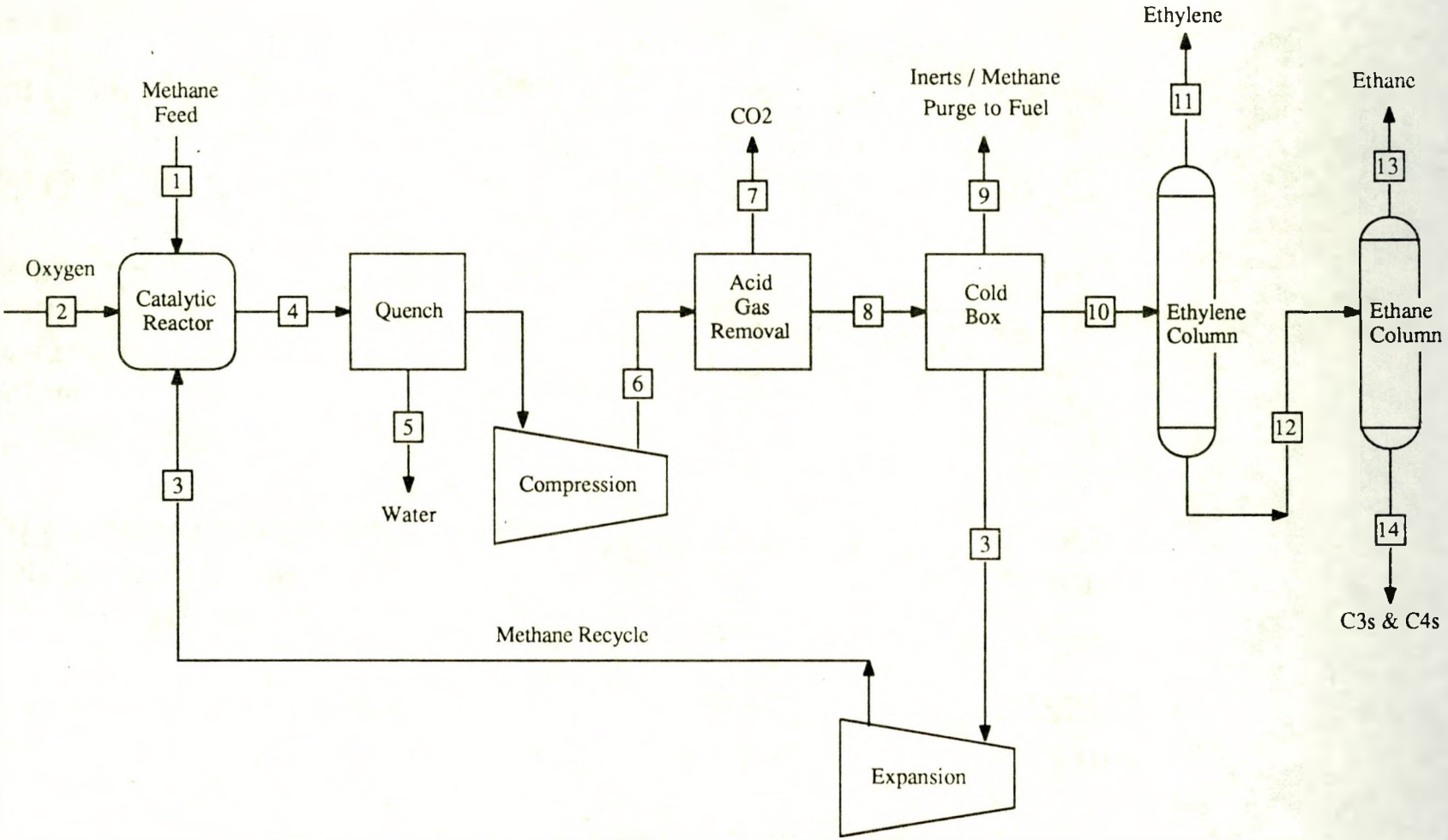


Exhibit 28

Methane Coupling Material Balance - Base Case

Stream	1 CH4 Feed	2 O2 Feed	3 CH4 Recycle	4 Rx Product	5 Quench Water	6 Comp Dischg	7 CO2 Purge
N2	2.6	6.5	80.6	89.7		89.7	
O2		285.8	0.8	0.9		0.9	
CO			0.8	0.9		0.9	
CO2	1.1			51.1		51.1	51.1
CH4	371.6		922.2	1003.7		1003.7	
C2H4			12.5	133.5		133.5	
C2H6	3.7		1.8	110.0		110.0	
C3H6				11.7		11.7	
C3H8				7.4		7.4	
C4s +				0.5		0.5	
H2O				280.7	280.7		
Total	**379.0**	**292.3**	**1018.7**	**1690.1**	**280.7**	**1409.4**	**51.1**

Stream	8 Cold Box Feed	9 Inert Purge	10 C2H4 RC Feed	11 C2H4 RC Make	12 C2H4 RC Tails	13 C2H6 RC Make	14 C2H6 RC Tails
N2	89.7	9.1					
O2	0.9	0.1					
CO	0.9	0.1					
CO2							
CH4	1003.7	81.4					
C2H4	133.5	0.1	120.9	119.8	1.1	1.1	
C2H6	110.0		108.1	0.1	108.0	107.8	0.2
C3H6	11.7		11.7		11.7	1.3	10.4
C3H8	7.4		7.4		7.4	0.1	7.3
C4s +	0.5		0.5		0.5		0.5
H2O							
Total	**1358.3**	**90.8**	**248.6**	**119.9**	**128.7**	**110.3**	**18.4**

Exhibit 29
Reactor Temperature Investment Costs

Case	1.0.3	1.0.0	1.0.4
Reactor Temperature, °C	**625**	**725**	**825**
Coupling Reaction System	75	83	98
Steam Cracking System			
Compression	86	86	87
Gas Pretreating	14	14	14
Cold Box & Methane Column	53	53	53
Refining	19	19	19
Refrigeration	64	64	65
Acetylene Hydrogenation	1	1	1
Air Compression System			
Total ISBL	**312**	**320**	**337**
Air Separation Unit	64	64	64
OSBL	150	154	160
Total Fixed Investment	**527**	**538**	**561**

All figures are $MM ± 25% for a unit producing 1,000 MMppy of ethylene.

Exhibit 30
Reactor Temperature Economics

Case	**1.0.3**	**1.0.0**	**1.0.4**
Reactor Temperature, °C	**625**	**725**	**825**
Total Fixed Investment	**527**	**538**	**561**
Working Capital	70	70	70
Total Utilized Investment	**597**	**608**	**631**
Operating Costs			
Methane	162	162	162
By-Product Credits	(102)	(102)	(102)
Utilities	27	27	27
Variable Cost	**87**	**87**	**87**
Fixed Cost	40	40	42
Total Cash Cost	**127**	**127**	**129**
ROIAT, %	**14.8**	**14.4**	**13.5**

All figures are $MM for a unit producing 1,000 MMppy of ethylene.
ROIAT is based on ethylene sales at $0.32/lb.

Exhibit 31
Reactor Pressure Investment Costs

Case	1.0.1	1.0.0	1.0.2
Reactor Pressure, psig	**80**	**150**	**240**
Coupling Reaction System	76	83	98
Steam Cracking System			
Compression	100	86	59
Gas Pretreating	14	14	14
Cold Box & Methane Column	53	53	54
Refining	19	19	19
Refrigeration	64	64	65
Acetylene Hydrogenation	1	1	1
Air Compression System			
Total ISBL	**327**	**320**	**311**
Air Separation Unit	64	64	64
OSBL	156	154	150
Total Fixed Investment	**547**	**538**	**525**

All figures are $MM ± 25% for a unit producing 1,000 MMppy of ethylene.

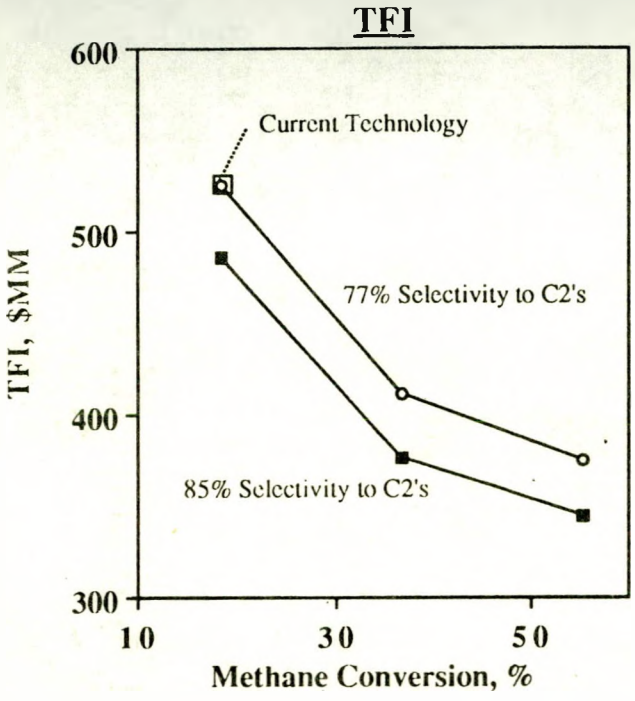
Exhibit 32
Reactor Pressure Economics

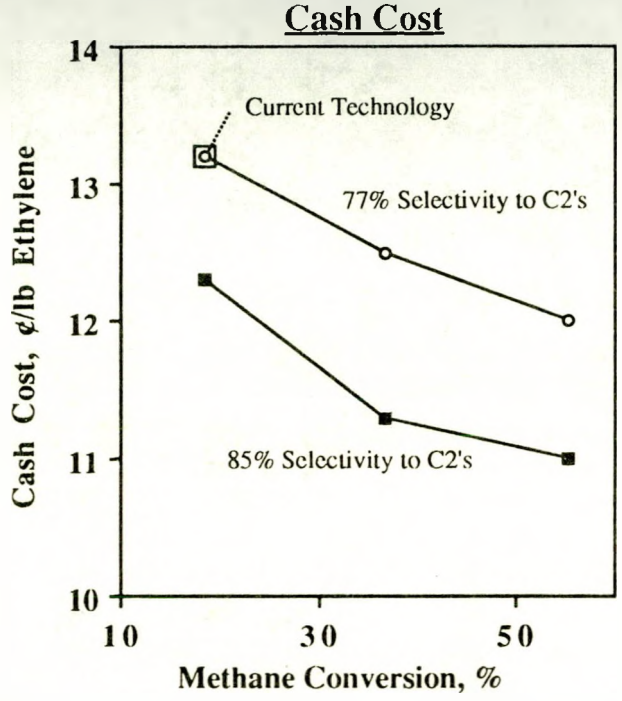
Case	**1.0.1**	**1.0.0**	**1.0.2**
Reactor Pressure, psig	**80**	**150**	**240**
Total Fixed Investment	**547**	**538**	**525**
Working Capital	71	70	69
Total Utilized Investment	**618**	**608**	**594**
Operating Costs			
Methane	162	162	162
By-Product Credits	(102)	(102)	(102)
Utilities	34	27	21
Variable Cost	**94**	**87**	**81**
Fixed Cost	41	40	40
Total Cash Cost	**135**	**127**	**121**
ROIAT, %	**13.3**	**14.4**	**15.6**

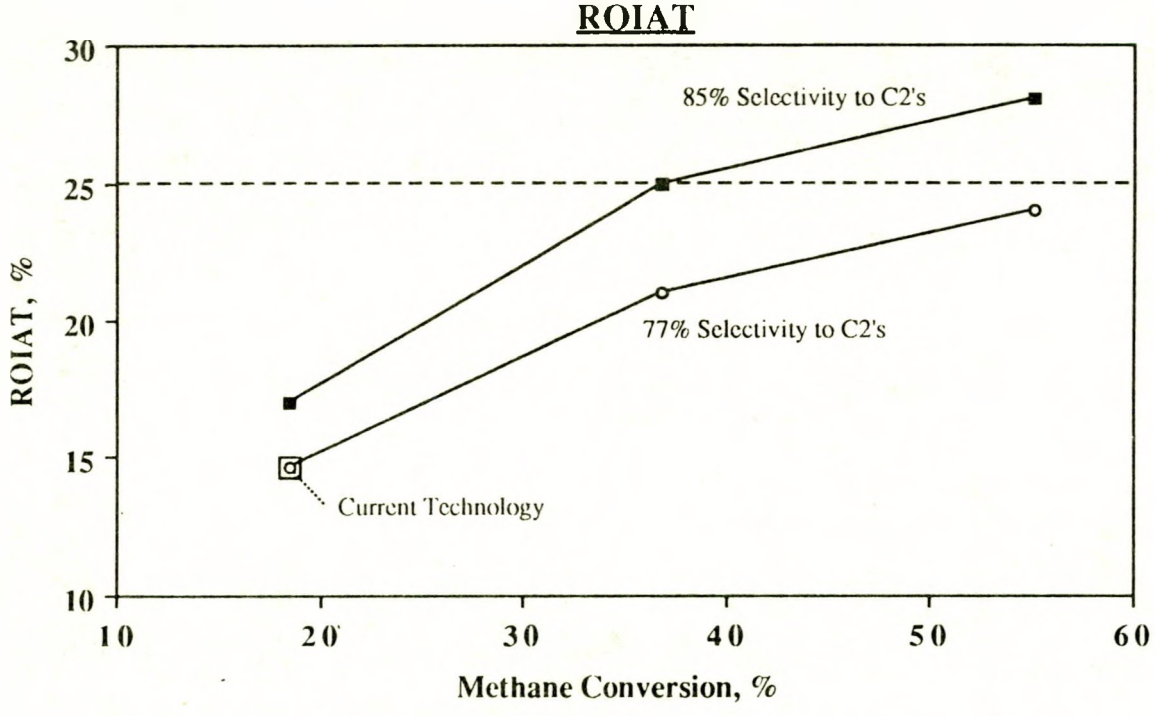
All figures are $MM for a unit producing 1,000 MMppy of ethylene.
ROIAT is based on ethylene sales at $0.32/lb.

Exhibit 33

Hypothetical Catalyst Performance Economics







Catalyst improvements should confer superior economics

Appendix J. PROCESS CONCEPTUALIZATION - METHANE TO LIQUID HYDROCARBON FUELS

TABLE J1

METHANOL FROM NATURAL GAS MATERIAL BALANCE

COMPARISON CASE

STREAM	1	2	3	4	5	6	7	8	9	10
Methane	176316	166484	9832	-	166484	25986	25986	-	179	-
Carbon Dioxide	2789	2631	158	-	2631	150315	7592	-	119840	-
Carbon Monoxide	-	-	-	-	-	182774	5410	-	-	-
Hydrogen	-	-	-	-	-	64616	19469	-	38	-
Nitrogen	2540	2399	141	-	2399	2399	2399	1132511	1135049	-
Ethane	9388	8870	518	-	8870	-	-	-	3	-
C_3^+	7620	7194	426	-	7194	-	-	-	3	-
Water	-	-	-	303196	607757	369245	1087	-	258168	672479
Oxygen	-	-	-	-	-	-	-	343594	36897	-
Methanol	-	-	-	-	-	-	1062	-	7	-
Dimethyl Ether	-	-	-	-	-	-	-	-	-	-
Higher Alcohols	-	-	-	-	-	-	-	-	-	-
Total	198653	187578	11074	303196	795335	795335	63005	1476105	1550184	672479

TABLE J1 (continued)

METHANOL FROM NATURAL GAS MATERIAL BALANCE

COMPARISON CASE

STREAM	11	12	13	14	15	16	17	18	19
Methane	166484	-	25986	515062	297577	243471	541048	-	-
Carbon Dioxide	2631	-	150315	150460	165427	135348	158052	-	-
Carbon Monoxide	-	-	182774	107236	159506	130504	112646	-	-
Hydrogen	-	-	64616	387034	248407	203243	406503	-	-
Nitrogen	2399	-	2399	46419	26850	21968	48818	-	-
Ethane	8870	-	-	-	-	-	-	-	-
C_3^+	7194	-	-	-	-	-	-	-	-
Water	304561	369283	77	764	463	378	59483	10638	68270
Methanol	-	-	-	21051	11578	9473	327087	-	304975
Dimethyl Ether	-	-	-	-	-	-	195	-	195
Higher Alcohols	-	-	-	-	-	-	361	-	361
Total	492139	369283	426167	1228026	909808	744385	1654193	10638	373801

STREAM	21	22	23	24	25	26	27	28
Water	2118944	1814383	122373	227621	16490	2684	246795	854667

TABLE J2

METHANOL TO OLEFINS MATERIAL BALANCE

COMPARISON CASE

STREAM	1	2	3	4	5	6	7	8
Carbon Dioxide	-	-	1090	1090	1090	-	-	1090
Methane	-	-	2586	2586	2586	2586	2586	-
Ethylene	-	-	69541	69541	69541	69541	69541	-
Ethane	-	-	1322	1322	1322	1322	1322	-
Propylene	-	-	34770	34770	34770	34770	34770	-
Propane	-	-	1322	1322	1322	1322	1322	-
Butene	-	-	15862	15862	15862	15862	15862	-
Pentene	-	-	6667	6667	6667	6667	6667	-
Water	68270	124754	364245	7523	861	861	-	-
Dimethyl Ether	195	27796	27796	22280	-	-	-	-
Methanol	304975	21422	22572	3216	17	17	-	-
Higher Alcohols	361	-	-	-	-	-	-	-
Total	373801	173972	547773	166179	134038	132948	132070	1090

STREAM	9	10	11	12	13	14	15
Water	362752	6030	104007	861	342866	103375	239491
Dimethyl Ether	6023	687	21593	-	-	-	-
Methanol	21079	1723	1993	17	1667	517	1150
Total	390034	8440	127593	878	344533	103892	240641

TABLE J3

MOGD MATERIAL BALANCE

COMPARISON CASE

STREAM	1	2	3	4	5	6	7	8	9	10	11
Methane	2586	1559	-	4145	4145	2586	-	-	-	2586	-
Ethylene	69541	2701	-	72242	4092	1391	-	-	-	1391	
Ethane	1322	4109	-	5431	5431	1322	-	-	-	1321	1
Propylene	34770	5622	-	40392	6317	695	-	-	-	347	348
Propane	1322	21192	-	22514	23347	2155	-	-	-	569	1586
Isobutane	-	18796	211	19007	19827	812	219	8	-	9	803
Butene	15862	8181	196	24239	8694	310	203	7	-	2	308
Butane	-	24386	1342	25728	26561	786	1389	47	-	4	782
Isopentane	-	545	17363	17908	18530	8	17977	614	-	-	8
Pentene	6667	65	3702	10434	3900	1	3834	132	-	-	1
Gasoline	-	-	424777	424777	440978	-	440978	15610	591	-	-
Distillate	-	-	25747	25747	130742	-	130742	949	104046	-	-
Total	132070	87156	473338	692564	692564	10066	595342	17367	104637	6229	3837

TABLE J4

MOGD MATERIAL BALANCE

CASE 2

STREAM	1	2	3	4	5	6	7	8	9	10	11
Methane	32	31	-	63	63	32	-	-	-	32	-
Ethylene	115971	2269	-	118240	4589	2320	-	-	-	2320	-
Ethane	61419	60074	-	121493	121493	61419	-	-	-	61418	1
Propylene	9294	182	-	9476	368	186	-	-	-	48	138
Propane	2779	3533	-	6312	7146	3613	-	-	-	418	3195
Isobutane	-	794	106	900	1721	817	110	4	-	3	814
Butene	1718	36	14	1768	84	33	15	1	-	-	33
Butane	-	764	1436	2200	3034	781	1489	53	-	1	780
Isopentane	-	8	16640	16648	17270	8	17254	614	-	-	8
Gasoline	-	-	426946	426946	443290	-	443290	15753	591	-	-
Distillate	-	-	25525	25525	130513	-	130513	942	104046	-	-
Total	191213	67691	470667	729571	729571	69209	592671	17367	104637	64240	4969

TABLE J5

METHANE TO METHANOL PRODUCT COST

COMPARISON CASE

VARIABLE COST	UNIT COST	CONSUMPTION/LB METHANOL	$MM/YR
Raw Materials			
Methane	$2.15/MMBTU	12033.0 BTU	62.19
Catalyst & Chemicals	-	-	2.43
Total			64.62
Utilities			
Steam Credit	$3.82/MLB	0.8259 LB	-7.58
Electricity	$43.00/MKWH	0.0151 KWH	1.56
Cooling Water	$0.010/MGAL	13.045 GAL	0.31
Process Water	$0.10/MGAL	0.140 GAL	0.03
Fuel Gas	$2.15/MMBTU	2774.8 BTU	14.32
Total			8.64
Total Variable Cost			73.26
PERIOD COST			
Operating Labor	10 Positions at $325M/Position		3.25
Maintenance	4% TFI		14.72
Laboratory	20% Operating Labor		0.65
Location Overhead	50% Maintenance & Labor		8.99
Total Period Cost			27.61

TABLE J6

METHANOL TO OLEFINS PRODUCT COST
COMPARISON CASE

VARIABLE COST	UNIT COST	CONSUMPTION/LB OLEFINS	$MM/YR
Raw Materials			
Catalyst	$1.60/LB	0.00183 LB	2.93
Utilities			
Steam	$3.82/MLB	1.347LB	5.15
Electricity	$43.00/MKWH	0.101 KWH	4.34
Cooling Water	$0.010/MGAL	13.35 GAL	0.13
Fuel Gas	$2.15/MMBTU	13.00 BTU	0.03
Total			9.65
Total Variable Cost			12.58
PERIOD COST			
Operating Labor	5 Positions at $325M/Position		1.63
Maintenance	4% TFI		2.97
Laboratory	20% Operating Labor		0.33
Location Overhead	50% Maintenance & Labor		2.30
Total Period Cost			7.23

TABLE J7

OLEFINS TO GASOLINE AND DISTILLATE PRODUCT COST

COMPARISON CASE

VARIABLE COST	UNIT COST	CONSUMPTION/LB GASOLINE & DISTILLATE	$MM/YR
Raw Materials			
Catalyst	$1.60/LB	0.00070 LB	1.08
Fuel Gas Credit	$2.15/MMBTU	-1066.9 BTU	-2.21
Total			-1.13
Utilities			
Steam	$3.82/MLB	0.0786 LB	0.29
Electricity	$43.00/MKWH	0.00887 KWH	0.37
Cooling Water	$0.010/MGAL	5.619 GAL	0.05
Fuel Gas	$2.15/MMBTU	1044.5 BTU	2.16
Total			2.87
Total Variable Cost			1.74
PERIOD COST			
Operating Labor	4 Positions at $325M/Position		1.30
Maintenance	4% TFI		1.95
Laboratory	20% Operating Labor		0.26
Location Overhead	50% Maintenance & Labor		1.62
Total Period Cost			5.13

TABLE J8

OVERALL PROCESS PRODUCT COST SUMMARY

COMPARISON CASE

	$MM			
	METHANE TO METHANOL	METHANOL TO OLEFINS	OLEFINS TO GASOLINE AND DISTILLATE	OVERALL PROCESS
METHANE	62.19	-	-2.21	59.98
OTHER RAW MATERIALS	2.43	2.93	1.08	6.44
UTILITIES	8.64	9.65	2.87	21.16
VARIABLE COST	73.26	12.58	1.74	87.58
PERIOD COST	27.61	7.23	5.13	39.97
PRODUCT COST	100.87	19.81	6.87	127.55

TABLE J9

RETURN ON INVESTMENT ANALYSIS

COMPARISON CASE

	¢/LB GASOLINE AND DISTILLATE	$MM/YR
SALES		
GASOLINE AND DISTILLATE	29.35 ($1.94/GAL)	282.35
LPG @ 7¢/LB	0.22	2.12
TOTAL SALES	29.57	284.47
VARIABLE COST	9.10	87.58
PERIOD COST	4.16	39.97
PRODUCT COST	13.26	127.55
ASSIGNED OVERHEAD @ 4.5% SALES	1.33	12.80
DEPRECIATION @ 10% TFI	5.10	49.09
LOCAL TAXES & INSURANCE @ 2% TFI	1.02	9.82
NIBT	8.86	85.21
NIAT @ 63% NIBT	5.58	53.68
ROIAT	10.0	10.0

	¢/LB GASOLINE AND DISTILLATE	$MM
INVESTMENT		
ISBL		
METHANE TO METHANOL	27.90	268.40
METHANOL TO OLEFINS	4.74	45.59
OLEFINS TO GASOLINE & DISTILLATE	3.61	34.75
TOTAL ISBL	36.25	348.74
OSBL		
METHANE TO METHANOL	10.35	99.60
METHANOL TO OLEFINS	2.98	28.63
OLEFINS TO GASOLINE & DISTILLATE	1.45	13.90
TOTAL OSBL	14.78	142.13
TOTAL FIXED INVESTMENT	51.03	490.87
WORKING CAPITAL	4.78	45.96
TOTAL UTILIZED INVESTMENT	55.81	536.83

TABLE J10

RETURN ON INVESTMENT ANALYSIS

HYPOTHETICAL CASE

	¢/LB GASOLINE AND DISTILLATE	$MM/YR
SALES		
GASOLINE AND DISTILLATE	24.68 ($1.63/GAL)	237.40
LPG @ 7¢/LB	0.22	2.12
TOTAL SALES	24.90	239.52
VARIABLE COST	7.99	76.87(1)
PERIOD COST	3.58	34.45
PRODUCT COST	11.57	111.32
ASSIGNED OVERHEAD @ 4.5% SALES	1.12	10.78
DEPRECIATION @ 10% TFI	4.15	39.89
LOCAL TAXES & INSURANCE @ 2% TFI	0.83	7.98
NIBT	7.23	69.55
NIAT @ 63% NIBT	4.55	43.82
ROIAT	10.0	10.0

	¢/LB GASOLINE AND DISTILLATE	$MM
INVESTMENT		
ISBL		
METHANE TO METHANOL	20.93	201.30(2)
METHANOL TO OLEFINS	4.74	45.59
OLEFINS TO GASOLINE & DISTILLATE	3.61	34.75
TOTAL ISBL	29.28	281.64
OSBL		
METHANE TO METHANOL	7.76	74.70(2)
METHANOL TO OLEFINS	2.98	28.63
OLEFINS TO GASOLINE & DISTILLATE	1.45	13.90
TOTAL OSBL	12.19	117.23
TOTAL FIXED INVESTMENT	41.47	398.87
WORKING CAPITAL	4.09	39.33
TOTAL UTILIZED INVESTMENT	45.56	438.20

NOTES: (1) Methane consumption and fuel gas usage is 86% of that shown for the Comparison Case in Table 8

(2) Investment for the conversion of methane to methanol is 75% of that required for the Comparison Case

TABLE J11

METHANE TO OLEFINS PRODUCT COST

CASE 2

VARIABLE COST	UNIT COST	CONSUMPTION/LB OLEFINS	$MM/YR
Raw Materials			
Methane	$2.15/MMBTU	34821.0 BTU(1)	74.95
Catalyst & Chemicals	-	-	1.00
Total			84.95
Utilities			
Electricity	$43.00/MKWH	0.229 KWH	9.84
Fuel Gas	$2.15/MMBTU	2685.3 BTU	5.78
Total			15.62
Total Variable Cost			91.57
PERIOD COST			
Operating Labor	6 Positions at $325M/Position		1.95
Maintenance	4% TFI		19.30
Laboratory	20% Operating Labor		0.39
Location Overhead	50% Maintenance & Labor		10.62
Total Period Cost			32.26

Note: (1) Net consumption based upon 12311.6 BTU/LB olefins fuel gas credit for the purge gas stream

TABLE J12

OLEFINS TO GASOLINE AND DISTILLATE PRODUCT COST

CASE 2

VARIABLE COST	UNIT COST	CONSUMPTION/LB GASOLINE & DISTILLATE	$MM/YR
Raw Materials			
Catalyst	$1.60/LB	0.00070LB	1.08
Utilities			
Steam	$3.82/MLB	0.6138 LB	2.26
Electricity	$43.00/MKWH	0.00887 KWH	0.37
Cooling Water	$0.010/MGAL	6.577 GAL	0.06
Fuel Gas	$2.15/MM BTU	1140.8 BTU	2.36
Total			5.05
Total Variable Cost			6.13
PERIOD COST			
Operating Labor	4 Positions at $325M/Position		1.30
Maintenance	4% TFI		2.23
Laboratory	20% Operating Labor		0.26
Location Overhead	50% Maintenance & Labor		1.76
Total Period Cost			5.55

TABLE J13

OVERALL PROCESS PRODUCT COST SUMMARY

CASE 2

	$MM		
	METHANE TO OLEFINS	OLEFINS TO GASOLINE AND DISTILLATE	OVERALL PROCESS
METHANE	74.95	-	74.95
OTHER RAW MATERIALS	1.00	1.08	2.08
UTILITIES	15.62	5.05	20.67
VARIABLE COST	91.57	6.13	97.70
PERIOD COST	32.26	5.55	37.81
PRODUCT COST	123.83	11.68	135.51

TABLE J14

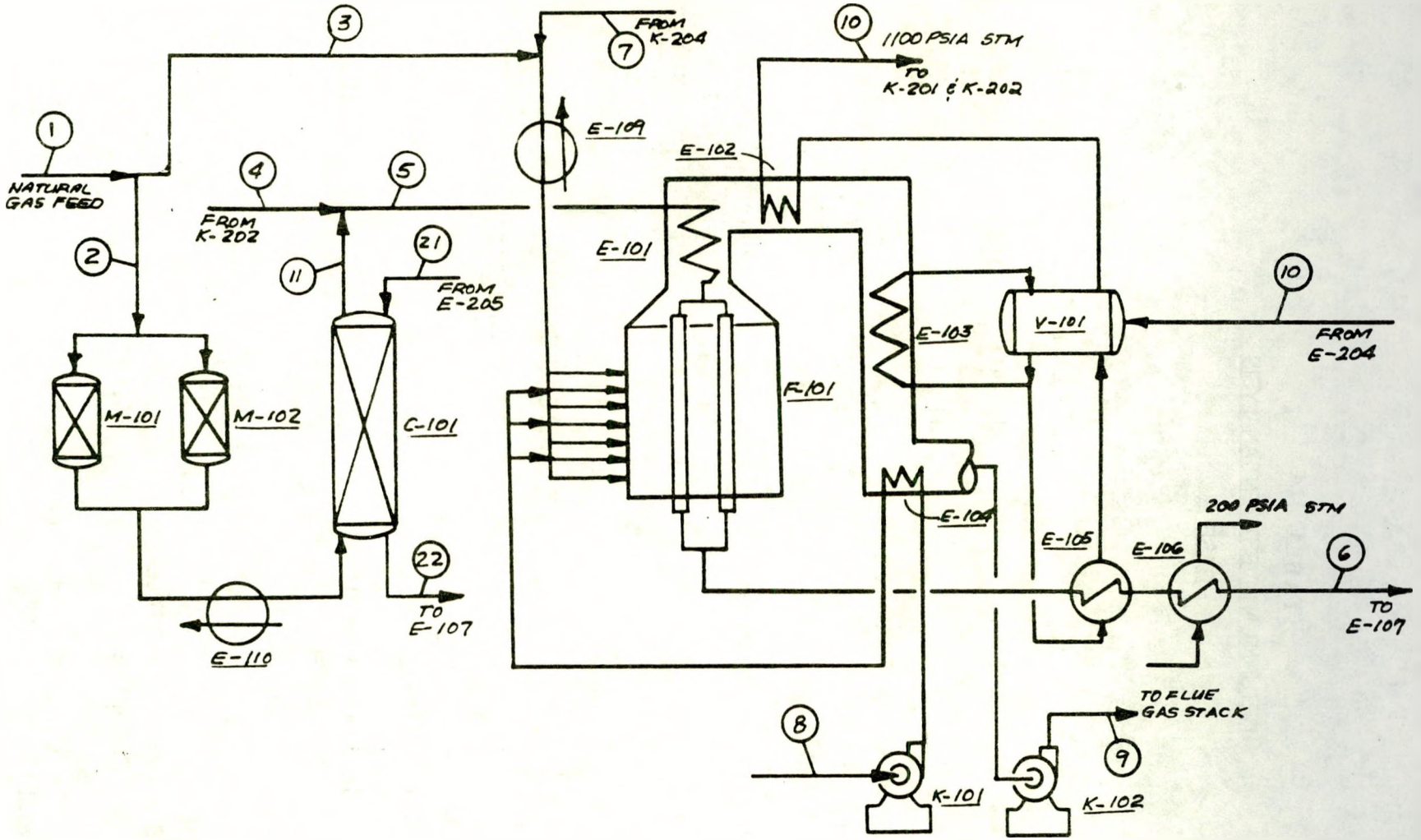
RETURN ON INVESTMENT ANALYSIS

CASE 2

	¢/LB GASOLINE AND DISTILLATE	$MM/YR
SALES		
GASOLINE AND DISTILLATE	31.74($2.09/GAL)	305.30
LPG @ 5¢/LB	0.20	1.96
TOTAL SALES	31.94	307.26
VARIBLE COST	10.16	97.70
PERIOD COST	3.93	37.81
PRODUCT COST	14.09	135.51
ASSIGNED OVERHEAD @ 4.5% SALES	1.44	13.83
DEPRECIATION @ 10% TFI	5.59	53.81
LOCAL TAXES & INSURANCE @ 2% TFI	1.12	10.76
NIBT	9.70	93.35
NIAT @ 63% NIBT	6.11	58.81
ROIAT	10.0	10.0

	¢/LB GASOLINE AND DISTILLATE	$MM
INVESTMENT		
ISBL		
METHANE TO OLEFINS	29.48	283.50
OXYGEN PLANT	6.35	61.10
OLEFINS TO GASOLINE & DISTILLATE	4.13	39.77
TOTAL ISBL	39.96	384.37
OSBL		
METHANE TO OLEFINS	11.79	113.40
OXYGEN PLANT	2.54	24.44
OLEFINS TO GASOLINE & DISTILLATE	1.65	15.91
TOTAL OSBL	15.98	153.75
TOTAL FIXED INVESTMENT	55.94	538.12
WORKING CAPITAL	5.23	50.27
TOTAL UTILIZED INVESTMENT	61.17	588.39

FIGURE J1. NATURAL GAS STEAM REFORMING (REACTION)



M-101 & M-102 HYDROGEN SULFIDE ABSORBERS	C-101 FEEDSTOCK WATER SATURATOR	E-110 NATURAL GAS FEED HEATER	E-109 FUEL PREHEATER	E-101 FEED PREHEATER	E-102 STEAM SUPERHEATER	E-103 FLUE GAS/ BOILER HEATER	E-104 AIR PREHEATER	E-105 REFORMED GAS/ HIGH PRESSURE STEAM EXCHANGER
				F-101 NATURAL GAS REFORMING FURNACE	K-101 AIR BLOWER	K-102 FLUE GASES EXTRACTOR	V-101 STEAM DRUM	E-106 REFORMED GAS/ LOW PRESSURE STEAM EXCHANGER

FIGURE J2. NATURAL GAS STEAM REFORMING (HEAT RECOVERY)

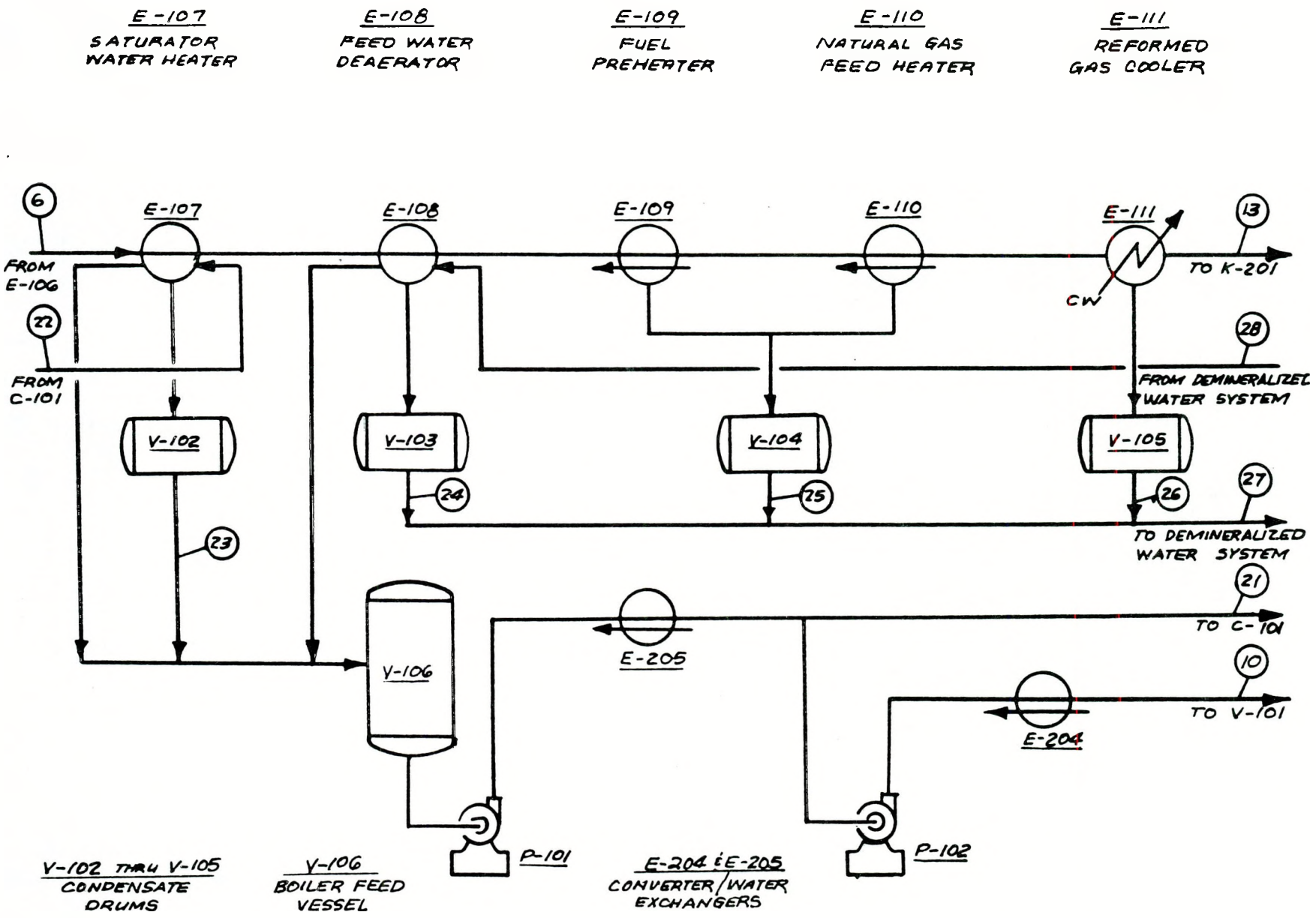


FIGURE J3. METHANOL SYNTHESIS

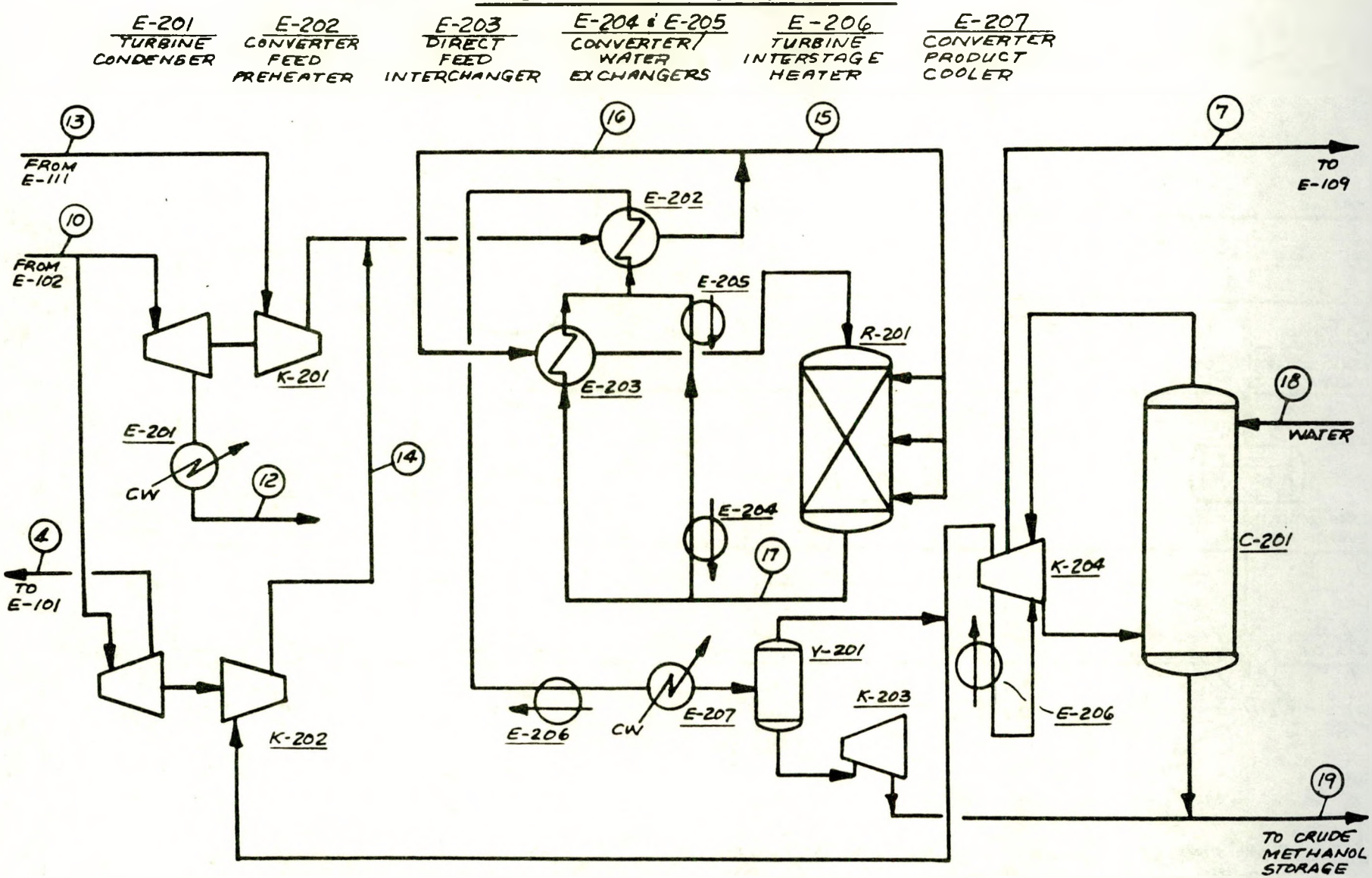


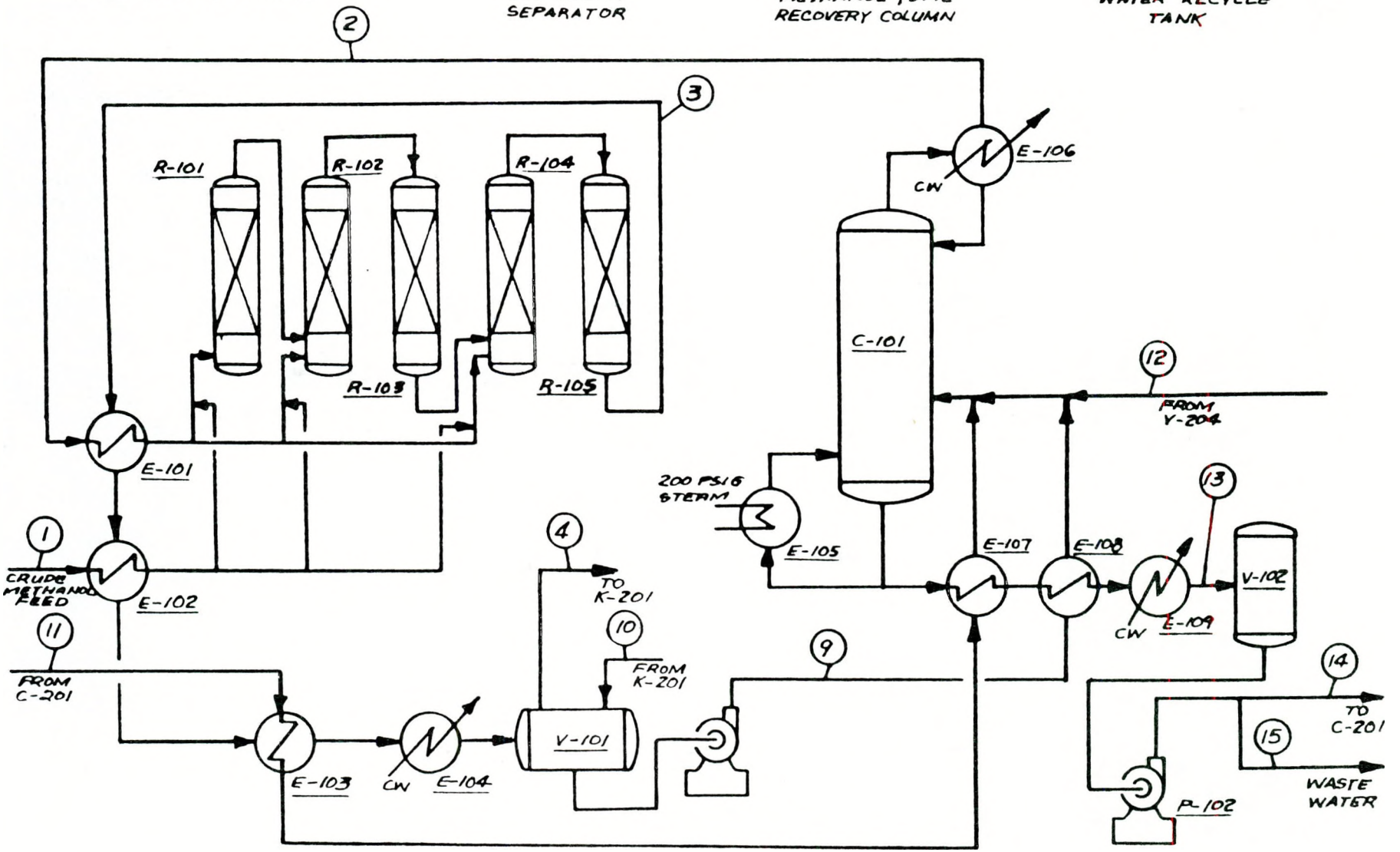
FIGURE J4. METHANOL TO OLEFINS (REACTION)

R-101 THRU R-105
FIXED BED REACTORS

V-101
EFFLUENT SEPARATOR

C-101
METHANOL / DME RECOVERY COLUMN

V-102
WATER RECYCLE TANK



E-101
RECYCLE/PRODUCT HEAT EXCHANGER

E-102
FEED/PRODUCT HEAT EXCHANGER

E-103
PRODUCT COOLER/ DME ABSORBER TAILS HEATER

E-104
PRODUCT COOLER

E-105
REBOILER

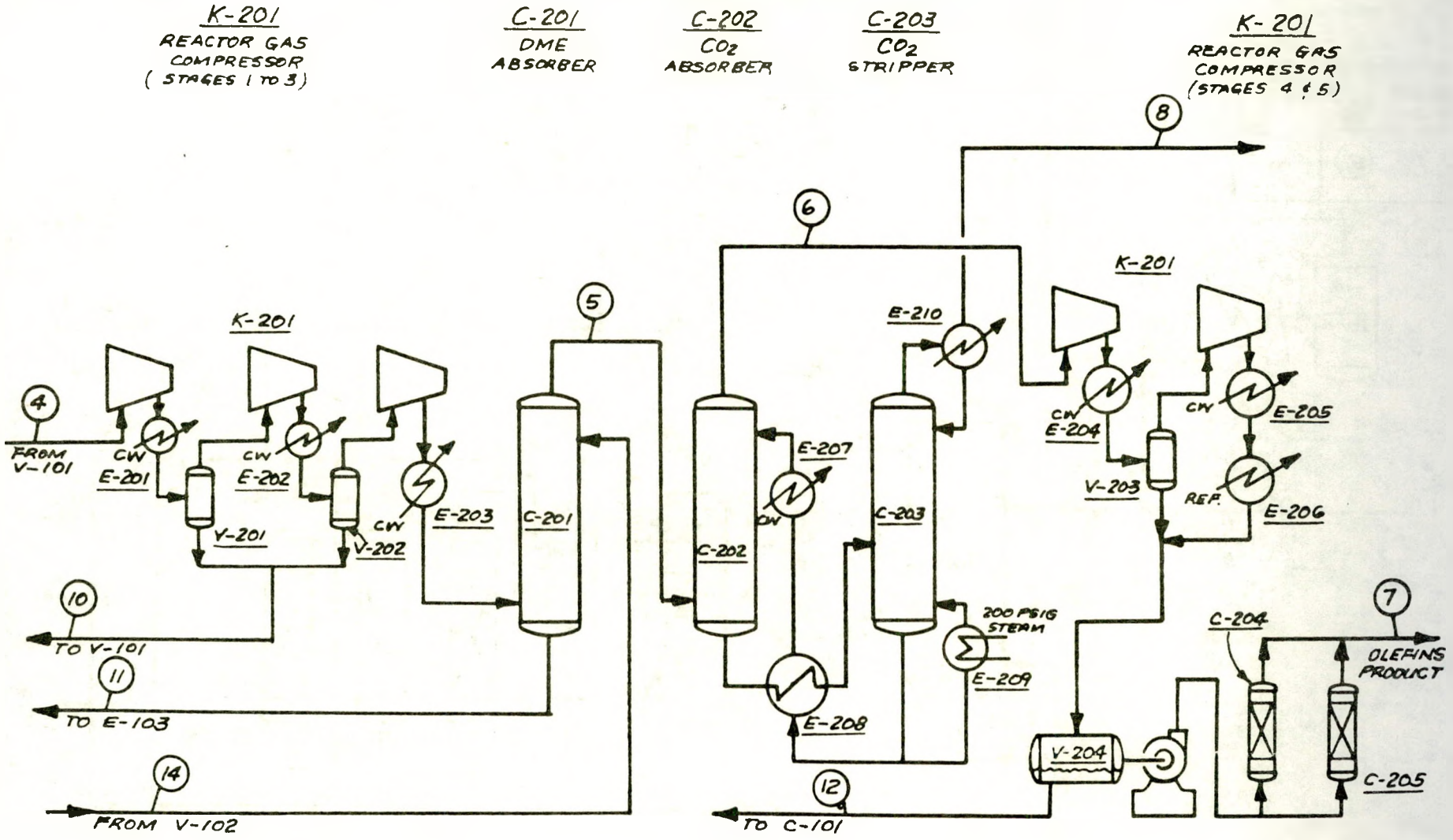
E-106
CONDENSER

E-107
TAILS COOLER/ DME ABSORBER TAILS HEATER

E-108
TAILS COOLER/ WATER RECYCLE HEATER

E-109
TAILS COOLER

FIGURE J5. METHANOL TO OLEFINS (COMPRESSION/CO_2 REMOVAL/DRYING)



E-201 THRU E-206 — INTERSTAGE COOLERS

V-201 THRU V-203 — KNOCKOUT DRUMS

E-207 — LEAN AMINE COOLER

E-208 — LEAN AMINE/RICH AMINE HEAT EXCHANGER

E-209 — REBOILER

E-210 — CONDENSER

V-204 — ORGANIC/WATER DECANTER

C-204 & C-205 — DRYERS

FIGURE J6. MOBIL OLEFINS TO GASOLINE AND DISTILLATE (MOGD)

R-101 THRU R-103 FIXED BED REACTORS

C-101 DEBUTANIZER COLUMN

K-101 DEETHANIZER COLUMN FEED COMPRESSOR

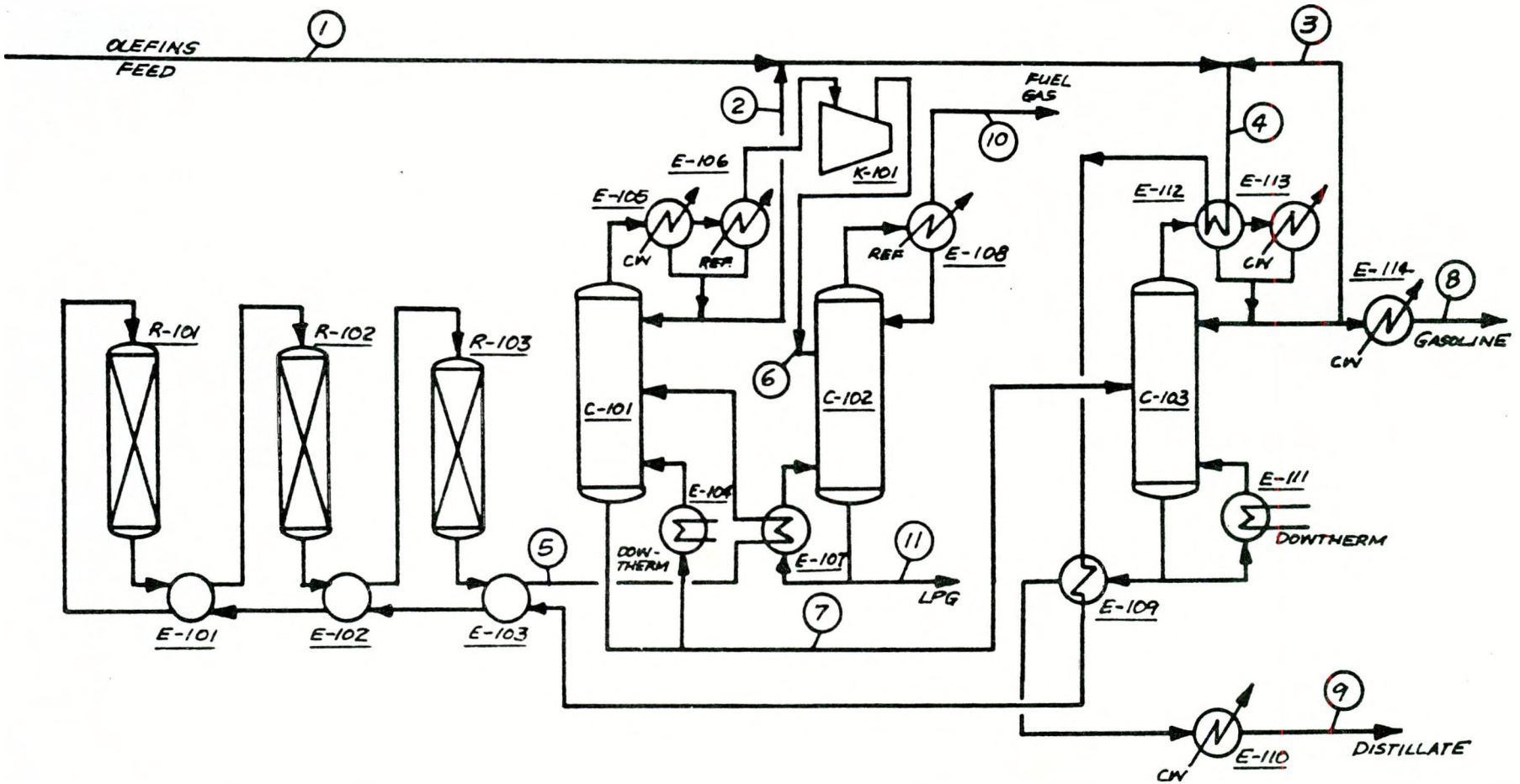
C-102 DEETHANIZER COLUMN

C-103 SPLITTER TOWER

E-112 SPLITTER TOWER PARTIAL CONDENSER

E-113 SPLITTER TOWER CONDENSER

E-114 GASOLINE PRODUCT COOLER



E-101 THRU E-103 REACTOR FEED/PRODUCT HEAT EXCHANGERS

E-104 DEBUTANIZER COLUMN REBOILER

E-105 DEBUTANIZER COLUMN WATER CONDENSER

E-106 DEBUTANIZER COLUMN REFRIGERATED CONDENSER

E-107 DEETHANIZER COLUMN REBOILER

E-108 DEETHANIZER COLUMN REFRIGERATED CONDENSER

E-109 REACTOR FEED/DISTILLATE HEAT EXCHANGERS

E-110 DISTILLATE PRODUCT COOLER

E-111 SPLITTER TOWER REBOILER

FIGURE J7. EFFECT OF METHANE COST ON LIQUID FUELS SALES PRICE-COMPARISON CASE

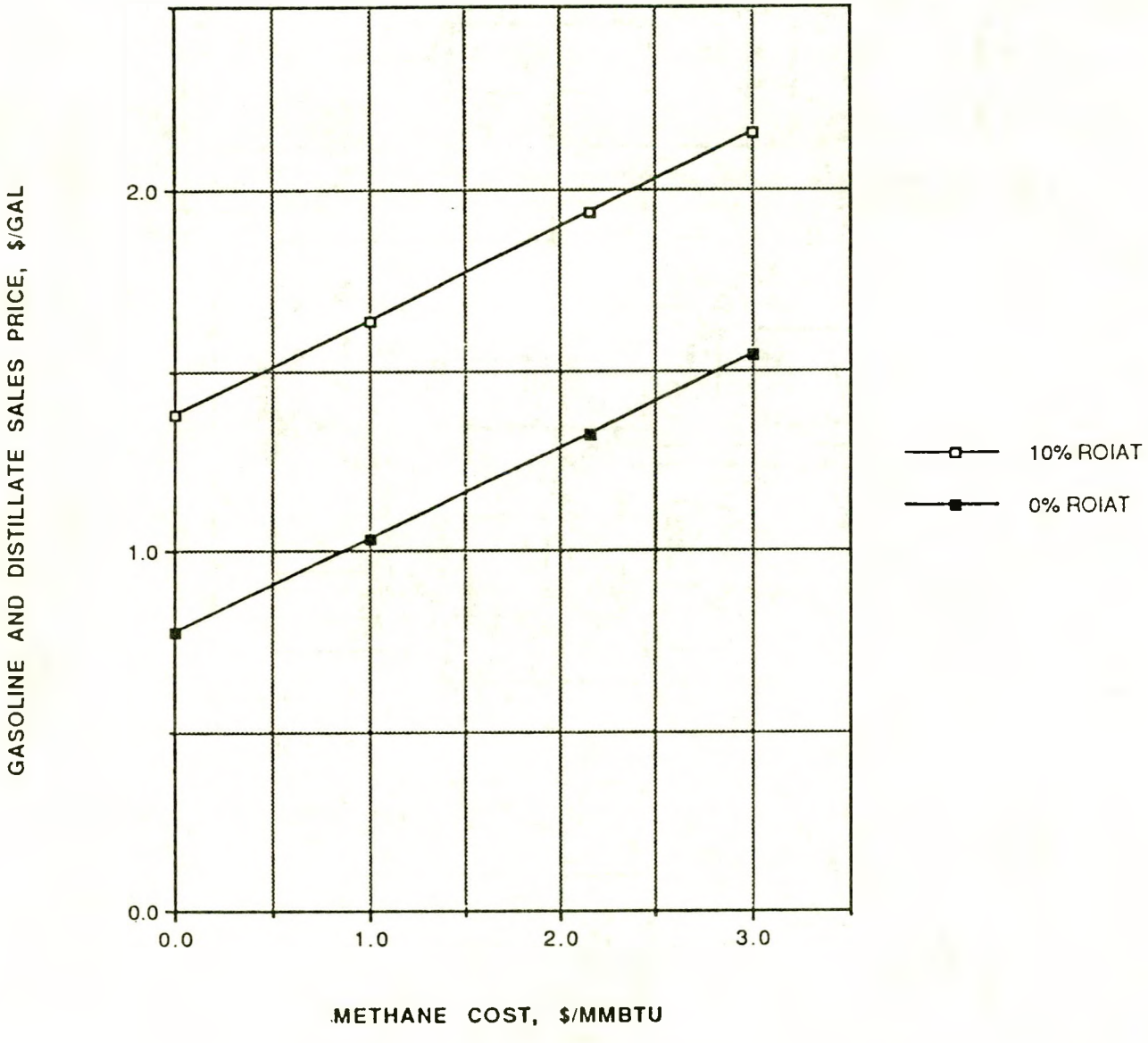


FIGURE J8. EFFECT OF METHANE COST ON LIQUID FUELS SALES PRICE-HYPOTHETICAL CASE

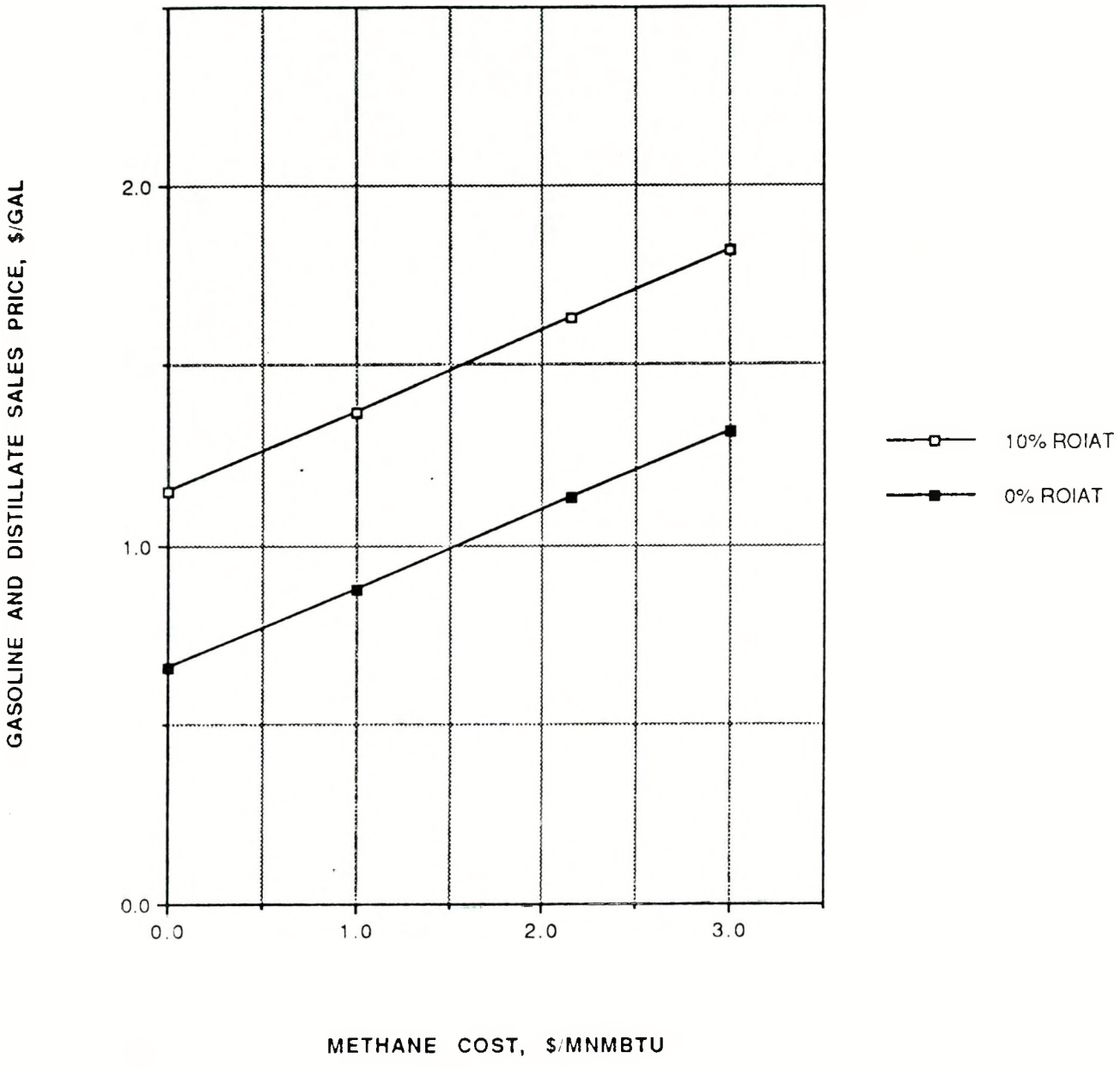
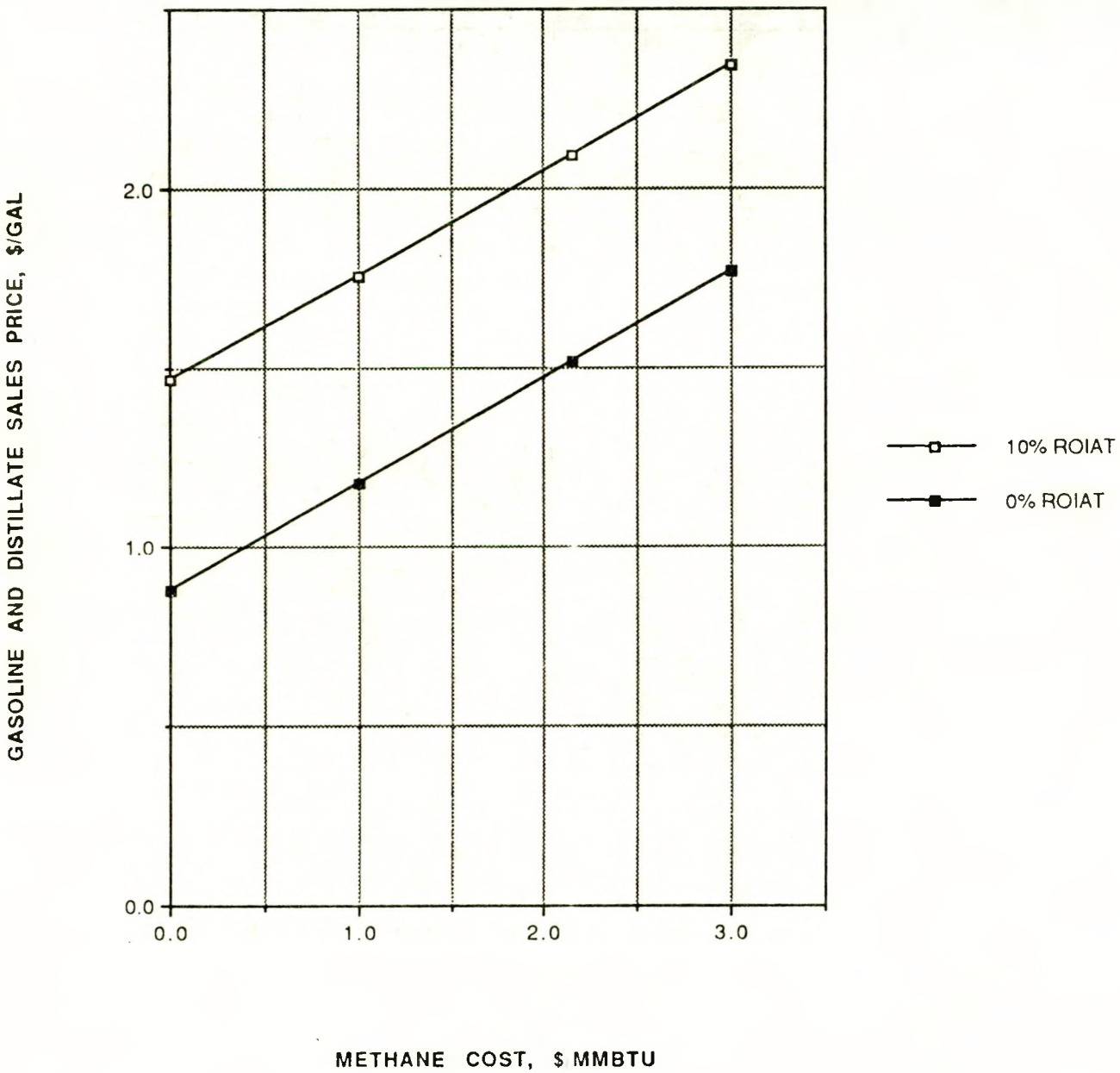


FIGURE J9. EFFECT OF METHANE COST ON LIQUID FUELS SALES PRICE-CASE 2



Appendix K. ENGINEERING ASSUMPTIONS, DEFINITIONS, METHODS, AND INDEX OF CASES

Assumptions and Definitions

Assumptions and definitions used for process economic evaluations are listed below:

Investment Estimate Basis: 1989 US Gulf Coast

Outside Battery Limits (OSBL) Investment:
40% of (Inside Battery Limits (ISBL) + Air Separation Unit Investments)
Total Fixed Investment: ISBL + Air Separation Unit + OSBL Investments

Working Capital: 10% of Sales + 20% of (Raw Materials + Utilities Costs)
Total Utilized Investment: Total Fixed Investment + Working Capital

Ethylene Value: 32 ¢/lb (used to compare among oxidative coupling cases)
Ethane Value: 16¢/gallon (5.39 ¢/lb, used to compare among oxidative coupling cases)
Propylene Value: 21 ¢/lb (used to compare among oxidative coupling cases)
Propane Value: 21.6 ¢/gallon (5.11 ¢/lb)
Crude C_4's Value: 25 ¢/gallon (5.13 ¢/lb)

Methane (Fuel Gas) Price: $2.15/MMBtu (5.13 ¢/lb)
Electricity Cost: $43.00/Mkhw

Variable Cost: Raw Material Cost - Co-Product Credits + Utilities

Fixed Costs:
Operating Labor: $325M per operating position
Maintenance: 4% of Total Fixed Investment
Laboratory: 20% of Operating Labor
Location Overhead: 50% of (Maintenance + Operating Labor)
Local Taxes and Insurance: 1% of Total Fixed Investment

Total Cash Cost: Variable Cost + Fixed Cost

Operating Income: Sales - Total Cash Cost
Depreciation: 10% of Total Fixed Investment
Taxes: 37% of (Operating Income - Depreciation)

ROIAT: (Operating Income - Depreciation - Taxes)/Total Utilized Investment

Methods

The Methane Coupling process configurations have been defined herein via Simplified Block Diagrams. Each process block represents one or more unit operations, and each unit operation, consists of one or more major equipment items. The arrangement of both the unit operations and the major equipment items within these blocks is subject to future optimization. But since this process conceptualization has been performed consistently throughout the Task 2 Engineering Program, differences in the economics between cases reflect real differences in assumptions, and are not likely to be affected significantly by any future optimization.

The Inside Battery Limits (ISBL) investment estimates, and the raw material and utility usages are based on the results of a heat and material balances for the process configurations. These balances are based on a combination of rigorous and approximate calculation methods. In general, compression and expansion operations, and vapor-liquid equilibrium separations such as distillations and single-stage flashes are modeled rigorously. Chemical reactions and special separations such as absorption and adsorption are modeled approximately.

The ISBL investment estimates are derived from approximate sizes and costs for each of the major equipment items included in the process configurations. Once the total major equipment cost for a process configuration has been determined, the total installed cost is determined by applying the following cost engineering factors which have been derived from UCC&P experience with similar processes:

Listed Major Equipment:	Total major equipment cost based on heat and material balance quantities
Unlisted Major Equipment:	12.5% of Listed Major Equipment
Direct Material:	89% of (Listed + Unlisted Major Equipment)

Indirect Material:	22% of (Listed + Unlisted Major Equipment)
Direct Labor:	63.7% of (Listed + Unlisted Major Equipment) (based on 1989 US Gulf Coast non-union construction)
Indirect Labor:	49.4% of Direct Labor
Subcontracts:	15% of (Listed + Unlisted Major Equipment)
Site Administration:	15.8% of Direct Labor
On-Site Cost:	Sum of Listed Major Equipment and all the above
Engineering:	27.6% of On-site Cost
Contingencies:	15% of (On-site Cost + Engineering)
Total ISBL Investment:	On-site Cost + Engineering + Contingencies

The methane raw material is assumed to be of the following composition:

Methane:	99.0 mole %
Ethane:	0.5 mole %
Nitrogen:	0.4 mole %
Carbon Dioxide:	0.1 mole %

The oxygen raw material is assumed to be of the following composition:

Oxygen	97.5 mole %
Nitrogen	2.5 mole %

The oxygen conversion per pass has been assumed to be 100% in all cases.

The raw material and utility usages are derived directly from the heat and material balances. Heat integration has been performed to minimize the heating and cooling that must be supplied via external utilities. In general, the exothermic heat of reaction generated in the oxidative coupling step is recovered as steam, which is then used to drive condensing turbines in the compression and refrigeration systems. The hot reaction product gas is cooled by heating the cold reaction feed gas up to a point, with the balance of the feed preheat supplied directly via gas-fired heaters. Purge gas from the process is most often the source of fuel for these heaters.

Single-pass cooling water is used for ambient temperature cooling. Refrigeration systems use propylene as the refrigerant down to -40 °C, and ethylene as the refrigerant down to -95 °C.

Index of Sensitivity Study Cases

The following list describes each case studied for methane coupling and refers to the pages in this report which discuss this case.

Case	Diluent	CH_4/O_2 Ratio	Notes	Pages	Exhibits
1.0.0	methane	9	Base Case	368-373	27-32
1.0.1	methane	9	Press = 80 psig	372-373	31-32
1.0.2	methane	9	Press = 240 psig	372-373	31-32
1.0.3	methane	9	Temp = 625 °C	370-371	29-30
1.0.4	methane	9	Temp = 825 °C	370-371	29-30
A1.1b	nitrogen	2		342-344, 351-353, 354-355, 360-361	5-6, 10-12, 13-14, 19-20
A1.1c	nitrogen	4		354-355, 360-361	13-14, 19-20
A1.1d	nitrogen	1		354-355, 360-361	13-14, 19-20
A1.2a	methane	7		342, 345-346, 351-353, 360-361, 362-363	5, 7, 10-12, 19-20, 21-22
A1.2b	methane	17	O_2 Conc = 5%	362-363	21-22
A1.3b	steam	2		342, 347-348, 351-353, 356-357, 360-361	5, 8, 10-12, 15-16, 19-20
A1.3c	steam	4		356-357, 360-361	15-16, 19-20
A1.3d	steam	1		356-357, 360-361	15-16, 19-20
A1.4b	sequential	5		342, 349-350, 351-353, 358-361, 364-367	5, 9, 10-12 17-20, 23-26
A1.4b.3	sequential	5	C_2H_6 is sold	366-367	25-26
A1.4b.4	sequential	5	$C_2H_4/C_2H_6 = 1$	364-365	23-24
A1.4b.5	sequential	5	$C_2H_4/C_2H_6 = 10$	364-365	23-24
A1.4c	sequential	2		360-361	19-20
A1.4d	sequential	7		360-361	19-20
A1.4e	sequential	10		360-361	19-20

DOE/PC/79817---8

DIRECT CONVERSION OF METHANE TO C_2's AND LIQUID FUELS

Final Technical Progress Report
for the Period October 1, 1987 - December 31, 1989

April 15, 1990

Work Performed Under DOE Contract Number DE-AC22-87PC79817
Pittsburgh Energy Technology Center

Industrial Chemicals Division

Solvents and Coatings Materials Division

Union Carbide Chemical and Plastics Company Inc.
South Charleston Technical Center
South Charleston, West Virginia 25303

Received by OSTI
JAN 07 1991